# komunikácie

COMMUNICATIONS

SCIENTIFIC LETTERS OF THE UNIVERSITY OF ŽILINA

Volume 24

UNIVERSITY
OF ŽILINA

ISSN 1335-4205

1953 70 2023

4/2022

# UNIVERSITY OF ŽILINA
## EDIS-Publishing House UNIZA

EDIS-Publishing House of the University of Žilina (UZ) is one of the University of Žilina's consituents. The beginning of its existence dates back to 1990. In the course of its work, the publishing house has published more than 4 700 titles of book publications, especially university textbooks, scientific monographs, scripts, prose, but also enriched the book market with titles of regional, children's and popular literature.

Students and professional public have the opportunity to purchase published titles in the „Selling Study Literature" directly on the premises of the University of Žilina, in the EDIS shop or upon order on a „cash on delivery" basis. All published titles are available at: www.edis.uniza.sk.

## EDIS-Publishing House of the University of Žilina offers book titles in English

*Lenka Černá, Jozef Daniš*
**APPLICATION OF COST CALCULATIONS IN THE TARIFF POLICY FORMATION IN RAILWAY TRANSPORT**
ISBN 978-80-554-1391-4 Price 7.61 €

*Jozef Gašparík et al.*
**RAILWAY TRAFFIC OPERATION**
ISBN 978-80-554-1281-8 Price 15.80 €

*Eva Nedeliaková, Jana Sekulová*
**EVALUATION OF QUALITY IN RAILWAY TRANSPORT**
ISBN 978-554-1272-6 Price 8.00 €

*Anna Tomová*
**ECONOMICS OF AIR NAVIGATION SERVICES**
ISBN 978-80-554-0905-4 Price 14.30 €

*Felix Fedorovič Rybakov, Alexander Nikolaevič Lyakin, Štefan Cisko et.al.*
**GLOBALIZATION AND DEVELOPMENT OF INFRASTRUCTURE**
ISBN 978-80-554-0719-7 Price 19.80 €

*Marica Mazurek*
**MODELS OF BRANDING AND THEIR APPLICATION**
ISBN 978-80-554-1705-9 Price 9.00 €

*Ján Bujňák, Ružica Nikolić, Jelena Djoković*
**STEEL STRUCTURES COLLECTION OF SOLVED PROBLEMS WITH EXCERPTS FROM THEORY**
ISBN 978-80554-0404-2 Price 9.34 €

*Martin Bugaj*
**Aeromechanics 1**
ISBN 978-80-554-1675-5 Price 14.50 €

*Michal Kvet, Karol Matiaško, Marek Kvet*
**USB - BECOME EXPERT IN MYSQL PRACTICES FOR DATABASE SYSTEMS IN MYSQL**
ISBN 978-80-554-1786-8 Price 13.50 €

*Tetiana Hovorushchenko et.al.*
**CD - INTELLIGENT INFORMATION-ANALYTICAL TECHNOLOGIES...**
ISBN 978-80-554-1729-5 Price 3.50 €

*Karol Matiaško, Michal Kvet, Marek Kvet*
**CD - Practices for database systems**
ISBN 978-80-554-1397-6 Price 2.20 €

*Jozef Melcer*
**Dynamics of structures**
ISBN 978-80-554-1698-4 Price 19.00 €

**EDIS-Publishing House UNIZA**
Univezitná 8215/1
010 26 Žilina
e-mail: edis_objednavky@uniza.sk, edis@uniza.sk
www.edis.uniza.sk

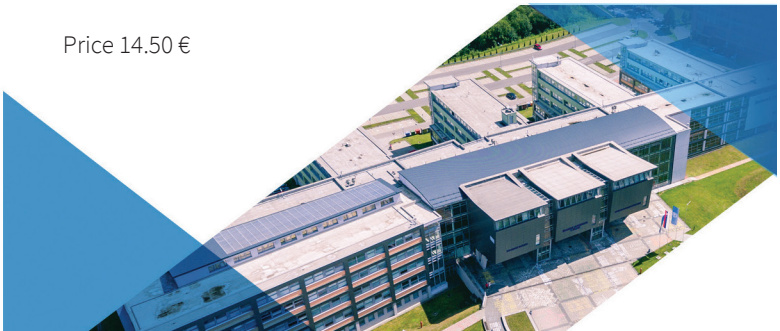

## A - OPERATION AND ECONOMICS



## B - MECHANICAL ENGINEERING



## D - CIVIL ENGINEERING IN TRANSPORT

## E - MANAGEMENT SCIENCE AND INFORMATICS



## F - SAFETY AND SECURITY ENGINEERING IN TRANSPORT

## G - TRAVEL AND TOURISM STUDIES IN TRANSPORT DEVELOPMENT

# A METHODOLOGICAL FRAMEWORK FOR EVALUATING SMART TRANSPORT APPLICABILITY IN ALGIERS

**Naima Labri *, Amal Baziz**

Department of Geography and Territorial Planning, LREAU Laboratory, USTHB (Houari Boumediene Sciences and Technology University), Algiers, Algeria

*E-mail of corresponding author: n-labri@live.fr

***Resume***

Intelligent transport systems (ITS), deriving from smart mobility concept, are emerging as a solution to transportation problems using information and communication technologies (ICT) to improve the transport performance and quality. The authors of this work aimed to propose a framework that evaluates applicability of ITS in the public transport sector, using Algiers as a case study and to discover eventual barriers to their implementation. The proposed framework is supported by literature contributing to the question of what barriers are encountered in developing versus developed countries when implementing ITS, this type of ignorance of contextual difficulties leads to calls for conceptual research in this regard. The methodology was illustrated using a matrix of indicators and measuring the applicability index. The result highlighted several barriers to technology adoption in Algiers public transport system and requires acting as a priority on governance and performance indicators according to Algiers context as a North African city.

***Article info***

Received 28 October 2021
Accepted 27 June 2022
Online 12 August 2022

***Keywords:***

ITS (Intelligent transport systems)
Algiers
public transport (PT)
smart mobility
framework

Available online: https://doi.org/10.26552/com.C.2022.4.A160-A171

ISSN 1335-4205 (print version)
ISSN 2585-7878 (online version)

## 1 Introduction

"Transportation systems are of strategic importance, for several reasons: they are the first tool of social cohesion, a powerful element in promoting economic and employment development and establishing an equilibrium between territorial areas with different levels of accessibility". [1] "The basis of its good functioning is to have enough adequate and timely information" [2]. The slightest problem that may affect them will impact negatively the quality of life of citizens and risk of compromising sustainable development objectives [3], which defines that, by 2030, governments should provide access for all to safe, effective, efficient and sustainable transport through the development of a digital environment or context [4].

Digital environment makes us think automatically of "Smart city, which is probably the most in vogue, debated and analyzed concept among researchers and governmental representatives from all over the world" [5].

The ICT enabled smart cities can play a key role in improving transport sustainability through controlling the systems more efficiently, facilitating behavioral changes and reducing energy consumption [6]. They are the source of fundamental changes in terms of travel, transport infrastructure and access to travel data providing the public stakeholders with new knowledge and new tools for control and management in favor of users as their journey can be better programmed in terms of time and combinations of modes, particularly at peak times.

"Intelligent Transport Systems (ITS) is the most common expression used to indicate the integrated application of ICTs to transport" [7] as one of the key tenets of mobility solutions, specialized for data collection, storage and processing and provide expertise in the planning, execution and assessment of the integrated initiatives and policies of smart mobility [8].

"They can be applied to all modes of transport, that is, air, ship, rail and road and to every element of a transport system, that is, the vehicle, the infrastructure and the driver or user, interacting together dynamically" [9]. "Their overall function is to support transport network controllers and other users (citizens, companies and city governments) in the decision-making process"

[10] by providing innovative services enabling them, to be better informed and to make safer, more coordinated and "intelligent" use of transport networks" [11].

"They include a large number of technologies and systems in various stages of development from research prototypes or even concepts, to commercially available products and applications" [12]. Their benefits are perceived significantly through their application particularly in the field of public transport [13].

In parallel with the commitment of the Algiers smart city project aiming to make the capital city smart by 2035, to achieve sustainability and to solve the major problems concerning Algiers, in order to transform it into a cleaner, safer, more modern, more accessible and more attractive city. Several actions have emerged, especially in the public transport, including the launch of the metro, tramway, the modernization of the commuter train and the upgrade of bus network [14]. The question to ask is the context of the transport sector in Algiers sufficiently favorable to the applicability of a smart transportation project? Which barriers need to be addressed for this challenge?

Authors were interested in this work, in exploring the question of technology in public transport in Algiers with an objective to design a framework to evaluate its applicability and draw up, to decision-makers, the priority dimension to be addressed and the conditions to be ensured for planning the transition toward its implementation. The importance of this work is to provide decision makers with a tool to guide their decisions; it should be specified that the framework established is adapted to Algiers as it eliminates obstacles that could affect technology implementation given its particularities, it is based on a comparative analysis between the two contexts (a developed and a developing context) to build up a tool for assessing the smart public transport policy that can be applied to other study cases while adapting it, depending on the objective of the study, by adding or removing indicators or variables. On the other hand, the transport sector is of the major importance in the urban policy in Algiers and the issue of technologies applied to public transport has rarely been addressed before.

## 2 Literature review

The objective of this step is to provide additional knowledge on the current state of smart mobility and its frameworks, considering the significant gaps in research, as it is still in its early stages [8].

Authors of [8] summarized smart mobility definitions and benefits. Many smart mobility initiatives have been noticed since its implementation, as well as in Germany, Spain, Netherlands, Italy, United Kingdom and France [8]. Intelligent transport system (ITS), as confirmed by previous scientific research, supports the urban smart mobility [9, 15-16]. They have been developed over the years, as a means to solve a variety of transportation problems [17]; particularly in Public Transport they can play a primary role to guarantee a high level of performance and quality of services [18].

For technology deployment in transportation, is highlighted in [18], that it implies appropriate knowledge and prior feasibility and applicability studies aiming to analyze if and how a certain application can be realized additively. Cambpell [19] explained the importance of putting IT in the hands of users who understand it, leveraging learning and mastering following its permanent evolution. However, technology alone does not guarantee successful results by itself; where the solution should extend beyond technology as its accompaniment [18], by an appropriate and functional organization on a permanent basis and by an effective day-by-day operation [20]. Another factor discussed in [18], is regarding the risks of the achievement of intelligent transportation, requiring an adapted approach by political leaders to support planning, transition and implementation process [21] or [22].

As stated in [23], some disappointment was noted according to smart mobility with regards to its techno-centric aspect that refers to the simple application of technology to the mobility system, confirmed also by [9] and its aspect centered on the user as a potential consumer of the services, making the concept too far from the reality of urban mobility in cities. Authors of [8] affirmed that there remains a large gap between the sustainability objectives of smart mobility and their study finds that the range of social, behavioral and cultural issues associated with smart mobility remain understudied. Authors of this article believe that reflection should be more focused on the citizen not just as user and his interaction with the digital world, a smart mobility solution is not just about using less energy or making use of ITC, it is about being able to function as an integral part of a larger system that also regards participation, urban and space quality, human capital, education and learning in urban environments [24], especially the community needs [25]. Then, it is recommended to develop an integrated approach of smart transportation, through the integration between technological and social innovations [26] and sustainability [27]. There are several transportation resources and procedures for intelligent cities that can be considered and adopted by urban centers, such as frameworks, which is a common methodology for the planning and assessment of smart mobility initiatives. With such a growing demand for urban travel comes the need for the scientific community to create tools that they can use to evaluate how practical, effective and safe these new modalities of transportation will be for the general public [8]. Such evaluations will protect different stakeholders involved in the process of developing smart transportation options. Success indicates the effectiveness of the framework put in place by the stakeholders when they see the project come to

fruition -from the planning phase of the project to its completion, confirming already the importance of the regulatory framework' [8].

Authors in [25-29] have adopted this methodology in their work. In [30] are defined six evaluation indicators and their acceptance rankings in the context of a feasibility study on the implementation of smart transportation, a methodological framework highlighting the smartness indicators derived from the capabilities of a smart system has been set up; the matrix of indicators is based on the 6 major criteria of a smart system. Authors of [31] developed a framework for evaluating smart mobility implementation and ranking initiatives in 11 Italian cities, based in three categories of smart mobility, which are accessibility, sustainability and ICT developed in 28 indicators. On the other hand, researchers in [32] introduced a taxonomy of 46 different smart mobility indicators to define the extent of ICT use and the related benefits. Indicators have become common elements in transport planning and policy making. So far, much research on transport indicators has been concerned with their function as suitable measurement tools for various planning and monitoring task, [33]. From the above it can be noticed that the choice of indicators reflects mainly the principles of a smart system, moreover it reflects the existence of an efficient urban transport system in terms of performance and that we are trying to make more efficient through technologies, which makes it very feasible and easy to implement, while in a context where there are constraints of different kinds, relating to urban transportation and ICT deployment, the environment becomes necessarily less favorable, such an environment characterizes the developing countries. It is precisely those constraints that constitute risks to compromise the expected results, as concluded by [18] affirming the need to consider and to deal with them, especially regarding the smart transportation investments.

Benchmarking is a widely used method of learning practices and performances from the best [34], this method is very common as a tool to promote urban policies and to learn from the experiences how to address the challenge of smart mobility on the condition of facing the limitations that may exist according to the contextual differences between the cities. Authors of [18] suggest to define ITS functionalities according to the specific objectives of PT Operators or Authorities and adapt them to the specific context, in particular

***Table 1*** *Matrix of indicators - part I*

| Indicators | | Extent of variables | Score |
|---|---|---|---|
| Governance | G1 | Availability of legal framework /NA, TP, PC, FC | |
| | G2 | Availability of strategic instruments / NA, TP, PC, FC | NA |
| | G3 | Availability of organising committee / NA, TP, PC, FC | NA |
| | G4 | Cooperation between actors and committee / NA, TP, | NA |
| | G5 | PC, FC | NA |
| | G6 | Periodic evaluation of committee actions / NA, TP, PC, | NA |
| | G7 | FC | NA |
| | G8 | Availability of standards and common language /NA, | NA |
| | G9 | TP, PC, FC | NA |
| | G10 | Coordination /NA, TP, PC, FC | (0) |
| | G11 | Consistency with existing laws /NA, TP, PC, FC | NA |
| | G12 | Return on investments | NA |
| | | Territorial coordination | NA |
| | | Development of specifications and standards | NA |
| | | Practice standards | |
| Social | S1 | Accessibility rate (all modes combined)/ NA, TP, PC, FC | PC |
| | S2 | Respect travel data's privacy / NA, TP, PC, FC | NA |
| | S3 | Availability of equipment at stations/ NA, TP, PC, FC | PC |
| | S3 | Availability of equipment at terminal / NA, TP, PC, FC | PC |
| | S4 | Security on board / NA, TP, PC, FC | PC |
| | S4 | Security at stations/ NA, TP, PC, FC | PC |
| | S4 | Security at terminals/ NA, TP, PC, FC | PC |
| | S5 | Safety against accidents/ NA, TP, PC, FC | TP |
| | S6 | Urgent interventions level at stations / NA, TP, PC, FC | TP |
| | S6 | Urgent interventions level on board/ NA, TP, PC, FC | TP |
| | S7 | Quality of services provided NA, TP, PC, FC | PC |
| | S8 | Comfort on board/ NA, TP, PC, FC | PC |
| | S8 | Comfort at stations/ NA, TP, PC, FC | PC |
| | S8 | Comfort at terminal/ NA, TP, PC, FC | PC |

***Table 2*** *Matrix of indicators - part II*

| Indicators | | Extent of variables | Score |
|---|---|---|---|
| Performance | P1 | Availability of exchange data between actors | TP |
| | P2 | Availability of real-time information for users at stations | TP |
| | P2 | Availability of real-time information for users on board | TP |
| | P3 | Reliability of real-time information for users at stations | TP |
| | P3 | Continuity of services at urban scale | TP |
| | P4 | Continuity of services at regional scale | TP |
| | P4 | Supply absorption | TP |
| | P5 | Energy efficiency | TP |
| | P5 | Feasibility study / (only for tramway, normal panels for the rest), | NA |
| | P6 | Risks study (only for tramway, normal panels for the rest) | NA |
| | P7 | Functional compatibility with existing public transport system | NA |
| | P8 | Functional compatibility with future perspectives of public transport system | NA |
| | P8 | Proportionality with urban planning context (land use planning) | NA |
| | P8 | Intermodality terminals availability | PC |
| | P9 | Integrated pricing and ticketing availability | PC |
| | P10 | Synchronization between modes | TP |
| | P11 | Cost efficiency | TP |
| | P12 | Data sharing and updating | TP |
| | P13 | Extent of coverage | TP |
| Smartness | I1 | Centralized system of controlling PT and data | PC |
| | I2 | Stations equipped with camera | PC |
| | I2 | Public vehicle equipped with camera | PC |
| | I3 | Stations equipped with electrical info device | PC |
| | I3 | Public vehicle equipped with electrical info device | PC |
| | I4 | Public vehicle equipped with sensors | NA |
| | I4 | Stations equipped with sensors | NA |
| | I5 | Terminals equipped with automatic ticket machine | PC |
| | I5 | Stations equipped with ticket validation device | PC |
| | I5 | public vehicle equipped with ticket validation device | PC |
| | I6 | Use of smart card | TP |
| | I6 | Track passenger's movement | NA |
| | I7 | Use of cellular application | TP |
| | I8 | Public vehicle equipped with functioning GPS | PC |

with regard to the role of the actors involved and the characteristics of the existing transport services.

Thus, this work is an opportunity to propose a framework that deals with those limitations to eliminate the barriers imposed by the context, especially when there is no an "one size fits-all" solution framework for smart cities [35] and each nation has its unique techniques to meet this challenge, [8].

## 3 Materials and methods

### 3.1 Measuring applicability index of smart transportation in Algiers

Using the matrix of indicators and variables (Table 1 and Table 2), appropriate scores for each variable of indicator were assigned. Then, we proceed to the measurement of the applicability index [30], according to:

$$Al_i = \frac{\sum_{i=1}^{J} Si}{V_i} \times 100\%, \quad (1)$$

where $Al_i$ is the applicability index of sub-system $i$, $S_i$ is score of indicators and $V_i$ is the total number of variables.

The variables are quantified by means of a qualitative scale of four categories [30], the values adopted are 0, 0.33, 0.67 and 1 and they reflect, respectively, the following data of variables of each indicator: NA - Not available (0), TP - Trail phase (0.33), PC - Partial coverage (0.67), FC - Full coverage (1)

It should be noted that variables, derived from the social, performance and smartness indicators, concern all the modes of transport combined (metro, tramway, train and bus); governance indicator reflects variables that concern transport public sector in general.

## 4 Results

The work is based, with the opinions of experts, on development of a framework with a matrix of indicators and variables to the calculation of the applicability index. It is then proceeded, using the Analytic Hierarchy Process method (AHP method), to prioritize the indicators selected for the framework to define the weights and rank the indicators.

**Smart Transportation Framework:** This framework was developed based on a depth analysis of the existing literature concerning intelligent transportation system, smart mobility and smart city as well as the experiences of other cities and experts' recommendations

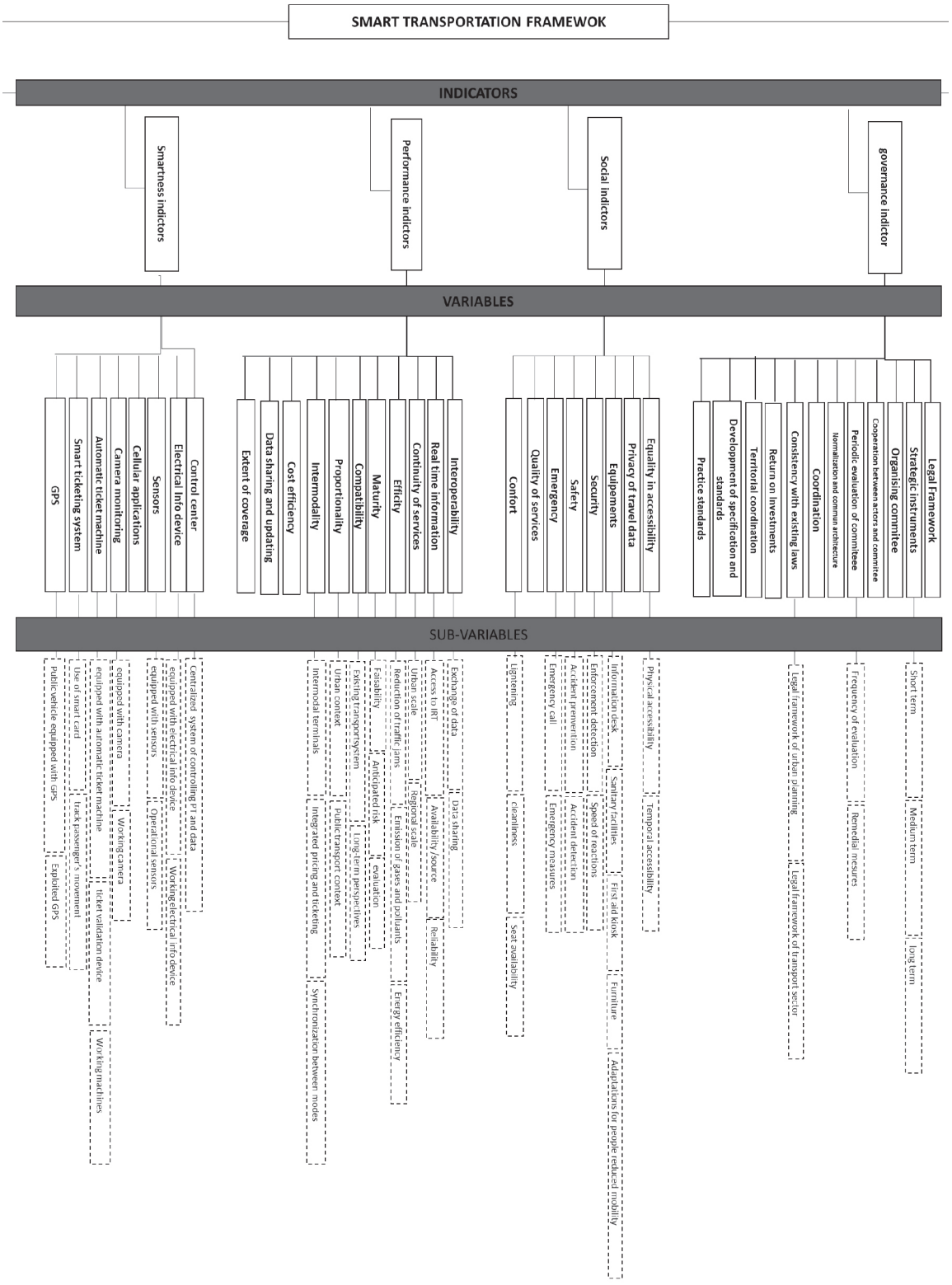


***Figure 1*** *Framework's structure*

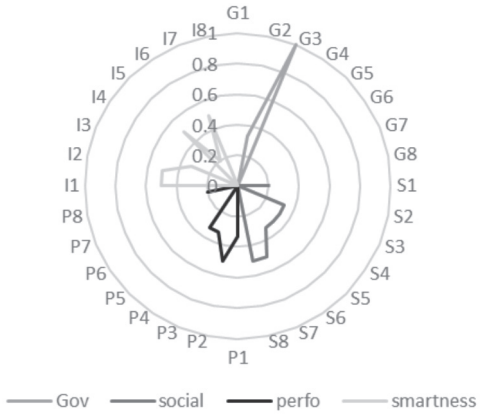


***Figure 2*** *Indicators share*

on the subject, it considers the particularities of the case study as a developing city. Beyond the technological aspects; authors were interested to find out what is the planning process within, since, it is nearly impossible to provide a framework for smart transportation deployment that can be applied everywhere, as there are differences that exist between cities, particularly in terms of transportation (the level of development, the level of transport infrastructure and the priorities set within the policy of each city) , the most important point to remember is that cities can learn from the experiences of others, as long as they take into account possible contextual differences and thus accelerate their own plans. The framework is based on chosen indicators, which are important tools for policymaking and revealing elements towards the key objectives [36]. The indicators that were chosen cover the essential dimensions of smart transportation integration and implementation that should be considered in terms of planning, management and functioning listed below. Each indicator has its own set of variables covering both quantitative and qualitative aspects leaving a final set of 39 variables as shown in Figure 1.

Governance indicator: referring to the policy and management principles of the transport system that should accompany the deployment of smart transportation in order to frame it, organize it, govern its operation and adapt it to the urban context, particularly on the social level, where solutions must be adopted in order to reward responsible behavior and punish the wrong attitude from users [37].

Social indicators: refer to characteristics that particularly affect the transport users, as long as they are the first concerned to be involved, informed and aware since they are the departure point and the purpose of any smart city project [38].

Performance indicators: refer to the functional characteristics of the transport system to ensure its performance in meeting current needs and its ability to make a change or transition to a technology-based strategy.

Smartness indicators: related to ICT technologies assigned to transport infrastructure as stated by [30], that the availability of a good level of infrastructure would indicate that the city has the potential to deploy the smart technologies.

### 4.1 Applicability index of smart transportation in Algiers

The result obtained through this work is presented below, a very low rate of applicability of technologies on public transport in Algiers (25.25 %), the parts of different indicators expressed by qualitative scale is very small, as shown in Figure 2. The indicator with the lowest share is governance followed by performance indicator, the social and smartness indicators have registered a slightly higher share than the previous ones, but in general remain low.

### 4.2 Prioritization of indicators

Using the Analytic Hierarchy Process method (AHP), [39] the binary comparison matrix was formed

***Table 3*** *Indicator weights*

| Indicators | Governance indicator | Performance indicators | Social indicator | Smartness indicator | Weights |
|---|---|---|---|---|---|
| Governance indicator | 0.800 | 0.662 | 0.535 | 0.096 | 0.4482 |
| Performance indicators | 0.277 | 0.220 | 0.321 | 0.872 | 0.4225 |
| Social indicator | 0.166 | 0.072 | 0.107 | 0.193 | 0.1345 |
| Smartness indicator | 0.055 | 0.906 | 0.035 | 0.010 | 0.2512 |

***Table 4*** *Classification of indicators*

| Indicators | Classification |
|---|---|
| Governance indicator | 2 |
| Performance indicators | 1 |
| Social indicator | 3 |
| Smartness indicator | 4 |

Coherence index = 0.0553

consistency ratio = 0.058 < 0.1(acceptable)

and then the weights of the different indicators were calculated (Table 3) considering the opinion of various researchers and experts working mainly in the transport sector in Algiers and researchers in this theme.

According to the results in Table 4, performance is the priority indicator for public transport to optimize the applicability of intelligent transport in Algiers, followed by governance, then social and smartness indicators.

## 5 Discussion

After getting the result of measuring the applicability of intelligent transportation system in Algiers and the share of each indicator, we opted to discuss the related causes behind that we will call barriers through investigations. The database of Algiers, relating to public transport, was not at our disposal, so we had to create one.

The low rate of governance indicator is related to the non-existence, in Algeria, of laws governing ITS deployment in the transport sector, as stated by [38] that current legislation is a major obstacle to ICT expansion in Algeria.

The low performance rate of public transport can be explained by the following realities gathered from our on-site investigations:

- A very limited radius of the multimodal offer of PT in Algiers has been noted, where only one municipality benefits from the four modes combined, 34 municipalities have access to only one mode, the bus. As previously discussed by [40] that the transport plan, defined in the Master plan for urban development and planning [41], is supposed to be multimodal, based on the metro, tramway and bus network in common areas. However, the rail network has not been integrated and services to new interior urban areas have not been considered. On the other hand, we also evoke the new city of Sidi Abdallah located in the southern suburbs of Algiers and designed to receive 320,000 inhabitants, leaving us to reflect on the flows to be generated and travel needs to be managed.
- The degree of interconnection between the four modes combined is very low and their synchronization in time is almost non-existent. It presents a problem previously studied by several researchers, including [40], who highlighted the lack of connections between the public transport lines and the inadequacy of multimodal services (ticketing, interoperability) applied to all the operators.
- The low territorial coverage of metro, tramway and train, explains the limited physical connection between them. To date, the bus is the dominant mode of transport in Algiers covering 62 % of the territory, including 59 municipalities and this is mainly due to the integration of private buses, which have improved the quantity but not the quality of the bus offer expected by users.
- Real-time information is indispensable nowadays, it offers the possibility to access the information system online via smartphones [5], we have noticed for the case of Algiers, restrictions in the sharing of data to users, as well as the inexistence of a smartphone application that provides data concerning public transport traffic. For this reason, users, once at stations, will be able to get information from signs or service agents.
- On board the train, metro and tramway, the information provided through micro-speaker concerns the route and the stations covered, while at stations only the tramway indicates reliable information concerning the arrival and departure times of vehicles. The routes and train schedules are fixed, but reflect a low level of reliability. There is no information about buses traffic and schedule either inside the vehicle or at stations, except the destination panels.

Social indicators are negatively impacted by endogenous and exogenous factors to the transport system affect users in terms of their interactions and exchanges in the ICT deployment process without losing sight of the risks resulting from their involvement. Authors of [38] found that, there can be no smart city without citizen involvement and participation. To discuss of the social indicators, share, a survey was conducted in this research, as a crowdsourcing technique for getting ideas and content from citizen through the internet-based platforms, [42]. It is increasingly used in academic research according to its easy access mode [43], known by many terminologies such as social search [44]. This method of survey research is widely used in Algiers by scholars due to the unavailability of comprehensive and up-to-date data and statistics in several public sectors, obliging researchers to remedy this either through field investigations or online surveys. The content analysis

is direct and qualitative and was carried out using SPHYNX IQ2 software, which allows to understand the data and clearly visualize the significant elements of the survey. The URL of surveys was distributed through social media in July 2019 concerning only Algiers. The public transport services analyzed were tramway, metro, commuter train and bus. (As for the rest of these modes, their share of urban travel is minimal compared to the modes mentioned above). The survey contained some questions related to users' travel habits and socio-economic characteristics: age, socio-professional category, reason for travel. Some changes have been made as removing inappropriate responses, changing the order of sections, reformulating the way some of them were introduced and so on. It led to the following findings:

- A large proportion of users have not been made aware of such deployment and are not yet familiar with technologies and have a poor grasp of the integration, to the digital world, whether through ignorance or lack of mastery, or they require access. Especially since the term, smart mobility, is still utopian for citizens who consider it far from the reality of the Algiers context, exactly as the case of the Smart City project, [38].
- To this end, the in-situ observation revealed public transport stations equipped with unattended ticketing machines where users prefer, due to a lack of mastering, to waste their time queuing, many machines have been out of order for a long time. According to authors' vision, it is believed that a significant portion of users do not trust the technology because they have not perceived its true benefits up to date.
- Accessibility (Physical and temporal accessibility): Another determining factor concerns the inequalities in terms of access to public transport; it is noted that bus is the only accessible mode in terms of time and distance, despite of other modes.
- Safety and security: Public transport systems can use ITS solutions to improve actions to prevent road accidents and fatalities, which are particularly common in developing cities such as Algiers [45]. Users have attested to the insecurity of public transport in Algiers particularly buses. The tramway with its easy physical access (without validation barriers and absence of security guards at all stations), has become more vulnerable to incidents, there have recently been traffic accidents that involved the tram and private vehicles, similarly, the commuter rail experienced an accident in November 2014 that resulted in one death and 63 injured people [46]. In addition, the fact that the traffic lights at intersections with the mechanical tracks are not checked and respected increases the risk of accidents.
- According to users, the safest mode of PT is the metro, since its access is conditional on the payment and validation of tickets and the permanent presence of security guards. As regards its safety against accidents, it is more satisfactory since it requires a dedicated site (no physical connection with other modes).
- Supply and services quality: The improvement of service quality does not only mean to invest money in advanced technologies, but to prioritize actions that influence the level of quality perceived by customers, as well, [47]. The entry into service of private bus operators in 2013 has increased the capacity to accommodate users, leaving a common handcrafted nature of their services [48-49], such as the appearance of a multitude of inexperienced operators; the heterogeneity of equipment (types and size of vehicles); the inadequacy of reception infrastructure for a good care of the users; the non-respect of stops, frequencies and schedules [50].
- Regarding users' satisfaction, metro users are more satisfied than tramway and commuter train users in all the common attributes characterizing the services.

The share of the smartness indicator can be explained by the current level of public transport infrastructures where we highlighted difficulties with the integration of technologies into public transport infrastructures regarding vehicles, stations and terminals detailed below. According to the on-site investigations and research, the following realities have been identified:

- Public buses have no functional GPS, cameras and sensors (15,000 buses in much deteriorated condition,) which are key elements providing users with the real-time data on arrivals and departures of public transport, [37].
- Bus stations have no ticket machine, cameras, receivers or electrical info devices and the sale of tickets is only done by agents inside public buses and by unqualified individuals inside private buses, sometimes or, as underlined in [37] that from a user's perspective, smart ticketing solutions may use smart cards or mobile phones to make ticketing more efficient. In some bus stations in Algiers, intelligent bus shelters were recently installed, whose interaction with buses for the display of IRT is not functional since buses are not adapted. It should be noted that there is a lack of cooperation by some users in terms of purchasing and validating tickets, the only mode in which tickets are validated is the metro, following the installation of validation barriers at the entrance, obliging users to buy and validate tickets to get there.
- For the tramway, there are no access barriers, the validation machines at the stations are no longer functional and users have become accustomed to not validating their tickets by using them for several journeys until counters have been installed at each station selling validated tickets valid only

for a single journey. There no internet applications in the public transport sector in Algiers, except for train.

- There are some applications developed by private individuals for example of TEMTEM, YASSIR and COURSA, conceived as UBER principle without a legal basis and concerning private transport, that are widely used, according to the survey, which accentuates the problems by further increasing the traffic as an alternative to public transportation. Some users make use of social media where administrators of some Facebook pages, for example of INFO TRAFIC ALGER, where subscribers share information about traffic during their travel (critical traffic points, accidents, siding in case of public works on the road…etc.).

After measuring the applicability index of smart transportation in Algiers and the scores of the selected indicators, the data collected from these investigations just confirmed the existence of barriers hindering Algiers' transition to a smart public transportation system, the most critical of them are:

- no laws, conventions or standards covering the deployment of smart transportation or ICT in transportation,
- The inexistence of equipment related to the smartness, such as detectors and sensors responsible for the reception and the detection,
- The existence of cognitive difficulties of the citizens related to the knowledge acquisition in terms of ICT deployment applied to transport,
- The existence of technical difficulties related to existing public transportation infrastructure that impact their synergy with smart technologies.

## 6 Conclusions

The overall objective of this article is to demonstrate the need for smart transportation integration in public transport in Algiers and to give importance to how it should be deployed by focusing on the adapted framework to be prepared for their implementation giving each constraint its right estimate.

To evaluate smart transportation applicability in public transports in Algiers, authors highlighted an adapted framework by benchmarking ITS deployment and then calculated its applicability index, which showed a very low rate.

Authors were then interested in ranking the indicators in order to decide on priorities for the coordinated adoption of smart transportation in public transport in Algiers, which highlighted public transport governance and performance as priorities that should be addressed first.

The main conclusion of the study is that the implementation of smart transportation should be included in the sector's priorities. Nonetheless, it may constitute a risk since many strategical objectives are not achieved acting as a barrier and making their achievement as important as smart transportation deployment particularly on the governance and performance plan.

The result of this study emphasizes the requirement of remedial priority actions related to governance and performance indicators in favor of preparation of a transition framework that accompanies smart transportation implementation in Algiers.

Authors suggest, to give priority firstly to the issues, as previously found by [49], at the institutional, organizational and regulatory level that hinder the current development of the transport system and secondly to the risks of smart transportation integration, particularly at the social level, since they condition the success of smart transportation and risks compromising their expected benefits. Thus, the confrontation of these barriers becomes a priority, such as the commitment to deployment of technologies in public transport, where technology cannot solve current problems but rather optimize their solutions, in other terms; they are more likely to complement each other.

The particularity of this work lies in the fact that it does not seek to propose intermediate or palliative solutions to transport problems, but rather to reflect on the process of adopting new technologies, especially with Algeria's commitment to a Smart City project where transport and mobility are key dimensions to be integrated into this project. In authors' opinion, these technologies can optimize definitive long-term solutions, while benefiting users primarily.

Another important aspect that was taken into consideration in this work is public participation through the survey recognizing the different views of public transport users in order to identify the cultural context, such as their attitudes and perception towards the transport technologies [51], as long as they constitute the basic element in the transport chain.

After being acquainted with the ITS deployment at the theoretical level, it would be opportune to direct the research perspective towards the most used technologies ICT [52], in order to define, in the case of Algiers, the applications most adapted to its context and try to customize them as they have an unavoidable contribution in the transportation sector.

One of the limitations in this study is the non-elaborative simulation and modelling exercise to predict the positive impact that the coordinated deployment of intelligent transport systems would have on public transport in Algiers and this is mainly due to the unavailability of sufficient data.

## References


[1] CASCETTA, E., PAGLIARA, F., PAPOLA, A. Governance of urban mobility: complex systems and integrated policies. *Advances in Complex Systems* [online]. 2007, **10**(supp02), p. 339-354. ISSN 0219-5259, eISSN 1793-6802. Available from: https://doi.org/10.1142/S0219525907001392

[2] JANUSOVA, L., CICMANCOVA, S. Improving safety of transportation by using intelligent transport systems. *Procedia Engineering* [online]. 2016, **134**, p. 14-22. ISSN 1877-7058. Available from:https://doi.org/10.1016/j.proeng.2016.01.031

[3] Sustainable development goals - United Nations [online]. Report. New York, 2016. Available from: https://unstats.un.org/sdgs/report/2016/the%20sustainable%20development%20goals%20report%202016.pdf

[4] JANOWSKI, T. Digital government evolution: from transformation to contextualization. *Government Information Quarterly* [online]. 2015, **32**(3), p. 221-236. ISSN 0740-624X. Available from: https://doi.org/10.1016/j.giq.2015.07.001

[5] TOMASZEWSKA, E. J., FLOREA, A. Urban smart mobility in the scientific literature - bibliometric analysis. *Engineering Management in Production and Services* [online]. 2018, **10**(2), p. 41-56. eISSN 2543-912X. Available from: https://doi.org/10.2478/emj-2018-0010

[6] BULL, R. ICT as an enabler for sustainable development: reflections on opportunities and barriers. *Journal of Information, Communication and Ethics in Society*. 2015, **13**(1), p. 19-23. ISSN 1477-996X. Available from: https://doi.org/10.1108/JICES-12-2014-0061

[7] MILES, J. C. Intelligent transport systems: overview and structure (history, applications and architectures) [online]. In: *Encyclopedia of Automotive Engineering*. John Wiley & Sons, Ltd., 2014. ISBN 9780470974025, eISBN 97811183ta179, p. 1-16. Available from: https://doi.org/10.1002/9781118354179.auto166

[8] BIYIK, C., ABARESHI, A., PAZ, A., RUIZ, R. A., BATTARRA, R., ROGERS, CH. D. F., LIZARRAGA, C. Smart mobility adoption: a review of the literature. *Journal of Open Innovation Technology Market and Complexity* [online]. 2021, **7**(2), 146. eISSN 2199-8531. Available from: https://doi.org/10.3390/joitmc7020146

[9] MANGIARACINA, R., PEREGO, A., SALVADORI, G., TUMINO, A. A comprehensive view of intelligent transport systems for urban smart mobility. *International Journal of Logistics Research and Applications* [online]. 2017, **20**(1), p. 39-52. ISSN 1367-5567, eISSN 1469-848X. Available from: https://doi.org/10.1080/13675567.2016.1241220

[10] ITS handbook [online]. 2. ed. Cedex, France: Piarc - World Road Association, 2012. Available from: https://www.piarc.org/en/News-Agenda-PIARC/News/2005-07-19,2910.htm

[11] Directive 2010/40/eu of the European Parliament and of the Council [online]. 2010. Available from: https://eur-lex.europa.eu/legal-content/EN/TXT/PDF/?uri=CELEX:32010L0040&rid=9

[12] GIANNOPOULOS, G. A. The application of information and communication technologies in transport. *European Journal of Operational Research* [online]. 2004, **152**(2), p. 302-320. ISSN 0377-2217. Available from: https://doi.org/10.1016/S0377-2217(03)00026-2

[13] JOHN, S. K., SIVARAJ, D., MUGELAN, R. Implementation challenges and opportunities of smart city and intelligent transport systems in India [online]. In: *Internet of things and big data analytics for smart generation*. Intelligent Systems Reference Library. Vol. 154. BALAS, V., SOLANKI, V., KUMAR, R., KHARI, M. (eds.). Cham: Springer, 2019. ISBN 978-3-030-04202-8, eISBN 978-3-030-04203-5, p. 213-235. Available from: https://doi.org/10.1007/978-3-030-04203-5_10

[14] BAOUNI, T., BERCHACHE, R. Intermodality and urban development in the agglomeration of Algiers: challenges, issues and perspectives / Intermodalite et developpement urbain dans l'agglomeration d'Alger: defis, enjeux et perspectives (in French). *Les Cahiers du CREAD*. 2011, **27**(97), p. 93-109. ISSN 2437-0568.

[15] PAPA, R., GARGIULO, C., RUSSO. L. The evolution of smart mobility strategies and behaviors to build the smart city. In: 5th IEEE International Conference on Models and Technologies for Intelligent Transportation Systems MT-ITS 2017: proceedings [online]. IEEE, 2017. Available from: https://doi.org/10.1109/MTITS.2017.8005707

[16] BATTARRA, R., ZUCARO, F., TREMITERRA, M. R. Smart mobility: an evaluation method to audit Italian cities. In: 5th IEEE International Conference on Models and Technologies for Intelligent Transportation Systems MT-ITS 2017: proceedings [online]. IEEE, 2017. Available from: https://doi.org/10.1109/MTITS.2017.8005709

[17] BARTH, M., BORIBOONSOMSIN, K. Environmentally beneficial intelligent transportation systems. *IFAC Proceedings Volumes* [online]. 2009, **42**(15), p. 342-345. ISSN 1474-6670. Available from: https://doi.org/10.3182/20090902-3-US-2007.0086

[18] AMBROSINO, G., FINN, B., GINI, S., MUSSONE, L. A method to assess and plan applications of ITS technology in Public Transport services with reference to some possible case studies. *Case Studies on Transport Policy* [online]. 2015, **3**(4), p. 421-430. ISSN 2213-624X. Available from: https://doi.org/10.1016/j.cstp.2015.08.005

[19] CAMPBELL, T. *Beyond smart city: how cities network, learn and innovate*. Earthscan, NY: Routledge, 2012. ISBN MUSCONE 9781849714266.

[20] FURTH, P. G., HEMILY, B., MULLER, T. H. J., STRATHMAN, J. G. Using archived AVL-APC data to improve transit performance and management. Transit Cooperative Research program (TCRP) Report 113. Washington: Transportation Research Board, 2006.
[21] KITCHIN, R. The promise and peril of smart cities. *Computers and Law: the Journal of the Society for Computers and Law*. 2015, **26**(2). ISSN 0140-3249.
[22] ANGELIDOU, M. Smart city policies: a spatial approach. *Cities* [online]. 2014, **41**(S1), p. S3-S11. ISSN 0264-2751. Available from: https://doi.org/10.1016/j.cities.2014.06.007
[23] PAPA, E., LAUWERS, D. Smart mobility: opportunity or threat to innovate places and cities. In: 20th international conference on urban planning and regional development in the information society REAL CORP 2015: proceedings. 2015. ISBN 978-3-9503110-9-9, eISBN 978-3-9503110-8-2, p. 543-550.
[24] SIEGELE, L. Mining the urban data. The Economist [online]. 2012. Available from: https://www.economist.com/news/2012/11/21/mining-the-urban-data
[25] BATTY, M., AXHAUSEN, K. W., GIANNOTTI, F., POZDNOUKHOV, A., BAZZANI, A., WACHOWICZ, M., OUZOUNIS, G., PORTUGALI, Y. Smart cities of the future. *The European Physical Journal Special Topics* [online]. 2012, **214**(1), p. 481-518. ISSN 1951-6355, eISSN 1951-6401. Available from: https://doi.org/10.1140/epjst/e2012-01703-3
[26] KANTER, R. M., LITOW, S. S. Informed and interconnected: a manifesto for smarter cities [online]. Harvard Business School General Management Unit Working Paper No. 09-141. 2009. Available from: https://www.hbs.edu/ris/Publication%20Files/09-141.pdf
[27] BANISTER, D. The sustainable mobility paradigm. *Transport Policy* [online]. 2008, **15**(2), p. 73-80. ISSN 0967-070X. Available from: https://doi.org/10.1016/j.tranpol.2007.10.005
[28] PIRO, G., CIANCI, I., GRIECO, L. A., BOGGIA, G., CAMARDA, P. Information centric services in smart cities. *Journal of Systems and Software* [online]. 2014, **88**, p. 169-188. ISSN 0164-1212. Available from: https://doi.org/10.1016/j.jss.2013.10.029
[29] MARLETTO, G., MAMELI, F. A participative procedure to select indicators of policies for sustainable urban mobility. Outcomes of a national test. *European Transport Research Review* [online]. 2012, **4**(2), p. 79-89. eISSN 1866-8887. Available from: https://doi.org/10.1007/s12544-012-0075-8
[30] DEBNATH, A. K., CHIN, H. CH., HAQUE, MD. M., YUEN, B. A methodological framework for benchmarking smart transport cities. *Cities* [online]. 2014, **37**, p. 47-56. ISSN 0264-2751. Available from: https://doi.org/10.1016/j.cities.2013.11.004
[31] BATTARRA, R., GARGIULO, C., TREMITERRA, M. R., ZUCARO, F. Smart mobility in Italian metropolitan cities: a comparative analysis through indicators and actions. *Sustainable Cities and Society* [online]. 2018, **41**, p. 556-567. ISSN 2210-6707. Available from: https://doi.org/10.1016/j.scs.2018.06.006
[32] BENEVOLO, C., DAMERI, R. P., D'AURIA, B. Smart mobility in smart city. In: *Empowering organizations: enabling platforms and artefacts* [online]. Lecture notes in information systems and organisations. Vol. 11. TORRE T., BRACCINI A., SPINELLI R. (eds.). Cham: Springer, 2016. ISBN 978-3-319-23783-1, eISBN 978-3-319-23784-8, p. 13-28. Available from: https://doi.org/10.1007/978-3-319-23784-8_2
[33] GUDMUNDSSON, H. Making concepts matter: sustainable mobility and indicator systems in transport policy. *International Social Science Journal* [online]. 2003, **55**(176), p. 199-217. eISSN 1468-2451. Available from: https://doi.org/10.1111/j.1468-2451.2003.05502003.
[34] GUDMUNDSSON, H., WYATT, A., GORDON, L. Benchmarking and sustainable transport policy: learning from the BEST network. *Transport Reviews* [online]. 2005, **25**(6), p. 669-690. ISSN 0144-1647, eISSN 1464-5327. Available from: https://doi.org/10.1080/01441640500414824
[35] HEATON, J., PARLIKAD, A. A conceptual framework for the alignment of infrastructure assets to citizen requirements within a smart cities framework. *Cities* [online]. 2019, **90**, p. 32-41. ISSN 0264-2751. Available from: https://doi.org/10.1016/j.cities.2019.01.041
[36] GUDMUNDSSON, H., SORENSEN, C. H. Some use - little influence? On the roles of indicators in European sustainable transport policy. *Ecological Indicators* [online]. 2013, **35**. p. 43-51. ISSN 1470-160X. Available from: https://doi.org/10.1016/j.ecolind.2012.08.015
[37] FLOREA, A., BERNTZEN, L., JOHANNESSEN, M. R., STOICA, D., NAICU, I. S., CAZAN, V. Low cost mobile embedded system for air quality monitoring. In: 6th International Conference on Smart Cities, Systems, Devices and Technologies SMART: proceedings. 2017. ISBN 978-1-61208-565-4, p. 5-12.
[38] AIT-YAHIA, K. G., GHIDOUCHE, F., N'GOALA, G. Smart city of Algiers: defining its context. In: *Smart city emergence*. ANTHOPOULOS, L. (ed.). Elsevier, 2019. ISBN 9780128161692, eISBN 9780128165843, p. 391-405.
[39] SAATY, T. L. Decision making with the analytic hierarchy process. *Scientia Iranica*. 2002, **9**(3), p. 215-229. ISSN 1026-3098, eISSN 2345-3605.

[40] TABTI-TALAMALI, A., BAOUNI, T. Public transportation in Algiers: towards a new governance approach. *Case Studies on Transport Policy* [online]. 2018, **6**(4), p. 706-715. ISSN 2213-624X. Available from: https://doi.org/10.1016/j.cstp.2018.08.009

[41] PDAU of Algiers, Orientation report, wilaya of Algiers, direction of the development of the territory, urban planning, prevention and resorption of the precaire habitat of the wilaya of Algiers /PDAU d'Alger, Rapport d'orientation, wilaya d'Alger, direction de l'amenagement du territoire, de l'urbanisme, de la prevention et de la resorption de l'habitat precaire de la wilaya d'Alger (in French). PARQUEXPO, L, 2015. 14.

[42] LIU, A. LU, S. C.-Y. A crowdsourcing design framework for concept generation. *CIRP Annals* [online]. 2016, **65**(1), p. 177-180. ISSN 0007-8506. Available from: https://doi.org/10.1016/j.cirp.2016.04.021

[43] HOSSAIN, M., KAURANEN, I. Crowdsourcing: a comprehensive literature review. *Strategic Outsourcing: An International Journal* [online]. 2015, **8**(1), p. 2-22. eISSN 1753-8297. Available from: https://doi.org/10.1108/SO-12-2014-0029

[44] DOAN, A., RAMAKRISHNAN, R., HALEVY, A.Y. Crowdsourcing systems on the world-wide web. *Communications of the ACM* [online]. 2011, **54**(4), p. 86-96. ISSN 0001-0782. Available from: https://doi.org/10.1145/1924421.1924442

[45] WELLE, B., SHARPIN, A. B., ADRIAZOLA-STEIL, C., BHATT, A., ALVEANO, S., OBELHEIRO, M., IMAMOGLU, C. T., JOB, S., SHOTTEN, M., BOSE, D. *Sustainable and safe: a vision and guidance for zero road deaths* [online]. 2018. ISBN 978-1-56973-927-7. Available from: https://www.wri.org/research/sustainable-and-safe-vision-and-guidance-zero-road-deaths

[46] MACHADO-LEON, J. L., ONA, R., BAOUNI, T., ONA, J. Railway transit services in Algiers: priority improvement actions based on users perceptions. *Transport Policy* [online]. 2017, **53**, p. 175-185. ISSN 0967-070X. Available from: https://doi.org/10.1016/j.tranpol.2016.10.004

[47] FREITAS, A. L. P. Assessing the quality of intercity road transportation of passengers: an exploratory study in Brazil. *Transportation Research Part A: Policy and Practice* [online]. 2013, **49**, p. 379-392. ISSN 0965-8564. Available from: https://doi.org/10.1016/j.tra.2013.01.042

[48] AOUDIA, O. A. Mastering and reviving the city : the Algiers metro / Maitriser et revivre la ville: le metro d'Alger (in French). 2012.

[49] SAFAR ZITOUN, M., TABTI-TALAMALI, A. Urban mobility in the agglomeration of Algiers: evolutions and perspectives / La mobilite urbaine dans l'agglomeration d'Alger: evolutions et perspectives (in French). International Bank for Reconstruction and Development, The World Bank, 2009.

[50] TABTI-TALAMALI, A. Strategies for the development of public transport: Cases of the Algiers tramway / Strategies de developpement des transports collectifs: cas du tramway d'Alger (in French). 2007.

[51] GIL, A., CALADO, H., BENTZ, J. Public participation in municipal transport planning processes - the case of the sustainable mobility plan of Ponta Delgada, Azores, Portugal. *Journal of Transport Geography* [online]. 2011, **19**(6), p. 1309-1319. ISSN 0966-6923. Available from: https://doi.org/10.1016/j.jtrangeo.2011.06.010

[52] ALAMSYAH, N., CHOU, T.-C., SUSANTO, T. D. ICT-mechanisms of intelligent transportation system in Taipei City as a smart city. *International Journal of Computer Science and Information Technology* [online]. 2016, **8**(3), p. 55-66. ISSN 0975-3826, eISSN 0975-4660. Available from: https://doi.org/10.5121/ijcsit.2016.8305

# IMPACT OF THE COVID-19 PANDEMIC ON CAR-SHARING IN POLAND

**Piotr Gorzelańczyk [1,*], Tomáš Kalina [2], Martin Jurkovič [2]**

[1]Stanislaw Staszic University of Applied Sciences in Pila, Pila, Poland
[2]Department of Water Transport, Faculty of Operation and Economics of Transport and Communications, University of Zilina, Zilina, Slovak Republic

*E-mail of corresponding author: piotr.gorzelanczyk@puss.pila.pl

***Resume***

The number of cars on Polish roads is increasing year by year. Currently, Poland is in second place in Europe in terms of the number of cars per 1000 inhabitants [1]. This causes problems in finding a place to park. In addition, during the pandemic, there was a problem with semis, which caused a sharp increase in the price of used cars and longer waiting times for new vehicles. The aim of this article is to find out the opinion of Polish residents on the Car-Sharing service during the CoVID-19 pandemic and how the pandemic has affected Car-Sharing not only in Poland, but also in Europe as a whole. For this purpose, a survey was conducted.

The research found that about 8% of people in Poland use the Car-Sharing service and that the pandemic had little impact on how this service was used. If someone needed to use this service, the pandemic was not an obstacle for them.

***Article info***

Received 22 March 2022
Accepted 29 June 2022
Online 12 August 2022

***Keywords:***

car-sharing
Poland
vehicle
COVID-19
pandemic

Available online: https://doi.org/10.26552/com.C.2022.4.A172-A186

ISSN 1335-4205 (print version)
ISSN 2585-7878 (online version)

## 1 Introduction

The automotive market in Poland is growing year on year. The exception is the year 2020 and the prevailing pandemic. In 2019, the number of registered passenger cars was 23.360.166 units [2]. This compares to 16.079.533 units just 10 years ago. The number of vehicles per 1.000 inhabitants is also increasing year on year. According to ACEA (European Automobile Manufactures Association) in 2011 Poland was in 15th place in Europe with the result of 470 vehicles per 1000 inhabitants. However, the latest data shows that in 2021 this number will increase to 747 vehicles and Poland will be on the 2nd place in Europe, just behind Luxembourg [3]. Based on ACEA data, the average age of cars on Polish roads exceeds 14 years, with an average of 11.5 years for the whole EU [4].

The large number of vehicles on the roads causes, among others, slowing down traffic, higher risk of accidents and problems with finding a place to park [5-9]. In addition, during the pandemic, there was a problem with semiconductors, which resulted in a sharp increase in the price of used cars and longer waiting times for new vehicles. For this reason, more and more people are starting to use Car-Sharing, the market for shared mobility. It grew rapidly between 2010 and 2011, when the total number of users exceeded one million. Based on Frost & Sullivan research, 10 million people were already using this service in 2017 [10]. This number is planned to reach 36 million in 2025, with an annual growth of 16.4% (Figure 1). However, these studies are shaken by the COVID-19 pandemic. Currently, the leading markets for shared mobility are Western Europe and the United States, and experts predict that the fastest growth in this area will take place in Asia [11].

COVID-19 is an infectious disease caused by coronavirus 2 of severe acute respiratory syndrome (SARS-CoV-2), the seventh coronavirus that can transmit between humans [12]. 11 March 2020. The World Health Organization (WHO) classified the COVID-19 outbreak as a global pandemic [13]. The new strain of coronavirus has reached the economic and social world on a scale not seen since the Great Depression (1929-1933) and is epidemic in nature compared to the Spanish flu of 1918 [14-15]. The spread of COVID-19 has reduced economic activity and led to a significant threat to the financial stability of many countries [16].

The development of the COVID-19 pandemic caused unprecedented restrictions on human mobility around the world [17]. Unprecedented measures restricting

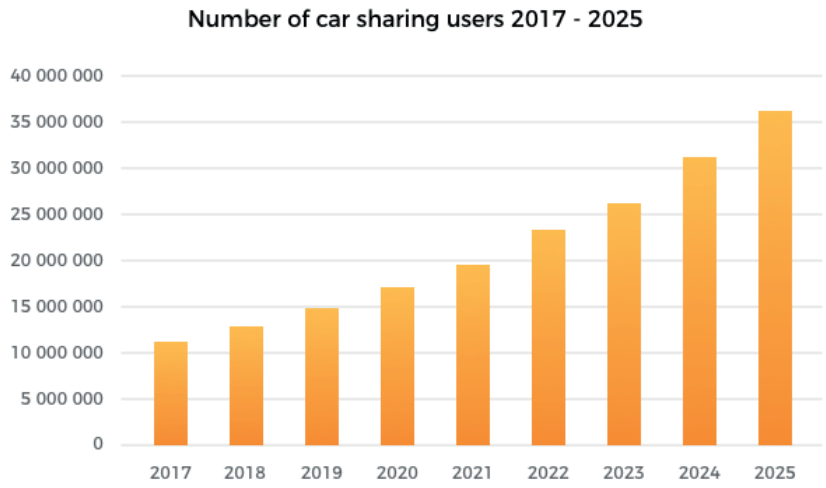


***Figure 1*** *Number of people using Car-Sharing [11]*

travel, movement and participation in activities have been introduced in many countries around the world [18]. These include staying at home, remote education, closed public institutions and workplaces, cancelled mass events and public gatherings, and restrictions on public transport, which have affected approximately 90% of the world's population [19-22] indicate a significant link between human mobility and government tightening of restrictions to contain the COVID-19 pandemic. Mobility restrictions vary between nations and regions due to their initial mobility patterns [23]. Schlosser et al [24] found that the COVID-19 pandemic resulted in reduced long-distance travel, which affected the spread process by "flattening" the epidemic curve and delaying spread to geographically remote regions.

The idea of ride-sharing originated in the United States during World War II, but gained particular popularity in the late 1970s. It was mainly used by commuting workers [25]. The idea of Car-Sharing has been considered by many researchers. For example, economic issues related to assets have been considered in works [26-29]. Identification of passenger transport platforms based on the concept of sharing economy and identification of possible space for development of this concept in Slovakia was presented in the work [30]. Mitrega and Malecka [31] presented an analysis of factors influencing the choice of sharing essence. Henrik Becker, Francesco Ciari, Kay W. Axhausen made a comparison of car-sharing systems used in Switzerland [32].

Most car-sharing related studies have focused on car-sharing services at stations, but there are also studies focusing on more advanced forms such as one-way car-sharing [33]. According to studies [34], the most suitable locations for car-sharing at stations are densely built-up urban areas with good public transport, and users are relatively young, affluent and well educated [35]. Considering the impact of car-sharing on the transport system, researchers have been able to confirm several positive effects, including fewer car trips and lower emissions [36-37], reduced parking demand [38-39], and promotion of the use of public transport and active transport modes [40].

According to a study by Hamari, Sjöklint, Ukkonen [41], there are 254 sharing economy platforms worldwide divided into several categories, of which the rental category includes the largest number of platforms (131 platforms).

## 2 Research

### 2.1 Purpose and scope of research

The aim of this article is to find out the transport preferences and the use of Car-Sharing services by the inhabitants of Poland and to try to answer how the pandemic influenced their preferences. Obtained results of the research can be the basis for the adoption of directions for the development of the Car-Sharing service, in case of a similar situation in the future. Due to the prevailing pandemic, the study was conducted using a survey method on a representative group of Polish residents in January 2021. In order to find out the preferences of European residents on the car-sharing service, similar research is being conducted in cooperation with the following research centres: University of Zilina, The Institute of Technology and Business in Ceske Budejovice, Budapest Univeristy of Technology and Economic and Ural State University of Economics.

### 2.2 Methodology of the research

The study was conducted by means of a survey. Firstly, a pre-survey was conducted to clarify the survey

questions and to fully understand the questions asked by the respondents. This was the only possible form of conducting this type of survey during the prevailing COVID-19 pandemic. The survey was conducted in an open manner, maintaining the anonymity of the respondents. The actual survey was conducted via the Internet. The survey was divided into two groups: those who use the car-sharing service and a second group that has never used the service. The survey contained a group of 22 common questions including age, gender, number of inhabitants, place of residence, education level, occupation and employment status. In addition, the survey asked about the Polish residents' destination, means of transport, distance to destination and duration of travel, as well as where they shopped before and during the pandemic. They were also asked about how they work and how they worked before the pandemic, whether they live in a "restricted zone" or near a paid car park, the number of household members and the number of cars in the household.

In the next item, respondents were asked: had they ever used a car-sharing service. Those who answered positively were asked to answer the following questions about car-sharing: how long, how often, when, why, which app they use. The most important question was: Did they use during the pandemic? Those who had not used car-sharing before were asked to indicate factors and reasons why they had not used the service. At the end of the survey, respondents were given the opportunity to give feedback on their experience with car-sharing. For the sake of accuracy, the survey was targeted at different audiences. Incomplete questionnaires were discarded. An important step during the implementation of the survey was the calculation of the research sample. For Poland (38162000 inhabitants), assuming a confidence level of 90% and a maximum error of 5%, the required number of people in the survey was 384 respondents. Therefore, 596 people participated in the study [42-43].

### 2.3 Results of tests

The subject of the survey were the inhabitants of Poland taking into account the place of residence, gender, number of inhabitants and their status on the labour market. The survey was conducted on a group of 2492 respondents, but only 596 correctly filled in questionnaires were used for further analysis. Women constituted 55% of respondents, men 34%. 11% of respondents did not answer the question about gender. Most of the respondents are adults. 29% of them are young people aged 18-35. Respondents aged 36-55 made up 58% and over 55 years old 13%. 5% were people under the age of 18. Most women (39%) and men (34%) were aged 36-45.

Most respondents lived in cities with up to 5 thousand inhabitants (38% of respondents) and the second group were people living in cities with 100-200 thousand inhabitants - 13%. 56% of respondents lived in a city and 44% lived in a village. Most women (41%) and men (33%) lived in towns with up to 5 thousand inhabitants (Table 1, 2).

The next question concerned labour market status. Over 89% were employed and almost 4% were self-employed. Among both men and women, 89% were working. The remaining group consisted of, respectively: unemployed, students, working students, pensioners, working pensioners, self-employed and people on maternity, parental and parental leaves.

Among the respondents almost 84% were people with

***Table 1*** *Socio-demographic characteristics of survey respondents - part 1*

| Category | n | % | Female | | Male | |
|---|---|---|---|---|---|---|
| | | | n | % | n | % |
| Sex: | | | | | | |
| Female | 328 | 55.00 | -- | -- | -- | -- |
| Male | 201 | 34.00 | -- | -- | -- | -- |
| No answer | 67 | 11.24 | -- | -- | -- | -- |
| Age: | | | | | | |
| under 18 years | 1 | 0.17 | 0 | 0.00 | 1 | 0.50 |
| 18-25 years | 30 | 5.03 | 16 | 4.88 | 11 | 5.47 |
| 26-35 years | 141 | 23.66 | 80 | 24.39 | 46 | 22.89 |
| 36-45 years | 216 | 36.24 | 127 | 38.72 | 68 | 33.83 |
| 46-55 years | 130 | 21.81 | 67 | 20.43 | 41 | 20.40 |
| 56-60 lat | 39 | 6.54 | 20 | 6.10 | 16 | 7.96 |
| above 60 lat | 39 | 6.54 | 18 | 5.49 | 18 | 8.96 |
| Place of residence: | | | | | | |
| urban area | 337 | 56.54 | 170 | 51.83 | 129 | 64.18 |
| rural area | 259 | 43.46 | 158 | 48.17 | 72 | 35.82 |

***Table 2*** *Socio-demographic characteristics of survey respondents - part 2*

| Category | n | % | Female | | Male | |
|---|---|---|---|---|---|---|
| | | | n | % | n | % |
| Educational level: | | | | | | |
| no education | 0 | 0.00 | 0 | 0.00 | 0 | 0.00 |
| primary | 3 | 0.50 | 2 | 0.61 | 1 | 0.50 |
| basic vocational | 9 | 1.51 | 3 | 0.91 | 6 | 2.99 |
| secondary technical | 51 | 8.56 | 21 | 6.40 | 24 | 11.94 |
| secondary | 33 | 5.54 | 21 | 6.40 | 12 | 5.97 |
| higher | 500 | 83.89 | 281 | 85.67 | 158 | 78.61 |
| Status on the labour market: | | | | | | |
| Pupil | 3 | 0.50 | 1 | 0.30 | 2 | 1.00 |
| Student | 8 | 1.34 | 5 | 1.52 | 3 | 1.49 |
| Working | 532 | 89.26 | 291 | 88.72 | 179 | 89.05 |
| Self-employed | 22 | 3.69 | 9 | 2.74 | 11 | 5.47 |
| Unemployed | 5 | 0.84 | 4 | 1.22 | 1 | 0.50 |
| Pensioner | 14 | 2.35 | 7 | 2.13 | 4 | 1.99 |
| maternity leave. parental leave. parental leave | 8 | 1.34 | 8 | 2.44 | 0 | 0.00 |
| other | 4 | 0.67 | 3 | 0.91 | 1 | 0.50 |
| Number of inhabitants: | | | | | | |
| up to 5.000 | 227 | 38.09 | 135 | 41.16 | 67 | 33.33 |
| 5.000 - 10.000 | 77 | 12.92 | 49 | 14.94 | 17 | 8.46 |
| 10.000 - 15.000 | 60 | 10.07 | 36 | 10.98 | 19 | 9.45 |
| 15.000 - 20.000 | 32 | 5.37 | 15 | 4.57 | 11 | 5.47 |
| 20.000 - 50.000 | 38 | 6.38 | 15 | 4.57 | 19 | 9.45 |
| 50.000 - 100.000 | 80 | 13.42 | 39 | 11.89 | 34 | 16.92 |
| 100.000 - 150.000 | 39 | 6.54 | 21 | 6.40 | 13 | 6.47 |
| 150.000 - 200.000 | 43 | 7.21 | 18 | 5.49 | 21 | 10.45 |
| 200.000 - 500.000 | 227 | 38.09 | 135 | 41.16 | 67 | 33.33 |
| above 500.000 | 77 | 12.92 | 49 | 14.94 | 17 | 8.46 |
| Work done - before the pandemic | | | | | | |
| traditionally. at the employer‘s premises | 566 | 94.97 | 310 | 94.51 | 190 | 94.53 |
| remotely | 6 | 1.01 | 3 | 0.91 | 2 | 1.00 |
| hybrid | 11 | 1.85 | 3 | 0.91 | 8 | 3.98 |
| other | 13 | 2.18 | 12 | 3.66 | 1 | 0.50 |
| Work done - during the pandemic | | | | | | |
| traditionally. at the employer‘s premises | 307 | 51.51 | 171 | 52.13 | 91 | 45.27 |
| remotely | 50 | 8.39 | 20 | 6.10 | 26 | 12.94 |
| hybrid | 228 | 38.26 | 129 | 39.33 | 81 | 40.30 |
| other | 11 | 1.85 | 8 | 2.44 | 3 | 1.49 |

higher education. 86% of female respondents had tertiary education, compared to 79% of male respondents. Before the pandemic, 95% of the respondents worked at their employer's premises, while during the pandemic this percentage dropped to 52%. On the other hand, during the pandemic 38% of respondents work in a hybrid way. Gender in this case does not matter. Most respondents work in public administration (65%) and education (7%).

When asked: Did your work situation change after the coronavirus outbreak? 85% of respondents answered no.

31% of respondents have four people in their household, 22% have two people and 21.5% have three people. 40% of respondents have one car and 39% have two cars in the household. 30% of women have four family members and one car (36%). Among men the proportions are: 32% and 49%.

Respondents were then asked to indicate the purpose of their daily trips, before and during the pandemic. In this case, respondents were able to choose one of seven answers, specifying the importance of the purpose. In the case analysed: 1 was the most frequent purpose, 5 the rarest and 6 not applicable. Before the pandemic, the most important goal for the respondents was work, followed by shopping, school and doctor. However, during the pandemic, a different hierarchy of respondents' goals emerged. Work and shopping came first, followed by doctor and social gatherings The above data corresponds with the previous questions regarding the age and work situation of the respondents. The above data are presented in Figures 2 and 3.

The main purpose of women's trips was work. This was 30% before the pandemic and 25% during the pandemic. The same was true for men: before the pandemic, work accounted for 25% and during the pandemic 19%. This is confirmed by the age of the respondents and also by the fact that 38% of them worked in a hybrid mode (Tables 3, 4).

Respondents were then asked which modes of transport they use. As in the previous case: 1 was the most frequent destination, 6 the rarest. Those asked, before and during the pandemic, used buses and trains most frequently. There was not much change during the pandemic. This may be influenced by the fact that the research was conducted in 2022, when the pandemic

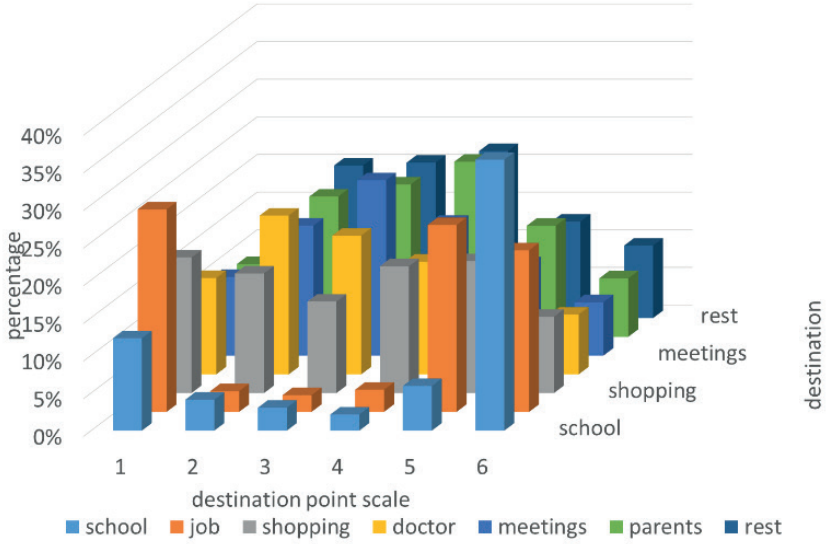


***Figure 2*** *Purpose of daily travel before the pandemic*

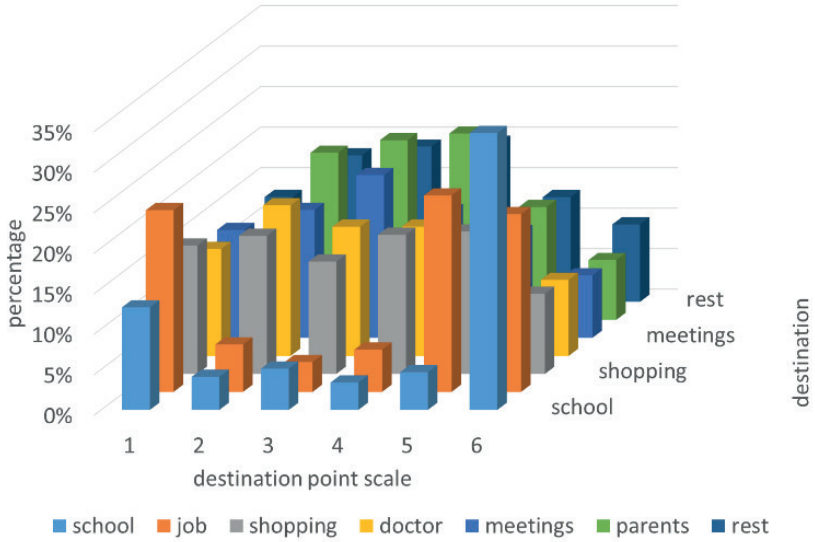


***Figure 3*** *The purpose of daily travel during a pandemic*

***Table 3*** *Purpose of women's daily travel before and during the pandemic*

| Destination | Before the pandemic [%] | | | | | | During a pandemic [%] | | | | | |
|---|---|---|---|---|---|---|---|---|---|---|---|---|
| | 1 | 2 | 3 | 4 | 5 | 6 | 1 | 2 | 3 | 4 | 5 | 6 |
| school | 11.29 | 4.32 | 3.31 | 0.53 | 6.60 | 36.20 | 12.22 | 3.87 | 5.24 | 3.11 | 4.13 | 33.62 |
| work | 29.12 | 2.70 | 2.21 | 1.59 | 23.35 | 18.10 | 24.66 | 5.52 | 2.86 | 4.15 | 22.74 | 18.52 |
| shopping | 20.09 | 17.30 | 11.76 | 13.23 | 16.50 | 10.39 | 17.19 | 18.78 | 15.24 | 11.92 | 17.57 | 10.54 |
| doctor | 9.93 | 18.92 | 20.22 | 19.05 | 13.71 | 9.20 | 9.95 | 20.44 | 16.67 | 19.17 | 14.73 | 10.54 |
| meetings | 7.90 | 17.84 | 23.53 | 17.46 | 13.96 | 8.01 | 10.86 | 16.02 | 20.95 | 15.54 | 15.25 | 8.55 |
| parents | 11.29 | 17.30 | 19.12 | 24.87 | 14.47 | 8.31 | 11.54 | 17.68 | 21.90 | 25.39 | 13.18 | 8.55 |
| leisure | 10.38 | 21.62 | 19.85 | 23.28 | 11.42 | 9.79 | 13.57 | 17.68 | 17.14 | 20.73 | 12.40 | 9.69 |
| max | 29.12 | 21.62 | 23.53 | 24.87 | 23.35 | 36.20 | 24.66 | 20.44 | 21.90 | 25.39 | 22.74 | 33.62 |

***Table 4*** *Purpose of men's daily travel before and during the pandemic*

| Destination | Before the pandemic [%] | | | | | | During a pandemic [%] | | | | | |
|---|---|---|---|---|---|---|---|---|---|---|---|---|
| | 1 | 2 | 3 | 4 | 5 | 6 | 1 | 2 | 3 | 4 | 5 | 6 |
| school | 12.00 | 4.55 | 2.87 | 3.57 | 6.18 | 34.85 | 13.17 | 4.73 | 4.00 | 4.21 | 6.06 | 35.11 |
| work | 24.80 | 3.03 | 2.87 | 4.29 | 25.48 | 23.74 | 19.34 | 7.10 | 5.71 | 8.42 | 24.24 | 23.40 |
| shopping | 15.60 | 14.39 | 12.07 | 18.57 | 19.69 | 10.61 | 14.40 | 15.98 | 10.86 | 20.00 | 19.48 | 10.11 |
| doctor | 17.60 | 24.24 | 15.52 | 9.29 | 9.65 | 7.07 | 18.11 | 17.75 | 13.14 | 11.58 | 12.12 | 7.98 |
| meetings | 14.00 | 15.15 | 24.71 | 17.14 | 9.65 | 5.56 | 16.87 | 13.02 | 21.14 | 15.79 | 10.39 | 6.91 |
| parents | 7.20 | 21.21 | 20.69 | 25.00 | 14.29 | 7.07 | 7.00 | 24.26 | 22.29 | 20.00 | 14.29 | 5.85 |
| leisure | 8.80 | 17.42 | 21.26 | 22.14 | 15.06 | 11.11 | 11.11 | 17.16 | 22.86 | 20.00 | 13.42 | 10.64 |
| max | 24.80 | 24.24 | 24.71 | 25.00 | 25.48 | 34.85 | 19.34 | 24.26 | 22.86 | 20.00 | 24.24 | 35.11 |

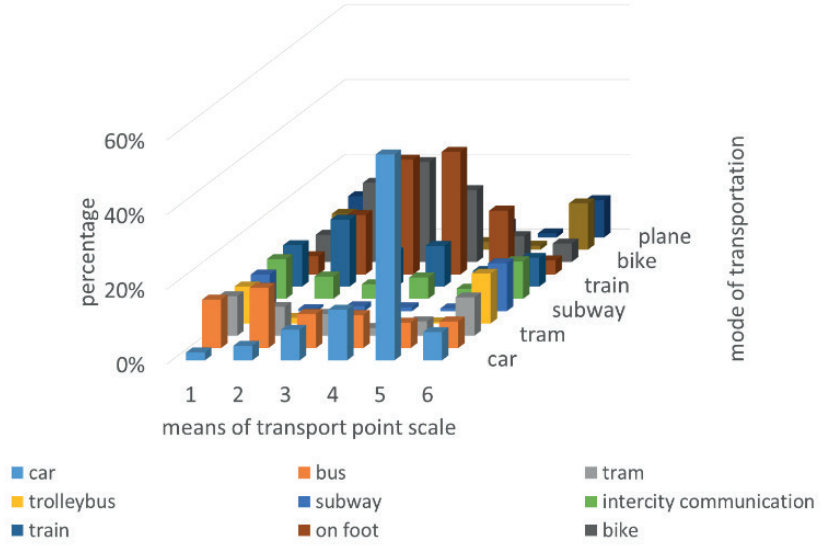


***Figure 4*** *Means of transport before the pandemic*

was already at an end. Previous studies by the author, indicate that most people used a car instead of public transport. The above results mainly refer to people's activities such as work or school and shopping. These data are presented in Figures 4 and 5. In the analysed case gender does not matter much. (Table 5, 6).

The next question asked about the distance from home to the destination before and during the pandemic. Most respondents before the pandemic outbreak indicated a distance of more than 20 km as their main travel destination (25%), this is mainly due to their place of work. After the pandemic outbreak, a distance of 1 to 5 km emerged as the main travel destination (25%). This is mainly due to commuting to work and shopping. After the pandemic outbreak, respondents abandoned visiting relatives and leisure activities, spending most of their time at home. These data are presented in Figure 6.

The next question asked how long did it take to travel to your main destination before and during the pandemic? In this case, before the pandemic outbreak,

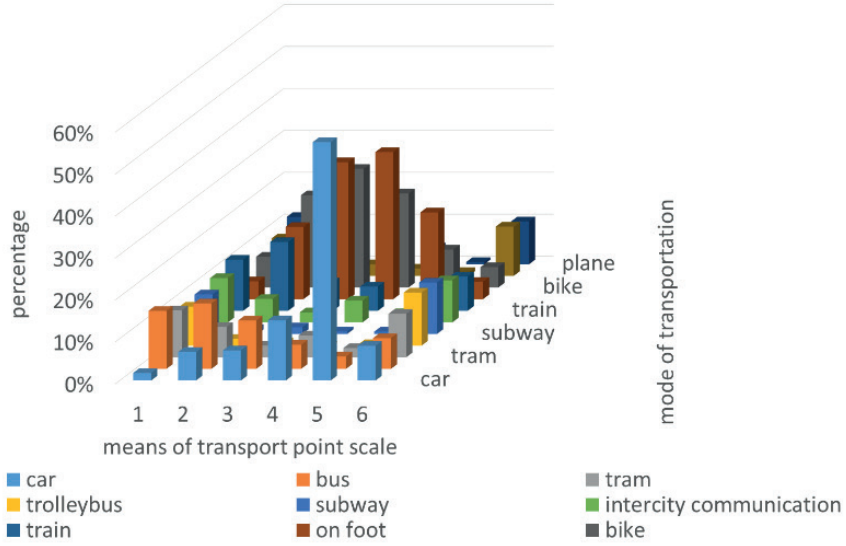


***Figure 5*** *Means of transport during a pandemic*

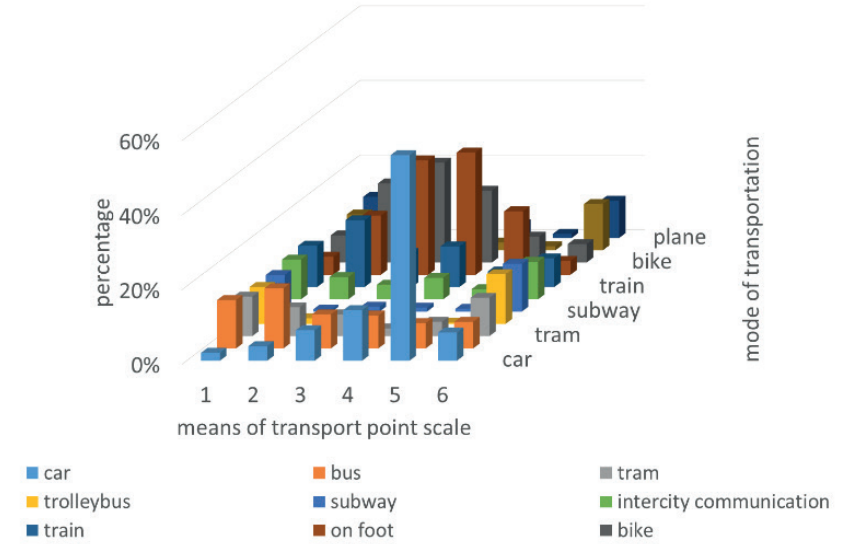


***Figure 4*** *Means of transport before the pandemic*

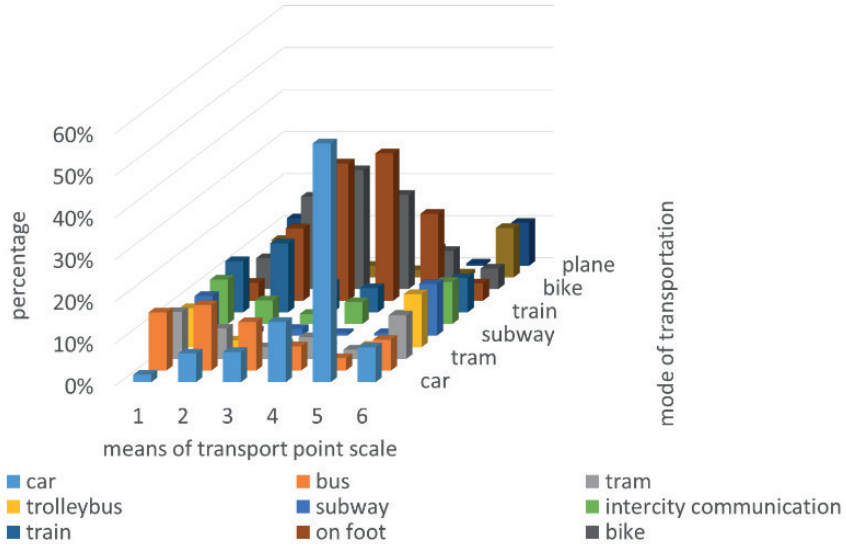


***Figure 5*** *Means of transport during a pandemic*

***Table 5*** *A means of transporting women before and during a pandemic*

| Means of transport | Before the pandemic [%] | | | | | | During a pandemic [%] | | | | | |
|---|---|---|---|---|---|---|---|---|---|---|---|---|
| | 1 | 2 | 3 | 4 | 5 | 6 | 1 | 2 | 3 | 4 | 5 | 6 |
| car | 1.96 | 3.47 | 5.81 | 13.54 | 55.59 | 6.78 | 1.70 | 4.72 | 6.35 | 16.85 | 58.75 | 7.55 |
| Bus | 12.68 | 17.34 | 9.68 | 7.29 | 6.39 | 7.29 | 14.06 | 18.90 | 8.73 | 2.25 | 2.31 | 7.64 |
| Tram | 9.80 | 9.83 | 5.16 | 3.13 | 3.19 | 10.83 | 10.51 | 8.66 | 2.38 | 3.37 | 1.65 | 10.75 |
| Trolleybus | 9.93 | 1.16 | 0.00 | 0.00 | 0.32 | 13.36 | 9.09 | 1.57 | 0.79 | 0.00 | 0.00 | 12.64 |
| Metro | 9.41 | 0.58 | 1.29 | 2.08 | 0.96 | 12.96 | 8.95 | 0.79 | 2.38 | 1.12 | 0.33 | 12.36 |
| Intercity transport | 10.59 | 5.20 | 5.16 | 6.25 | 2.56 | 10.43 | 10.37 | 6.30 | 2.38 | 5.62 | 1.65 | 10.47 |
| Train | 11.63 | 13.29 | 9.03 | 11.46 | 3.51 | 8.20 | 12.36 | 15.75 | 4.76 | 4.49 | 2.97 | 8.68 |
| By foot | 6.01 | 17.92 | 31.61 | 30.21 | 18.21 | 3.14 | 5.54 | 17.32 | 34.13 | 38.20 | 21.45 | 3.30 |
| Bike | 7.58 | 21.97 | 29.03 | 21.88 | 7.03 | 4.35 | 7.81 | 20.47 | 32.54 | 22.47 | 9.57 | 3.96 |
| Motorbike | 9.67 | 0.58 | 0.00 | 0.00 | 1.60 | 12.55 | 8.81 | 1.57 | 2.38 | 0.00 | 1.32 | 12.08 |
| Plane | 10.72 | 8.67 | 3.23 | 4.17 | 0.64 | 10.12 | 10.80 | 3.94 | 3.17 | 5.62 | 0.00 | 10.57 |
| max | 12.68 | 21.97 | 31.61 | 30.21 | 55.59 | 13.36 | 14.06 | 20.47 | 34.13 | 38.20 | 58.75 | 12.64 |

***Table 6*** *A means of transporting men before and during a pandemic*

| Means of transport | Before the pandemic [%] | | | | | | During a pandemic[%] | | | | | |
|---|---|---|---|---|---|---|---|---|---|---|---|---|
| | 1 | 2 | 3 | 4 | 5 | 6 | 1 | 2 | 3 | 4 | 5 | 6 |
| car | 2.70 | 5.15 | 11.38 | 14.29 | 53.37 | 7.60 | 2.13 | 9.71 | 10.31 | 8.96 | 55.19 | 8.08 |
| Bus | 13.72 | 14.71 | 8.13 | 11.69 | 7.30 | 6.71 | 13.65 | 11.65 | 14.43 | 8.96 | 3.28 | 7.07 |
| Tram | 11.23 | 5.88 | 6.50 | 1.30 | 4.49 | 9.89 | 11.73 | 5.83 | 3.09 | 7.46 | 2.73 | 9.93 |
| Trolleybus | 9.77 | 0.74 | 0.00 | 0.00 | 0.00 | 13.78 | 9.38 | 0.97 | 0.00 | 0.00 | 0.00 | 13.13 |
| Metro | 10.19 | 0.74 | 1.63 | 0.00 | 0.00 | 12.90 | 9.81 | 1.94 | 1.03 | 0.00 | 0.00 | 12.46 |
| Intercity transport | 10.40 | 7.35 | 3.25 | 6.49 | 2.81 | 9.72 | 10.45 | 5.83 | 3.09 | 5.97 | 2.19 | 9.43 |
| Train | 10.40 | 24.26 | 10.57 | 7.79 | 5.62 | 7.07 | 11.94 | 17.48 | 11.34 | 5.97 | 4.37 | 7.74 |
| By foot | 3.74 | 13.97 | 27.64 | 33.77 | 17.98 | 4.06 | 2.99 | 17.48 | 27.84 | 31.34 | 22.95 | 4.55 |
| Bike | 6.86 | 19.85 | 24.39 | 18.18 | 7.30 | 5.30 | 7.04 | 23.30 | 23.71 | 23.88 | 8.74 | 5.56 |
| Motorbike | 9.15 | 1.47 | 1.63 | 3.90 | 0.00 | 12.72 | 8.74 | 1.94 | 3.09 | 4.48 | 0.00 | 11.78 |
| Plane | 11.85 | 5.88 | 4.88 | 2.60 | 1.12 | 10.25 | 12.15 | 3.88 | 2.06 | 2.99 | 0.55 | 10.27 |
| max | 13.72 | 24.26 | 27.64 | 33.77 | 53.37 | 13.78 | 13.65 | 23.30 | 27.84 | 31.34 | 55.19 | 13.13 |

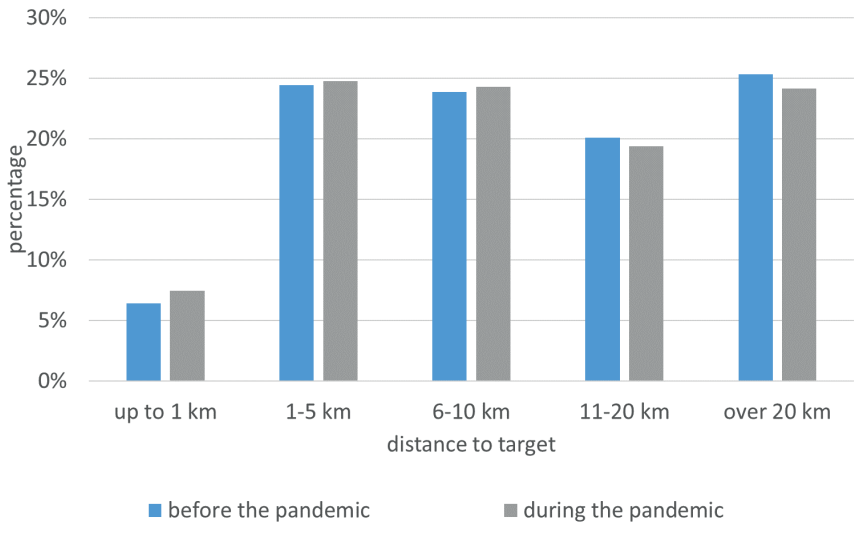


***Figure 6*** *Distance to destination before and during a pandemic*

most people commuted to their main destination, usually work, within 15-30 minutes (33%). During the epidemic and reduced traffic, this time is up to 15 minutes (36%). This is closely related to the previous question on the distance from home to the main destination and is shown in Figure 7.

Another question concerned the monthly costs spent on the car - before and during the pandemic. In this case, before the outbreak of the pandemic, most people spent up to 250€ (70%); during the pandemic, this value decreased minimally to 68%. This was mainly due to the fact that people started using their own cars instead of public transport (Figure 8).

Respondents were then asked how many kilometres they travelled annually: before and during the pandemic. Based on Table 7, it can be seen that the highest number of respondents travelled a distance of 10-15.000 km before the pandemic (27%), and during the pandemic and restricted mobility, this value dropped slightly to 5-10.000 km (26%). This is largely due to public fear of contagion and restricted mobility. Considering gender, the pandemic did not change the mobility behaviour of men and women.

The next question asked respondents about the frequency of car use before and during the pandemic. The majority of respondents used the car practically every day before and during the pandemic. The frequency of car use was not significantly affected by the pandemic (Figure 9).

Additionally, respondents were asked if they lived in a restricted traffic zone and in the vicinity of a paid car park. Negative answers were given by (95%) and (92%) of respondents respectively. Another question concerned driving an electric car. Over 90% of respondents, including 95% of women and 84% of men, have never driven an electric car. Among the respondents, 37% park

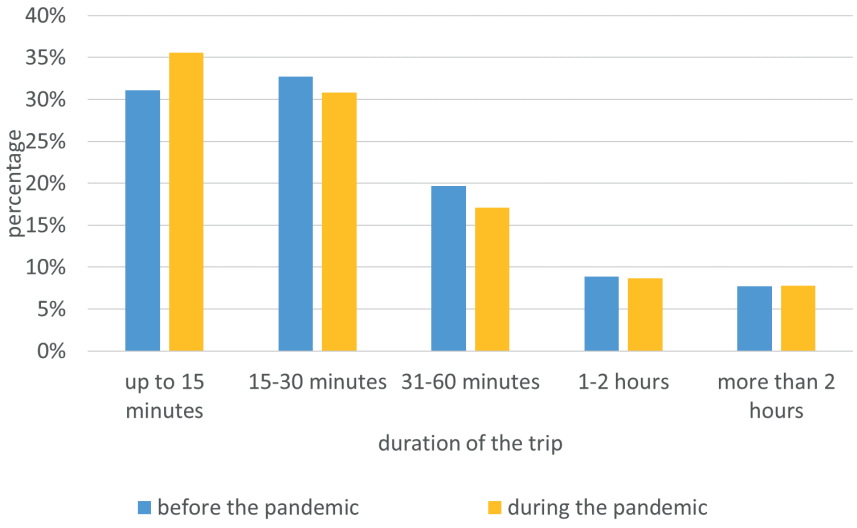


***Figure 7*** *Duration of the trip before and during the pandemic*

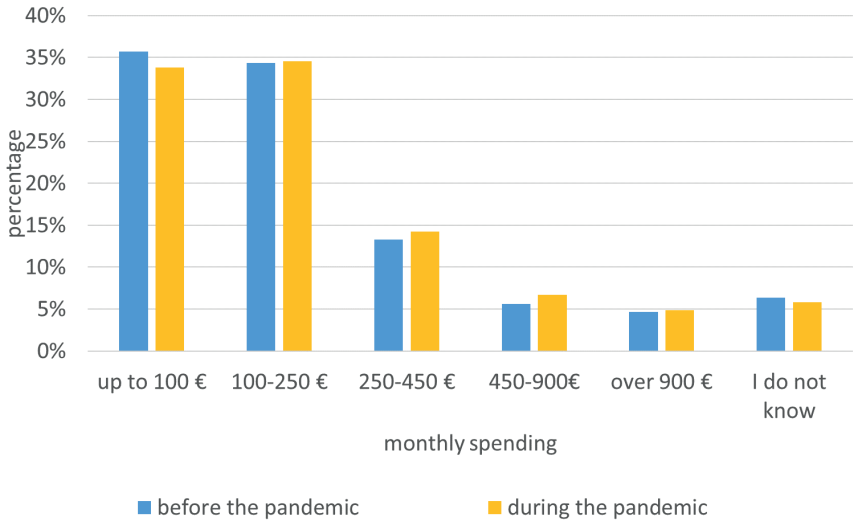


***Figure 8*** *Monthly costs spent on car - before and during the pandemic*

***Table 7*** *Number of kilometres travelled annually by respondents*

| Category | before the pandemic | | during a pandemic | | before the pandemic | | during a pandemic | |
|---|---|---|---|---|---|---|---|---|
| | n | % | n | % | Female [%] | Male [%] | Female [%] | Male [%] |
| Less than 5000 km | 109 | 16.59 | 135 | 21.29 | 21.20 | 9.00 | 26.18 | 13.74 |
| 5.001 - 10.000 km | 171 | 26.03 | 167 | 26.34 | 25.92 | 27.49 | 27.02 | 26.07 |
| 10.001 - 15.000 km | 174 | 26.48 | 160 | 25.24 | 24.87 | 28.44 | 21.73 | 29.38 |
| 15.001 - 20.000 km | 115 | 17.50 | 100 | 15.77 | 15.45 | 20.38 | 13.37 | 19.91 |
| above 20.000 km | 88 | 13.39 | 72 | 11.36 | 12.57 | 14.69 | 11.70 | 10.90 |

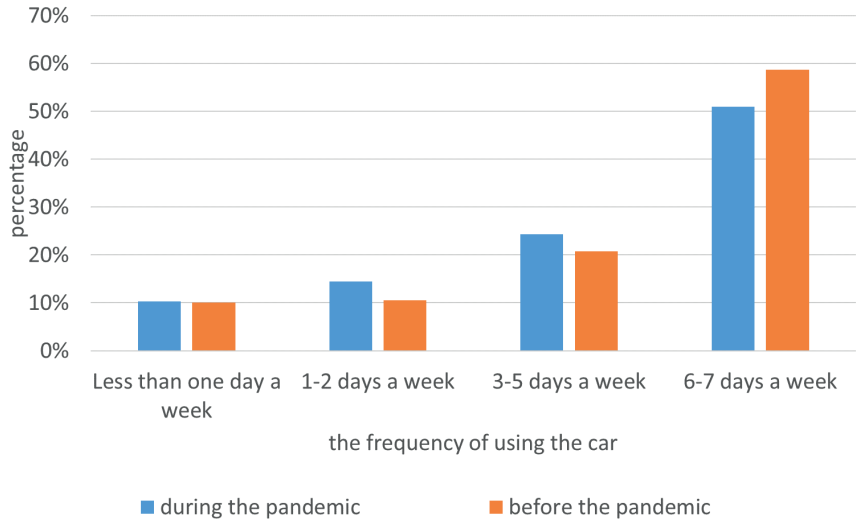


***Figure 9*** *Frequency of car use*

***Table 8*** *Answers given by respondents*

| Category | n | % | Female | | Male | |
|---|---|---|---|---|---|---|
| | | | n | % | n | % |
| Limited traffic zone | | | | | | |
| yes | 33 | 5.54 | 22 | 6.71 | 8 | 3.98 |
| no | 563 | 94.46 | 306 | 93.29 | 193 | 96.02 |
| Paid parking | | | | | | |
| yes | 50 | 8.39 | 24 | 7.32 | 21 | 10.45 |
| no | 546 | 91.61 | 304 | 92.68 | 180 | 89.55 |
| Electric car driving | | | | | | |
| Yes. I have one | 6 | 1.01 | 3 | 0.91 | 2 | 1.00 |
| Yes. I have owned one in the past | 1 | 0.17 | 0 | 0.00 | 1 | 0.50 |
| Yes. I have borrowed one from a friend | 51 | 8.56 | 14 | 4.27 | 29 | 14.43 |
| No. never | 538 | 90.27 | 311 | 94.82 | 169 | 84.08 |
| Parking place of the car | | | | | | |
| On the street | 97 | 16.28 | 46 | 14.02 | 44 | 21.89 |
| In a shared garage | 45 | 7.55 | 27 | 8.23 | 15 | 7.46 |
| In a fenced area of the property | 172 | 28.86 | 101 | 30.79 | 54 | 26.87 |
| In an individual garage | 219 | 36.74 | 120 | 36.59 | 73 | 36.32 |
| In a secure car park | 11 | 1.85 | 4 | 1.22 | 4 | 1.99 |
| not applicable | 52 | 8.72 | 30 | 9.15 | 11 | 5.47 |

***Table 9*** *Answers given by respondents*

| Category | n | % | Female [%] | Male [%] |
|---|---|---|---|---|
| Using Car-Sharing | | | | |
| yes | 48 | 8.05 | 5.18 | 12.94 |
| no | 548 | 91.95 | 94.82 | 87.06 |
| How long have respondents been using car-sharing? | | | | |
| less than 1 year | 12 | 25.00 | 17.65 | 20.83 |
| 1 to 2 years | 13 | 27.08 | 17.65 | 33.33 |
| 2 to 3 years | 9 | 18.75 | 23.53 | 20.83 |
| more than 3 years | 14 | 29.17 | 41.18 | 25.00 |
| Use during a pandemic | | | | |
| yes | 32 | 66.67 | 52.94 | 76.92 |
| no | 16 | 33.33 | 47.06 | 23.08 |
| Determinants of car-sharing | | | | |
| Price of the service | 18 | 29.51 | 18.52 | 26.09 |
| Avoiding costs associated with car ownership | 14 | 22.95 | 29.63 | 10.87 |
| Accessibility | 32 | 52.46 | 29.63 | 50.00 |
| Environmental factor | 2 | 3.28 | 3.70 | 2.17 |
| Economic factor | 8 | 13.11 | 7.41 | 8.70 |
| Other | 5 | 8.20 | 11.11 | 2.17 |

***Table 10*** *Advantages of Car-sharing*

| Category | The importance of the advantages of car-sharing [%] | | | | | | | | | |
|---|---|---|---|---|---|---|---|---|---|---|
| | 1 | 2 | 3 | 4 | 5 | 6 | 7 | 8 | 9 | 10 |
| has a positive impact on the environment | 5.05 | 15.15 | 11.63 | 14.29 | 14.29 | 8.33 | 10.00 | 3.57 | 8.70 | 15.25 |
| no need to have your own vehicle | 15.15 | 18.18 | 11.63 | 4.76 | 7.14 | 4.17 | 0.00 | 10.71 | 13.04 | 11.86 |
| Guarantees easy access to the vehicle. | 9.09 | 6.06 | 9.30 | 11.90 | 16.67 | 20.83 | 35.00 | 3.57 | 13.04 | 3.39 |
| lower costs compared to using your own vehicle | 8.08 | 9.09 | 9.30 | 14.29 | 9.52 | 16.67 | 0.00 | 14.29 | 21.74 | 6.78 |
| Possibility of parking in various locations | 11.11 | 15.15 | 6.98 | 16.67 | 4.76 | 8.33 | 10.00 | 14.29 | 13.04 | 8.47 |
| Guarantees no parking fees. | 15.15 | 9.09 | 9.30 | 16.67 | 0.00 | 0.00 | 10.00 | 14.29 | 13.04 | 10.17 |
| gives the opportunity to use new models of cars of different brands | 11.11 | 12.12 | 13.95 | 9.52 | 7.14 | 8.33 | 5.00 | 7.14 | 4.35 | 13.56 |
| reduces the number of other vehicles in the city | 10.10 | 6.06 | 11.63 | 7.14 | 19.05 | 16.67 | 5.00 | 14.29 | 8.70 | 6.78 |
| has an easy-to-use application | 7.07 | 9.09 | 16.28 | 4.76 | 19.05 | 16.67 | 15.00 | 10.71 | 0.00 | 5.08 |
| my employer pays for the use of Car-sharing | 8.08 | 0.00 | 0.00 | 0.00 | 2.38 | 0.00 | 10.00 | 7.14 | 4.35 | 18.64 |

their car in a garage and 29% park it on the property (Table 8).

The next questions in the survey were about car-sharing. Among the respondents, only 8% used car-sharing. Among them there were 5% women and almost 13% men. Most respondents used the service up to 10 times, which confirms the fact that this service is not very popular in Poland. People who use the car-sharing service most often use it for up to 2 years (52%). Women use the service longer. The pandemic has reduced the use of car-sharing. In addition, 33% of respondents have stopped using the service, this is particularly noticeable

***Table 11*** *Determinants of not using car-sharing*

| Category | n | % | Female [%] | Male [%] |
|---|---|---|---|---|
| lack of available parking spaces | 49 | 6.14 | 6.40 | 4.96 |
| high costs of car-sharing | 60 | 7.52 | 6.64 | 9.54 |
| difficulties in car-sharing | 94 | 11.78 | 12.09 | 12.60 |
| complexity of finding available cars when needed | 36 | 4.51 | 3.08 | 6.11 |
| the service is not available in my area | 337 | 42.23 | 44.31 | 39.31 |
| mistrust of unknown cars (reliability. safety. etc.) | 78 | 9.77 | 9.48 | 10.69 |
| fear of damaging the rented vehicle | 88 | 11.03 | 12.80 | 9.92 |
| lack of need | 21 | 2.63 | 0.95 | 4.20 |
| own car | 24 | 3.01 | 2.37 | 2.29 |
| lack of information about the service | 8 | 1.00 | 0.24 | 0.00 |

***Table 12*** *Answers to the question: why have you never used a car sharing service?*

| Category | n | % | Female [%] | Male [%] |
|---|---|---|---|---|
| I have never needed such a service | 317 | 40.54 | 42.79 | 40.16 |
| I cannot give up using my private car | 45 | 5.75 | 3.95 | 7.48 |
| I am afraid that in case of need I will not find a free car | 41 | 5.24 | 3.95 | 7.09 |
| I am not familiar with the service / am not informed | 126 | 16.11 | 17.44 | 12.99 |
| The service is not available in my area | 209 | 26.73 | 26.74 | 25.98 |
| Risks associated with unknown cars (reliability. safety. etc.) | 39 | 4.99 | 4.19 | 5.91 |
| Other | 5 | 0.64 | 0.93 | 0.39 |

among women. Most respondents use the car-sharing service less than once a month or several times a month. They use it mainly when they do not have a car or other means of transport are not available and instead of a private car for short trips. Respondents decided to use car-sharing mainly because of the availability of the service (53%). They also mentioned the price of the service (30%) and the avoidance of costs associated with owning a car (23%). The gender of the respondents did not matter much (Table 9).

Respondents were also given the opportunity to indicate which advantages of car-sharing are most important to them? In this case 1 means the most important and 10 the least important. The most important for the respondents is the possibility not to own a car, the guarantee of free parking and the possibility to park in many places and to use new car models of different brands. Environmental impact and functionality of applications are not considered at all by respondents (Table 10).

Residents in Poland use various car-sharing applications (BlaBlaCar, Bolt, Easyshare, EcoShare, InnogyGO!, Panek CarSharing, Miimove, Traficar, 4mobility). Many of them use at least one of these. Panek CarSharing and Traficar are used by 66% of respondents. On a scale of 1 to 6, respondents rate the performance of the app highly. 37% of respondents rate it 4 and 29% rate it 5. Gender is not important in rating the app's performance. Men and women rate it 4.48.

Another group of questions concerns people who do not use car-sharing. Respondents were asked why they do not use this service. Respondents were given a choice of multiple answers. Most of them (42%) answered that the service is not available in my area. This is mainly due to the fact that the car-sharing service is still underdeveloped in Poland and available only in bigger cities, and among the respondents there were also inhabitants of small towns. The second answer was that it is difficult for me to share a car (12%). This is a serious problem because it is difficult to change people's mental behaviour. Everyone wants to have their own car and does not want to share it. In this case it will be difficult to convince such people to use this service. Another answer given was the fear of damage to the rented vehicle (11%). Although the cars are insured and with proper use nothing should happen to them, people are afraid to use them. (Table 11).

Respondents were then asked why they had never used a car sharing service? The majority of respondents said they did not need such a service (41%). This question is consistent with ACEA data, which confirms that there are more and more cars in Poland. For this reason everyone drives their own car and there is no need to rent one. Respondents also stated that the service is not available in my area (27%) and they do not know what car-sharing is and how it works (16%). It shows that the car-sharing service is poorly developed and poorly advertised in Poland (Table 12).

The last question, for all, concerned other comments on the functioning of car-sharing in Poland not mentioned in the survey. Respondents pointed out above all the

limited access to the car-sharing service and its high cost. People using the service also pointed out that there are vehicles damaged by other users, e.g. jammed handbrake or incomplete equipment, as well as dirty cars inside.

## 3 Conclusions

After the COVID-19 outbreak, the mobility of the Polish population changed, especially in cities where public transport existed and people stayed at home or started using their own cars. In smaller towns and villages, where there is no public transport, people still mainly use cars because they are dependent on it. Research has found that around 8% of people in Poland use car-sharing. The pandemic has caused a decrease in the use of car-sharing. More than 30% of those surveyed have given up using it because of health concerns. In addition, limited availability is an obstacle to the use of this service. It is mainly developed in big cities, while in smaller towns people do not even know about its existence. The number of vehicles in Poland, which is growing year on year, confirms the fact that Poles prefer to use their own car rather than a car driven by other people. This may change in the future, as the growing number of cars in cities makes it difficult to find parking spaces, and it is very often the case that car-sharing companies have spaces purchased for this purpose. In addition, a large proportion of car-sharing cars are electric, which means that in some cities there is the possibility of using bus lanes.

## Acknowledgement

This publication was created thanks to support under the Operational Program Integrated Infrastructure for the project: Identification and possibilities of implementation of new technological measures in transport to achieve safe mobility during a pandemic caused by COVID-19 (ITMS code: 313011AUX5), co-financed by the European Regional Development Fund.

## References

[1] Road accidents - Police statistics [online] [accessed 2021-08-11] Available from: https://statystyka.policja.pl/st/ruch-drogowy/76562,Wypadki-drogowe-raporty-roczne.html
[2] Local data bank [online] [accessed 2021-08-11] Available from: https://bdl.stat.gov.pl/BDL/dane/podgrup/tablica
[3] Motorisation rates in the EU, by country and vehicle type [online] [accessed 2021-08-11] Available from: https://www.acea.be/statistics/tag/category/vehicles-per-capita-by-country/
[4] Passenger cars in the EU [online] [accessed 2021-08-11] Available from: http://bityl.pl/rmYCs
[5] BARTUSKA, L., HANZL, J., LIZBETINOVA, L. Possibilities of using the data for planning the cycling infrastructure. *Procedia Engineering* [online]. 2016, **161**, p. 282-289. ISSN 1877-7058. Available from: https://doi.org/10.1016/j.proeng.2016.08.555
[6] LIZBETINOVA, L., LEJSKOVA, P., NEDELIAKOVA E., CAHA, Z., HITKA, M. The growing importance of ecological factors to employees in the transport and logistics sector. *Economic Research / Ekonomska IstraZivanja* [online]. 2021, latest articles. ISSN 1331-677X, eISSN 1848-9664. Available from: https://doi.org/10.1080/1331677X.2021.2013275
[7] SVADLENKA, L., SIMIC, V., DOBRODOLAC, M., LAZAREVIC, D., TODOROVIC, G. Picture fuzzy decision-making approach for sustainable last-mile delivery. *IEEE Access* [online]. 2020, **8**, p. 209393-209414. eISSN 2169-3536. Available from: https://doi.org/10.1109/ACCESS.2020.3039010
[8] CUBRANIC-DOBRODOLAC M, SVADLENKA L, CICEVIC S, TRIFUNOVIC A, DOBRODOLAC M. Using the interval type-2 fuzzy inference systems to compare the impact of speed and space perception on the occurrence of road traffic accidents. *Mathematics* [online]. 2020, **8**(9), 1548. eISSN 2227-7390. Available from: https://doi.org/10.3390/math8091548
[9] CUBRANIC-DOBRODOLAC, M., SVADLENKA, L., CICEVIC, S., DOBRODOLAC, M. Modelling driver propensity for traffic accidents: a comparison of multiple regression analysis and fuzzy approach. *International Journal of Injury Control and Safety Promotion* [online]. 2020, **27**(2), p. 156-167. ISSN 1745-7300, eISSN 1745-7319. Available from: https://doi.org/10.1080/17457300.2019.1690002
[10] FROST & SULLIVAN, Future of Car Sharing Market to 2025 [online] [accessed 2022-02-18] Available from: https://store.frost.com/future-of-carsharing-market-to-2025.html
[11] Car sharing and transportation trends [online] [accessed 2022-02-18] Available from: https://www.futuremind.com/blog/car-sharing-and-transportation-trends
[12] ANDERSEN, K., RAMBAUT, A., LIPKIN, I. W., HOLMES, E., GARRY, R. The proximal origin of SARS-CoV-2. *Nature Medicine* [online]. 2020, **26**, p. 450-52. ISSN 1078-8956, eISSN 1546-170X. Available from: https://doi.org/10.1038/s41591-020-0820-9

[13] MAIER, B. F., BROCKMANN, D. Effective containment explains subexponential growth in recent confirmed COVID-19 cases in China. *Science* [online]. 2020, **368**, p. 742-46. ISSN 0036-8075, eISSN 1095-9203. Available from: https://doi.org/10.1126/science.abb4557

[14] BARRO, R., URSUA, J., WENG, J. The coronavirus and the great influenza pandemic: lessons from the "spanish flu" for the coronavirus's potential effects on mortality and economic activity. NBER Working Papers 26866. Cambridge, MA, USA: National Bureau of Economic Research, 2020.

[15] LAING, T. The economic impact of the coronavirus 2019 (Covid-2019): implications for the mining industry. *The Extractive Industries and Society* [online]. 2020, **7**(2), p. 580-82. ISSN 2214-790X. Available from: https://doi.org/10.1016/j.exis.2020.04.003

[16] BOOT, A., CARLETTI, E., HASELMANN, R., KOTZ, H.-H., KRAHNEN, J. P., PELIZZON, L., SCHAEFER, S., SUBRAHMANYAM, M. The Coronavirus and financial stability [online]. SAFE Policy Letter. Vol. 78. Frankfurt: Leibniz Institute for Financial Research SAFE, 2020. Available from: https://safe-frankfurt.de/policy-center/policy-publications/policy-publ-detailsview/publicationname/the-coronavirus-and-financial-stability.html

[17] WARREN, M. S., SKILLMAN, S. W. Mobility changes in response to COVID-19 [online]. arXiv:2003.14228. 2020. Available from: https://doi.org/10.48550/arXiv.2003.14228

[18] DE VOS, J. The effect of COVID-19 and subsequent social distancing on travel behavior. *Transportation Research Interdisciplinary Perspectives* [online]. 2020, **5**, 100121. ISSN 2590-1982. Available from: https://doi.org/10.1016/j.trip.2020.100121

[19] GOSSLING, S., SCOTT, D., HALL, M. C. Pandemics, tourism and global change: a rapid assessment of COVID-19. *Journal of Sustainable Tourism* [online]. 2020, **19**(1), p. 1-20. ISSN 0966-9582, eISSN 1747-7646. Available from: https://doi.org/10.1080/09669582.2020.1758708

[20] BONACCORSI, G., PIERRI, F., CINELLI, M., FLORI, A., GALEAZZI, A., PORCELLI, F., SCHMIDT, A. L., VALENSISE, C. M., SCALA, A., QUATTROCIOCCHI, W., PAMMOLLI, F. Economic and social consequences of human mobility restrictions under COVID-19. *Proceedings of the National Academy of Sciences* [online]. 2020, **117**, p. 15530-15535. eISSN 1091-6490. Available from: https://doi.org/10.1073/pnas.2007658117

[21] PULLANO, G., VALDANO, E., SCARPA, N., RUBRICHI, S., COLIZZA, V. Population mobility reductions during COVID-19 epidemic in France under lockdown. *The Lancet Digital Health* [online]. 2020, **2**(12), p. E638-E649. ISSN 2589-7500. Available from: https://doi.org/10.1016/S2589-7500(20)30243-0

[22] QUEIROZ, L., MELO, J. L., BARBOZA, G., URBANSKI, A. H., NICOLAU, A., OLIVA, S., NAKAYA, H. Large-scale assessment of human mobility during COVID-19 outbreak [online]. Open Science Framework. 2020. Available from: https://doi.org/10.31219/osf.io/nqxrd

[23] GALEAZZI, A., CINELLI, M., BONACCORSI, G., PIERRI, F., SCHMIDT, A. L., SCALA, A., PAMMOLLI, F., QUATTROCIOCCHI, W. Human mobility in response to COVID-19 in France, Italy and UK. *Scientific Reports* [online]. 2021, **11**, 13141. eISSN 2045-2322. Available from: https://doi.org/10.1038/s41598-021-92399-2

[24] SCHLOSSER, F., MAIER, B. F., HINRICHS, D., ZACHARIAE, A., BROCKMANN, D. COVID-19 lockdown induces structural changes in mobility networks - implication for mitigating disease dynamics. arXiv:2007.01583v1. 2020.

[25] FERGUSON, E. The rise and fall of the American carpool: 1970-1990. *Transportation* [online]. 1997, **24**(4), p. 349-376. ISSN 0049-4488.

[26] STOFKOVA, J., STRICEK, I., STOFKOVA, K. Data analysis in quality management of the network enterprise. In: *Production management and engineering sciences*. 2016. p. 273-278. ISBN 978-1-138-02856-2

[27] VARTIAK, L., JANKALOVA, M. The business excellence assessment. *Procedia Engineering* [online]. 2017, **192**, p. 917-922. ISSN 1877-7058. Available from: https://doi.org/10.1016/j.proeng.2017.06.158

[28] VEENEMAN, W. The sharing economy and the relevance for transport. In: *Advances in Transport Policy and Planning*. FISHMEN, E. (ed.). Vol. 4. 1. ed. Elsevier, 2019. ISBN 978-0128162101, p. 39-57.

[29] GARBAROVA, M., HOLLA BACHANOVA, P. Sharing economy as a new form of business in global environment. In: 18th International Scientific Conference Globalization and its Socio-Economic Consequences: proceedings. 2018. ISBN 978-80-8154-249-7, ISSN 2454-0943, p. 103-110.

[30] GARBAROVA M., VARTIAK L. Consequences of the sharing economy on passenger transport. *Transportation Research Procedia* [online]. 2021, **55**, p. 57-62. ISSN 2352-1465. Available from: https://doi.org/10.1016/j.trpro.2021.06.006

[31] MITREGA V., MALECKA A. Conditions for participation in the so-called ride sharing - blablacar user research results. *Scientific Journals of the University of Szczecin. No. 875 Problems of management, finance and marketing* [online]. 2015, **41**(2), p. 153-164. ISSN 1509-0507, eISSN 2353-2874. Available from: https://doi.org/10.18276/pzfm.2015.41/2-13

[32] BECKER, H., CIARI, F., AXHAUSEN, K. W. Comparing car-sharing schemes in Switzerland: user groups and usage patterns. *Transportation Research Part A: Policy and Practice* [online]. 2017, **97**, p. 17-29. ISSN 0965-8564. Available from: https://doi.org/10.1016/j.tra.2017.01.004

[33] SHAHEEN, S. A., CHAN, N. D., MICHEAUX, H. One-way carsharing's evolution and operator perspectives from the Americas. *Transportation* [online]. 2015, **42**, p. 519-536. ISSN 0049-4488. Available from: https://doi.org/10.1007/s11116-015-9607-0

[34] STILLWATER, T., MOKHTARIAN, P. L., SHAHEEN, S. A. Carsharing and the built environment, geographic information system-based study of one U.S. operator. *Transportation Research Record: Journal of the Transportation Research Board* [online]. 2008, **2110**, p. 27-34. ISSN 0361-1981, eISSN 2169-4052. Available from: https://doi.org/10.3141/2110-04

[35] BURKHARDT, J. E., MILLARD-BALL, A. Who is attracted to carsharing? *Transportation Research Record: Journal of the Transportation Research Board* [online]. 2006, **1986**, p. 98-105. ISSN 0361-1981, eISSN 2169-4052. Available from: https://doi.org/10.1177/0361198106198600113

[36] CERVERO, R., TSAI, Y. City Carshare in San Francisco, California - second-year travel demand and car ownership impact. *Transportation Research Record: Journal of the Transportation Research Board* [online]. 2004, **1887**, p. 117-127. ISSN 0361-1981, eISSN 2169-4052. Available from: https://doi.org/10.3141/1887-14

[37] SHAHEEN, S. A. The impact of carsharing on public transit and non-motorized travel: an exploration of North American carsharing survey data. *Energies* [online]. 2011, **4**(11), p. 2094-2114. ISSN 1996-1073. Available from: https://doi.org/10.3390/en4112094

[38] MILLARD-BALL, A., MURRAY, G., TER SCHURE, J., FOX, C., BURKHARDT, J. Car-sharing: where and how it succeeds [online]. Technical report 108. Transit Cooperative Research Program. Washington, D.C.: Transportation Research Board, 2005. Available from: https://ccdcboise.com//wp-content/uploads/2016/02/Document-D1-TCRP-Car-sharing-Where-and-How-It-Succeeds.pdf

[39] SHAHEEN, S. A., RODIER, C., MURRAY, G., COHEN, A., MARTIN, E. Carsharing and public parking policies: assessing benefits, costs, and best practices in North America [online]. Technical report CA-MTI-10-2612. San Jose, California: Mineta Transportation Institute, 2010. Available from: https://transweb.sjsu.edu/sites/default/files/2612_Carsharing-Parking.pdf

[40] SIOUI, L., MORENCY, C., TREPANIER, M. How carsharing affects the travel behavior of households: a case study of Montreal, Canada. *International Journal of Sustainable Transportation* [online]. 2013, **7**(1), p. 52-69. ISSN 1556-8318, eISSN 1556-8334. Available from: https://doi.org/10.1080/15568318.2012.660109

[41] HAMARI, J., SJOKLINT, M., UKKONEN, A. The sharing economy: why people participate in collaborative consumption. *Journal of the Association for Information Science and Technology* [online]. 2016, **67**(9), p. 2047-2059. eISSN 2330-1643. Available from: https://doi.org/10.1002/asi.2355

[42] BABBIE, E. R. The practice of social research. Belmont: Wadsworth Cengage, 2010. ISBN 9780495598411.

[43] Research sample selection [online] [accessed 2/21/2020]. Available from: https://www.naukowiec.org/dobor.html

# MODELING THE BEHAVIOR IN CHOOSING THE TRAVEL MODE FOR LONG-DISTANCE TRAVEL USING SUPERVISED MACHINE LEARNING ALGORITHMS

**Khondhaker Al Momin [1,*], Saurav Barua [1], Omar Faruqe Hamim [2], Subrata Roy [3]**

[1]Department of Civil Engineering, Daffodil International University, Dhaka, Bangladesh
[2]Department of Civil Engineering, Bangladesh University of Engineering and Technology, Dhaka, Bangladesh
[3]Department of Civil Engineering, University of Information Technology and Sciences, Dhaka, Bangladesh

*E-mail of corresponding author: momin.ce@diu.edu.bd

***Resume***

The long-distance travel (LDT) mode choice modeling is important for transportation planners. This study investigated alternative mode choice behavior for the LDT between the intercity buses and trains. A questionnaire survey, consisting of important mode choice attributes, was conducted on various groups of people in Bangladesh. Numerous travel mode choice contributing features (e.g., travel time, travel costs, origin-destination, comfort, safety, travel time reliability, ticket availability and schedule flexibility) were considered and the LDT mode choice models were developed using various machine learning algorithms typically applied for classification problems. With 95.31% accuracy and 0.95 F1-score, Random Forest model was the best performing model for the dataset. According to the findings of this study, the intercity bus is preferred over the intercity train for LDT in Bangladesh.

***Article info***

Received 23 May 2022
Accepted 2 August 2022
Online 8 September 2022

***Keywords:***

long distance travel
mode choice
supervised machine learning
intercity train
intercity bus

Available online: https://doi.org/10.26552/com.C.2022.4.A187-A197

ISSN 1335-4205 (print version)
ISSN 2585-7878 (online version)

## 1 Introduction

Understanding the causal variables is vital in predicting the travel demand in the transportation planning domain. Factors such as individual traits, household type, security, comfort level, weather and built environment affect a person's travel mode choice [1-3]. Two of the most competitive public transport modes for the long-distance travel (LDT) within a country are intercity train and intercity bus. Bus uses shared road space with other vehicles on highways, whereas the train uses exclusive right-of-way with high ridership potential without occupying any road space [4]. Hence, prioritizing the train services will lead to more efficient use of land for transportation than bus services. On the contrary, intercity buses provide more accessibility and flexibility than intercity trains. Besides, construction, operation and improvement of the bus service systems are less expensive and time-consuming than the intercity train systems [5]. It has been argued by Kampf et. al. [6] that different modes of transport are essential parts of a sustainable transport system. Therefore, there is a need for research to assess peoples' preferences between intercity train and intercity bus services.

In travel behavior research, discrete choice models, such as the multinomial logit model [7], are usually used. According to Cheng et al. [8] machine learning (ML) methods are a viable alternative to statistical models to predict the mode preferences for traveling. Many researchers have employed the ML techniques to predict travel mode preference behavior in recent years. However, differences can be identified between ML and conventional statistical methodologies in terms of understanding the data structure [9]. A logit model presupposes the data structure using assumptions regarding behavior and statistics, whereas many popular ML methods are non-parametric, devoid of theoretical assumptions about the underlying data structure and rely on computers for analyzing the data [10]. Hence, more flexible structures can be formed using the ML algorithms to yield better predictive ability on test samples. Several recent works in travel behavior research have shown that ML models are outperforming logit models in predictive capacity, especially in research related to travel behavior [8-9, 11-13].

Preference for travel mode or modal split has been studied over the past few decades for transportation planning and policymaking. Mode choice depends on

several features, such as time required for travel, travel expenses, level of comfort, safety, convenience and so on [14-15]. Each feature has underlying relation with the mode choice model individually and in combination. The mode choice model varies with demographics, socioeconomic and geographic conditions. Two of the most significant factors in choosing among available alternative travel modes are found to be the adequacy of transportation infrastructure and level of service [16].

The LDT differs from short-distance daily travel in various aspects. According to the European DATELINE study [17], the LDT is defined as trips that cover 100 kilometers or more, whereas the US Bureau of Transportation Statistics [18] defines LDT as trips greater or equal to 50 miles (83.33 kilometers) travel from the origin. Though few prior pieces of literature have been found to distinguish clearly between the different features and aspects of LDT than short-distance travel, it is apparent that people used to make a distinctive choice for both cases. Short-distance travels are typically work trips, non-work trips, shopping trips which are most frequent, whereas the LDT is mostly infrequent and subjected to non-work trips and vacation trips.

Several studies performed nested logit model [19], structured equation model [20], neural network [21], decision tree (DT) [10] and random forest (RF) algorithm [8, 12, 22] to understand modal split behavior. Each of the models has its pros and cons. This research aimed to use popular supervised ML algorithms. used for classification problems such as Naive Bayes (NB), Support Vector Machine (SVM), K-Nearest Neighbors (KNN), RF and DT models, to develop a mode preference model for LDT, using stated preference survey data. Further, the attributes important in predicting the travel mode preference have been identified by investigating the users' LDT mode choice behavior using the best-performing ML-based classification method in the context of Dhaka, the capital city of Bangladesh. According to the authors' knowledge, none has performed such study for modeling the LDT mode choice using ML approaches in a low-income country like Bangladesh.

## 2 Literature review

The growing challenge of increasing demand for travel, safety concerns, energy exhaustion, emission of deadly gases and environmental deterioration has prompted transportation engineers to adopt ML techniques to solve these dynamic problems [23]. The ML is an assemblage of methodologies or algorithms that allow computers to program the development of the data-driven model by detecting patterns in statistically significant data [24]. Recently, a variety of ML approaches have been employed for modeling the travel mode choice. Using artificial neural networks, Pulugurta et al. [25] were able to incorporate human knowledge and activities at the cognitive level into mode choice behavior; Tang et al. [26] discussed the travel mode switching behavior of people who were only given two options using DTs. On the other hand, Cheng et al. [8] modeled the behavior in travel mode preference using the RF algorithm. Instead of using logit model, travel mode preference can be modeled using a classification problem-based approach. Many researchers have argued that ML classifiers can effectively model individual travel behavior [8-9, 11, 13].

Across the world, many researchers have focused on revealing different factors affecting the LDT. Moeckel et al. [27] explained why it is important to predict and understand the LDT mode in terms of vehicle miles traveled, as well as looked at different logit and combined choice models for proposing a new (modified $R^3$ logit) nested multinomial logit model to predict LDT mode for the state of North Carolina, USA. A study conducted in Japan by Shen [28] found that the Latent Class Model performed better than the Mixed Logit Model when it came to choosing transport mode among monorail, car and bus. Bok et al. [29] conducted an empirical study for LDT in Portugal by car, train, or bus. Similarly, many researchers for example Rohr et al. [30] in the UK, MVA [31] in the Netherlands, De Jong and Gunn [32] in Italy, Mandel et al. [33] in Germany and RAVE [34] in Portugal, conducted studies regarding the long-distance travel using different logit models. Furthermore, Gasparik et al. [35] explored the technical and non-technical obstacles to the operation of long-distance rail services in the European Union.

In addition, ML classifiers have been found to outperform conventional logit models in forecasting the travel-mode preferences, e.g., RF classifier achieves better accuracy in less computational time and with less modeling effort than the multinomial logit model (MNL) [12, 36]. ML models increase compatibility with the empirical data by allowing flexible model structures, whereas logit models work on a predetermined model structure; thus, ML models perform better than logit models in predicting mode preferences for travel [9, 37]. This is due to the fact that the logit model prioritizes the estimation of the parameter to increase the predictive precision of the model [38]. Wang and Ross [39] compared the performance between extreme gradient boosting (XGB) and the MNL model in predicting travel mode choice and found that in overall, the XGB model is better at making predictions than the MNL model, especially when the data set is not extremely unbalanced. Omrani [40] applied four ML methods (neural net-RBF, neural net-MLP, multinomial logistic regression and SVM) to predict how people in Luxembourg will choose to travel and found that the ML methods perform better.

Despite showing a significant overall model fit, the mixed logit model was found to have worse prediction accuracy than the simpler multinomial logit model [41]. According to Mullainathan and Spiess [38], although the ML approaches yield better predictive accuracy, these are

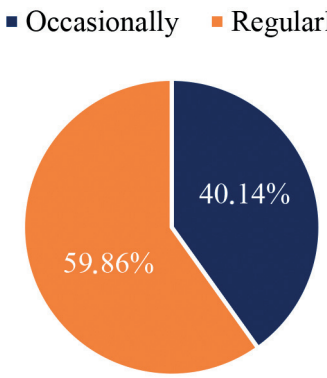


***Figure 1*** *Frequency of travel on the route*

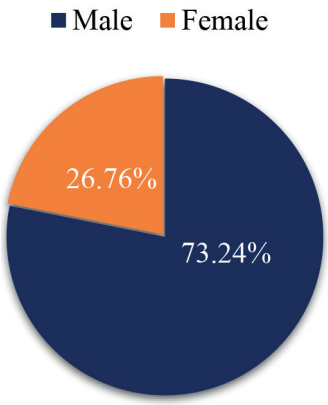


***Figure 2*** *Gender*

often thought to have a lower level of explanatory power. Furthermore, the ML models are termed as hard to be explainable due to their inability to facilitate behavioral interpretation [42]. However, a development has been made recently in the ML domain to facilitate decision-making with the availability of various interpretation tools which can be applied in extracting knowledge from these uninterpretable models [43-44].

Variable importance is being commonly used as an aid to ML tools for modeling the mode preferences for travel [8, 10, 12]. Recently, Hagenauer and Helbich [12] distinguished the variable importance results between the ML methods and the multinomial logit model. Cheng et al. [8] have assessed the relative value of the explanatory variables of RF model by using the variable importance tool to formulate transportation policies. Therefore, it is clear that the analysis of the variable outputs of ML models can show which factors drive prediction decisions. This research focuses on identifying the attributes affecting travel mode choice for LDT in Bangladesh.

## 3 Methodology

### 3.1 Data collection

In this study, four routes have been considered to understand the LDT mode choice behavior. The origin node of the routes selected for this study is Dhaka, the capital city of Bangladesh and the destination nodes are four other major metropolitans of Bangladesh, i.e., Chittagong, Rajshahi, Khulna and Sylhet. The distances between Dhaka and Chittagong, Rajshahi, Khulna and Sylhet are 244 kilometers, 247.7 kilometers, 270.3 kilometers and 240.5 kilometers, respectively; therefore, these trips can be considered as long-distance trips according to the Bureau of Transportation Statistics [18]. A total of 852 responses have been collected, out of which 302 responses were collected through an online questionnaire survey circulated via google forms and the remaining 550 responses were collected in person by a group of enumerators from different bus stands and railway stations. The questionnaire survey is designed with close-ended multiple-choice questions containing two segments. The questions in the questionnaire have been adapted from similar research [45-46] performed to model travel mode choice for the LDT.

The first part of the questionnaire includes general questions regarding route traveling, frequency of travel and demographic information such as gender and income level. The second portion asks about travel mode preference and various features related to mode choice, e.g., the time required for travel, i.e., travel time, expenses incurred for travel, i.e., travel costs, comfort during journey, safety, reliability of journey time, stop or station closer (proximity) to destination, stop or station closer (proximity) to origin, availability of tickets and flexible schedule. The respondents were asked to choose between intercity train and intercity bus mode for LDT in the questions related to each of the features.

Figures 1 and 2 show the distribution of respondents in terms of the travel frequency and gender. It is observed from Figure 1 that 59.86% of respondents regularly travel while 40.14% are occasional travelers and among them, 73.24% are male and 26.76% are female respondents (ref. Figure 2). Female passengers in Bangladesh rarely travel long distances alone, which explains the less dominance of female respondents in the survey.

According to monthly household income and origin-destination of the journey, the distributions of respondents are represented in Figures 3 and 4. Among the income group, 38.50% of the respondents have a monthly income of less than 20,000 Bangladeshi Taka (BDT) (equivalent to 212 USD, currency conversion rate as of 16 July, 2022) and 37.09% have a monthly income between 50,000 BDT (equivalent to 578 USD) to 1,00,000 BDT (equivalent to 1,156 USD), 19.13% earn 20,000 BDT (equivalent to 231 USD) to 50,000 BDT (equivalent to 532 USD) on a monthly basis and only 5.28% have a monthly household income over 1,00,000 BDT (equivalent to 1,064 USD).

From Figure 4 can be observed that the portion of respondents traveling from Dhaka to four major metropolitan cities of Bangladesh in descending order

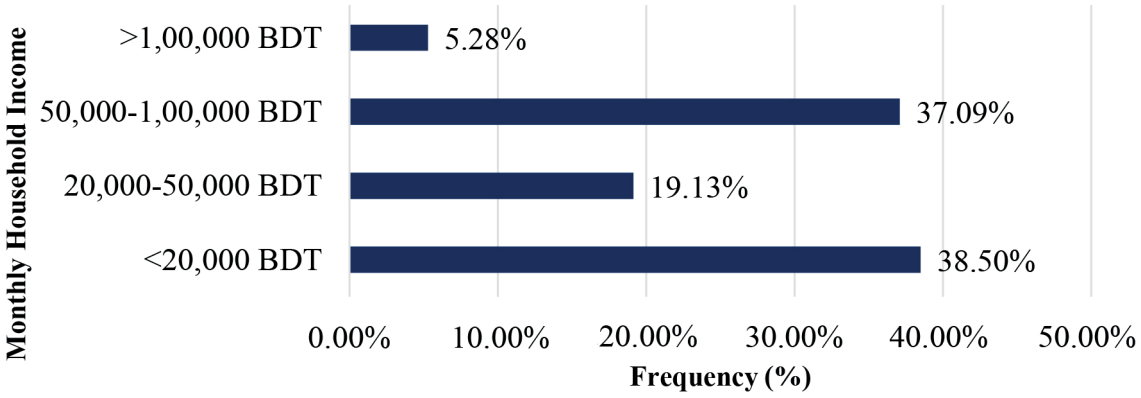


***Figure 3*** *Monthly household income*

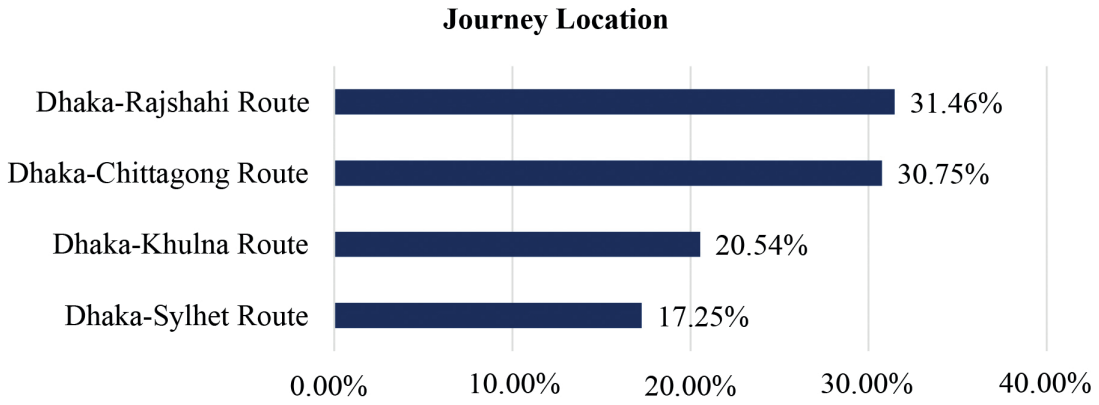


***Figure 4*** *Origin-destination of journey*

are Rajshahi (31.46 %), Chittagong (30.75 %), Khulna (19.54%) and Sylhet (15.89 %).

### 3.2 Data preprocessing

The collected data stored in google forms is exported as comma-separated values (.csv) file and then the data is converted to categorical dummy variables. The travel mode choice option "Intercity Train" was converted to 0 and "Intercity Bus" was converted to 1, the four different routes, i.e. Dhaka-Rajshahi, Dhaka-Chittagong, Dhaka-Khulna and Dhaka-Sylhet, are coded as 0, 1, 2 and 3 respectively, frequency of travel being occasionally or regularly is converted to 0 and 1, age of the respondents classified as less than 18 years, 18 to 40 years and more than 40 years are coded as 0, 1 and 2, males are coded as 0, in contrast, females are coded as 1, monthly household income being less than BDT 20,000 is converted to 0 and similarly, income levels of BDT 20,000 to 50,000, BDT 50,000 to 1,00,000 and more than BDT 1,00,000 are converted to 1, 2 and 3, the occupation of the respondents classified as service holder, student, businessman and housewife are coded as 0, 1, 2 and 3. For training the model, 70% of the dataset was chosen randomly and the rest was used for testing purposes. Using various python libraries, i.e., NumPy, Pandas, Matplotlib, Seaborn and Scikit-learn, the preprocessed dataset has been used in ML algorithms for further analysis.

### 3.3 Travel mode choice classification model development

A labeled dataset of 852 participants is used to classify travel mode choice to train different supervised ML algorithms, i.e., NB, SVM, DT, RF and KNN. NB, based on Bayes' theorem [47], is a classification strategy that predicts the probability of an occurrence on the basis of past knowledge about associated factors [48]. It works best in two scenarios: features that are fully independent and features that are functionally dependent [49]. The DT classifier creates a tree-like structure by categorizing the data set into smaller nodes, with terminal nodes indicating decision outcomes [48, 50]. The RF is an ensemble classifier that is made up of numerous DTs, similar to a forest being made up of many trees [51]. Distinct parts of the dataset used for training are employed to train various DTs of an RF model. The RF classifier selects the classification that receives the greatest number of votes if the outcome is discrete and the mean of all trees is considered for numeric categorization [48]. In an m-dimensional space, an SVM generates a separation hyperplane, where m is the number of features. These hyperplanes

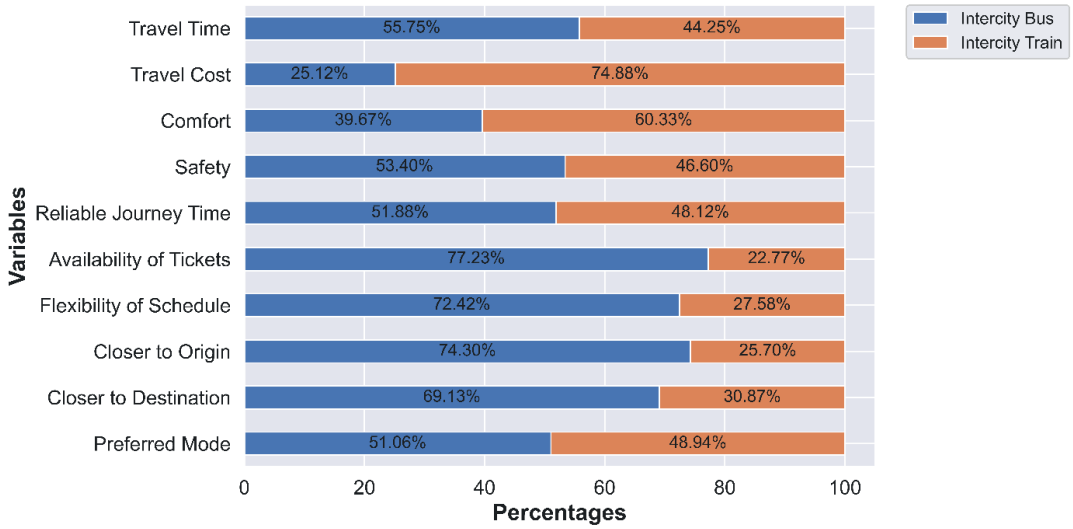


***Figure 5*** *Mode choice preferences by the respondents in terms of different variables*

function as decision boundaries for classifying both linear and non-linear data points. All the data are first mapped onto an m-dimensional feature space, then the SVM determines the separation hyperplane having the maximum margin with minimum classification errors [48, 52]. The KNN algorithm is a simplified form of the NB classifier where probability values are not required [48, 53]. The letter K in the KNN stands for the number of nearest neighbors who are regarded to be eligible to receive a 'vote' from the algorithm. In some cases, differing values for the variable K can result in different categorization results for the same datasets.

To evaluate which model is the best suited to the datasets used in this study, the accuracy and F1-score of each model are compared to one another. The hyperparameters of the model achieving the highest accuracy and F1-score are tuned to obtain an optimized model. Furthermore, the receiver operating characteristic (ROC) curve, F1-score, confusion matrix, precision, recall and area under the curve (AUC) of the selected ML model are all examined to evaluate its overall performance. Additionally, variable importance scores are computed to identify the most significant factors in predicting the travel mode choice.

## 4 Results

### 4.1 Mode choice preferences

Mode choice preferences stated by the respondents corresponding to nine independent variables (i.e., station closer to origin or destination, flexibility of travel schedule, availability of tickets, reliability of travel time, safety, comfort, travel costs and time required for travel) and one dependent variable (preferred travel mode for a particular route) are summarized in Figure 5. In terms of the mode choice for LDT, 55.75% of the respondents preferred to use the bus, while 44.25% preferred to travel by train. More people choose to travel by bus than by train as it takes less time for travel and gives more reliable journey time, safety, availability of tickets, flexible travel schedules, proximity of stations to origin and destination. On the other side, in terms of less travel costs and comfort, traveling by train is preferred compared to traveling by bus. It is evident from this analysis that both modes have some advantages and disadvantages corresponding to different factors associated with LDT.

### 4.2 Mode choice classification models

A variety of supervised ML algorithms have been used to classify the preferences for the LDT mode choice. The accuracy and F1-score achieved by different methods are depicted in Table 1. It shows that the RF classifier produces the highest accuracy and F1-score among all of the methods tested. Hence, the RF classifier is selected as the best method for classifying mode choice preferences for LDT considering the F1-score and accuracy achieved in the testing dataset. Besides that, the RF method can determine out-of-bag accuracy by measuring the average prediction accuracy obtained from the trees whose samples are not considered in the bootstrap sample. Therefore, the over-fitting problem can be detected by observing the out-of-bag accuracy. The out-of-bag accuracy of RF classifier was found to be 93.12% which is very high, so it is evident that the model does not suffer from an over-fitting problem. Table 1 shows that the accuracy and F1-scores of various algorithms are very close and Grandini et al. [54] showed that the accuracy and F1-score might be the same in some cases.

Furthermore, a random search cross-validation technique has been utilized to discover the optimum hyperparameters for refining the RF model's performance in order to improve its accuracy. From a grid of a range of

***Table 1*** *Accuracies and F1-scores achieved by various classification methods*

| Method | Accuracy (%) | F1-Score |
|---|---|---|
| NB | 87.11 | 0.87 |
| DT | 93.75 | 0.94 |
| SVM | 93.75 | 0.94 |
| KNN | 92.97 | 0.94 |
| RF | 95.31 | 0.95 |

***Table 2*** *Classification outcomes of optimized RF model*

| No. of trees | Maximum no. of features for splitting a node | Maximum depth of trees | Minimum no. of samples for splitting a node | Minimum no. of samples used in each leaf | Method for sampling datapoints | Testing accuracy (%) | Out-of-bag accuracy (%) |
|---|---|---|---|---|---|---|---|
| 1828 | 3.87 | 233 | 5 | 1 | Bootstrap | 95.31 | 93.46 |

***Table 3*** *Confusion matrix for testing dataset using optimized RF model*

| | | Predicted | |
|---|---|---|---|
| | | 0 (Intercity Train) | 1 (Intercity Bus) |
| Observed | 0 (Intercity Train) | 115 | 5 |
| | 1 (Intercity Bus) | 7 | 129 |

***Table 4*** *Performance evaluation of optimized RF model*

| | Precision | Recall | F1-Score | Support |
|---|---|---|---|---|
| 0 (Intercity Train) | 0.94 | 0.96 | 0.95 | 120 |
| 1 (Intercity Bus) | 0.96 | 0.95 | 0.96 | 136 |
| | Accuracy | | 0.95 | 256 |
| Average (Macro) | 0.95 | 0.95 | 0.95 | 256 |
| Average (Weighted) | 0.95 | 0.95 | 0.95 | 256 |

different hyperparameters, i.e. the total number of trees used, maximum number of features used to split a node, the maximum number of steps performed in each DT, the minimum points placed in a node before splitting the node, the minimum number of points a leaf node can hold, methodology (with or without replacement) used to sample data points, samples are randomly picked from the grid and ten-fold cross-validation is performed with each combination of values using Scikit-Learn's RandomizedSearchCV method. A summary of the hyperparameter values used, testing accuracy and validation accuracy of the RF model after optimization is presented in Table 2.

After optimizing the RF model, the testing accuracy has been unchanged, but the out-of-bag accuracy has improved by 0.36 %. Confusion matrix for the testing dataset generated by the optimized model is shown in Table 3.

From the confusion matrix for the testing dataset, presented in Table 3, can be observed that only seven testing instances of the bus are falsely predicted as train and five testing samples of the train are falsely predicted as bus. In contrast, the 115 testing samples of train and 129 samples of train are correctly classified. The performance evaluation report of the optimized RF model in terms of different metrics is provided in Table 4.

Table 4 portrays different metrics, i.e., precision, recall and F1-score, for evaluating the performance of the optimized RF model. The support values for class 0 and class 1 are very close. This makes the testing dataset a balanced set leading to similar precision, recall and F1 scores for the classifier. The precision value of 0.95 reveals that 95 % of the positive predictions made by the model are also positive observations, the recall value of 0.95 means that 95 % of the positive observations are also predicted as positive labels by the model and the F1-score of 0.95 explains that 95 % of the positive predictions are correctly classified. All of these metrics are close to 1.0, representing a good predictive power of the developed classification model. Figure 6 shows the ROC curve of the optimized RF model.

An ROC curve denotes connection amid false positive (FP) rate and true positive (TP) rate where the FP rate = FP/ (FP + true negative) and TP rate = TP/ (TP + false negative). The AUC is used to summarize the ROC curve since it measures the capacity of a classifier to distinguish between different classes. The AUC

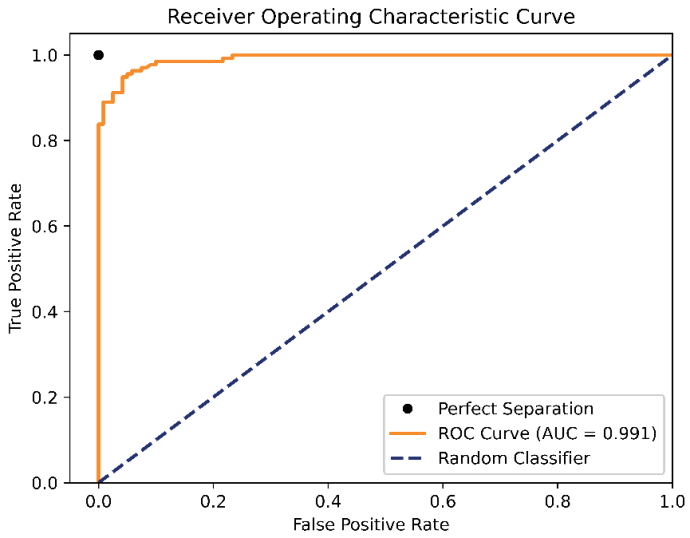


***Figure 6*** *ROC curve of the optimized RF model*

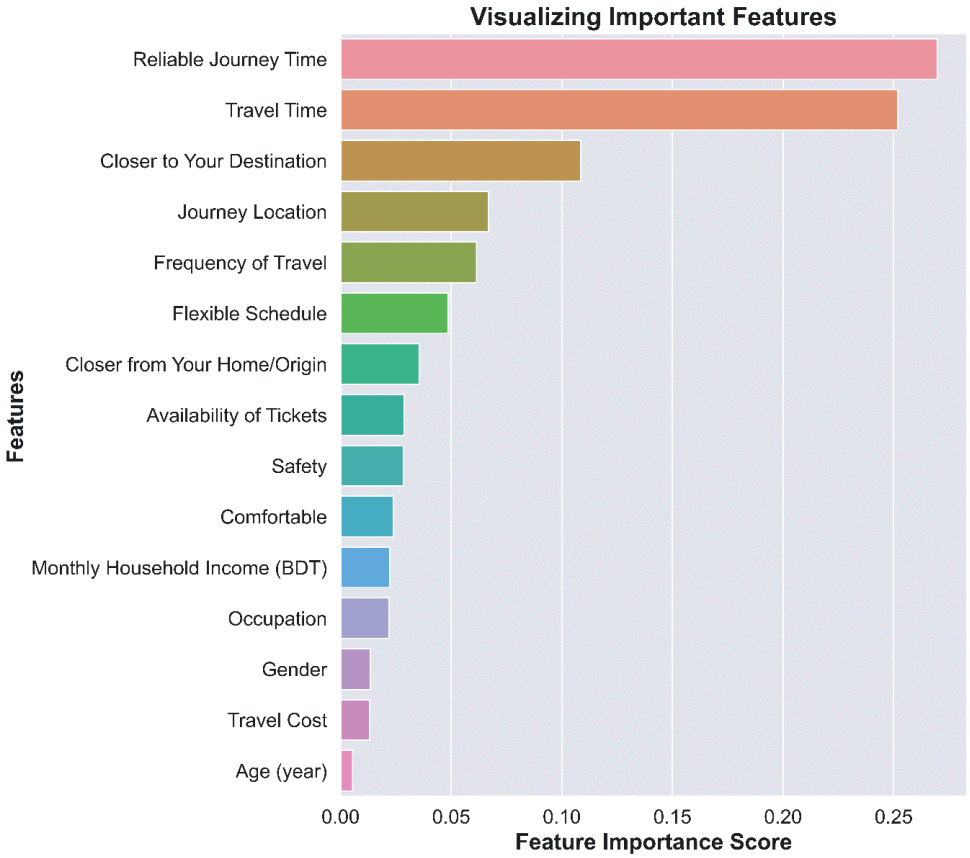


***Figure 7*** *Feature importance scores of the optimized RF model*

reveals how satisfactorily the model differentiates amid positive and negative classes. As AUC increases, so does the model performance. Usually, the AUC value ranges between 0.5 and 1.0. From Figure 6 can be observed that the ROC curve of the optimized RF model is way above the random classifier line and very close to the perfect separation point. In addition, the AUC score of the developed model is 0.991, which is very close to 1.0, representing the perfect classifier. As a result, the model can be considered as effective in distinguishing between two classes.

### 4.3 Determining important features

In order to determine the important features in choosing a travel mode for LDT, the feature importance scores of all the features used in developing the

classification model are plotted in Figure 7. The feature importance score represents the contribution of the feature in making the decision regarding the travel mode choice for LDT.

In the RF classification model, Gini importance, or mean decrease in impurity, is used to measure the importance of features [55]. The features shown in Figure 7 are ranked as per decreasing importance score. Reliable journey time is the most important feature for the proposed LDT mode choice, time required for travel, stop or station closer to destination, journey location and frequency of travel are the second, third, fourth and fifth most important features. The other features, deemed important in deciding on the travel mode, are flexible schedule, stop or station closer to the origin, availability of tickets, safety, comfortability, monthly household income, occupation, gender, travel costs and age of the respondent in descending order of importance.

So, it is evident that for the LDT, travelers in Bangladesh emphasize more the reliable journey time, time required for travel, stop or station closer to destination, journey location and frequency of travel compared to other factors. On the other hand, flexible schedule, stop or station closer to the origin, availability of tickets, safety, comfortability, monthly household income, occupation, gender, travel costs and age of the respondent have less influence in choosing travel mode for LDT. Although the intercity trains are more preferable to intercity buses in terms of comfort and travel costs, buses are more preferred by the respondents in overall (see Figure 5). This is because these two factors contribute less in deciding on the travel mode in comparison to other factors. Hence, the intercity bus is the preferred mode of LDT over intercity train in Bangladesh, especially due to less reliable journey time, time required for travel, stop or station closer to destination, journey location and frequency of travel. However, it is to be kept in mind that flexible roads have been found to deteriorate early in Bangladesh [56-57], if such situation continues to degrade in the future, people's mode choice in the LDT might get changed.

## 5 Limitations of the study

One of the limitations of this study is that it only considered two modes of the long-distance travel, i.e., bus and train. There are two other modes of transportation available for long-distance travel in Bangladesh, i.e., airways and waterways. The railway network in Bangladesh covers approximately 2877.10 kilometers connecting 44 of the 64 districts, whereas only eight districts are connected by air and only a few districts in the Barishal division have waterways (launch) for long-distance travel. So, buses and trains represent most of the long-distance travel in Bangladesh, while the long-distance travel by airways and waterways can be considered as a future scope of the study. Besides, only machine learning models have been used to model the mode choice preferences. As an extension of this study, discrete choice modeling techniques can be used and compared to the performance of the machine learning models.

## 6 Conclusions

This study investigates travelers' alternative mode choice behavior between the intercity trains and intercity buses for the LDT. Data related to demographics, socioeconomic status of the respondents and various features of mode choice are collected from a questionnaire survey conducted on various groups of people in the capital city, Dhaka, in Bangladesh. Among the features considered for modeling travel mode choice, time required for travel, costs associated with travel, the proximity of origin or destination from stop or station, comfort, safety, reliability of journey time, availability of tickets and flexibility of schedule have been considered. Using the acquired data, several ML algorithms are used to predict the travel mode choice behavior. Considering the model accuracy and F1-score, the RF model outperformed all the others, with 95.31% accuracy and 0.95 F1-score. Further, the model has been optimized by tuning different hyper-parameters, which led to an unchanged accuracy but an increased out-of-bag accuracy of 93.46%. The feature importance score determined from the model revealed that reliable journey time, time required for travel, stop or station closer to destination, journey location and frequency of travel are the most critical features in forecasting travel mode choice.

**Nomenclature**

| | |
|---|---|
| AUC | Area Under the Curve |
| DT | Decision Tree |
| FP | False Positive |
| KNN | K-Nearest Neighbors |
| LDT | Long Distance Travel |
| ML | Machine Learning |
| MLP | Multi-Layer Perceptron |
| MNL | Multinomial Logit |
| NB | Naive Bayes |
| RBF | Radial Basis Functions |
| RF | Random Forest |
| ROC | Receiver Operating Characteristic |
| SVM | Support Vector Machine |
| TP | True Positive |
| UK | United Kingdom |
| USA | United States of America |
| XGB | Extreme Gradient Boosting |

**Declaration of competing interests**

The authors declare that they have no known competing financial interests or personal relationships that could have appeared to influence the work reported in this paper.

**Acknowledgments**

The authors of this paper would like to thank the Department of Civil Engineering, Daffodil International University, for the technical assistance in conducting this research.

**References**

[1] SPRUMONT, F., VITI, F., CARUSO, G., KONIG, A. Workplace relocation and mobility changes in a transnational metropolitan area: the case of the University of Luxembourg. *Transportation Research Procedia* [online]. 2014, **4**, p. 286-299. ISSN 2352-1465. Available from: https://doi.org/10.1016/j.trpro.2014.11.022

[2] ARBELAEZ, O. Modeling the choice of public and private bicycles in cities / Modelacion de la eleccion de la bicicleta publica y privada en ciudades (in Spanish). MSc. Thesis. Medellin: Department of Civil Engineering, Universidad Nacional de Colombia, 2015.

[3] BOCKER, L., VAN AMEN, P., HELBICH, M. Elderly travel frequencies and transport mode choices in greater Rotterdam, the Netherlands. *Transportation* [online]. 2016, **44**(4) p. 831-852. ISSN 0049-4488, eISSN 1572-9435. Available from: https://doi.org/10.1007/s11116-016-9680-z

[4] MANDOKI, P., LAKATOS, A. Quality evaluation of the long-distance bus and train transportation in Hungary. *Transportation Research Procedia* [online]. 2017, **27**, p. 365-372. ISSN 2352-1465. Available from: https://doi.org/10.1016/j.trpro.2017.12.086

[5] VEENEMAN, W. W., VAN DE VELDE, D. M., SCHIPHOLT, L. L. The value of bus and train: public values in public transport. In: European Transport Conference: proceedings. 2006. p. 18-20.

[6] KAMPF, R., GASPARIK, J., KUDLACKOVA, N. Application of different forms of transport in relation to the process of transport user value creation. *Periodica Polytechnica Transportation Engineering* [online]. 2012, **40**(2), p. 71-75. ISSN 0303-7800, eISSN 1587-3811. Available from: https://doi.org/10.3311/pp.tr.2012-2.05

[7] MCFADDEN, D. Conditional logit analysis of qualitative choice behavior. In: *Frontiers in Econometrics*. ZAREMBKA, P. (ed.). NY: Academic Press, 1973. ISBN 978-0127761503.

[8] CHENG, L., CHEN, X., DE VOS, J., LAI, X., WITLOX, F. Applying a random forest method approach to model travel mode choice behavior. *Travel Behaviour and Society* [online]. 2019, **14**, p. 1-10. ISSN 2214-367X. Available from: https://doi.org/10.1016/j.tbs.2018.09.002

[9] ZHAO, X., YAN, X., YU, A., VAN HENTENRYCK, P. Prediction and behavioral analysis of travel mode choice: A comparison of machine learning and logit models. *Travel Behaviour and Society* [online]. 2020, **20**, p. 22-35. ISSN 2214-367X. Available from: https://doi.org/10.1016/j.tbs.2020.02.003

[10] ZHAO, X., ZHOU, Z., YAN, X., VAN HENTENRYCK, P. Distilling black-box travel mode choice model for behavioral interpretation. ArXiv [online]. 2019, arXiv:1910.13930. Available from: https://doi.org/10.48550/arXiv.1910.13930

[11] LINDNER, A., PITOMBO, C. S., CUNHA, A. L. Estimating motorized travel mode choice using classifiers: an application for high-dimensional multicollinear data. *Travel Behaviour and Society* [online]. 2017, **6**, p. 100-109. eISSN 2214-367X. Available from: https://doi.org/10.1016/j.tbs.2016.08.003

[12] HAGENAUER, J., HELBICH, M. A comparative study of machine learning classifiers for modeling travel mode choice. *Expert Systems with Applications* [online]. 2017, **78**, p. 273-282. ISSN 0957-4174. Available from: https://doi.org/10.1016/j.eswa.2017.01.057

[13] GOLSHANI, N., SHABANPOUR, R., MAHMOUDIFARD, S. M., DERRIBLE, S., MOHAMMADIAN, A. Modeling travel mode and timing decisions: comparison of artificial neural networks and copula-based joint model. *Travel Behaviour and Society* [online]. 2018, **10**, p. 21-32. ISSN 2214-367X. Available from: https://doi.org/10.1016/j.tbs.2017.09.003

[14] CHEN, J., LI, S. Mode choice model for public transport with categorized latent variables. *Mathematical Problems in Engineering* [online]. 2017, **2017**, 7861945. ISSN 1024-123X, eISSN 1563-5147. Available from: https://doi.org/10.1155/2017/7861945

[15] ZHANG, R., YE, X., WANG, K., LI, D., ZHU, J. Development of commute mode choice model by integrating actively and passively collected travel data. *Sustainability* [online]. 2019, **11**(10), 2730. eISSN 2071-1050. Available from: https://doi.org/10.3390/su11102730

[16] VAN ACKER, V., KESSELS, R., PALHAZI CUERVO, D., LANNOO, S., WITLOX, F. Preferences for long-distance coach transport: evidence from a discrete choice experiment. *Transportation Research*

*Part A: Policy and Practice* [online]. 2020, **132**(C), p. 759-779. ISSN 0965-8564. Available from: https://doi.org/10.1016/j.tra.2019.11.028

[17] BROG, W., ERL, E., SAMMER, G., SCHULZE, B. Design and application of a travel survey for long-distance trips based on an international network of expertise - concept and methodology. In: 10th International Conference on Travel Behaviour Research: proceedings. 2003.

[18] Long-distance travel - Bureau of transportation statistics [online]. 2017. Available from: https://www.bts.gov/bts/archive/publications/highlights_of_the_2001_national_household_travel_survey/section_03

[19] BASTARIANTO, F. F., IRAWAN, M. Z., CHOUDHURY, C., PALMA, D., MUTHOHAR, I. A tour-based mode choice model for commuters in Indonesia. *Sustainability* [online]. 2019, **11**(3), 788. eISSN 2071-1050. Available from: https://doi.org/10.3390/su11030788

[20] WANG, Y., YAN, X., ZHOU, Y., XUE, Q. Influencing mechanism of potential factors on passengers' long-distance travel mode choices based on structural equation modeling. *Sustainability* [online]. 2017, **9**(11), 1943. eISSN 2071-1050. Available from: https://doi.org/10.3390/su9111943

[21] NAM, D., KIM, H., CHO, J., JAYAKRISHNAN, R. A model based on deep learning for predicting travel mode choice. In: 96th Annual Meeting Transportation Research Board: proceedings. 2017. p. 8-12.

[22] HASEGAWA, H., NAITO, T., ARIMURA, M., TAMURA, T. Modal choice analysis using ensemble learning methods (in Japanese). *Journal of Japan Society of Civil Engineering* [online], 2012, **68**(5), p. 773-780. eISSN 2185-6540. Available from: https://doi.org/10.2208/jscejipm.68.I_773

[23] ABDULJABBAR, R., DIA, H., LIYANAGE, S., BAGLOEE, S. Applications of artificial intelligence in transport: an overview. *Sustainability* [online]. 2019, **11**(1), 189. eISSN 2071-1050. Available from: https://doi.org/10.3390/su11010189

[24] BHAVSAR, P., SAFRO, I., BOUAYNAYA, N., POLIKAR, R., DERA, D. Machine learning in transportation data analytics. In: *Data analytics for intelligent transportation system* [online]. CHOWDHURY, M., APON, A., DEY, K. (eds.). Elsevier, 2017. ISBN 978-0-12-809715-1, p. 283-307. Available from: https://doi.org/10.1016/B978-0-12-809715-1.00012-2

[25] PULUGURTA, S., ARUN, A., ERRAMPALLI, M. Use of artificial intelligence for mode choice analysis and comparison with traditional multinomial logit model. *Procedia - Social and Behavioral Sciences* [online]. 2013, **104**, p. 583-592. ISSN 1877-0428. Available from: https://doi.org/10.1016/j.sbspro.2013.11.152

[26] TANG, L., XIONG, C., ZHANG, L. Decision tree method for modeling travel mode switching in a dynamic behavioral process. *Transportation Planning and Technology* [online]. 2015, **38**(3), p. 833-850. ISSN 0308-1060, eISSN 1029-0354. Available from: https://doi.org/10.1080/03081060.2015.1079385

[27] MOECKEL, R., FUSSELL, R., DONNELLY, R. Mode choice modeling for long-distance travel. *Transportation Letters* [online]. 2015, **7**(1), p. 35-46. ISSN 1942-7867, eISSN 1942-7875. Available from: https://doi.org/10.1179/1942787514y.0000000031

[28] SHEN, J. Latent class model or mixed logit model? A comparison by transport mode choice data. *Applied Economics* [online]. 2009, **41**(22), p. 2915-2924. ISSN 0003-6846, eISSN 1466-4283. Available from: https://doi.org/10.1080/00036840801964633

[29] DE BOK, M., COSTA, A., MELO, S., PALMA, V., FRIAS, R. Estimation of a mode choice model for long distance travel in Portugal. In: World Conference of Transport Research: proceedings. 2010.

[30] ROHR, C., DALY, A., PATRUNI, B., TSANG, F. The importance of frequency and destination choice effects in long-distance travel behaviour: what choice models can tell us. In: International Choice Modelling Conference: proceedings. 2009.

[31] MVA. The specification of the long distance travel model. Final project report. Rotterdam: Dutch Ministry of Transports and Public Works, 1985.

[32] DE JONG, G., GUNN, H. Recent evidence on car cost and time elasticities of travel demand in Europe. *Journal of Transport Economics and Policy (JTEP)* [online]. 2001, **35**(2), p. 137-160. eISSN 0022-5258.

[33] MANDEL, B, GAUDRY, M., ROTHENGATTER, W. A disaggregate Box-Cox logit mode choice model of intercity passenger travel in Germany and its implications for high-speed rail demand forecasts. *The Annals of Regional Science* [online]. 1997, **31**, p. 99-120. ISSN 0570-1864, eISSN 1432-0592. Available from: http://dx.doi.org/10.1007/s001680050041

[34] RAVE. Study of demand in the corridors of the high-speed rail network / Estudo da procura nos corredores da rede ferroviaria de alta velocidade (in Spanish). Study for high speed rail network / Study for rede ferroviaria de alta velocidade. Lisbon: AT Kearney, 2003.

[35] GASPARIK, J., MESKO, P., ZAHUMENSKA, Z. Methodology for tendering the performances in long distance rail passenger transport. *Periodica Polytechnica Transportation Engineering* [online]. 2019, **47**(1), p. 19-24. ISSN 0303-7800, eISSN 1587-3811. Available from: https://doi.org/10.3311/PPtr.11192

[36] LHERITIER, A., BOCAMAZO, M., DELAHAYE, T., ACUNA-AGOST, R. Airline itinerary choice modeling using machine learning. *Journal of Choice Modelling* [online]. 2018, **31**, p. 198-209. ISSN 1755-5345. Available from: https://doi.org/10.1016/j.jocm.2018.02.002

[37] BISHOP, CH. M. *Pattern recognition and machine learning*. Vol. 4. New York: Springer-Verlag, 2006. ISBN 978-1-4939-3843-8.

[38] MULLAINATHAN, S. SPIESS, J. Machine learning: an applied econometric approach. *Journal of Economic Perspectives* [online]. 2017, **31**(2), p. 87-106. ISSN 0895-3309, eISSN ISSN 1944-7965. Available from: https://doi.org/10.1257/jep.31.2.87

[39] WANG, F., ROSS, C. L. Machine learning travel mode choices: comparing the performance of an extreme gradient boosting model with a multinomial logit model. *Transportation Research Record* [online]. 2018, **2672**(47), p. 35-45. ISSN 0361-1981, eISSN 2169-4052. Available from: https://doi.org/10.1177/0361198118773556

[40] OMRANI, H. Predicting travel mode of individuals by machine learning. *Transportation Research Procedia* [online]. 2015, **10**, p. 840-849. ISSN 2352-1465. Available from: https://doi.org/10.1016/j.trpro.2015.09.037

[41] CHERCHI, E., CIRILLO, C. Validation and forecasts in models estimated from multiday travel survey. *Transportation Research Record* [online]. 2010, **2175**(1), p. 57-64. ISSN 0361-1981, eISSN 2169-4052. Available from: https://doi.org/10.3141/2175-07

[42] KARLAFTIS, M. G., VLAHOGIANNI, E. I. Statistical methods versus neural networks in transportation research: differences, similarities and some insights. *Transportation Research Part C: Emerging Technologies* [online]. 2011, **19**(3), p. 387-399. ISSN 0968-090X. Available from: https://doi.org/10.1016/j.trc.2010.10.004

[43] ATHEY, S. Beyond prediction: using big data for policy problems. *Science* [online]. 2017, **355**(6324), p. 483-485. ISSN 0036-8075. Available from: https://doi.org/10.1126/science.aal4321

[44] MOLNAR, C. *Interpretable machine learning: a guide for making black box models explainable* [online]. 2. ed. Independently published, 2022. ISBN 979-8411463330. Available from: https://christophm.github.io/interpretable-ml-book/

[45] DE PALMA, A., ROCHAT, D. Mode choices for trips to work in Geneva: an empirical analysis. *Journal of Transport Geography* [online]. 2000, **8**(1), p. 43-51. ISSN 0966-6923. Available from: https://doi.org/10.1016/s0966-6923(99)00026-5

[46] ASHALATHA, R., MANJU, V. S., ZACHARIA, A. B. Mode choice behavior of commuters in Thiruvananthapuram City. *Journal of Transportation Engineering* [online]. 2013, **139**(5), p. 494-502. ISSN 2473-2907, eISSN 2473-2893. Available from: https://doi.org/10.1061/(asce)te.1943-5436.0000533

[47] LINDLEY, D. V. Fiducial distributions and Bayes' theorem. *Journal of the Royal Statistical Society: Series B (Methodological)* [online]. 1958, **20**(1), p. 102-107. eISSN 1467-9868. Available from: https://doi.org/10.1111/j.2517-6161.1958.tb00278.x

[48] UDDIN, S., KHAN, A., HOSSAIN, M. E., MONI, M. A. Comparing different supervised machine learning algorithms for disease prediction. *BMC Medical Informatics and Decision Making* [online]. 2019, **19**(1), 281. ISSN 1472-6947. Available from: https://doi.org/10.1186/s12911-019-1004-8

[49] RISH, I. An empirical study of the naive Bayes classifier. In: Workshop on Empirical Methods in Artificial Intelligence IJCAI 2001: proceedings. 2001. p.41-46.

[50] QUINLAN, J. R. Induction of decision trees. *Machine Learning* [online]. 1986, **1**(1), p. 81-106. ISSN 0885-6125, eISSN 1573-0565. Available from: https://doi.org/10.1007/bf00116251

[51] BREIMAN, L. Random forests. *Machine Learning* [online]. 2001, **45**, p. 5-32. ISSN 0885-6125, eISSN 1573-0565. Available from: https://doi.org/10.1023/A:1010933404324

[52] JOACHIMS, T. Making large-scale SVM learning practical [online]. Technical report no. 1998,28. Dortmund: University Dortmund, 1998. ISSN 0943-4135. Available from: http://hdl.handle.net/10419/77178

[53] COVER, T., HART, P. Nearest neighbor pattern classification. *IEEE Transactions on Information Theory* [online]. 1967, **13**(1), p. 21-27. ISSN 0018-9448, eISSN 1557-9654. Available from: https://doi.org/10.1109/TIT.1967.1053964

[54] GRANDINI, M., BAGLI, E., VISANI, G. Metrics for multi-class classification: an overview. ArXiv [online]. 2020, abs/2008.05756. Available from: https://doi.org/10.48550/arXiv.2008.05756

[55] KANG, K., RYU, H. Predicting types of occupational accidents at construction sites in Korea using random forest model. *Safety Science* [online]. 2019, **120**, p. 226-236. ISSN 0925-7535. Available from: https://doi.org/10.1016/j.ssci.2019.06.034

[56] HAMIM, O. F., HOQUE, M. S. Prediction of pavement life of flexible pavements under the traffic loading conditions of Bangladesh. In: International Airfield and Highway Pavements Conference: proceedings [online]. 2019. ISBN 9780784482452. Available from: https://doi.org/10.1061/9780784482452.003

[57] HAMIM, O. F., ANINDA, S. S., HOQUE, M. S., HADIUZZAMAN, M. Suitability of pavement type for developing countries from an economic perspective using life cycle cost analysis. *International Journal of Pavement Research and Technology* [online]. 2021, **14**, p. 259-266. ISSN 1996-6814, eISSN 1997-1400. Available from: https://doi.org/10.1007/s42947-020-0107-z

# EVALUATION OF THE PARKING SYSTEM EFFICIENCY BASED ON THE JADWIZYN SETTLEMENT IN PILA IN THE LIGHT OF SUSTAINABLE DEVELOPMENT

**Piotr Gorzelańczyk *, Karol Matuszak**

Stanislaw Staszic State University of Applied Sciences in Pila, Pila, Poland

*E-mail of corresponding author: piotr.gorzelanczyk@ans.pila.pl

***Resume***

The aim of the article is to assess the efficiency of the parking system on the example of the Jadwizyn estate in Pila in the light of sustainable development. For this purpose, an organoleptic test of the use of the parking space was carried out for 7 consecutive days, at three different times of the day (morning, noon, evening) in December and January.

The conducted research has shown that the parking system in the analyzed estate is not effective for the community living in the estate and the sustainable development guidelines were not taken into account during its planning. In the discussed case, it is necessary to introduce changes to the estate's parking policy, for example by implementing new parking solutions in the form of parking automation or building a multi-level structure providing more parking spaces.

***Article info***

Received 22 March 2022
Accepted 2 August 2022
Online 20 September 2022

***Keywords:***

parking
parking system
housing estate
Pila
sustainable development

Available online: https://doi.org/10.26552/com.C.2022.4.A198-A215

ISSN 1335-4205 (print version)
ISSN 2585-7878 (online version)

## 1 Introduction and literature review

With the development of the automotive industry and the number of registered vehicles (Figure 1), the needs and expectations of the road infrastructure users also increased, especially those related to parking spaces [1]. The concept of a parking lot is understood as a place intended for parking cars [2]. More precisely, it is a place that allows one to park vehicles that are currently not in motion.

Sustainable development [4-5] is a concept and way of thinking in economics that assumes the level and quality of life at the level guaranteed by civilization. The idea of sustainable development is summarized and presented in the first sentence of the WCED report (also known as the "Brundtland Commission") of 1987 - "Our Common Future". Sustainable development is development that meets the needs of the present without compromising the capabilities of the future. generations to meet their own needs.

Sustainable development supports, protects and restores the health and integrity of the Earth's ecosystem without jeopardizing the ability to meet the needs of future generations [6-7]. It illustrates economic growth that leads to social cohesion and an increase in the value of the natural environment [8-9] and sustainable business as capable of "prospering indefinitely" [10]. The concept of sustainable development [11] covers everyone and everything - it concerns various aspects of human activity and human relations with the environment [12].

A sustainable urban transport system is essential for the proper development of a society and parking is an important element of this. The literature on sustainable parking management systems is extensive and mainly focuses on Park-and-Ride systems [13], planning and use of parklets [14] and the increasingly used Intelligent Transport Systems (ITS) [15-16]. In the case of car parks, the aim is to use them as efficiently as possible [17], with the possibility of introducing new solutions such as shared parking. This idea leads to the most efficient use of parking spaces. The allocation of parking spaces [18-19], the use of shared parking [20-22] and the design of a shared parking platform [23-24] have received much attention in the literature.

Over the years, the approach to parking policy planning and the perception of parking systems in cities has changed. Initially, it was based on transport infrastructure, striving for its greatest functionality, fluidity and capacity. Furthermore, city officials have started to see other important aspects - how existing

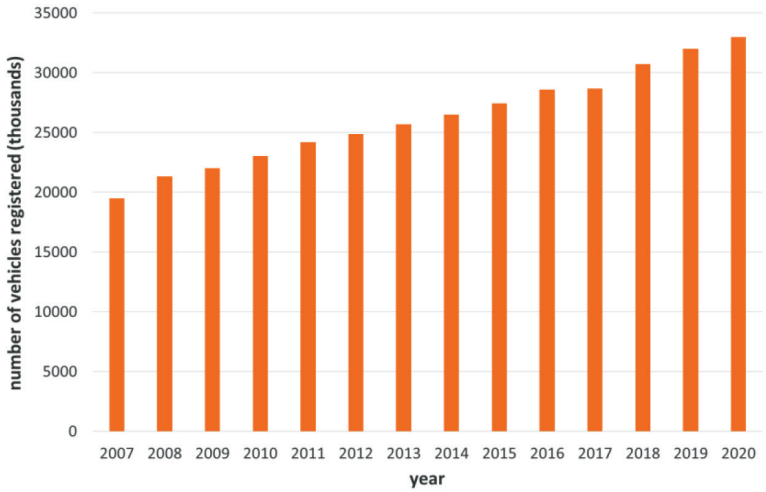


***Figure 1*** *The number of vehicles registered in Poland in 2007-2019 [3]*


***Figure 2*** *Location of the town of Pila on the map of Poland [28]*

transport systems and road infrastructure affect the quality of life of city dwellers, are they functional for people with disabilities and businesses and how they affect the environment. To determine whether a city's transport policy is sustainable, it must meet the different conditions [25].

Therefore, it can be concluded that an efficiently operating road infrastructure, which can be described as sustainable, encourages to quit of the most popular means of transport, which is a passenger car and encourages the use of public transport. This, in consequence, is expected to result in a healthier life for the inhabitants and an increase in the cleanliness of cities [26].

There are studies in the literature on urban engineering that confirm that the use of sustainable urban transport has a positive impact on development of cities and satisfaction of their inhabitants. An example is the transport assessment study carried out in the city of Czestochowa, Poland, which implements subsequent steps to improve the road infrastructure in a sustainable manner, encouraging the use of public urban transport. The respondents of the presented study emphasized that the advantages affecting the superiority of passenger car transport over the city transport are greater comfort, destination and shorter travel time. Nevertheless, the respondents were not clearly negative in the context of public transport, which may lead to conclusions that specific changes in the structure and functioning of this mode of transport could change their opinions and encourage them to use it in the future.

The problems with the road capacity visible on Polish roads allow to conclude that the comfort of traveling by individual passenger transport is still greater than traveling by public means of transport, therefore most road infrastructure users still prefer to travel in this way [26].

In terms of the sustainable development of urban transport, an important element is the parking control system. It includes parking solutions that facilitate the management of available parking spaces, e.g. make it easier for the driver to find a free parking space. Such systems significantly contribute to the more effective use of the parking lot, reducing the time for the driver to find a free space, which is particularly problematic in places with a large parking lot.

## 2 Materials and methods

The city of Pila is located in the northern part of the Wielkopolska Province (Figure 2) on the border with the Zachodniopomorskie Province. In 2020, Pila

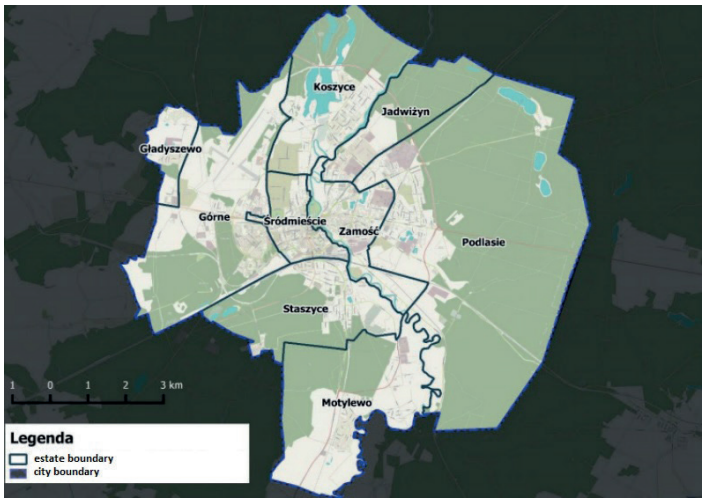


***Figure 3*** *Map of the town of Pila with a breakdown by housing estates [31]*

was inhabited by 69.411 inhabitants, which is about 5.000 less than in 2002 when the population was 75.197 [27]. Thanks to the data provided by the Pila City Hall, a downward trend in the number of inhabitants of the city can be observed.

The city covers an area of 103 km$^2$ and the population density is 674 people / km$^2$ [29]. In 2011, the city consisted of nine districts, the largest was and still is Podlasie (Figure 3). Other districts are: Gorne, Koszyce, Srodmiescie, Gladyszewo, Zamoscie, Staszyce, Motylewo and Jadwizyn, of which auxiliary units of the communes of Jadwizyn, Srodmiescie and Zamosc housing estates were abolished in 2011 [30].

The concept of the city is based on maintaining sustainable development by improving the economy, infrastructure and educational and recreational offer. Pila is the leader of investment attractiveness (Forbes 2007/2008 ranking), it is the most business-friendly city (in 2012, 1st place in the Wielkopolska and the 12th in Poland according to the Newsweek weekly), 16th city in the country in the national ranking of the Self-Government of Sustainable Development conducted under the aegis of the Foundation of the Promotional Emblem TERAZ POLSKA [32].

The Smart City idea is being implemented in Pila, which involves the use of information and communication technologies supporting, among others social integration and sustainable development. According to the development strategy of the city of Pila until 2035, it was planned to modernize car parks in the city, as well as to build a park & ride car park with places for disabled people and nanny with children, kiss & ride parking spaces and a parking lot for bicycles and to build parking information systems. An information and promotion campaign is also planned about the built infrastructure, its values and possibilities of using it, as part of the promotion of sustainable mobility [33].

The Jadwizyn estate (Figure 3) was established pursuant to two resolutions of August 29 and 31, 2006. The estate was also granted the statute at that time. Nevertheless, the resolutions lost their force due to the new resolution No. XIV / 195/11 introduced on November 29, 2011, which called for the abolition of the auxiliary unit of the Jadwizyn estate. The city authorities argued their move with the residents' lack of interest in initiatives aimed at developing the individual. The inhabitants of the estate showed a lack of support for local government bodies in organizational matters, which resulted in the abolition of the estate in its legal form [34].

Nevertheless, the estate still exists in the social sphere of inhabitants and the city authorities of Pila continue to keep statistics for the indicated area, for example regarding the number of inhabitants. The boundaries of the estate indicated on the city map are still valid as the Jadwizyn estate has not been liquidated in the spatial and functional zone, but has only been deprived of its administrative unit.

According to the data published on the website of the Pila City Hall, 4.564 people lived in Jadwizyn in 2017. Its area is approximately 566.44 ha. This space is dominated by multi-storey residential buildings, although there are detached buildings at Jana and Jedrzeja Sniadeckich Streets. Additionally, also in the south-west part of the estate, which includes ul. Dabrowskiego (from number 92 to 150), ul. Grazyny, ul. Jagiellonska, ul. Jozefa Bema, ul. Kwidzynska, ul. Malgorzaty, ul. Olsztynska, pl. Jagielly, ul. Zelazna, houses only free-standing buildings.

The second, frequently used intersection in the estate is the intersection of Sniadeckich Street with Laczna Street located next to the education building, but no major problems related to the traffic flow have been observed there.

The estate has 63 multi-storey buildings and a total of 899 parking spaces. In the context of the diversity of parking systems, the estate can be described as diverse. There are systems such as private underground car parks and garage spaces on it

At the Jadwizyn estate, one would not meet the

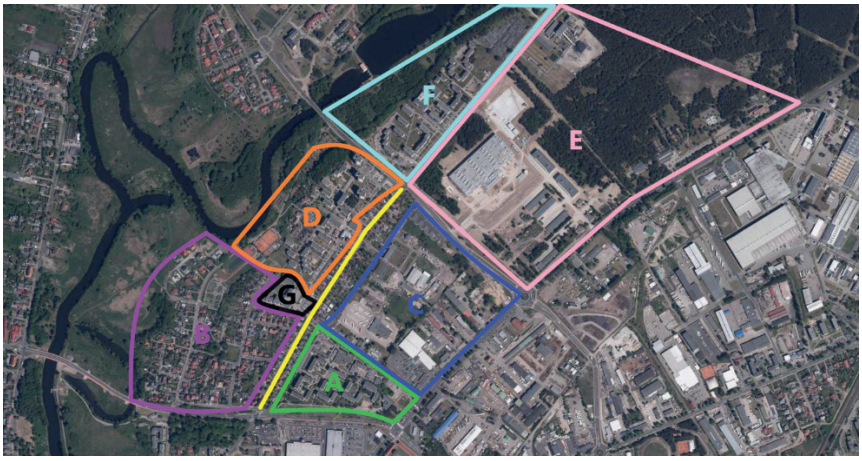


***Figure 4*** *The Jadwizyn estate divided into 8 parking zones [35]*

most modern parking solutions that operate in a fully automated manner, but it can be seen that along with newer buildings, among others, underground car parks with a view to making the best use of parking spaces.

## 3 Research results

The purpose of the research was to analyze the effectiveness of the parking system in the Jadwizyn estate in Pila in the light of sustainable development. The subject of the research were car parks located in the estate at the following streets: Laczna, Dabrowskiego, Grazyny, Jagiellonska, Jozefa Bema, Kwidzynska, Malgorzata, Olsztynska, Jagiely, Zelazna, Krolowej Jadwigi, Sniadeckich and at Aleja Powstancow Wielkopolskich (Figure 4) and the volume flow of vehicles occupying parking spaces at specified intervals, in such a way as to best check the actual efficiency of the currently functioning parking system solutions. Consequently, the research aimed to present a proposal to improve the directions of development of local road infrastructure.

With the help of the presented scientific literature on the subject, it can be noticed the existence of problems related to the failure to adapt to the needs of residential communities regarding parking infrastructure. It is about too large distances between residential buildings and the grouping of parking spaces. Another problem is the outdated road infrastructure, which probably stems from an inaccurate forecast of the number of cars owned by a selected housing estate. As a result, the number of places in a given grouping often turns out to be insufficient to meet the needs of the inhabitants. Moreover, the car parks do not have parking aids, which is another problematic issue. There are also doubts relating to safety issues, such as blocking access roads by incorrectly parked vehicles, as well as mismatching the distance between parking spaces and other objects not related to the parking infrastructure, such as trees, stones or poles, which consequently pose a threat to parking spaces, drivers and other infrastructure users.

Based on the above observations, obtained thanks to the presented scientific literature and for the needs of the research, a hypothesis is formulated that the parking system operating in the Jadwizyn estate in Pila

***Table 1*** *The structures of separated zones in the Jadwizyn estate of 30.12.2020 - part 1 [31]*

| Street name | Zone | Age range | Women | Men | Number of multi-family buildings | Number of single-family buildings | Total number of parking spaces |
|---|---|---|---|---|---|---|---|
| Laczna street | A | 0-18 | 61 | 88 | 17 | 0 | 200 |
| | | 19-55 | 198 | 229 | | | |
| | | 56-63 | 58 | 31 | | | |
| | | 64 and above | 167 | 124 | | | |
| | | Sum | 956 | | | | |
| Dabrowskiego street, Grazyny street, Jagiellonska street, Jozefa Bema, Kwidzynska street, Malgorzaty street, Olsztynska square, Jagielly street, Zelazna street | B | 0-18 | 51 | 50 | 0 | 160 | 4 |
| | | 19-55 | 135 | 184 | | | |
| | | 56-63 | 35 | 27 | | | |
| | | 64 and above | 57 | 54 | | | |
| | | Sum | 593 | | | | |

***Table 2*** *The structures of separated zones in the Jadwizyn estate of 30.12.2020 - part 2 [31]*

| Street name | Zone | Age range | Women | Men | Number of multi-family buildings | Number of single-family buildings | Total number of parking spaces |
|---|---|---|---|---|---|---|---|
| Powstancow Wielkopolskich Avenue to Lukasiewicz roundabout, Przeswit street | C | 0-18 | 0 | 0 | 0 | 0 | 0 |
| | | 19-55 | 0 | 0 | | | |
| | | 56-63 | 0 | 0 | | | |
| | | 64 and above | 0 | 0 | | | |
| | | Sum | 0 | | | | |
| Krolowej Jadwigi street | D | 0-18 | 109 | 128 | 24 | 16 | 273 |
| | | 19-55 | 309 | 321 | | | |
| | | 56-63 | 121 | 65 | | | |
| | | 64 and above | 228 | 185 | | | |
| | | Sum | 1466 | | | | |
| Aleja Powstancow Wielkopolskie from the Lukasiewicz roundabout to the height of the production plant, Philips street | E | 0-18 | 0 | 0 | 0 | 0 | 19 |
| | | 19-55 | 0 | 0 | | | |
| | | 56-63 | 0 | 0 | | | |
| | | 64 and above | 0 | 0 | | | |
| | | Sum | 0 | | | | |
| Sniadeckich street | F | 0-18 | 82 | 97 | 22 | 0 | 337 |
| | | 19-55 | 226 | 235 | | | |
| | | 56-63 | 72 | 70 | | | |
| | | 64 and above | 112 | 102 | | | |
| | | Sum | 996 | | | | |
| School at Krolowej Jadwigi street | G | 0-18 | 0 | 0 | 0 | 0 | 40 |
| | | 19-55 | 0 | 0 | | | |
| | | 56-63 | 0 | 0 | | | |
| | | 64 and above | 0 | 0 | | | |
| | | Sum | 0 | | | | |
| Sniadeckich street with buildings along the street | H | 0-18 | 32 | 38 | 0 | 69 | 0 |
| | | 19-55 | 88 | 91 | | | |
| | | 56-63 | 28 | 27 | | | |
| | | 64 and above | 44 | 39 | | | |
| | | Sum | 387 | | | | |
| Sum | | | 2932 | | 63 | 245 | 873 |

is ineffective in relation to the needs of its residents.

The study consisted of observation of the parking infrastructure in the Jadwizyn estate, divided into 8 parking zones, shown in Figure 4. The individual zones cover the following streets:

- Zone A - ul. Laczna.
- Zone B - ul. Dabrowskiego (from number 92 to 150), ul. Grazyny, ul. Jagiellonian. ul. Jozefa Bemq, ul. Kwidzynska, ul. Malgorzaty, ul. Olsztynska, pl. Jagielly, ul. Zelazna.
- Zone C - Aleja Powstancow Wielkopolskich to the Lukasiewicza roundabout, ul. Przeswit.
- Zone D - ul. Krolowej Jadwigi.
- Zone E - Aleja Powstancow Wielkopolskich from the Lukasiewicza roundabout to the height of the Philips production plant, ul. Frits Philips.
- Zone F - ul. Sniadeckich covering the northern zone of the estate, which is characterized by multi-family buildings.
- Zone G - includes a car park adjacent to the school

at ul. Krolowej Jadwigi.

- Zone H - runs through the main street of the estate (Sniadeckich Street), which in this part is characterized by single-family houses.

The research was performed in the periods from November 30 to December 6, 2020 and January 11 to 17, 2021. Each of them lasted 7 days in 3 time intervals: 6.00-8.00, 14.00-16.00 and 21.00-23.00. Measurements made in both dates are characterized by taking into account the following parameters for each zone: total number of parking spaces, the average number of occupied and vacant spaces, including the number of spaces for disabled people, the number of cars parked incorrectly, the number of multi-family and single-family buildings and the number of residents. Data from the Pila City Hall on 30/12/2020 [31] obtained for the purposes of this article, regarding the structures in individual zones, are presented in Tables 1 and 2.

The studied area of the Jadwizyn estate is inhabited by 2.932 residents in 63 multi-family buildings and 245 single-family buildings, which include 873 parking spaces. In order to facilitate research, the estate has been divided into 8 zones: A-H. The description of the zones can be found later in the article. The indicator method [36] was used to analyze the neighbourhood parking system. By default, it adopts three criteria, however, due to the lack of access to restricted parking zones, the subject criterion, which uses the restricted parking zone share index, was not taken into account. Therefore, two criteria were used: subjective and functional, presented in Table 3 and were calculated based on the data presented in Tables 1 and 2. The parking intensity indicator expresses the ratio of the number of parked vehicles to the total number of parking spaces as a percentage and represents the total degree of occupied parking spaces for the examined area. The parking correctness index is also expressed as a percentage, it is the ratio of the number of incorrectly parked vehicles to the number of parked vehicles. As improperly parked cars are understood all the vehicles in the area of a given test that were left in a manner that deviates from the correct one in a given system, e.g. in a forbidden place, hindering pedestrian traffic, green areas or outside the designated parking stand.

In Table 4 the subjective criterion was presented along with the indicator of the number of parking spaces per 100 inhabitants for each zone. A zero result in zones C and H results from the lack of parking spaces and a zero result for zones E and G due to the zero number of inhabitants.

Moreover, the method of direct systematic observation was adopted in the study [36]. The task was to observe the phenomenon of how residents leave their cars at designated parking spaces, in order to notice the relationship between their behaviour, the functionality of existing parking lots in relation to the needs of residents and the effectiveness of parking systems.

The first zone is inhabited by 956 residents in 17 multi-family buildings with 200 parking spaces and 67 private garages. The zone is presented in Figure 5.

In Table 5 is shown the parking intensity and correctness indicators in zone A for the 1st and 2nd measurement period. The number of parking spaces for the first indicator on individual days at three different times of the day was presented and the correctness of parked vehicles was presented, which means that on November 30, in the evening hours, the number of incorrectly parked vehicles was 5.5% of the total number of parking spaces, i.e. 10 cars in this case. For poorly parked vehicles, cases were counted that took places outside the designated parking spaces, e.g. in a prohibited place. It was observed that some vehicles blocked the access to the dumpster shelters and were left in forbidden places, thus making it difficult for, for example, emergency services to access individual

***Table 3*** *Criteria and indicators for the evaluation of the estate parking system [36]*

| Criterion | Name | Formula |
|---|---|---|
| Subjective | The indicator of the number of parking spaces per 100 inhabitants [place / 100 inhabitants] | $W_{B2} = \frac{M_C}{U_C} * 100$ |
| Functional | Parking intensity indicator [%] | $W_{C1} = \frac{P_C}{M_C} * 100$ |
| | Parking correctness indicator [%] | $W_{C2} = \frac{P_N}{P_C} * 100$ |

$M_C$ - number of parking spaces,

$U_C$ - number of residents,

$P_C$ - number of parked vehicles,

$P_N$ - number of vehicles parked incorrectly.

***Table 4*** *Indicator of the number of parking spaces per 100 inhabitants, divided into zones*

| Indicator | Zone | | | | | | | |
|---|---|---|---|---|---|---|---|---|
| | A | B | C | D | E | F | G | H |
| $W_{B2}$ [1 place for 100 people] | 20.9 | 0.7 | 0 | 18.6 | 0 | 33.8 | 0 | 0 |

***Figure 5*** *Zone A with marked parking spaces [35]*

***Table 5*** *Indicators of parking intensity and correctness for zone A*

| First measurement | | | | | | | | | |
|---|---|---|---|---|---|---|---|---|---|
| Indicator [%] | Time | 30.Nov | 01.Dec | 02. Dec | 03. Dec | 04. Dec | 05. Dec | 06. Dec | Average |
| $W_{c1}$ | 06.00-08.00 | 67.5 | 60.5 | 64.5 | 63 | 66 | 82.5 | 85 | 69.9 |
| $W_{c2}$ | | 3 | 0.8 | 1.6 | 3.2 | 2.3 | 1.8 | 2.4 | 2.1 |
| $W_{c1}$ | 14.00-16.00 | 71 | 77.5 | 89 | 81.5 | 86.5 | 84.5 | 84 | 82 |
| $W_{c2}$ | | 0.7 | 2.6 | 2.8 | 1.8 | 1.2 | 3 | 3 | 2.2 |
| $W_{c1}$ | 21.00-23.00 | 90.5 | 94 | 95.5 | 92 | 93 | 94.5 | 96.5 | 93.7 |
| $W_{c2}$ | | 5.5 | 6.9 | 4.2 | 3.8 | 3.2 | 2.1 | 4.7 | 4.3 |
| Second measurement | | | | | | | | | |
| Indicator [%] | Time | 11.Jan | 12.Jan | 13.Jan | 14.Jan | 15.Jan | 16.Jan | 17.Jan | Average |
| $W_{c1}$ | 06.00-08.00 | 82.5 | 79 | 77.5 | 76.5 | 75.5 | 80 | 83.5 | 79.2 |
| $W_{c2}$ | | 5.5 | 7.3 | 4.8 | 7.9 | 7.3 | 6.7 | 7.9 | 6.8 |
| $W_{c1}$ | 14.00-16.00 | 92.5 | 89.5 | 88 | 90.5 | 86.5 | 88.5 | 89.5 | 89.3 |
| $W_{c2}$ | | 6.7 | 6.1 | 6.1 | 9.7 | 8.5 | 6.1 | 8.5 | 7.4 |
| $W_{c1}$ | 21.00-23.00 | 94 | 91.5 | 94.5 | 94 | 92 | 93.5 | 96 | 93.6 |
| $W_{c2}$ | | 7.9 | 8.5 | 7.3 | 11.5 | 9.1 | 8.5 | 10.9 | 9.1 |

buildings. The last column shows the average for a given time of day and indicator. In the second period of the study, an increase in the average intensity in the morning and afternoon hours, as well as a similar result for the evening hours was noticed.

Development of the zone B consists of 160 single-family buildings inhabited by 593 people. Due to the single-family development of the zone, which distinguishes this part of the estate from the rest, the number of parking spaces is limited to 4, located next to the grocery store. The boundaries of zone B are set out in Figure 6.

Table 6 shows the traffic intensity index for the zone B for the 1st and 2nd measurements. Increased use of parking spaces in the afternoon by store customers has been noticed. Incorrectly parked vehicles were not observed. During the study, it was noticed that residents leave their cars in private parking lots within the property. There are no designated parking spaces for disabled people in this zone and no incorrect parking has been observed. Depending on the time of day, the average number of occupied parking spaces varies from 1 to 2. During the research on the second date, there were no badly parked vehicles and the highest intensity occurred in the afternoon. Comparing the results of the measurements, a minimal increase in parking space in the second period was noticed.

Zone C is the service and retail part of the estate (Figure 7), which consists of the IBI shopping mall, MZK Pila bus depot, car wash, Altvater garbage dump and small local businesses. In this part, there is one parking system with 194 parking spaces, which belongs

***Figure 6*** *Zone B with marked parking spaces [35]*

***Table 6*** *Parking intensity and correctness indicator for zone B*

| First measurement | | | | | | | | | |
|---|---|---|---|---|---|---|---|---|---|
| Indicator [%] | Time | 30.Nov | 01.Dec | 02. Dec | 03. Dec | 04. Dec | 05. Dec | 06. Dec | Average |
| $W_{c1}$ | 06.00-08.00 | 25 | 25 | 25 | 25 | 25 | 25 | 0 | 21.4 |
| $W_{c2}$ | | - | - | - | - | - | - | - | - |
| $W_{c1}$ | 14.00-16.00 | 50 | 25 | 100 | 25 | 75 | 25 | 0 | 42.9 |
| $W_{c2}$ | | - | - | - | - | - | - | - | - |
| $W_{c1}$ | 21.00-23.00 | 25 | 75 | 25 | 25 | 50 | 50 | 0 | 35.7 |
| $W_{c2}$ | | - | - | - | - | - | - | - | - |
| Second measurement | | | | | | | | | |
| Indicator [%] | Time | 11.Jan | 12.Jan | 13.Jan | 14.Jan | 15.Jan | 16.Jan | 17.Jan | Average |
| $W_{c1}$ | 06.00-08.00 | 25 | 25 | 0 | 25 | 25 | 50 | 25 | 25 |
| $W_{c2}$ | | - | - | - | - | - | - | - | - |
| $W_{c1}$ | 14.00-16.00 | 25 | 75 | 50 | 25 | 50 | 50 | 50 | 46.4 |
| $W_{c2}$ | | - | - | - | - | - | - | - | - |
| $W_{c1}$ | 21.00-23.00 | 0 | 25 | 50 | 50 | 50 | 50 | 50 | 39.3 |
| $W_{c2}$ | | - | - | - | - | - | - | - | - |

to a shopping mall, but it was not included in the study, because it is largely used by residents of other parts of the city and its use is different than in residential areas. An interesting tendency of owners of vehicles from zone A was noticed to leave them outside the designated positions, in the IBI gallery, especially in the place bordering zone A.

Due to the lack of parking spaces, the purpose of which is to leave cars by residents while they are in their place of residence, the test results for the entire zone C have not been prepared as a vehicle parked incorrectly, because they did not occupy the designated positions (Table 7). Based on the presented results, it can be concluded that in the morning and evening hours there is the largest number of incorrectly parked vehicles by the inhabitants of Zone A.

The zone D is inhabited by 1.466 people. The vast majority of zones are the multi-family buildings, the number of which is 26 (Figure 8). With regard to the single-family housing, it was calculated that there are 16

***Figure 7*** *Zone C [35]*

***Table 7*** *Average of incorrectly parked vehicles at particular times of the day*

| First measurement | | | | | | | | |
|---|---|---|---|---|---|---|---|---|
| Time/Data | 30.Nov | 01.Dec | 02. Dec | 03. Dec | 04. Dec | 05. Dec | 06. Dec | Average |
| 6:00-8:00 | 2 | 3 | 3 | 2 | 1 | 3 | 4 | 2.57 |
| 14:00-16:00 | 0 | 1 | 2 | 2 | 2 | 2 | 3 | 1.71 |
| 21:00-23:00 | 5 | 4 | 4 | 4 | 6 | 5 | 5 | 4.71 |
| Second measurement | | | | | | | | |
| Time/Data | 11.Jan | 12.Jan | 13.Jan | 14.Jan | 15.Jan | 16.Jan | 17.Jan | Average |
| 6:00-8:00 | 1 | 2 | 3 | 3 | 3 | 2 | 3 | 2.43 |
| 14:00-16:00 | 2 | 2 | 0 | 1 | 2 | 1 | 3 | 1.57 |
| 21:00-23:00 | 6 | 5 | 5 | 3 | 4 | 4 | 4 | 4.43 |

buildings of this type in the zone. There are 273 parking spaces in this zone. In this part of the estate there is one local grocery store with 8 parking spaces. There is a church near the grocery store, but it does not have a dedicated parking lot. There are also single garage car parks in the zone, of which there are 55 in total.

A large number of incorrectly parked cars took place on sidewalks, green belts and places with no parking. In the evening hours, one can observe significant difficulties related to the movement of the vehicle in the designated zone, which is related to incorrect parking, presented by the parking correctness indicator in Table 8. It shows that on November 30, in the evening hours, the number of poorly parked vehicles was 14.6% of the number of occupied parking spaces. In this case, it is nearly 40 vehicles parked in prohibited places. This could be due to the start of the weekend and the arrival of more people at home. The high parking intensity index occurs for all the test hours, while the highest result can be observed in the evening hours, along with the highest parking correctness index.

There are no residential buildings in zone E. There are a facility of the military unit and the Municipal Heat Engineering. These centers have 6 and 13 parking spaces, respectively, which are probably used only by employees of the centers (Figure 9). It is worth noting that there are no dedicated parking spaces for disabled people, despite the fact that the car parks are located near two workplaces.

In Table 9 the parking intensity index for zone E was taken into account together with the average for each of the three times of the day. Due to the lack of incorrectly parked vehicles, the correctness index was not calculated. The discussed zone is characterized by the highest parking intensity in the morning, probably due to the hours in which employees of nearby workplaces work.

The zone F (Figure 10) includes only multi-family residential buildings. Their number is 22. There are 337 parking places for this number of buildings. Due to the newer housing development of two buildings, they also have underground garages for use by residents. Underground garage car parks are available only to people who have them, which made it impossible to take them into account in the study. There are also 180 single garage car parks in this zone, which are monitored and entry to their area is prohibited, which is preceded by a no-entry sign, excluding people with garage spaces.

***Figure 8*** *Zone D with marked parking spaces [35]*

***Table 8*** *Indicator of intensity and correctness of parking for zone D*

| First measurement | | | | | | | | | |
|---|---|---|---|---|---|---|---|---|---|
| Indicator [%] | Time | 30.Nov | 01.Dec | 02. Dec | 03. Dec | 04. Dec | 05. Dec | 06. Dec | Average |
| $W_{c1}$ | 06.00-08.00 | 63.4 | 60.8 | 66.7 | 62.3 | 61.5 | 80.2 | 84.6 | 68.5 |
| $W_{c2}$ | | 12.7 | 10.2 | 7.7 | 9.4 | 8.9 | 7.3 | 7.8 | 9.2 |
| $W_{c1}$ | 14.00-16.00 | 87.9 | 90.1 | 84.6 | 93.4 | 85.7 | 85.7 | 90.5 | 88.3 |
| $W_{c2}$ | | 10.8 | 9.8 | 12.1 | 8.2 | 10.3 | 11.5 | 8.1 | 10.1 |
| $W_{c1}$ | 21.00-23.00 | 95.2 | 94.9 | 97.1 | 94.5 | 96.3 | 97.1 | 99.6 | 96.4 |
| $W_{c2}$] | | 14.6 | 8.5 | 11.3 | 14 | 10.6 | 12.1 | 12.9 | 12 |
| Second measurement | | | | | | | | | |
| Indicator [%] | Time | 11.Jan | 12.Jan | 13.Jan | 14.Jan | 15.Jan | 16.Jan | 17.Jan | Average |
| $W_{c1}$ | 06.00-08.00 | 79.9 | 75.8 | 72.9 | 79.9 | 82.1 | 76.9 | 76.2 | 77.7 |
| $W_{c2}$ | | 11 | 8.2 | 12.1 | 6 | 8.5 | 10.5 | 9.1 | 9.3 |
| $W_{c1}$ | 14.00-16.00 | 88.3 | 90.5 | 89 | 84.2 | 88.3 | 86.8 | 90.5 | 88.2 |
| $W_{c2}$ | | 5.8 | 10.5 | 11.5 | 10 | 11.2 | 14.8 | 10.9 | 10.7 |
| $W_{c1}$ | 21.00-23.00 | 92.7 | 91.2 | 93.8 | 90.8 | 94.5 | 96 | 97.1 | 93.7 |
| $W_{c2}$ | | 12.6 | 12.9 | 10.2 | 10.9 | 12 | 15.6 | 13.6 | 12.5 |

The indicators of the occupied parking spaces intensity and the correctness of parked vehicles for zone F are presented in Table 10, showing the variable number of cars on different days, taking into account three tests during the day. The highest number of parked vehicles was recorded in the evening hours; however, it is worth noting that the indicator in the afternoon hours is also high for both analyzed periods of time. Comparing the test results, an increase in the index was noted in the morning and evening hours and a slight decrease in the evening hours for the second period of the study.

Zone G is a part of the estate (Figure 11), where the education building is located, "Queen Jadwiga". The building includes a parking lot with 43 parking spaces. The main assumption is that the car park is to be used by the employees of the facility to park vehicles during their work, as well as for parents who take their children to school or come to meetings with teachers. It is worth noting that during the study, the school institution conducted remote classes for its students, so it was not fully used by their parents and other people.

In Table 11, the intensity index in zone G was marked, the parking correctness index was not included, because during the tests, no irregularities related to leaving the vehicles were observed and the highest intensity of parking was recorded in the evening hours in both cases. Comparing the research results, it can be stated that for each time of the day an increase in

***Figure 9*** *Zone E with marked parking spaces [35]*

***Table 9*** *Indicator of intensity and correctness of parking for zone E*

| First measurement | | | | | | | | | |
|---|---|---|---|---|---|---|---|---|---|
| Indicator [%] | Time | 30.Nov | 01.Dec | 02. Dec | 03. Dec | 04. Dec | 05. Dec | 06. Dec | Average |
| $W_{c1}$ | 06.00-08.00 | 63.2 | 63.2 | 73.7 | 63.2 | 57.9 | 26.3 | 21.1 | 52.6 |
| $W_{c2}$ | | - | - | - | - | - | - | - | - |
| $W_{c1}$ | 14.00-16.00 | 21.1 | 26.3 | 42.1 | 31.6 | 26.3 | 15.8 | 10.5 | 24.8 |
| $W_{c2}$ | | - | - | - | - | - | - | - | - |
| $W_{c1}$ ] | 21.00-23.00 | 5.3 | 15.8 | 15.8 | 26.3 | 26.3 | 15.8 | 0 | 15 |
| $W_{c2}$ | | - | - | - | - | - | - | - | - |
| Second measurement | | | | | | | | | |
| Indicator [%] | Time | 11.Jan | 12.Jan | 13.Jan | 14.Jan | 15.Jan | 16.Jan | 17.Jan | Average |
| $W_{c1}$ | 06.00-08.00 | 47.4 | 68.4 | 57.9 | 57.9 | 68.4 | 63.2 | 52.6 | 59.4 |
| $W_{c2}$ | | - | - | - | - | - | - | - | - |
| $W_{c1}$ | 14.00-16.00 | 15.8 | 21.1 | 31.6 | 26.3 | 21.1 | 5.3 | 15.8 | 19.5 |
| $W_{c2}$ | | - | - | - | - | - | - | - | - |
| $W_{c1}$ | 21.00-23.00 | 10.5 | 10.5 | 10.5 | 5.3 | 10.5 | 15.8 | 5.3 | 9.8 |
| $W_{c2}$ | | - | - | - | - | - | - | - | - |

parking intensity was recorded in the second research period.

The zone H was separated for the purposes of the study (Figure 12) in order to separate the residential buildings belonging to it from other zones, because the adjacent single-family houses are directed towards the main Sniadeckich Street starting from zones A and B and continuing to the end of zones F and E, adjacent to each of the zones described above. The division is aimed at increasing the correctness of the research by subtracting the number of inhabitants of zone H from the inhabitants of other zones, because they park only on their properties, the entrance to which is from the main street. The number of buildings per zone is 69.

For the H zone, no table was prepared containing data from the research carried out from 30/11/2020 to 6/12/2020, because the zone did not have any parking spaces and the residents of this zone parked their vehicles on their properties with single-family houses.

The conducted research was aimed at assessing the effectiveness of the parking system at the Jadwizyn estate in Pila in the light of sustainable development. At the very beginning, it is worth noting that the study was carried out during the SARS-CoV-2 coronavirus pandemic, which significantly limited the movement of the population since the introduction of the epidemic and preventive measures limiting the spread of the virus. The situation could have contributed to an increase in the intensity of the use of parking lots due to the transfer of many works from stationary to remote mode (the so-called home office) and due to the limitation or closure of some workplaces, or staying in home quarantine in accordance with the government's recommendations. Therefore, the tests in the first period were carried out on November 30, 2020 after lifting some restrictions, including opening of shopping malls, however operating under the sanitary regime limiting the maximum number of customers.

***Figure 10*** *Zone F with marked parking spaces [35]*

***Table 10*** *Indicator of intensity and correctness of parking for zone F*

| First measurement | | | | | | | | | |
|---|---|---|---|---|---|---|---|---|---|
| Indicator [%] | Time | 30.Nov | 01.Dec | 02. Dec | 03. Dec | 04. Dec | 05. Dec | 06. Dec | Average |
| $W_{c1}$ | 06.00-08.00 | 52.2 | 50.1 | 54.9 | 54.3 | 47.2 | 68.2 | 72.4 | 57.1 |
| $W_{c2}$ | | 3.4 | 1.2 | 5.4 | 2.2 | 1.3 | 2.6 | 2.9 | 2.7 |
| $W_{c1}$ | 14.00-16.00 | 81.3 | 76.3 | 81.9 | 68.8 | 73 | 77.4 | 85.5 | 77.7 |
| $W_{c2}$ | | 4 | 2.3 | 2.2 | 1.3 | 1.2 | 1.5 | 3.1 | 2.2 |
| $W_{c1}$ | 21.00-23.00 | 86.6 | 87.8 | 84.6 | 88.7 | 82.8 | 84.9 | 86.9 | 86.1 |
| $W_{c2}$ | | 4.8 | 5.1 | 3.5 | 4 | 2.9 | 4.2 | 3.8 | 4 |
| Second measurement | | | | | | | | | |
| Indicator [%] | Time | 11.Jan | 12.Jan | 13.Jan | 14.Jan | 15.Jan | 16.Jan | 17.Jan | Average |
| $W_{c1}$ | 06.00-08.00 | 60.2 | 58.8 | 52.5 | 56.4 | 55.2 | 71.2 | 74.5 | 61.3 |
| $W_{c2}$ | | 3.4 | 2.5 | 5.1 | 3.2 | 2.2 | 4.2 | 6.4 | 3.8 |
| $W_{c1}$ | 14.00-16.00 | 73.6 | 77.7 | 76.6 | 79.8 | 81 | 78.3 | 85.2 | 78.9 |
| $W_{c2}$ | | 4 | 3.1 | 3.1 | 2.6 | 3.3 | 4.9 | 2.8 | 3.4 |
| $W_{c1}$ | 21.00-23.00 | 84.6 | 86.4 | 84.3 | 84 | 85.8 | 88.4 | 87.2 | 85.8 |
| $W_{c2}$ | | 6.7 | 6.9 | 5.6 | 3.5 | 4.5 | 6 | 5.1 | 5.5 |

On the other hand, the tests in the second period, on January 11-17, 2021, took place after the announcement of further restrictions prohibiting the normal operation of such facilities as shopping malls and gyms. Table 12 compares the average parking intensity indicators for each of the zones in the first and second study periods.

The test results are presented collectively in Table 13 and 14 for both studies, simultaneously gathering all the zones of the Jadwizyn estate. They contain intensity indicators. Each research day is divided into 3 time periods in which the research was carried out. The higher the intensity index, the more parking spaces have been occupied. The average daily intensity was calculated for each test day. At the end of the statement, the correctness index was given in the form of an arithmetic mean, taking into account the entire period of testing of a given table, whereas in Table 15 is the intensity index with the average for each of the 3 series of time intervals for the entire test period. This allows one to visualize the intensity that occurs at certain times of the day. A1 means the 1st measurement, A2 means the 2nd measurement, etc.

The analysis of the research results (Table 12) allows to state that zone D together with zone A had the highest parking intensity indicator. This is due to the highest number of multi-family buildings in these zones. In addition, these buildings have old buildings that are not equipped with, for example, underground parking spaces and the size of the existing parking lots is not adapted to the current needs of residents. Zone D was characterized by the greatest use of parking spaces in the afternoon and evening hours. It is worth

***Figure 11*** *Zone G with marked parking spaces [35]*

***Table 11*** *The intensity and correctness index for zone G*

| First measurement | | | | | | | | | |
|---|---|---|---|---|---|---|---|---|---|
| Indicator [%] | Time | 30.Nov | 01.Dec | 02. Dec | 03. Dec | 04. Dec | 05. Dec | 06. Dec | Average |
| $W_{c1}$ | 06.00-08.00 | 12.5 | 12.5 | 10 | 17.5 | 10 | 25 | 30 | 16.8 |
| $W_{c2}$ | | - | - | - | - | - | - | - | - |
| $W_{c1}$ | 14.00-16.00 | 22.5 | 17.5 | 22.5 | 20 | 22.5 | 35 | 27.5 | 23.9 |
| $W_{c2}$ | | - | - | - | - | - | - | - | - |
| $W_{c1}$ | 21.00-23.00 | 32.5 | 30 | 27.5 | 35 | 32.5 | 40 | 40 | 33.9 |
| $W_{c2}$ | | - | - | - | - | - | - | - | - |
| Second measurement | | | | | | | | | |
| Indicator [%] | Time | 11.Jan | 12.Jan | 13.Jan | 14.Jan | 15.Jan | 16.Jan | 17.Jan | Average |
| $W_{c1}$ | 06.00-08.00 | 27.5 | 30 | 22.5 | 30 | 20 | 32.5 | 37.5 | 28.6 |
| $W_{c2}$ | | - | - | - | - | - | - | - | - |
| $W_{c1}$ | 14.00-16.00 | 20 | 27.5 | 27.5 | 27.5 | 37.5 | 40 | 35 | 30.7 |
| $W_{c2}$ | | - | - | - | - | - | - | - | - |
| $W_{c1}$ | 21.00-23.00 | 32.5 | 35 | 32.5 | 40 | 35 | 45 | 47.5 | 38.2 |
| $W_{c2}$ | | - | - | - | - | - | - | - | - |

***Table 12*** *Average rate of parking correctness for the two research periods*

| Indicator | Time | Zone | | | | | | | |
|---|---|---|---|---|---|---|---|---|---|
| | | A | B | C | D | E | F | G | H |
| $W_{c1}$ [%] | 30.11-06.12.2020 | 81.9 | 33.3 | - | 84.4 | 30.8 | 73.6 | 24.9 | - |
| | 11.01-17.01.2021 | 87.4 | 36.9 | - | 86.5 | 29.6 | 75.3 | 32.5 | - |

noting that this zone is inhabited by the largest number of inhabitants, which accounts for half of the entire estate.

Although the zone D is inhabited by 1.466 people, zone F has more parking spaces by 64 parking spaces. Additionally, zone F has 137 more parking spaces than zone A, despite the similar number of inhabitants. The largest number of parking spaces in zone F is the result of the renovation of local car parks by the city authorities, thus increasing the number of available spaces. While in zones D and A, there are only old, dense buildings that prevent creation of new places, which could involve the construction of parking spaces in close proximity to residential buildings and their windows and this would be against Polish law.

Comparing the three zones with the highest number of inhabitants, A, D and F, the last one was the one that recorded the lowest number of occupied zones at any time of the day. This is due to the largest number of parking spaces per 100 inhabitants; in this case it amounts to almost 34, where for zone A it is almost 21 and for zone D more than 18 parking spaces per 100 people. In addition, zone F has the latest development compared to the rest of the estate zones, making it easier

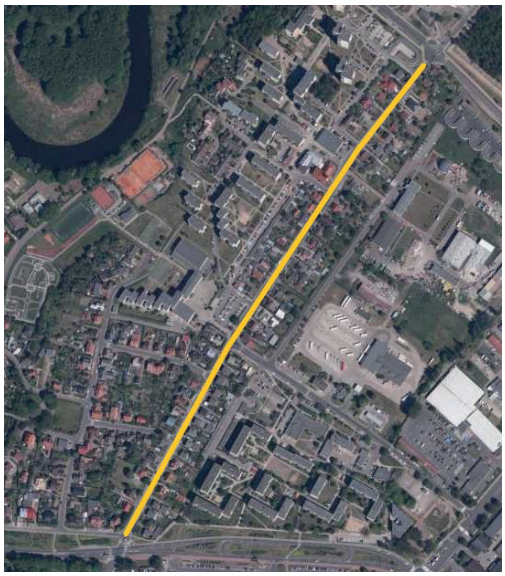

***Figure 12*** *Zone H [35]*

***Table 12*** *List of indicators for all the zones of the Jadwizyn estate during the study period from 30/11/2020 to 06/12/2020*

| Date | Time | Zone | | | | | | | | |
|---|---|---|---|---|---|---|---|---|---|---|
| | | A | | B | D | | E | F | | G |
| | | $W_{c1}$ [%] | $W_{c2}$ [%] | $W_{c1}$ [%] | $W_{c1}$ [%] | $W_{c2}$ [%] | $W_{c1}$ [%] | $W_{c1}$ [%] | $W_{c2}$ [%] | $W_{c1}$ [%] |
| 30.Nov | 06.00-08.00 | 67.5 | 3.0 | 25.0 | 63.4 | 12.7 | 63.2 | 52.2 | 3.4 | 12.5 |
| | 14.00-16.00 | 71.0 | 0.7 | 50.0 | 87.9 | 10.8 | 21.1 | 81.3 | 4.0 | 22.5 |
| | 21.00-23.00 | 90.5 | 5.5 | 25.0 | 95.2 | 14.6 | 5.3 | 86.6 | 4.8 | 32.5 |
| | Average | 76.3 | 3.1 | 33.3 | 82.2 | 12.7 | 29.8 | 73.4 | 4.1 | 22.5 |
| 01.Dec | 06.00-08.00 | 60.5 | 0.8 | 25.0 | 60.8 | 10.2 | 63.2 | 50.1 | 1.2 | 12.5 |
| | 14.00-16.00 | 77.5 | 2.6 | 25.0 | 90.1 | 9.8 | 26.3 | 76.3 | 2.3 | 17.5 |
| | 21.00-23.00 | 94.0 | 6.9 | 75.0 | 94.9 | 8.5 | 15.8 | 87.8 | 5.1 | 30.0 |
| | Average | 77.3 | 3.4 | 41.7 | 81.9 | 9.5 | 35.1 | 71.4 | 2.9 | 20.0 |
| 02. Dec | 06.00-08.00 | 64.5 | 1.6 | 25.0 | 66.7 | 7.7 | 73.7 | 54.9 | 5.4 | 10.0 |
| | 14.00-16.00 | 89.0 | 2.8 | 100.0 | 84.6 | 12.1 | 42.1 | 81.9 | 2.2 | 22.5 |
| | 21.00-23.00 | 95.5 | 4.2 | 25.0 | 97.1 | 11.3 | 15.8 | 84.6 | 3.5 | 27.5 |
| | Average | 83.0 | 2.8 | 50.0 | 82.8 | 10.4 | 43.9 | 73.8 | 3.7 | 20.0 |
| 03.Dec | 06.00-08.00 | 63.0 | 3.2 | 25.0 | 62.3 | 9.4 | 63.2 | 54.3 | 2.2 | 17.5 |
| | 14.00-16.00 | 81.5 | 1.8 | 25.0 | 93.4 | 8.2 | 31.6 | 68.8 | 1.3 | 20.0 |
| | 21.00-23.00 | 92.0 | 3.8 | 25.0 | 94.5 | 14.0 | 26.3 | 88.7 | 4.0 | 35.0 |
| | Average | 78.8 | 2.9 | 25.0 | 83.4 | 10.5 | 40.4 | 70.6 | 2.5 | 24.2 |
| 04.Dec | 06.00-08.00 | 66.0 | 2.3 | 25.0 | 61.5 | 8.9 | 57.9 | 47.2 | 1.3 | 10.0 |
| | 14.00-16.00 | 86.5 | 1.2 | 75.0 | 85.7 | 10.3 | 26.3 | 73.0 | 1.2 | 22.5 |
| | 21.00-23.00 | 93.0 | 3.2 | 50.0 | 96.3 | 10.6 | 26.3 | 82.8 | 2.9 | 32.5 |
| | Average | 81.8 | 2.2 | 50.0 | 81.2 | 9.9 | 36.8 | 67.7 | 1.8 | 21.7 |
| 05.Dec | 06.00-08.00 | 82.5 | 1.8 | 25.0 | 80.2 | 7.3 | 26.3 | 68.2 | 2.6 | 25.0 |
| | 14.00-16.00 | 84.5 | 3.0 | 25.0 | 85.7 | 11.5 | 15.8 | 77.4 | 1.5 | 35.0 |
| | 21.00-23.00 | 94.5 | 2.1 | 50.0 | 97.1 | 12.1 | 15.8 | 84.9 | 4.2 | 40.0 |
| | Average | 87.2 | 2.3 | 33.3 | 87.7 | 10.3 | 19.3 | 76.9 | 2.8 | 33.3 |
| 06.Dec | 06.00-08.00 | 85.0 | 2.4 | 0.0 | 84.6 | 7.8 | 21.1 | 72.4 | 2.9 | 30.0 |
| | 14.00-16.00 | 84.0 | 3.0 | 0.0 | 90.5 | 8.1 | 10.5 | 85.5 | 3.1 | 27.5 |
| | 21.00-23.00 | 96.5 | 4.7 | 0.0 | 99.6 | 12.9 | 0.0 | 86.9 | 3.8 | 40.0 |
| | Average | 88.5 | 3.3 | 0.0 | 91.6 | 9.6 | 10.5 | 81.6 | 3.2 | 32.5 |
| Average | | 81.9 | 2.9 | 33.3 | 84.4 | 10.4 | 30.8 | 73.6 | 3.0 | 24.9 |

***Table 13*** *List of indicators for all the zones of the Jadwizyn estate during the study period from 30/11/2020 to 06/12/2020*

| Date | Time | Zone | | | | | | | | |
|---|---|---|---|---|---|---|---|---|---|---|
| | | A | | B | D | | E | F | | G |
| | | $W_{c1}$ [%] | $W_{c2}$ [%] | $W_{c1}$ [%] | $W_{c1}$ [%] | $W_{c2}$ [%] | $W_{c1}$ [%] | $W_{c1}$ [%] | $W_{c2}$ [%] | $W_{c1}$ [%] |
| 11.Jan | 06.00-08.00 | 82.5 | 5.5 | 25.0 | 79.9 | 11.0 | 47.4 | 60.2 | 3.4 | 27.5 |
| | 14.00-16.00 | 92.5 | 6.7 | 25.0 | 88.3 | 5.8 | 15.8 | 73.6 | 4.0 | 20.0 |
| | 21.00-23.00 | 94.0 | 7.9 | 0.0 | 92.7 | 12.6 | 10.5 | 84.6 | 6.7 | 32.5 |
| | Average | 89.7 | 6.7 | 16.7 | 86.9 | 9.8 | 24.6 | 72.8 | 4.7 | 26.7 |
| 12.Jan | 06.00-08.00 | 79.0 | 7.3 | 25.0 | 75.8 | 8.2 | 68.4 | 58.8 | 2.5 | 30.0 |
| | 14.00-16.00 | 89.5 | 6.1 | 75.0 | 90.5 | 10.5 | 21.1 | 77.7 | 3.1 | 27.5 |
| | 21.00-23.00 | 91.5 | 8.5 | 25.0 | 91.2 | 12.9 | 10.5 | 86.4 | 6.9 | 35.0 |
| | Average | 86.7 | 7.3 | 41.7 | 85.8 | 10.5 | 33.3 | 74.3 | 4.2 | 30.8 |
| 13.Jan | 06.00-08.00 | 77.5 | 4.8 | 0.0 | 72.9 | 12.1 | 57.9 | 52.5 | 5.1 | 22.5 |
| | 14.00-16.00 | 88.0 | 6.1 | 50.0 | 89.0 | 11.5 | 31.6 | 76.6 | 3.1 | 27.5 |
| | 21.00-23.00 | 94.5 | 7.3 | 50.0 | 93.8 | 10.2 | 10.5 | 84.3 | 5.6 | 32.5 |
| | Average | 86.7 | 6.1 | 33.3 | 85.2 | 11.2 | 33.3 | 71.1 | 4.6 | 27.5 |
| 14.Jan | 06.00-08.00 | 76.5 | 7.9 | 25.0 | 79.9 | 6.0 | 57.9 | 56.4 | 3.2 | 30.0 |
| | 14.00-16.00 | 90.5 | 9.7 | 25.0 | 84.2 | 10.0 | 26.3 | 79.8 | 2.6 | 27.5 |
| | 21.00-23.00 | 94.0 | 11.5 | 50.0 | 90.8 | 10.9 | 5.3 | 84.0 | 3.5 | 40.0 |
| | Average | 87.0 | 9.7 | 33.3 | 85.0 | 9.0 | 29.8 | 73.4 | 3.1 | 32.5 |
| 15.Jan | 06.00-08.00 | 75.5 | 7.3 | 25.0 | 82.1 | 8.5 | 68.4 | 55.2 | 2.2 | 20.0 |
| | 14.00-16.00 | 86.5 | 8.5 | 50.0 | 88.3 | 11.2 | 21.1 | 81.0 | 3.3 | 37.5 |
| | 21.00-23.00 | 92.0 | 9.1 | 50.0 | 94.5 | 12.0 | 10.5 | 85.8 | 4.5 | 35.0 |
| | Average | 84.7 | 8.3 | 41.7 | 88.3 | 10.6 | 33.3 | 74.0 | 3.3 | 30.8 |
| 16.Jan | 06.00-08.00 | 80.0 | 6.7 | 50.0 | 76.9 | 10.5 | 63.2 | 71.2 | 4.2 | 32.5 |
| | 14.00-16.00 | 88.5 | 6.1 | 50.0 | 86.8 | 14.8 | 5.3 | 78.3 | 4.9 | 40.0 |
| | 21.00-23.00 | 93.5 | 8.5 | 50.0 | 96.0 | 15.6 | 15.8 | 88.4 | 6.0 | 45.0 |
| | Average | 87.3 | 7.1 | 50.0 | 86.6 | 13.6 | 28.1 | 79.3 | 5.0 | 39.2 |
| 17.Jan | 06.00-08.00 | 83.5 | 7.9 | 25.0 | 76.2 | 9.1 | 52.6 | 74.5 | 6.4 | 37.5 |
| | 14.00-16.00 | 89.5 | 8.5 | 50.0 | 90.5 | 10.9 | 15.8 | 85.2 | 2.8 | 35.0 |
| | 21.00-23.00 | 96.0 | 10.9 | 50.0 | 97.1 | 13.6 | 5.3 | 87.2 | 5.1 | 47.5 |
| | Average | 89.7 | 9.1 | 41.7 | 87.9 | 11.2 | 24.6 | 82.3 | 4.8 | 40.0 |
| Average | | 87.4 | 7.7 | 36.9 | 86.5 | 10.9 | 29.6 | 75.3 | 4.2 | 32.5 |

***Table 14*** *Cumulative intensity indicator for all the zones of the Jadwizyn estate*

| Indicator | Time | Zone | | | | | | | | | | | | | | | |
|---|---|---|---|---|---|---|---|---|---|---|---|---|---|---|---|---|---|
| | | A1 | A2 | B1 | B2 | C1 | C2 | D1 | D2 | E1 | E2 | F1 | F2 | G1 | G2 | H1 | H2 |
| $W_{c1}$ [%] | 06.00-08.00 | 69.9 | 79.2 | 21.4 | 25 | - | - | 68.5 | 77.7 | 52.6 | 59.4 | 57.1 | 61.3 | 16.8 | 28.6 | - | - |
| | 14.00-16.00 | 82 | 89.3 | 42.9 | 46.4 | - | - | 88.3 | 88.2 | 24.8 | 19.5 | 77.7 | 78.9 | 23.9 | 30.7 | - | - |
| | 21.00-23.00 | 93.7 | 93.6 | 35.7 | 39.3 | - | - | 96.4 | 93.7 | 15 | 9.8 | 86.1 | 85.8 | 33.9 | 38.2 | - | - |
| | Average | 81.90 | 87.40 | 33.30 | 36.90 | - | - | 84.40 | 86.50 | 30.80 | 29.60 | 73.60 | 75.30 | 24.90 | 32.50 | - | - |

to leave cars, e.g. thanks to underground parking lots that belong to new multi-family buildings.

The highest percentage of incorrectly parked cars was in zones A, D and F. It was observed that incorrectly parked cars were most often located in close proximity to residential buildings and therefore often made it difficult to move around parking lots, e.g. by obstructing other vehicles and garbage arbors, leaving narrow passages that forced users to perform additional manoeuvres with the vehicle in order to park or leave the parking lot. The available parking spaces in the evening hours were most often located far from the places of residential buildings, which was an inconvenience for the residents and they preferred to leave the vehicle in the wrong place, rather than park it correctly. It is worth mentioning that some of the cars parked incorrectly did not hinder the movement of other vehicles and pedestrians, standing in unused places, e.g. neglected parts of sidewalks, which due to their width are able to accommodate several vehicles.

In zone B, despite the lack of public parking spaces intended for residents, there were no incorrectly parked vehicles and parking spaces under the local store were used mainly by the store's customers. It follows that the lack of publicly available parking solutions is the result of the residents of the zone having parking spaces on private properties, which fully covers their needs. Moreover, zone B, due to its distance from multi-family housing, is not an interesting place to leave a vehicle for people living in other zones. The situation of the H zone is similar, because here we are also dealing with single-family houses, which have parking spaces on the property and the residents of these houses do not need to leave their cars in public parking spaces available throughout the estate.

Zone G, despite having a car park, which was originally intended for use by employees of the educational institution, was used mainly in the afternoon and evening hours, most likely by residents of the nearby zones A, D and H. This is the result of an insufficient number of places in the zones mentioned, especially at times when the largest number of residents spent their time at home. It is worth taking into account that due to the situation related to the prevailing pandemic, school classes were held mainly remotely, which could result in a decrease in the intensity of parking spaces used in this area in the morning.

Zone E has parking spaces located at workplaces. It can be concluded that the car parks located in this zone are used only by plant employees, as indicated by the highest traffic hours. The largest number of parked cars was between 6 AM and 8 AM and with each subsequent hour of testing, their number decreased. The evening average number of cars parked in this zone was the lowest. No incorrectly parked vehicles were observed, which allows to conclude that the parking spaces are sufficient to meet the needs of employees or that they also have parking lots at their disposal at the workplace.

Despite the failure to carry out the research for the entire C-zone due to the purpose of the parking system to meet the needs of the mall's customers, during the research for the rest of the estate, it was noticed that the C-zone car park, which belongs to the "IBI" shopping center, was filling up in the evening hours when the gallery was closed. These cars remained there until the very morning, which may indicate that the residents of the estate, especially zone A, decided to leave the car in the parking lot belonging to the store due to the insufficient number of parking spaces in their zone. Another issue indicating such a possibility is the drivers leaving their cars in parking spaces located as close as possible to zone A.

Summarizing the collected conclusions, evaluation of the effectiveness of the parking system allows to conclude that the discussed system is insufficient in individual zones of the Jadwizyn estate, in particular for zones A and D, where the situation prevailing during the research allowed for the practically complete use of available parking spaces, especially in the form of the parking intensity indicator in the second observation period, which increased on average by 5.5% for zone A and by 2.1% for the second zone. This is particularly evident when comparing the data from the first and second dates. The observed increase in parking space in the second period of the study results from the imposed restrictions, related to, inter alia, with the closure of large-format stores and shopping malls. This limited the swinging movement between the place of work, education and trade and the place of residence. The situation allowed to "test" the efficiency of the parking systems existing on the estate.

Referring to the idea of sustainable urban transport, it can be stated that the parking system at the Jadwizyn estate does not fit in with this transport policy. First of all, the infrastructure was created with the current needs of the inhabitants of that time in mind and not for the long-term use. At the same time, it confirms that no analyses, concerning the condition of the infrastructure and the increasing interest in means of individual communication, had been carried out before. Moreover, the fact that drivers spend a lot of time driving around the neighbourhood in order to find a vacant place is contrary to the assumption of sustainable urban transport, which aims to reduce the negative effects caused by the excessive movement of combustion vehicles.

## 4 Conclusion

The conducted research made it possible to notice that the problem of urban aging is not a problem faced only by large agglomerations, but also by smaller cities and towns. The technical progress that took place in the automotive world was not foreseen at the time when the Polish architecture was reconstructed after World War II, the effects of which are still felt by

drivers of vehicles involved in road traffic [37]. The basic conclusion regarding the ineffectiveness of the Pila car park in the Jadwizyn estate also concerns the archaic structure of the existing systems, which do not meet the expectations and needs of residents, contributing to their general dissatisfaction. This is a problem especially visible in periods when the public spends a lot of time in their home areas (holidays, pandemic restrictions, weekends).

However, attention should be paid to difficulties that occurred during the examination. By examining the intensity of the car park and its demand, authors were not able to determine whether each parked vehicle belongs to people living in multi-family buildings, visitors or families living in single-family buildings.

Using the research, it was possible to assess the effectiveness of the parking system that exists in the Jadwizyn estate in Pila and to refer to the idea of sustainable development with the presented results. The conducted study proved that the system is not effective for the community living in the estate and allows to draw a conclusion that changes in the parking policy of the estate should be made, for example by implementing new parking solutions in the form of parking automation or building a multi-level structure providing more parking spaces. Continuation of the research in the field presented would certainly help to implement even more accurate solutions that would result in implementation of the most effective parking systems, tailored both to the structure of the estate and the needs of its residents, this type of research could be carried out with help of a survey conducted among residents.

## References


[1] GOLASZEWSKI, A., KUKULSKI, J., TOWPIK, K. *Vehicle transport infrastructure*. Warsaw: Publishing House of the Warsaw University of Technology, 2006. ISBN 9788372075901.

[2] PWN [online] [accessed 2020-06-10]. 2020. Available from: https://sjp.pwn.pl/slowniki/parking.html

[3] Police statistical data [online] [accessed 2019-10-10]. 2019. Available from: http://www.statystyka.policja.pl/

[4] UNCED. Agenda 21. In: United Nations Conference on Environment and Development UNCED: proceedings. United Nations. 1992.

[5] KATES, R. W., CORELL, R. HALL, J. M., JAEGER, C. C., LOWE, I., MCCARTHY, J. J., SCHELLNHUBER, H. J., BOLIN, B., DICKSON, N. M., FAUCHEUX, S., GALLOPIN, G. C., GRÜBLER, A., HUNTLEY, B., JAGER, J., JODHA, N. S., KASPERSON, R. E., MABOGUNJE, A., MATSON, P., MOONEY, H., MOORE III, B., O'RIORDAN, T., SVEDIN, U. Sustainability science. *Science* [online]. 2001, 292(5517), p. 641-642. ISSN 0036-8075. Available from: https://doi.org/10.1126/science.1059386

[6] STAPPEN, R. Brundtland report. New York, NY, USA: Oxford University Press, 2006.

[7] GALLOPIN, G. A. Systems approach to sustainability and sustainable development; sustainable development and human settlements division ECLAC [online] [accessed 2020-06-10]. Santiago, Chile: Government of the Netherlands Project NET / 00/063 "Sustainability Assessment in Latin America and the Caribbean", 2003. Available from: https://repositorio.cepal.org/bitstream/handle/11362/5759/S033119_en.pdf

[8] GERWIN, M. Sustainable development plan for Poland: local developmental initiatives [online] [accessed 2020-06-10]. 2020. Available from: http://www.sopockainitiative.org/earth/pdf/LIR-new.pdf

[9] KOZLOWSKI, S. *The future of eco-development*. Lublin, Poland: John Paul II Catholic University of Lublin, 2005. ISBN 83-7363-312-X.

[10] PEZZEY, J. C. V., TOMAN, M. A. *The economics of sustainability* [online]. 1. ed. London: Routledge, 2002. eISBN 9781315240084. Available from: https://doi.org/10.4324/9781315240084

[11] BORIS, T., BRZOZOWSKI, T. Analysis of the existing statistical data in terms of their usefulness for determining the level of sustainable transport development with a proposal for their extension. Report on the implementation of the expertise. Jelenia Gora-Warsaw. *Logistyka*. 2014, **3**, p. 7254-7260. ISSN 1231-5478.

[12] SZTANGRET, I. Systemic sustainable development in the transport service sector. *Sustainability* [online]. 2020, **12**(22), 9525. eISSN 2071-1050. Available from: https://doi.org/10.3390/su12229525

[13] ORTEGA, J., MOSLEM, S., PALAGUACHI, J., ORTEGA, M., CAMPISI, T., TORRISI, V. An integrated multi criteria decision making model for evaluating park-and-ride facility location issue: A case study for Cuenca City in Ecuador. *Sustainability* [online]. 2021, **13**(13), 7461. eISSN 2071-1050. Available from: https://doi.org/10.3390/su13137461

[14] CAMPISI, T., CASELLI, B., ROSSETTI, S., TORRISI, V. The evolution of sustainable mobility and urban space planning: exploring the factors contributing to the regeneration of car parking in living spaces. *Transportation Research Procedia* [online]. 2022, **60**, p. 76-83. ISSN 2352-1465. Available from: https://doi.org/10.1016/j.trpro.2021.12.011

[15] WU, E. H. K., LIU, C. Y., SAHOO, J., JIN, M. H., LIN, S. H. Agile urban parking recommendation service for intelligent vehicular guiding system. *IEEE Intelligent Transportation Systems Magazine* [online]. 2014, **6**, p. 35-49. ISSN 1939-1390, eISSN 1941-1197. Available from: https://doi.org/10.1109/MITS.2013.2268549

[16] TORRISI, V., IGNACCOLO, M., INTURRI, G. Innovative transport systems to promote sustainable mobility: Developing the model architecture of a traffic control and supervisor system. *Lecture Notes in Computer Science* [online]. 2018, **10962**, p. 622-638. ISSN 0302-9743, eISSN 1611-3349. Available from: https://doi.org/10.1007/978-3-319-95168-3_42
[17] LITMAN, T. *Parking management best practices*. 2. ed. New York, NY, USA: Routledge, 2020. ISBN 9781351178686.
[18] CAI, Y., CHEN, J., ZHANG, C., WANG, B. A parking space allocation method to make a shared parking strategy for appertaining parking lots of public buildings. *Sustainability* [online]. 2019, **11**(1), 120. eISSN 2071-1050. Available from: https://doi.org/10.3390/su11010120
[19] HUANG, X., LONG, X., WANG, J., HE, L. Research on parking sharing strategies considering user overtime parking. *PLoS ONE* [online]. 2020, **15**, e0233772. ISSN 1932-6203. Available from: https://doi.org/10.1371/journal.pone.0233772
[20] HAO, J., CHEN, J., CHEN, Q. Floating charge method based on shared parking. *Sustainability* [online]. 2019, **11**(1), 72. eISSN 2071-1050. Available from: https://doi.org/10.3390/su11010072
[21] ZHAO, P., GUAN, H., WEI, H., LIU, S. Mathematical modelling and heuristic approaches to optimize shared parking resources: a case study of Beijing, China. *Transportation Research Interdisciplinary Perspectives* [online]. 2021, **9**, 100317. ISSN 2590-1982. Available from: https://doi.org/10.1016/j.trip.2021.100317
[22] DUAN, M., WU, D., LIU, H. Bi-level programming model for resource-shared parking lots allocation. *Transportation Letters* [online]. 2019, **12**, p. 501-511. ISSN 1942-7867, eISSN 1942-7875. Available from: https://doi.org/10.1080/19427867.2019.1631596
[23] JIAN, S., LIU, W., WANG, X., YANG, H., WALLER, S. T. On integrating carsharing and parking sharing services. *Transportation Research Part B: Methodological* [online]. 2020, **142**, p. 19-44. ISSN 0191-2615. Available from: https://doi.org/10.1016/j.trb.2020.09.013
[24] JI, Y., DONG, J., LAI, Z., FENG, Q. Optimal allocation of shared parking spaces for hospital parkers considering parking choice behaviour under bounded rationality. *Transportation Letters* [online]. 2020, latest articles, p. 1-12. ISSN 1942-7867, eISSN 1942-7875. Available from: https://doi.org/10.1080/19427867.2022.2048226
[25] BIENCZAK, M., FIEREK, S., KICINSKI, M., MERKISZ-GURANOWSKA, A., ZMUDA-TRZEBIATOWSKI, P. Calming traffic in historic city quarters. Case study: Poznan. Poznan: Poznan University of Technology, Department of Transport Systems, 2018.
[26] BRZESZCZAK A., IMIOLCZYK, J., CZUMA-IMIOLCZYK, L. Sustainable public transport - social assessment of collective transport in Czestochowa. *Urban Studies*. 2018, **30**, p. 85-98. ISSN 2082-4793.
[27] History of the town of Pila [online] [accessed 2020-06-10]. 2020. Available from: http://www.pila.pl/pl/historia.html
[28] Generating localization [online] [accessed 2020-06-10]. 2020. Available from: https://geohack.toolforge.org/
[29] Pila poviat, Statistical vademecum of the local government - Pila municipal commune [online] [accessed 2020-06-10]. 2020. Available from: https://poznan.stat.gov.pl/
[30] Bulletin of public information - Pila City Hall [online] [accessed 2020-06-10]. 2020. Available from: http://bip.pila.pl/
[31] Pila City Hall [online] [accessed 2020-06-10]. 2020. Available from: http://www.pila.pl
[32] Pila economy [online] [accessed 2020-06-10]. 2020. Available from: http://www.pila.pl/pl/48-gospodarka.html
[33] Development strategy of the city of Pila until 2035 [online] [accessed 2020-06-10]. 2020. Available from: http://www.pila.pl/pl/strategia-rozaran-miasta-pily-do-2035-roku.html
[34] Resolution No. XIV/195/11 of the Pila City Council [online] [accessed 2020-06-10]. 2020. Available from: http://www.bip2.um.pila.pl
[35] Geoportal [online] [accessed 2020-06-10]. 2020. Available from: https://mapy.geoportal.gov.pl/
[36] JEDYNAK, Z., KOZDRAS, K. Assessment of the parking system of the housing estate F. Kotula in Rzeszow. *Logistyka*. 2015, **4**, p. 3867-3874. ISSN 1231-5478.
[37] GACA, S., SUCHORZEWSKI W., TRACZ M. *Road traffic engineering. Theory and practice*. Warsaw: Publishing House of Communications and Communications in Warsaw, 2008. ISBN 978-83-206-1947-8.

# FORECASTING THE ROAD ACCIDENT RATE AND THE IMPACT OF THE COVID 19 ON ITS FREQUENCY IN THE POLISH PROVINCES

**Piotr Gorzelańczyk [1], Martin Jurkovič [2,*], Tomáš Kalina [2], Malaya Mohanty [3]**

[1]Stanislaw Staszic University of Applied Sciences in Pila, Pila, Poland
[2]Department of Water Transport, Faculty of Operation and Economics of Transport and Communications, University of Zilina, Zilina, Slovak Republic
[3]KIIT - Kalinga Institute of Industrial Technology, Odisha, India

*E-mail of corresponding author: martin.jurkovic@uniza.sk

***Resume***

The COVID-19 pandemic has significantly affected the development of road transport, not only in Poland, but also worldwide. Limited mobility, especially at the beginning of the pandemic, had a large impact on the number of road accidents. The aim of the present study is to predict the number of road accidents in Poland and to assess the impact of the COVID-19 pandemic on variability of the number of road accidents. To attain the objective, annual data on the road accidents for every province in Poland were collected and analysed. Based on historical crash data, obtained from the police, the number of road accidents was forecasted for both pandemic and non-pandemic scenarios. Selected time series models and exponential models were used to forecast the number of accidents.

***Article info***

Received 1 July 2022
Accepted 26 August 2022
Online 20 September 2022

***Keywords:***

road accident
COVID 19
forecasting
Brownian model
Holt model
Winters model

Available online: https://doi.org/10.26552/com.C.2022.4.A216-A231

ISSN 1335-4205 (print version)
ISSN 2585-7878 (online version)

## 1 Introduction and literature review

The road traffic accidents are events that cause not only injuries or death to road users, but the damage to property, as well. According to the WHO, approximately 1.3 million people die each year as a result of traffic accidents. Traffic accidents account for around 3% of their GDP for most of the countries in the world. Road traffic accidents are the leading cause of death for minors and young people aged 5-29 [1]. One of the most frequent causes of traffic accidents is the young age of drivers. Hudec et al. (2021) dealt with the fatal traffic accidents in the period 2017-2019, caused by drivers who have held driving licenses for less than five years [2]. The UN General Assembly has set an ambitious goal of halving the number of road deaths and injuries by 2030.

Traffic forecasting has always been important, considering the long-term strategy or design and therefore has been a field, which has attracted a lot of researchers around the world. Few of the important studies are described in the following part of this section.

Szumska et al. (2020) presented the road safety issues in Poland over the years 2009-2019, with a detailed consideration of the data on side, front and rear accidents, as well as the characteristics of perpetrators of road accidents in terms of gender and age of drivers [3].

Okutani et al. (1984) used Kalman filtering theory to forecast the traffic volume [4]. The authors using the Kalman theory computed 3 error indices (a) mean relative error, which indicates the expected error as a fraction of the measurement, (b) root relative square error and (c) maximum relative error and compared it to UTCS-2, which was previously determined as the best of the most widely used algorithms. They also found that all the new prediction models perform substantially (up to 80%) better than UTCS-2. Davis and Nihan (1991) reviewed the problem of the short-term traffic forecasting as a non-parametric regression method, by utilising the nearest neighbor (k-NN) approach [5]. According to the authors, this technique might sidestep some of the problems inherent in parametric forecasting approaches. Lavrenz et al. (2018) stated that last two decades have led to growing need for the short-term prediction of traffic parameters [6]. According to them, prediction models should be embedded in a real-time

intelligent transportation systems environment. The authors examined various forecasting models and their findings showed significant sensitivity of ARIMA models in dealing with missing values. Kashyap et al. (2022) reviewed various traffic forecasting models related to deep learning techniques [7]. Their article reviewed some of the latest works in deep learning for the traffic flow prediction. They talked about the rising popularity of hybrid methods. Lana et al. (2018) aimed to summarize the efforts to date towards extracting the main comparing criteria in traffic forecasting and challenges in this field [8]. Williams and Hoel (2003) used a seasonal ARIMA process to model and forecast vehicular traffic flow [9]. This article presents the theoretical basis for modelling univariate traffic condition data streams as seasonal auto regressive integrated moving average processes. Demissie et al. (2013) focused on study of the smart urban mobility in Oporto, Portugal, leveraging on the existing sensing capabilities to collect historical traffic sensing data through traffic counters [10]. The program used by authors is Porto LivingLab, which is a smart city initiative that aims to study urban dynamics. More specifically, this study analyses urban mobility by using historical data from road-mounted traffic counters to predict future vehicular traffic behaviour. Ali et al. (2021) used the machine learning to forecast and predict traffic crashes and their associated injuries and fatalities from a traffic safety standpoint [11]. The model consists of four terms: trend component, cyclical, seasonal and irregular components. The trend component was natural due to increase in population, which was directly proportional to traffic accidents. The cyclical component demonstrated an increase in the number of accidents, with the highest increase (28.9 %) in February 2011 and then it showed a decline in accident number per month. The decrement of accidents happened because the fixed speed camera system was widely applied on major roads. The seasonal component showed seasonal effects where more accidents occurred in July, August and September (summer season) and less accidents occurred in February, March and April (winter season). Many countries have their own guidelines to forecast the road accidents. For instance, in India, IRC 108 is a guideline by Indian Roads Congress for traffic forecasting on highways. The various methodologies discussed in the guideline are forecasting techniques like ADT, AADT, ARIMA, linear regression etc. Salisu and Oyesiku (2020) examined traffic survey analysis on major highways in Ogun State, Nigeria using manual traffic count method for estimation of traffic volume and flow pattern [12].

Time series forecasting and decision trees have been used extensively in the field of accident forecasts by various researchers [13-17]. The three widely used time series methods are Exponential smoothening technique, Holt-Winters method and seasonal ARIMA. According to Wu et al. (2017), Winters method has the highest forecasting accuracy, as compared to other methods [18]. According to Dutta et al. (2022), empirical results from exponential smoothening models assert the importance of their application in accident forecasting [16]. Yadav and Nath (2017) reported that MAPE values for exponential smoothening technique is much lesser than ARIMA techniques and hence provides better fit for forecasted data [19]. Along with these time series analyses, Artificial Neural Networks (ANN) and its various types are used a lot for traffic forecasting. Yang et al. (2022) proposed a multi-node Deep Neutral Network (DNN) to predict different levels of severity of injury, death and property loss with great accuracy [20]. Similarly, study by Biswas et al. (2019) used the Random Forest regression to predict the number of road accidents, where the authors opined the smaller groups to be favored over larger groups [21]. Chudy-Laskowska and Pisula (2014) used an autoregressive model with quadratic trend for forecasting the road incidents [22]. According to Kashpruk (2010), moving average techniques can also be used for accident forecasting; however, the prediction accuracy is too low [23]. As discussed earlier, time series analyses like ARIMA or SARIMA are also used for forecasting [24-27]. A limitation to ARIMA is the linear nature of the model by Dudek (2013) [28]. Hadoop is a new prediction technique, which was used by Kumar et al. (2019) [29]. The disadvantage of this method is its inability to work with small data files. Karlaftis and Vlahogianni (2009) used the Garch model for prediction [24]. However, they found the method to be very complex and complicated [30-31]. Various researchers [32-33] have also used the Data-Mining techniques for forecasting, which usually have the disadvantage of huge sets of general descriptions [34]. One also encounters the combination of models proposed by Sebego et al. as a combination of different models [35]. Parametric models were also proposed in the work of Bloomfield (1973) [36]. From the literature, it can be safely assumed that Time-series analyses and neural networks are better forecasting methods. Between them, time series analyses have more dynamics and types to choose from based on the type of date one is dealing with.

Regarding the sources of accident data, the most commonly, they are collected and analyzed by government authorities through relevant government agencies. Data are collected through police reports, insurance databases or hospital records. Partial information on the road accidents is then processed for the transport sector on a larger scale [37]. Another important source of data collection in today's era is the use of Intelligent transport systems (ITS). The GPS devices in vehicles are used for the collection of such data [38]. Vehicle number plate recognition system also helps in collecting large amounts of traffic data over a monitored period of time, which however is a tedious job [39]. In the present study, different data sources have been combined with major inputs from the police data since they provide the most trustworthy information.

***Table 1*** *Area and population by province in Poland in 2020*

| Provinces | Area | | Population | |
|---|---|---|---|---|
| | in ha | in km² | total | per 1 km² |
| Poland | 31,270,525 | 312,705 | 38,265,013 | 122 |
| Lower Silesia | 1,994,670 | 19,947 | 2,891,321 | 145 |
| Kuyavia-Pomerania | 1,797,134 | 17,971 | 2,061,942 | 115 |
| Lublin Province | 2,512,246 | 25,123 | 2,095,258 | 83 |
| Lubusz Province | 1,398,793 | 13,988 | 1,007,145 | 72 |
| Lodz Province | 1,821,895 | 18,219 | 2,437,970 | 134 |
| Lesser Poland | 1,518,279 | 15,183 | 3,410,441 | 225 |
| Masovia | 3,555,847 | 35,559 | 5,425,028 | 153 |
| Opole Province | 941,187 | 9,412 | 976,774 | 104 |
| Subcarpathia | 1,784,576 | 17,846 | 2,121,229 | 119 |
| Podlasie Province | 2,018,702 | 20,187 | 1,173,286 | 58 |
| Pomerania | 1,832,368 | 18,323 | 2,346,671 | 128 |
| Silesia | 1,233,309 | 12,333 | 4,492,330 | 364 |
| Holy Cross | 1,171,050 | 11,710 | 1,224,626 | 105 |
| Warmia-Masuria | 2,417,347 | 24,173 | 1,416,495 | 59 |
| Greater Poland | 2,982,650 | 29,826 | 3,496,450 | 117 |
| West Pomerania | 2,290,472 | 22,905 | 1,688,047 | 74 |

## 2 Materials and methods

Poland is inhabited by over 38 million people. Poland covers an area of 312 705 km² and is divided into 16 provinces (Table 1, Figure 1). Based on the police road crash data, it may be stated that the number of road accidents on Polish roads is decreasing year by year. For all the studied provinces in the analysed period 2001-2021 the average decrease is more than 56 %. This is most visible in Kuyavia-Pomerania province (70 %) and Podlasie province (69 %, and least in the Lubusz province (32 %). The number of road accidents depends on the number of inhabitants in each province [40].

In some provinces there are fluctuations in the number of accidents, with a downward trend. In comparison with the European Union the number of accidents in Poland is still very high.

During the pandemic, a decrease in the number of road accidents is observed. Compared to 2019, there were on average 21 % fewer road accidents in 2020 and comparing the statistics of 2021 compared to 2019, the decrease is more than 23 %. Figure 2 graphically shows the trend of road accidents in Poland between 2001 and 2021 for the analysed provinces. The number of road accidents depends on the province. The rate of accidents per 100,000 inhabitants in 2021 is presented in Figure 3. The highest number of accidents per 100,000 inhabitants can be observed in the Lodz (95) and Masovia (79.3) provinces and the lowest in the Podlasie (37) and Kuyavia-Pomerania (38.8) provinces [41].

Selected exponential equalization models were used to forecast the number of road accidents for each province in Poland. The essence of these methods is that the time series of the forecast variable is pronounced with a weighted moving average and the weights are determined according to the exponential function. These weights were optimally selected by Statistica software, in which the applied analyses were performed.

The forecast of the number of accidents for the analysed provinces was based on the weighted average of the current and historical series. The obtained results of the forecast using these methods depend on the choice of a model and its optimal values of parameters. Forecasting the number of accidents in Poland by provinces was carried out using the selected time series models.

The following errors of expired forecasts determined from Equations (1) to (5) were used to calculate measures of analytical forecasting perfection:

- ME - mean error

$$ME = \frac{1}{n}\sum_{i=1}^{n}(Y_i - Y_p), \tag{1}$$

- MAE -mean average error

$$MAE = \frac{1}{n}\sum_{i=1}^{n}|Y_i - Y_p|, \tag{2}$$

- MPE -mean percentage error

$$MPE = \frac{1}{n}\sum_{i=1}^{n}\frac{Y_i - Y_p}{Y_i}, \tag{3}$$

- MAPE - mean absolute percentage error

$$MAPE = \frac{1}{n}\sum_{i=1}^{n}\frac{|Y_i - Y_p|}{Y_i}, \tag{4}$$


***Figure 1*** *Location of provinces in Poland (Division of Poland, 2022)*

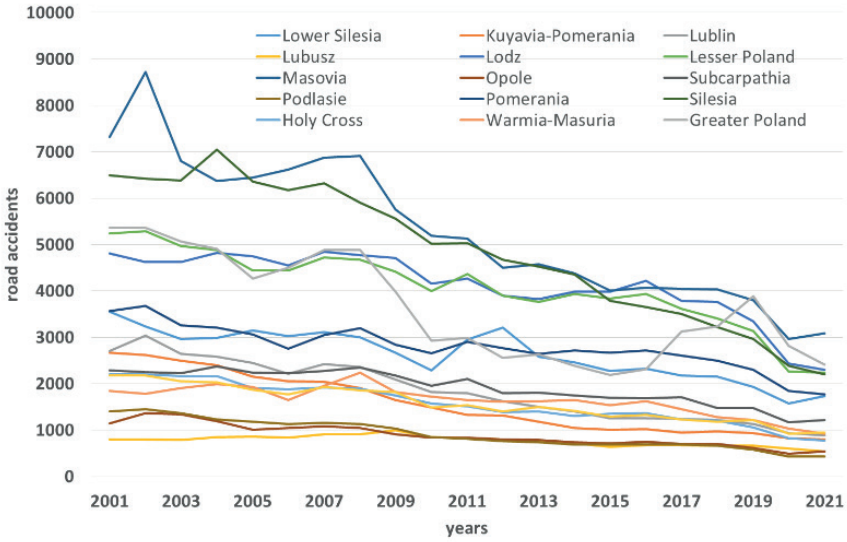


***Figure 2*** *Comparison of the number of accidents in Poland between 2001 and 2021*

- SSE - mean square error

$$SSE = \sqrt{\frac{1}{n}\sum_{i=1}^{n}(Y_i - Y_p)^2}, \quad (5)$$

where:
n - the length of the forecast horizon,
Y - observed value of the road accidents,
$Y_p$ - forecasted value of the road accidents.

In order to compare the number of accidents in case of pandemic and if it did not exist, the mean percentage error was minimized.

## 3 Research results

The variability of the number of road accidents per day was examined by the Kruskall - Wallis test. The value of the test statistic is 14.4 with a test probability of $p < 0.05$. This value indicates that, according to

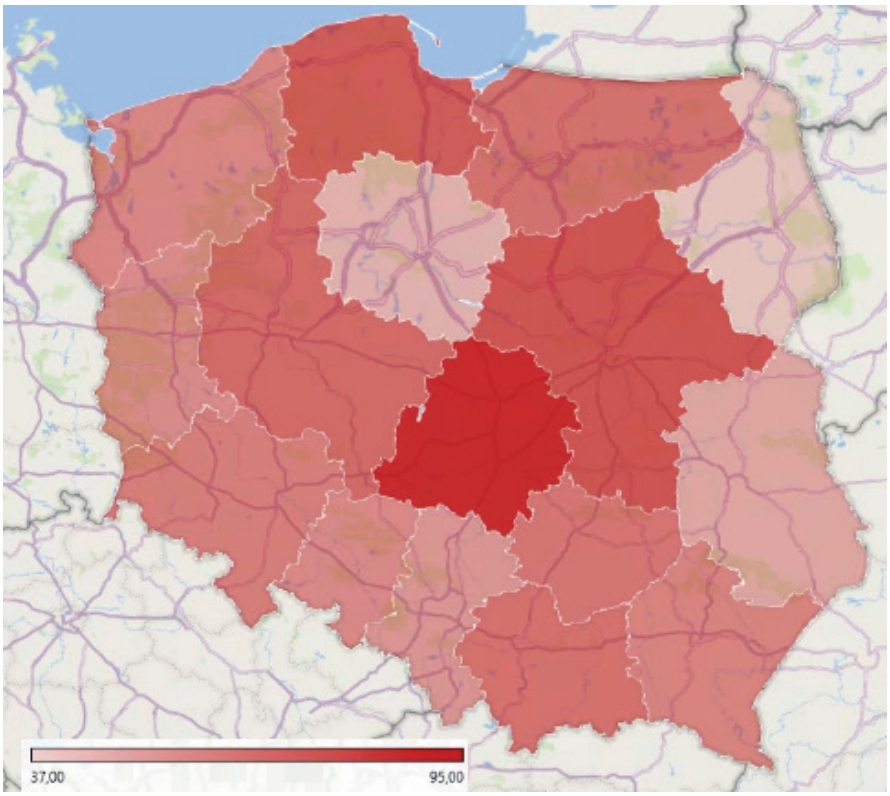


***Figure 3*** *Accident rate per 100,000 inhabitants in 2021 (Statistice Police, 2022)*

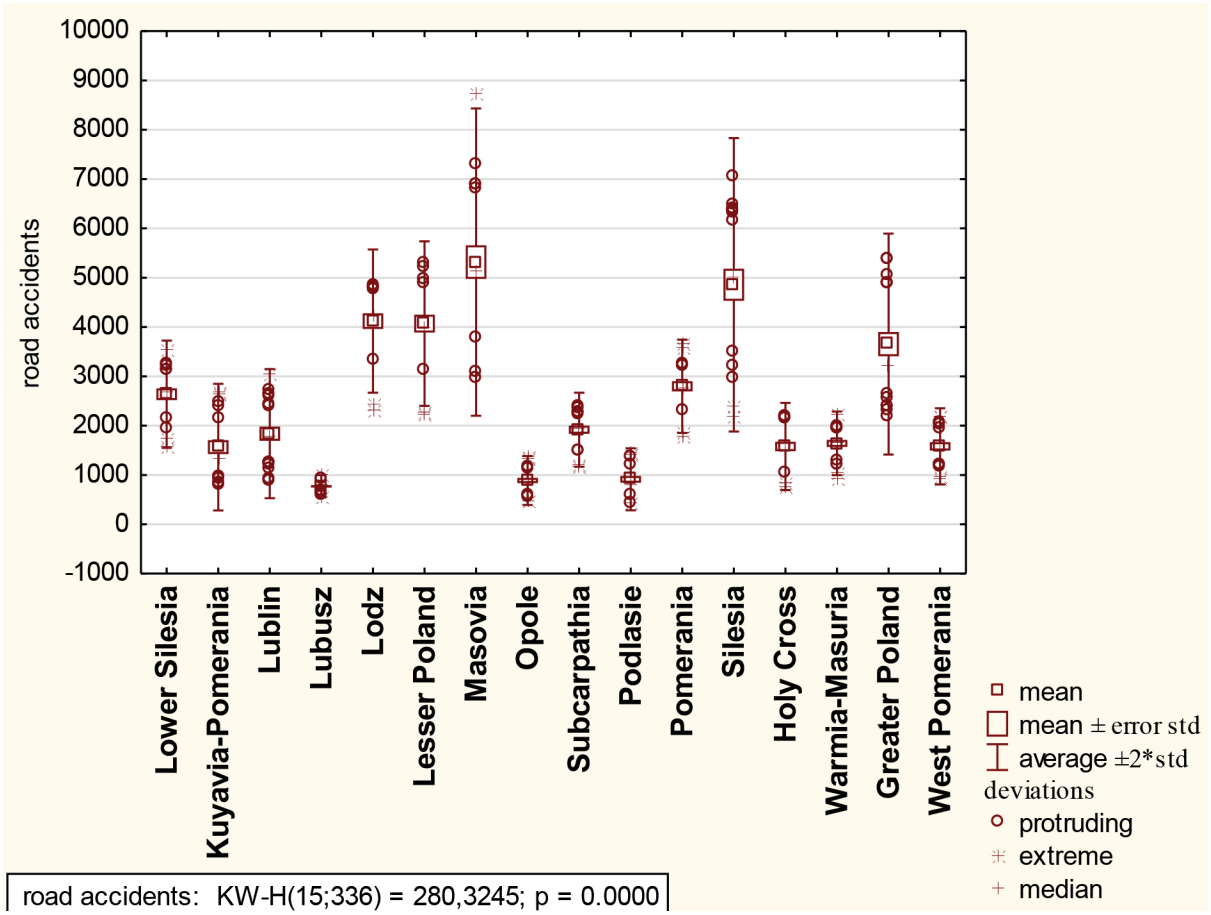


***Figure 4*** *Comparison of the average number of road accidents in Poland by province in the years 2001-2021*

the hypothesis, the equality of the average level of road accidents should be rejected. This means that the number of accidents in Poland show a systematic decrease in the average level of accidents over the years. Furthermore, there is a clear variation in the number of accidents per day, as shown in Figure 4.

Figure 4 clearly shows that the highest number of road accidents occurs at weekends, on Fridays and Saturdays. This is due to the increased traffic at weekends, which causes a high number of road accidents. The least number of road accidents occur on Sundays because workplaces are closed on this day, resulting in less traffic on the roads.

Based on the analysis of the number of road accidents, it can be concluded that they have a seasonal character. Therefore, the selected time series models for forecasting the number of road accidents were used for further analysis.

### 3.1 Forecasting road accidents in the province

To forecast the number of accidents in each province, data from the Polish Police from 2001 to 2021 were used. To examine the impact of the pandemic on the number of road accidents in the analysed provinces, the study was divided into two-time frames:

- From 2001 to 2021 (considering the occurrence of pandemic) and
- From 2001 to 2019 (considering that there were no pandemic).

The study assumes that the start of the pandemic is in 2020, due to the lack of police statistics on the number of road accidents by province and month. The forecast results for each province with pandemic impact (up to 2021) are shown in Figures 5-20. Similarly, accident forecasts for each province without pandemic data (up to 2019) are shown in Figures 21-36. The individual forecasting methods used in the study are coded M1, M2, ....., Mn. The individual forecasting techniques used in the study are as follows:

M1 - moving average method 2-points,
M2 - moving average method 3-points,
M3 - moving average method 4-points,
M4 - exponential smoothing no trend seasonal component: none,
M5 - exponential smoothing no trend seasonal component: additive,
M6 - exponential smoothing no trend seasonal component: multiplicative,
M7 - exponential smoothing linear trend seasonal component: none HOLTA,
M8 - exponential smoothing linear trend seasonal component: additive,
M9 - exponential smoothing linear trend seasonal component: multiplicative WINTERSA,

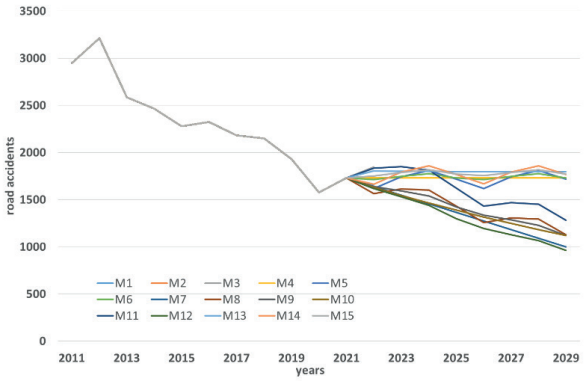


***Figure 5*** *Forecasting the number of road accidents in the Lower Silesian Province in 2022-2029*

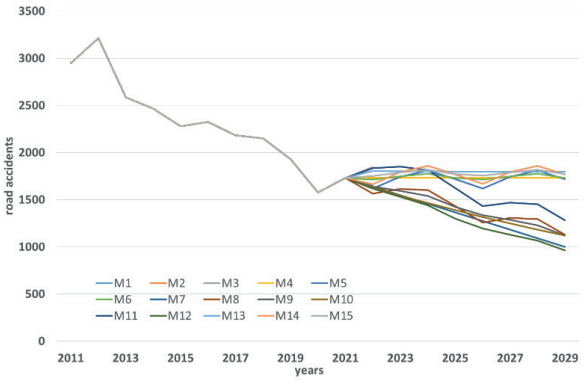


***Figure 5*** *Forecasting the number of road accidents in the Lower Silesian Province in 2022-2029*

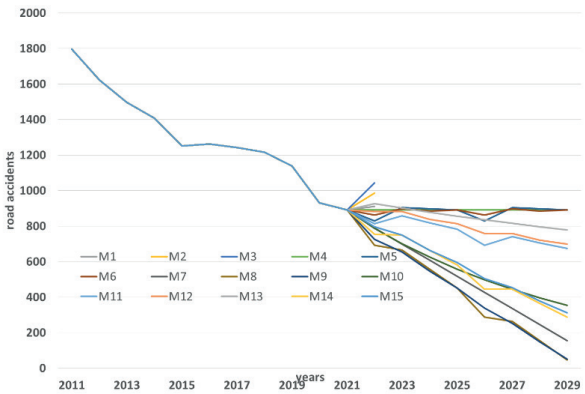


***Figure 6*** *Forecasting the number of road accidents in Lublin Province in 2022-2029*

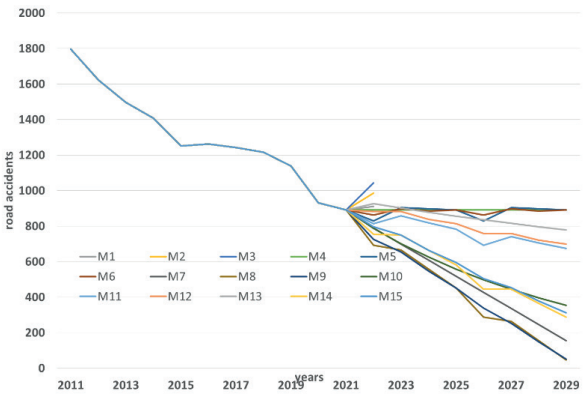


***Figure 6*** *Forecasting the number of road accidents in Lublin Province in 2022-2029*

M10 - exponential smoothing exponential seasonal component: none,
M11 - exponential smoothing exponential seasonal component: additive,
M12 - exponential smoothing exponential seasonal component: multiplicative,
M13 - exponential smoothing fading trend seasonal component: none,
M14 - exponential smoothing fading trend seasonal component: additive,
M15 - exponential smoothing fading trend seasonal component: multiplicative)

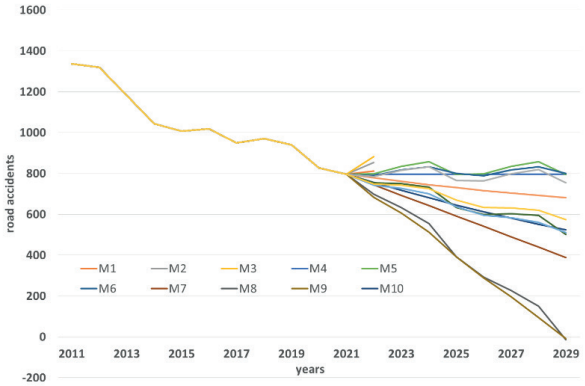


***Figure 7*** *Forecasting the number of road accidents in Kuyavia-Pomerania Province in 2022-2029*

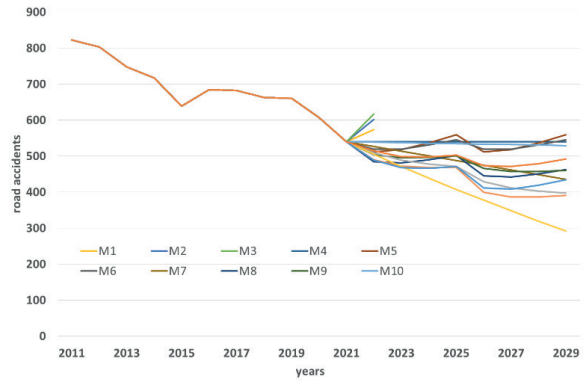


***Figure 8*** *Forecasting the number of road accidents in Lubusz Province in 2022-2029*

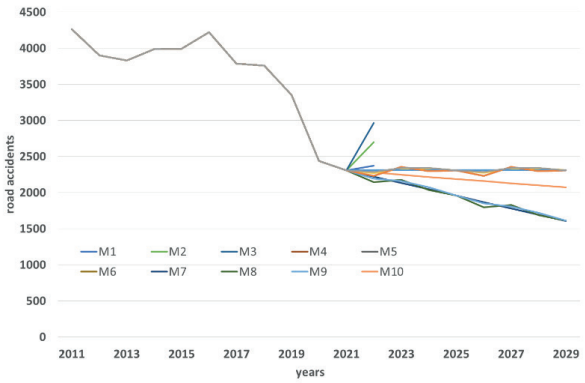


***Figure 9*** *Forecasting the number of road accidents in the Lodz Province in the years 2022-2029*

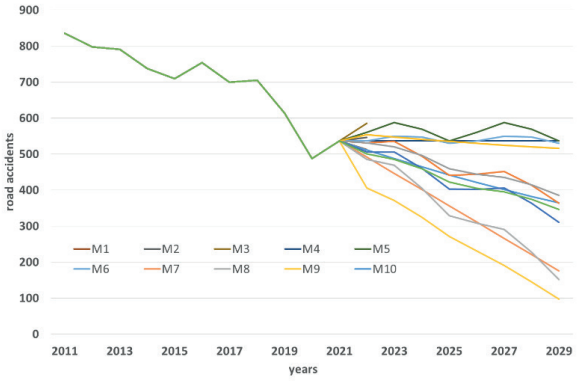


***Figure 10*** *Forecasting the number of road accidents in Opole Province in 2022-2029*

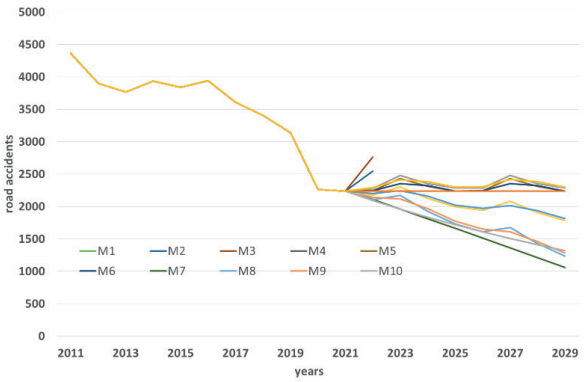


***Figure 11*** *Forecasting the number of road accidents in the Lesser Poland in the years 2022-2029*

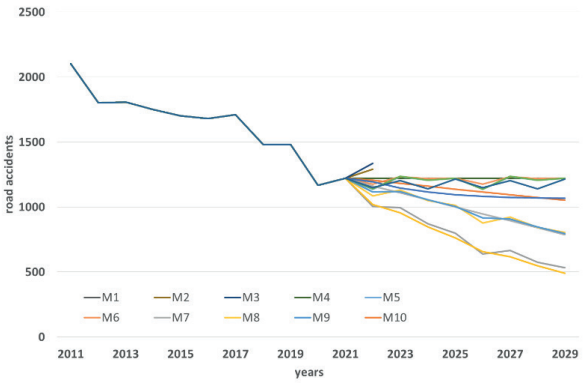


***Figure 12*** *Forecasting the number of road accidents in Subcarpathia Province in 2022-2029*

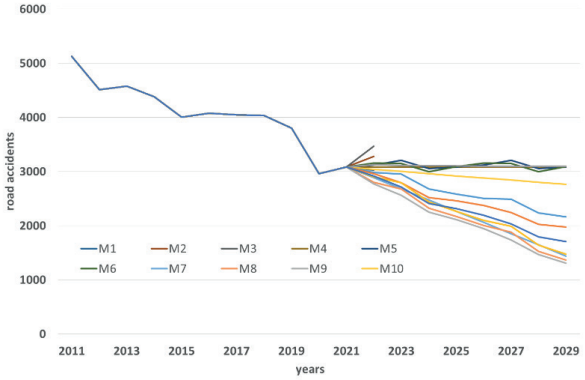


***Figure 13*** *Forecasting the number of road accidents in Masovia Province in 2022-2029*

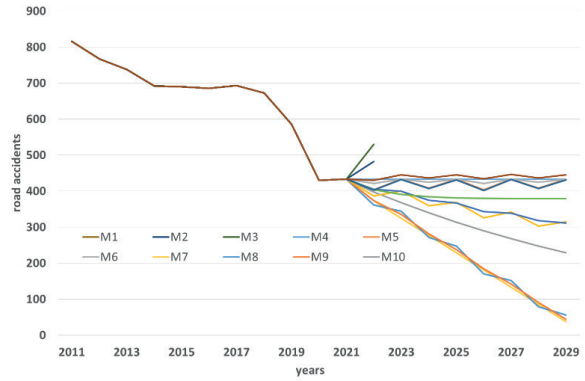


***Figure 14*** *Forecasting the number of road accidents in Podlasie Province in 2022-2029*

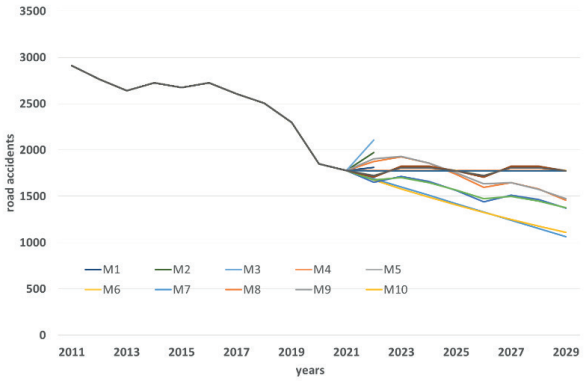


***Figure 15*** *Forecasting the number of road accidents in Pomerania Province in 2022-2029*

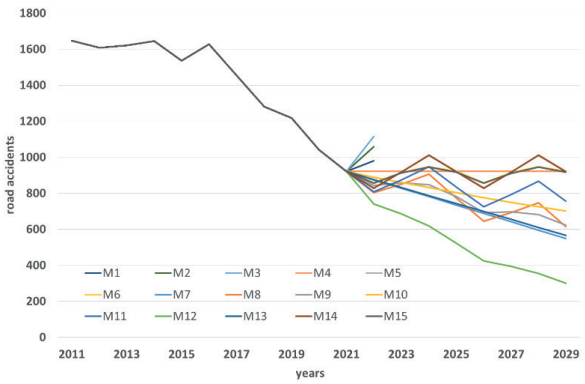


***Figure 16*** *Forecasting the number of road accidents in Warmia-Masuria Province in 2022-2029*

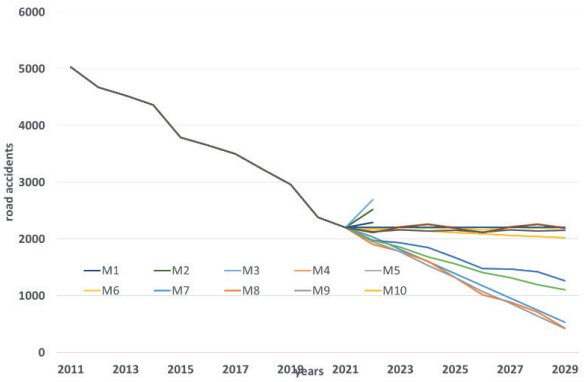


***Figure 17*** *Forecasting the number of road accidents in Silesia Province in 2022-2029*

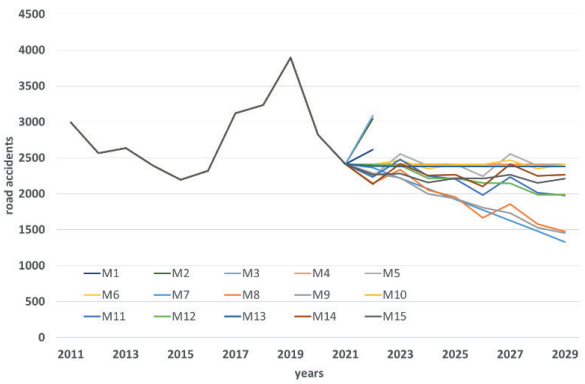


***Figure 18*** *Forecasting the number of road accidents in Greater Poland Province in 2022-2029*

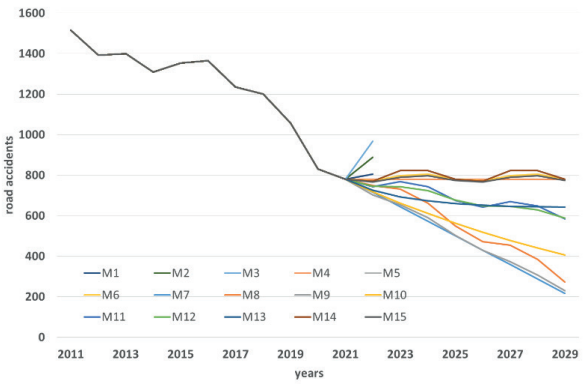


***Figure 19*** *Forecasting the number of road accidents in the Holy Cross Province in 2022-2029*

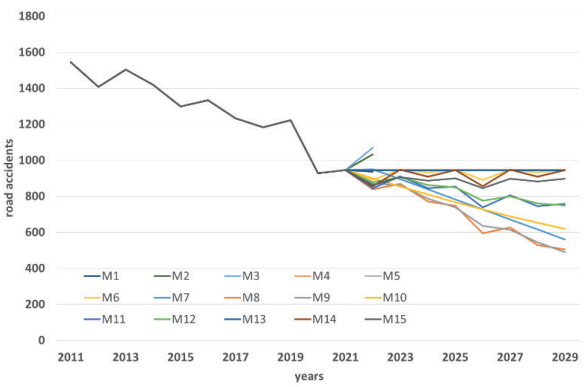


***Figure 20*** *Forecasting the number of road accidents in the West Pomeranian Province in the years 2022-2029*

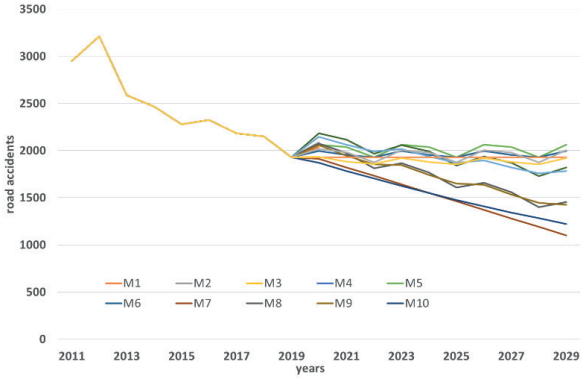


***Figure 21*** *Forecasting the number of road accidents in the Lower Silesian Province in 2020-2029 if there were no pandemic*

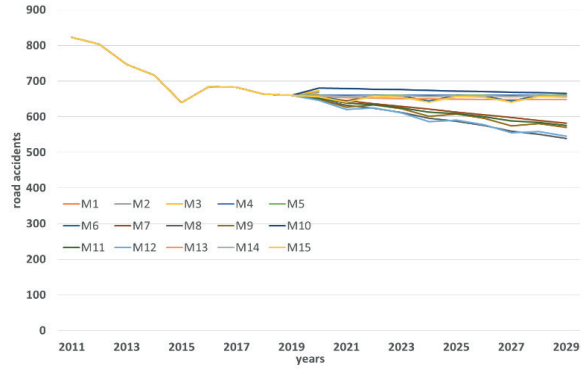


***Figure 22*** *Forecasting the number of road accidents in Lubusz Province in 2020-2029 if there was no pandemic*

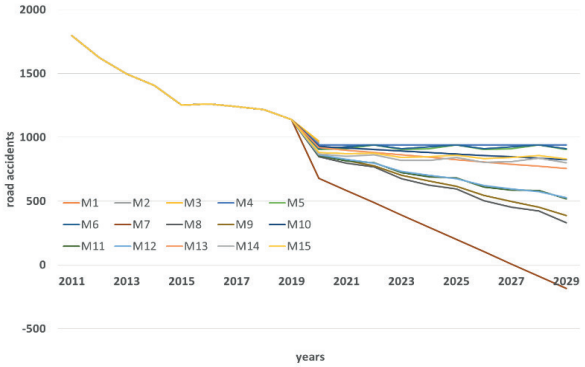


***Figure 23*** *Forecasting the number of road accidents in Kuyavia-Pomerania province in 2020-2029 if there was no pandemic*

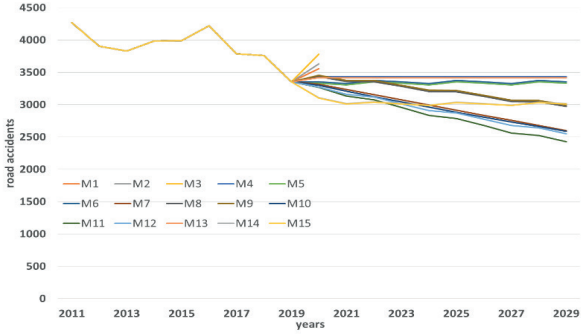


***Figure 24*** *Forecasting the number of road accidents in Lodz Region in the y ears 2020-2029 if there was no pandemic*

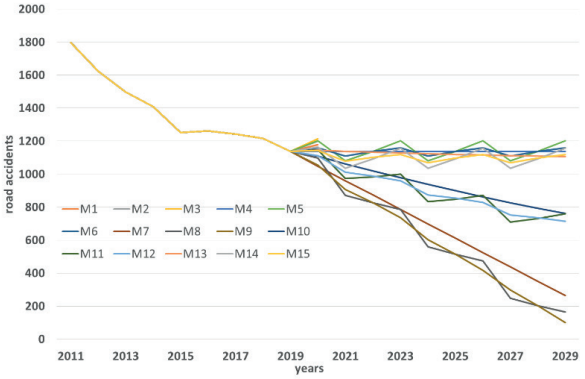


***Figure 25*** *Forecasting the number of road accidents in Lublin province in 2020-2029 if there was no pandemic*

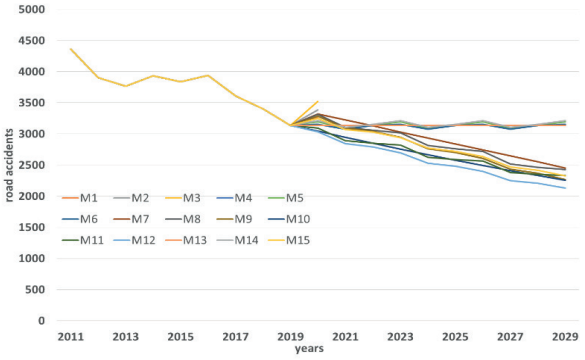


***Figure 26*** *Forecasting the number of road accidents in Lesser Poland province in 2020-2029 if there was no pandemic*

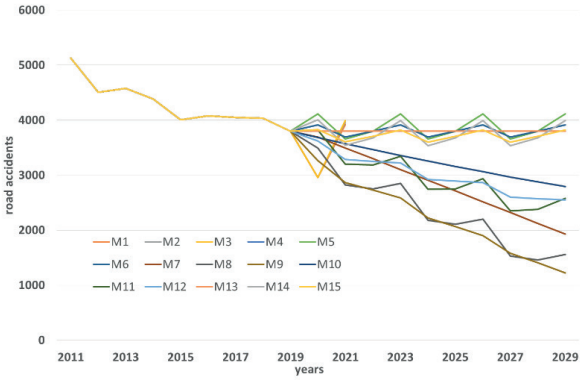


***Figure 27*** *Forecasting the number of road accidents in Masovia province in 2020-2029 if there was no pandemic*

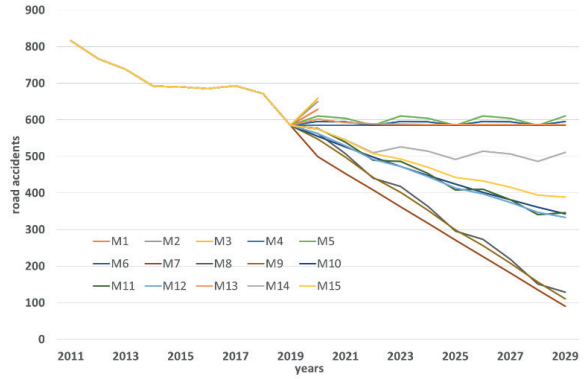


***Figure 28*** *Forecasting the number of road accidents in Podlasie Province in 2020-2029 if there was no pandemic*

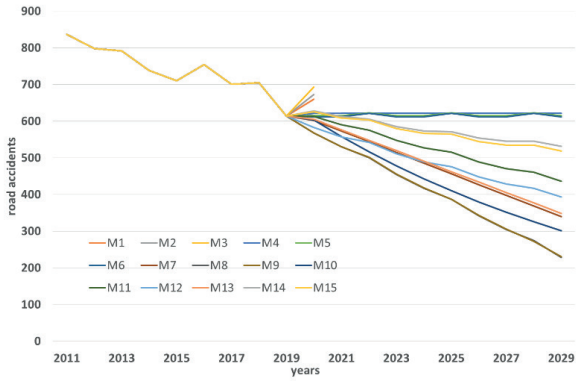


***Figure 29*** *Forecasting the number of road accidents in Opole Province in 2020-2029 if there was no pandemic*

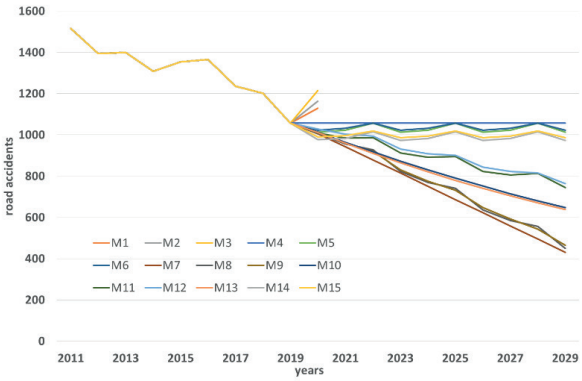


***Figure 33*** *Forecasting the number of road accidents in Holy Cross Province in 2020-2029 if there was no pandemic*

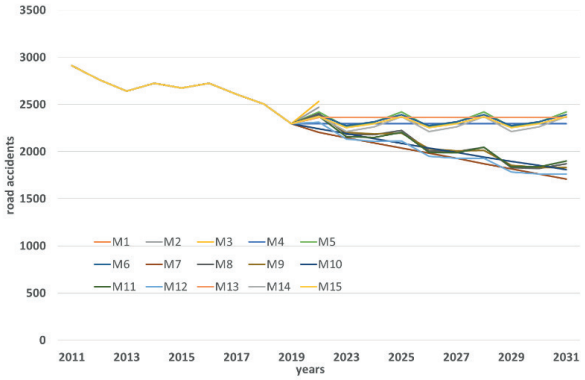


***Figure 30*** *Forecasting the number of road accidents in Pomerania Province in 2020-2029 if there was no pandemic*

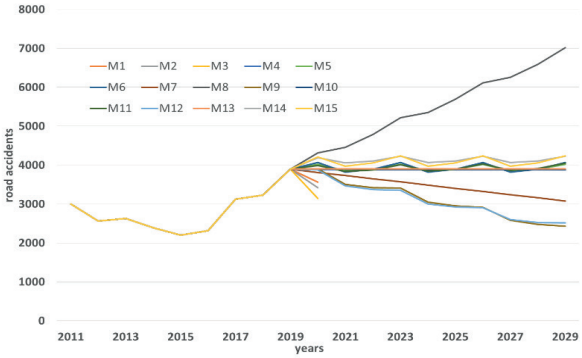


***Figure 34*** *Forecasting the number of road accidents in Greater Poland Province in 2020-2029 if there was no pandemic*

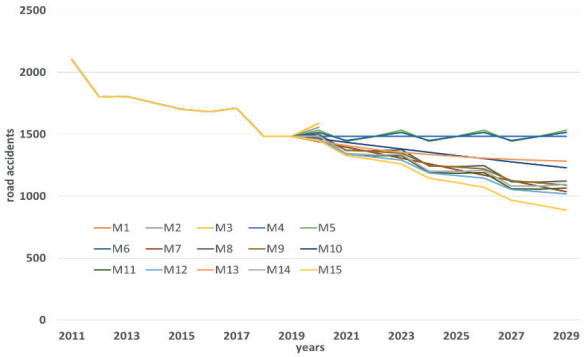


***Figure 31*** *Forecasting the number of road accidents in Subcarpathia province in 2020-2029 if there was no pandemic*

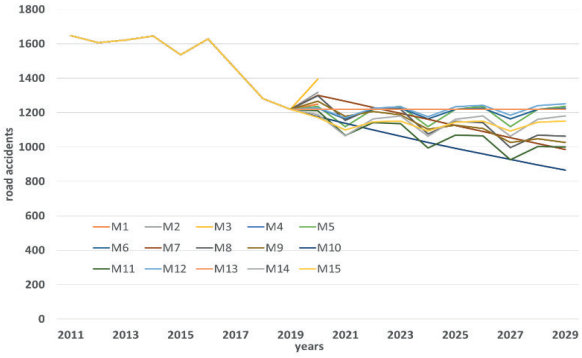


***Figure 35*** *Forecasting the number of road accidents in Warmia-Masuria Province in 2020-2029 if there was no pandemic*

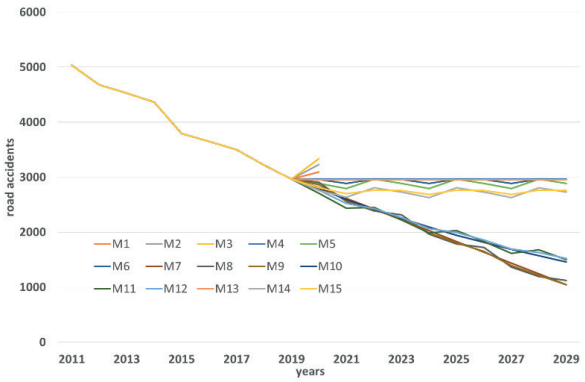


***Figure 32*** *Forecasting the number of road accidents in Silesia Province in 2020-2029 if there was no pandemic*

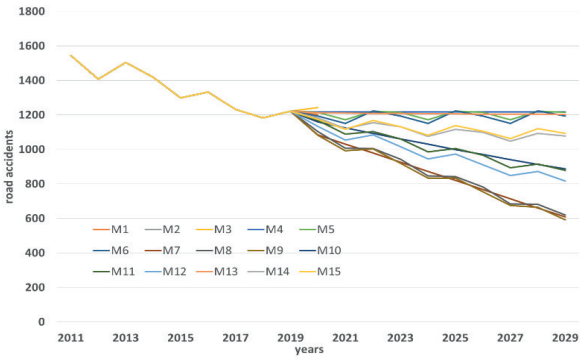


***Figure 36*** *Forecasting the number of road accidents in the West Pomerania Province in 2020-2029 if there were no pandemic*

Based on the results of the pandemic study, the number of road accidents projected at the end of the analysed period 2029 ranges from 44 to 2313 depending on the province and the forecasting technique used. This confirms the fact that the number of road accidents in the studied provinces will decrease year over year.

To compare the number of road accidents depending on the studied province during the pandemic and in the absence of pandemic, the forecast of the number of road accidents was made based on different forecasting techniques, for which the average percentage error is the smallest. The following methods were selected as the best forecasting methods for each province:

- The occurrence of a pandemic: Lower Silesia - M8, Kuyavia-Pomerania - M11, Lublin - M7, Lubusz - M7, Lodz - M12, Lesser Poland - M7, Masovia - M7, Opole - M7, Subcarpathia - M7, Podlasie - M9, Pomerania - M11, Silesia - M9, Holy Cross - M8, Warmia-Masuria - M10, Greater Poland - M7, West Pomerania - M8,
- No pandemic: Lower Silesia - M11, Kuyavia-Pomerania - M12, Lublin - M11, Lubusz - M8, Lodz - M7, Lesser Poland - M11, Masovia - M8, Opole - M12, Subcarpathia - M7, Podlasie - M7, Pomerania - M12, Silesia - M9, Holy Cross - M7, Warmia-Masuria - M7, Greater Poland - M7, West Pomerania - M11,

In the next step the forecast of the number of road accidents for the following years was made in each province in the case no pandemic was there. The research was conducted to answer the question how the pandemic influenced the number of road accidents in the analysed provinces. In order to do so, the Police data containing the number of road accidents in the years 2001-2019 were used [41].

Based on the conducted research, it can be concluded that the estimated number of road accidents by province for the year 2029 ranges from 89 to 3077 depending on the method used and the province. Based on the obtained results of the research, it can be concluded that the number of road accidents in Poland will decrease from year to year in individual provinces.

## 4 Discussion

The projected number of road accidents in 2020 and 2021 in each province was compared to the actual number of road accidents reported by the police (black line in Figures 37 to 52) [41]. Those data are presented in Figures 37 to 52.

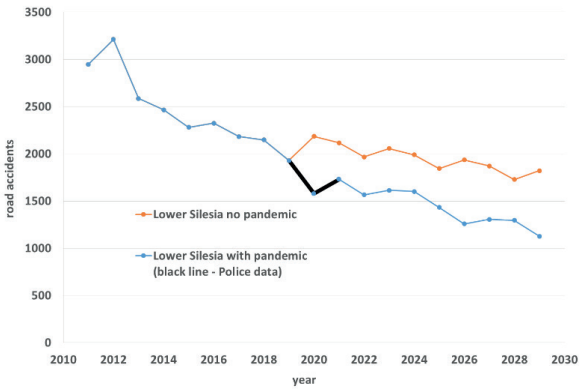


***Figure 37*** *Comparison of the number of road accidents in the Lower Silesian Province with and without the pandemic*

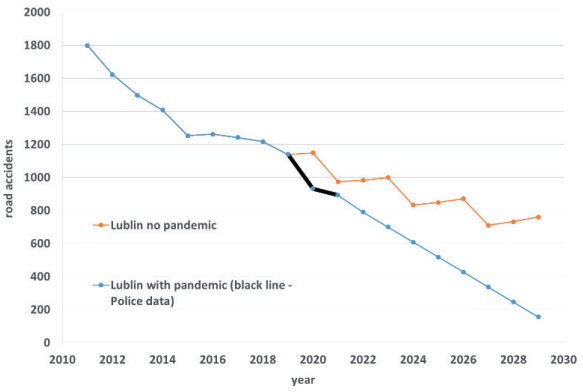


***Figure 39*** *Comparison of the number of road accidents in Lublin Province with and without the pandemic*

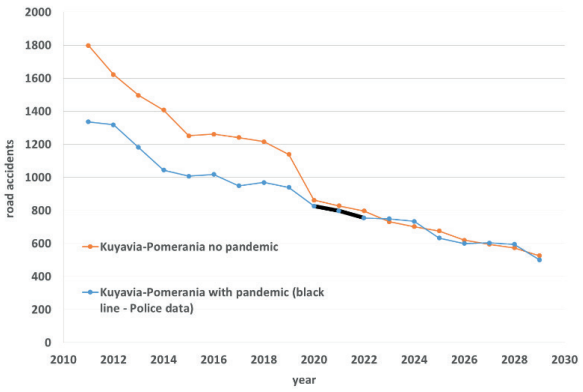


***Figure 38*** *Comparison of the number of road accidents in Kuyavia-Pomerania province with and without the pandemic*

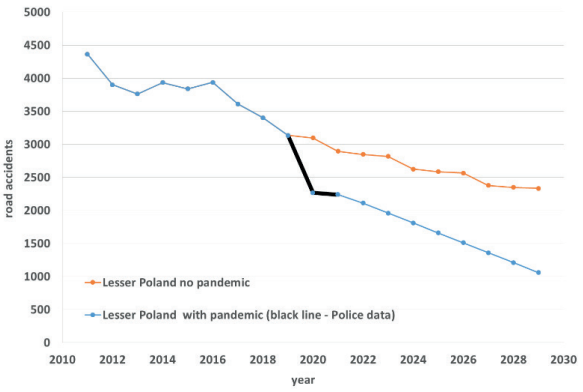


***Figure 40*** *Comparison of the number of road accidents in Lesser Poland province with and without the pandemic*

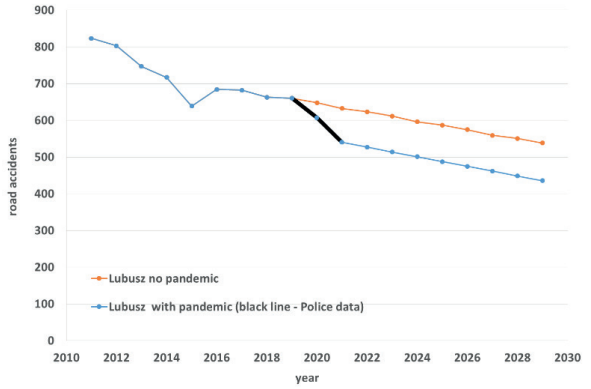


***Figure 41*** *Comparison of the number of road accidents in Lubusz province with and without the pandemic*

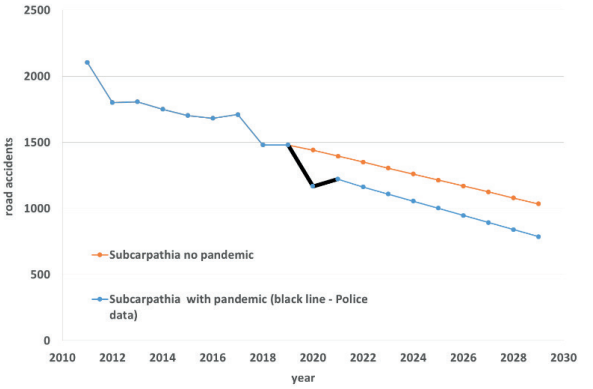


***Figure 45*** *Comparison of the number of road accidents in Subcarpathia province with and without the pandemic*

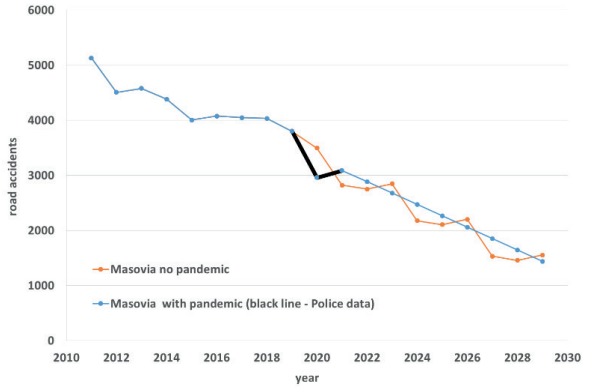


***Figure 42*** *Comparison of the number of road accidents in Masovia province with and without the pandemic*

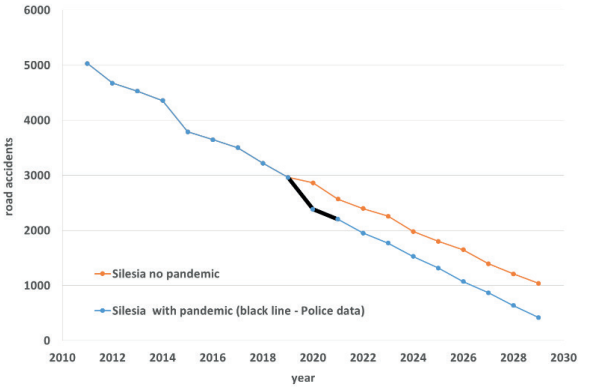


***Figure 46*** *Comparison of number of road accidents in Silesia with and without the pandemic*

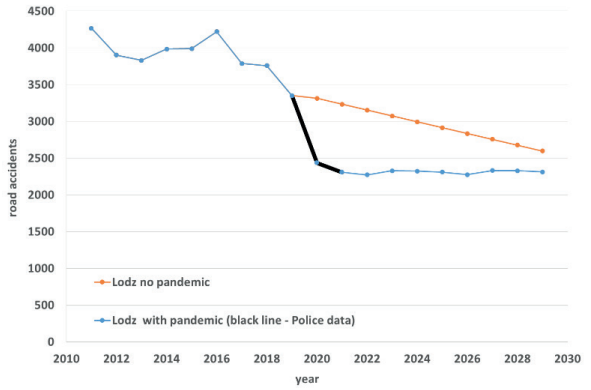


***Figure 43*** *Comparison of the number of road accidents in Lodz Province with and without the pandemic*

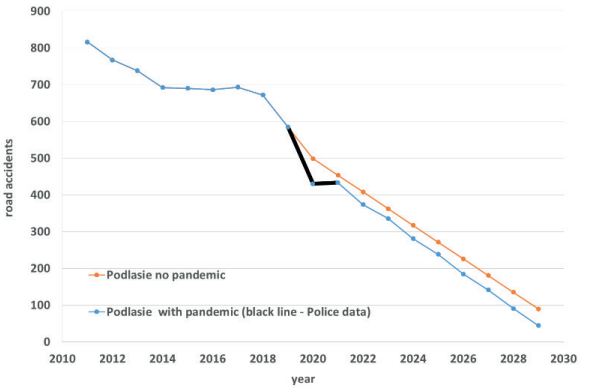


***Figure 47*** *Comparison of the number of road accidents in Podlasie province with and without the pandemic*

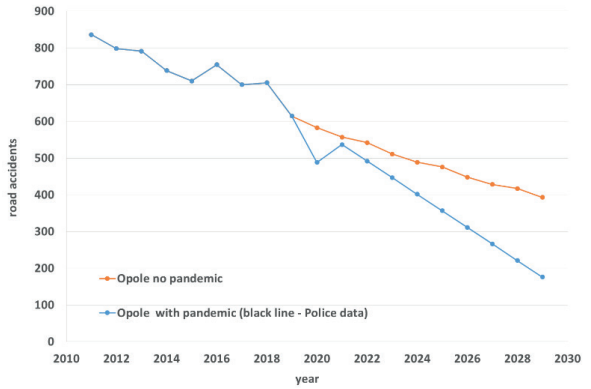


***Figure 44*** *Comparison of the number of road accidents in the Opole Province with and without the pandemic*

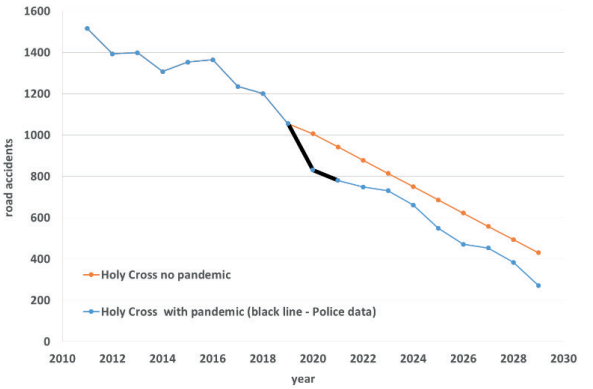


***Figure 48*** *Comparison of the number of road accidents in the Holy Cross Province with and without the pandemic*

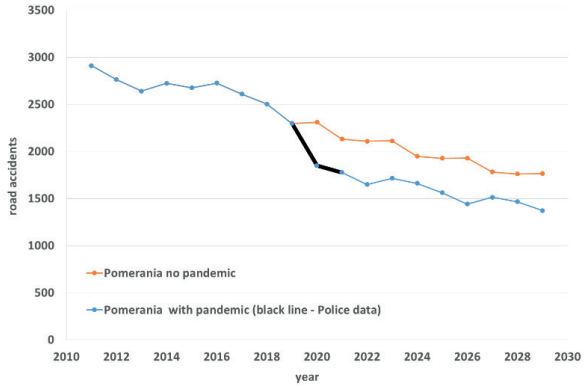


***Figure 49*** *Comparison of the number of road accidents in Pomerania Province with and without the pandemic*

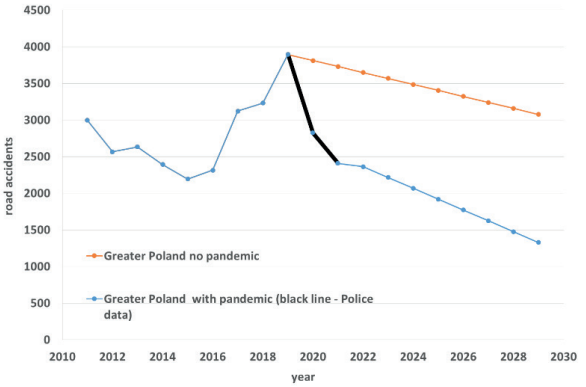


***Figure 51*** *Comparison of the number of road accidents in Greater Poland Province with and without the pandemic*

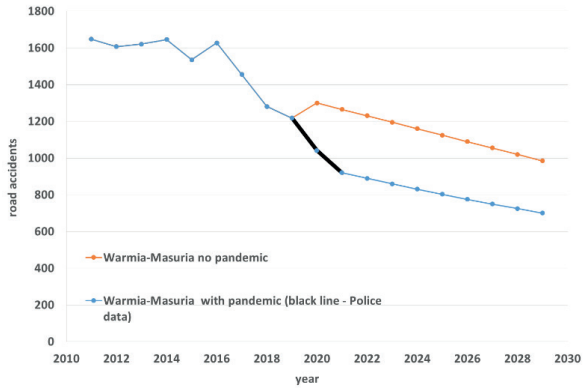


***Figure 50*** *Comparison of the number of road accidents in Warmia-Masuria Province with and without the pandemic*

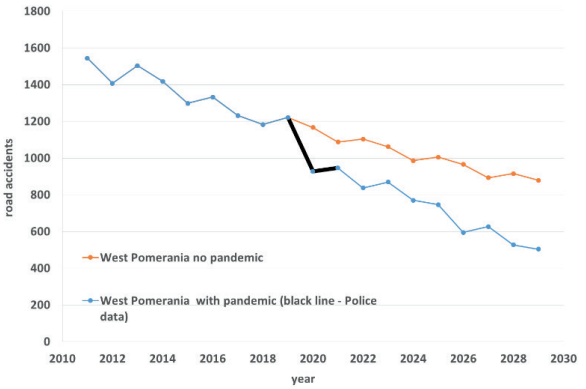


***Figure 52*** *Comparison of the number of road accidents in the West Pomeranian Province with and without the pandemic*

Based on the obtained data, it can be concluded that the pandemic caused a decrease in the number of road accidents in Poland by 21% on average. The ranges depending on the province narrow in the range: 10% for Lubusz province to almost 53% for Lublin province. The most visible decrease is observed in Lublin, Greater Poland and Lesser Poland Provinces. Moreover, the forecasts show, that in the current situation further decrease in the number of road accidents in Poland can be expected.

## 5 Conclusion

The forecasted number of accidents in Poland in individual provinces was determined by the exponential equalization method using the Statistica software. The applied weights were estimated by the program in such a way to minimize the mean absolute error and mean absolute percentage error.

To forecast the number of accidents in individual provinces, Polish Police data from 2001-2021 were used. To examine the impact of the pandemic on the number of road accidents in the analysed provinces, the study was divided into two time frames: 2001- 2021 (with pandemic) and 2001-2019 (without pandemic).

Based on the forecast considering the pandemic, it can be concluded that the forecasted number of road accidents at the end of the analysis period 2029, varies from 44 to 2313 depending on the province and on the forecasting technique used. The forecasted data also confirms the fact that the number of the road accidents in the studied provinces will decrease year by year.

In the next step, the prognosis of the number of road accidents for the following years in each province in the absence of the pandemic was forecasted. The aim of this forecasting analysis was to understand the actual effect of pandemic and its influence on the number of road accidents in the studied provinces. In order to do this, the Police statistics defining the number of road accidents in the years 2001-2019 were used.

Based on the research, it can be concluded that the estimated number of road accidents in each province for 2029 ranges from 89 to 3077, depending on the method used and the province. Based on the presented results of the research it can be concluded that the number of road accidents in Poland will decrease year by year in each province. However, the forecast without the pandemic gives a higher value of crashes as compared to forecasted values with effect of pandemic.

Based on obtained data, it may be stated that the pandemic caused decrease in the number of road accidents in Poland by 21% on average. The variation and spread varies across voivodship areas in the range:

10% for Lubuskie Province to almost 53% for Lubelskie Province. The most visible decrease is observed in the voivodships: Lubelskie, Wielkopolskie and Małopolskie. Moreover, the forecasts indicate that in the current situation further decrease in the number of road accidents in Poland can be expected.

Furthermore, based on analysis of the obtained results it may be stated, that the forecasts of the number of road accidents in Poland for the next year's show a downward tendency, especially in relation to the arrival of Covid-19 virus pandemic. Comparison of forecast to the actual data proved accuracy of the used models. Another important conclusion from the analysis is that there is a significant variation in the number of accidents in individual provinces. Moreover, depending on the voivodeship for which the forecasting is carried out, certain types of forecasting techniques turn out to be more accurate.

**Acknowledgemet**

This publication was created thanks to support under the Operational Program Integrated Infrastructure for the project: Identification and possibilities of implementation of new technological measures in transport to achieve safe mobility during a pandemic caused by COVID-19 (ITMS code: 313011AUX5), co-financed by the European Regional Development Fund.

**References**

[1] *The global status on road safety* [online]. Geneva: World Health Organization, 2018. ISBN 978-92-4-156568-4. Available from: https://www.who.int/publications/i/item/9789241565684

[2] HUDEC, J., SARKAN, B., CABAN, J., STOPKA, O. The impact of driving schools' training on fatal traffic accidents in the Slovak Republic. *Scientific Journal of Silesian University of Technology. Series Transport* [online]. 2021, **110**, p. 45-57. ISSN 0209-3324. Available from: https://doi.org/10.20858/sjsutst.2021.110.4

[3] SZUMSKA, E., FREJ, D., GRABSKI, P. Analysis of the causes of vehicle accidents in Poland in 2009-2019. *LOGI - Scientific Journal on Transport and Logistics* [online]. 2020, **11**(2), p. 76-87. eISSN 2336-3037. Available from: https://doi.org/10.2478/logi-2020-0017

[4] OKUTANI, I., STEPHANEDES, Y. J. Dynamic prediction of traffic volume through Kalman filtering theory. *Transportation Research Part B: Methodological* [online]. 1984, **18**(1), p. 1-11. ISSN 0191-2615. Available from: https://doi.org/10.1016/0191-2615(84)90002-X

[5] DAVIS, G. A., NIHAN, N. L. Nonparametric regression and short-term freeway traffic forecasting. *Journal of Transportation Engineering* [online]. 1991 **117**(2), p. 178-188. ISSN 2473-2907, eISSN 2473-2893. Available from: https://doi.org/10.1061/(ASCE)0733-947X(1991)117:2(178)

[6] LAVRENZ, S., VLAHOGIANNI, E., GKRITZA, K., KE, Y. Time series modeling in traffic safety research. *Accident Analysis and Prevention* [online]. 2018, **117**, p. 368 -380. ISSN 0001-4575, eISSN 1879-2057. Available from: https://doi.org/10.1016/j.aap.2017.11.030

[7] KASHYAP, A. A., RAVIRAJ, S., DEVARAKONDA, A., NAYAK K, S. R., K V, S., BHAT, S. J. Traffic flow prediction models -A review of deep learning techniques. *Cogent Engineering* [online]. 2022, **9**(1), 2010510. eISSN 2331-1916. Available from: https://doi.org/10.1080/23311916.2021.2010510

[8] LANA, I., OLABARRIETA, I. I., VELEZ, M., DEL SER, J. On the imputation of missing data for road traffic forecasting: new insights and novel techniques. *Transportation Research Part C: Emerging Technologies* [online]. 2018, **90**, p. 18-33. ISSN 0968-090X. Available from: https://doi.org/10.1016/j.trc.2018.02.021

[9] WILLIAMS, B. M., HOEL, L. A. Modeling and forecasting vehicular traffic flow as a seasonal ARIMA process: theoretical basis and empirical results. *Journal of Transportation Engineering* [online]. 2003, **129**(6), p. 664-672. ISSN 2473-2907, eISSN 2473-2893. Available from: https://doi.org/10.1061/(ASCE)0733-947X(2003)129:6(664)

[10] DEMISSIE, M. G., DE ALMEIDA CORREIA, G. H., BENTO, C. Exploring cellular network handover information for urban mobility analysis. *Journal of Transport Geography* [online]. 2013, **31**, p. 164-170. ISSN 0966-6923. Available from: https://doi.org/10.1016/j.jtrangeo.2013.06.016

[11] ALI, E. S., HASAN, M. K., HASSAN, R., SAEED, R. A., HASSAN, M. B., ISLAM, S., NAFI, N. S., BEVINAKOPPA, S. Machine learning technologies for secure vehicular communication in internet of vehicles: recent advances and applications. *Security and Communication Networks* [online]. 2021, **2021**, 8868355. ISSN 1939-0114, eISSN 1939-0122. Available from: https://doi.org/10.1155/2021/8868355

[12] SALISU, U., OYESIKU, O. Traffic survey analysis: implications for road transport planning in Nigeria. *LOGI - Scientific Journal on Transport and Logistics* [online]. 2020 **11**(2) p. 12-22. eISSN 2336-3037. Available from: https://doi.org/10.2478/logi-2020-0011

[13] PANDE, A., ABDEL-ATY, M., DAS, A. A classification tree-based modeling approach for segment related crashes on multilane highways. *Journal of Safety Research* [online]. 2010, **41**(5), p. 391-397. ISSN 0022-4375. Available from: https://doi.org/10.1016/j.jsr.2010.06.004

[14] BORUCKA, A., KOZLOWSKI, E., OLESZCZUK, P., SWIDERSKI, A. Predictive analysis of the impact of the time of day on road accidents in Poland. *Open Engineering* [online]. 2021, **11**(1), p. 142-150. ISSN 2391-5439. Available from: https://doi.org/10.1515/eng-2021-0017

[15] YOUSEFZADEH-CHABOK, S., RANJBAR-TAKLIMIE, F., MALEKPOURI, R., RAZZAGHI, A. A time series model for assessing the trend and forecasting the road traffic accident mortality. *Archives of Trauma Research* [online]. 2016, **5**(3), p. 1-6. ISSN 2251-953X, eISSN 2251-9599. Available from: https://doi.org/10.5812/ATR.36570

[16] DUTTA, B., BARMAN, M. P., PATOWARY, A. N. Exponential smoothing state space innovation model for forecasting road accident deaths in India. *Thailand Statistician* [online]. 2022, **20**(1), p. 26-35. ISSN 1685-9057, eISSN 2351-0676. Available from: https://ph02.tci-thaijo.org/index.php/thaistat/article/view/245847

[17] DERETIC, N., STANIMIROVIC, D., AWADH, M. A., VUJANOVIC, N., DJUKIC, A. SARIMA modelling approach for forecasting of traffic accidents. *Sustainability* [online]. 2022, **14**(8), 4403. eISSN 2071-1050. Available from: https://doi.org/10.3390/su14084403

[18] WU, L., GAO, X., XIAO, Y., LIU, S., YANG, Y. Using grey Holt -Winters model to predict the air quality index for cities in China. *Natural Hazards* [online]. 2017, **88**(2), p. 1003-1012. ISSN 0921-030X, eISSN 1573-0840. Available from: https://doi.org/10.1007/s11069-017-2901-8

[19] YADAV, V., NATH, S. Forecasting of PM 10 using autoregressive models and exponential smoothing technique. *Asian Journal of Water, Environment and Pollution* [online]. 2017, **14**(4), p. 109-113. ISSN 0972-9860, eISSN 1875-8568. Available from: https://doi.org/10.3233/ajw-170041

[20] YANG, Z., ZHANG, W., FENG J. Predicting multiple types of traffic accident severity with explanations: a multi-task deep learning framework. *Safety Science* [online]. 2022, **146**, 105522, ISSN 0925-7535, Available from: https://doi.org/10.1016/j.ssci.2021.105522

[21] BISWAS, A.A., MIA, J., MAJUMDER, A. Forecasting the number of road accidents and casualties using random forest regression in the context of Bangladesh. In: 10th International Conference on Computing, Communication and Networking Technologies ICCCNT: proceedings [online]. IEEE. 2019. Available from: https://doi.org/10.1109/ICCCNT45670.2019.8944500

[22] CHUDY-LASKOWSKA, K., PISULA, T. Forecast of the number of road accidents in Poland. *Logistyka / Logistics*. 2014, **6**. ISSN 1231-5478. Available from:

[23] KASHPRUK, N. Comparative research of statistical models and soft computing for identification of time series and forecasting. Opole: Opole University of Technology, 2010.

[24] PROCHAZKA, J., FLIMMEL, S., CAMAJ, M., BASTA, M. Modelling the number of road accidents. Wroclaw: Publishing house of the University of Economics in Wroclaw, 2017.

[25] SUNNY, C. M., NITHYA, S., SINSHI, K. S., VINODINI, V. M. D. ,LAKSHMI, A. K. G., ANJANA, S., MANOJKUMAR, T. K. Forecasting of road accident in Kerala: a case study. In: 2018 International Conference on Data Science and Engineering ICDSE: proceedings [online]. IEEE. 2018. Available from: https://doi.org/10.1109/ICDSE.2018.8527825

[26] DUTTA, B., BARMAN, M. P., PATOWARY, A. N. Application of ARIMA model for forecasting road accident deaths in India. *International Journal of Agricultural and Statistical Sciences* [online]. 2020, **16**(2), p. 607-615. ISSN 0973-1903, eISSN 0976-3392. Available from: https://connectjournals.com/03899.2020.16.607

[27] KARLAFTIS, M., VLAHOGIANNI, E. Memory properties and fractional integration in transportation timeseries. *Transportation Research Part C: Emerging Technologies* [online]. 2009, **17**(4), p. 444-453. ISSN 0968-090X. Available from: https://doi.org/10.1016/j.trc.2009.03.001

[28] DUDEK, G. Exponential smoothing models for short-term power system load forecasting. *Energy Market*. 2013, **3**, 106. ISSN 1425-5960.

[29] KUMAR, S., VISWANADHAM, V., BHARATHI, B. Analysis of road accident. *IOP Conference Series Materials Science and Engineering* [online]. 2019, **590**(1), 012029. ISSN 1757-8981, eISSN 1757-899X. Available from: https://doi.org/10.1088/1757-899X/590/1/012029

[30] PERCZAK, G., FISZEDER, P. GARCH model - using additional information on minimum and maximum prices. Bank and Credit. Num. 2. 2014.

[31] FISZEDER, P. GARCH class models in empirical financial research. Torun: Scientific Publishers of the Nicolaus Copernicus University, 2009.

[32] PATIL, D., FRANKLIN, R., DESHMUKH, S., PILLAI, S., NASHIPUDIMATH, M. Analysis of road accidents using data mining techniques: a survey. *International Research Journal of Engineering and Technology*. 2020, 7(5), p. 6859-6862. ISSN 2395-0072, eISSN 2395-0056.

[33] LI, L, SHRESTHA, S., HU, G. Analysis of road traffic fatal accidents using data mining techniques. In: 2017 IEEE 15th International Conference on Software Engineering Research, Management and Applications SERA: proceedings [online]. 2017. p. 363-370. Available from: https://doi.org/10.1109/SERA.2017.7965753

[34] MARCINKOWSKA, J. Statistical methods and data mining in assessing the occurrence of syncope in the group of narrow-QRS tachycardia (AVNRT and AVRT) [online]. Poznan: Medical University of Karol Marcinkowski in Poznan, 2015 Available from: http://www.wbc.poznan.pl/Content/373785/index.pdf

[35] SEBEGO, M., NAUMANN, R. B., RUDD, R. A., VOETSCH, K., DELLINGER A. M., NDLOVU, C. The impact of alcohol and road traffic policies on crash rates in Botswana, 2004 -2011: time-series analysis. *Accident Analysis and Prevention* [online]. 2008, **70**, p. 33 -39. ISSN 0001-4575, eISSN 1879-2057. Available from: https://doi.org/10.1016/j.aap.2014.02.017

[36] BLOOMFIELD, P. An exponential model in the spectrum of a scalar time series. *Biometrika* [online]. 1973, **60**(2), p. 217 -226 eISSN 1464-3510. Available from: https://doi.org/10.1093/biomet/60.2.217

[37] GORZELANCZYK, P., PYSZEWSKA, D., KALINA, T., JURKOVIC, M. Analysis of road traffic safety in the Pila Poviat. *Scientific Journal of Silesian University of Technology. Series Transport* [online]. 2020, **107**, p. 33-52. ISSN 0209-3324. Available from: https://doi.org/10.20858/sjsutst.2020.107.3

[38] CHEN, C. Analysis and forecast of traffic accident big data. *ITM Web of Conferences* [online]. 2017, **12**, 04029. eISSN 2271-2097. Available from: https://doi.org/10.1051/itmconf/20171204029

[39] RAJPUT, H., SOM, T., KAR, S. An automated vehicle license plate recognition system. *Computer* [online]. 2015, **48**(8), p. 56-61. ISSN 0018-9162, eISSN 1558-0814. Available from: https://doi.org/10.1109/MC.2015.244

[40] Central Statistical Office [online] [accessed 2022-03-15]. Available from: www.gus.pl

[41] Statistic Road Accident [online] [accessed 2022-02-12]. Available from: https://statystyka.policja.pl/

# URBAN ROAD TRANSPORT NETWORK ANALYSIS: MACHINE LEARNING AND SOCIAL NETWORK APPROACHES

**Emre Kuşkapan [1], M. Yasin Çodur [2], Ahmet Tortum [3], Giovanni Tesoriere [4], Tiziana Campisi [4,*]**

[1]Department of Civil Engineering, Engineering and Architecture Faculty, Erzurum Technical University, Erzurum, Turkey
[2]College of Engineering and Technology, American University of the Middle East, Kuwait
[3]Department of Civil Engineering, Engineering Faculty, Ataturk University, Erzurum, Turkey
[4]Faculty of Engineering and Architecture, Kore University of Enna, Enna, Italy

*E-mail of corresponding author: tiziana.campisi@unikore.it

***Resume***

Traffic congestion is one of the most significant problems in urban transportation. It has been increasing, especially in regions close to intersections. Several methods have been developed to reduce the traffic congestion. One of the analysis methods is social network analysis (SNA). This method, which has increased use in transportation, can quickly identify the most central intersections in transportation networks. Improvements to central intersections, identified in a road network structure, speed up the traffic flow across the entire network structure. In this study, the Istanbul highway transportation network has been examined and values for a series of network centrality measures have been calculated using the SNA. The accuracy and error scales of the centrality values were compared using a machine learning algorithm. The Bonacich power centrality has been the best performance. Based on the study results the most central intersections in Istanbul have been determined.

Available online: https://doi.org/10.26552/com.C.2022.4.A232-A245

***Article info***
Received 7 May 2022
Accepted 20 September 2022
Online 17 October 2022

***Keywords:***
central intersections
machine learning
transportation planning
urban transportation

ISSN 1335-4205 (print version)
ISSN 2585-7878 (online version)

## 1 Introduction

The traffic congestion is one of the important problems in daily life, in cities. Traffic jams can prevent people from getting where they want to go on time. In order to prevent this situation, it is necessary to carry out studies that would minimize the congestion. A wide range of detailed information is required to estimate congestion and to evaluate solutions for transport planning. The traditional method is to calculate the traffic manually and to report the traffic situations. This method's application has significantly decreased in recent years. Traditional models can require a lot of time and effort; consequently, they are not economical [1-2]. In addition, traffic congestion negatively impacts drivers through increased travel time and delayed destination arrival. To reduce these negative effects, many transport studies were conducted. For example, improvements at intersections where the traffic congestion is intense can provide more permanent solutions for the road network [3]. At the same time, to understand the network performance and design the best transportation planning, it is imperative for transport planners to consider many factors (for instance traffic volume, location of intersections and the connection of roads). Travelers' travel times are variables affected by traffic incidents and bad weather conditions. Therefore, it is difficult to analyze and model different traffic conditions [4].

Various numerical traffic data must be provided for these analyses and models. Thanks to development of technology and intelligent transportation systems, vehicle counting hoses, motion detector cameras, computers and counting units used, it is very easy to obtain traffic volume data [5]. With development of these counting methods, traffic counts and analyses have become quite practical. In the past several years, the analysis of network traffic has become a subject of continuous research in various sub-fields of computer networks. Many researchers have implemented effective network traffic algorithms for analysis and the prediction of network traffic [6-7]. Similarly, technical information used in these analyses is useful to formulate the relationship between the traffic composition and the ring road safety and to formulate recommendations for designing the vehicle safety improvement strategies

[8]. As an example of this situation, analyses to investigate the effects of hazardous substances on road transportation and the effects of risk factors leading to accidents can provide theoretical support for adoption of effective measures to reduce the risks associated with road transportation [9]. Likewise, traffic problems can be seriously prevented through the correct usage and analysis of traffic data. Thanks to this, delays can be minimized by reducing the traffic congestion on the roads during the traffic peak hours. Additionally, the optimum order can be achieved by examining how drivers behave and react to bottlenecks with varying traffic capacities from time to time, user balance and optimal traffic order of the system. For this reason, it is very important to provide the traffic data and conduct analyses using this data [10].

## 2 Literature review

Traffic analysis methods have gained prominence in recent years. Social network analysis (SNA) technique has recently been utilized to analyze traffic data for traffic analysis. The SNA is frequently used in many fields, such as sociology, anthropology, social psychology, communication, economics and mathematics. The SNA, which is an interdisciplinary field of study, examines the structure of communities, tries to describe the network structure and visualizes the relationships that cannot be easily observed between the communities by modeling the existing connections [11].

The SNA-based approach focuses on links and relationships within the community. It can be observed that studies on SNA have proliferated in recent years and researchers' interest in the subject remains strong. Some of the studies in which the SNA has been applied in the field of transportation are included in this study. In one of the existing studies, the dynamic development of taxi sharing behaviors and the social network structure focused on taxi sharing were investigated. The advantages of taxi sharing based on a social network, an increasing match ratio and a satisfaction level comparable to the satisfaction level associated with trip-based methods were demonstrated [12]. In another study, Pritchard et al. [13], underlined the importance of considering the social aspects of accessibility and mobility when planning for urban transport systems using the SNA. Cheng et al. [14], investigated the use of centralities to identify central nodes in a transport network to improve the design of the transport network and address network failures. They implemented these centralities in the Singapore subway network and compared them to traditional topology-based centralization measures. In another study, a road network was constructed using the SNA. Three types of centralities were calculated: degree centrality, closeness centrality and betweenness centrality. These node centralities explain how important a node is in a network [15]. Watts and Witham, [16] used the SNA method to analyze the communication networks of organizations that promote sustainable transport policy in the UK. At the end of the study, they found that different types of centrality, such as degree and betweenness centrality, have stronger relations to influence than closeness centrality. Networks offer many different roles for organizations that need to be effective. For this reason, organizations should carefully consider which role they want to play and how they can properly position themselves in the context of their network. El-adaway [17], considered the most important step in the implementation of the SNA in the field of transportation. He used the SNA to analyze the intersections in Louisiana in the United States, modeling the intersections as nodes and modeling the streets as edges. Using the volume maps for the connection forces between the node points, he obtained four different centrality measures for all the intersections in each case study. By interpreting those centrality values, he identified the most central intersections in the road network structure. The results indicated that the SNA intersection modeling aligns with current congestion studies and Regional Transportation Planning decisions in Louisiana. At the end of the study, the SNA is cited as an important method for analyzing and improving transport networks. El-adaway et al. [18], also mentions that the use of the SNA, which is practical and economic, will create a new perspective that will allow for making more effective infrastructure network decisions when adopted alongside traditional transport network analysis techniques.

When similar studies on this line of research are examined, few studies on SNA in transportation engineering have been conducted. This paper presents one of the few studies to have focused on this issue. In addition, unlike in other studies, the effect of a new road, added to a road network, on the whole network structure was examined. Using the traffic volume data, two different case studies were investigated from before and after the construction of the 3rd Bosphorus Bridge and the Northern Ring Motorway. The five different centrality values, obtained for both cases, were compared by using support vector machine, which is a machine learning algorithm and the most central intersections in the Istanbul road network were detected. Using the SNA as the first analysis step to identify central intersections will assist decision-makers in better focusing their more detailed analyses using traditional methods in such areas only compared to the overall network. This will significantly decrease the invested resources in transportation planning and will create a more integrated and comprehensive perspective for evaluating the transportation networks.

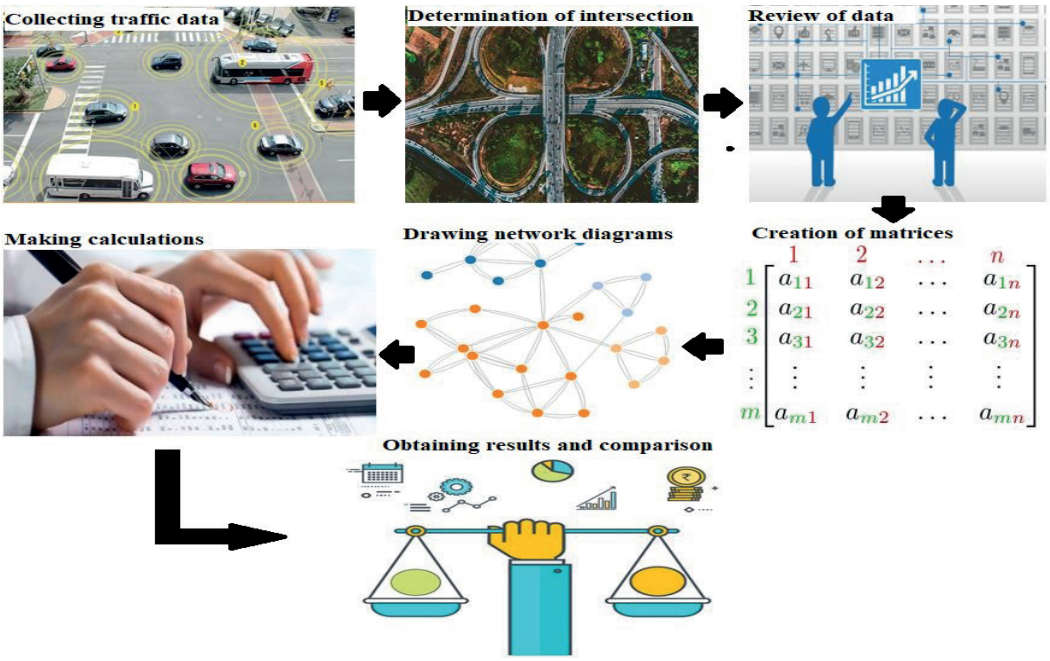


***Figure 1*** *Flow chart of SNA application in transportation planning*

## 3 Method and network model

The SNA examines the relationships between individuals or objects in terms of political, formal-informal, familial, geographical, or any other factors. SNA, which also means the digitization and scientific making of interpersonal relations, is used to explore the relations between various organizations, or the networks formed by these organizations and important events [19]. Therefore, the network analysis allows for examining how the elements, organizations, or systems within a network affect the way the network functions. The advantage of SNA is that, unlike many other methods, it focuses on interactions (rather than individual behavior); it is also less time-consuming and more practical than many other methods. In addition, it is an interdisciplinary analysis method that can be applied in many areas, such as social networks, political networks, electricity networks and transportation networks. The SNA can be especially important to a country's policies when it is applied to transportation networks because it is an indisputable fact that innovative strategies for transportation policies contribute to sustainable economic growth [20]. Implementation of the SNA in transportation networks is provided, as shown in Figure 1.

### 3.1 Centrality

Centrality focuses on the following question: "Who is the most important and centralized actor (node) in the network?" Measures of local centrality are those that examine the very close environment of the individual; however, to understand an individual's position in the social network, it is necessary to examine its place within the general structure of the network. In the SNA, the node point with the highest centrality value is called the most central (important) node [21]. Similarly, the most central intersection points in the road network structure are called the most central intersections. When determining the most central intersections, not only the traffic volume values of the intersections are considered. At the same time, the location of the intersection points in the network structure and the neighbor status of the intersections are also examined. Therefore, each concept of centrality examines the network in a different way.

#### 3.1.1 Closeness centrality

This centrality measures the degree of closeness (or distance) of a node in the network to (or from) other nodes, either directly or indirectly. Closeness is a sum of individual's shortest distances to other individuals in the network and the ability to access information reflects how quickly a node can connect to other nodes in the network. Additionally, the closeness measure can calculate the weakness or strength of the connections between the nodes [22]. It is calculated using equations (1) and (2). In this centrality, the concept is not necessary for a node to have a high degree and closeness. Closeness centrality defined as $C_C(i)$ in Equation (1). Normalized closeness centrality defined as $C_c'(i)$ in Equation (2). Where $d$ $(i, j)$ represents the distance between vertices $i$ and $j$; N represents the number of nodes in the network.

$$C_C(i) = \left[\sum_{j=1}^{N} d(i,j)\right]^{-1}, \quad (1)$$

$$C_c'(i) = (C_C(i))/(N-1). \quad (2)$$

### 3.1.2 Degree centrality

Degree centrality is equal to the number of ties (links) of a node to other nodes. It not only reflects the connectivity of each node to other nodes, but it also relies on the network size. In other words, the larger the network, the higher the maximum degree of centralization [23]. Thus, a certain degree of centrality indicates that a node either has many connections in a small network or has only a small number of ties in a large network. When the degree of centrality of any node is calculated, the sum of the tie values to that node is calculated as shown in Equation (3). $X$ is the factor, $i$ and $j$ are the network nodes.

$$C_d(i) = \sum_j X_{ij}. \quad (3)$$

### 3.1.3 Betweenness centrality

This centrality addresses how the relationships between the binary elements that are not directly connected are controlled or directed by other nodes. Betweenness centrality is an important indicator of excessive information exchange within a network or control of the flow of resources. This measurement is based on the shortest number of ties passing through a node [24]. It is calculated using Equations (4) and (5).

$$C_b(i) = \sum_{j<k} g_{jk}(i)/g_{jk}, \quad (4)$$

usually normalized by:

$$C_b'(i) = C_b(i)/[(n-1)(n-2)/2], \quad (5)$$

where $g_{jk}g_{jk}$ is the shortest number of ties connecting $jk$ and $g_{jk}$ is the number that node $i$ is on.

### 3.1.4 Eigenvector centrality

Eigenvector centrality shows the importance of a node in the network. The eigenvector center is not equal to all the connections in the network; it assumes that efficient nodes act on less effective nodes to which they are associated. It depends on the number of connections and the quality of the ties. If a node has a small number of high-quality connections, it can cross a node with a large number of medium-quality connections. For network G = (V, E), with |V| as the number of nodes, let the adjacency matrix A = ($a_{v,t}$). M(v) is a set of neighbors of v, $a_{v,t}$ = 1 if node v is tied to node t and $a_{v,t}$ = 0 otherwise, λ is a constant [25]. The eigenvector centrality value of v is obtained by equation (6):

$$x_v = \frac{1}{\lambda}\sum_{t\in M(V)} x_t = \frac{1}{\lambda}\sum_{t\in G} a_{v,t}x_t. \quad (6)$$

### 3.1.5 Bonacich power centrality

Bonacich power is a measure that determines the node centrality based on the degree centrality of adjacent nodes, where a node's degree centrality is its summed connections to others, weighted by their centralities. This centrality depends not only on how many connections a node has but also on how many connections its neighbors have (and on how many connections its neighbors' neighbors have and so on). The highest value found here represents the most powerful node on the network, as shown in equation (7) [26].

$$C(\alpha,\beta) = \alpha(I-\beta R)^{-1}R1, \quad (7)$$

where R is the adjacency matrix (can be valued), β reflects the extent to which you weight the centrality of nodes tied to the studied node, I is the identity matrix, α is a scaling vector, 1 is a vector of all ones.

## 3.2 Ucinet and netdraw

Ucinet is a comprehensive package for analysis of the social networks. It can read and write in several formatted text and Excel files. In addition, it can create a network model (i.e. using Netdraw), constitute centrality measures, conduct a matrix analysis and conduct a statistical analysis based on permutation. The Netdraw Software is also included in this package to integrate with Ucinet and allow for drawing diagrams of social networks. No additional program is needed to create network diagrams from data in the Ucinet Software as well as in the Netdraw Software. Since this program is free, it is frequently preferred in the SNA [27].

## 3.3 Support vector machine (SVM)

In machine learning, the SVM is a supervised learning algorithm. It can be used for classification, as well as for regression. It is very efficient for many applications in science and engineering, especially for classification problems (pattern recognition). The main objective is to identify a hyper-plane that can classify the data points distinctively. The SVM classifier can be made non-linear by mapping the input variables to a higher dimension space and then applying the algorithm to the processed parameters [28]. This mapping is done using the SVM kernels. Two kernels are evaluated, radial basis function (RBF) and polynomial. Expressions for radial basis function (RBF) and polynomial in Scikit-

learn are shown in equations (8) and (9), respectively [29].

$$K(x,z) = \exp(-y\|x-z\|^2), \tag{8}$$

$$K(x,z) = (y(x^T z) + c)^d. \tag{9}$$

In equations (8) and (9), K is the kernel function, $x$ and $z$ are vectors in the input space, $c$ is the coefficient, $d$ is the order of the polynomial and $\gamma$ is the kernel parameter. The kernel parameter $\gamma$ gives the influence of a single training data point [30].

It is necessary to compare the accuracy values of the order of the central intersections determined by the concepts of centrality. Performance analysis can be performed for each concept of centrality using the Kappa statistics, mean absolute error (MAE) and root mean squared error (RMSE) values. MAE and RMSE represent error scales and Kappa statistic expresses the accuracy value [31]. These calculations can be made easily with Weka (Waikato Environment for Knowledge Analysis).

The Kappa statistics is frequently used to test interrater reliability. The importance of rater reliability lies in the fact that it represents the extent to which the data collected in the study are correct representations of the variables measured. One may compare two or more tests or examinations to measure their agreement beyond that caused by chance. The Kappa statistic is formulated as :

$$K = \frac{p_o - p_e}{1 - p_e}, \tag{10}$$

where $p_o$ and $p_e$ are expectation and observation, respectively. The meaning of this calculation has come into question and ranges for the measure vary. However, an example would include the following: $K$ < 0.20 = poor agreement; $K$ = 0.21 to 0.40 is fair; $K$ = 0.41 to 0.60 is moderate; $K$ = 0.61 to 0.80 is substantial; and $K$ > 0.81 is good [32].

The MAE is a measure of errors between paired observations expressing the same phenomenon. To put it shortly, it is the average of all the absolute errors and a model evaluation metric used with regression models. MAE error of a model with respect to a test set is the mean of the absolute values of the individual prediction errors on over all the instances in the test set. Each prediction error is the difference between the true value and the predicted value for the instance. It also measures closeness of the predictions to the eventual outcomes. Examples of Y versus X include comparisons of predicted versus observed, subsequent time versus initial time and one technique of measurement versus an alternative one. It can be expressed by equation (11), where $x_{f,i}$ and $x_{o,i}$ are the i-th expectation and observation, respectively:

$$MAE = \frac{1}{N}\sum_{1=1}^{N}|x_{f,i} - x_{o,i}|. \tag{11}$$

The RMSE is the square root of mean squared error; it measures the differences between values predicted by a hypothetical model and the observed values. In other words, it measures the quality of the fit between the actual data and the predicted model. The RMSE is one of the most frequently used measures of the goodness of fit of generalized regression models. It can be expressed as: $x_{f,i}x_{o,i}$

$$RMSE = \sqrt{\frac{1}{N}\sum_{1=1}^{N}(x_{f,i} - x_{o,i})^2}. \tag{12}$$

### 3.4 Case studies

Traffic counts represent the volume of traffic in both directions in a 24-hour period. Traffic counting systems are categorized into two main groups: road systems and roadside systems. Roadside systems, such as pneumatic hose systems, magnetic loop systems and systems with piezoelectric sensors are used by the General Directorate of Highways [33]. The most commonly used roadside systems are manual counting systems. In recent years, advances in traffic management applications within the scope of intelligent transportation systems have fostered roadside counting systems using technologies such as video visual systems, passive and active infrared, ultrasonic, radar, laser and microwave. Traffic volume values are obtained using these counting systems. For the traffic volume, the most common method on wide roads is the counting method, using hoses laid on the roads. The calculated traffic volume is obtained using these counting methods, as well as the calculation of average estimated value. These data are derived from the annual average daily traffic values. In this study, the compound of the state roads and ring roads in Istanbul traffic volume maps were used. Traffic volume values were obtained from the General Directorate of Highways and Transport Management Center of Istanbul Metropolitan Municipality [34-35]. The left side of Istanbul is located on the European continent and the right side is located on the Asian continent.

There are three Bosphorus Bridges connecting the two continents. The 1st and 2nd Bosphorus Bridges (i.e. the 1st is 15 Temmuz Sehitler Bridge and the 2nd is Fatih Sultan Mehmet Bridge) are old structures, while the 3rd Bosphorus Bridge (Yavuz Sultan Selim Bridge) was constructed recently. Accordingly, two different situations were investigated to determine the effect of the newly constructed 3rd Bosphorus Bridge on the traffic of Istanbul. The traffic volumes from before and after the construction of the 3rd Bosphorus Bridge and the Northern Ring Motorway are illustrated in Figures 2 and 3 as the first and second case studies. In the first case, 13 intersections have formed, belonging to the transportation network consisting of ring roads and state roads. In the second case, 14 intersections (added I node) have formed because new roads have been added to the network. The 3rd Bosphorus Bridge added to


***Figure 2*** *The first case study; traffic volume map from before the construction of the 3rd Bosphorus Bridge and the Northern Ring Motorway*


***Figure 3*** *The second case study; traffic volume map from after the construction of the 3rd Bosphorus Bridge and the Northern Ring Motorway (Connection of I and M intersections)*

the highway network structure has reduced the traffic load of the other two Bosphorus Bridges. Traffic flow has accelerated in the 1st and 2nd Bosphorus Bridges, especially due to the obligation to cross the 3rd Bosphorus Bridge for heavy land vehicles. With this situation, the 3rd Bosphorus Bridge has become an important transit point as it facilitates access to settlements in the regions near A, F, I and M intersections. Thus, the highway network structure gained momentum in the north direction.

The reason for investigating their situation before and after is to determine whether the new road added to the network structure has changed the central intersection. If the central intersection has changed, it has to move a little closer to the route newly added to the network structure, since the centrality of the network structure is expected to shift in that direction. At the same time, the new central intersection is expected not to go far from the existing central intersection. In addition to this situation, it is expected that the central intersection will be close to the middle points in the network structure and the traffic volume value will be high. The application method giving results suitable to these conditions increases the accuracy of the method.

It is very important to determine the central intersection in a highway network structure. Thanks to the improvement of the central intersection determined for the network structure, the entire network structure is optimally affected. For this reason, the central intersections can be prioritized in order to obtain maximum efficiency from investments in the road network. In order to detect these central intersections, the SNA method was used in the study. Current transportation analysis tools are expensive and time consuming and require rigorous data

***Table 1*** *Adjacency matrices of the first case study*

| | A | B | C | D | E | F | G | H | J | K | L | M | N |
|---|---|---|---|---|---|---|---|---|---|---|---|---|---|
| A | 0 | 0 | 0 | 1 | 0 | 1 | 0 | 0 | 0 | 0 | 0 | 0 | 0 |
| B | 0 | 0 | 1 | 0 | 1 | 0 | 0 | 0 | 0 | 0 | 0 | 0 | 0 |
| C | 0 | 1 | 0 | 0 | 1 | 0 | 0 | 0 | 0 | 0 | 0 | 0 | 0 |
| D | 1 | 0 | 0 | 0 | 1 | 0 | 1 | 0 | 0 | 0 | 0 | 0 | 0 |
| E | 0 | 1 | 1 | 1 | 0 | 0 | 0 | 1 | 0 | 0 | 0 | 0 | 0 |
| F | 1 | 0 | 0 | 0 | 0 | 0 | 1 | 0 | 1 | 0 | 0 | 0 | 0 |
| G | 0 | 0 | 0 | 1 | 0 | 1 | 0 | 1 | 1 | 0 | 0 | 0 | 0 |
| H | 0 | 0 | 0 | 0 | 1 | 0 | 1 | 0 | 0 | 0 | 1 | 0 | 0 |
| J | 0 | 0 | 0 | 0 | 0 | 1 | 1 | 0 | 0 | 1 | 0 | 0 | 0 |
| K | 0 | 0 | 0 | 0 | 0 | 0 | 0 | 0 | 1 | 0 | 1 | 1 | 0 |
| L | 0 | 0 | 0 | 0 | 0 | 0 | 0 | 1 | 0 | 1 | 0 | 0 | 1 |
| M | 0 | 0 | 0 | 0 | 0 | 0 | 0 | 0 | 0 | 1 | 0 | 0 | 1 |
| N | 0 | 0 | 0 | 0 | 0 | 0 | 0 | 0 | 0 | 0 | 1 | 1 | 0 |

***Table 2*** *Adjacency matrices of the second case study*

| | A | B | C | D | E | F | G | H | I | J | K | L | M | N |
|---|---|---|---|---|---|---|---|---|---|---|---|---|---|---|
| A | 0 | 0 | 0 | 1 | 0 | 1 | 0 | 0 | 0 | 0 | 0 | 0 | 0 | 0 |
| B | 0 | 0 | 1 | 0 | 1 | 0 | 0 | 0 | 0 | 0 | 0 | 0 | 0 | 0 |
| C | 0 | 1 | 0 | 0 | 1 | 0 | 0 | 0 | 0 | 0 | 0 | 0 | 0 | 0 |
| D | 1 | 0 | 0 | 0 | 1 | 0 | 1 | 0 | 0 | 0 | 0 | 0 | 0 | 0 |
| E | 0 | 1 | 1 | 1 | 0 | 0 | 0 | 1 | 0 | 0 | 0 | 0 | 0 | 0 |
| F | 1 | 0 | 0 | 0 | 0 | 0 | 1 | 0 | 1 | 0 | 0 | 0 | 0 | 0 |
| G | 0 | 0 | 0 | 1 | 0 | 1 | 0 | 1 | 0 | 1 | 0 | 0 | 0 | 0 |
| H | 0 | 0 | 0 | 0 | 1 | 0 | 1 | 0 | 0 | 0 | 0 | 1 | 0 | 0 |
| I | 0 | 0 | 0 | 0 | 0 | 1 | 0 | 0 | 0 | 1 | 0 | 0 | 1 | 0 |
| J | 0 | 0 | 0 | 0 | 0 | 0 | 1 | 0 | 1 | 0 | 1 | 0 | 0 | 0 |
| K | 0 | 0 | 0 | 0 | 0 | 0 | 0 | 0 | 0 | 1 | 0 | 1 | 1 | 0 |
| L | 0 | 0 | 0 | 0 | 0 | 0 | 0 | 1 | 0 | 0 | 1 | 0 | 0 | 1 |
| M | 0 | 0 | 0 | 0 | 0 | 0 | 0 | 0 | 1 | 0 | 1 | 0 | 0 | 1 |
| N | 0 | 0 | 0 | 0 | 0 | 0 | 0 | 0 | 0 | 0 | 0 | 1 | 1 | 0 |

for reliable results. Accordingly, a quick and inexpensive methodology to preliminarily analyze traffic networks is beneficial to better direct more detailed transportation analyses. Due to its ability to grasp the full complexity and connectivity of networks in a timely and cost effective manner, SNA can fulfill this requirement. The SNA approach has been able to easily and quickly determine the most central intersections in the investigated transportation networks. Previous research reveals that the road network structures, examined using the SNA, give correct results and provide high efficiency in improving traffic flow. Accordingly, SNA is believed to be an effective and innovative tool in transportation analysis [36].

The first important step in SNA is to create an adjacency matrix. In both case studies, after creating a map where the nodes and the traffic volume values were processed, an adjacency matrix was created for the nodes. During the creation of the adjacency matrix, if there was a transition state between the two nodes, a value of 1 was entered in the matrix and if there was no transition between two nodes, a value of 0 was entered. At this stage, a point needs to be written in the field 0 corresponding to each node. Tables 1 and 2 show the adjacency matrices for both case studies.

The traffic volume values for each node were entered in the generated adjacency matrix. Once the generated adjacency matrix had been loaded into the Ucinet Software, a graph of the road network was obtained from the Netdraw Software, a tab of Ucinet [37]. This process was performed for both case studies and the two different road networks are presented in Figures 4 and 5. In the first case, 13 nodes were formed in the road network; in the second case, with the addition of the I node, the road network consisted of 14 nodes. The I node was located between the F, J and M nodes. In addition, the first case consisted of 18 ties, while 20 ties were formed in the second case.

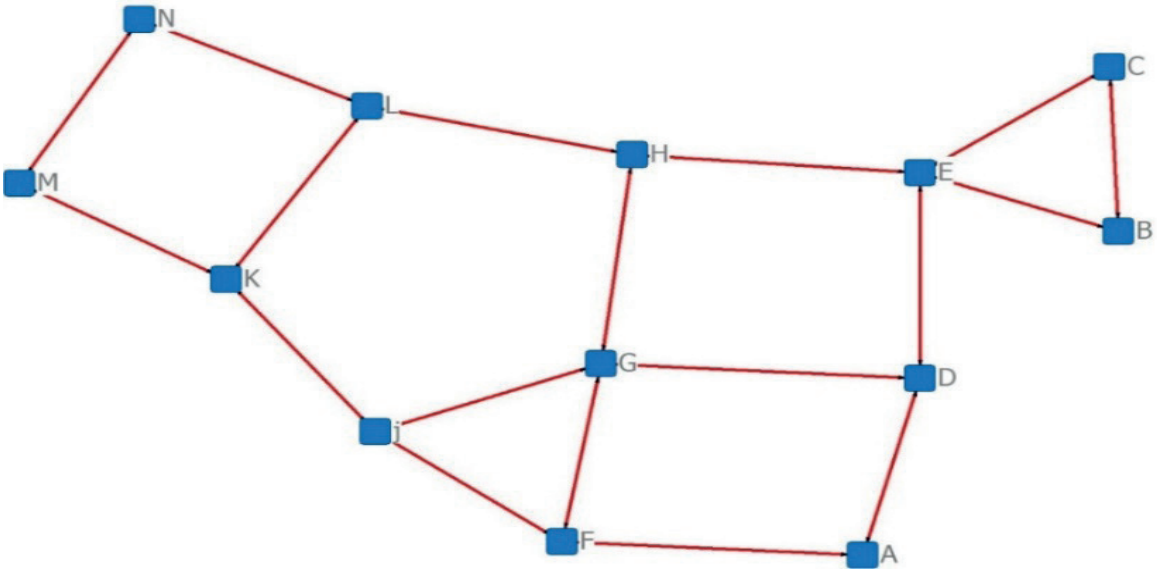


***Figure 4*** *The first case study network structure*

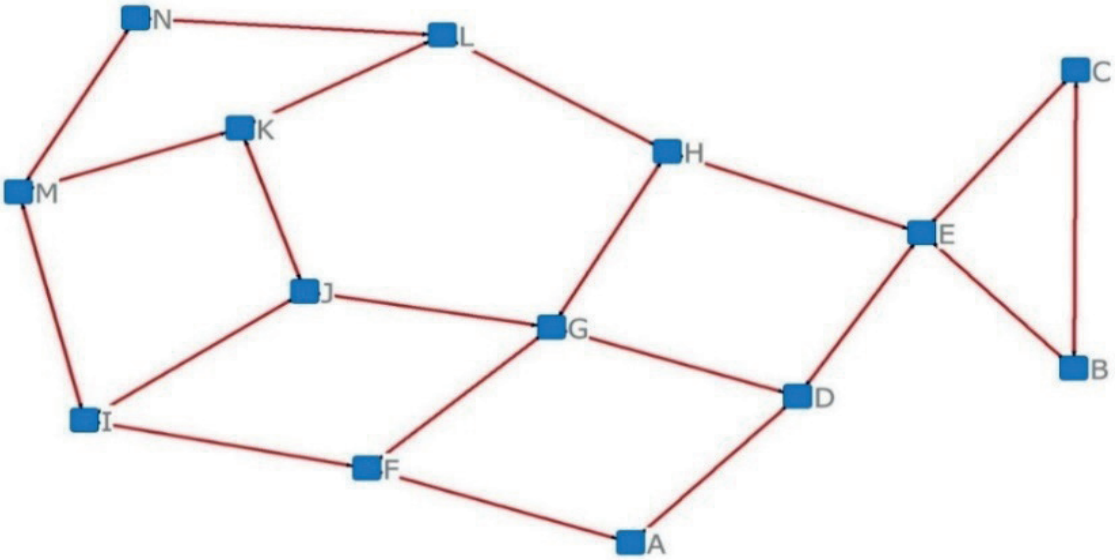


***Figure 5*** *The second case study network structure*

## 4 Results and discussion

Once the road network has been established, it was available to examine the situations of centralization for SNA. After the centrality values has been compared, the first 10 nodes with the highest values in the network have been determined. One of the most basic concepts of centrality is the closeness centrality. In this centrality, the tie values in the network are not important; rather, the structure of the network is important. The geodesic distances between nodes need to be determined correctly when calculating this centrality. It is easy to calculate the closeness centrality values when the closeness matrix with the shortest distances has been determined. Tables 3 and 4 present the closeness matrices, which were formed according to the location of the nodes in the network.

Closeness centrality values calculated for both cases are given in Table 5. In the first case, the value of node H was slightly higher than that of node G, but both values were the same in the second case. As mentioned previously, the closeness centrality is higher in the regions at the midpoints of the network. Another main centrality measure is the degree centrality. In this centrality, the sum of the tie values of each node in the network is calculated. Unlike in the case of the closeness centrality in the case of this centrality, the location of the node in the network structure is not important. All that matters is that the tie values connect the nodes. When the degree of centrality values was examined, it was observed that the value of the node L was higher in both cases, since in both cases the traffic volume values on the road network reached their maximum levels at node L. At the same time, the traffic volume

***Table 3*** *Closeness centrality matrix of the first case study*

| | A | B | C | D | E | F | G | H | J | K | L | M | N |
|---|---|---|---|---|---|---|---|---|---|---|---|---|---|
| A | 0 | 3 | 3 | 1 | 2 | 1 | 2 | 3 | 2 | 3 | 4 | 4 | 5 |
| B | 3 | 0 | 1 | 2 | 1 | 4 | 3 | 2 | 4 | 5 | 3 | 5 | 4 |
| C | 3 | 1 | 0 | 2 | 1 | 4 | 3 | 2 | 4 | 4 | 3 | 5 | 4 |
| D | 1 | 2 | 2 | 0 | 1 | 2 | 1 | 2 | 2 | 3 | 3 | 4 | 4 |
| E | 2 | 1 | 1 | 1 | 0 | 3 | 2 | 1 | 3 | 3 | 2 | 4 | 3 |
| F | 1 | 4 | 4 | 2 | 3 | 0 | 1 | 2 | 1 | 2 | 3 | 3 | 4 |
| G | 2 | 3 | 3 | 1 | 2 | 1 | 0 | 1 | 1 | 2 | 2 | 3 | 3 |
| H | 3 | 2 | 2 | 2 | 1 | 2 | 1 | 0 | 2 | 2 | 1 | 3 | 2 |
| J | 2 | 4 | 4 | 2 | 3 | 1 | 1 | 2 | 0 | 1 | 2 | 2 | 3 |
| K | 3 | 5 | 4 | 3 | 3 | 2 | 2 | 2 | 1 | 0 | 1 | 1 | 2 |
| L | 4 | 3 | 3 | 3 | 2 | 3 | 2 | 1 | 2 | 1 | 0 | 2 | 1 |
| M | 4 | 5 | 5 | 4 | 4 | 3 | 3 | 3 | 2 | 1 | 2 | 0 | 1 |
| N | 5 | 4 | 4 | 4 | 3 | 4 | 3 | 2 | 3 | 2 | 1 | 1 | 0 |

***Table 4*** *Closeness centrality matrix of the second case study*

| | A | B | C | D | E | F | G | H | I | J | K | L | M | N |
|---|---|---|---|---|---|---|---|---|---|---|---|---|---|---|
| A | 0 | 3 | 3 | 1 | 2 | 1 | 2 | 3 | 2 | 3 | 4 | 4 | 3 | 4 |
| B | 3 | 0 | 1 | 2 | 1 | 4 | 3 | 2 | 5 | 4 | 5 | 3 | 5 | 4 |
| C | 3 | 1 | 0 | 2 | 1 | 4 | 3 | 2 | 5 | 4 | 4 | 3 | 5 | 4 |
| D | 1 | 2 | 2 | 0 | 1 | 2 | 1 | 2 | 3 | 2 | 3 | 3 | 4 | 4 |
| E | 2 | 1 | 1 | 1 | 0 | 3 | 2 | 1 | 4 | 3 | 3 | 2 | 4 | 3 |
| F | 1 | 4 | 4 | 2 | 3 | 0 | 1 | 2 | 1 | 2 | 3 | 3 | 2 | 3 |
| G | 2 | 3 | 3 | 1 | 2 | 1 | 0 | 1 | 2 | 1 | 2 | 2 | 3 | 3 |
| H | 3 | 2 | 2 | 2 | 1 | 2 | 1 | 0 | 3 | 2 | 2 | 1 | 3 | 2 |
| I | 2 | 5 | 5 | 3 | 4 | 1 | 2 | 3 | 0 | 1 | 2 | 3 | 1 | 2 |
| J | 3 | 4 | 4 | 2 | 3 | 2 | 1 | 2 | 1 | 0 | 1 | 2 | 2 | 3 |
| K | 4 | 5 | 4 | 3 | 3 | 3 | 2 | 2 | 2 | 1 | 0 | 1 | 1 | 2 |
| L | 4 | 3 | 3 | 3 | 2 | 3 | 2 | 1 | 3 | 2 | 1 | 0 | 2 | 1 |
| M | 3 | 5 | 5 | 4 | 4 | 2 | 3 | 3 | 1 | 2 | 1 | 2 | 0 | 1 |
| N | 4 | 4 | 4 | 4 | 3 | 3 | 3 | 2 | 2 | 3 | 2 | 1 | 1 | 0 |

***Table 5*** *Closeness and degree centrality values of case studies*

| Degree centrality | | | | Closeness Centrality | | | |
|---|---|---|---|---|---|---|---|
| First Case | | Second Case | | First Case | | Second Case | |
| L | 516549 | L | 508555 | H | 0.52 | G | 0.50 |
| J | 421119 | K | 402090 | G | 0.5 | H | 0.50 |
| K | 401575 | J | 395673 | E | 0.46 | L | 0.43 |
| N | 166094 | N | 163792 | L | 0.44 | J | 0.43 |
| G | 142994 | G | 154385 | J | 0.44 | D | 0.43 |
| H | 106491 | H | 118348 | D | 0.44 | E | 0.433 |
| E | 65959 | M | 96047 | K | 0.41 | F | 0.42 |
| M | 45230 | E | 73950 | F | 0.40 | K | 0.39 |
| D | 45077 | D | 51787 | A | 0.36 | I | 0.38 |
| C | 20812 | I | 40762 | C | 0.33 | A | 0.37 |

***Table 5*** *Closeness and degree centrality values of case studies*

| Degree centrality | | | | Closeness Centrality | | | |
|---|---|---|---|---|---|---|---|
| First Case | | Second Case | | First Case | | Second Case | |
| L | 516549 | L | 508555 | H | 0.52 | G | 0.50 |
| J | 421119 | K | 402090 | G | 0.5 | H | 0.50 |
| K | 401575 | J | 395673 | E | 0.46 | L | 0.43 |
| N | 166094 | N | 163792 | L | 0.44 | J | 0.43 |
| G | 142994 | G | 154385 | J | 0.44 | D | 0.43 |
| H | 106491 | H | 118348 | D | 0.44 | E | 0.433 |
| E | 65959 | M | 96047 | K | 0.41 | F | 0.42 |
| M | 45230 | E | 73950 | F | 0.40 | K | 0.39 |
| D | 45077 | D | 51787 | A | 0.36 | I | 0.38 |
| C | 20812 | I | 40762 | C | 0.33 | A | 0.37 |

***Table 6*** *Betweenness and eigenvector centrality values of case studies*

| Betweenness centrality | | | | Eigenvector centrality | | | |
|---|---|---|---|---|---|---|---|
| First Case | | Second Case | | First Case | | Second Case | |
| E | 33.76 | E | 30.98 | L | 0.55 | L | 0.57 |
| H | 33.61 | H | 29.74 | K | 0.53 | K | 0.52 |
| L | 24.95 | G | 25.83 | J | 0.43 | J | 0.39 |
| G | 21.82 | L | 19.02 | H | 0.32 | H | 0.38 |
| K | 17.15 | D | 15.66 | N | 0.25 | N | 0.25 |
| D | 15.25 | F | 12.67 | G | 0.23 | G | 0.19 |
| J | 14.87 | I | 10.58 | F | 0.09 | M | 0.09 |
| F | 7.48 | J | 10.19 | M | 0.06 | I | 0.08 |
| M | 3.79 | K | 7.59 | D | 0.04 | E | 0.05 |
| N | 3.79 | M | 7.59 | E | 0.04 | D | 0.03 |

values reached their second highest level at node J in the first case study, but reached their second highest level at node K in the second case study. It was observed that the tie values attached to the I node added in the network structure were not high. Therefore, the I node in the second case study did not much affect the other nodes in terms of the degree centrality.

Like closeness centrality, betweenness centrality is a shortest-path-based centrality concept. The difference is that a node is located based on the extent to which it takes part in the shortest paths between the other nodes rather than based on its closeness to the other nodes. For example, when calculating the betweenness centrality of a node, the shortest distances between the other nodes and how many of them pass through that node are determined. The more the node takes part in the shortest paths, the higher its betweenness centrality value. The most important factor to consider while calculating the betweenness centrality of the nodes is that there may be more than one shortest path between the nodes. It can be seen that the E node had the highest betweenness centrality value in Table 4. This is because there was no alternative to the E node for the transition to the C and B nodes. At the same time, like the closeness centrality values of nodes G, L and H, the betweenness centrality values of nodes G, L and H seemed to be high. In the second case, the I node attached to the network induced a change in the order of the other nodes, especially since it facilitated the transition to the M and N nodes.

Eigenvector centrality is a measurement of centrality that takes degree centrality a step further. In this concept, the importance of a node depends not only on the number of ties it has but on the importance of its neighbors, as well. In this way, eigenvector centrality can yield results that reflect the network structure more accurately than degree centrality. The nodes with the highest eigenvector centrality, as revealed in Table 6, appeared to be ranked in the same way as the nodes with the highest degree centrality. Since the concept of eigenvector centrality is similar to the concept of degree centrality, it was seen in the results that the rankings were similar. The L node ranked first in both working positions because it had both high degree centrality and neighbors with high degree centrality. In both situations, the K node had a higher eigenvector centrality value than the J node. This is because the K node was a neighbor to the L node, which had the high

***Table 7*** *Bonacich power centrality values of case studies*

| First Case | | Second Case | |
|---|---|---|---|
| L | 78160776 | K | 80128328 |
| K | 77112864 | L | 68472496 |
| N | 57223936 | J | 60620028 |
| J | 53638424 | H | 50518176 |
| H | 49054532 | N | 33966540 |
| G | 31645060 | G | 32196792 |
| F | 11707991 | M | 15508986 |
| M | 11152561 | I | 13719325 |
| E | 5692315 | E | 7213459 |
| D | 5371831 | D | 5668435 |

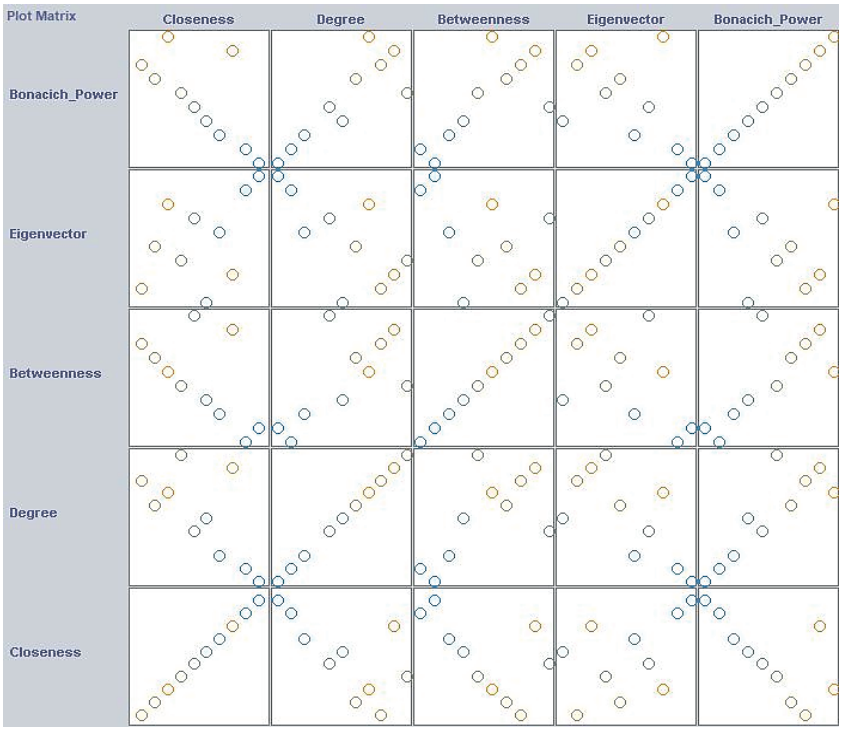


***Figure 6*** *Plot matrix of centrality concepts*

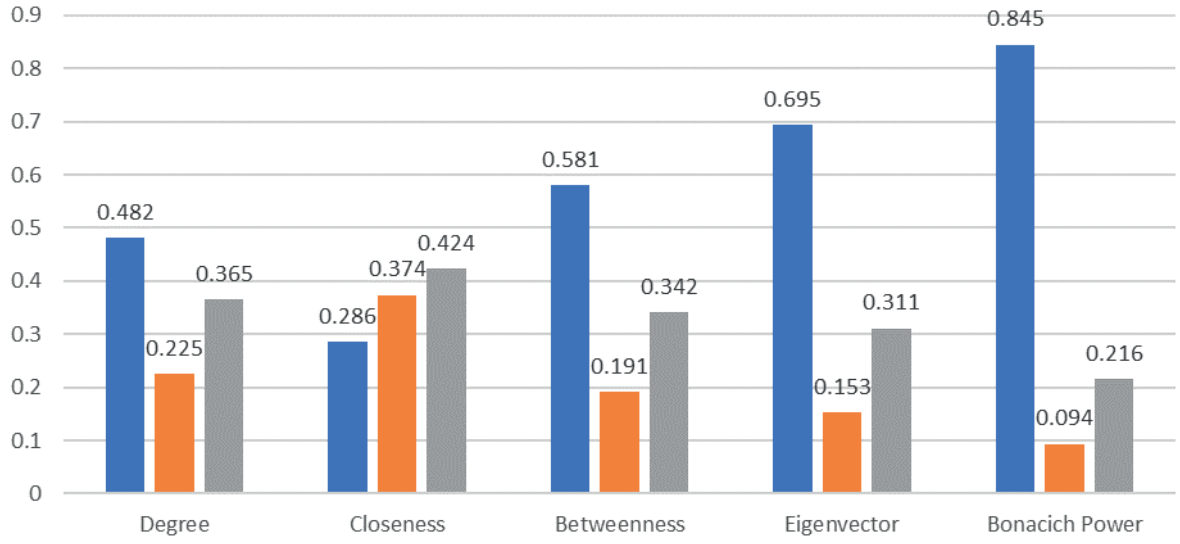


***Figure 7*** *Error scales and accuracy value*

degree centrality. In addition, it was observed that the addition of the I node to the network structure barely affected this centrality measure because the order of the nodes with the six highest eigenvector centrality values did not change.

Bonacich power was proposed by Phillip Bonacich as an important method in SNA because it considers the tie values and location of the nodes in the network structure. The node in the network structure is a comprehensive method that considers the neighbors of the nodes in the whole network, not merely their neighbors [38]. When the Bonacich power centrality values of this study, as presented in Table 7, were examined, it was observed that the L node had the highest value in the first case. Although the L node, with the highest volume value, ranked first in eigenvector centrality and degree centrality in both case studies, the K node had the highest Bonacich power centrality value in the second case study. It was observed that the highest Bonacich power centrality value passed from the L node to the K node with the addition of the I node in the second case study. In other words, the node moved to a more northern point. These results reflected the reality that the new bridge and the node that was added to the network structure are located in the northern part of the city of Istanbul.

Each centrality measure examines the network structure from different approaches. For this reason, it should be determined which centrality criterion gives better results by using the results obtained. The concept of centrality, which gives the best results, will be more suitable for the road network structure. The SVM algorithm was used to perform this operation. First of all, the relationship between this algorithm and the concepts of centrality was examined. The relationship of each centrality concept with each other is shown in Figure 6. After this process, Kappa statistical value and error scales for each centrality criterion, were calculated using the SVM. These results are shown in the graph in Figure 7. The column in dark blue represents the kappa statistical value, the column in orange represents the MAE value and the column in gray represents the RMSE value.

The Bonacich power centrality has values of 0.094 MAE, 0.216 RMSE. Accordingly, the centrality value with the lowest error rate was the Bonacich power centrality. Similarly, the Kappa statistic value is 0.845. This value is quite high compared to other centrality concepts. Bonacich power centrality has the best results in terms of both error scales and accuracy.

As a result of these analyses and comparisons, it was decided that the centrality indicator that provided the most appropriate results for this transportation network structure is the Bonacich power centrality, which examined the network structure in terms of both centrality and degree. Furthermore, this concept of centrality examined the network structure completely rather than locally. For these reasons, it was observed that the Bonacich power centrality values provided more realistic results than the other centrality measurements in determining the most central intersection of the transportation road network.

## 5 Conclusions

With the global increase in traffic congestion, modeling and analyzing the road networks have become very important. Various modeling and analysis methods have been developed for this purpose. In this study, the traffic networks were modeled and analyzed using Netdraw and Ucinet, which are SNA Software with a practical and innovative structure. The results were compared using support vector machine with Weka Software, a machine learning program. When the measures of centrality were examined, it was observed that the most appropriate concept of centrality for the transportation network analyzed in this study was Bonacich power centrality, which has examined the nodes in a network structure both in terms of their positions and degrees. This situation is very suitable for the road network structure. Since in determining the most central intersection in road network structures, both the locations of the intersections and the traffic volume values are taken as basis. For the first case study, the L intersection on the south of the Anatolian side was identified as the most central intersection using this centrality measure. This intersection is at the intersection point of the ongoing ring road of 2nd Bosphorus Bridge and the extension of the 1st Bosphorus Bridge. In the second case study, the K intersection was identified as the most central intersection. This intersection is also on the Anatolian side and closer to the midpoints, compared to the L intersection. It is located at an important point in the intersection zone of the 2nd Bosphorus Bridge. Both nodes are in the transition zone to the bridges and they are at intersections with high traffic volumes. The 3rd bridge and new road added to the road traffic in Istanbul caused the most central intersection to change. All these situations support the idea that these nodes are the central points.

Overall, improvements made at the most central intersection in the road network structure can reduce traffic congestion and delays in the entire network structure. The results of this study can guide the local governments. Decision makers can prioritize the idea of practical implementation and useful methods such as SNA when planning the improvement of any transport network. Additionally, the future line of research can measure how improvements could occur at central intersections and the overall impact of these improvements on traffic. This article proposes application of the SNA method in engineering studies involving the relationship between transport networks and nodes the need to identify the most central nodes in the network structure.

## References


[1] LIU, X., WANG, J., LIU, T., XU, J. Forecasting spatiotemporal boundary of emergency-event-based traffic congestion in expressway network considering highway node acceptance capacity. *Sustainability* [online]. 2021, **13**(21), 12195. eISSN 2071-1050. Available from: https://doi.org/10.3390/su132112195

[2] BECKMANN, M. J. Traffic congestion and what to do about it. *Transportmetrica B: Transport Dynamics* [online]. 2013, **1**(1), p. 103-109. ISSN 2168-0566, eISSN 2168-0582. Available from: https://doi.org/10.1080/21680566.2013.780988

[3] MATHEW, T. V., BOMBAY, I. T. Automated traffic measurement. Transportatin System Engineering [online] [accessed 2021-09-11]. Lecture notes and presentations. Available from: https://www.civil.iitb.ac.in/tvm/1100_LnTse/ceTseLn/ceTseLn.html

[4] KIM, J., SARKAR, S., VENKATESH, S. S., RYERSON, M. S., STAROBINSKI, D. An epidemiological diffusion framework for vehicular messaging in general transportation networks. *Transportation Research Part B: Methodological* [online]. 2020, **131**, p. 160-190. ISSN 0191-2615. Available from: https://doi.org/10.1016/j.trb.2019.11.004

[5] WANG, D. Z. W., XIE, D. F. Reliable transportation network design considering uncertain demand variability. *Journal of Sustainable Transportation* [online]. 2016, **10**(8), p. 752-763. ISSN 1556-8318, eISSN 1556-8334. Available from: https://doi.org/10.1080/15568318.2016.1149644

[6] Traffic counting systems - General Directorate of Highways [online] [accessed 2022-03-21]. Available from: http://www.kgm.gov.tr/SiteCollection Documents /KGMdocuments/Istatistikler/TrafikveUlasimBilgileri/17TrafikUlasimBilgileri.pdf

[7] KOC, E., CETINER, B., ROSE, A. SOIBELMAN, L., TACIROGLU, E., WEI, D. CRAFT: Comprehensive resilience assessment framework for transportation systems in urban areas. *Advanced Engineering Informatics* [online]. 2020, **46**, 101159. ISSN 1474-0346. Available from: https://doi.org/10.1016/j.aei.2020.101159

[8] GAUTHIER, P., FURNO, A., EL FAOUZI, N. E. Road network resilience: how to identify critical links subject to day-to-day disruptions. *Transportation Research Record* [online]. 2018, **2672**, p. 54-65. ISSN 0361-1981, eISSN 2169-4052. Available from: https://doi.org/10.1177/03611981187921

[9] WEN, H., SUN, J., ZENG, Q., ZHANG, X., YUAN, Q. The effects of traffic composition on freeway crash frequency by injury severity: a Bayesian multivariate spatial modeling approach. *Journal of Advanced Transportation* [online]. 2018, **2018**, 6964828. ISSN 0197-6729, eISSN 2042-3195. Available from: https://doi.org/10.1155/2018/6964828

[10] HADAS, Y., GNECCO, G., SANGUINETI, M. An approach to transportation network analysis via transferable utility games. *Transportation Research Part B: Methodological* [online]. 2017, **105**, p. 120-143. ISSN 0191-2615. Available from: https://doi.org/10.1016/j.trb.2017.08.029

[11] ZHANG, X., ZHANG, H. M., LI, L. Analysis of user equilibrium traffic patterns on bottlenecks with time-varying capacities and their applications. *International Journal of Sustainable Transportation* [online]. 2010, **4**(1), p. 56-74. ISSN 1556-8318, eISSN 1556-8334. Available from: https://doi.org/10.1080/15568310601060036

[12] FREEMAN, L. C. *The development of social network analysis*. Vancouver, BC Canada: Empirical Press, 2014. ISBN 1-59457-714-5.

[13] PRITCHARD, J. P., MOURA, F., ABREU E SILVA, J. Incorporating social network data in mobility studies: benefits and takeaways from an applied survey methodology. *Case Studies on Transport Policy* [online]. 2016, **4**(4), p. 279-293. Available from: https://doi.org/10.1016/j.cstp.2016.09.002

[14] CHENG, Y. Y., LEE, R. K. W., LIM, E. P., ZHU, F. Measuring centralities for transportation networks beyond structures [online]. In: *Applications of Social Media and Social Network Analysis*. KAZIENKO, P., CHAWLA, N. (eds.). Lecture Notes in Social Networks. Cham: Springer, 2015. ISBN 978-3-319-19002-0, eISBN 978-3-319-19003-7, p. 23-39. Available from: https://doi.org/10.1007/978-3-319-19003-7_2

[15] COOPER, C. H. V. Predictive spatial network analysis for high-resolution transport modeling applied to cyclist flows, mode choice and targeting investment. *International Journal of Sustainable Transportation* [online], 2018, **12**(10), p. 714-724. ISSN 1556-8318, eISSN 1556-8334. Available from: https://doi.org/10.1080/15568318.2018.1432730

[16] WATTS, R., WITHAM, A. Social network analysis of sustainable transportation organizations [online]. Available from: http://www.uvm.edu/~transctr/research/trc_reports/UVM-TRC-12008.pdf 2012

[17] EL-ADAWAY, I. Analyzing traffic layout using dynamic social network analysis. NCITEC Project, 2014.

[18] EL-ADAWAY, I. H., ABOTALEB, I., VECHAN, E. Identifying the most critical transportation intersections using social network analysis. *Transportation Planning and Technology* [online]. 2018, **41**(4), p. 353-374. ISSN 0308-1060, eISSN 1029-0354. Available from: https://doi.org/10.1080/03081060.2018.1453456

[19] UYGUN, M. Stakeholders analysis of health tourism in Turkey: social network analysis approach practice in Ankara. Ankara: Yildirim Beyazit University, 2018.

[20] YAPICIOGLU, B., MOGBO, O. N., YITMEN, I. Innovative strategies for transport policies in infrastructure development: Nigerian stakeholders' perspective. *International Journal of Civil Engineering* [online]. 2017, **15**, p. 747-761. ISSN 1735-0522, eISSN 2383-3874. Available from: https://doi.org/10.1007/s40999-017-0172-0

[21] STORTO, C. An SNA-DEA prioritization framework to identify critical nodes of gas networks: the case of the US interstate gas infrastructure. *Energies* [online]. 2019, **12**, 4597. eISSN 1996-1073. Available from: https://doi.org/10.3390/en12234597

[22] KEMAL, Y. Increasing the effect of marketing from mouth to mouth with the social network analysis method: application on data sets. Ege University, 2011.

[23] OPSAHL, T., AGNEESSENS, F., SKVORETZ, J. Node centrality in weighted networks: generalizing degree and shortest paths. *Social Networks* [online]. 2010, **32**(3), p. 245-251. ISSN 0378-8733. Available from: https://doi.org/10.1016/j.socnet.2010.03.006

[24] FALZON, L., QUINTANE, E., DUNN, J., ROBINS, G. Embedding time in positions: temporal measures of centrality for social network analysis. *Social Networks* [online]. 2018, **54**, p. 168-178. ISSN 0378-8733. Available from: https://doi.org/10.1016/j.socnet.2018.02.002

[25] SABAH, L. Social network analysis and outbreak modeling. Duzce University, 2018.

[26] BONACICH, P. Some unique properties of eigenvector centrality. *Social Networks* [online]. 2007, **29**(4), p. 555-564. ISSN 0378-8733. Available from: https://doi.org/10.1016/j.socnet.2007.04.002

[27] HSIEH, M. Simple network analysis with UCINET - Engineering Systems Division [online]. Available from: https://ocw.mit.edu/courses/engineering-systems-division/esd-342-network-representations-of-complex-engineering-systems-spring-2010/tools/ucinet_slides.pdf. 2006

[28] LENDEL, V., PANCIKOVA, L., FALAT, L., MARCEK, D. Intelligent modelling with alternative approach: application of advanced artificial intelligence into traffic management. *Communications-Scientific Letters of the University of Zilina* [online]. 2017, **19**(4), p. 36-42. ISSN 1335-4205, eISSN 2585-7878. Available from: https://doi.org/10.26552/com.C.2017.4.36-42

[29] BUITINCK, L., LOUPPE, G., BLONDEL, M., PEDREGOSA, F., MUELLER, A., GRISEL, O., NICULAE, V., PRETTENHOFER, P., GRAMFORT, A., GROBLER, J., LAYTON, R., VANDERPLAS, J., JOLY, A., HOLT, B., VAROQUAUX, G. API design for machine learning software: experiences from the scikit-learn project. 2013. p. 1-15.

[30] KARANDIKAR, J. Machine learning classification for tool life modeling using production shop-floor tool wear data. *Procedia Manufacturing* [online]. 2019, **34**, p. 446-454. ISSN 2351-9789. Available from: https://doi.org/10.1016/j.promfg.2019.06.192

[31] GALDI, P., TAGLIAFERRI, R. Data mining: accuracy and error measures for classification and prediction [online]. In: *Encyclopedia of Bioinformatics and Computational Biology*. RANGANATHAN, S., GRIBSKOV, M., NAKAI, K., SCHONBACH, CH. (eds.). Vol. 1. Elsevier, 2018. ISBN 978-0-12-811432-2, p. 431-436. Available from: https://doi.org/10.1016/B978-0-12-809633-8.20474-3

[32] MCHUGH, M. L. Lessons in biostatistics interrater reliability : the kappa statistic. *Biochemica Medica* [online]. 2012, **22**(3), p. 276-282. ISSN 1330-0962, eISSN 1846-7482. Available from: https://doi.org/10.11613/BM.2012.031

[33] SAMMUT, C., WEBB, G. I. Mean absolute error [online]. In: *Encyclopedia of Machine Learning*. SAMMUT, C., WEBB, G. I. (eds.). Boston, MA: Springer US, 2010. ISBN 978-0-387-30768-8, eISBN 978-0-387-30164-8. Available from: https://doi.org/10.1007/978-0-387-30164-8_525

[34] Traffic density map - Istanbul Metropolitian Municipality [online] [accessed 2021-10-04]. Available from: https://uym.ibb.gov.tr/YHarita/ Harita_tr.aspx

[35] Traffic volume maps - General Directorate of Highways [online] [accessed 2021-09-26]. Available from: http://www.kgm.gov.tr/Sayfalar/KGM/SiteTr/ Trafik/TrafikHacimHaritasi.aspx

[36] EL-ADAWAY, I. H., ABOTALEB, I. S., VECHAN, E. Social network analysis approach for improved transportation planning. *Journal of Infrastructure Systems* [online]. 2017, **23**(2), p. 1-14. ISSN 1076-0342, eISSN 1943-555X. Available from: https://doi.org/10.1061/(ASCE)IS.1943-555X.0000331

[37] HART, M. G., YPMA, R. J. F., ROMERO-GARCIA, R., PRICE, S. J., SUCKLING, J. Graph theory analysis of complex brain networks: new concepts in brain mapping applied to neurosurgery. *Journal of Neurosurgery* [online]. 2016, **124**(6), p. 1665-1678. ISSN 0022-3085, eISSN 1933-0693. Available from: https://doi.org/10.3171/2015.4.JNS142683

[38] KUSKAPAN, E., CODUR, M. Y., TORTUM, A. Identifying the most critical intersections in transportation networks. *Technical Gazette* [online]. 2021, **28**(6), p. 1920-1926. ISSN 1330-3651, eISSN 1848-6339. Available from: https://doi.org/10.17559/TV-20201117162526

**Dear colleague,**

Journal Communications - Scientific Letters of the University of Zilina are a well-established open-access scientific journal aimed primarily at the topics connected with the field of transport. The main transport-related areas covered include Civil engineering, Electrical engineering, Management and informatics, Mechanical engineering, Operation and economics, Safety and security, Travel and tourism studies. The full list of main topics and subtopics is available at: *https://komunikacie.uniza.sk/artkey/inf-990000-0500_Topical-areas.php*

Journal Communications - Scientific Letters of the University of Zilina are currently indexed by EBSCO and SCOPUS.

We would like to invite authors to submit their papers for consideration. We have an open-access policy and there are no publication, processing or other fees charged for published papers. Our journal operates a standard double-blind review procedure, the successful completion of which is a prerequisite for paper publication.

The journal is issued four times a year (in January, in April, in July and in October).

I would also like to offer you the opportunity of using already published articles from past issues as source of information for your research and publication activities. All papers are available at our webpage: *http://komunikacie.uniza.sk*, where you can browse through the individual volumes.

For any questions regarding the journal Communications - Scientific Letters of the University of Zilina please contact us at: *komunikacie@uniza.sk*

We look forward to future cooperation.

Sincerely

Branislav Hadzima
editor-in-chief

# STUDYING THE PROCESS OF THE INTERNAL COMBUSTION ENGINE EXHAUST GAS PURIFICATION BY AN ELECTRIC PULSE

Adil Kadyrov [1], Yevgeniy Kryuchkov [1,*], Kirill Sinelnikov [1], Alexandr Ganyukov [1], Rustem Sakhapov [2], Aliya Kukesheva [1]

[1]Abylkas Saginov Karaganda Technical University, Karaganda, Kazakhstan
[2]Kazan State University of Architecture and Engineering, Kazan, Russia

*E-mail of corresponding author: kryuchkov.yevgeniy94@gmail.com

***Resume***
The article deals with method of purifying the exhaust gases in an automobile muffler or other transport equipment using electrical pulses. Electrical pulses are formed between the two ring electrodes (anode and cathode) installed in series along the gas flow. The physical picture of the process is described. A mathematical model has been developed and studied. A deterministic relationship has been established between the engine volume, the number of the crankshaft revolutions, the electric field strength and the charge strength and dynamic viscosity of the gas. Experimental studies have been carried out. The goal of the experiment was to confirm the hypothesis of impact ionization of exhaust gases. The effectiveness of electrical pulse purification has been proven.

***Article info***
Received 27 April 2022
Accepted 15 August 2022
Online 8 September 2022

***Keywords:***
transport equipment
vehicle
internal combustion engine
muffler
ionization
electrodes
exhaust gas purification

Available online: https://doi.org/10.26552/com.C.2022.4.B275-B287

ISSN 1335-4205 (print version)
ISSN 2585-7878 (online version)

## 1 Introduction

Motor vehicles are the main source of air pollution in cities. Pollution is caused by the emission of exhaust gases into the atmosphere. The toxic component of exhaust gases is nitric oxide, soot that contains a carcinogenic substance, benzopyrene, as well as other substances. These substances cause asthma, vascular-cardiac stroke, neurology and other cardiovascular diseases in the population [1-2]. Mufflers equipped with a purification system can reduce polluting emissions [3].

The requirements to neutralization of exhaust gases from internal combustion engines are growing from year to year. The analysis of the state of work for neutralization of exhaust gases of internal combustion engines suggests that the following methods can be further classified among the promising ways of its development: flame neutralization, liquid neutralization, thermal catalytic neutralization and a number of others, the development of which was dealt with in a number of studies [3].

Liquid neutralization of exhaust gases has become widespread in vehicles and self-propelled equipment operating in confined spaces. The disadvantages of liquid neutralizers include the difficulty of operating vehicles at negative ambient temperatures, since the solution can freeze when the engine is not running. Liquid neutralization is difficult to operate: it requires daily removal and disposal of the used liquid and sludge, flushing the system and filling it with a fresh liquid [4].

Thermal catalytic neutralization of exhaust gases has been developed quite well, has proven itself to be a high degree of purification, especially from nitrogen oxides. On the other hand, thermal catalytic converters are bulky, heavy, they cannot be placed instead of mufflers, the fuel consumption of the engine with thermal catalytic converters increases by 15%. Mounting, the thermal catalytic converters on vehicles requires a reliable automation system to ensure the coordination of the exhaust gas heating system with the engine operating modes [5].

Flame neutralization of exhaust gases is uncompetitive for vehicles because it requires additional fuel consumption, energy costs to maintain the flame, air supply. In addition, the flame neutralization has a low efficiency of exhaust gas purification from $NO_2$, $C_xH_4$, CO and soot and a high fire hazard. Meanwhile, this method effectively purifies exhaust gases. Its efficiency can be improved by increasing the proportion of oxygen in exhaust gas [6].

Neutralization of exhaust gases by ultrasound in mufflers is not yet used but relevant studies have been carried out by Kazakh scientists, [7].

A whole area is dealing with the gas purification including exhaust electrostatic precipitators using an electric field and electrical breakdown of gas: a corona discharge [8].

The hypothesis of this study consists in increasing the impact ionization of exhaust gas particles due to its counter movement from the muffler and the electrical discharge directed in the opposite direction. This reduces the opacity (turbidity) of exhaust gases due to the electrons attaching and sticking.

A number of constructive solutions for purifying gases with an electric pulse were proposed [9]. The development of the research hypothesis was preceded by the analysis of a number of patent decisions. For the most part, those solutions are not intended for vehicle mufflers [10].

In some patents designed specifically for purification of the exhaust gases of internal combustion engines, there are the following design features:

- in the design of patent SU1404664A, the liquid injection into a special chamber is proposed [11];
- patent CRU 2398328C2 also proposes to arrange a separate chamber for needle electrodes [12];
- patent SU 1470985 proposes an annular chamber device [13];
- patent RU 2132471C1 implies annealing of exhaust gases with their subsequent processing by an electric field.

The disadvantage of these patents is the need to introduce an additional chamber in front of the muffler into the design of a vehicle. This complicates the design of the muffler and purification system and makes it impossible to upgrade the existing fleet of vehicles.

As a result of analyzing the patented solutions, the authors propose placing the electrodes directly in the muffler, moreover, not flat but annular ones that are mounted not on the inner surfaces of the muffler but along its central axis. This arrangement provides an oncoming movement of gas particles when the discharge is directed from the electrode towards the engine collector. The counter motion increases the impact ionization of gas molecules, the attachment and detachment of electrons.

The purpose of this study is to establish dependences that describe the process of ionization and purification of exhaust gases by providing a corona discharge in the muffler.

To achieve the goal, the objectives of the study include:

- developing and studying a mathematical model for the movement of gas particles in the muffler;
- obtaining deterministic dependences that relate the volume of the engine combustion chambers, the number of revolutions of the crankshaft, the electric field strength and the dynamic viscosity of the gas;
- developing experimental benches, carrying out experiments to determine the opacity and composition of exhaust gases under the action of an electric discharge;
- processing the results of the experiment.

Scientific novelty is determined by obtaining theoretical and experimental relationships between the magnitude of the electrical pulse, gas pressure, particle velocity and dynamic viscosity of the gas, which determine the degree of exhaust gases purification.

The practical usefulness consists in obtaining the data for developing an engineering method of calculating the operating mode of an electric pulse in a muffler.

The obtained data and dependences are of scientific and practical importance.

## 2 Materials and methods

The physics of the corona discharge process has been sufficiently studied [14]. The charge development begins with application of the high voltage to the charging electrode and producing electrons through the impact ionization. Subsequently, avalanche or chain ionization occurs, the essence of which lies in the fact that a free electron that has a greater energy of communication, when colliding with an atom, knocks out one electron from it and forms one positively charged ion. After the collision, the electron will gain energy and in the next collision, four electrons will appear, then eight, then sixteen and so on. The electrons will move towards the anode and positive ions towards the cathode.

In this case, the number of electrons n obeys the exponential law [15]:

$$n = n_0 \cdot \exp(\alpha x), \tag{1}$$

where $x$ is the particle movement; $n_0$is the number of free electrons with the run x = 0; $\alpha$ is the coefficient of ionization probability.

The counter movement increases the impact ionization of the gas molecules, attaching and sticking the electrons. The coefficient α increases rapidly with increasing the temperature and the field strength. Free electrons ionize gas atoms or stick to particles and this process is the most active near the corona electrode.

A number of studies determine the relationship between the electric charge density, ion mobility, ionization current, electric field strength E [16].

To prove the hypothesis put forward, it is necessary to study the patterns of particle motion in the muffler design proposed (Figure 1). The electromotive force $F_e$ and the friction force $F_c$ on other particles act on the gas particle located between the two electrodes [17].

The unusualness of the proposed design solution consists in placing the ring electrodes along the central axis of the muffler that allows increasing the friction force of particles determined by the Stokes law:

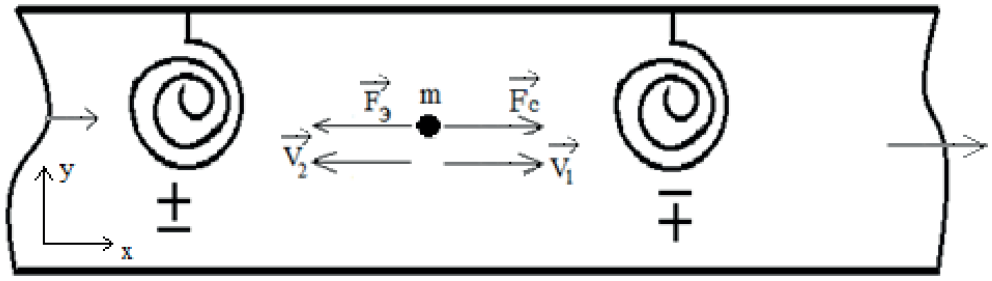


***Figure 1*** *Forces acting on the gas particle in the muffler*

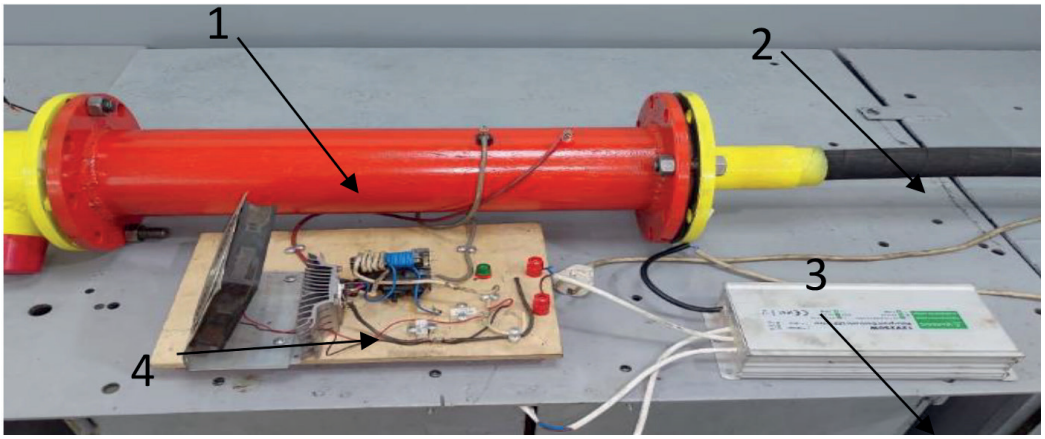


*1 - bench body, 2 - pipeline to the vehicle muffler, 3 - electric current source, 4 - instrument cooling radiator*

***Figure 2*** *Experimental bench*

$$F_c = 6\pi r\mu V\,, \tag{2}$$

where $\mu$ is the dynamic viscosity of the gas particles; $r$ is the particle radius; $V$ is the total velocity after the particles collision [18].

When determining the friction force, it is necessary to take into account the velocity of the particles collision, that is, when the EMF is directed opposite to the movement of the gas

$$V = V_1 + V_2, \tag{3}$$

where $V$ is the total velocity after the collision; $V_1$ is the particle motion velocity determined by the EMF; $V_2$ is the velocity of the particle motion provided by the engine operation. The "+" sign in the equation means that the particles move to each other, the "-" sign means that they move in the same direction [19].

It is natural that, when adding velocities, the Stokes friction force increases (Figure 1). The ring shape of the electrodes allows providing an annular corona discharge that increases the efficiency of ionization [20].

The magnitude of the electromotive force is determined by the expression:

$$F_э = Eq\,, \tag{4}$$

where $E$ is the intensity; $q$ is the charge value.

To analyze the relationship of ionization parameters with the engine crankshaft speed and the capacity of the internal combustion engine chambers, there is the following dependence:

$$V = \frac{\omega \cdot Q}{\pi R^2}\,, \tag{5}$$

where $\omega$ is the number of the crankshaft revolutions; Q is the total capacity of the combustion chamber; R is the average radius of the muffler [21].

An important issue is accounting for the probability in the equation of particle motion. Taking into account Equations (1) to (5), the following system of equations is obtained:

$$\begin{cases} m\ddot{x} = Eq \pm 6\pi r\mu V, \\ V = \dfrac{\omega \cdot Q}{\pi r^2}, \\ n = n_0\, e^{-\alpha x}, \end{cases} \tag{6}$$

where the first equation of the system of Equations (6) presents a differential equation of the gas particle motion under the action of forces $F_c$ and $F_э$ in the muffler (Figure 1); $x$ is the particle motion; t is the particle life time [22].

The preliminary analysis of the system of equations in (6) leads to the following conclusions:

- analytically, it is necessary to determine the value of X: the law of particle motion;
- experimentally, there is determined the value and pattern of changing the probability α.

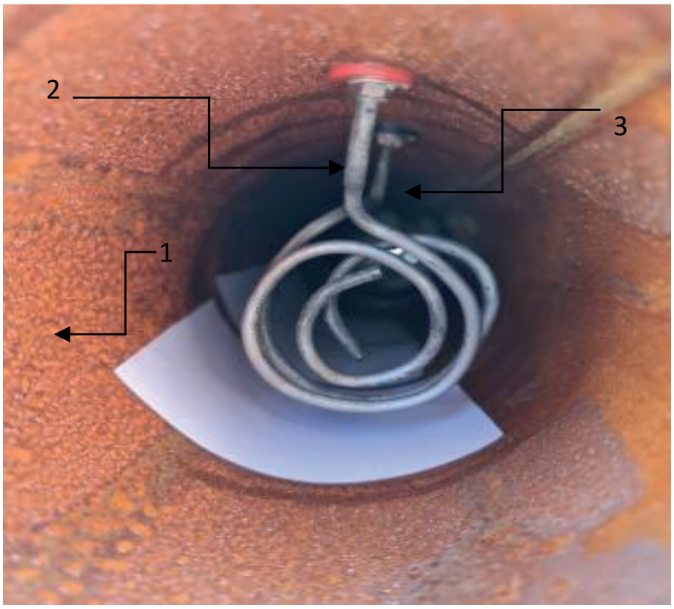


*1 - inner surface of the steel pipe wall, 2 - anode, 3 - cathode*
***Figure 3*** *Location of the spiral electrodes inside the experimental bench*

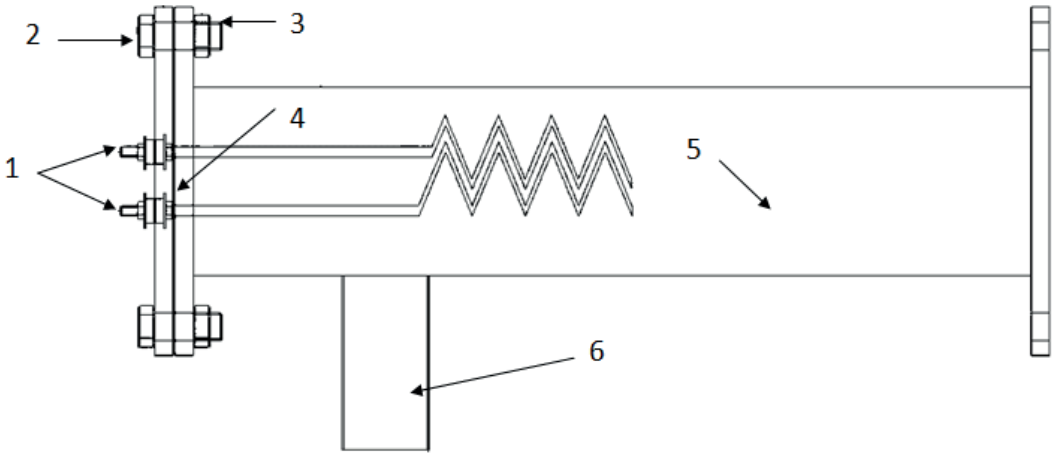


*1 - electric pulse electrodes, 2 - bolt, 3 - nut, 4 - flange, 5 - steel pipe, 6 - inlet pipe*
***Figure 4*** *Diagram of the bench for reducing the exhaust gases of the diesel engine toxicity*

Therefore, to achieve these objectives and goals of the study, the analytical and experimental research methods were used [23].

An experimental bench has been made for the experiments. The bench (Figure 2) is a steel pipe of the diameter of 110 mm, the length of 500 mm and the wall thickness of 1.5 mm. Flat flanges with the outer diameter of 205 mm, the inner diameter of 110 mm and the thickness of 15 mm are attached to the pipe by means of a bolted connection [24].

The electrodes, as mentioned, are placed inside the tube of the bench (Figure 3).

The diagram of the experimental bench for reducing the toxicity of the exhaust gases of a diesel vehicle is shown in Figure 4.

The electrical circuit of the bench consists of such elements as a source of high voltage electric current (20 kV) (Figure 5) and two metal plates twisted into a spiral arranged parallel to each other that are separated from each other by air (Figure 3). This device is an air condenser, thus the electric current will not flow in such a circuit, because the layer of air between the plates, as well as other gases, is not capable of conducting electricity. However, by communicating the necessary potential difference to the metal plates, the galvanometer connected to this circuit begins to record the electric current passing due to ionization of the air layer between these plates. In the presented set, the exhaust gases have been cleaned due to impact ionization of the exhaust gas [25].

The goal of the experiment was to confirm the hypothesis of impact ionization of exhaust gases. To achieve the goal, the following tasks have been performed:

- developing and manufacturing an experimental bench;
- developing and assembling an electrical circuit for operation of the electrodes;

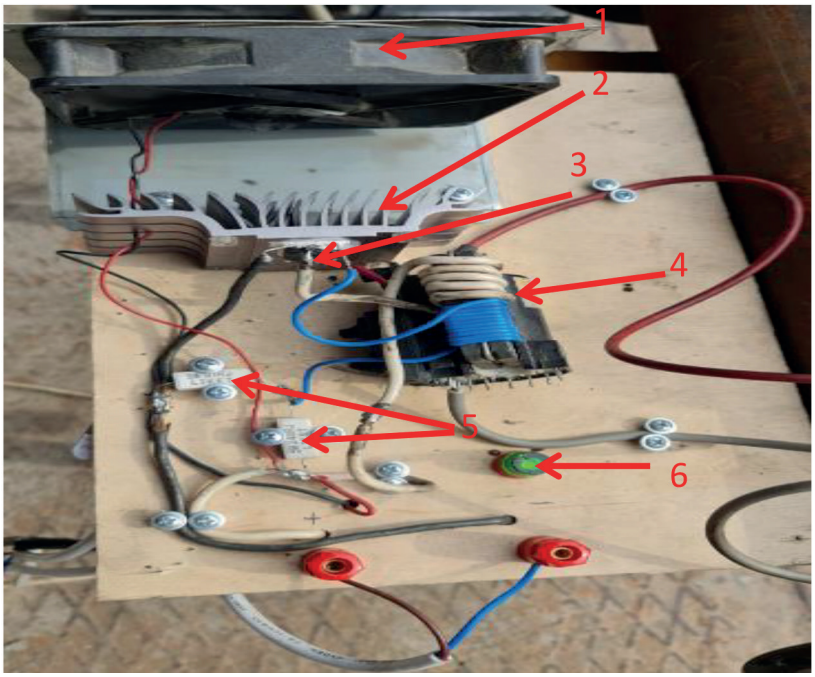


*1 - cooler; 2 - radiator; 3 - transistor; 4 - multiplier; 5 - resistance (ceramic resistors); 6 - device operation indicator*

***Figure 5*** *High voltage electric current source*


***Figure 6*** *BOSCH FSA 740 diagnostic center*

- preparing the electrodes;
- selecting the equipment for measuring the composition of exhaust gases;
- selecting the equipment for measuring the exhaust smoke.

The experiment has been carried out in two stages as follows:

- at the first stage, the smoke of exhaust gases has been measured before the impact of the ionizer and 60 seconds after the impact of the ionizer depending on the range of rotation of the engine crankshaft (810, 1080 and 1486 rpm);
- at the second stage, there have been measured the contents of oxygen, carbon dioxide and carbon monoxide gases, hydrocarbons with the use of the gas analyzer before and after exposure to the ionizer [26].

The measurements have been made by the diagnostic center "BOSCH FSA 740" (Figure 6).

The experimental bench has been connected to the vehicle with a rubber hose to the inlet pipe 1 for supplying the exhaust gases to the set (Figure 7). With the ionizer turned on, the exhaust gas has been exposed to a high voltage electric field.

To perform the high-precision toxicity measurements during the experiment, the BOSCH FSA 740 diagnostic complex has been used. The diagnostic complex "BOSCH" includes a diagnostic scanner "KTS 560", a gas analyzer


***Figure 7*** *The process of connecting the vehicle to the diagnostic complex*

"BEA 050", an optical smoke meter "BEA 070". With the help of the KTS 560 scanner, the speed of the vehicle engine has been monitored to fix the data at a certain moment of the engine crankshaft speed. On the BEA 050 gas analyzer, the composition of the exhaust gases has been determined, namely the content of oxygen in the exhaust gases, carbon dioxide, hydrocarbon and carbon monoxide. The data from the "BEA 070" optical opacity meter has been used to determine the percentage of smoke in the exhaust gases of a diesel engine.

## 3 Results

As a result of integration of the first differential equation of system of equations in (6), the function of particle displacement between the electrodes has been obtained:

$$X(t) = \left(v_0 - \frac{Eq}{6\pi r\mu}\right)\cdot\left(1 - e^{-\frac{6\pi r\mu}{m}t}\right) + \frac{Eq}{6\pi r\mu}t\,. \qquad (7)$$

Taking into account that the $\left(1 - e^{-\frac{6\pi r\mu}{m}t}\right)$ tends to zero at t → 0, the trend of the X variation law has the form:

$$X = \frac{Eq}{6\pi r\mu}t\,, \qquad (8)$$

where t is the electron life time.

Based on the dependence, it follows that the path of a particle between the electrons can be the greater, the greater the charge strength and intensity, but it decreases with increasing the Stokes force.

The ionization rate has been determined by the derivative of Equation (8); it is equal to:

$$V = \frac{Eq}{6\pi r\mu}\,. \qquad (9)$$

From the third equation of system of equations in (6), by taking a logarithm, the dependence of the probability α on the X displacement and the quantities characterizing the process is determined:

$$\alpha = \frac{X}{\ln\frac{n_0}{n}}\,. \qquad (10)$$

The main result of mathematical modeling is obtaining a dependence that determines the relationship between all the process parameters.

The speed of the particle, from the condition of ionization and dynamic friction in Equation (9), should be equal to the speed of movement developed by the engine Equation (5):

$$\frac{Eq}{6\pi r\mu} = \frac{\omega\cdot Q}{\pi R^2} \qquad (11)$$

or

$$\frac{Eq}{\pi r\mu} = \frac{\omega\cdot Q}{R^2}\,. \qquad (12)$$

Equation (12) relates EMF (*Eq*), dynamic viscosity (μ), the crankshaft speed (ω), the engine combustion chamber capacity (Q ), the muffler size (R) .

Thus, knowing such characteristics of the engine as the cylinder capacity Q, the crankshaft speed ω, the muffler radius and the reference values of dynamic viscosity μ, one can determine the magnitude of the pulse *Eq*.

At the first stage of the experiment, the opacity of the exhaust gases of a diesel vehicle has been measured.

There have been made 3 measurements of the exhaust gas smoke before exposure to a high-voltage electric field and 3 measurements after exposure to different engine operating ranges of 750, 1000, 1550 rpm. The recorded readings of the exhaust smoke are shown in Table 1. According to the smoke readings, a diagram has been created (Figure 8) that shows the degree of changing the smoke of the exhaust gas of a diesel engine depending on the speed of the crankshaft.

The impact of the high voltage electric field on the

***Table 1*** *BEA 070 smoke meter readings for diesel engines*

| Impact type | Crankshaft rotation speed, rpm | Period of operation, s | Opacity, % |
|---|---|---|---|
| Before the exposure to a high voltage electric field | 750 | | 21.5 |
| After the exposure to a high voltage electric field | 750 | | 15.7 |
| Before the exposure to a high voltage electric field | 1000 | | 30.2 |
| After the exposure to a high voltage electric field | 1000 | | 28 |
| Before the exposure to a high voltage electric field | 1550 | | 32.4 |
| After the exposure to a high voltage electric field | 1550 | 60 | 30.6 |

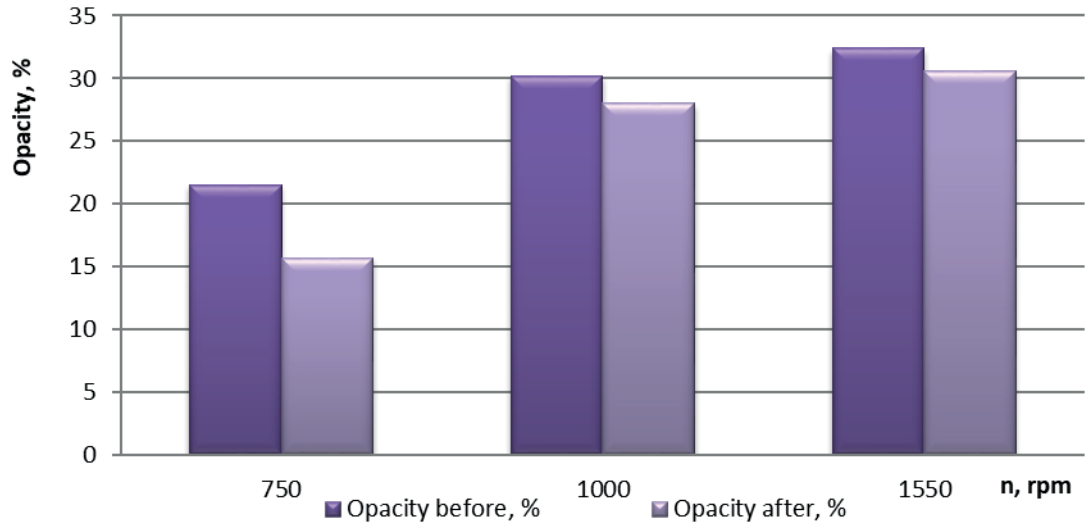


***Figure 8*** *Diagram of changing the degree of opacity (turbidity) of diesel exhaust gas*

***Table 2*** *BEA 050 gas analyzer readings before the exposure to a high voltage electric field*

| No | Rotation speed, 1/min | $O_2$ %vol | $CO_2$ %vol | HC ppm vol | CO %vol | Measurement time, s |
|---|---|---|---|---|---|---|
| 1 | 750 | 17.18 | 2.38 | 22 | 0.026 | |
| 2 | 1000 | 17.41 | 2.28 | 24 | 0.051 | |
| 3 | 1550 | 17.63 | 2 | 29 | 0.065 | 60 |

***Table 3*** *BEA 050 gas analyzer readings after the exposure to a high voltage electric field*

| No | Rotation speed, 1/min | $O_2$ %vol | $CO_2$ %vol | HC ppm vol | CO %vol | Measurement time, s |
|---|---|---|---|---|---|---|
| 1 | 750 | 17.27 | 2.35 | 22 | 0.019 | |
| 2 | 1000 | 17.46 | 2.27 | 25 | 0.049 | |
| 3 | 1550 | 17.61 | 2.1 | 30 | 0.062 | 60 |

exhaust smoke of a diesel engine has been proven in accordance with the diagram shown in Figure 8. After the impact of a high voltage electric field on the exhaust gas of a vehicle, decreasing the smoke concentration has been detected. In particular, with the engine crankshaft speed of 750 rpm, decrease the smoke concentration by 27 % has been revealed. With the engine operating range at 1000 rpm, decrease of the smoke concentration by 7.3 % has been noted. With the engine speed of 1600 rpm, the smoke concentration decreased by 5.56 %.

As a result of the field experiment, decreasing the degree of turbidity of the exhaust gas has been more than 5 %. The physical process is explained by the impact ionization of the gaseous medium, which is proven by experiment.

At the second stage of the experiment, 6 measurements have been made to determine the composition of the exhaust gases of the vehicle. Measurements have been

made before the impact of the ionizer on the engine operating ranges of 750, 1000, 1550 rpm. The data are shown in Table 2. Then, the experiment has been carried out after the exposure to the ionizer. Measurements of the exhaust gases composition have been recorded and presented in Table 3.

At the second stage of the experiment, according to the data from the diagrams of Figures 9-12, it has been revealed that the high voltage electric field affects the composition of the exhaust gases. With the engine speed of 750 rpm, the effect of impact ionization on the composition of the vehicle exhaust gas has been proven, namely, increasing the percentage of oxygen in the exhaust gases by 0.52% and decreasing carbon dioxide content of 1.26%, decreasing carbon monoxide content of 27% have also been recorded. When the engine has been running at 1000 rpm, increasing the concentration of oxygen by 0.29% and hydrocarbons by 1 unit of carbon concentration in ppm by volume of gas, decreasing carbon dioxide 1.26% and decreasing carbon monoxide by 3.92% have been recorded. During the operation of the engine at 1550 rpm, it has been found that the content of oxygen and carbon monoxide decreased by 0.11% and 4.62% respectively. The carbon dioxide content in the exhaust gases increased by 4.76% and hydrocarbons increased by 1 unit of carbon concentration in ppm by volume of gas.

The hypothesis about the possibility of reducing the toxicity of exhaust gases of a diesel engine under the influence of a high voltage electric field was confirmed.

Figure 13 shows that the humidity of the exhaust

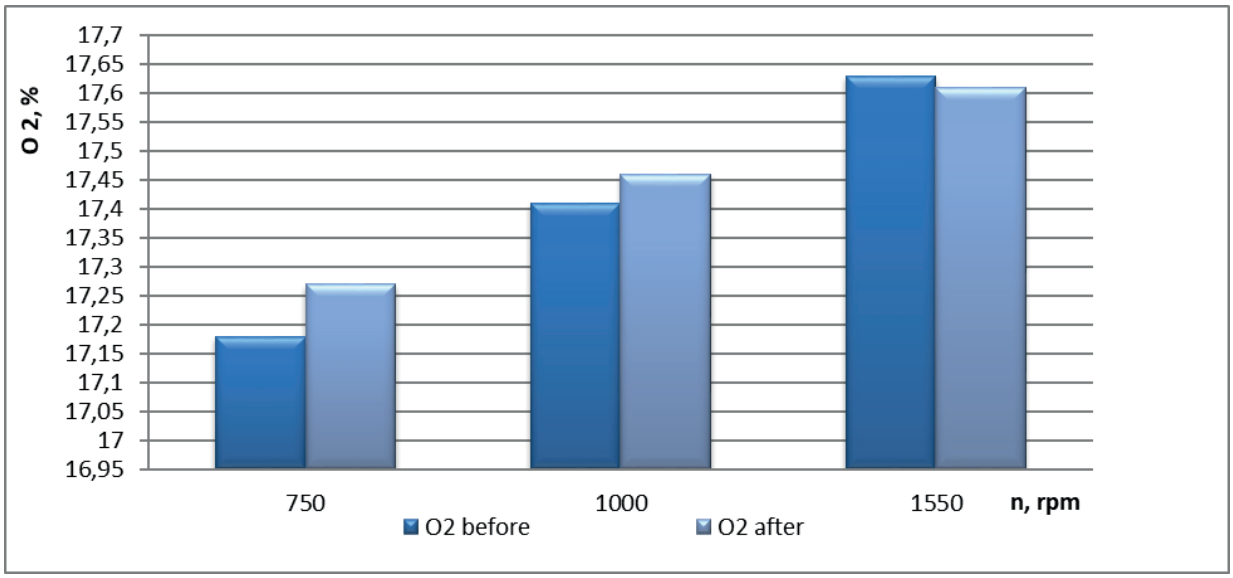


***Figure 9*** *Diagram of the oxygen content in the exhaust gases before and after the exposure to a high voltage electric field*

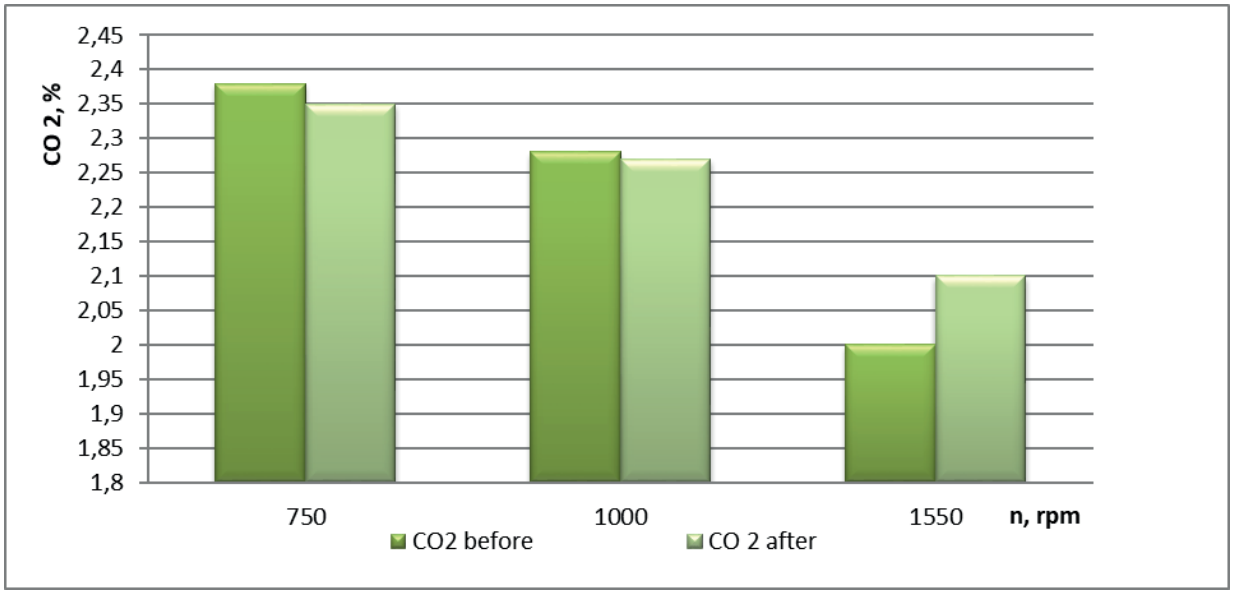


***Figure 10*** *Diagram of the carbon dioxide content before and after the exposure to a high voltage electric field*

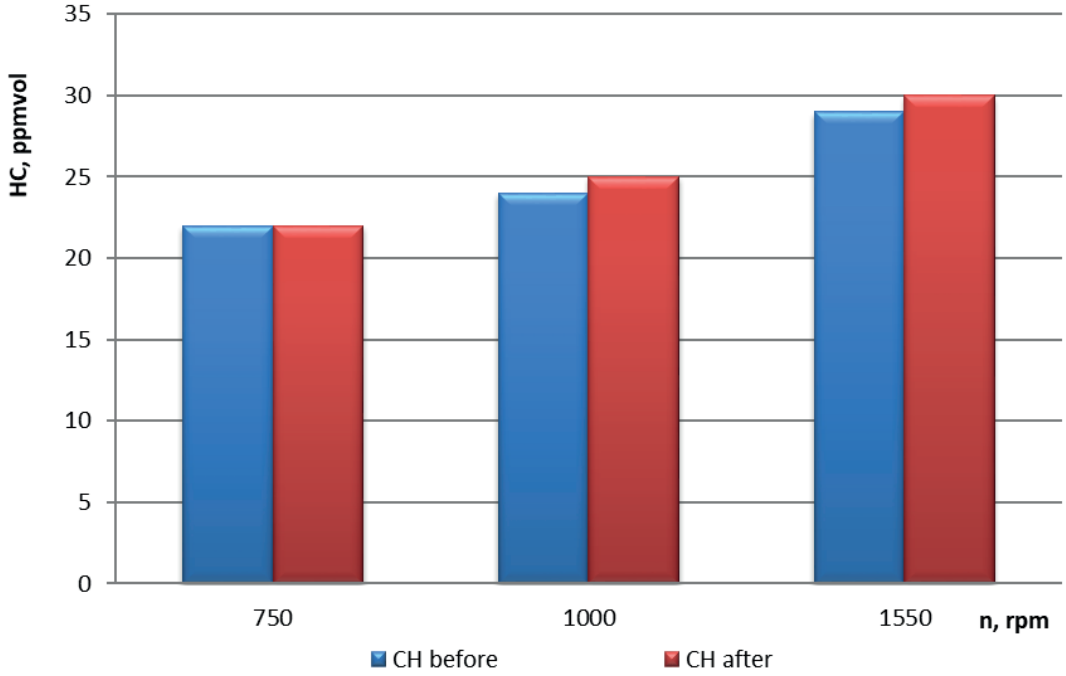


***Figure 11*** *Diagram of the hydrocarbon content before and after the exposure to a high voltage electric field*

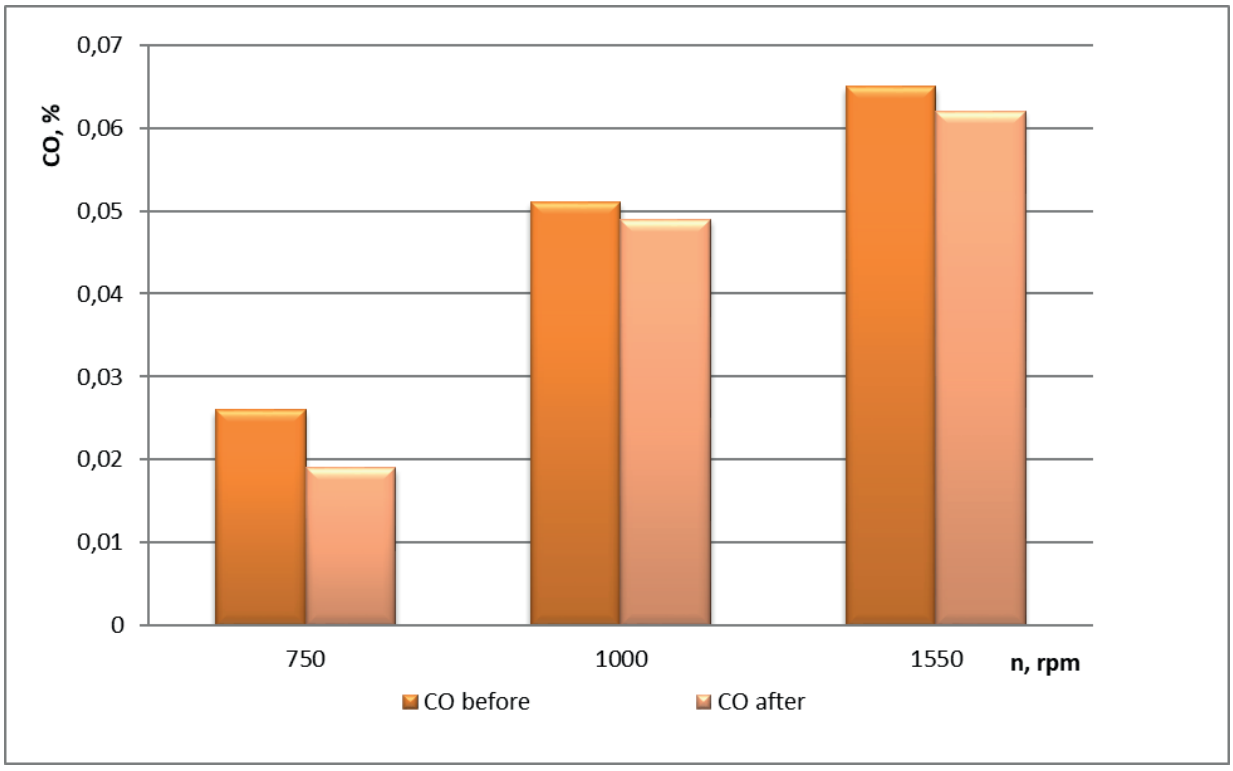


***Figure 12*** *Diagram of the carbon monoxide content before and after the exposure to a high voltage electric field*

gases increases sharply after the influence of a high voltage electric field.

Figures 14-17 show graphs of the dependence of changes in humidity and gas concentration on the number of revolutions.

As the speed increases, the oxygen content increases and the humidity decreases. This is due to the fact that the electrical pulse purifies the gas.

The amount of hydrocarbon increases due to the increase in oxygen, favorable conditions arise for the chemical reaction of the combination of oxygen with hydrogen.

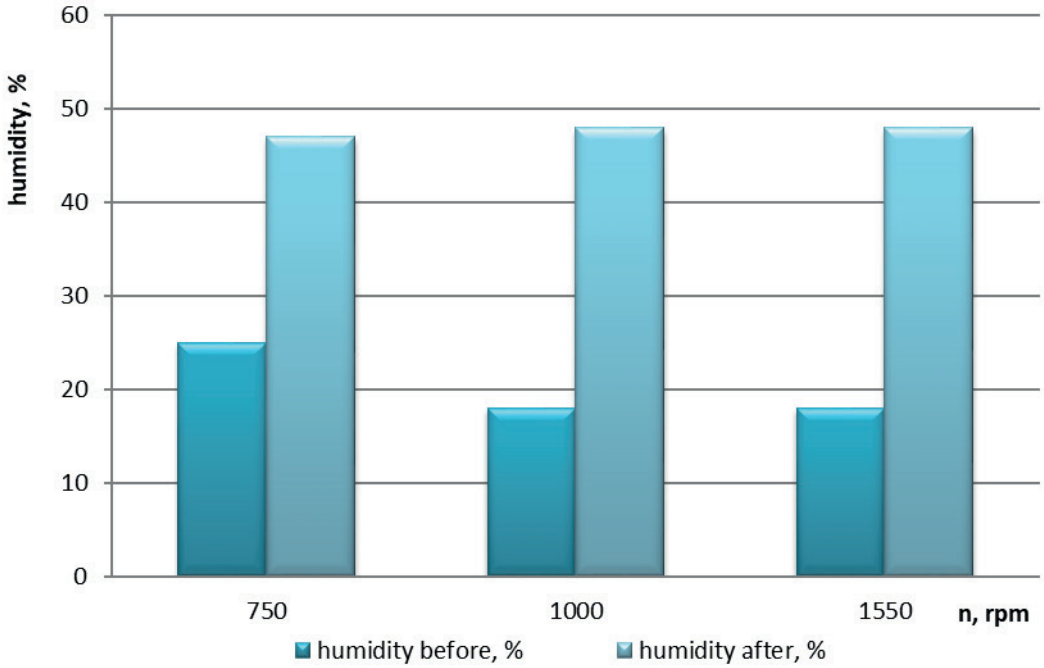


***Figure 13*** *Diagram of the humidity variation*

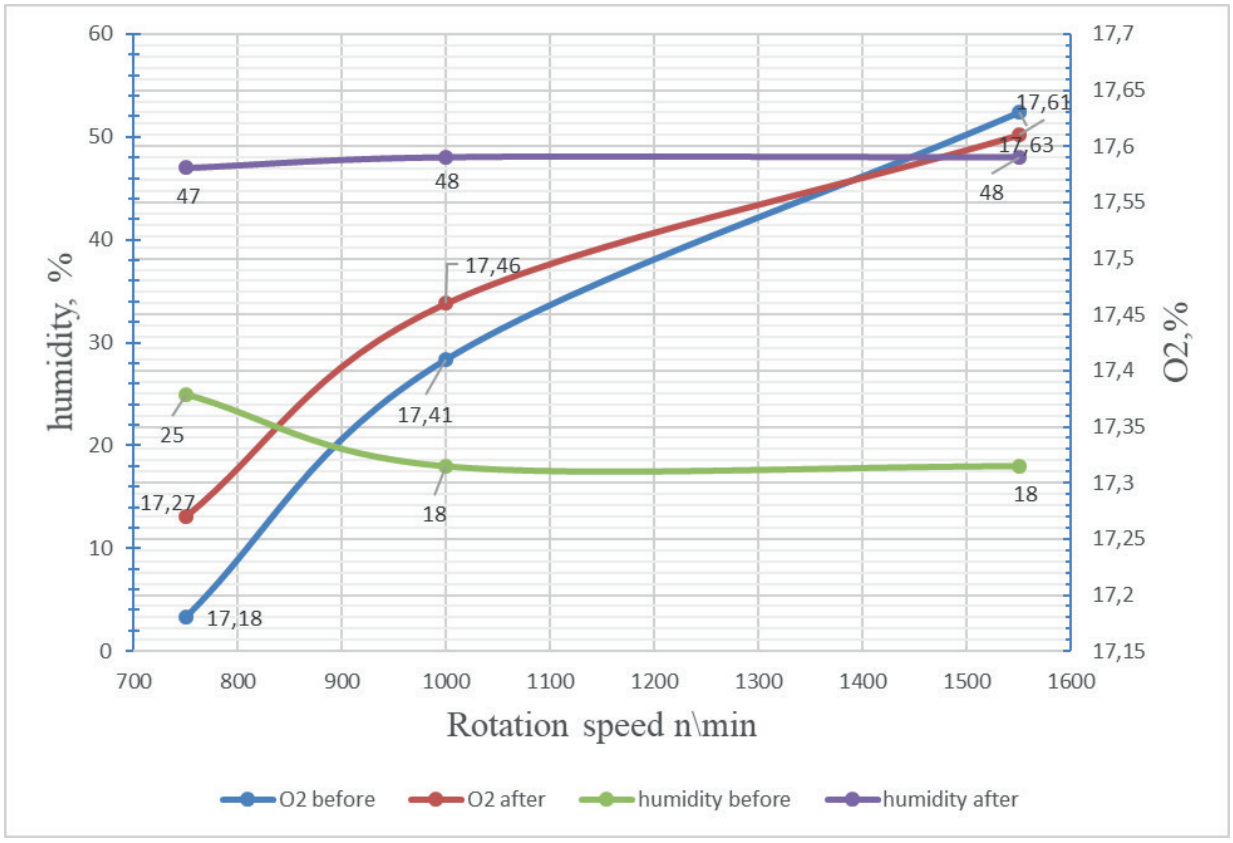


***Figure 14*** *Changing the oxygen content and humidity before and after the exposure to a high voltage electric field*

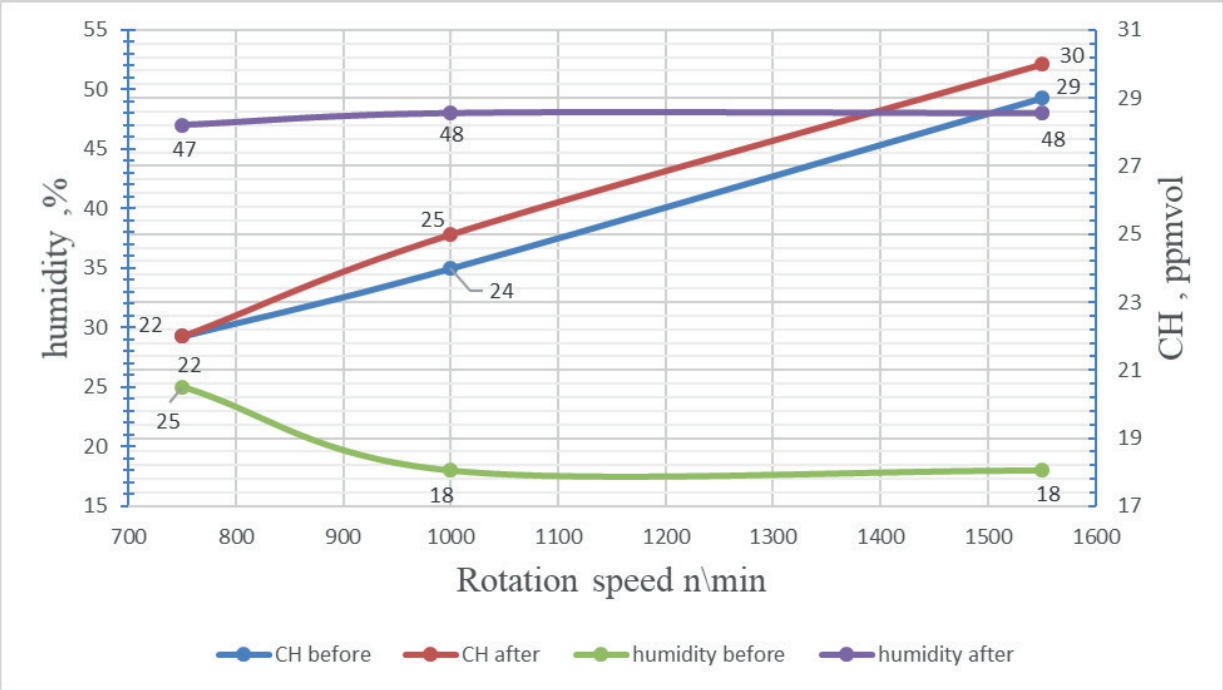


***Figure 15*** *Changing the hydrocarbon content and humidity before and after the exposure to a high voltage electric field*

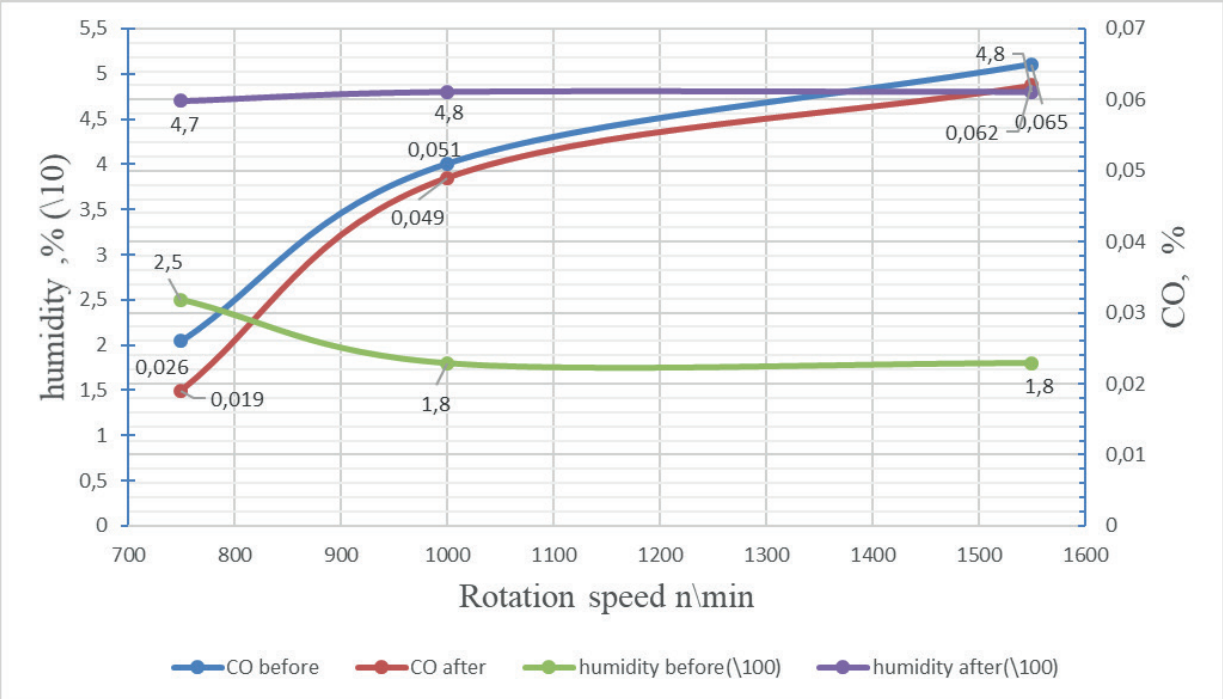


***Figure 16*** *Changing the carbon monoxide content and humidity before and after the exposure to a high voltage electric field*

The content of carbon monoxide and carbon dioxide decreased after exposure to an electric field. From the analysis of the graphs (Figures 14-17) it follows:

- after the pulse impact, the content of carbon monoxide and carbon dioxide decreases;
- the oxygen content increases, as the air is ozonized;
- increasing the oxygen content in the gas, together with the presence of water molecules and ionization, forms conditions for decomposing heavy organic gas molecules, which leads to increasing the hydrocarbon content.

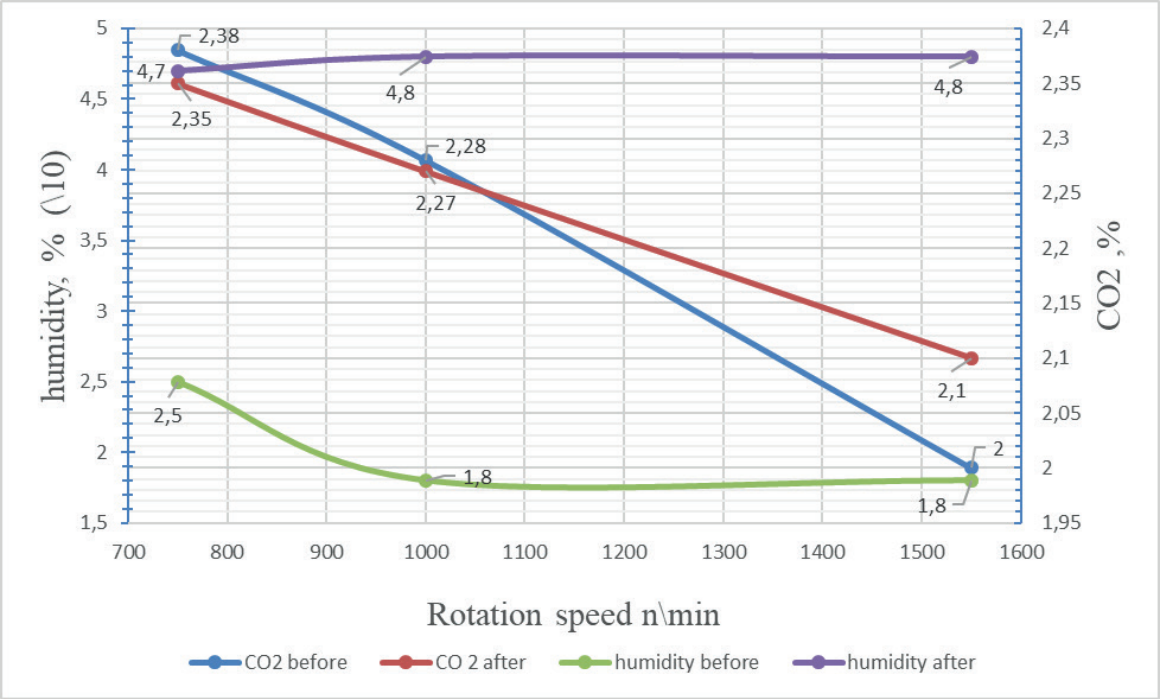


***Figure 17*** *Changing the carbon dioxide content and humidity before and after the exposure to a high voltage electric field*

## 4 Conclusions

Based on the results of the studies, the hypothesis of the possibility of purifying the exhaust gases of internal combustion engines by exposing it to a corona discharge in an electric field has been confirmed.

A mathematical model for the movement of gas particles in a muffler has been developed and studied.

A deterministic relationship between the capacity of the combustion chambers, the discharge parameters and the engine speed has been obtained.

An experimental bench has been developed and manufactured. The constructive decision on the location of two ring electrodes along the axis of gas movement and when it moves in the opposite direction from the collector and the discharge has been justified.

With increasing the engine speed and with a constant discharge, the oxygen content increases and that of carbon monoxide and carbon dioxide decreases. The hydrocarbon formation reaction takes place.

In general, the results obtained have practical and scientific significance. The obtained materials form the basis for the calculation method for the design of automobile mufflers with an electric impulse effect on exhaust gases.

## References

[1] KADYROVA, I. A., MINDUBAEVA, F. A., GRJIBOVSKI, A. M. Prediction of outcomes after stroke: a systematic review. *Human Ecology*. 2015, **2015**(10), p 55-64. ISSN 1728-0869.

[2] KADYROV, A., GANYUKOV, A., PAK, I., SULEYEV, B., BALABEKOVA, K. Theoretical and experimental study of operation of the tank equipment for ultrasonic purification of the internal combustion engine exhaust gases. *Communications - Scientific Letters of the University of Zilina* [online]. 2021, **23**(3), p. B219-B226. ISSN 1335-4205, eISSN 2585-7878. Available from: https://doi.org/10.26552/com.C.2021.3.B219-B226

[3] KADYROV, A. S., AMANGELDIYEV, N. E. New specifications of the theory of ground cutting. *Periodico Tche Quimica*. 2019, **16**(31), p. 922-936. ISSN 1806-0374.

[4] IBATOV, M. K., KADYROV, A. S., PAK, I. A., KADYROVA, I. A., ASKAROV, B. S. The results of experimental studies of the capacitive equipment of ultrasonic cleaning of exhaust gases of vehicles. *Ugol / Coal* [online]. 2020, **2**, p. 73-78. ISSN 0041-5790. Available from: https://doi.org/10.18796/0041-5790-2020-2-73-78

[5] KADYROV, A., GANYUKOV, A., IMANOV, M., BALABEKOVA, K. Calculation of constructive elements of mobile overpass. *Current Science* [online]. 2019, **116**(9), p. 1544-1550. ISSN 0011-3891. Available from: https://doi.org/10.18520/cs/v116/i9/1544-1550

[6] KADYROV, A., KUNAEV, V., GEORGIADI, I., KHAIBULLIN, R. Advanced methods for solving the problems of road construction in central Kazakhstan. *Tehnicki Vjesnik – Technical Gazette* [online]. 2019, **26**(4), p. 1159-1163.

ISSN 1330-3651. Available from: https://doi.org/10.17559/TV-20170225144013
[7] KADYROV, A., SARSEMBEKOV, B., GANYUKOV, A., ZHUNUSBEKOVA, Z., ALIKARIMOV, K. Experimental research of the coagulation process of exhaust gases under the influence of ultrasound. *Communications - Scientific Letters of the University of Zilina* [online]. 2021, **23**(4), p. B288-B298. ISSN 1335-4205, eISSN 2585-7878. Available from: https://doi.org/10.26552/com.C.2021.4.B288-B298
[8] KADYROV, A. S., KUNAYEV, V. A., GEORGIADI, I. V. Prospects for processing of ferrous metallurgical waste based on ArcelorMittal Temirtau experience. *Metallurgist* [online]. 2018, **62**(1-2), p. 22-28. ISSN 0026-0894. Available from: https://doi.org/10.1007/s11015-018-0620-3
[9] GANYUKOV, A., KADYROV, A., BALABEKOVA, K., KURMASHEVA, B. Tests and calculations of structural elements of temporary bridges / Badania i obliczenia elementów konstrukcyjnych mostów tymczasowych (in Polish). *Roads and Bridges / Drogi i Mosty* [online]. 2018, **17**(3), p. 215-226. ISSN1643-1618. Available from: https://doi.org/10.7409/rabdim.018.014
[10] KADYROV, A. S., KUNAYEV, V. A., GEORGIADI, I. V. Ferrous metallurgy waste and waste technical fluids for obtaining the material of road bases. *Ecology and Industry of Russia* [online]. 2017, **21**(12), p. 44-48. ISSN 1816-0395. Available from: https://doi.org/10.18412/1816-0395-2017-12-44-48
[11] Patent of USSR №1404664. Method for cleaning exhaust gases of an internal combustion engine. 1985
[12] Patent of Russian Federation №2398328. Gas ionization method. 2008
[13] Patent of USSR №1470985. Method for neutralizing exhaust gases of an internal combustion engine and a device for its implementation. 1986
[14] Patent of Russian Federation №2132471. Method for reducing the toxicity of exhaust gases of an internal combustion engine and a device for its implementation. 1999
[15] KADYROV, A., BALABEKOVA, K., GANYUKOV, A., AKHMEDIYEV, S. The constructive solution and calculation of elements of the unified module of the mobile bridge overcrossing. Transport Problems [online]. 2017, **12**(3), p. 59-69. ISSN 1896-0596. Available from: https://doi.org/10.20858/tp.2017.12.3.6
[16] KADYROVA, I. A., KADYROV, A. S. Alterations of serum neurospecific proteins concentrations in patients with metabolic syndrome. *Journal of Neurology and Psychiatry named after S. S. Korsakov* [online]. 2016, **116**(11), p. 92-97. ISSN 1997-7298. Available from: https://doi.org/10.17116/jnevro201611611192-97
[17] ZHUNUSBEKOVA, Z. Z., KADYROV, A. S. Study of digging machine flat element loading in clay solution. *Scientific Bulletin of National Hirnichoho University*. 2016, **2**, p. 30-33. ISSN 2071-2227.
[18] Patent of the Republic of Kazakhstan No. 3194. Device for ultrasonic purification of exhaust. 2018.
[19] KADYROV, A. S., PAK, I. A., KADYROVA, I. A., GANYUKOV, A. A. Physics of the process of ultrasonic coagulation of exhaust gases of internal combustion engines of motor vehicles. *Bulletin of PSU. Energy Series*. 2020, **1**, p. 219-230. ISSN 1811-1858.
[20] KADYROV, A., PAK, I., GANYUKOV, A., IMANOV, M., BALABEKOVA, K. Research of operation of equipment for ultrasonic purification of exhaust gases of internal combustion engines. *Journal of Engineering Physics and Thermophysics* [online]. 2021, **94**(6), p. 1407-1414. ISSN 1062-0125, eISSN 1573-871X. Available from: https://doi.org/10.1007/s10891-021-02447-x
[21] KADYROV, A., GANYUKOV, A., BALABEKOVA, K. Development of constructions of mobile road overpasses. *MATEC Web of Conferences* [online]. 2017, **108**, 16002. eISSN 2261-236X. Available from: https://doi.org/10.1051/matecconf/201710816002
[22] KHODZHIBERGENOV, D. T., ESIRKEPOV, A., SHEROV, K. T. Rational milling of metals. *Russian Engineering Research*. 2015, 35(1), p. 43-45. ISSN 1068-798X.
[23] NASAD, T. G., SHEROV, K. T., ABSADYKOV, B. N., TUSUPOVA, S. O., SAGITOV, A. A. ABDUGALIYEVA, G. B., OKIMBAYEVA, A. E. Formation management in parts processing regenerated by surfacing. *News of the National Academy of Sciences of the Republic of Kazakhstan, Series of Geology and Technical Sciences*. 2019, **3**(435), p. 102-108. eISSN 2518-170X.
[24] KADYROV, A., KARSAKOVA, A., DONENBAYEV, B., BALABEKOVA, K. Establishing the strength characteristics of the lifting-leveling device structures of the VPO-3-3000 machines for the track straightening. *Communications - Scientific Letters of the University of Zilina* [online]. 2020, **22**(4), p. 70-79. ISSN 1335-4205, eISSN 2585-7878. Available from: [2] https://doi.org/10.26552/com.C.2020.4.70-79
[25] IBATOV, M. K., KADYROV, A. S., PAK, I. A., KADYROVA, I. A., ASKAROV, B. S. Results of experimental studies of the operation of capacitive equipment for ultrasonic cleaning of vehicle exhaust gases. *Ugol / Coal* [online]. 2020, 2, p. 73-78. ISSN 0041-5790. Available from: https://doi.org/10.18796/0041-5790-2020-2-73-78
[26] KADYROV, A., ZHUNUSBEKOVA, Z., GANYUKOV, A., KADYROVA, I., KUKESHEVA, A. General characteristics for loading the working elements of drilling and milling machines when moving in the clay solution. *Communications - Scientific Letters of the University of Zilina* [online]. 2021, **23**(2), p. B97-B105. ISSN 1335-4205, eISSN 2585-7878. Available from: https://doi.org/10.26552/com.C.2021.2.B97-B105

# STUDYING THE PROCESS OF TRANSPORT EQUIPMENT COOLING SYSTEM ULTRASONIC CLEANING

Adil Kadyrov [1], Kirill Sinelnikov [1,*], Rustem Sakhapov [2], Alexandr Ganyukov [1], Bakyt Kurmasheva [1], Shinpolat Suyunbaev [3]

[1]Karaganda Technical University, Karaganda, Kazakhstan
[2]Kazan State University of Architecture and Engineering, Kazan, Russia
[3]Tashkent State Transport University, Tashkent, Uzbekistan

*E-mail of corresponding author: coolzero7777@gmail.com

***Resume***
The article deals with the existing methods of cleaning vehicle radiators from sedimentary scale. A method of cleaning radiator tubes by ultrasonic radiation is proposed. An experimental bench has been developed for studying ultrasonic cleaning processes. Based on the results of the experiment, dependences have been obtained that determine the efficiency of the process depending on the mass of scale removed and the liquid outflow rate from the tubes. There are proposed the purification degree coefficients. The hypothesis about the possibility of cleaning radiators with ultrasonic vibrations has been confirmed.

***Article info***
Received 27 April 2022
Accepted 28 July 2022
Online 16 September 2022

***Keywords:***
vehicle
transport equipment
radiator
cooling system
internal combustion engine
ultrasound
cleaning

Available online: https://doi.org/10.26552/com.C.2022.4.B288-B300

ISSN 1335-4205 (print version)
ISSN 2585-7878 (online version)

## 1 Introduction

A radiator is an element of the cooling systems of the internal combustion engine of road transport that consists of thin-walled tubes through which the coolant flows, and tanks-reservoirs connecting the tubes into a single unit (Figure 1) [1]. The radiator provides the desired temperature range of the engine coolant by giving off excess heat to the flow of air passing through the radiator.

Radiators for various purposes are mounted on road transport depending on the design of the vehicle:

- a radiator of the engine cooling system;
- the vehicle interior heater radiator;
- an oil radiator;
- the air conditioning and evaporator radiators;
- an intercooler radiator.

These radiators can be significantly different in appearance but fundamentally of the same design [1]. The main designs of automobile radiators are shown in Figure 2.

Reliable operation of the internal combustion engine in transport equipment is impossible without a good cooling system [2]. Proper maintenance of the cooling system increases the engine life. Maintenance of the cooling system is mainly reduced to the timely replacement of the coolant and flushing the cooling system. Deterioration of the technical condition of the engine leads to deterioration in the environmental situation, a large emission of exhaust gases into the atmosphere. This in turn contributes to the development of pulmonary, cardiac and other diseases [3].

The operation of the internal combustion engine cooling system consists in cooling the engine by removing excess heat and transferring it to the radiator that releases it into the atmosphere [4]. A coolant, such as antifreeze, constantly circulates in the cooling system keeping the engine temperature within a certain range.

Antifreezes do not form scale but they are dangerous from a different point of view: they decompose over time, and their decomposition products affect adversely the cooling system. Rust, oxides and layers of various organic substances form on the internal surfaces of the metal components of the cooling system.

In the engine cooling system, metals of various properties are used. So, the radiator is made of brass or galvanized steel, the engine block head is made of aluminum alloy, and the cylinder block is made of cast iron or aluminum alloy. When cleaning, the reaction must occur between scale and a chemical reagent without affecting the

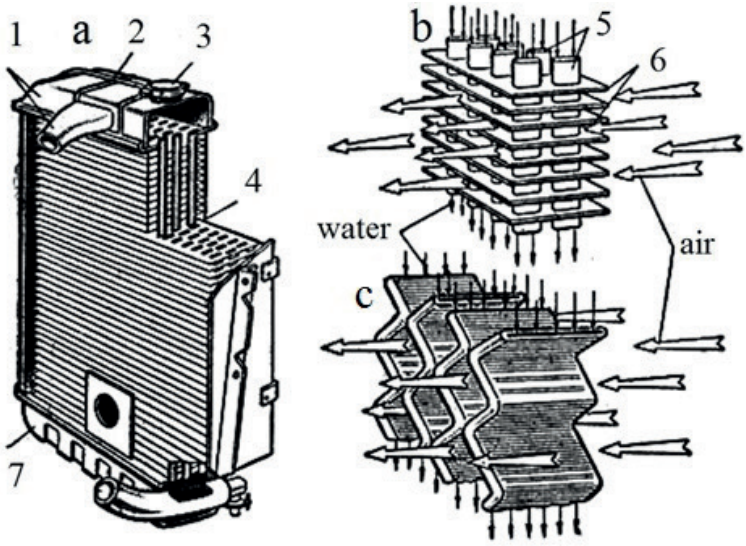


*a - vehicle radiator device, b - tubular core, c - lamellar core,* 1 *- upper tank with a pipe,* 2 *- steam pipe,* 3 *- filler neck with a plug,* 4 *- core,* 5 *- tubes,* 6 *- transverse plates,* 7 *- lower tank with a pipe*

***Figure 1*** *Vehicle radiator arrangement*

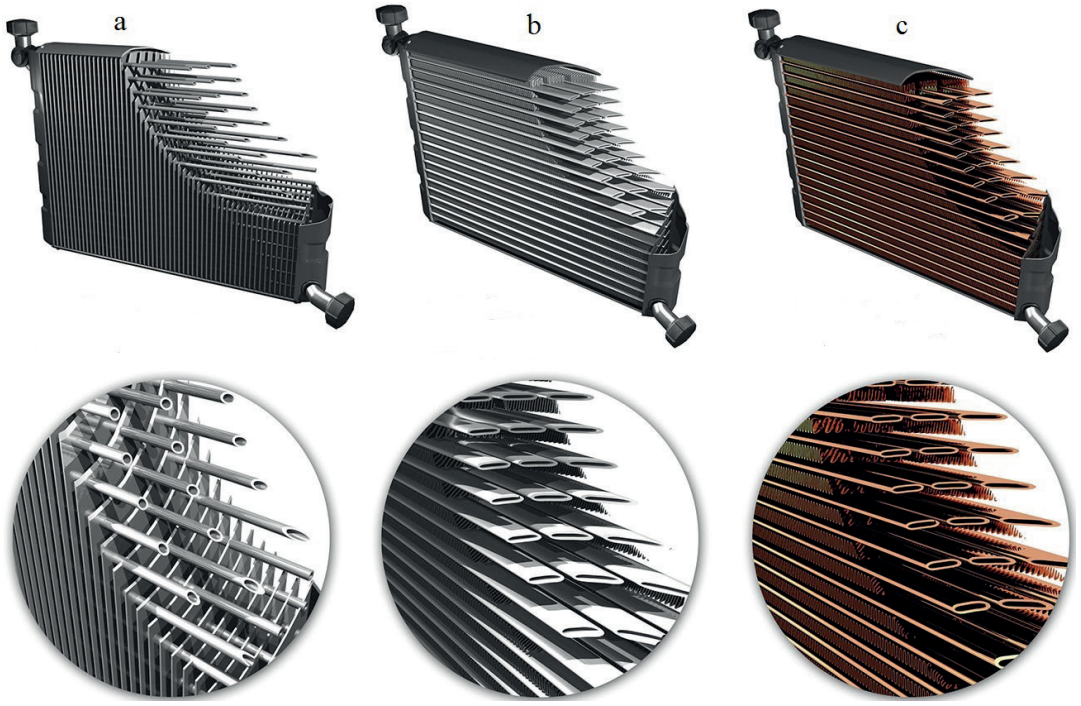


*a - aluminum tubular-plate prefabricated radiator, b - aluminum tubular-band brazed radiator, c - copper-brass tubular-band brazed radiator*

***Figure 2*** *Automobile radiators designs*

metal; this cannot be done because each type of pollution requires its own chemical action [5-8].

A variety of contaminants of different kinds penetrate into the cooling system: oils and other contaminants, detergents, dust, etc. Sealants that are often used to quickly repair damage to radiators and pipes sealants, which are often used for quick repairing damages to radiators and pipes, pollute seriously the system.

Scale, rust, oil-organic contaminants are deposited on the internal surfaces of the cooling system components. They have worse thermal conductivity compared to that of metals, they narrow the clearance of thin tubes (Figure 3). This leads to decreasing the efficiency of the cooling system and as a result, to engine overheating [9].

A labor-intensive process of maintaining the cooling system of motor vehicles is the cleaning of radiators from


1 - *interior heater radiator,* 2 - *tube,* 3 - *scale,* 4 - *scale-metal boundary*

***Figure 3*** *Scale deposits on the radiator tubes*

scale deposits formed on the walls of the radiator tubes. To date, the radiators of the internal combustion engine cooling system are cleaned by the chemical and mechanical methods. These methods have a number of significant drawbacks due to high complexity of the process, the detrimental effect on the components and the impossibility of using the method due to the design and type of the radiator [10].

The chemical method of cleaning radiators involves washing the radiator with distilled water and adding etching acids to it. At this, washing the radiator can be performed directly on the vehicle; to obtain the best result it is possible to dismantle the radiator from the vehicle [11-13].

After flushing the radiator, the flushing liquid is drained and clean water is poured, the procedure is repeated until the clean liquid flows from the stove radiator; then the radiator cleaning is considered complete. There is always a risk of damaging the vehicle radiator using chemicals to clean it that results in smudges and microcracks.

With the mechanical cleaning method, the remaining liquid is first drained from the cooling system and then the radiator is removed. To gain access to the tubes, at least one of the radiator tanks is unsoldered. The work for mechanical cleaning of tubes consists in the fact that a steel bar of the appropriate section and length is inserted into each tube, then a reciprocating movement is performed along the entire length of the tube while removing scale and internal deposits. If it is impossible to clean the tubes on one side, the second radiator tank is soldered and cleaned on the other side. The mechanical cleaning method is characterized by high labor intensity and the associated high costs of time and money for the cleaning process [14]. The radiator tubes are often damaged, and it comes into disrepair.

The authors propose to use ultrasonic vibrations to clean the radiator tubes. Ultrasonic cleaning is a method of cleaning the surface of solids in flushing liquid s or water, due to the impact of ultrasonic vibrations on them.

The cleaning process is characterized by the joint manifestation of various nonlinear effects that occur in the liquid when exposed to ultrasonic vibrations. These effects include cavitation, acoustic currents, sound pressure and sound capillary effect [15-17]. In particular, in the process of cleaning the radiator tubes, the effect of cavitation is observed that is accompanied by the formation of cavitation bubbles pulsating and collapsing near pollution, thereby destroying the layer of scale and other deposits [18-19].

The method of ultrasonic cleaning does not require significant use of manual labor and other mechanical influences from the side and greatly simplifies the cleaning process. This removes flammable and toxic solvents from the cleaning process.

In this regard, the proposed method of cleaning the vehicle radiator from scale is relevant.

The hypothesis of the study is assumption of the possibility of cleaning the vehicle radiator from scale by ultrasonic action.

The purpose of the work is studying the process of ultrasonic cleaning, namely: establishing the dependences linking the exposure time of the ultrasonic generator to the mass of scale washed out from the heater radiator of a passenger vehicle, the temperature of the flushing fluid and the exposure time. For the initial study, the authors have selected a passenger car interior heater radiator.

To achieve the goal of the study, the following tasks have been solved: the analysis of literature sources has been performed on the possibility of cleaning the radiators of the cooling system of motor vehicles using ultrasonic waves; an experimental bench for ultrasonic cleaning the radiator has

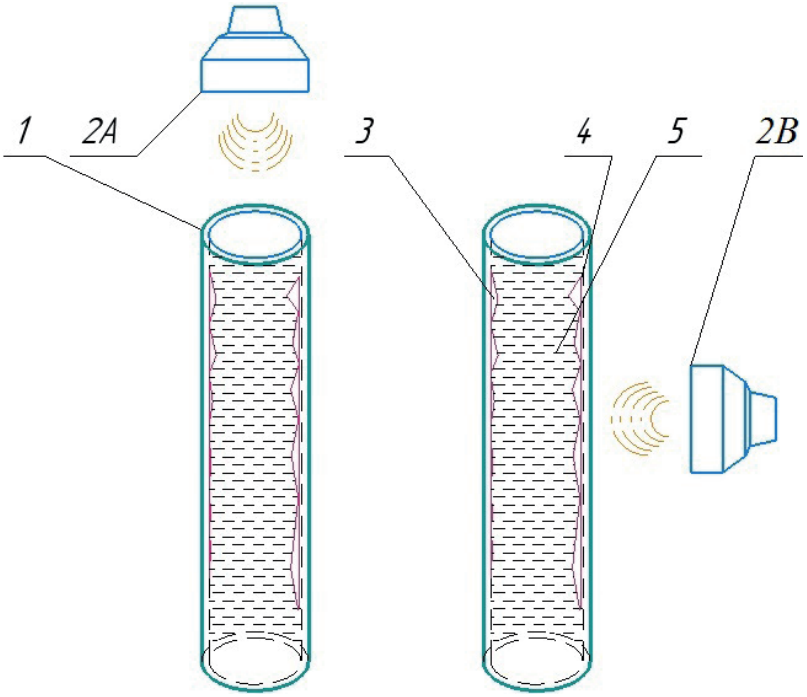


*1 - tube, 2A - longitudinal ultrasonic transducer, 2B - transverse ultrasonic transducer, 3 - scale, 4 - scale-metal boundary, 5 - water*

***Figure 4*** *Diagram of the ultrasonic wave impact on the radiator tube*

been developed and the analysis of the results obtained has been carried out. The dependences have been obtained that determine the intensity of cleaning.

## 2 Materials and methods

Ultrasound is mechanical vibration of particles above 20 kHz. Ultrasound travels in the form of waves. To move ultrasound, unlike electromagnetic waves, an elastic medium is needed: a solid body, a gas, a liquid [20].

The main characteristics of ultrasonic waves are the length λ, the oscillation period T, the frequency of oscillations $f$, the speed of sound C in the propagation medium. There are longitudinal and transverse ultrasonic waves. Longitudinal waves coincide with the direction, displacement and velocity of the medium particles, and transverse waves propagate in the direction perpendicular to the plane, the direction of displacement and velocity of the body [21].

An important indicator is the power of ultrasound, that is, the energy transmitted by the wave through the surface under consideration per unit of time.

Ultrasonic dispersion is fine grinding of solids or liquids under the action of ultrasonic vibrations. Liquid dispersion in gases is called atomization, and liquid dispersion in liquids is called emulsification. Ultrasonic dispersion makes it possible to obtain highly dispersed mixtures with the particle size smaller than 1 μm, while mechanical dispersion allows obtaining particles with the particle size of up to 1-10 μm [21].

Grinding substances occurs under the action of shock waves and violation of the materials continuity. This helps to accelerate the cleaning of surfaces immersed in a liquid medium from contamination [22].

The difference between the proposed method and others consists in the fact that here the cleaning takes place without pouring a chemical liquid into the radiator and mechanical impacts but under the action of ultrasound on the tank wall scale [23].

In addition, the turbulent mode of fluid movement caused by ultrasonic vibrations is of great importance in the ultrasonic dispersion method [24].

For the occurrence of the phenomenon of cavitation, the radiator tubes are filled with a liquid. The liquid has minimum viscosity, a sufficiently high temperature and is saturated with air. Plain water has a variable value of dynamic viscosity: at 0°C - 1.977 Pa·s, at 40°C - 0.655 Pa·s, at 80°C - 0.357 Pa·s [25]. In this regard, water is needed for cleaning.

Since cavitation is the process of the air bubbles explosion in the liquid medium, the more saturated the water with air, the more efficient the process.

The ultrasound impact can be along the tube and across the tubes of the radiator (Figure 4). When exposed along the tubes, a longitudinal wave arises, and when the effect is transverse, a transverse wave arises.

With a transverse wave, it is necessary to cross the interface of the media several times: twice the walls of each tube, which leads to rapid attenuation of the wave. Preliminary experiments have been carried out that proved that the action of a longitudinal wave is more effective [26].

***Figure 5*** *experimental bench for ultrasound cleaning the car radiator*

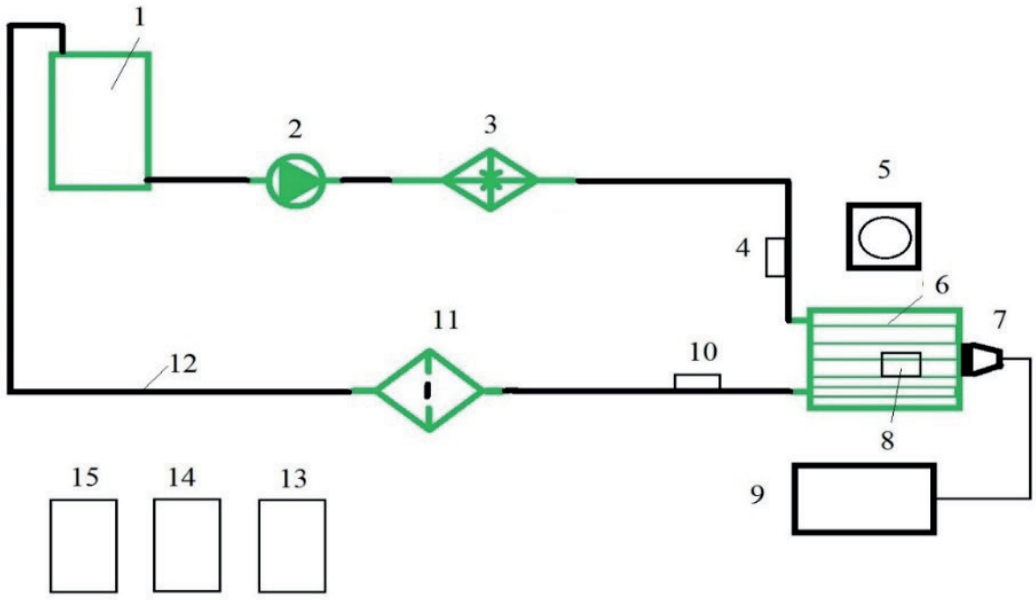


*1- reservoir for liquid; 2 - circulation pump; 3 - heating element; 4 - liquid temperature sensor on the inlet pipe of the radiator; 5 - axial fan; 6 - interior heater radiator; 7 - ultrasonic emitter; 8 - temperature sensor of the air flow passing through the radiator; 9 - ultrasonic generator; 10 - liquid temperature sensor on the outlet pipe of the radiator; 11 - filter; 12 - rubber pipes; 13 - device for controlling the temperature flow of the air passing through the radiator; 14 - device for monitoring the temperature of the liquid entering the radiator; 15 - device for monitoring the temperature of the liquid leaving the radiator*

***Figure 6*** *Scheme of the experimental setup for car radiators ultrasound cleaning*

To test the effectiveness of ultrasonic cleaning, the authors have used experimental research methods.

The purpose of the experiment has been to confirm the proposed hypothesis.

The experiment has been carried out on a specially designed experimental bench for ultrasonic cleaning of car radiators (Figures 5-7).

The bench is a unit for cleaning radiators that consists of the following elements: a liquid reservoir, rubber pipes, a heating element, a circulation pump, a filter, an ultrasonic


*1 - interior heater radiator; 2 - ultrasonic emitter; 3 - axial fan; 4 - circulation pump with a heating element; 5 - filter; 6 - reservoir for liquid; 7 - devices for temperature control; 8 - rubber pipes*

***Figure 7*** *Placing the emitter on the interior heater radiator*

100 watt 40 kHz generator, an ultrasonic 50 watt 40 kHz emitter, temperature measuring instruments, an axial fan, a passenger car interior heating radiator (Figure 7).

The scheme of the experimental setup for ultrasonic cleaning of car radiators is shown in Figure 6.

Water with the lowest viscosity have been used as a flushing liquid for the heater radiator of a passenger car. Cavitation occurs most rapidly in water. Water of different temperatures has been used to determine the optimal temperature range.

The procedure of the experiment consist of two stages. At the first stage, the experiment has the following tasks:

1. Determining the parameters of pure water.
2. Determining the ultrasonic wave impact along the radiator tubes on the experimental becnh.
3. Determining water parameters after exposure to ultrasound.
4. Processing the obtained results.

The second stage of the experiment consisted of the following tasks:

1. Determining the parameters of pure water.
2. The ultrasonic wave impact along the tubes of the radiator with air saturation into water on an experimental bench.
3. Determining water parameters after ultrasonic exposure with saturation of additional air into the liquid.
4. Processing the obtained results.

In this regard, the following actions have been carried out at both stages of the experiment:

- the antifreeze has been drained from the radiator and antifreeze residues have been washed out with water;
- clean water has been poured into the radiator;
- the water has been drained from the radiator, the flow rate, mass and volume of the water have been measured to determine its density (Figures 8-9);
- the water has been poured, the ultrasonic exposure has been performed, the rate of water outflow, its density and the mass of scale released after exposure to ultrasound have been measured;
- the temperature of the inlet and outlet fluid passing through the radiator before and after exposure to ultrasound has been determined;
- the temperature of the air flow passing through the radiator developed by the axial fan has been determined.

To determine the efficiency of cleaning the radiator using ultrasonic exposure, the rate of water outflow from the tubes has been measured before and after exposure to the ultrasonic wave. By weighing, the mass and density of water and pulp (water + scale) have been determined.

The mass of scale has been determined in the following way: the mass of pure water has been taken from the mass


***Figure 8*** *Determining the liquid volume using a volumetric flask and the mass of liquid on the balance*


***Figure 9*** *Determining the liquid outflow rate through the radiator*

of the pulp and the mass of the washed scale has been obtained. The pulp is a liquid with scale obtained after exposure to an ultrasonic wave on the radiator. The scale is a solid deposit formed on the surfaces of heat exchange elements, on which the liquid is heated and cooled. Scale formation occurs not only due to decomposition of the coolant but also due to the ingress of engine oil, gasoline, grease, etc.

The same experiment has been carried out for water of various temperatures, and after saturation of the liquid with air. The water has been saturated with air by forcing it through a hose with a compressor.

The performance of a car radiator was determined by monitoring the temperature of the passing liquid at the inlet and outlet pipes of the radiator. With the help of a fan, a stream of air has been forced through the radiator that produced heat exchange between the air and the radiator. The air flow temperature has been controlled.

## 3 Results

The first stage of the experiment provides the effect of ultrasound on water that is poured into the radiator within 600, 1200, 1800 seconds.

The mass of the liquid, the pulp outflow time, its flow rate and temperature have been measured depending on

***Table 1*** *Parameters measured under the action of ultrasound*

| Measured parameter | Unit of measurement | Exposure time, s. | | | |
|---|---|---|---|---|---|
| | | 0 | 600 | 1200 | 1800 |
| Liquid mass (M) | Gram (g) | 44.57 | 44.60 | 44.63 | 44.69 |
| Liquid volume (V) | Milliliter (ml) | 45 | 45 | 45 | 45 |
| Liquid density (P) | Gram/cubic centimeter (g/cm$^3$) | 0.9904 | 0.9911 | 0.9917 | 0.9931 |
| Liquid outflow time (t) | Second (s) | 1 liter within 9.93 seconds | 1 liter within 9.73 seconds | 1 liter within 9.22 seconds | 1 liter within 9.20 seconds |
| Liquid outflow rate (U) | Milliliter/second (ml/s) | 100.7 | 102.7 | 108.45 | 108.69 |
| Liquid temperature (°C) | Celsius degree | 51 | 51 | 50 | 51 |

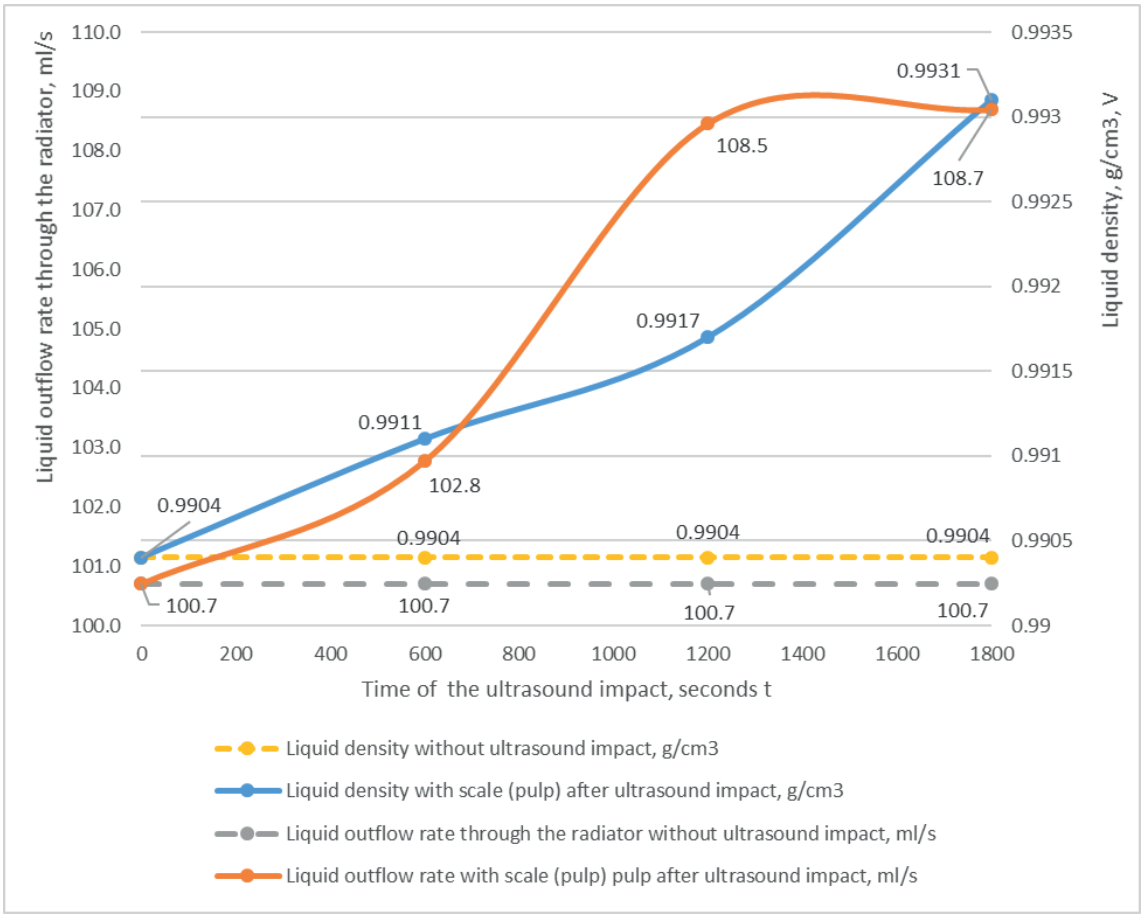


***Figure 10*** *Changing the liquid density outflow rate through the car radiator depending on the time of exposure to ultrasound*

***Table 2*** *Changing the mass of the pulp depending on the time of exposure to ultrasound*

| Impact on the radiator | Liquid mass | Liquid mass increasing after the impact |
|---|---|---|
| Before exposure to ultrasonic wave, 0 seconds | 44.57 grams | 0 grams |
| After the first exposure to ultrasonic wave, 600 seconds | 44.60 grams | 0.03 grams |
| After the second exposure to the ultrasonic wave, 1200 seconds | 44.63 grams | 0.06 grams |
| After the third exposure to the ultrasonic wave, 1600 seconds | 44.69 grams | 0.12 grams |

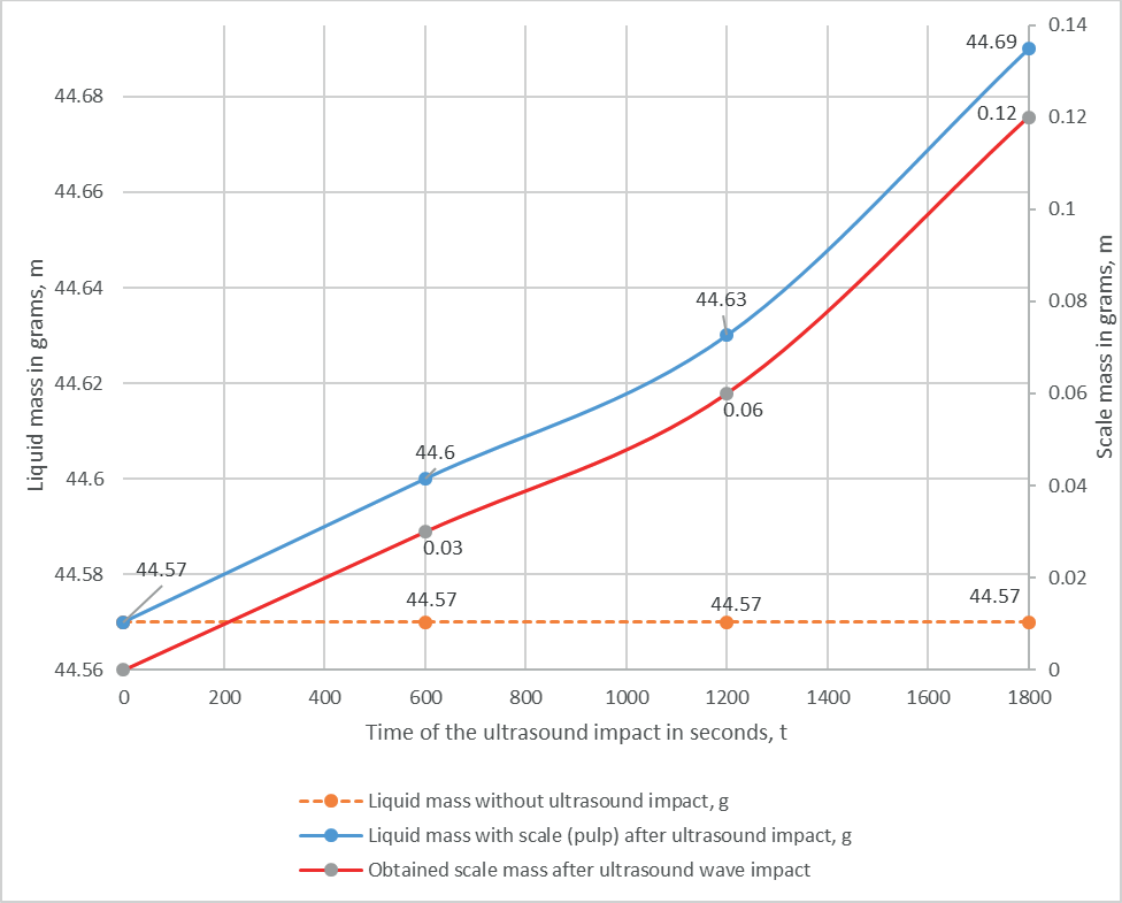


***Figure 11*** *The mass of pulp obtained depending on the ultrasound impact time*

the time of exposure to ultrasound. These parameters are shown in Table 1.

The processing of the experimental results made it possible to obtain the dependence of the fluid outflow rate through the car radiator and its density, which allows determining the intensity of tube cleaning (Figure 10).

It follows from the dependence in Figure 10 that, with increasing the time of exposure to ultrasound, the liquid outflow rate with scale (pulp) in comparison with pure water increases curvilinearly with the extremum in the area of the time of ultrasound impact of 1400 s.

Reducing the flow rate in the area of 1600...1800 s is determined by the fact that the radiator has been cleaned. The density of the pulp also increases with increasing the time of exposure to ultrasound and, consequently, with a greater transfer of energy.

Table 2 shows changing the mass of the pulp depending on the time of exposure to ultrasound

Figure 11 shows that there takes place increasing the pulp mass. This growth is curvilinear. According to the measurements, a graph of changing the mass of the pulp has been obtained. Subtracting the mass of pure water from the mass of the pulp, there has been obtained the mass of the washed scale.

The dependences obtained in Figure 11 confirm the assumption that it is possible to clean the radiator tubes with ultrasound. The scale content in the liquid increases in a curvilinear manner with increasing the time of exposure to ultrasound on the heater radiator of a passenger car.

During the experiment, the dependence of the outflow rate of the flushing liquid on the temperature has been established (Table 3), From the resulting graph (Figure 12) it follows that the outflow rate of the pulp almost linearly increases with increasing the temperature of the poured water. This is caused by decreasing its dynamic viscosity.

The optimum temperature for the ultrasonic dispersion

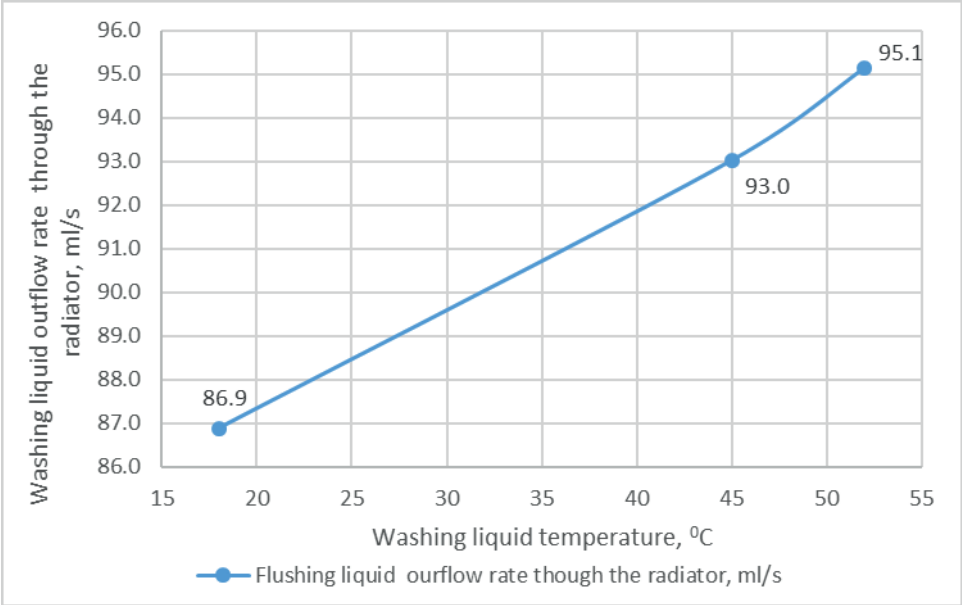


***Figure 12*** *Changing the liquid outflow rate through the radiator depending on the liquid temperature*

***Table 3*** *Coefficients that characterize the efficiency of the radiator cleaning*

| Measured parameter | Exposure time, s. | | | |
|---|---|---|---|---|
| Ultrasonic exposure time | 0 | 600 | 1200 | 1800 |
| Fluid flow rate increase factor after exposure to ultrasound ($K_0$) | 1 | 1.019860973 | 1.076961271 | 1.079344588 |
| The coefficient of increase in the mass of the washed scale after exposure to ultrasound (Km) | 1 | 1.000673 | 1.001346 | 1.002692 |
| The coefficient of increase in the density of the liquid after exposure to ultrasound ($K_p$) | 1 | 1.000707 | 1.001313 | 1.002726 |

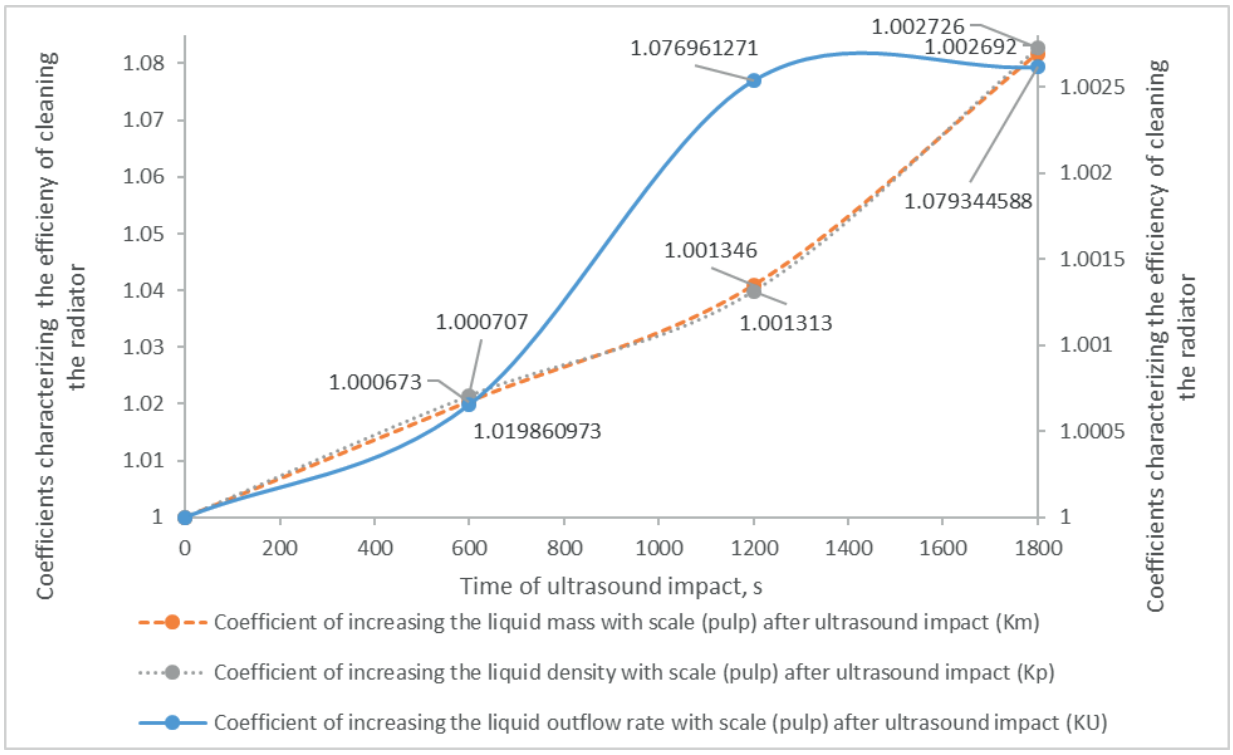


***Figure 13*** *Coefficients characterizing the efficiency of radiator cleaning*

***Table 4*** *Parameters measured under ultrasound impact with air*

| Measured parameter | Unit of measurement | Impact time, s. | | |
|---|---|---|---|---|
| | | 0 | Ultrasound impact, 600 s. | Ultrasound +air impact, 600 c. |
| Liquid mass (M) | Grams (g) | 44.52 | 44.57 | 44.65 |
| Liquid volume (V) | Milliliters (ml) | 45 | 45 | 45 |
| Liquid Density (P) | Grams per cubic centimeter (g/cm$^3$) | 0.9893 | 0.9904 | 0.9922 |
| Liquid outflow time (t) | Seconds (s) | 1 liter within 9.21 seconds | 1 liter within 9.18 seconds | 1 liter within 9.17 seconds |
| Liquid flow rate (U) | Milliliter per second (ml/s) | 108.6 | 108.9 | 109.1 |
| Liquid temperature (°C) | Celsius degrees (°C) | 50 | 51 | 51 |

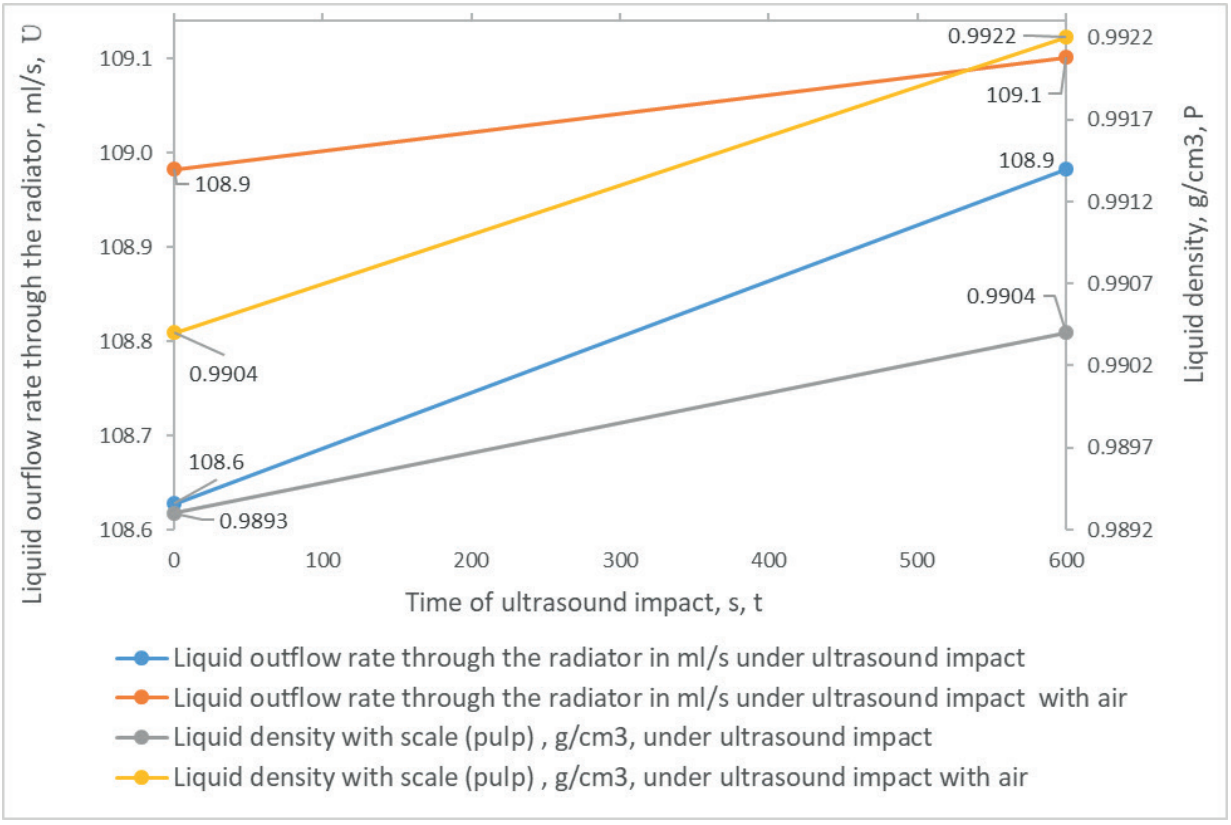


***Figure 14*** *Changing the density and the liquid outflow rate through the car radiator when the water is saturated with air*

process is 40…60 Celsius degrees [26]. When the specified temperature is exceeded, the rate of grinding scale particles decreases, therefore, the process of cleaning the car radiator will decrease. For the experiment, the temperature range of 50-51 °C has been selected.

According to the ratios of the scale mass to the liquid outflow rate with different periods of impact, the coefficients of cleaning efficiency have been determined (Figure 13):

$$K_m = \frac{m_{1...3} \times 100\%}{m_0},$$
$$K\upsilon = \frac{\upsilon_{1...3} \times 100\%}{\upsilon_0}, \quad (1)$$
$$K_p = \frac{p_{1...3} \times 100\%}{p_0},$$

where: Km, $K_U$ and $K_p$ are coefficients that characterize increasing the scale mass, the density and the liquid outflow rate from the radiator depending on the time of ultrasound impact;

$m_{1...3}$ is the scale mass depending on the time of ultrasound impact;

$U_{1...3}$ in the liquid ourflow rate depending on the time of ultrasound impact;

$P_{1...3}$ is the pulp density depending on the time of ultrasound impact.

The obtained coefficients in Figure 13 characterize the efficiency of cleaning the radiator. The physical meaning of the coefficients Km, $K_U$ and Kp consist in reflecting the processes occurring under the impact of liquid cavitation

under the action of ultrasound and characterize the efficiency of scale destruction in the radiator tubes.

At the second stage of the experiment, water has been saturated with air using a compressor. Then the experiment has been repeated according to the first plan, and according to the obtained measurable parameters (Table 4), a graph has been built (Figure 14).

The dependences obtained in Figure 14 indicate increasing the liquid cavitation when saturated with air. When exposed to an ultrasonic wave and saturating the flushing liquid with air using a compressor, it improves the process of cleaning the radiator tubes.

## 4 Conclusion

The literature analysis of ultrasonic cleaning systems carried out led to the conclusion that such ultrasonic effects were not used to clean the radiators of the motor vehicle cooling system.

The hypothesis about the possibility of developing a method of cleaning radiator tubes from scale using ultrasonic exposure has been experimentally proven, while the results of the experiment have shown the following:

- the rate of fluid outflow from the radiator tubes after ultrasonic exposure increases. This is caused by increasing the internal section of the tubes as a result of descaling;
- the density of the pulp is higher than the density of water and, according to the curvilinear dependence, it increases with the time of exposure to ultrasound;
- the mass of scale released also depends on the cleaning time;
- when the water temperature rises, the cleaning process accelerates, as the intensity of cavitation increases;
- the more water is saturated with air, the more intensive the cleaning process. The impact is almost linear.

The results obtained make it possible to prove scientific and practical significance for the development of a methodology of calculating the parameters of the technological process of maintaining the radiators.

## References

[1] VAKHLAMOV, V. K. *Cars: the basics of design: a textbook for students of institutions of secondary vocational education*. Moscow: Academy, 2007. ISBN 978-5-7695-4230-5.

[2] PUCHIN, E. A., GADZHIEV, A. A., KONONENKO, A. Repair of radiators of the cooling system of internal combustion engines. Textbook. Moscow: FGOU VPO MGAU, 2006.

[3] KADYROVA, I. A., MINDUBAYEVA, F. A., GRJIBOVSKI, A. M. Prediction of outcomes after stroke: a systematic review. *Human Ecology*. 2015, **2015**(10), p. 55-64. ISSN 1728-0869.

[4] KADYROV, A., GANYUKOV, A., PAK, I., SULEYEV, B., BALABEKOVA, K. Theoretical and experimental study of operation of the tank equipment for ultrasonic purification of the internal combustion engine exhaust gases. *Communications - Scientific Letters of the University of Zilina* [online]. 2021, **23**(3), p. B219-B226. ISSN 1335-4205, eISSN 2585-7878. Available from: https://doi.org/10.26552/com.C.2021.3.B219-B226

[5] KADYROV, A., ZHUNUSBEKOVA, Z., GANYUKOV, A., KADYROVA, I., KUKESHEVA, A. General characteristics for loading the working elements of drilling and milling machines when moving in the clay solution. *Communications - Scientific Letters of the University of Zilina* [online]. 2021, **23**(2), p. B97-B105. ISSN 1335-4205, eISSN 2585-7878. Available from: https://doi.org/10.26552/com.C.2021.2.B97-B105

[6] KADYROV, A., SARSEMBEKOV, B., GANYUKOV, A., ZHUNUSBEKOVA, Z., ALIKARIMOV, K. Experimental research of the coagulation process of exhaust gases under the influence of ultrasound. *Communications - Scientific Letters of the University of Zilina* [online]. 2021, **23**(4), p. B288-B298. ISSN 1335-4205, eISSN 2585-7878. Available from: https://doi.org/10.26552/com.C.2021.4.B288-B298

[7] KADYROV, A. S., KUNAYEV, V. A., GEORGIADI, I. V. Ferrous metallurgy waste and waste technical fluids for obtaining the material of road bases. *Ecology and Industry of Russia* [online]. 2017, **21**(12), p. 44-48. ISSN 1816-0395. Available from: https://doi.org/10.18412/1816-0395-2017-12-44-48

[8] [8]KADYROV, A., KARSAKOVA, A., DONENBAYEV, B., BALABEKOVA, K. Establishing the strength characteristics of the lifting-leveling device structures of the VPO-3-3000 machines for the track straightening. *Communications - Scientific Letters of the University of Zilina* [online]. 2020, **22**(4), p. 70-79. ISSN 1335-4205, eISSN 2585-7878. Available from: [9] https://doi.org/10.26552/com.C.2020.4.70-79

[10] IBATOV, M. K., KADYROV, A. S., PAK, I. A., KADYROVA, I. A., ASKAROV, B. S. The results of experimental studies of the capacitive equipment of ultrasonic cleaning of exhaust gases of vehicles. *Ugol / Coal* [online]. 2020, **2**, p. 73-78. ISSN 0041-5790. Available from: https://doi.org/10.18796/0041-5790-2020-2-73-78

[11] KADYROV, A., GANYUKOV, A., IMANOV, M., BALABEKOVA, K. Calculation of constructive elements of mobile overpass. *Current Science* [online]. 2019, **116**(9), p. 1544-1550. ISSN 0011-3891. Available from: https://doi.org/10.18520/cs/v116/i9/1544-1550

[12] KADYROV, A., KUNAEV, V., GEORGIADI, I., KHAIBULLIN, R. Advanced methods for solving the problems of road construction in central Kazakhstan. *Tehnicki Vjesnik* [online]. 2019, **26**(4), p. 1159-1163. ISSN 1330-3651. Available from: https://doi.org/10.17559/TV-20170225144013

[13] KADYROV, A. S., AMANGELDIYEV, N. E. New specifications of the theory of ground cutting. *Periodico Tche Quimica*. 2019, **16**(31), p. 922-936. ISSN 1806-0374.

[14] KADYROV, A. S., KUNAYEV, V. A., GEORGIADI, I. V. Prospects for processing of ferrous metallurgical waste based on arcelormittal temirtau experience. *Metallurgist* [online]. 2018, **62**(1-2), p. 22-28. ISSN 0026-0894. Available from: https://doi.org/10.1007/s11015-018-0620-3

[15] GANYUKOV, A., KADYROV, A., BALABEKOVA, K., KURMASHEVA, B. Tests and calculations of structural elements of temporary bridges / Badania i obliczenia elementów konstrukcyjnych mostów tymczasowych (in Polish). *Roads and Bridges* / *Drogi i Mosty* [online]. 2018, **17**(3), p. 215-226. ISSN1643-1618. Available from: https://doi.org/10.7409/rabdim.018.014

[16] KADYROV, A., BALABEKOVA, K., GANYUKOV, A., AKHMEDIYEV, S. The constructive solution and calculation of elements of the unified module of the mobile bridge overcrossing. Transport Problems [online]. 2017, **12**(3), p. 59-69. ISSN 1896-0596. Available from: https://doi.org/10.20858/tp.2017.12.3.6

[17] ZHUNUSBEKOVA, Z. Z., KADYROV, A. S. Study of digging machine flat element loading in clay solution. *Scientific Bulletin of National Hirnichoho University*. 2016, **2**, p. 30-33. ISSN 2071-2227.

[18] KADYROV, A., PAK, I., GANYUKOV, A., IMANOV, M., BALABEKOVA, K. Research of operation of equipment for ultrasonic purification of exhaust gases of internal combustion engines. *Journal of Engineering Physics and Thermophysics* [online]. 2021, **94**(6), p. 1407-1414. ISSN 1062-0125, eISSN 1573-871X. Available from: https://doi.org/10.1007/s10891-021-02447-x

[19] NASAD, T. G., SHEROV, K. T., ABSADYKOV, B. N., TUSUPOVA, S. O., SAGITOV, A. A. ABDUGALIYEVA, G. B., OKIMBAYEVA, A. E. Formation management in parts processing regenerated by surfacing. *News of the National Academy of Sciences of the Republic of Kazakhstan, Series of Geology and Technical Sciences*. 2019, **3**(435), p. 102-108. ISSN 2224-5278.

[20] Patent of the Republic of Kazakhstan No. 3194. Device for ultrasonic purification of exhaust. 2018.

[21] BALDEV, R., RAJENDRAN, V., PALANICHI, P. *Applications of ultrasound*. Moscow: Technosphere, 2006. ISBN 5-94836-088-1.

[22] BERGMAN, L. *Ultrasound and its application in science and technology*. BERGMAN, L., GRIGORIEVA, V. S., ROSENBERG, L. D. Moscow: Publishing House of Foreign Literature, 1957.

[23] KHODZHIBERGENOV, D. T., ESIRKEPOV, A., SHEROV, K. T. Rational milling of metals. *Russian Engineering Research*. 2015, **35**(1), p. 43-45. ISSN 1068-798X.

[24] KADYROV, A., GANYUKOV, A., BALABEKOVA, K. Development of constructions of mobile road overpasses. *MATEC Web of Conferences* [online]. 2017, **108**, 16002. eISSN 2261-236X. Available from: https://doi.org/10.1051/matecconf/201710816002

[25] KADYROVA, I. A., KADYROV, A. S. Alterations of serum neurospecific proteins concentrations in patients with metabolic syndrome. *Journal of Neurology and Psychiatry named after S. S. Korsakov* [online]. 2016, **116**(11), p. 92-97. ISSN 1997-7298. Available from: https://doi.org/10.17116/jnevro201611611192-97

[26] KADYROV, A. S., PAK, I. A., KADYROVA, I. A., GANYUKOV, A. A. Physics of the process of ultrasonic coagulation of exhaust gases of internal combustion engines of motor vehicles. *Bulletin of PSU. Energy Series*. 2020, **1**, p. 219-230. ISSN 1811-1858.

[27] IBATOV, M. K., KADYROV, A. S., PAK, I. A., KADYROVA, I. A., ASKAROV, B. S. Results of experimental studies of the operation of capacitive equipment for ultrasonic cleaning of vehicle exhaust gases. *Ugol* / *Coal* [online]. 2020, 2, p. 73-78. ISSN 0041-5790. Available from: https://doi.org/10.18796/0041-5790-2020-2-73-78

# THE STABILITY INDICATORS OF THE SECTION ARTICULATED BUSES

Vladimir Sakhno [1], Juraj Gerlici [2], Viktor Polyakov [1], Anatolii Korpach [1], Oleksii Korpach [1], Kateryna Kravchenko [2,*]

[1]National Transport University M. Omelianovicha-Pavlenka, Kiev, Ukraine
[2]University of Zilina, Zilina, Slovak Republic

*E-mail of corresponding author: kateryna.kravchenko@fstroj.uniza.sk

***Resume***
The mathematical model of a multi-section articulated bus has been improved in the article, which allowed to determine the stability indicators of the two and three-section articulated buses for the Metrobus system. The critical speed for the three-section articulated bus was 28.06 m/s and for the two-section articulated bus - 30.89 m/s. Since the motion of multi-section articulated buses will be carried out on separate lanes with a speed of 25 - 28 m/s, one can assume that the stability of rectilinear traffic of both two and three-section buses is provided. In non-stationary modes of motion with two-section articulated buses, the lateral speed of the first bus decreases by almost 8.5% compared to the three-section and the second trailer-bus increases by almost 9.5% compared to the three-section. In this case, the motion stability of multi-section articulated buses can be considered satisfactory, as the lateral accelerations in the center of mass of all sections do not exceed 0.45 g.

Available online: https://doi.org/10.26552/com.C.2022.4.B301-B309

***Article info***
Received 12 May 2022
Accepted 13 September 2022
Online 29 September 2022

***Keywords:***
two and three-section
articulated bus
stability
trailer
acceleration

ISSN 1335-4205 (print version)
ISSN 2585-7878 (online version)

## 1 Formulation of the problem

One of the main problems of the modern big city is the global crisis of normal functioning of the urban environment due to the structural growth of the motorization level, oversaturation of the road network with traffic flows. This leads to a sharp deterioration in transport services, traffic jams, rising noise and air pollution, a practical drop in speed, rising energy costs, increasing the victim's number of road accidents [1-9].

Recently, many cities around the world have introduced so-called BRT (Bus Rapid Transit) systems [2-4]. These systems have become a cheaper alternative to the subway and other rail transport, including trams. The BRT transport now operates in more than 200 cities around the world. The advent of Metrobus system will help evolve "minibuses" from cities and move to a more progressive model of urban transport.

The main economic advantage of a high-speed bus over a regular one is much lower fuel consumption per passenger [1-9]. This is achieved through rational, specially designed driving modes. On the BRT line, as a rule, multi-section articulated bus run especially large capacity (18 or 22, 24, 25 m), but the main difference from the usual city routes is that they run on a separate (dedicated) lane at short intervals, for example, 1 minute. Along with the undeniable advantages of bi-articulated buses and trolleybuses, they also have disadvantages - worse manoeuvrability and stability. Therefore, solving issues related to improving the manoeuvrability and stability of multi-section articulated buses is an urgent task.

## 2 Analysis of scientific publications

Stability of motion belongs to the properties of motor vehicles that do not have a strict certainty in terminology, requirements, indicators and methods of assessment. In practice, they use experimental characteristics that determine the stability of vehicles during movement and in theory, direct and indirect indicators and their dependences, among which the main ones are the critical speed of movement and lateral accelerations acting in the center of mass of individual sections. At present, the problem of determining the stability conditions for the semi-trailer trucks has been sufficiently studied. Thus, in [10-11], a simplified analysis of the manoeuvrability and stability of vehicle combinations, such as a tractor in combination with

one or two semitrailers or a truck and a full trailer, was carried out. Vehicle combinations are considered linear dynamic systems with two degrees of freedom for each unit. The motion equations are derived taking into account the effect of braking and acceleration and the characteristic equation for motion with constant speed is obtained. In [12], the three-dimensional dynamic models of a truck and a trailer were developed, based on which a dynamic model of the semi-trailer truck was constructed. Based on the first-order approximation theory of ordinary differential equations and the theory of Hopf bifurcation, the linear and nonlinear stability of each element and the semi-trailer truck as a whole under rectilinear motion is studied. Numerical results show that for the nonlinear and linear models the critical velocities differ little from each other. In [13], the equations of vertical and lateral dynamics of a semi-trailer truck with 6 degrees of freedom are reduced to a matrix form. The motion of such a vehicle in the vertical and lateral planes has been investigated. It is shown that the developed method can be applied to analyze the stability of the motion, in particular, of passenger trains. In [14], a multivariate extension of the D2-IBC (Data Driven - Inversion Based Control) method is considered and its application to control the stability of the motion of the semi-trailer trucks is discussed in detail. In [15], a model of the semi-trailer truck with 31 freedom degrees was constructed using the AutoSum package and the directions of improving the semi-trailer truck stability are shown. At the same time, it is shown that its stability can be significantly improved by using an inerter, which is considered effective for increasing the stability and performance of multi-section road trains. However, as practice shows, determining the system's behavior nature in the field of instability and identifying the causes of their occurrence has not lost its relevance.

The characteristics of the maneuverability and stability of the vehicle motion, as is known, are determined by a combination of the operational, mass-geometric and design parameters of its modules (vehicle for the Metrobus system) and their control systems. In general, the desired combinations of these parameters from the point of view of stability, even for the same vehicle in the range of operational loads and run speeds, are different. As a consequence, it is difficult to obtain accurate design parameters and quantitative indicators according to the stability criteria of its motion at the early stages of the design of vehicles. Success in solving such problems depends on how well the mathematical model is chosen and its essential parameters that describe the dynamic system behavior in different modes of motion. Therefore, the aim of the work is a comparative assessment of the two and three-section articulated buses in both stationary and non-stationary modes.

Figure 1 shows the general view (a) and the calculation scheme of the three-section articulated bus (b). Metrobus consists of a driving link, which has front steering wheels and can have rear driving wheels, both swivel and non-swivel. Both the first and the second trailing single-axle link can have both rotating and non-rotating wheels. At the point $O_0'$, the first towing link rests on the leading one, at the second point $O_1'$, the towing link rests on the first. Interaction forces between the links of the road train arise at the coupling points $O_0'$ and $O_1'$.

## 3 Comparative assessment of the motion stability of the two and three-section articulated buses

In [16], a system of differential equations was obtained by the sections method, which describes the plane-parallel motion of the sections of a three-section articulated bus, Figure 1 (b). This system of equations is written in the form:

$$\begin{aligned}
&m(\dot{v} - u\omega) = -X_2 + XA - XB\cos\gamma_1 + \\
&+ YB\sin\gamma_1; \\
&m(\dot{u} + v\omega)Y_2 + YA - YB\cos\gamma_1 + XB\sin\gamma_1; \\
&J\dot{\omega} = aYA - bY_2 - c(YB\cos\gamma_1 + XB\sin\gamma_1) + \\
&+ M_1 + M_2; \\
&J_1\dot{\omega}_1 = -YA\lambda\cos\gamma_0 + XA\lambda\sin\theta - M_1 = 0; \\
&J_2\dot{\omega}_2 = d_1 YB - b_1 Y_3 + \\
&+ c_1(YC\cos\gamma_2 + XC\sin\gamma_2) - M_3; \\
&J_3\dot{\omega}_3 = d_2 YC - b_2 Y_4 + M_2 - M_3.
\end{aligned} \tag{1}$$

The reactions at the connection points of the three-section articulated bus sections are defined as follows:

$$\begin{aligned}
&XC = m_3\dot{v}_3 - m_3\omega_3 u_3 + X_4; \\
&YC = m_3\dot{u}_3 + m_3\omega_3 v_3 - Y_4; \\
&XB = m_2\dot{v}_2 - m_2\omega_2 u_2 + m_3\dot{v}_3\cos\gamma_2 - \\
&- m_3\omega_3 u_3\cos\gamma_2 - X_4\cos\gamma_2 + X_3 - m_3\dot{u}_3\sin\gamma_2 - \\
&- m_3\omega_3 v_3\sin\gamma_2 + Y_4\sin\gamma_2; \\
&XA = m_1\dot{u}_1\sin\theta + m_1\omega_1 v_1\sin\theta - Y_1\sin\theta - \\
&- m_1\dot{v}_1\cos\theta + m_1\omega_1 u_1\cos\theta - X_1\cos\theta; \\
&YA = -m_1\dot{u}_1\cos\theta - m_1\omega_1 v_1\cos\theta + Y_1\cos\theta - \\
&- m_1\dot{v}_1\sin\theta + m_1\omega_1 u_1\sin\theta - X_1\sin\theta.
\end{aligned} \tag{2}$$

In the systems of Equations in (1) and (2), the following designations are accepted:

- $a$ – the distance from the front axle to the center of the bus mass;
- $b$ – the distance from the rear axle to the center of the bus mass;
- $c$ – the distance from the center of the bus mass to the coupling point with the first trailer;
- $\lambda$ – the side shift of the front controlled wheels of the bus, due to the longitudinal inclination of the pivot axis;

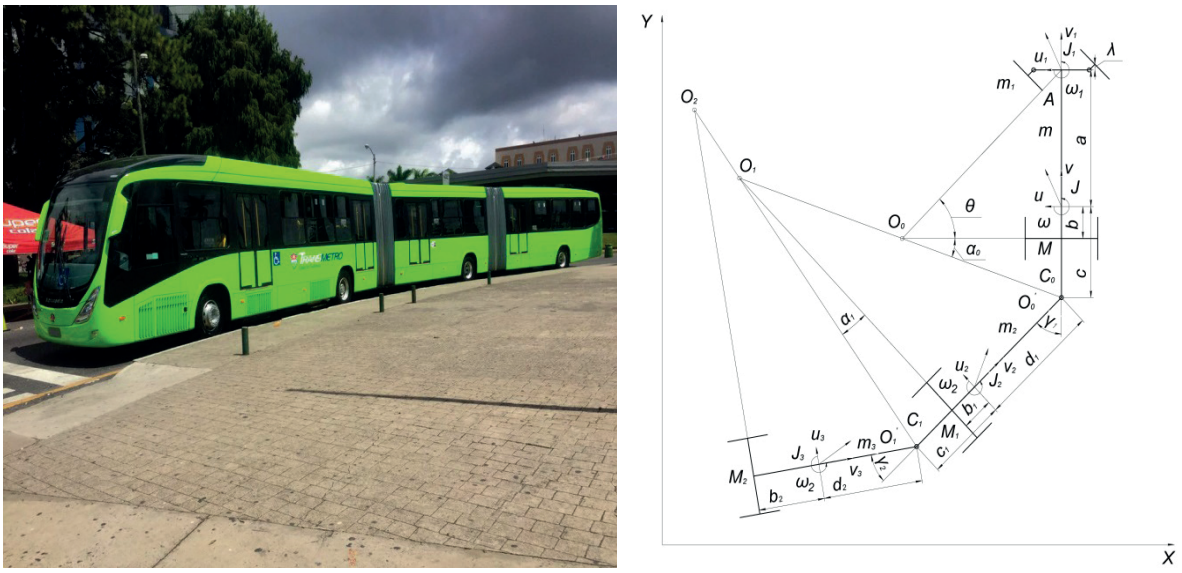


a) b)

***Figure 1*** *Van Hool ExquiCity Metrobus (a); the estimated scheme of the three-section articulated bus for Metrobus system*

$\theta$ – the rotation angle of the front axle wheels of the bus;

$\gamma_1, \gamma_2$ – the first and second joint angles;

$b_1$ – the distance from the mass center of the first trailer to its axis;

$c_1$ – the distance from the mass center of the first trailer to the coupling point with the second trailer;

$d_1$ – the distance from the mass center of the first trailer to the coupling point with the bus;

$b_2$ – the distance from the mass center of the second trailer to its axis;

$d_2$ – the distance from the mass center of the second trailer to the coupling point with the first trailer;

$m$, $m_1$, $m_2$, $m_3$ – the mass of the controlled module of the bus, first and second trailer, respectively;

$J$ – the central moment of the bus;

$\nu, u$ – the longitudinal and cross projections of the velocity vector of the mass center on the axes associated with the bus, respectively;

$\omega$ – the bus angular velocity along the vertical axis;

$J_1$ – the central moment of inertia of the wheel control module of the bus;

$\nu_1, u_1$ – the longitudinal and cross projections of the velocity vector of the mass center of the control wheel module of the bus, respectively;

$\omega_1$ – the angular velocity of the control wheel module of the bus;

$J_2$ – the central moment of first trailer inertia;

$\nu_2, u_2$ – the longitudinal and cross projections of the velocity vector of the mass center of the first trailer, respectively;

$\omega_3$ – the angular velocity of the first trailer;

$J_3$ – the central moment of second trailer inertia;

$\nu_3, u_3$ – the longitudinal and cross projections of the velocity vector of the mass center of the second trailer, respectively;

$\omega_3$ – the angular velocity of the second trailer.

The system of equations in (1) includes lateral forces acting on the wheels of the axles of the multi-section articulated bus. Today, there are several analytical approximations of the dependence of the lateral reaction applied in the wheel contact patch on the side-slip angle, but the most widespread is the following formula [17]:

$$Y_i = \frac{k_i \delta_i}{\sqrt{1 + k_i \delta_i^2 \left(\varphi^2 G_i^2\right)^{-1}}}, \tag{3}$$

where

$\delta_i, Y_i$ – the side-slip angles of the bus axles wheels and lateral force, respectively;

$j$ – the coefficient of lateral adhesion between the wheel tire and the supporting surface;

$k_i$ – the side-slip resistance coefficient.

The need to take into account the nonlinearity is explained by the fact that only in a very narrow range the dependence between the forces acting on the axle and the axle retraction angles is close to linear, while for other values of the side-slip angles this dependence is nonlinear and the lateral force cannot exceed the adhesion forces Y*. As the lateral force approaches its maximum value, partial slip in the lateral direction begins and then full slip. In accordance with this, the maximum value of the lateral force $Y = Y^*$ can be found based on the fact that

$$\lim_{\delta \to +\infty} Y(\delta) = \frac{k}{\chi} = Y^*, \Rightarrow \chi = \frac{k}{Y^*}, Y = \varphi G, \tag{4}$$

where

$\varphi$ – the lateral adhesion coefficient between the tire and the ground;

$G$ – the vertical wheel load.

If one denotes the resistance coefficient to the side-slip in the absence of longitudinal forces acting on the wheel through $k_0$, then the value of $k$ will be determined as:

$$k = k_o \cdot \frac{\sqrt{1 - \left(\frac{X}{\varphi G}\right)^2}}{1 + 0.375\frac{X}{G}}, \tag{5}$$

where

$X$ – the longitudinal force acting on the wheel, the value of which is determined by the ratio

$$\begin{aligned} X &= \frac{M}{r},\ if\ \frac{M}{r} < \varphi G, \\ X &= \varphi G,\ if\ \frac{M}{r} \geq \varphi G, \end{aligned} \tag{6}$$

where

$M$ – the traction (braking) moment that is applied to the wheel.

In the absence of traction (braking) moment on the wheels of the bus axles, the lateral forces on the wheels of its axles are determined by relationships, respectively:

$$Y_i = \frac{k_i \delta_i}{\sqrt{1 + \chi_i^2 \delta_i^2}},\ \chi_i = \frac{k_i}{\varphi Z_i}, \tag{7}$$

where

$Z_i$ – the normal reaction of the supporting surface to the i-th axle of the bus.

The wheel side-slip angles of the multi-section articulated bus axles are defined as

$$\begin{aligned} &\delta_1 = -arctg\frac{u_1}{v_1} - arctg \times \\ &\times \nu \sin\theta + (u + a\omega)\cos\theta - \\ &\frac{-(\omega + \dot{\theta})\lambda + b_1(\omega + \dot{\gamma}_1)}{\nu\cos\theta + (u + a\omega)\sin\theta}, \\ &\delta_2 = arctg[(-u + b\omega)/\nu], \\ &\delta_3 = arctg(-u_2 + b_1\omega/v_2) = arctg \times \\ &\nu\sin\gamma_1 - (u - c\omega)\cos\gamma_1 + \\ &\frac{+(\omega + \dot{\gamma}_1)d_1 + b_1(\omega + \dot{\gamma}_1)}{\nu\cos\gamma_1 + (u - c\omega)\sin\gamma_1}, \\ &\delta_4 = [(-u_3 + b_2\omega_3)/v_3] = arctg \times \\ &\times\{[\nu\cos\gamma_1 + (u - c\omega)\sin\gamma_1]\sin\gamma_2 - \\ &-[\nu\sin\gamma_1 + (u - c\omega)\cos\gamma_1 - (\omega + \dot{\gamma}_1)]\times \\ &\times\cos\gamma_2 + (\omega + \dot{\gamma}_1 + \dot{\gamma}_2)d_2\}/ \\ &/\{[\nu\cos\gamma_1 + (u - c\omega)\sin\gamma_1]\cos\gamma_2 + \\ &+\begin{bmatrix} -\nu\sin\gamma_1 + (u - c\omega)\cos\gamma_1 - \\ -(\omega + \dot{\gamma}_1)d_1 - c_1(\omega + \dot{\gamma}_1) \end{bmatrix}\sin\gamma_2\Big\}. \end{aligned} \tag{8}$$

The moment of resistance to turning the wheels of the controlled module of the bus is proportional to the angles of its turning:

$$M_{h1} = h_1 \cdot \dot{\theta}, \tag{9}$$

where

$h_1$ – the coefficient of viscous friction in the steering parts.

The resistance moments of turning of the bus sections are defined as

$$M_{0i} = \frac{2}{3} Z_{0i}\mu\frac{R_i^2 - r_i^2}{R_i^2 + r_i^2}, \tag{10}$$

where

$Z_{0i}$ – the vertical load in the coupling device;

$\mu$ – the friction coefficient in the coupling device;

$R_i$, $r_i$ – the larger and smaller radius of the coupling device, respectively.

The longitudinal forces on the wheels of the axles of the bus are determined by the known dependence

$$X_i = f \cdot Z_i, \tag{11}$$

where

$f$ – the rolling resistance coefficient of bus wheels.

The obtained system of equations allows to study the behavior of a three-section articulated bus in both stationary and non-stationary mode motions, as well as to determine the critical speed $v_{cr}$ of the bus, which has two approaches to its quantitative estimation [16]: the first is associated with the study of characteristic equations (the 1st Lyapunov's method) or Lyapunov's functions (the 2nd Lyapunov's method), the second - with the output of the motion parameters for the allowable range. The critical speed $v_{cr}$, as a stability criterion, connects the design and operational parameters of the multi-section articulated bus and its speed and allows you to find its maximum value, exceeding which leads to the loss of the motion stability.

Analytical expressions for variables $U(\gamma_i), \omega(\gamma_i)$ corresponding to steady mode motions $(\dot{U} = 0, \dot{\omega} = 0, \dot{\gamma}_i = 0, \ddot{\gamma}_i = 0 (i = 1,2))$ can be obtained from the system of equations in (1) on a circular trajectory of sufficiently large radius, provided that $v = const$:

$$\begin{cases} (m + m_1 + m_2 + m_3)\omega\nu = Y_1 + Y_2 + Y_3 + Y_4; \\ -c(m + m_2 + m_3)\omega\nu = \\ aY_1 - bY_2 - c(Y_3 + Y_4) + M_{h1}; \\ [mc + m_2 d_1 + m_3 d_2]\omega\nu = d_1 Y_3 + d_2 Y_4 + \\ + M_{h1} - M_{01}; \\ m_2 d_2 \omega\nu = Y_3(d_2 + b_2) + M_{02}; \\ m_3 d_3 \omega\nu = I_3 Y_4 + M_{03} - M_{02}; \end{cases} \tag{12}$$

It is impossible to solve the system of equations in (12) in general form and analyze the dependences of the lateral and angular velocities $(U\ and\ \omega)$ of the bus and the joint angles $\gamma_i$ of the articulated bus on its design parameters due to the complexity of the disclosure of the sixth-order determinant and the cumbersomeness of the expressions themselves. Therefore, to calculate the determinants of the system in (12), it is necessary to use

numerical methods, for example, the Maple software. Then the variables obtained using the Maple software will make it possible to determine the influence of various design and operational factors on the stability indicators of the articulated bus.

According to the linearity of the lateral slip forces $Y_{ij}$, as a function of the side-slip angle $\delta_i$, the solutions of the equations system in (12) will be the values of the variables appropriating to stationary modes, namely:

$$U = \frac{\Delta_U}{\Delta}; \omega = \frac{\Delta_\omega}{\Delta}; \gamma_1 = \frac{\Delta_{\gamma 1}}{\Delta}; \gamma_2 = \frac{\Delta_{\gamma 2}}{\Delta}, \tag{13}$$

where

$\Delta$ – the main determinant of the system;

$\Delta_U, \Delta_\omega, \Delta_{\gamma 1}, \Delta_{\gamma 2}$ – determinants of the system to find the appropriate variables.

The roots of characteristic equations can be determined by numerical methods. Note that the description of the articulated bus motion, which is actually a nonlinear object, linear equations are a replacement for one problem with another, with which the first may have nothing to do (due to nonlinearity of assignments and terms of the equations of motion higher than the first order).

Hence the following task: to establish the necessary and sufficient conditions for stability on the first approximation. According to Lyapunov's theorem on the stability of a steady mode motion by the first approximation [14], if all the characteristic equation roots of the first approximation system of the perturbed motion equations have negative real parts, then the undisturbed motion is stable and asymptotically stable, no matter what the higher orders in the differential equations of perturbed motion.

The conditions under which all the roots have negative real parts are determined by the Liénard-Shipard criterion: for the characteristic equation to have all the roots with negative real parts, it is necessary and sufficient that:

1) all the characteristic equation coefficients were positive;
2) the main diagonal minors of the Hurwitz matrix compiled for the given characteristic equation were positive. Those conditions are fulfilled if all the denominators of Equation (13) - the main determinants of the system, are positive. What it looks like:

$$\nu < \nu_{cr} = \frac{\beta}{-\alpha}, \tag{14}$$

where $\alpha$ and $\beta$ in Equation (14) will be defined as

$$\beta = \| \beta_{ij} \|_1^4; \ \alpha = \| \alpha_{ij} \|_1^4. \tag{15}$$

Taking into account the fact that the stationary mode motions of the articulated bus are not only rectilinear modes, but the circular modes, as well, then for the realizability of such a motion it is necessary to fulfill the condition $R > 0$. The turning radius $R = \nu/\omega$ in the theory of wheeled vehicles is usually called the curvature radius of the trajectory point of the longitudinal axis of the driving link, the speed of which is directed along the axis [16]. For the radius R one has:

$$R = \frac{\begin{array}{l} -\left\{\begin{array}{l} m(k_3 d_1 + M_{o2})(k_4 d_2 + M_{o3}) \times \\ \times (M_{h1} - M_{o2}) + [c(k_1 + k_2) + \\ + M_{h1} - M_{o1}[m_1 M_{02}(k_4 d_2 + M_{03}) - \\ - m_2 M_{03}(k_3 c_1 - M_{02})] \end{array}\right\} \times \\ \times \nu^2 + [c(k_1 + k_2) + M_{h1} - M_{o1}] \times \\ \times \left\{\begin{array}{l} (k_4 d_2 + M_{03})[M_{o2}(M_{o2} + M_{o3}) - \\ - k_1(\mu_1 + c_1 M_{h1})] + k_4 \\ \times (k_3 c_1 - M_{02}) \times d_2 M_{o3} \end{array}\right\} + \\ + (k_3 d_1 + M_{o2})(k_4 d_2 + M_{o3})[(k_1 + k_2)\mu_1 - \\ -(M_{h1} - M_{01})^2 \end{array}}{\begin{array}{l} (k_1 + k_2) G_2 - (M_{h1} - M_{o1})\gamma_{10}] \times \\ \times (k_3 d_1 + M_{o2})(k_4 d_2 + M_{03}) - \\ -[c(k_1 + k_2) + M_{h1} - M_{01}] \times \\ \times [(k_4 d_2 + M_{03}) k_3 G_2)] \end{array}} \tag{16}$$

where

$k_i$ – the sum of the resistance wheels coefficients of the i-th axis;

$\gamma_{10} = k_{1i}\gamma_0; M_1 = k_{1i}a; M_2 = k_{2ii}b; M_3 = k_{3i}d_1;$
$M_4 = k_{4i}d_2; \mu_1 = k_{1i}a^2; \mu_2 = k_{2i}b^2; \mu_3 = k_{3i}d_1^2;$
$\mu_4 = k_{4i}d_2^2; G_2 = \sum_i k_{1i}a_i\gamma_i.$

As follows from Equation (16), the turning radius of the three-section articulated bus depends on the mass and geometric parameters of its sections, as well as the resistance coefficients of the wheels of the axles of the first $k_3$ and the second trailer-bus section $k_4$.

Equation (16) is presented in the form:

$$R = \frac{l}{\gamma_0} - \nu^2 \varphi\begin{pmatrix} k_{1i}, k_{2i}, k_{3i}, k_{4i}, \gamma_i, m, m_1, m_2, \\ a, b, c, c_1, d_1, d_2 \end{pmatrix}, \tag{17}$$

Since $\varphi(\infty, \infty, \infty, \infty, \gamma_i, m, m_1, m_2, a, b, c, c_1, d_1, d_2) = 0$, then Equation (17) includes, as a special case, a linearized expression $R = l/\gamma_0$ for the radius of trajectory curvature of the bus rear axle on wheels rigid in the lateral direction. If $\varphi(\infty, \infty, \infty, \infty, \gamma_i, m, m_1, m_2, a, b, c, c_1, d_1, d_2) < or > 0$, then $R$ will be greater or less than 0 and the three-section articulated bus will have insufficient or excessive agility. If $\varphi(\infty, \infty, \infty, \infty, \gamma_i, m, m_1, m_2, a, b, c, c_1, d_1, d_2) = 0$ the three-section articulated bus is neutral with respect to understeer: its turning radius is the same as in the multi-articulated bus on rigid lateral wheels.

For $\gamma_i > 0$, the denominator of Equation (16) will be greater than 0, respectively, the condition of the feasibility of circular motion and the stability of rectilinear motion is satisfied only if $\nu < \nu_{cr}$. From Equation (15) one obtains:

$$\xi v^2 + \eta > 0; \eta > -\xi v^2; v^2 < \frac{\eta}{-\xi} \Rightarrow v_{cr}^2 = \frac{\eta}{-\xi},$$

where

$$v_{cr}^2 = \frac{\begin{array}{l}[c(k_1+k_2)+M_{h1}-M_{o1}\{(k_4d_2+M_{o3})\times \\ \times[M_{o2}(M_{o2}+M_{o3})-k_3(\mu_3+c_1M_{o3})]+ \\ +k_4(k_3c_1-M_{o2})(d_2M_{o3}+\mu_4)\}+ \\ +(k_3d_1+M_{o2})(k_4d_2+M_{o3})[(k_1+k_2)\times \\ \times(\mu_1+\mu_2)-(M_{h1}-M_{o1})^2\end{array}}{\begin{array}{l}m(k_3d_1+M_{o2})(k_4d_2+M_{o3})(M_{h1}-M_{o1})+ \\ +[c(k_1+k_2)+M_{h1}-M_2][m_1M_{o2}\times \\ \times(k_4d_2+M_{o3})-m_2M_{o3}(k_3c_1-M_{o2})\end{array}} \quad (18)$$

According to Equation (18), calculations of the critical speed of motion of the three and two-section articulated buses are performed. The calculations were performed on the following initial data:

$v = 5\text{m/s}, \lambda = -0.023m, a = 3.68\,m; b = 2.32\,m;$
$c = 8.71\,m; c_1 = 3.7\,m; d_1 = 4.17\,m; d_2 = 4.17\,m;$
$R = 1.1\,m; r = 0.2\,m; m = 18000\,kg; J = 38500\,kg \cdot m^2;$
$m_1 = 400\,kg; J_1 = 18.5\,kg \cdot m^2; m_2 = 9500\,kg \cdot m^2;$
$J_2 = 31200\,kg \cdot m^2; m_3 = 9500\,kg \cdot m^2; J_3 = 31200\,kg \cdot m^2;$
$k_f = 0; k_1 = 160000\,\text{N/rad}; k_2 = 320000\,\text{N/rad};$
$k_3 = 180000\,\text{N/rad}; k_4 = 320000\,\text{N/rad}; h = 30,$
$\varphi = 0.8; \gamma_0 = 0; \theta = \theta_0 + k_\theta \cdot n; k_\theta = 0.05;$
$n = 1,2\ldots10; \nu := 0; X1 = X2 = X3 = X4 = 0.$

In the case of the two-section articulated bus, should be accepted:
$c_1 = 0, b_2 = 0, d_2 = 0, m_3 = 0, J_3 = 0, k_4 = 0.$

For the multi-section articulated bus selected for calculation, the critical speed was:

- for the three-section articulated bus - 28.06 m/s;
- for the two-section articulated bus - 30.89 m/s.

Despite the fact that the motion of the multi-articulated bus by the Metrobus system is carried out

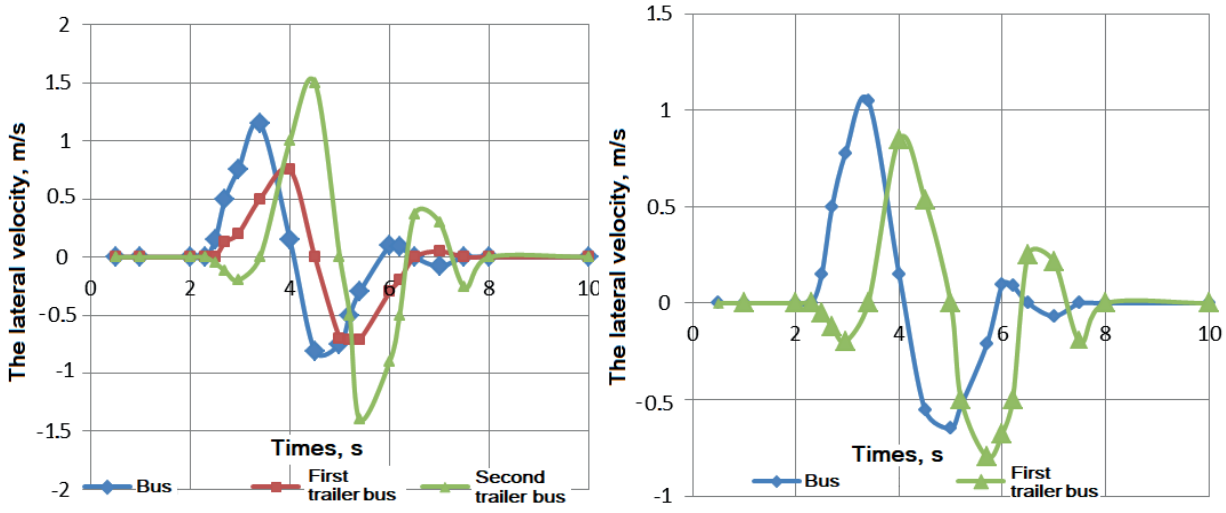


*a)* *b))*

***Figure 2*** *The lateral velocity of the articulated bus during the "jerk the steering wheel" manoeuver: a - three-section articulated bus; b - two-section articulated bus*

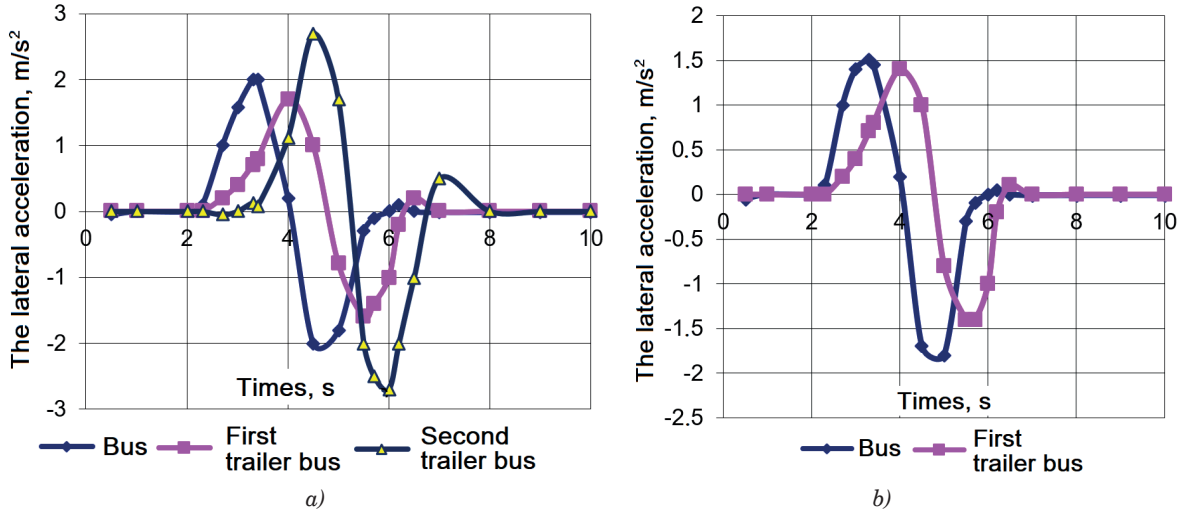


*a)* *b)*

***Figure 3*** *The lateral acceleration of the mass centers of multi-section articulated bus during the "jerk the steering wheel" manoeuver: a - three-section articulated bus; b - two-section articulated bus*

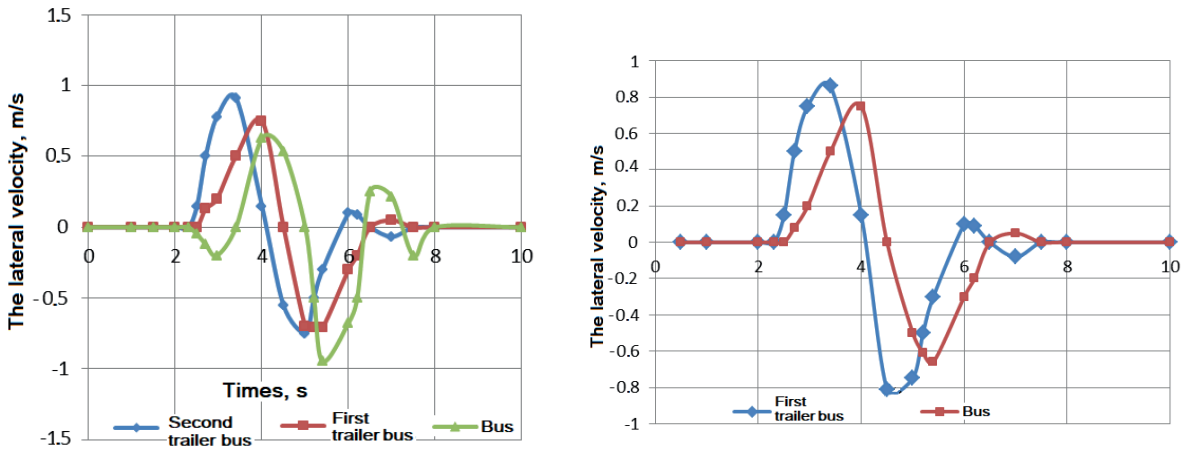


*a)* *b)*

***Figure 4*** *The lateral velocity of the articulated bus during the "displacement" manoeuver: a - three-section articulated bus; b - two-section articulated bus*

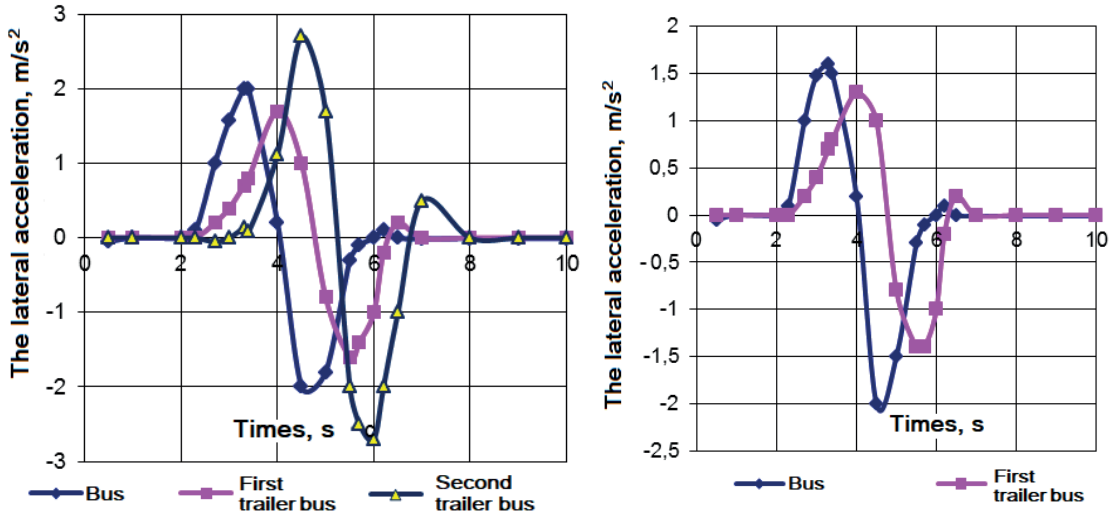


*a)* *b)*

***Figure 5*** *The lateral acceleration of the mass centers of multi-section articulated bus during the "displacement" manoeuver: a - three-section articulated bus; b - two-section articulated bus*

on separately allocated lanes at a speed of 25-28 m/s, it can be considered that the stability of the rectilinear motion of both two and three-sections articulated buses in Metrobus system is ensured.

The stability of the multi-section articulated bus in the non-stationary modes of motion can be judged by the lateral speed of individual sections of the multi-section articulated bus and the value of lateral accelerations when it performs various maneuvers, in particular, the "jerk of the steering wheel - turning the steering wheel with an angular speed of at least 19 rad/s" and "displacement" Figures 2 to 5.

From the given Figures 2 to 5 it follows that the limiting factor for the lateral speed in the case of a three-section articulated bus is the third trailer bus (its lateral speed is almost 20.5% higher than of the first). In the case of a two-section articulated bus, the lateral speed of the first bus decreases by almost 8.5% compared to the three-section and the second trailer bus increases by almost 9.5% compared to the three-section). However, the stability of motion can be judged to a greater extent by the value of the lateral acceleration acting in the center of mass of the individual sections. According to literary sources, the motion stability can be considered satisfactory if the lateral accelerations at the center of mass of the section do not exceed 0.45g. In addition, the damping nature of the oscillations also indicates the stability of the multi-section articulated bus motion. In this case, the limiting factor, when performing the "jerk of the steering wheel" maneuver, is the mass center acceleration of the second trailer section in the case of a three-section articulated bus and a bus in the case of the two-section articulated bus.

## 4 Conclusion

An improved mathematical model of the three-section articulated bus is presented, which made it possible to determine the stability indicators of both

the two-section articulated bus and the three-section articulated bus. Thus, the critical speed for the three-section articulated was 28.06 m/s and for the two-section articulated bus - 30.89 m/s. Despite the fact that the motion by the multi-section articulated bus in the Metrobus system is carried out on separately allocated lanes at a speed of 25-28 m/s, it can be considered that the stability of the rectilinear motion of both two and three-section buses is ensured. In the non-stationary modes of motion with the two-section articulated buses, the lateral speed of the first bus decreases by almost 8.5 % compared to the three-section and the second trailer-bus increases by almost 9.5 % compared to the three-section. At the same time, the motion stability of both multi-sections articulated buses can be considered satisfactory, since the lateral accelerations in the center of mass of all sections do not exceed 0.45 g. In addition, the damping nature of the oscillations also indicates the stability of the multi-section articulated bus motion.

## 5 Discussion of research results

The mathematical model of the plane-parallel movement of the two- and three-lane Metrobuses developed in the work made it possible to achieve the goal of the study. As noted in [18], the kinetic models, to which the developed model belongs, are better in high-precision simulators and in control problems related to «dynamic» tasks (for example, preventing overturning, ensuring stability, braking without sliding, etc.). A reasonable choice of the model should be the result of a compromise between the price of use and efficiency. A complication of the model, as shown in [7], is not always justified, because increasing the degrees of freedom of the system leads to an increase in the number of initial parameters that must be determined with a sure accuracy, which cannot always be achieved. Linearization of the model to determine the maximum speed (critical for stability) did not lead to significant errors. Thus, three-dimensional dynamic models of a car and a trailer were developed in work [12], based on which a dynamic train model was built, which is used to study the linear and non-linear stability of each element and the autotrain as a whole during rectilinear movement. numerical results show that for the nonlinear and linear models, the critical velocities are a little different from each other. However, when studying the stability of the Metrobus in transient traffic modes, it is necessary to use the three-dimensional models, which will be the subject of further research.

## References

[1] OMELNICKIJ, O. E. Analysis of the design of metro buses. *Scientific and Industrial Journal Highway Truck of Ukraine / Naukovo - Vyrobnychyy Zhurnal Avtoshliakhovyk Ukrayiny*. 2018, **3**, p. 7-11. ISSN 0365-8392.

[2] PEKEL, E., KARA, S. S. Simulation-based fleet scheduling in the Metrobus. *International Journal of Simulation and Process Modelling* [online]. 2016, **11**(3-4), p. 326-333. ISSN 1740-2123. Available from: https://doi.org/10.1504/IJSPM.2016.078523

[3] ORTEGON-SANCHEZ A., TYLER N. Towards multi-modal integrated mobility systems: views from Panama City and Barranquilla. *Research in Transportation Economics* [online]. 2016, **59**, p. 204-217. ISSN 1740-2123. Available from: https://doi.org/10.1016/j.retrec.2016.03.001

[4] AVALOS-BRAVO, V., ARELLANO, C. C., PEREZ, D. A. P., CRUZ, M. H. Forecasting people's influx on Mexico City metrobus line 1 using a fractal analysis. In: *Communications in Computer and Information Science* [online]. MATA-RIVERA, M. F., ZAGAL-FLORES, R., ARELLANO VERDEJO, J., LAZCANO HERNANDEZ, H. E. (eds.). Vol. 1276. Cham: Springer, 2016. ISBN 978-3-030-59871-6, eISBN 978-3-030-59872-3, p. 92-105. Available from: https://doi.org/10.1007/978-3-030-59872-3_7

[5] DIZO, J., BLATNICKY, M. Investigation of ride properties of a three-wheeled electric vehicle in terms of driving safety. *Transportation Research Procedia* [online]. 2019, **40**, p. 663-670. ISSN 2352-1457. Available from: https://doi.org/10.1016/j.trpro.2019.07.094

[6] DIZO, J., BLATNICKY, M. Evaluation of vibrational properties of a three-wheeled vehicle in terms of comfort. *Manufacturing Technology* [online]. 2019, **19**(2), p. 197-203. ISSN 1213-2489. Available from: https://doi.org/10.21062/ujep/269.2019/a/1213-2489/MT/19/2/197

[7] STASTNIAK, P. Freight long wagon dynamic analysis in S-curve by means of computer simulation. *Manufacturing Technology* [online]. 2015, **15**(5), p. 930-935. ISSN 1213-2489. Available from: https://doi.org/10.21062/ujep/x.2015/a/1213-2489/MT/15/5/930

[8] GECHEV, T., MRUZEK, M., BARTA, D. Comparison of real driving cycles and consumed braking power in suburban Slovakian driving. *MATEC Web of Conferences* [online]. 2017, **133**, 02003. ISSN 2261-236X. Available from: https://doi.org/10.1051/matecconf/201713302003

[9] DIZO, J., BLATNICKY, M., BARTA, D., MELNIK, R. Application of simulation computations in investigation of vibration properties of a tricycle. *Diagnostics / Diagnostyka* [online]. 2019, **20**(3), p. 97-104. ISSN 1641-6414. Available from: https://doi.org/10.29354/diag/111827

[10] SCHMID, I. Engineering approach to truck and tractor train stability. *SAE Transactions* [online]. 1967, **76**, p. 1-26. ISSN 0148-7191. Available from: https://doi.org/10.4271/670006
[11] KOLESNIKOVICH, A. N., VYGONNYJ, A. G. Stability of a trailer road train of increased length (25.25 m) in straight-line motion. *Actual Problems of Mechanical Engineering*. 2018, **7**, p. 96-100. ISSN2306-3084.
[12] LUO, R., ZENG, J. Hunting stability analysis of train system and comparison with single vehicle model. *Jixie Gongcheng Xuebao / Chinese Journal of Mechanical Engineering* [online]. 2008, **44**(4), p. 184-188. ISSN 0577-6686. Available from: https://doi.org/10.3901/JME.2008.04.184
[13] HALES, F. D. *The vertical motion lateral stability of road vehicle trains*. Ukraine: Transport and Road Research Laboratory (TRRL) Technology University, 1972.
[14] GALLUPPI, O., FORMENTIN, S., NOVARA, C., SAVARESI, S. M. Nonlinear stability control of autonomous vehicles: a MIMO D2-IBC solution. *IFAC-PapersOnLine* [online]. 2017, **5**(1), p. 3691-3696. ISSN 2405-8963. Available from: https://doi.org/10.1016/j.ifacol.2017.08.563
[15] CHEN, H.-J., SU, W.-J., WANG, F.-C. Modelling and analyses of a connected multi-car train system employing the inerter. *Advances in Mechanical Engineering* [online]. 2017, **9**(8), p. 1-13. ISSN 1687-8132. Available from: https://doi.org/10.1177/16878140177017
[16] SAHNO, V., MYROVANY, I., POLJAKOV, V., MISKO, E. To comparative assessment of three-unit lorry passenger trains. *Advances in Mechanical Engineering and Transport.* 2019, **2**(13), p. 146-155. ISSN 2313-5425.
[17] HREBET, V. G., MISKO, E. M., VERBICKIJ, V. G. To the experimental determination of the dependences of the lateral slip forces of a two-axle vehicle in the oversteer curves. In: 10th International Scientific and Practical Conference Modern Technologies and Prospects for the Development of Road Transport: proceedings. 2017. ISBN 978-966-641-707-0, p. 126-128.
[18] ZHANG, Y., KHAJEPOUR, A., HUANG, Y. Multi-axle/articulated bus dynamics modeling: a reconfigurable approach. *Vehicle System Dynamics* [online]. 2018, **56**(9), p. 1315-1343. eISSN 1744-5159. Available from: https://doi.org/10.1080/00423114.2017.1420205

# EXPERIMENTAL STUDY OF MAXIMUM STRESSES IN THE STATIONARY HOIST DESIGN IN THE ANSYS SOFTWARE ENVIRONMENT

Aidana Donenbaykyzy Kassymzhanova [1], Marat Kenesovich Ibatov [1], Oyum Temirgalievich Balabayev [1,*], Bakytzhan Serikovich Donenbaev[1], Daurenbek Ikhtiyarovich Ilessaliyev [2]

[1]Abylkas Saginov Karaganda Technical University, Karaganda, Kazakhstan
[2]Tashkent State Transport University, Tashkent, Uzbekistan

*E-mail of corresponding author: balabaev.ot@mail.ru

***Resume***
The authors have studied the methods of loading bulk cargo in the railway transport. The developed method of loading bulk cargoes into containers transported by railway platforms has been developed. The article deals with experimental studies of maximum stresses in the design of the proposed stationary hoist. The studies have been carried out in the ANSYS software environment with development of simulation models of the hoist design.

***Article info***
Received 14 July 2022
Accepted 3 October 2022
Online 24 October 2022

***Keywords:***
railway transport
railway platform
container
bulk cargo loading
stationary hoist
simulation modeling
export

Available online: https://doi.org/10.26552/com.C.2022.4.B310-B318

ISSN 1335-4205 (print version)
ISSN 2585-7878 (online version)

## 1 Introduction

The growth of container traffic is a global trend; this is also typical for the countries of Central Asia (Kazakhstan, Afghanistan, Tajikistan, Uzbekistan). A special role is played by the general advantages of containers: their convenience and economy in the freight transportation. Economic and geographical factors, development of the Central Asia countries' economies, as well as development of the Chinese economy resulted in the railway freight traffic with Europe becoming very important. Thus, development of a method to improve the efficiency of loading operations for containers transported by railway platforms is an urgent task.

In 2010, at the meeting, representatives of the NC "Kazakhstan Temir Zholy" JSC (Kazakhstan Railways) and the Ministry of Railways of China decided that wheat would be transported in containers and a necessary condition for transportation would be tare the cargo in 50 kg bags [1]. However, this is a very time-consuming process, since it is necessary to transship each bag at transshipment points. Despite the fact that bulk cargo requires bulk transportation, the decision to transport bagged wheat is due to the lack of the necessary infrastructure to ensure the loading and unloading of bulk cargo into containers.

The COVID-19 pandemic has shown that China began demanding to deliver grain in containers loaded in big bags, where the human presence during loading and unloading operations is minimized and forklifts came to the rescue. The practice has shown that containers arriving at the station are promptly accepted, unloaded, overloaded by the Chinese side, so, there are fewer delays. Since the issue of loading wheat into rail containers in bulk has not been fully resolved, one can confidently say that the potential of container transportation in rail transport is not fully used.

Considering the difference in railway gauge, when transporting goods through the new Asia-European Continental Bridge, it is necessary to transship cargo twice during the transportation to Europe. As a result, duration of the goods' transportation increases accordingly, at the transshipment point of the border port, goods are likely to be delayed. A certain difference in gauge exists in Asian and European countries. One of the solutions will be containerization and development of the intermodal transportation.

It is obvious that the increase in intermodal

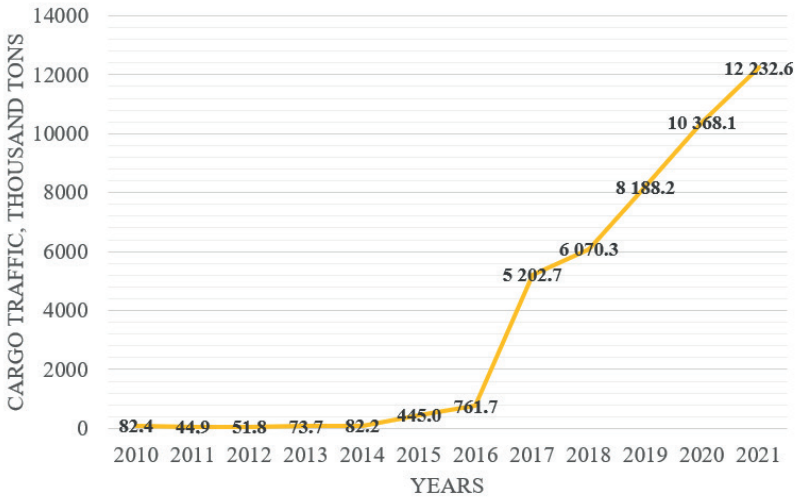


***Figure 1*** *Cargo traffic in containers using all types of transport*

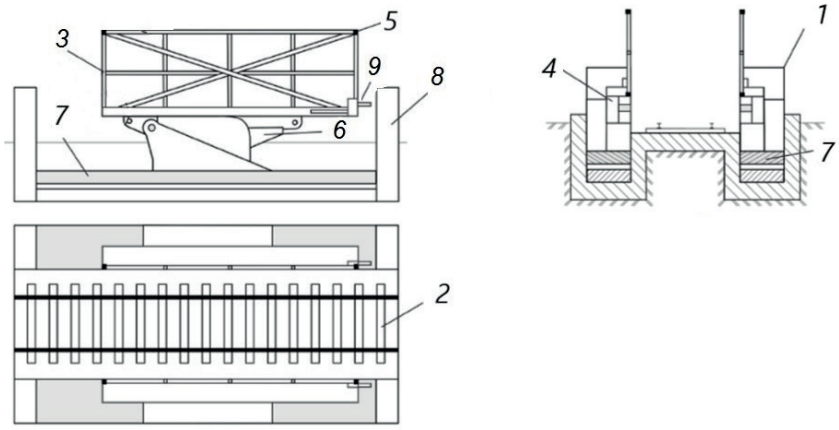


***Figure 2*** *The structure diagram of the developed stationary hoist with indication of the main nodes: 1 - hydraulic lift, 2 - railway track, 3 - load-handling frames, 4 - horizontal drives, 5 - locks, 6 - vertical drives, 7 - supporting frames, 8 - lifting drives, 9 - devices for opening and closing the hatches of the container*

transport is a natural phenomenon [2]. When analyzing the freight transportation in containers, in the Republic of Kazakhstan over the past years, a sharp increase in container traffic was observed since 2017, while since 2018 this figure has been growing with an arithmetic progression (Figure 1) [3].

The growth dynamics of container traffic shows that, if needed, it is possible to organize the loading of returnable containers from the bulk cargo with other types of imported cargo in order to exclude empty containers from entering the country or to organize multimodal transportation along other routes, Figure 1.

As a result of reviewing and analyzing design solutions of loading and unloading bulk cargoes [4-5], it can be said that the developed devices only perform loading into road or rail vehicles and there are currently no devices for loading bulk cargoes into containers for their transportation by railway platforms. A good solution to the problem could be the use of tractor-trailers, the so-called reach stackers, by the way, the work of which is mentioned in the paper of colleagues, where the process associated with the operation conducted on intermodal transport units, for example a large type A container, including inter alia: simple operations and combinations of operations (so-called combined cycles) were presented [6]. However, this transport and technological system, where a tractor-trailer is used, cannot be implemented when loading the bulk cargo into containers on railway tracks, in the cramped conditions of agricultural elevators.

The solution of this problem would contribute to the growth dynamics of the export potential of bulk cargoes, by improving the transport infrastructure.

To solve this problem, at Abylkas Saginov Karaganda Technical University, the authors of this article have developed the design of a stationary hoist (Figure 2) for loading containers transported by railway platforms [7].

The technical result of the invention is to increase the efficiency of loading the bulk cargo into containers transported by railway platforms. The specified technical

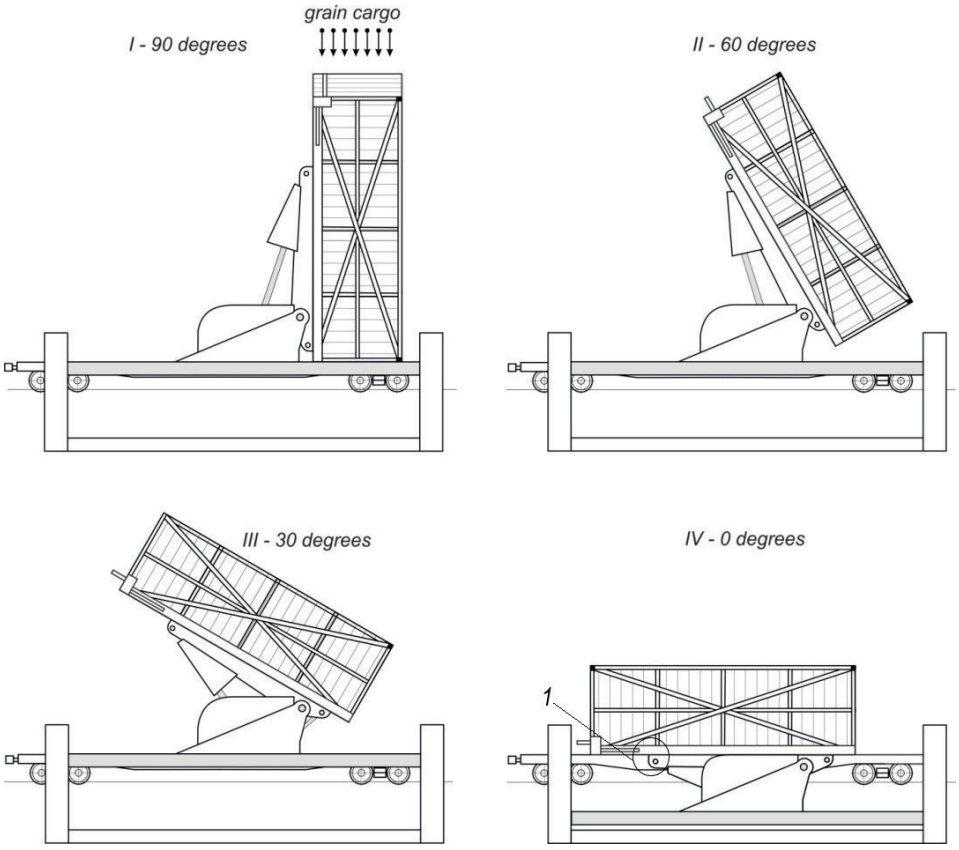


***Figure 3*** *Test positions of the stationary hoist (1 - section with maximum stress, figures 5 to 8)*

result is achieved by the fact that the following changes have been made to the considered method of loading containers transported by railway platforms: a lift is mounted on the railway track; it is equipped with devices for rotating and mounting a container with the end wall on the railway platform for loading bulk cargo [7].

The research methodology is provided by:

- planning the procedure for carrying out experimental studies;
- establishing the influencing factors and output indicators;
- selecting the number of test trials and test positions;
- performing experimental studies with calculations and design of simulation models in the ANSYS software environment;
- comparation of the experimental studies' results to results of theoretical studies performed in the Mathcad software environment.

To determine the rational design parameters, the article presents a detailed study of the proposed lift design with development of a simulation model in the ANSYS software environment.

## 2 Purpose and plan of experimental studies

The purpose of experimental studies was to confirm the operability of the proposed design of a stationary hoist (Figure 2) for loading the grain cargo into containers on railway platforms.

To achieve this purpose, it is necessary to solve the following tasks [8]:

- to plan the procedure for carrying out experimental studies of the "container-hoist" system;
- to establish the influencing factors and output indicators;
- to select the number of test trials and test positions [8-9];
- to perform experimental studies with calculations and development of simulation models in the ANSYS software environment;
- to compare the results of experimental studies to results of theoretical studies performed in the Mathcad software environment.

Experimental studies of the "container-hoist" system include the following stages:

1. Establishing the influencing factors and output indicators. The influencing factor is the force that is loaded on a certain area of the structure of the developed stationary hoist ($F_i/S$, MPa). The output indicator, as the most important characteristics of the process under study, considered in the design of a stationary hoist after the application of a force, is selected: mechanical stresses ($\sigma_{Ei}$, MPa) that occur in the design of a stationary hoist.
2. Selecting the number of test trials and test positions. The object of experimental studies is

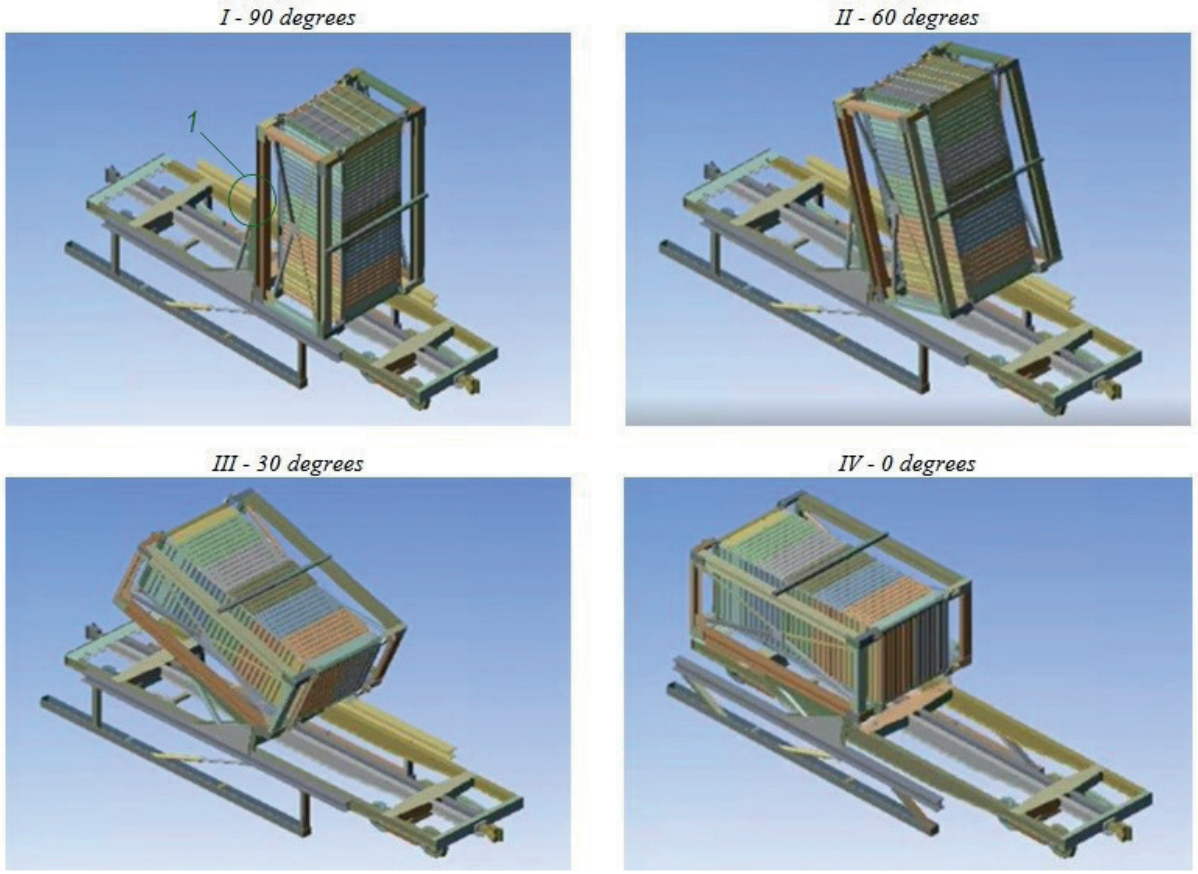


***Figure 4*** *Simulation 3D modeling of the developed stationary hoist in the ANSYS software environment (1 - section with maximum stress, figures 5-8)*

the "container-hoist" system, implemented in the form of simulation models in the ANSYS software environment [10], which have been designed to solve the goal of the experiment. This system can be represented as a "black box" of a single-factor experiment, where the input influencing factor is the stress ($F_i/S$, MPa) and the output parameter (response function) is mechanical stress ($\sigma_{Ei}$, MPa). Thus, the registration of the output parameter in a single-factor experiment is carried out with considering the influence of one factor and determining one value of the output parameter. Based on the above conditions and according to the Methodology of rational planning of experiments [11], for obtaining the results, it is necessary to perform $N=1^1=1$ experiments for each planned loading: 25 t; 35 t; 45 t; 55 t; 65 t; 75 t; 85 t; 95 t. Thus, for experimental studies, it is accepted to carry out 8 loadings for the selected positions of the developed stationary hoist (Figure 3), i.e. 32 test trials for 4 test positions environment [10].

3. Carrying out experimental studies in the ANSYS software environment.

When performing the experimental studies in the ANSYS software environment, it is necessary to:

- perform the simulation modeling of the stationary hoist design;
- carry out 32 test trials of the stationary hoist design for 4 test positions with 8 loadings;
- receive reports of test results.

## 3 Experimental studies

Simulation computations represent a very effective tool for investigating operational characteristics and behaviours of constructions without having a real product [12]. Simulation modeling of the design of a stationary hoist in the ANSYS software environment has begun with development of sketches by size and then, using the ANSYS tools, the simulation models of the developed stationary hoist in 4 test positions were obtained (Figure 4).

After developing the simulation models for the design of the developed stationary hoist in the ANSYS software environment, when carrying out experimental studies:

- the properties of construction materials have been set;
- the forces and directions of forces acting on the structure have been given;
- the process of calculation by the finite element method has been performed, taking into account all the specified parameters.

***Table 1*** *Maximum stresses in the structure according to 32 test trials for 4 tested positions*

| Test trials | | No.1 | No.2 | No.3 | No.4 | No.5 | No.6 | No.7 | No.8 |
|---|---|---|---|---|---|---|---|---|---|
| Loadings to the structure, $m$ / $F_i/S$, ton / MPa | | 25 / 245.250 | 35 / 343.350 | 45 / 441.450 | 55 / 539.550 | 65 / 637.650 | 75 / 735.750 | 85 / 833.850 | 95 / 931.950 |
| Stresses in the test positions, $\sigma_{Ei}$, MPa | I | 25.043 | 37.484 | 48.491 | 65.679 | 80.003 | 92.078 | 106.650 | 121.230 |
| | II | 14.237 | 20.221 | 22.443 | 27.665 | 30.144 | 32.418 | 34.448 | 36.351 |
| | III | 54.022 | 70.103 | 87.192 | 103.230 | 120.700 | 137.200 | 154.200 | 170.690 |
| | IV | 75.393 | 102.990 | 130.340 | 157.480 | 183.430 | 209.490 | 239.480 | 267.470 |

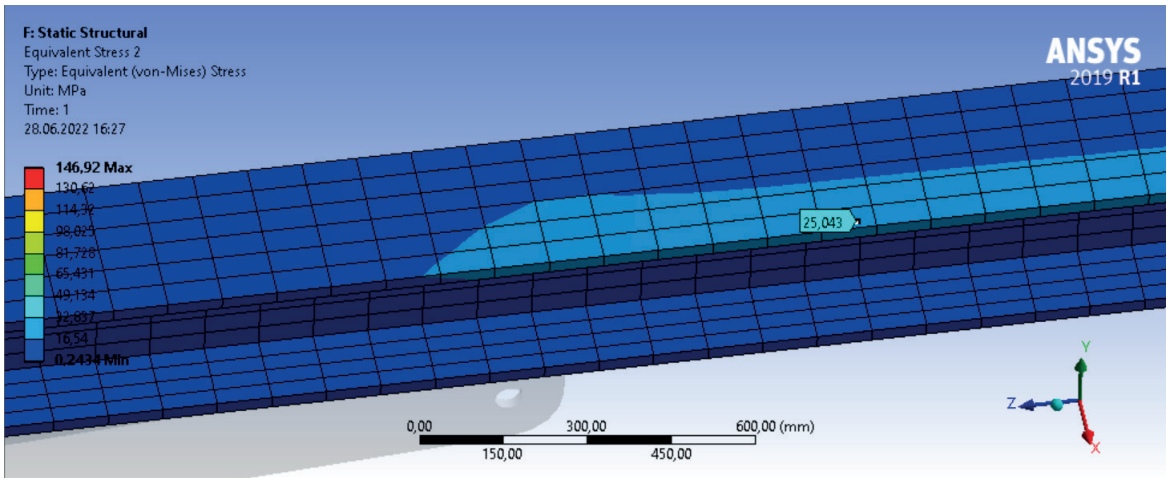


***Figure 5*** *Results of the first test trial for a position I - 90° (see* ***Table 1****)*

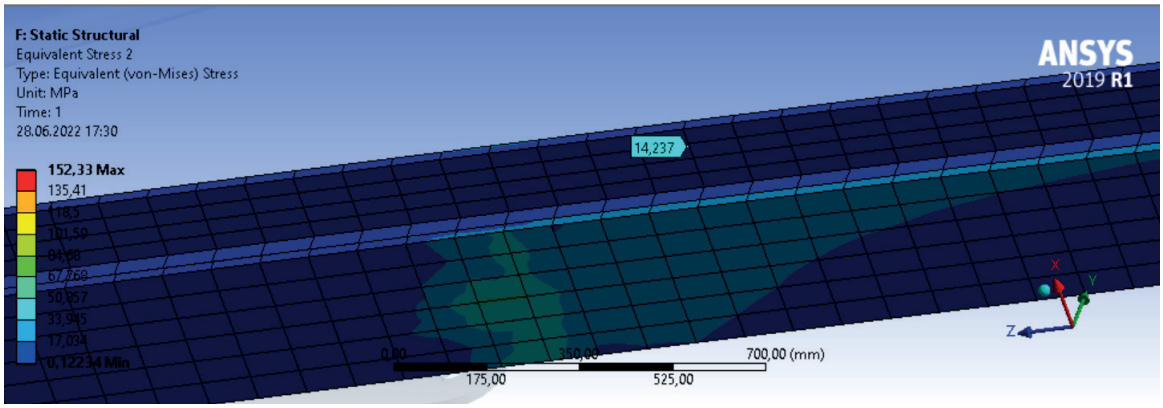


***Figure 6*** *RResults of the first test trial for position II - 60°*

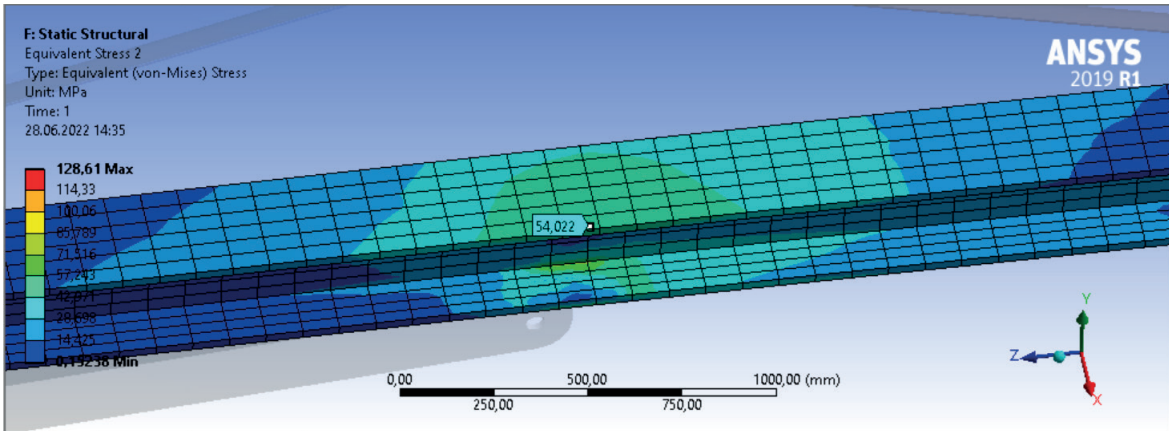


***Figure 7*** *Results of the first test trial for position III - 30°*

## 4 Results of experimental studies

When carrying out experimental studies of the "container-hoist" system, 32 test runs have been performed (Table 1) for 4 test positions (Figures 2 and 3): I - at 90 degrees; II - at 60 degrees; III - at 30 degrees; IV - at 0 degrees. The 8 planned loadings have been performed: 25 t; 35 t; 45 t; 55 t; 65 t; 75 t; 85 t; 95 t. At the end of each test run, the ANSYS application program produced the stress diagrams in the load-handling frame

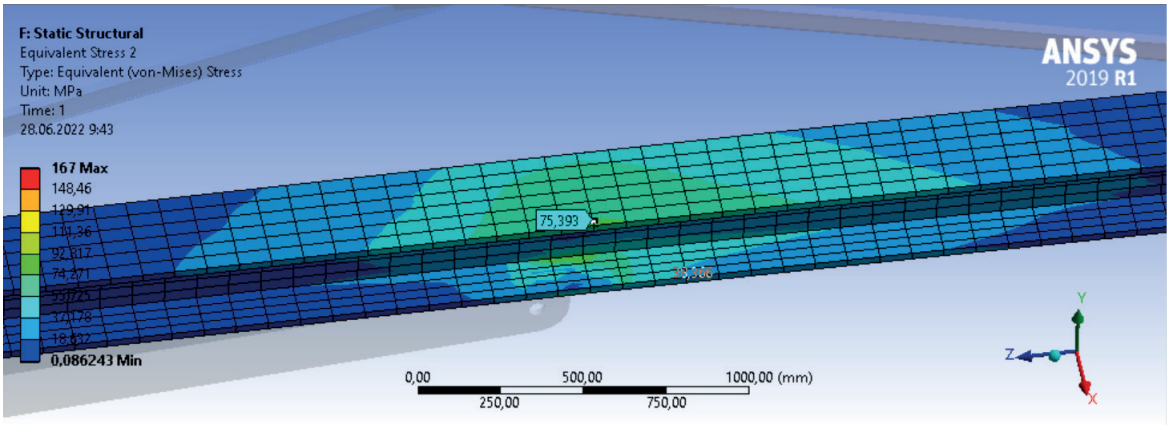


***Figure 8*** *Results of the first test trial for position IV - 0°*

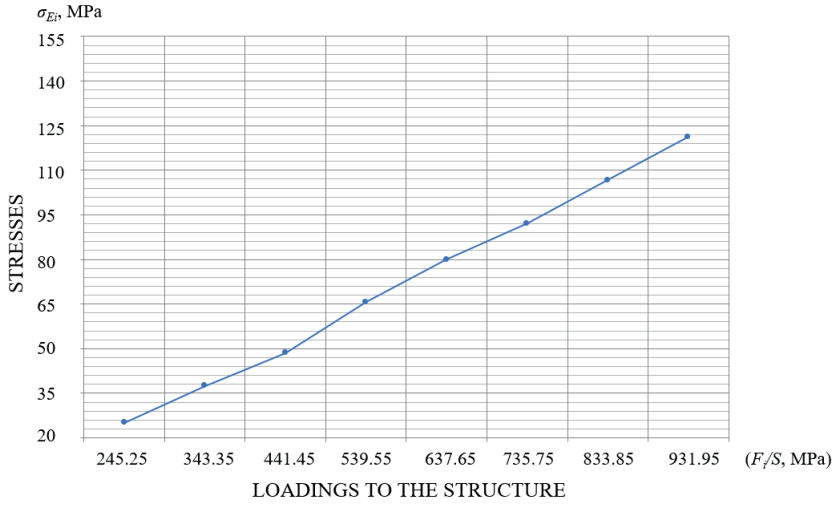


***Figure 9*** *Experimental dependence of output indicators ($\sigma_{Ei}$, MPa) on the influencing factors ($F_i/S$, MPa) in test position I at 90°*

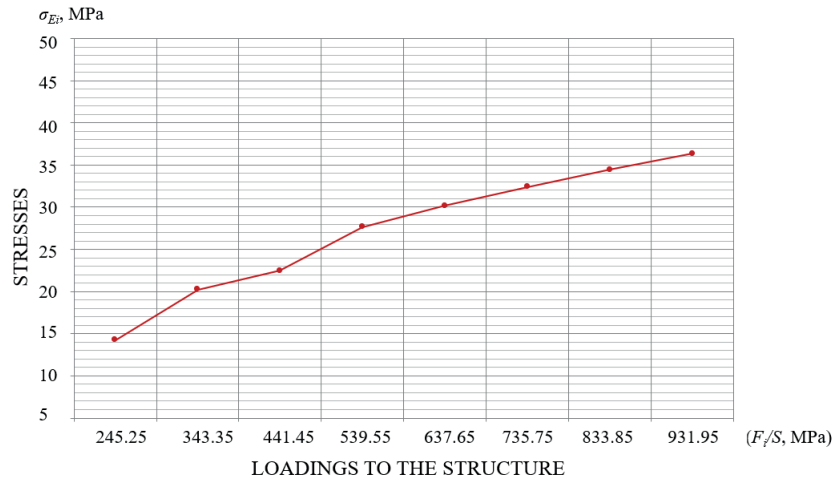


***Figure 10*** *Experimental dependence of output indicators ($\sigma_{Ei}$, MPa) on the influencing factors ($F_i/S$, MPa) in test position ($F_i/S$, MPa) in test position II at 60°*

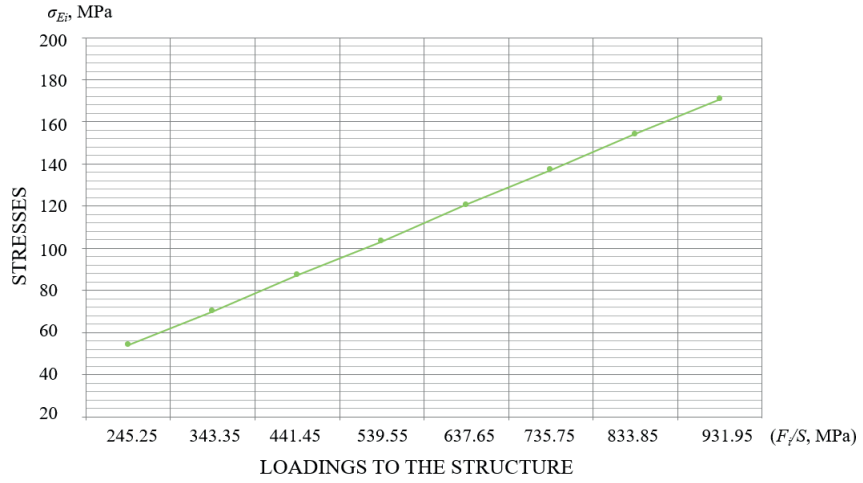


***Figure 11*** *Experimental dependence of output indicators ($\sigma_{Ei}$, MPa) on the influencing factors ($F_i/S$, MPa) in test position III at 30°*

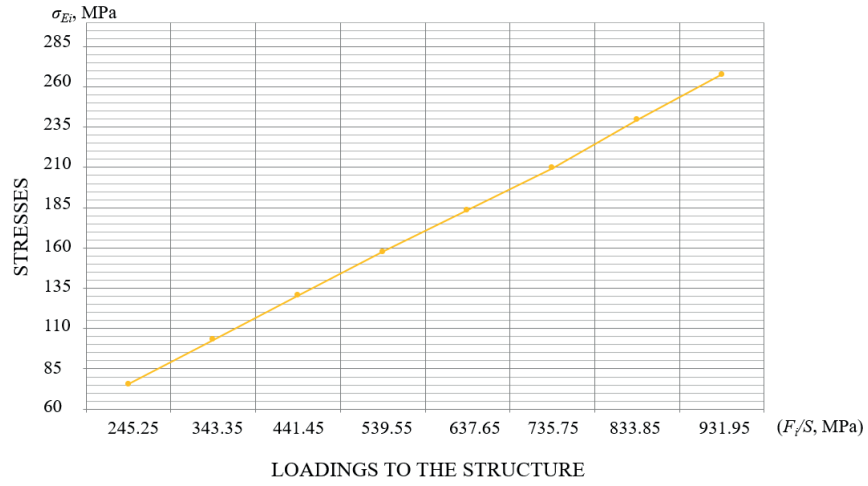


***Figure 12*** *Experimental dependence of output indicators ($\sigma_{Ei}$, MPa) on the influencing factors ($F_i/S$, MPa) in test position IV at 0 degrees*

***Table 2*** *Convergence of experimental (Ansys) and theoretical indicators (Mathcad)*

| Test No. | Experimental and theoretical indicators | | | | | | | | | | | |
|---|---|---|---|---|---|---|---|---|---|---|---|---|
| | I - at 90 degrees | | | II - at 60 degrees | | | III - at 30 degrees | | | IV - at 0 degrees | | |
| | $y_{ei}$ | $y_{thi}$ | % | $y_{ei}$ | $y_{thi}$ | % | $y_{ei}$ | $y_{thi}$ | % | $y_{ei}$ | $y_{thi}$ | % |
| 1 | 25.043 | 28.335 | 0.12 | 14.237 | 11.267 | -0.26 | 54.022 | 42.873 | -0.26 | 75.393 | 62.990 | -0.20 |
| 2 | 37.484 | 39.669 | 0.06 | 20.221 | 15.774 | -0.28 | 70.103 | 60.022 | -0.17 | 102.990 | 88.186 | -0.17 |
| 3 | 48.491 | 51.003 | 0.05 | 22.443 | 20.281 | -0.11 | 87.192 | 77.171 | -0.13 | 130.340 | 113.382 | -0.15 |
| 4 | 65.679 | 62.337 | -0.05 | 27.665 | 24.788 | -0.12 | 103.230 | 94.320 | -0.09 | 157.480 | 138.578 | -0.14 |
| 5 | 80.003 | 73.671 | -0.09 | 30.144 | 29.295 | -0.03 | 120.700 | 111.469 | -0.08 | 183.430 | 163.775 | -0.12 |
| 6 | 92.078 | 85.005 | -0.08 | 32.418 | 33.802 | 0.04 | 137.200 | 128.618 | -0.07 | 209.490 | 188.971 | -0.11 |
| 7 | 106.650 | 96.339 | -0.11 | 34.448 | 38.308 | 0.10 | 154.200 | 145.767 | -0.06 | 239.480 | 214.167 | -0.12 |
| 8 | 121.230 | 107.673 | -0.13 | 36.351 | 42.815 | 0.15 | 170.690 | 162.916 | -0.05 | 267.470 | 239.363 | -0.12 |

structure with the results of calculating the output indicators (Figures 5 to 8).

After carrying out experimental studies of the "container-hoist" system, the results of 32 test trials for 4 test positions have been plotted on a grid of rectangular coordinates and connected by experimental points into experimental dependences $\sigma_{Ei} = f(F_i/S)$. Figures 9 to 12 show experimental dependences for 32 test runs (Table 2) for 4 test positions. The graphs show that the mechanical stresses ($\sigma_{Ei}$, MPa), which arise in the design

of a stationary hoist increase as the load increases.

A comparison of the theoretical calculations results, performed in the Mathcad application program (***Table 2***), to results of experimental studies (Table 1), performed in the ANSYS software environment, has in general confirmed the adequacy of the calculated values and the error does not exceed 30 %.

## 5 Conclusions

To increase the export potential of the bulk cargoes of the Republic of Kazakhstan, the authors of this article have proposed a stationary hoist design for loading the bulk cargo into containers transported by railway platforms. The proposed method was patented in the Derwent patent database, Clarivate Analytics [7].

To determine the rational design parameters, the stationary hoist operation has been simulated in the ANSYS software environment. Total of 32 test trials for 4 test positions of experimental studies were carried out. They have proved that the stationary hoist design is able to withstand emerging mechanical stresses ($\sigma_{Ei}$, MPa) up to 833.85 MPa, or 85 t, while the yield strength of the selected construction material (Structural Steel) is 250 MPa. The convergence of the experimental indicators, presented in the article with the theoretical data obtained in the Mathcad application program, has confirmed the adequacy of the calculated values and the error does not exceed 30 %.

## Acknowledgement

This research has was funded by the Science Committee of the Ministry of Science and Higher Education of the Republic of Kazakhstan (Grant No. AP14869550, "Design and study of a stationary hoist for loading grain cargo into containers transported by railway platforms").

## References

[1] CHERNOMOROV, A. G. Creation of a transshipment system at Dostyk station for the purpose of transporting grain cargoes in international traffic. *The Bulletin of Kazakh Academy of Transport and Communications named after M. Tynyshpayev*. 2011, 3, p. 44-46. ISSN 1609-1817.

[2] ZAJAC, M., SWIEBODA, J. Analysis of the process of unloading containers at the inland container terminal. In: *Safety and reliability: methodology and applications*. NOWAKOWSKI, T., MLYNCZAK, M., JODEJKO-PIETRUCZUK, A., WERBINSKA-WOJCIECHOWSKA, S. (eds.). London, UK: Taylor and Francis Group, 2014. eISBN 9780429226823, p. 1237-1241.

[3] Official website of the Agency for Strategic planning and reforms of the Republic of Kazakhstan Bureau of National Statistics. Transportation of goods in containers by all modes of transport. [online] [accessed 2022-07-07]. Available from: https://www.stat.gov.kz/search/transportation of goods in containers by all modes of transport

[4] Patent RU 2 127 703 C1 Method of loading and unloading containers transported by railway platforms. 1999.

[5] Patent WO/2005/030622 A method and system for filling the entire volume of 20 feet steel shipping containers. 2005.

[6] KOSTRZEWSKI, M., KOSTRZEWSKI, A. Analysis of operations upon entry into intermodal freight terminals. *Applied Sciences* [online]. 2019, **9**(12), 2558. eISSN 2076-3417. Available from: https://doi.org/10.3390/app9122558

[7] VITVITSKII, E. E., GUMAROV, G. S., BALABAEV, O. T., ABISHEV, K. K., SARZHANOV, D. K., KASSYMZHANOVA, A. D. Method of loading bulk goods in containers transported by railway. Patent number(s): RU2654439-C1 for invention. Derwent primary accession number: 2018-53628L. Database: Derwent innovations index of Web of Science maintained by Clarivate Analytics.

[8] KASSYMZHANOVA, A. D. Certificate of the Republic of Kazakhstan on including the information into the State register of rights to objects protected by copyright. Methods of carrying out experimental studies of the stress-strain state of the design of a stationary hoist designed for loading grain cargo into containers on railway platforms. No. 26526. 2022.

[9] KADYROV, A., KARSAKOVA, A., DONENBAYEV, B., BALABEKOVA, K. Establishing the strength characteristics of the lifting-leveling device structures of the VPO-3-3000 machines for the track straightening. *Communications - Scientific Letters of the University of Zilina* [online]. 2020, **22**(4), p. 70-79. ISSN 1335-4205, eISSN 2585-7878. Available from: https://doi.org/10.26552/com.C.2020.4.70-79

[10] KASSYMZHANOVA, A. D. Certificate of the Republic of Kazakhstan on including the information into the state register of rights to objects protected by copyright. Methods of carrying out experimental studies of the stress-strain state of the design of a stationary hoist designed for loading grain cargo into containers on railway platforms [online]. No. 26526. 2022. Available from: https://copyright.kazpatent.kz/?!.iD=wQEy

[11] PROTODYAKONOV, M. M., TEDER, R. I. *Methods of rational planning of experiments*. Moscow: Science, 1970.

[12] DIZO, J., BLATNICKY, M., HARUSINEC, J., SUCHANEK, A. Assessment of dynamics of a rail vehicle in terms of running properties while moving on a real track model. *Symmetry* [online]. 2022, **14**(3), 536. eISSN 2073-8994. Available from: https://doi.org/10.3390/sym14030536

# COMPRESSIVE STRENGTH ANALYSIS OF A STEEL BOLTED CONNECTION UNDER BOLT LOSS CONDITIONS

**Rafał Grzejda** [1,*], **Rafał Perz** [2]

[1]Faculty of Mechanical Engineering and Mechatronics, West Pomeranian University of Technology in Szczecin, Szczecin, Poland
[2]Institute of Aeronautics and Applied Mechanics, Warsaw University of Technology, Warsaw, Poland

*E-mail of corresponding author: rafal.grzejda@zut.edu.pl

***Resume***
The aim of the study is the numerical analysis of a bolted connection under the conditions of loss of bearing capacity of some fasteners in this connection. The joined plates in the connection were made of the 3D finite elements, while the fasteners were treated as hybrid models consisting of rigid heads and nuts and flexible beams between them. A model of unilateral contact with friction was used between the joined plates. The bolted connection was first preloaded according to three different tensioning sequences and with a normalised force. After all the bolts were tensioned, the selected bolts were removed, simulating bolt damage under connection loading conditions. The connection was tested for external compressive loads up to 210 kN. The effect of the loosening of the connection on the load in the remaining bolts at the stage of the connection operation was investigated.

***Article info***
Received 11 July 2022
Accepted 5 October 2022
Online 24 October 2022

***Keywords:***
structural health monitoring
bolted connection
preload
fastener damage
finite element method

Available online: https://doi.org/10.26552/com.C.2022.4.B319-B327

ISSN 1335-4205 (print version)
ISSN 2585-7878 (online version)

## 1 Introduction

In the current literature, much attention is paid to monitoring the technical condition of various engineering structures. This applies especially to systems with structural nodes such as: bolted [1], riveted [2], adhesively bonded [3] or welded connections [4]. These issues are generally referred to as structural health monitoring (SHM). An overview of the methods used in this area is presented, inter alia, in [5].

Structural condition assessment can be carried out on the existing system in real time. Sometimes, however, it is justified to carry out such an assessment numerically, for example in the case of large-size systems or in the case of simulating gradual structural damage in a complex process involving geometric nonlinearity, nonlinear material performance, damage evolution and dynamics [6].

There are two main issues in structural health monitoring of bolted connections and bolts. The first is their analysis of the loss of bearing capacity of some load-bearing elements, such as a column. If one or more of these columns fails under abnormal loads, the vertical load transfer paths are cut off and internal forces would be transferred to adjacent structural members. In this case, there is a need for solidity of the remaining structure in order to evenly and effectively distribute the loads. Otherwise, local damage may cause a chain of damage that results in disproportionate damage or even collapse of the entire structure, which is termed progressive collapse. Consequently, numerous studies on progressive collapse have been carried out using numerical simulations. The most frequently used method in this case was the finite element method (FEM), which is implemented in many analyses of various structures [7-10].

Sadek et al. [11] have conducted a computational study of simple composite shear connections in the column loss scenario. The analyses showed that the composite floor system designed in accordance with the current guidelines is susceptible to collapse due to a loss of the middle column. Kim and Kim [12] have developed a finite element model of a steel frame resistant to bending. A nonlinear dynamic analysis of the FEM-based model under the column loss conditions has been performed. The numerical results showed that the location of the column removal had a significant impact on the behaviour of the panel zone. Lu et al.

[13] have proposed the coupled finite element-discrete element method to account for the influence and heaping of fragments in the progressive collapse analysis. Kwasniewski [14] has developed a detailed 3D model with a large number of finite elements for an existing multi-story structure. Based on the numerical results, modelling parameters that affect the potential for progressive collapse have been identified. Sasani et al. [15] have concluded that a method ignoring the effects of the bending moment and the axial force in the beams would underestimate the anti-collapse resistance of the structure. Fu [16] has built a 3D finite element model of a tall building that can represent the performance of a frame structure to prevent collapse in a column loss scenario. Helmy et al. [17] have performed a dynamic analysis of the gradual collapse of the structure using the applied-element method. The results showed that ignoring the floors in the gradual collapse analysis can lead to wasteful design. Gu et al. [18] have developed a progressive discrete element based collapse simulation system. With the help of this system, the collapse mode and the decomposition of debris after the collapse can be obtained. Based on the experimental results, Gao et al. [19] have carried out a numerical analysis taking into account the material fracture in order to predict the ultimate behaviour of the composite frame under column loss. Tang et al. [20] have conducted research on the progressive collapse of fully bolted beam-to-column connections. Wang et al. [21] have performed similar tests for different types of connections. Rodriguez et al. [22] have carried out an analysis of the fragility and sensitivity of steel frames with bolted-angle connections in conditions of progressive collapse.

The second main issue, related to the structural health monitoring of bolted connections and bolts, is their analysis of the loss of bearing capacity of some fasteners in the connection. However, there are only a few papers devoted to FE-modelling of phenomena occurring in bolted connections due to damage of fasteners. Rucka et al. [23] have applied the wave propagation in diagnostics of the steel bolted bridge parts. Qin and Chu [24] and Qin et al. [25] have performed a quasi-static finite element analysis of a typical disc-drum connection used in rotors of large rotating machines, provided that some bolts were removed from the connection model. Blachowski and Gutkowski [26] have investigated the variability of the connection stiffness, caused by the damage of several bolts and its effect on the displacements in the case of a selected tele-communications tower. Patil et al. [27] have presented the results of a transient analysis of a frame with bolted connections after removing one of the bolts, while Hasni et al. [28] have described the structural health monitoring of a steel frame, in which the damage was simulated by loosening the bolts and creating cracks on its members. The above-mentioned papers concerned the FEM analysis of connections with symmetrical bolt distribution.

Due to the fact that a small number of published papers related to the assessment of the health condition of bolted connections on the basis of modelling was noticed, this subject was taken up in the presented paper. The established numerical finite element model of the selected bolted connection made it possible to provide some assessments about the drop of the bearing capacity of the damaged connection system owing to the loss of one or two of fasteners. The paper is concerned with the bolted connection of plates with a ground contact surface, the experimental studies of which have been described in [29-30]. The scope of the paper covers two connection stages: preload and operation. The novelty, in relation to the above-mentioned articles, is that in this paper an asymmetric connection was modelled. The subject addressed in this paper is worthy of investigation both from a scientific point of view and for practical applications. All the calculations were performed using the Midas NFX 2020 R2 finite element commercial software.

The remainder of this paper is organised as follows: Section 2 briefly presents the models of the bolted connection selected for calculations. Section 3 describes the research procedure including the ways of tensioning of the bolts and their damage. Section 4 provides and discusses the experimental results. Section 5 concludes the paper.

## 2 Models of the bolted connection

### 2.1 3D model

The subject of research and analysis is a bolted connection, which is a pair of plates joined with $i$ fasteners, shown in Figure 1 (for $i$ = 1, 2, …, 7). The fasteners are of the M10 × 1.25 type. Each of the bolt-nut pair is treated as one part without creating threads, as existing studies [31] have shown that threadless bolt models can reproduce most of the mechanical response of threaded bolt models and effectively reduce computational time. This approach to fasteners modelling is often used by other researchers, as well [26, 32-33].

The joined plates are fastened to the upper and lower bases. The thickness of all the joined elements is equal to 28 mm. The connection is sloped horizontally at 60 degrees to introduce coexistence of compressive and shear stresses (for comparison, see [34]). The total height of the structure is approximately 266 mm. The plates and bases are made of 1.0577 steel [35]. The bolts are made in the class of mechanical properties 8.8 and the nuts in the class of mechanical properties 8.

The area of the contact surface between the joined plates and the established numbering of the bolts are presented in Figure 2. This area is within a circle with a radius of 90 mm and its size does not exceed $9 \times 10^3$ mm$^2$.

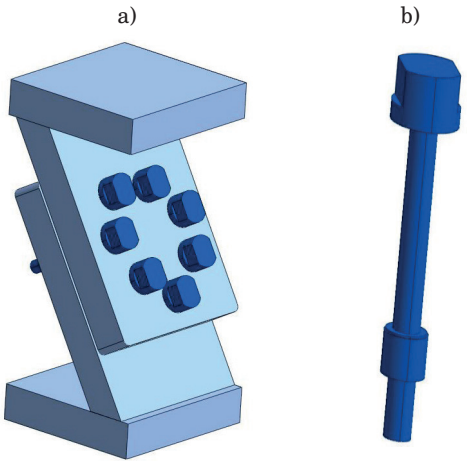


***Figure 1*** *The 3D model of the bolted connection (a) and 3D model of the single fastener (b)*

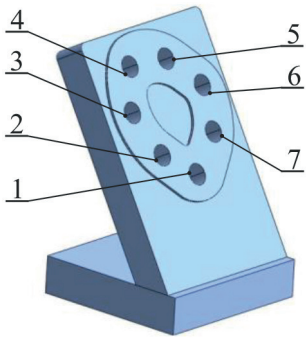


***Figure 2*** *Contact surface between the joined plates and the established bolt numbering*

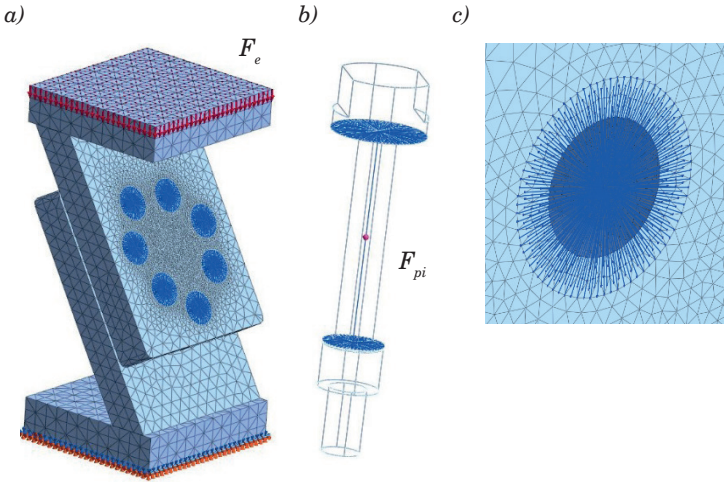


***Figure 3*** *The FEM-based model of the bolted connection (a), FEM-based model of the single fastener (b) and bolt to plate connection (c)*

***Table 1*** *Parameters of materials used in the model of the bolted connection*

| Parameter | Joined elements | Fasteners |
|---|---|---|
| Elastic modulus, GPa | 210 | 210 |
| Poisson's ratio | 0.30 | 0.28 |

## 2.2 FEM-based model

Using the Midas NFX 2020 R2 finite element system tools, a model of the bolted connection was made, shown in Figure 3. The joined plates were divided into 3D tetragonal finite elements, while the fasteners were modelled as flexible beams with rigid heads and nuts. In particular, the fastener models were obtained by connecting with rigid links the nodes of the beams and the nodes in the mesh of the joined plates lying within the heads of the bolts and nuts (for comparison, see [36-37]).

The individual parts of the bolted connection were assigned linear materials suitable for the steels listed in Section 2.1. Details on the parameters of these materials are given in Table 1.

General surface-to-surface contact elements were applied between the joined plates. They allow for the nonlinear analysis taking into consideration the possibility of separating the joined plates in the vertical direction and the occurrence of sliding in the horizontal direction. The following values of the contact layer parameters were adopted, appropriate for joining ground surfaces [38-39]:

- normal stiffness factor equal to 10,
- tangential stiffness factor equal to 1,
- coefficient of static friction equal to 0.14.

Welded type contact elements were applied between the plates and the bases to prevent the elements from moving relative to each other, in any direction.

The whole model of the bolted connection was built with 78750 elements and 133162 nodes. The model was

constrained by taking away all degrees of freedom at the bottom of the lower base (Figure 3a). The preload of the bolts $F_{pi}$ was applied using the "pretension" function available in the Midas NFX 2020 R2 system (marked by a red dot in Figure 3b). The external compressive load $F_e$ was applied perpendicularly to the top surface of the upper base and its value increased from 0 to 210 kN (Figure 3a).

## 3 Research procedure

The research was divided into the following stages:

1. Preloading the bolted connection in succession in three tensioning sequences in one pass. (Details of the assembly are provided in Table 2.)
2. Entering the damage state by removing the selected bolt according to the diagram shown in Table 3 (after each method of tensioning the bolted connection). Characterisation of changes in the value of forces in the bolts remaining in the bolted connection.
3. Loading the bolted connection in the operating condition. Comparison of the bolt forces values for a healthy and damaged connection.

The value of the preload of bolts $F_{pi}$ of 22 kN was calculated based on the PN-EN 1993-1-8 standard [40] and the analysis of the maximum surface pressure values between fasteners and joined plates was performed.

## 4 Research results and discussion

The graphical presentation of the calculation results for sequences A, B and C, respectively, is shown in Figures 4 to 6. The values of the operating forces in the selected bolts, related to the preload of the bolts, were compared for a healthy and damaged connection (after each state of damage). It is clear from the graphs that the drops in operating forces in the damaged connection occur faster than in the healthy connection. The analysis of this phenomenon can be performed based on the $Z_1$ indicator in the form:

$$Z_1 = \left| \frac{F_{bi}^h - F_{bi}^f}{F_{bi}^h} \right| \cdot 100\,, \tag{1}$$

where: $F_{bi}^h$ is the operating force in the $i$-th bolt in the considered distribution of forces at the end of the loading process of the healthy connection and $F_{bi}^f$ is an analogous force in the $i$-th bolt in the case of the damaged connection.

The greatest drop in operating force occurred in bolt No. 3 and it did not exceed 3 % in the first damaged state and 10 % in the second damaged state, for all the method of tensioning the bolted connection (Table 4). The bolt tensioning method has a slight effect on differences in these drops.

The total bolts tension at the end of the connection loading process was also compared. For this purpose, the $Z_2$ indicator was introduced by the formula:

$$Z_2 = \left| \frac{F_t^h - F_t^f}{F_t^h} \right| \cdot 100\,, \tag{2}$$

where: $F_t^h$ is the total force in the bolts in the considered distribution of forces at the end of the process of loading the healthy connection and $F_t^f$ is an analogous force in the case of the damaged connection.

The greatest drops in total force do not exceed 1 % in the first damaged state and 4 % in the second damaged state, for all the methods of tensioning the bolted connection (Table 5). The bolt tensioning method has a slight effect on the differences in these drops.

The last comparisons of the graphs, shown in

***Table 2*** *Sequences of tensioning of the bolted connection*

| Path type | Sequence (see Figure 2) |
|---|---|
| A | 1-3-5-7-2-4-6 |
| B | 1-4-7-3-6-2-5 |
| C | 1-5-2-6-3-7-4 |

***Table 3*** *Simulation of the damage of the bolted connection*

| State 1 | State 2 |
|---|---|
| 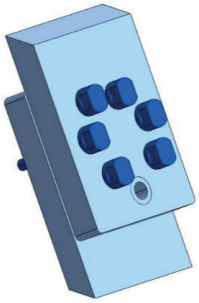 | 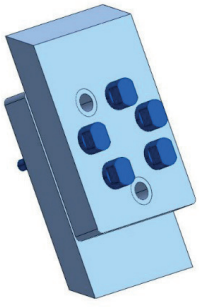 |

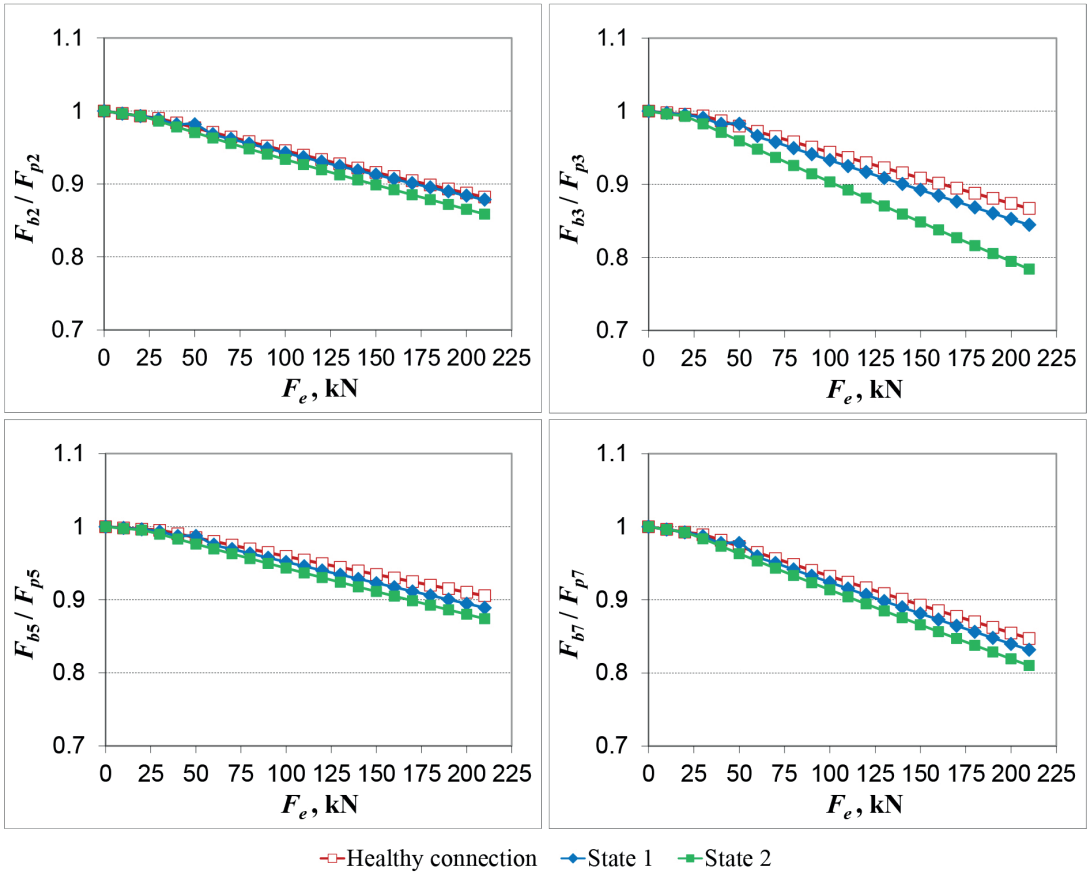


***Figure 4*** *Bolt forces in the connection tensioned according to the sequence of type A*

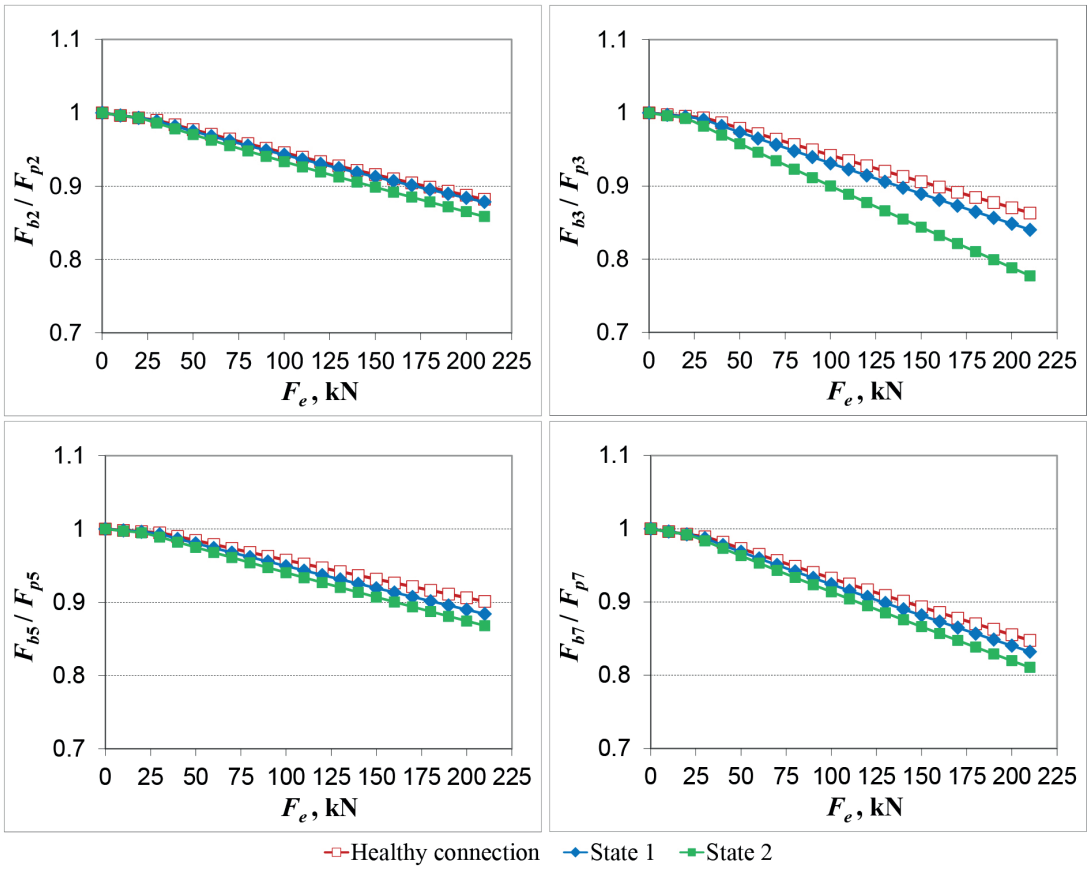


***Figure 5*** *Bolt forces in the connection tensioned according to the sequence of type B*

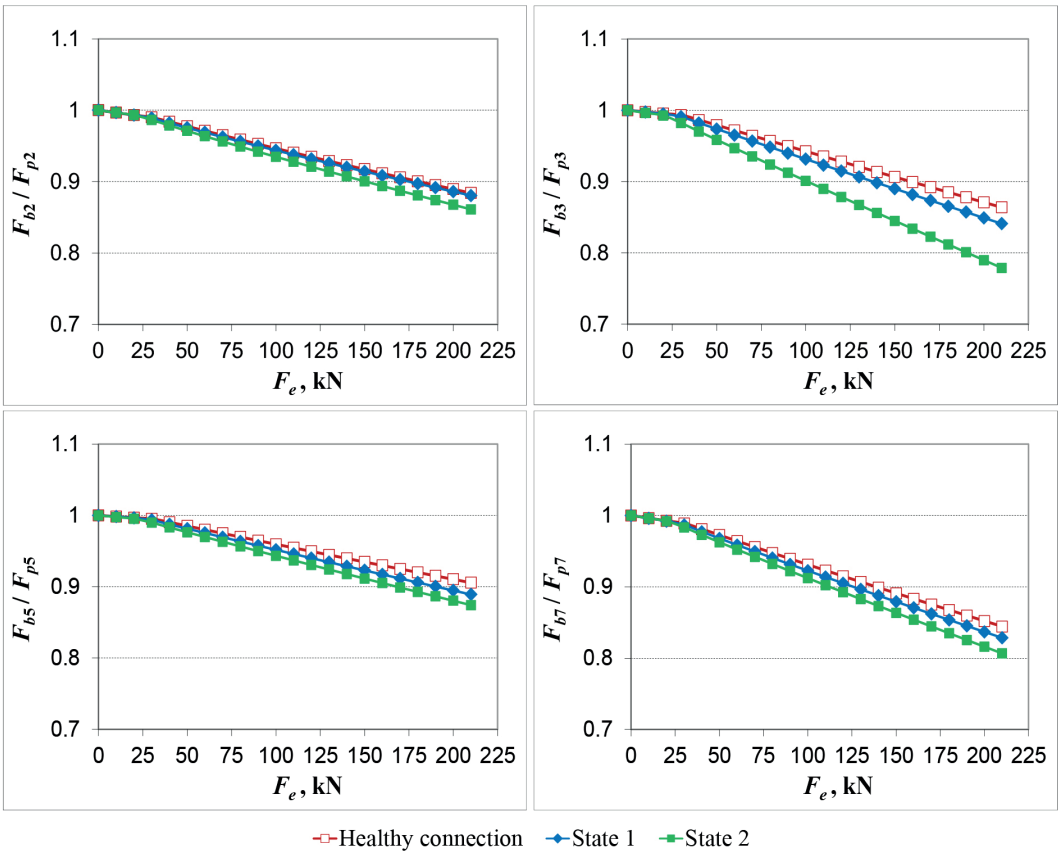


***Figure 6*** *Bolt forces in the connection tensioned according to the sequence of type C*

***Table 4*** *$Z_1$ indicator values (%)*

| Path type | State 1 | | | |
|---|---|---|---|---|
| | Bolt number | | | |
| | 2 | 3 | 5 | 7 |
| A | 0.41 | 2.58 | 1.82 | 1.83 |
| B | 0.41 | 2.65 | 1.91 | 1.82 |
| C | 0.40 | 2.64 | 1.82 | 1.87 |
| | State 2 | | | |
| Path type | Bolt number | | | |
| | 2 | 3 | 5 | 7 |
| A | 2.65 | 9.58 | 3.48 | 4.37 |
| B | 2.66 | 9.94 | 3.69 | 4.36 |
| C | 2.60 | 9.83 | 3.48 | 4.45 |

***Table 5*** *$Z_2$ indicator values (%)*

| Path type | State 1 | State 2 |
|---|---|---|
| A | 0.87 | 3.27 |
| B | 0.87 | 3.33 |
| C | 0.87 | 3.28 |

Figures 4 to 6, were aimed at determining the value of the external load $F_e$ at which the operating forces in the bolts in the damaged connection reach the values corresponding to the final load condition in the healthy connection. The results of these analyses are summarised in Table 6. Based on that, it can be concluded that the bearing capacity of the connection in the first damage state decreased by approximately 14 % and in the second damage state by approximately 37 %. The bolt tensioning method has a slight effect on the

***Table 6*** *External load values (kN)*

| State 1 | | | | |
|---|---|---|---|---|
| Path type | Bolt number | | | |
| | 2 | 3 | 5 | 7 |
| A | 203.6 | 181.9 | 180.5 | 191.1 |
| B | 203.5 | 181.9 | 180.6 | 191.1 |
| C | 203.5 | 181.9 | 180.5 | 191.1 |
| State 2 | | | | |
| Path type | Bolt number | | | |
| | 2 | 3 | 5 | 7 |
| A | 174.8 | 133.1 | 159.1 | 170.1 |
| B | 174.6 | 132.6 | 158.7 | 170.0 |
| C | 174.7 | 133.0 | 159.1 | 170.1 |

value of the bearing capacity.

In the literature cited in the introduction, the differences in the displacements of the joined elements, as a result of the removal of selected bolts, were studied rather than the differences in the values of forces in the bolts not removed from the connection. However, similar to the results of the other researchers, is the fact that the stiffness of the bolted connection decreases after its damage, i.e. after removing a bolt or a few bolts [24-26].

## 5 Conclusions

The paper presents an example of modelling the preloaded asymmetric bolted connections under damage and external force load conditions. Consideration of the connection with an arbitrary bolt system is original in relation to the works carried out so far. The results of the study lead to the following conclusions:

1. The drops in operating forces in a damaged connection loaded with external force occur faster than in a healthy connection. The differences in the values of the operating forces can be as high as 10 % (in the case of the two out of seven bolts failure).
2. The bearing capacity of a damaged connection (caused by the failure of two out of seven bolts) may be reduced by approximately 37 %.
3. The method of tensioning the connection has a slight effect on the magnitude of drops in the values of bolt forces and the bearing capacity of the connection in its damage state.
4. It is possible to carry out experimental tests verifying the presented bolted connection model using the stand described in [29-30].
5. The presented method can be used in assessing the health of bolted connections.

## References

[1] GRZEJDA, R., PARUS, A. Health assessment of a multi-bolted connection due to removing selected bolts. *FME Transactions* [online]. 2021, **49**(3), p. 634-642 [accessed 2022-07-11]. ISSN 1451-2092. Available from: https://doi.org/10.5937/fme2103634G

[2] DEMETGUL, M., SENYUREK, V. Y., UYANDIK, R., TANSEL, I. N., YAZICIOGLU, O. Evaluation of the health of riveted joints with active and passive structural health monitoring techniques. *Measurement* [online]. 2015, **69**, p. 42-51 [accessed 2022-07-11]. ISSN 0263-2241. Available from: https://doi.org/10.1016/j.measurement.2015.03.032

[3] MEDEIROS, R., SOUZA, G. S. C., MARQUES, D. E. T., FLOR, F. R., TITA, V. Vibration-based structural monitoring of bi-clamped metal-composite bonded joint: experimental and numerical analyses. *The Journal of Adhesion* [online]. 2021, **97**(10), p. 891-917 [accessed 2022-07-11]. ISSN 0021-8464. Available from: https://doi.org/10.1080/00218464.2020.1711742

[4] IJAZ, M., QAYYUM, F., ELAHI, H., ULLAH, M., EUGENI, M., BADSHAH, S., GAUDENZI, P. Effect of natural aging and fatigue crack propagation rate on welded and non-welded aluminum alloy (AA2219-T87). *Advances in Science and Technology - Research Journal* [online]. 2019, **13**(3), p. 129-143 [accessed 2022-07-11]. ISSN 2080-4075. Available from: https://doi.org/10.12913/22998624/110737

[5] BARSKI, M., KEDZIORA, P., MUC, A., ROMANOWICZ, P. Structural health monitoring (SHM) methods in machine design and operation. *Archive of Mechanical Engineering* [online]. 2014, **61**(4), p. 653-677 [accessed 2022-07-11]. ISSN 0004-0738. Available from: https://doi.org/10.2478/meceng-2014-0037

[6] GAO, S. Nonlinear finite element failure analysis of bolted steel-concrete composite frame under column-loss. *Journal of Constructional Steel Research* [online]. 2019, **155**, p. 62-76 [accessed 2022-07-11]. ISSN 0143-974X. Available from: https://doi.org/10.1016/j.jcsr.2018.12.020

[7] MAZURKIEWICZ, L., MALACHOWSKI, J., DAMAZIAK, K., TOMASZEWSKI, M. Evaluation of the response of fibre reinforced composite repair of steel pipeline subjected to puncture from excavator tooth. *Composite Structures* [online]. 2018, **202**, p. 1126-1135 [accessed 2022-07-11]. ISSN 0263-8223. Available from: https://doi.org/10.1016/j.compstruct.2018.05.065

[8] MIELOSZYK, J., TARNOWSKI, A., KOWALIK, M., PERZ, R., RZADKOWSKI, W. Preliminary design of 3D printed fittings for UAV. *Aircraft Engineering and Aerospace Technology* [online]. 2019, **91**(5), p. 756-760 [accessed 2022-07-11]. ISSN 1748-8842. Available from: https://doi.org/10.1108/AEAT-07-2018-0182

[9] GRZYWINSKI, M., SELEJDAK, J., DEDE, T. Shape and size optimization of trusses with dynamic constraints using a metaheuristic algorithm. *Steel and Composite Structures*. 2019, **33**(5), p. 747-753. ISSN 1229-9367.

[10] WYSMULSKI, P., DEBSKI, H., FALKOWICZ, K. Sensitivity of compressed composite channel columns to eccentric loading. *Materials* [online]. 2022, **15**(19), 6938 [accessed 2022-10-13]. ISSN 1996-1944. Available from: https://doi.org/10.3390/ma15196938

[11] SADEK, F., EL-TAWIL, S., LEW, H. S. Robustness of composite floor systems with shear connections: modeling, simulation and evaluation. *Journal of Structural Engineering*. 2008, **134**(11), p. 1717-1725. ISSN 0733-9445.

[12] KIM, T., KIM, J. Progressive collapse-resisting capacity of steel moment frames considering panel zone deformation. *Advances in Structural Engineering*. 2009, **12**(2), p. 231-240. ISSN 1369-4332.

[13] LU, X., LIN, X., YE, L. Simulation of structural collapse with coupled finite element-discrete element method. In: *Computational structural engineering*. 1. ed. Dordrecht: Springer, 2009, p. 127-135. ISBN 978-90-481-2822-8.

[14] KWASNIEWSKI, L. Nonlinear dynamic simulations of progressive collapse for a multistory building. *Engineering Structures* [online]. 2010, **32**(5), p. 1223-1235 [accessed 2022-07-11]. ISSN 0141-0296. Available from: https://doi.org/10.1016/j.engstruct.2009.12.048

[15] SASANI, M., KAZEMI, A., SAGIROGLU, S., FOREST, S. Progressive collapse resistance of an actual 11-story structure subjected to severe initial damage. *Journal of Structural Engineering*. 2011, **137**(9), p. 893-902. ISSN 0733-9445.

[16] FU, F. 3-D nonlinear dynamic progressive collapse analysis of multi-storey steel composite frame buildings - parametric study. *Engineering Structures* [online]. 2011, **32**(12), p. 3974-3980 [accessed 2022-07-11]. ISSN 0141-0296. Available from: https://doi.org/10.1016/j.engstruct.2010.09.008

[17] HELMY, H., SALEM, H., MOURAD, S. Computer-aided assessment of progressive collapse of reinforced concrete structures according to GSA code. *Journal of Performance of Constructed Facilities*. 2013, **27**(5), p. 529-539. ISSN 0887-3828.

[18] GU, X., WANG, X., YIN, X., LIN, F., HOU, J. Collapse simulation of reinforced concrete moment frames considering impact actions among blocks. *Engineering Structures* [online]. 2014, **65**, p. 30-41 [accessed 2022-07-11]. ISSN 0141-0296. Available from: https://doi.org/10.1016/j.engstruct.2014.01.046

[19] GAO, S., GUO, L., FU, F., ZHANG, S. Capacity of semi-rigid composite joints in accommodating columns loss. *Journal of Constructional Steel Research* [online]. 2017, **139**, p. 288-301 [accessed 2022-07-11]. ISSN 0143-974X. Available from: https://doi.org/10.1016/j.jcsr.2017.09.029

[20] TANG, H., DENG, X., JIA, Y., XIONG, J., PENG, C. Study on the progressive collapse behavior of fully bolted RCS beam-to-column connections. *Engineering Structures* [online]. 2019, **199**, 109618 [accessed 2022-07-11]. ISSN 0141-0296. Available from: https://doi.org/10.1016/j.engstruct.2019.109618

[21] WANG, F., YANG, J., PAN, Z. Progressive collapse behaviour of steel framed substructures with various beam-column connections. *Engineering Failure Analysis* [online]. 2020, **109**, 104399 [accessed 2022-07-11]. ISSN 1350-6307. Available from: https://doi.org/10.1016/j.engfailanal.2020.104399

[22] RODRIGUEZ, D., BRUNESI, E., NASCIMBENE, R. Fragility and sensitivity analysis of steel frames with bolted-angle connections under progressive collapse. *Engineering Structures* [online]. 2021, **228**, 111508 [accessed 2022-07-11]. ISSN 0141-0296. Available from: https://doi.org/10.1016/j.engstruct.2020.111508

[23] RUCKA, M., ZIMA, B., KEDRA, R. Application of guided wave propagation in diagnostics of steel bridge components. *Archives of Civil Engineering* [online]. 2014, **60**(4), p. 493-515 [accessed 2022-07-11]. ISSN 1230-2945. Available from: https://doi.org/10.2478/ace-2014-0033

[24] QIN, Z., CHU, F. Numerical studies on time-varying stiffness of disk-drum type rotor with bolt loosening. *Journal of Physics: Conference Series* [online]. 2015, **628**, 012076 [accessed 2022-07-11]. ISSN 1742-6588. Available from: https://doi.org/10.1088/1742-6596/628/1/012076

[25] QIN, Z., HAN, Q., CHU, F. Bolt loosening at rotating joint interface and its influence on rotor dynamics. *Engineering Failure Analysis* [online]. 2016, **59**, p. 456-466 [accessed 2022-07-11]. ISSN 1350-6307. Available from: https://doi.org/10.1016/j.engfailanal.2015.11.002

[26] BLACHOWSKI, B., GUTKOWSKI, W. Effect of damaged circular flange-bolted connections on behaviour of tall towers, modelled by multilevel substructuring. *Engineering Structures* [online]. 2016, **111**, p. 93-103 [accessed 2022-07-11]. ISSN 0141-0296. Available from: https://doi.org/10.1016/j.engstruct.2015.12.018

[27] PATIL, C. S., ROY, S., JAGTAP, K. R. Damage detection in frame structure using piezoelectric actuator. *Materials Today: Proceedings* [online]. 2017, **4**(2), Part A, p. 687-692 [accessed 2022-07-11]. ISSN 2214-7853. Available from: https://doi.org/10.1016/j.matpr.2017.01.073

[28] HASNI, H., JIAO, P., ALAVI, A. H., LAJNEF, N., MASRI, S. F. Structural health monitoring of steel frames using a network of self-powered strain and acceleration sensors: A numerical study. *Automation in Construction* [online]. 2018, **85**, p. 344-357 [accessed 2022-07-11]. ISSN 0926-5805. Available from: https://doi.org/10.1016/j.autcon.2017.10.022

[29] GRZEJDA, R., PARUS, A. Experimental studies of the process of tightening an asymmetric multi-bolted connection. *IEEE Access* [online]. 2021, **9**, p. 47372-47379 [accessed 2022-07-11]. ISSN 2169-3536. Available from: https://doi.org/10.1109/ACCESS.2021.3067956

[30] GRZEJDA, R., PARUS, A., KWIATKOWSKI, K. Experimental studies of an asymmetric multi-bolted connection under monotonic loads. *Materials* [online]. 2021, **14**(9), 2353 [accessed 2022-07-11]. ISSN 1996-1944. Available from: https://doi.org/10.3390/ma14092353

[31] CAO, Z., BRAKE, M. R. W., ZHANG, D. The failure mechanisms of fasteners under multi-axial loading. *Engineering Failure Analysis* [online]. 2019, **105**, p. 708-726 [accessed 2022-07-11]. ISSN 1350-6307. Available from: https://doi.org/10.1016/j.engfailanal.2019.06.100

[32] WALCZAK, R., PAWLICKI, J., ZAGORSKI, A. Tightness and material aspects of bolted flange connections with gaskets of nonlinear properties exposed to variable loads. *Archives of Metallurgy and Materials* [online]. 2016, **61**(3), p. 1409-1416 [accessed 2022-07-11]. ISSN 1733-3490. Available from: https://doi.org/10.1515/amm-2016-0231

[33] JASZAK, P. Prediction of the durability of a gasket operating in a bolted-flange-joint subjected to cyclic bending. *Engineering Failure Analysis* [online]. 2021, **120**, 105027 [accessed 2022-07-11]. ISSN 1350-6307. Available from: https://doi.org/10.1016/j.engfailanal.2020.105027

[34] CHAN, J. L. Y., LO, S. H. Direct analysis of steel frames with asymmetrical semi-rigid joints. *Steel and Composite Structures*. 2019, **31**(1), p. 99-112. ISSN 1229-9367.

[35] PN-EN 10025-1, Hot rolled products of structural steels, Part 1: General technical delivery conditions. Warsaw: Polish Committee for Standardization, 2007.

[36] GRZEJDA, R. FE-modelling of a contact layer between elements joined in preloaded bolted connections for the operational condition. *Advances in Science and Technology - Research Journal* [online]. 2014, **8**(24), p. 19-23 [accessed 2022-07-11]. ISSN 2080-4075. Available from: https://doi.org/10.12913/22998624/561

[37] PALENICA, P., POWALKA, B., GRZEJDA, R. Assessment of modal parameters of a building structure model. *Springer Proceedings in Mathematics and Statistics*. 2016, **181**, p. 319-325. ISSN 2194-1009.

[38] GRZESIK, W. Effect of the machine parts surface topography features on the machine service (in Polish). *Mechanik* [online]. 2015, **88**(8-9), p. 587-593 [accessed 2022-07-11]. ISSN 0025-6552. Available from: https://doi.org/10.17814/mechanik.2015.8-9.493

[39] GRZEJDA, R., WARZECHA, M., URBANOWICZ, K. Determination of pretension in bolts for structural health monitoring of multi-bolted connection: FEM approach. *Lubricants* [online]. 2022, **10**(5), 75 [accessed 2022-07-11]. ISSN 2075-4442. Available from: https://doi.org/10.3390/lubricants10050075

[40] PN-EN 1993-1-8, Eurocode 3: Design of steel structures, Part 1-8: Design of joints. Warsaw: Polish Committee for Standardization, 2006.

# STRUCTURAL BEHAVIOR OF PRESTRESSED CONCRETE BRIDGE GIRDER WITH MONOLITHIC JOINT

**Assylkhan Jalairov [1], Dauren Kumar [2,*], Khaini-Kamal Kassymkanova [3], Gulzhan Nuruldaeva [3], Arailym Imankulova [1]**

[1]Department of Transport, Construction, Bridges and Tunnels, Kazakh University of Way Transport, Almaty, Republic of Kazakhstan
[2]Department of Cartography and Geoinformatics, Al-Farabi Kazakh National University, Almaty, Republic of Kazakhstan
[3]Satbayev University, Almaty, Republic of Kazakhstan

*E-mail of corresponding author: daurendkb@gmail.com

***Resume***

The paper presents the results of a test on a composite bridge girder of a length of 42.0 m, which was performed to assess its resistance, stiffness and crack resistance. Composite reinforced concrete beam with three blocks is joined by the two monolithic joints. When testing a beam with monolithic joint in terms of stiffness, crack resistance and strength, a load of 943.5 kN was achieved without cracking, which is 26.8 % higher than the required one.

***Article info***

Received 30 January 2022
Accepted 24 August 2022
Online 19 September 2022

***Keywords:***

composite bridge prestressed
concrete beam
monolithic joint
beam strength
beam stiffness
beam crack resistance

Available online: https://doi.org/10.26552/com.C.2022.4.D150-D159

ISSN 1335-4205 (print version)
ISSN 2585-7878 (online version)

## 1 Introduction

Composite prestressed concrete bridge beams are used when it is impossible or difficult to deliver solid beams to the construction site. In comparison to the whole transported ones, a number of requirements are imposed on the composite ones, associated with the manufacture of a stand for an even, practical ideal connection of beam blocks on the slipway

The nature of the shear at the interface between the high-strength precast concrete of a bridge beam and concrete used as a material for grouting bridge connections or as a repair material for the bridge decks was studied in the work [1]. The test results show that refurbishment concrete has excellent adhesion to precast concrete, which is higher than the guideline values.

The long-term behavior of joints of a prestressed concrete composite beam with precast and monolithic bridge decks is described in [2]. The results show that the normal stress of concrete in joints after pouring can develop over time from compressive stress to tensile stress and the effect of creep and shrinkage of assembled concrete decks over time can play a significant role.

Simulation of the glue lines showed that joints glued with plastic glue strongly depend on the shape of the cohesive zone models and that the trapezoidal shape is the best fit with experimental data [3]. On the other hand, when using the brittle adhesives, it is allowed to neglect the shape of the cohesive zone models.

## 2 Materials and methods

Control tests of a prototype of a composite bridge girder of a length of 42.0 m were carried out at the production base of the Almaty Plant of Bridge Structures (APBS).

The prototype composite along the length of the beam consists of three blocks - two outer and one middle, joined together by means of the two monolithic joints 0.2 m wide (Figure 1). Figures 2 and 3 show the formwork dimensions of the outer and middle beam blocks. The length of the outer block is 13.9 m, the length of the middle block is 13.8 m. The joints connecting the blocks are made of monolithic reinforced concrete 0.2 m wide.

The prototype of a composite beam with monolithic joints also consists of three blocks - two outer and

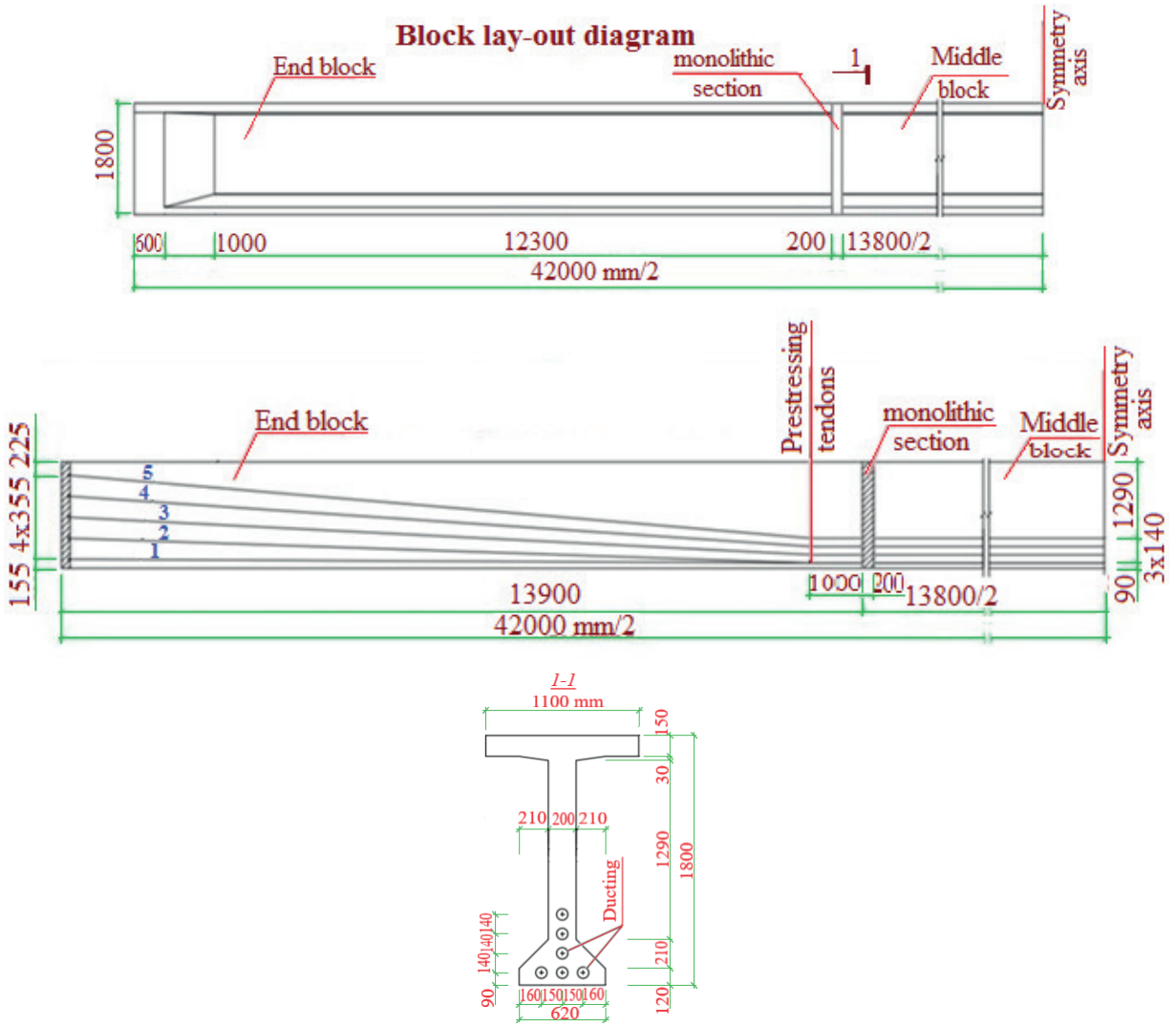


***Figure 1*** *General data, block layout diagram and the position of the prestressing tendons*

one middle (Figure 4). The length of the outer blocks is 14000 mm. The middle block has the shape of an inverted trapezoid - at the top the block has a length equal to 14010 mm, at the bottom - 14000 mm.

In the cross-section, the beam blocks have a T-section with an extended part at the bottom to accommodate beams prestressing steel.

The class of concrete for beam blocks is B40 according to [4].

When reinforcing a composite beam with prestressing steel, six tendons were designed, where each tendon consisted of seven strands K-7 of a diameter of 15 mm of Beloretsk Metallurgical Plant, having increased physical and mechanical characteristics in comparison to the characteristics given in the normative document "GOST 13840-68*. Reinforced steel ropes 1 × 7. Specifications". According to the document, for a single wire rope of a diameter of 15 mm, the force at the conditional yield strength is $P_{0.2} \geq 197$ kN and the conditional yield strength is $\sigma_{0.2} \geq 1410$ MPa. The controlled force in one prestressing tendon was taken equal to 1292 kN [5].

Figures 4 and 5 show the zones of monolithic joints No. 1 and No. 2 for combining the middle block with the two outer blocks. The class of concrete of a monolithic joint is taken equal to B40 with a strength range from 523.9 MPa to 589 MPa.

Before joining, the blocks of the composite beam were installed on the platform and the strands were pushed through the channeling blocks of the blocks. Figure 6 shows a general view of the end of the end block with the tendons laid in the assembly.

The joining of the blocks of the composite beam with each other in the staple was carried out by tensioning the beams of the prestressing tendons. The outer blocks are combined with the middle block using the two monolithic joints 0.2 m wide. Figure 7 shows the formwork of a monolithic joint.

After concreting the joints of the blocks and gaining their characteristic strength, the beams were gradually tensioned. The upper tendon was tensioned first, using a DN-7 hydraulic jack (Figure 8). The last were tensioned tendons in the lower row of the prestressing tendons. After tensioning each tendon was anchored. At the next stage of work, after prestressing the beams, cement

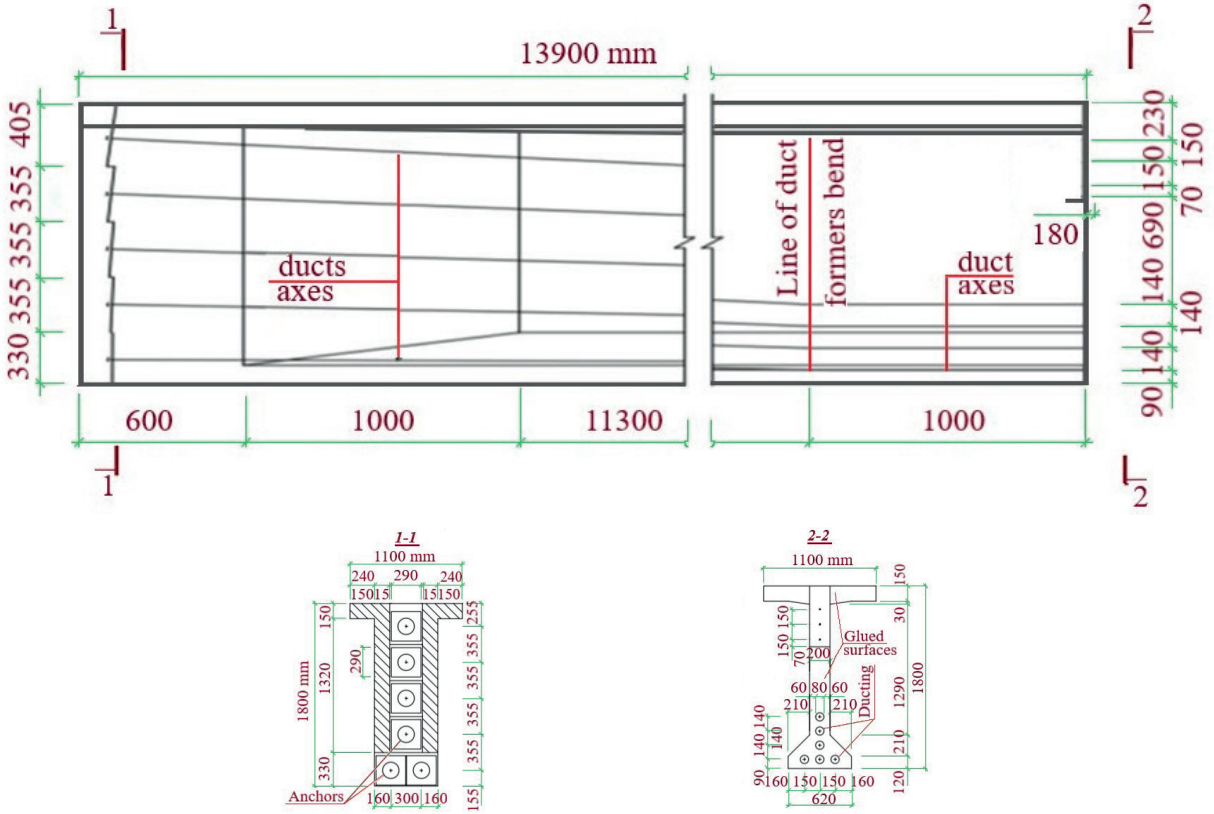


***Figure 2*** *Dimensions of formwork, front of the end block*

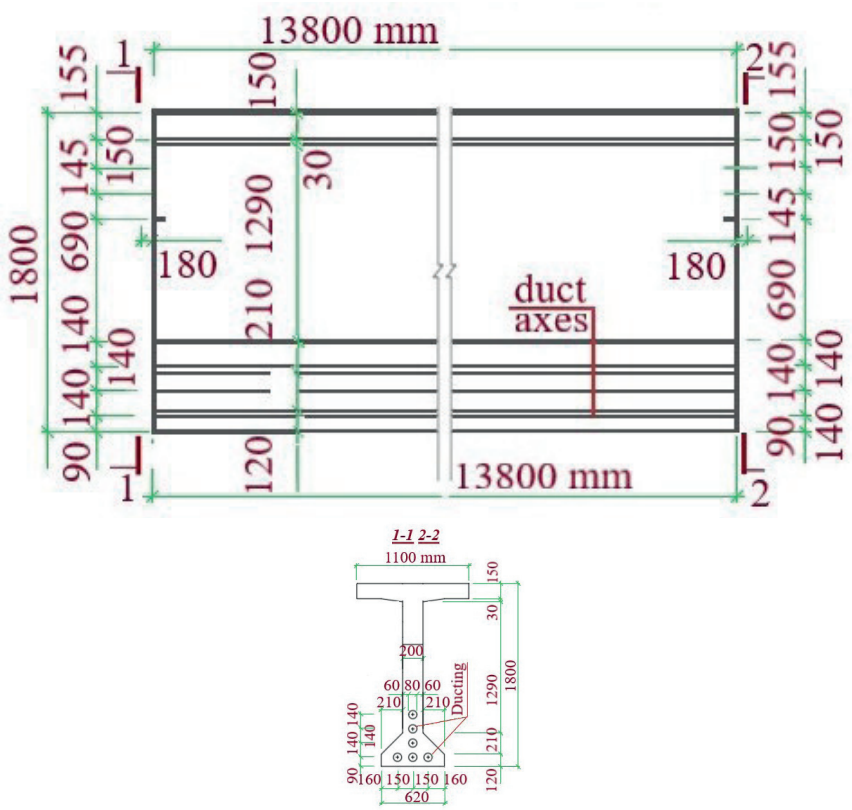


***Figure 3*** *Dimensions of formwork, middle block facade*

grout was injected into the ducts (Figure 9).

With the concrete age of the end blocks of 14 and 15 days and the middle block of 17 days, the actual concrete strength was tested. The strength of concrete was evaluated by the shock pulse method in accordance with State standard GOST 22690 "Concrete. Determination of the strength by mechanical methods of non-destructive testing "using an electronic meter of concrete strength IPS-MG4.03, developed by OOO "SKB" (Limited Liability Company "Construction Design Bureau") "Stroypribor" (Chelyabinsk, Russian Federation) was carried out.

The actual concrete strength of the outer blocks was B55 and B45 [4] and the middle block was B50. The strength of the concrete of the monolithic joints was B50.

To obtain the monolithic concrete of class B50,

***Figure 4*** *Joint zone No. 1 between the blocks before tensioning strands and concreting the joint (see Figure 1)*

***Figure 5*** *Joint zone No. 2 between the blocks before tensioning strands and concreting the joint (see Figure 1)*

***Figure 6*** *General view of the end block with tendons embedded in the ducts*

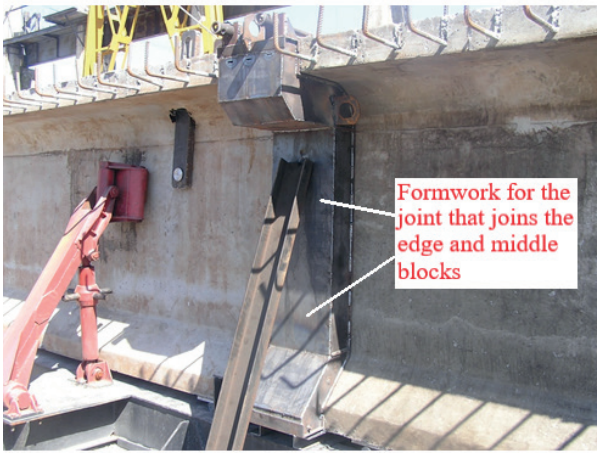


***Figure 7*** *Formwork for casting the joint*

***Figure 8*** *Tensioning of the upper tendon by a hydraulic jack DN-7*

***Figure 9*** *Injection of cement grout into the second duct*

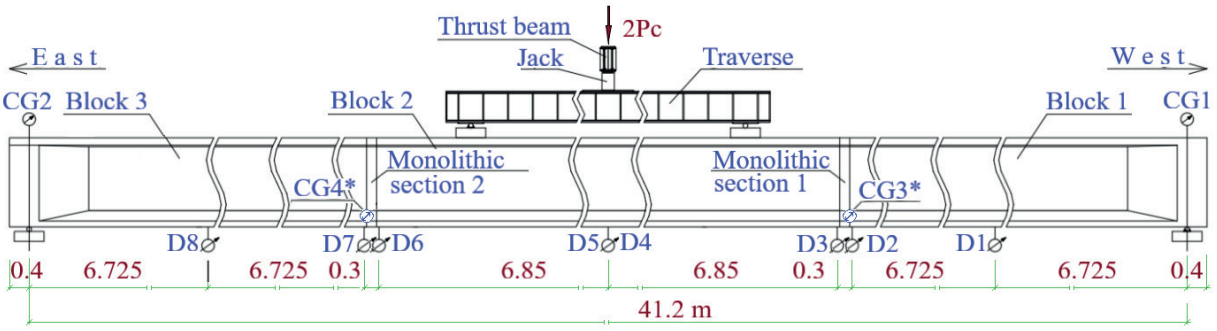


***Figure 10*** *Scheme of a composite beam of a length of L = 42.0 m with loading devices and mechanical indicators: ∅ - Deflection meters (D1 - D8 ); ⤢ - Clock type gauge (CG1-CG2) with a division value of 0.01 mm; ⤢ - Clock type gauge (CG3*-CG4*) with a division value of 0.001 mm*

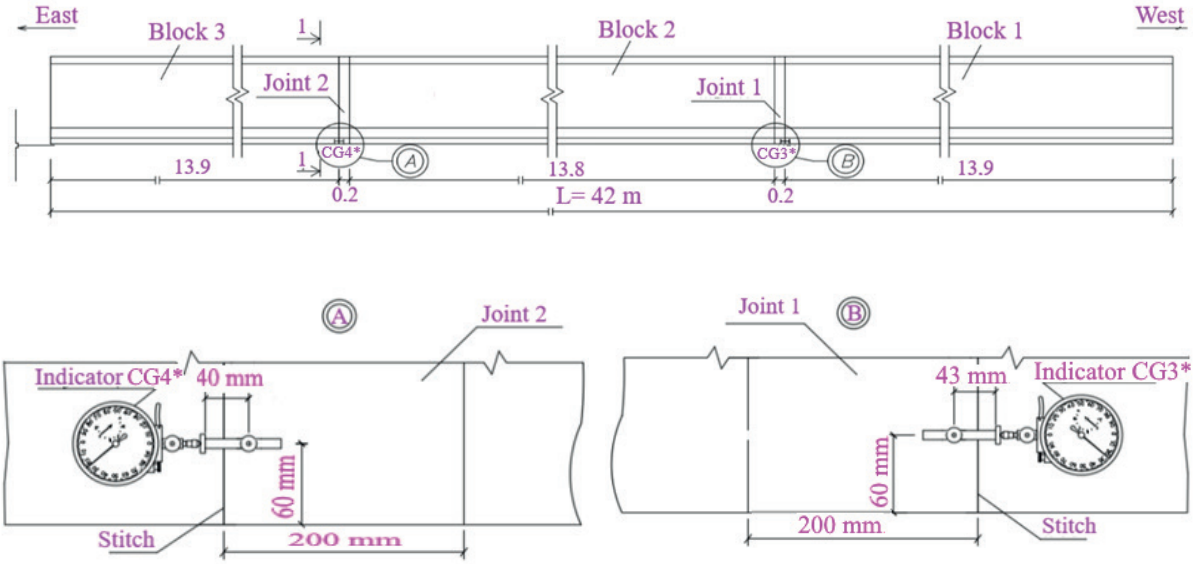


***Figure 11*** *Arrangement of dial gauges in the interface of joints 1 and 2 in a beam with a monolithic joints: CG3 * and CG4 * - with a graduation of 0.001 mm*

Portland cement of Topki plant (Russia) of grade M500 was used as a binder and as the main cladding additive - polycarboxylate hyper plasticizer Glenium 116, produced by BASF with a consumption of 1.2 % by mass of cement.

The effect of chemical additives on the rheological properties of fresh concrete is given in [6]. The rheometric workability tests (RWT) on standard construction mortars were conducted. The results confirmed the effectiveness of the RWT for evaluation of modified concretes.

The effect of organo-mineral modifier for concrete of transport constructions is given in [7]. The introduction of the modified cement system reduced the porosity to 3-5 %, depending on the composition of the concrete mixture. Tests of the repair layer of concrete with the modifier increased water resistance to W14 and frost resistance to grade F300.

Control measurements of the blocks showed that their geometric dimensions correspond to the design data.

Prior to testing, the bottom of the composite beam was surveyed using geodetic instruments to determine the camber of the beam. Instrumental survey was carried out using the tacheometer SOKKIA level of C3030 model and a geodetic rod.

Figure 10 shows a composite beam with a length of 42.0 m with loading devices and mechanical devices installed on the experimental structure. The mass of the loading devices was 49 kN. The effective length of the experimental beam, adopted in the tests, was 41.2 m, i.e. the axes of the supporting parts were located at a distance equal to 0.4 m from the ends of the outer blocks of the composite beam. In the middle part of the span, at a distance of 5.0 m from its centre, the test load was transferred in the form of two concentrated forces P (Figure 10).

To assess the stress-strain state of the monolithic joints No. 1 and No. 2 the middle block with the end ones and the possibility of fixing the opening of the joints in the process of loading, dial indicators were installed with a graduation rate of 0.001 and 0.01 mm (Figure 11 - at the joint zone).

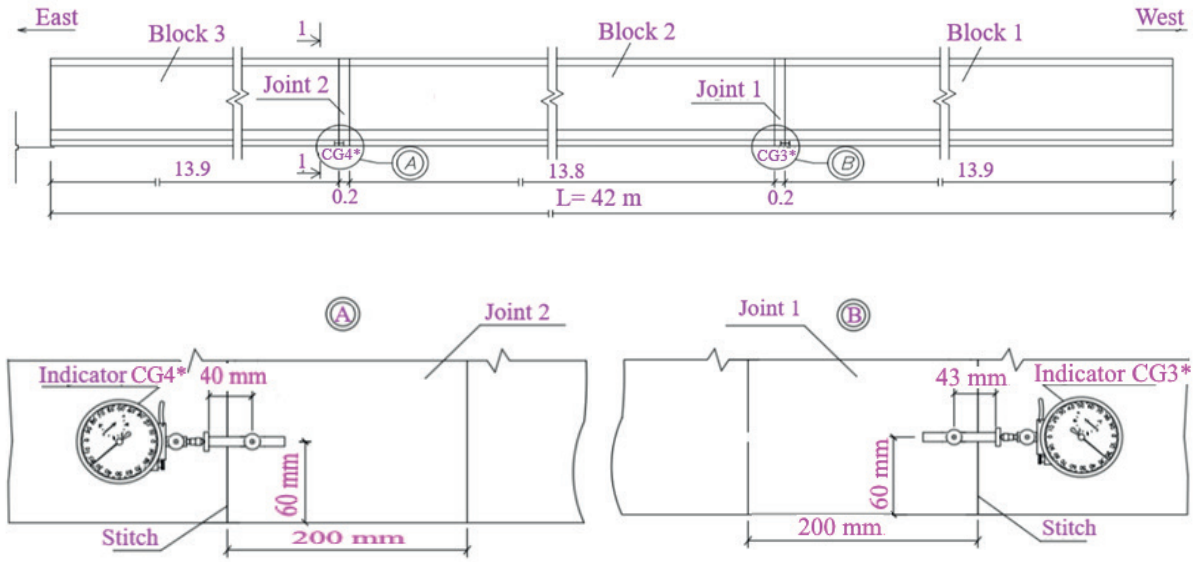


***Figure 11*** *Arrangement of dial gauges in the interface of joints 1 and 2 in a beam with a monolithic joints: CG3 * and CG4 * - with a graduation of 0.001 mm*

***Figure 12*** *Fragment of a composite beam 42.0 m long with installed strain gages and deflection meters in a beam with a monolithic joint*

Figure 12 shows the strain gauges glued to concrete beams to determine concrete strains along the height of the beam during the testing and mechanical devices installed on a composite beam to determine its deflections during the testing. The settlement of the supports was controlled using dial indicators with a graduation of 0.01 mm.

The results of experimental and numerical studies of the prefabricated bridge beam MDP for a span of 38 m with combined prestressing are given in [8]. The design of the beam is the result of a collaboration between the University of Zilina and a design company.

## 3 Results and discussion

### 3.1 Test results of a beam with a monolithic joints

In accordance with standard GOST 8829-94 "Reinforced concrete prefabricated concrete building products. Loading test methods. Rules for assessing, stiffness and crack resistance" [9] the values of control loads when testing a composite beam for stiffness, crack resistance and strength were adopted as follows:

1. When tested for stiffness:

- ❑ upon reaching the load $2P_c$ = 436 kN the deflection in the middle of the span a composite beam should not exceed a value equal to $f_c$ = 83 mm.

2. When tested for fracture toughness:
   - ❑ upon reaching the load $2P_c$ = 534 kN the opening of cracks in concrete of a composite beam should not exceed the value $a_{cr}$ = 0.15 mm.
3. When tested for strength:
   - ❑ upon reaching the load $2P_c$ = 744 kN the strength of the composite beam shall be ensured

Before the start of the tests, the lower edge of the 42.0 m long composite beam was leveled to determine the outline of its deformation. The deformation of the composite beam in the middle of the span, taking into account the preliminary rise of the middle block equal to 40 mm, was 103 mm.

To create and control the magnitude of the load when testing the composite beam, a power plant was used, which included a hydraulic jack DG100P230G with a lifting capacity of 1000 kN, a pressure cylinder, high-pressure tubes and a manual pumping station.

During the tests, the deflections of the beam were measured and recorded using the deflection meters. The possible opening of the joint at interface was recorded using dial indicators with a graduation rate of 0.001 mm. The settlement of the supports during the tests was controlled using the dial indicators with a graduation of 0.01 mm.

To control the moment of cracking, the side surfaces of the middle block of the composite beam were additionally covered with a thin layer of lime mortar. The crack width was determined using a Brinell microscope.

The load was applied to the composite beam in stages. After each stage of loading, readings were taken from the strain gauges, deflection meters and dial indicators.

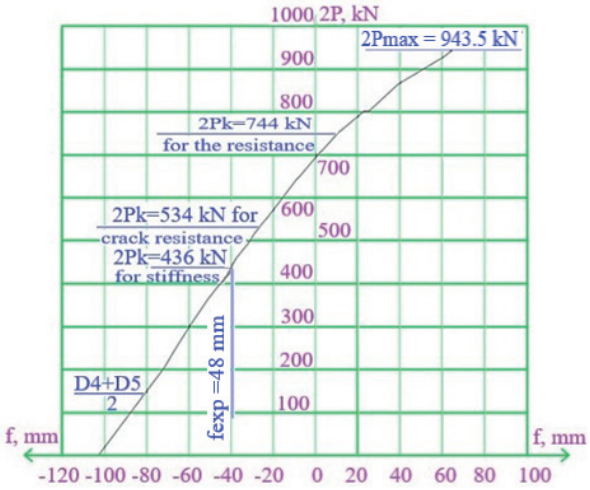


***Figure 13*** *- Load deflection graph of a composite beam in the middle of the span during its loading (D4 and D5 - deflection meters)*

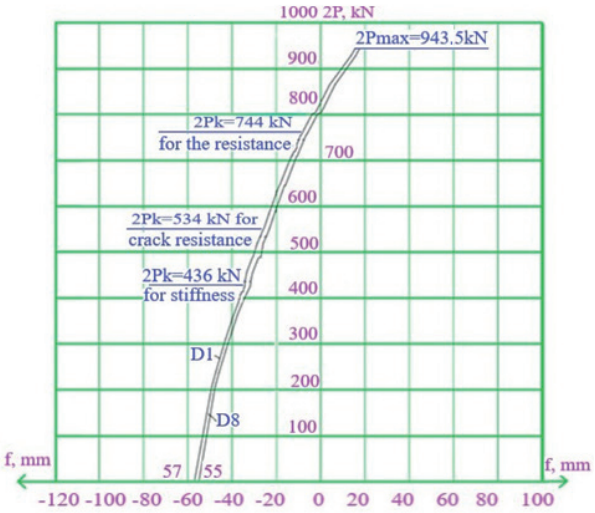


***Figure 14*** *Load deflection graph of a composite beam at a distance of 6.725 m from the axes of the supporting parts during its loading (D1 and D8 - deflection meters)*

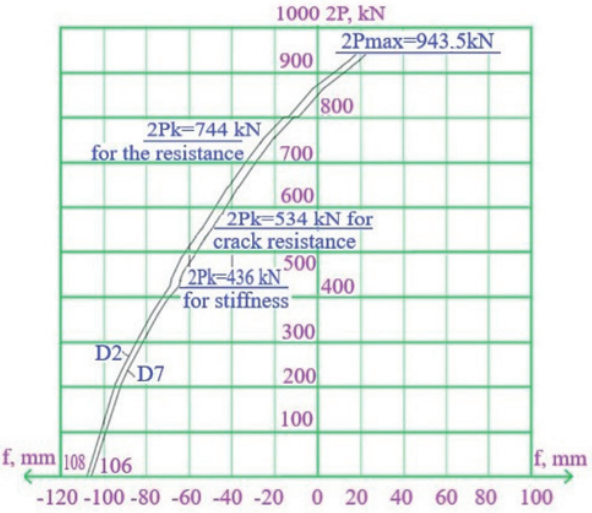


***Figure 15*** *Load deflection graph of a composite beam at a distance of 13.45 m from the axes of the supporting parts during its loading: in the joint zone 1 deflection meter D2, in the joint zone 2 deflection meter D7*

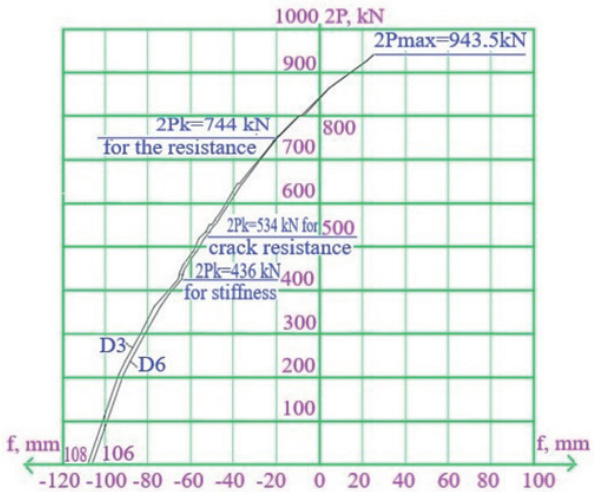


***Figure 16*** *The Load deflection graph of a composite beam at a distance of 13.75 m from the axes of the supporting parts during its loading: in the joint zone 1 deflector D3, in the joint zone 2 deflector D6*

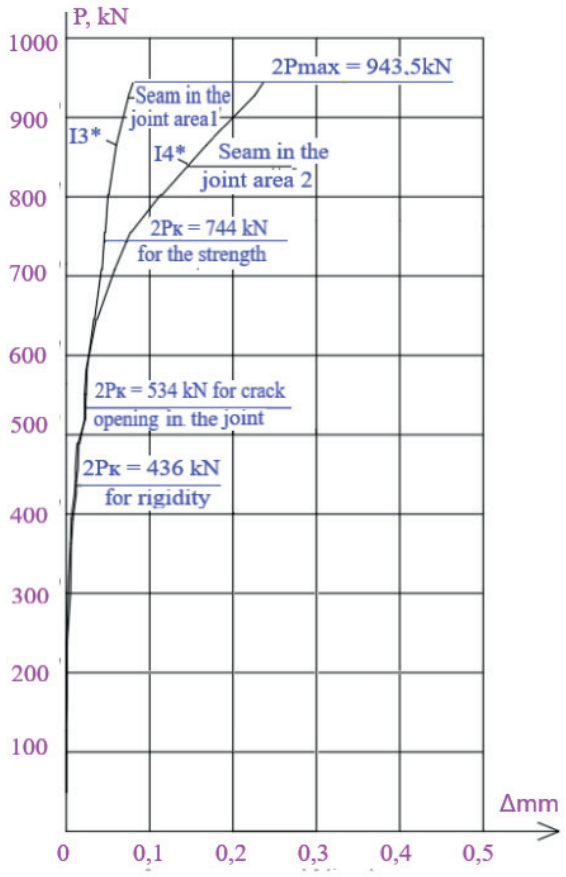


***Figure 17*** *Load-joint opening graph for the monolithic joints 1 and 2*

As an example, Figures 13 - 16 show the load-deflection graphs of a composite beam in the middle of the span during its loading.

Figure 17 shows a graph of the opening of the monolithic joint in the area of joints No. 1 and No. 2 of a composite beam during its loading, which were recorded by the dial indicators with a division value of 0.001 mm.

At the first stage of testing, the stiffness of the composite beam was evaluated. With a control load in terms of rigidity equal to $2P_c$ = 436 kN, the experimental deflection of a composite beam in the middle of the span should not exceed the control value of the deflection equal to $f_c$ = 83 mm. Upon reaching the control load equal to $2P_c$ = 436 kN, the experimental deflection in the middle of the span of the composite beam had a value equal to $f_{exp}$ = 48.0 mm, which was 57.9 % of the permitted control deflection (see Figure 13).

In terms of rigidity, a composite beam with a length of 42.0 m meets the requirements of the bridge standards SNiP 2.05.03-84* [10] and GOST 8829-94.

At the second stage of testing, the crack resistance of the concrete of the composite beam itself was evaluated. Upon reaching the control load $2P_c$ = 534 kN, the crack opening width should not exceed the control value equal to $a_{cr}$ = 0.15 mm

Upon reaching the control load equal to $2P_c$ = 534 kN in the concrete of the beam in the middle of the span, in the zone of maximum bending moments, there were no cracks.

At the same time, the possible opening of the joint at interface during the loading was monitored using dial indicators with a graduation rate of 0.001 mm. When the control load for the crack resistance was reached, equal to $2P_c$ = 534 kN, there was an opening of the joints No1 and No2. The size of the opening of the seams was 0.022 mm, which is lower than the value equal to $a_{cr}$ = 0.15 mm.

In terms of the crack resistance, a beam 42.0m long meets the requirements of the bridge norms SNiP 2.05.03-84 * and GOST 8829-94.

At the last, the third stage of testing, the strength of the beam was tested. According to the design calculations, the control load when assessing the strength of the beam was $2P_c$ = 744 kN.

During the tests, an experimental load of $2P_c$ = 943.5 kN was achieved, which, when checking the strength of a composite beam, which exceeded the control load equal to $2P_c$ = 744 kN. The exceeded value of the experimental load achieved during the tests over the reference strength load was 26.8 %.

The nature of the increase in the deflection curves in the composite beam (Figure 15) and the assessment of its stress-strain state indicated that the limiting state was not reached in it and the experimental structure still had reserves in bearing capacity [11-12].

In terms of strength, a composite beam of a length of 42.0 m meets the requirements of the bridge standards SNiP 2.05.03-84 * [10] and GOST 8829-94 [9].

During the tests, the possible displacement (pulling) of the prestressing steel, relative to the concrete of the composite beam, was monitored. At all the stages of loading a composite beam, no displacement (pulling) of the beams of prestressing steel relative to the concrete of the experimental structure was observed.

## 4 Conclusions

1. The control load, when checking a beam with a monolithic joint in terms of stiffness, was $2P_c$ = 436 kN. At a given load, the control deflection of the beam should not exceed a value equal to $f_c$ = 83.0 mm. With a load of $2P_c$ = 436 kN, the experimental deflection of the beam in the middle of the span had a value equal to $f_{exp}$ = 48.0 mm, which was 57.9 % of the permitted value for the control deflection.
   In terms of stiffness, the composite beam meets the requirements of the bridge standards SNiP 2.05.03-84 * and GOST 8829-94.
2. The control load, when checking a beam with monolithic joints for crack resistance, was equal to $2P_c$ = 534 kN. At a given load, the crack opening should not exceed a value equal to $a_{cr}$ = 0.15 mm. Upon reaching the control load equal to $2P_c$ = 534 kN, no cracks were formed in the concrete of the beam in the zone of maximum moments.
   In terms of crack resistance, the beam meets the requirements of the bridge standard SNiP 2.05.03-84 * and GOST 8829-94.
3. The control load, when checking a beam with monolithic joints in terms of strength, was equal to 2 $P_c$ = 744 kN. During the tests, an experimental load of 2 $P_{max}$ = 943.5 kN was achieved, which, when checking the strength of a composite beam, exceeded the control load equal to 2 $P_c$ = 744 kN. The assessment of the stress-strain state at the achieved experimental load equal to 2 $P_{max}$ = 943.5 kN indicated that the limiting state was not reached in the beam and the prototype still had reserves for bearing capacity.
   In terms of strength, the composite beam meets the requirements of the bridge standard SNiP 2.05.03-84 * and GOST 8829-94.

## References


[1] SEMENDARY, A. A., HAMID, W. K., STEINBERG, E. B., KHOURY, I. Shear friction performance between high strength concrete (HSC) and ultra high performance concrete (UHPC) for bridge connection applications. *Engineering Structures* [online]. 2020, **205**, 110122. ISSN 0141-0296. Available from: https://doi.org/10.1016/j.engstruct.2019.110122

[2] HUANG, D., WEI, J., LIU, X., DU, Y., ZHANG, S. Experimental study on influence of post-pouring joint on long-term performance of steel-concrete composite beam. *Engineering Structures* [online]. 2019, **186**, p. 121-130. ISSN 0141-0296. Available from: https://doi.org/10.1016/j.engstruct.2019.02.003

[3] CAMPILHO, R. D. S. G., BANEA M. D., NETO, J. A. B. P., DA SILVA, L. F. M. Modelling adhesive joints with cohesive zone models: effect of the cohesive law shape of the adhesive layer. *International Journal of Adhesion and Adhesives* [online]. 2013, **44**, p. 48-56. Available from: https://doi.org/10.1016/j.ijadhadh.2013.02.006

[4] Interstate Standard GOST 26633 - 2015 Heavy-weight and sand concretes. Specifications (in Russian). Moscow, 2019.

[5] JALAIROV, A., KUMAR, D., KASSYMKANOVA, K.-K., SARSEMBEKOVA, Z., NURULDAEVA, G., JANGULOVA, G. Structural behavior of prestressed concrete bridge girder with epoxy joint. *Communications - Scientific Letters of the University of Zilina* [online]. 2022, **24**(2), p. D59-D71. ISSN 1335-4205, eISSN 2585-7878. Available from: https://doi.org/10.26552/com.C.2022.2.D59-D71

[6] SZWABOWSKI, J., GOLASZEWSKI, J. Designing workability of high performance concrete using rheometrical workability test. *Communications - Scientific Letters of the University of Zilina* [online]. 2002, **4**(3), p. 35-40. ISSN 1335-4205, eISSN 2585-7878. Available from: https://doi.org/10.26552/com.C.2002.3.35-40

[7] PSHINKO, O., SHCHERBAK, A., RUDENKO, D. Research of operational properties of modified specialized concrete for transport constructions. *Communications - Scientific Letters of the University of Zilina* [online]. 2019, **21**(4), p. 90-96. ISSN 1335-4205, eISSN 2585-7878. Available from: https://doi.org/10.26552/com.C.2019.4.90-96

[8] MORAVCIK, M., BUJNAKOVA, P. New precast bridge girder with combined prestressing. *Communications - Scientific Letters of the University of Zilina* [online]. 2011, **13**(3), p. 19-23. ISSN 1335-4205, eISSN 2585-7878. Available from: https://doi.org/10.26552/com.C.2011.3.19-23

[9] State standard GOST 8829-94. Reinforced concrete and prefabricated concrete building products. Loading test methods. Assessment of strength, rigidity and crack resistance (in Russian). Moscow, 1998.

[10] SNiP 2.05.03-84*. Bridges and pipes (in Russian). Moscow, 2005.

[11] ABDALLA, L. B., GHAFOR, K., MOHAMMED, A. Testing and modeling the young age compressive strength for high workability concrete modified with PCE polymers. *Results in Materials* [online]. 2019, **1**, 100004. ISSN 2590-048X. Available from: https://doi.org/10.1016/j.rinma.2019.100004

[12] IBRAGIMOV, R., FEDIUK, R. Improving the early strength of concrete: effect of mechanochemical activation of the cementitious suspension and using of various superplasticizers. *Construction and Building Materials* [online]. 2019, **226**, p. 839-848. ISSN 0950-0618. Available from: https://doi.org/10.1016/j.conbuildmat.2019.07.313

# INSPECTION AND PREPARATION FOR TESTING OF THE ROAD OVERPASS OF THE ALMATY-KAPSHAGAI HIGHWAY AFTER THE VEHICULAR IMPACTS

Assylkhan Jalairov [1], Dauren Kumar [2,*], Gulzhan Nuruldaeva [3], Khaini-Kamal Kassymkanova [3], Bakdaulet Kumar [3], Yermek Zhalgasbekov [2]

[1]Department of Transport, Construction, Bridges and Tunnels, Kazakh University of Way Transport, Almaty, Republic of Kazakhstan
[2]Department of Cartography and Geoinformatics, Al-Farabi Kazakh National University, Almaty, Republic of Kazakhstan
[3]Satbayev University, Almaty, Republic of Kazakhstan

*E-mail of corresponding author: daurendkb@gmail.com

***Resume***

The 33.0 m long reinforced concrete bridge beams of the overpass superstructure after vehicular impacts were taken as a research object. The overpass consists of 14 beams, six of which were repaired by restoring the widened lower part with EMACO FAST TIXO, manufactured by BASF. The remaining 8 beams were completely dismantled and replaced with new ones. The new beams have been fully tested for the perception of vehicular loads.

The fully reconstructed span structure showed compliance with the design loads of A14, NK-120 and NK-180 based on test results.

***Article info***

Received 11 April 2022
Accepted 23 August 2022
Online 26 September 2022

***Keywords:***

overpass
superstructure
detailed survey
beam damage
beam testing
FEM

Available online: https://doi.org/10.26552/com.C.2022.4.D160-D173

ISSN 1335-4205 (print version)
ISSN 2585-7878 (online version)

## 1 Introduction

The present article brings the survey results of the bridge beams damages of a prestressed concrete girders double-span structure of a length of 33 m, caused by vehicle impacts in the Almaty-Kapshagai highway overpass section.

The basic goal of the constructed bridge structure survey was to establish its compliance with the project plans and the regulatory requirements on the operation quality.

The road overpass is located on a straight section in the plane and on a longitudinal axis in the i = 5 ‰ profile. As per the project, the angle of intersection of the longitudinal axis of the road overpass with the existing highway is 66° (Figure 1). The bridge scheme was adopted as 33+33 m. The total length of the bridge according to the project is 66.91 m [1].

The overpass superstructures are made of 33 m long pre-stressed VTK-33U beams (VTK - VTK - Russian abbreviation for High-Tech Construction).

On the top of superstructures beams, a laid-on slab made of monolithic reinforced concrete with grouting joints along the slab of the roadway of the VTK-33u beams was installed.

## 2 Materials and methods

A detailed examination of the damaged VTK-33 beams at the superstructure No. 1 was performed after the accident. As can be seen from Figure 2, most of the VTK-33 beams were significantly damaged.

Figure 2 shows that all fourteen VTK-33u beams were damaged as a result of vehicle impacts. Along with the destruction of the widened lower part of the beams, the destruction of the bottom flanges of the beams took place with the formation of cracks in them along the longitudinal axis of the beams.

Table 1 lists data on the presence of longitudinal cracks in beams ribs and their length.

The destruction of the widened lower part and the flange of the beam No. 1 are present with a rupture of the wire of the ropes K-7 (Figures 3 and 4).

A significant damage in beams 2, 3, 4 and 11 are present (Figures 5-8). In them, the bottom flange is


***Figure 1*** *The general view of the overpass from the Kapshagai city side: 1 and 2 - superstructure numbers*


***Figure 2*** *The general view of the damaged superstructure No. 1 from the Kapshagai city side*

destroyed, ruptures of the reinforcement of a smooth and periodic profile took place. Longitudinal cracks of various lengths were revealed in the flanges of those beams.

Authors presented the results of a damage survey and an assessment of the prestressed concrete girders viaduct repair works, damaged as a result of a vehicle impact [2]. It has been analytically proven that the structure can be strengthened by assembling prestressed reinforced concrete beams at both ends.

Beams 5, 6, 7 and 8 have a lower degree of damage (Figures 9-12). In them, the destruction of the widened lower part of the beams is mainly present.

***Table 1*** *The numbers of beams, the presence of cracks and the length of their stretch in bottom flanges*

| Numbers when counting from the Kapshagai city towards Almaty city | 1 | 2 | 3 | 4 | 5 | 6 | 7 | 8 | 9 | 10 | 11 | 12 | 13 | 14 |
|---|---|---|---|---|---|---|---|---|---|---|---|---|---|---|
| The presence of longitudinal cracks in the ribs of the beams at the base of the upper part of bottom flange and the length of their stretch, m | + 8.6 | + 6.2 | + 9.2 | + 3.3 | - - | - - | - - | - - | - - | - - | + 3.9 | + 6.2 | + 5.4 | + 3.2 |

Note:

«+» - longitudinal cracks are present in the flange of the beams;

«-» - no longitudinal cracks are present in the flange of the beams.

***Figure 3*** *A general view of the destruction in beam No. 1 from the Kapshagai side (Destruction of the bottom flange of beam and its widened lower part. A longitudinal crack was revealed in the upper part of the beam flange of a length of about 8.6 m)*

***Figure 4*** *Fragment of destruction in beam No. 1 and damage with wire rupture of K-7 ropes from the Kapshagai side*

***Figure 5*** *A general view of the destruction of the bottom flange of the beam No. 2 (The reinforcement of the smooth and periodic profile is damaged. The bundle of prestressed reinforcement is exposed)*

***Figure 6*** *Destruction of the widened lower part of beam No. 3 from the Kapshagai side (Smooth and periodic profile reinforcement was torn. A longitudinal crack was revealed in the upper part of the beam rib of a length of about 9.2 m)*

***Figure 7*** *Destruction of the widened lower part of the beam No. 4 from the side of Almaty (The reinforcement of the smooth and periodic profile is torn. A longitudinal crack was revealed in the upper part of the beam rib of a length of about 3.3 m)*

***Figure 8*** *Destruction of the widened lower part of the beam No. 11 from the Kapshagai side (The reinforcement of the smooth and periodic profile is damaged. A longitudinal crack was revealed in the upper part of the beam rib of a length of about 3.9 m)*

***Figure 9*** *Fragment of the destroyed widened lower part of beam No. 5 from the Kapshagai side (The reinforcement is torn; the bundle of prestressing reinforcement is exposed)*

***Figure 10*** *Damage of the protective concrete cover in the widened lower part of beam No. 6 from the Kapshagai side (The longitudinal smooth reinforcement is damaged)*

***Figure 11*** *Damage of the protective concrete cover in the widened lower part of beam No. 7 from the Kapshagai side*

***Figure 12*** *Destruction of the widened lower part of the beam No. 8 from the Kapshagai side*

## 3 Technical assessment of the superstructure beams No. 1

The obtained survey results of the VTK-33U beams of the superstructure No. 1 showed that destruction of the widened lower part of the beams (bottom flange), rupture of smooth and periodic reinforcement, rupture of wires and exposure of K-7 ropes of the pre-stressing reinforcement took place in them. Additionally, damage to ribs in a number of beams with the formation of longitudinal cracks at the base of the upper haunch were present.

Article [3] presents the results of inspections of reinforced concrete bridges in the north of Slovakia after 40-50 years of operation. Based on the results of residual life calculation, recommendations for further bridge operation are given. An assessment model for determining the priority strategy for bridge maintenance is described in [4]. The publications [5-6] present the results of the analysis of damage to bridges with box girders and risk assessment for the bridge structures using a fuzzy structure in a car explosion.

The following notes should be considered based on the analysis of damage in the VTK-33U beams:

- in beam 1, the destruction of the rib, the lower widened part and the rupture of the wires of the K-7 ropes are present;
- in the beams 5, 6, 7, 8, 9, 10 destructions of the widened lower part, damage to the reinforcement of a smooth and periodic profile, exposure of bundles of strained reinforcement have occured;
- in the beams 2, 3, 4, 11, 12, 13, 14 there were destructions of the widened lower part, damage to the reinforcement of a smooth and periodic profile, exposure of bundles of stressed reinforcement and longitudinal cracks of various lengths in the edge of the beams at the base of the upper part of bottom flange.

Bridge damage detection based on the visual data was performed by revealing the undamaged areas, that make up more than 80-90 % of the total surface area. Next, the contour masks were created to refine the classification in the surface texture. The mentioned method reduced the search space for the inspector by 90.1 % [7].

The results of reinforcement models of reinforced concrete T-beams are presented in [8]. It is shown that reinforcement with one MBrace® S&P CFK 150/2000 bend lamella and three S&P C-Sheet 640 100 mm wide improves the bending strength of the models.

Damaged beams, excluding the beam No. 1, could be repaired. At the same time, in the beams No. 1, 2, 3, 4, 11, 12, 13 and 14, along with the damage to the lower widened part, there were longitudinal cracks of various lengths in the bottom flange of the beams, at the base of the upper sides. The presence of those cracks significantly reduced the bearing capacity of those beams. Given the presence of such damage, it was recommended to dismantle these beams, which was done.

In beams No. 5, 6, 7, 8, 9 and 10, only the lower broadened part of the beams was damaged, caused by the destruction of the protective layer of concrete. A detailed examination revealed that the bundles of stressed reinforcement in the lower widened part of the beams were not damaged, which did not cause the reduction of the bearing capacity of these structures, the presence of such damage gave reason to recommend the repair of those beams.

For repairment of beams No. 5, 6, 7, 8, 9 and 10, BASF's EMACO FAST TIXO was recommended. This material is a non-shrinking, fast-hardening dry mix of a thixotropic type, containing polymer fibers, intended for structural repairs of concrete and reinforced concrete.

In article [9] are cited and described the methods and repair materials applied towards the improvement of prestressed concrete beams performance.

Application of organomineral modifier for the transport structures is given in [10]. On an example of concrete samples of brands M50 and M100 40×40×160 mm with W/C = 0.5 it is shown that the bending strength of modified concretes is higher on the average by 89-104%.

The use of fiber-based repair compounds can slow down the corrosion in loaded reinforced concrete beams [11], improve the operation of reinforced concrete structural elements under extreme conditions [12].

## 4 Bridge beam testing

### 4.1 Beam testing preparation

As stated in section 3, beams No. 1, 2, 3, 4, 11, 12, 13 and 14 were recommended to be dismantled. These beams were dismantled and replaced by the new prestressed concrete bridge beams VTK-33u, 33 m long, manufactured by Magnetik LLP (Zarechny village, Almaty region, Kazakhstan). Those beams are designed for superstructures of road bridges designed for the impact of temporary mobile loads A14, NK-120 and NK-180.

As per the project, the VTK-33u beam concrete class is B35 according to [13]. Figure 13 demonstrates a longitudinal section and cross sections of the VTK-33u beam. Seven-wire strands K-7 with a diameter of 15 mm according to GOST 13840-68 "Steel reinforcing ropes 1x7. Specifications" [14], combined by four strands into a cables (7 wires) and two strands, combined into one cables (Table 2, Figure 13). The area of the prestressing tendons, adopted in the project when reinforcing the beam, is $A_p$ = 4170 mm$^2$. Three rods with a diameter of 14 mm of class A 400 according to GOST 34028-2016 are accepted as working longitudinal non-stressed reinforcement [15]. The area of the non-stressed reinforcement adopted in the project when reinforcing the beam is As = 462 mm$^2$.

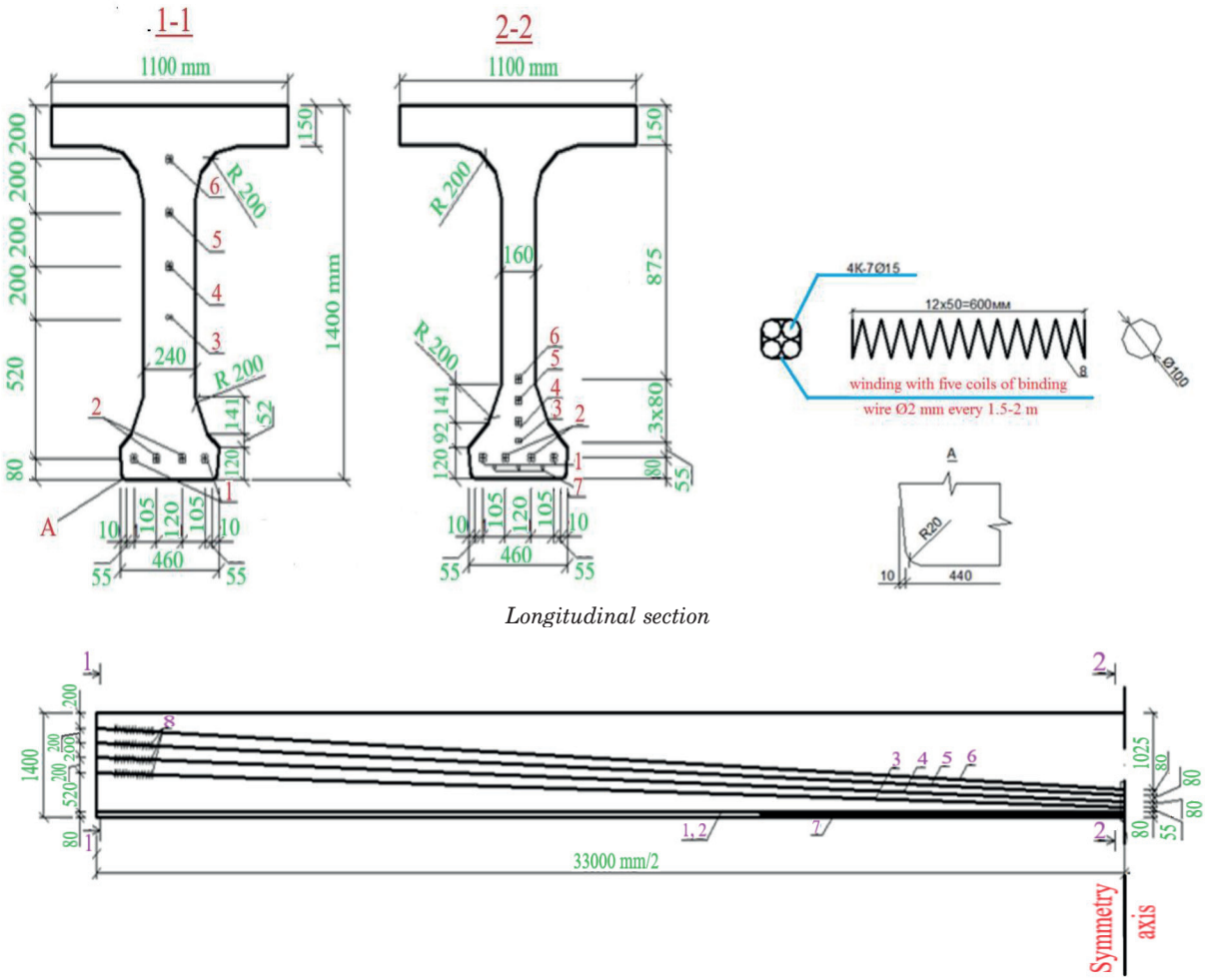


***Figure 13*** *Longitudinal section and cross sections of the VTK-33u beam*

***Table 2*** *Specification of the beam reinforcement elements*

| No. | Title | Elements | Quantity | Weight, kg |
|---|---|---|---|---|
| 1 | Cables of 4 strands K-7 Ø 15 mm as per GOST 13840-68* | L=34200 | 2 | 301 |
| 2 | | L=34200 | 2 | 301 |
| 3 | | L=34200 | 1 | 150.5 |
| 4 | | L=34200 | 1 | 150.5 |
| 5 | | L=34200 | 1 | 150.5 |
| 6 | | L=34200 | 1 | 150.5 |
| 7 | Longitudinal bars | Ø 14 A 400 L=11700 | 3 | 43 |
| 8 | Helix | Ø 6 240 L=4500 | 16 | 16 |

As per Construction Directives and Rules 2.05.03-84* "Bridges and Pipes"[16], the beam testing control loads were:

- Stiffness - $2P_c$ = 280 kN;
- Crack resistance - $2P_c$ = 360 kN;
- Strength - $2P_c$ = 630 kN.

Prior to the start of the tests, an instrumental survey of the bottom of the beam was done using a geodetic tool in order to determine the beam deflection. Instrumental survey was carried out using a SOKKIA C3030 level and a geodetic rod.

The experimental bending of the beam in the middle of the span, loading devices mass included was 42 mm and the loading devices mass excluded was- 45.4 mm.

The difference between the calculated and experimental bending of the beam made $\Delta$ = 45.8 - 45.4 = 0.4 mm, which indicates a satisfactory convergence.

Figure 14 demonstrates the design scheme of the experimental product and the outline of the beam bottom in the presence of loading devices on it. Review of the beam deflection curve indicates a satisfactory shape of the formwork bottom.

On the day of testing, the actual strength of the

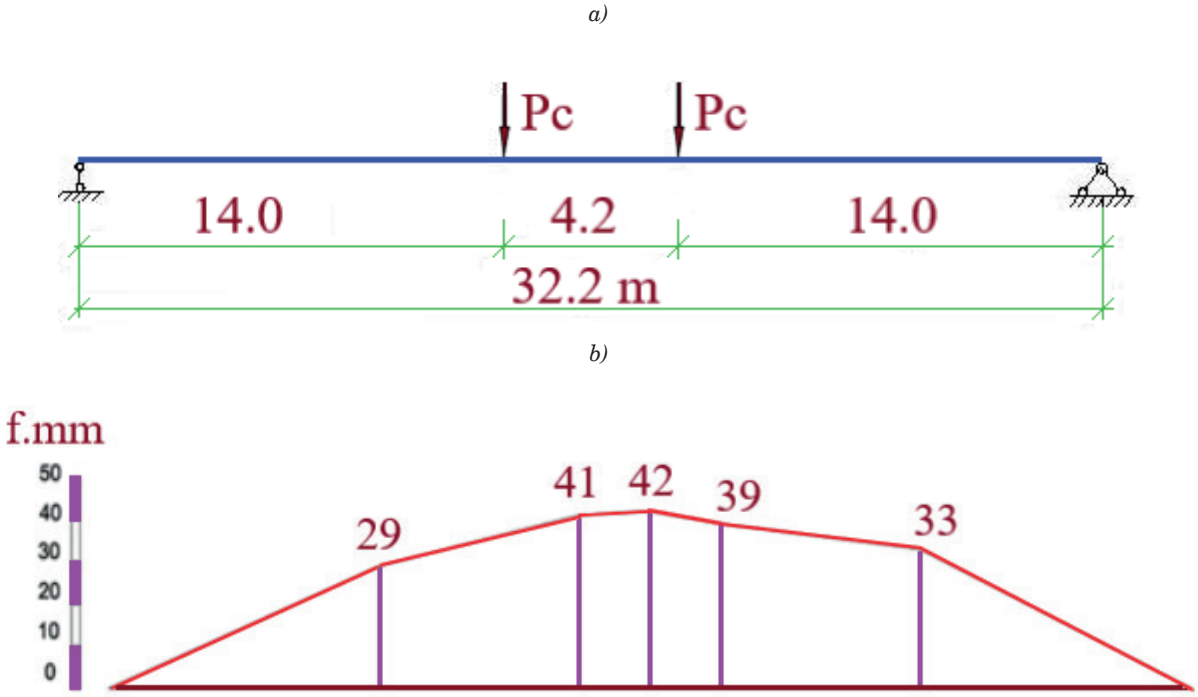


***Figure 14*** *The design scheme of a 32.2 m long composite beam (a) and the outline of its lower face, loading devices weight included (b)*

***Table 3*** *Concrete beams experimental grades*

| Item No. | Structure name | Number of experimental single values, n | Average value of concrete strength R̂, MPa | Standard σ, MPa | Variation coefficient, v | Experimental concrete grade, B |
|---|---|---|---|---|---|---|
| 1 | 2 | 3 | 4 | 5 | 6 | 7 |
| 1 | VTK-33u | 34 | 46.47 | 5.397 | 0.116 | 37.33 |

beam concrete was determined. The strength of concrete was evaluated by the shock pulse method, as per GOST 22690-88 "Concrete" standard. Determination of strength by mechanical methods of non-destructive testing" [17] using an electronic concrete strength meter IPS-MG4.03, developed by SKB Stroypribor LLC (Chelyabinsk, Russian Federation).

Table 3 presents the processing results of the concrete strength experimental values. The experimental grade of the beam concrete at the day of testing made B37.33. The concrete strength corresponds to the nearest B35 grade.

### 4.2 Beam testing

Control (certification) tests of the reinforced concrete structures are carried out according to the schemes provided for in the design documentation, both before the start of mass production of structures and periodically in the process of their manufacture.

A certified power stand of Magnetik LLP was used for testing. To create and control the magnitude of the vertical load during the testing of a beam, a power plant was used, a hydraulic jack DP140G300, a pressure gauge, high pressure hoses and a pumping station included.

The estimated length of the prototype, adopted in the tests was 32.2 m, i.e. the axes of the supporting parts were located at a distance equal to 0.4 m from the ends of the beam. In the middle part of the span, at a distance made 2.1 m from its middle, the test load on the prototype was applied in the form of the two concentrated forces P. The test scheme for the VTK-33u beam corresponded to the scheme adopted in the project.

During the tests, the deflections of the beam were determined in the middle of the span, under two loads P and at a distance of 8.05 m from the axis of the beam supports. Beam deflections were recorded using deflectometers of Aistov system and Kucherenko Central Research Institute of Building Structures (Moscow, Russia). The subsidence of the supports was controlled using dial indicators with a division value of 0.01 mm.

In the course of testing, the possible slippage

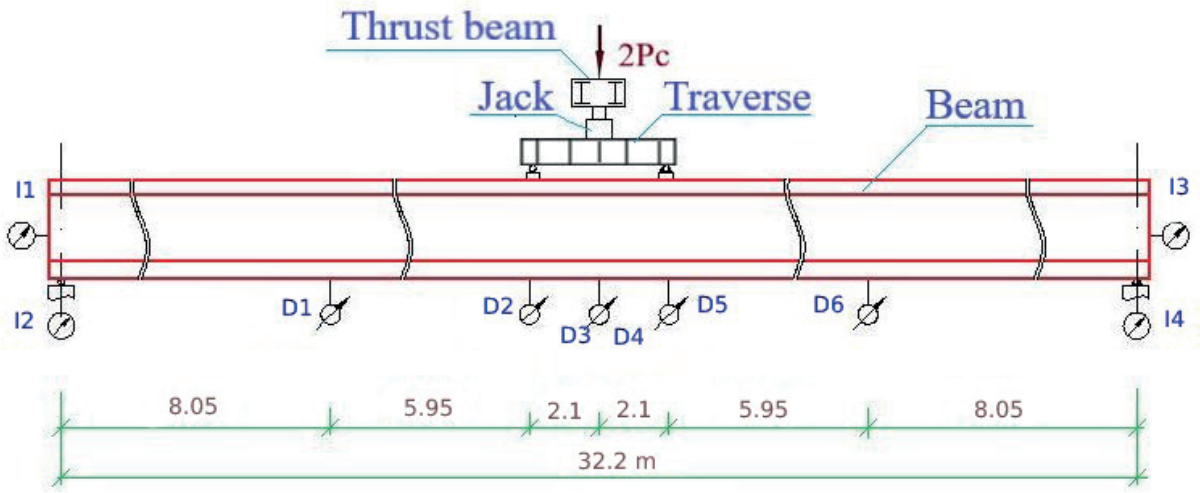


- deflectometers (D1-D6); - dial gauge (I1-I4)

***Figure 15*** *Experimental product scheme with the loading equipment and mechanical devices*

***Figure 16*** *General view of the power stand and the VTK-33u tested beam*

***Figure 17*** *The support zone of the VTK-33u beam with dial indicators*

of prestressing reinforcement beams relative to the concrete of the beam was controlled using dial indicators with a division value of 0.01 mm, installed at the ends of the beam. Figure 15 shows the design scheme for testing the VTK-33u beam and the scheme of an experimental product with loading devices.

To control the moment of a crack formation, the side surfaces of the slab in the middle of the span were additionally covered with a thin layer of lime solution. The crack extension width was determined using a Brinell microscope.

A phased load was applied to the experimental beam. After each phase of loading, readings were taken on deflectometers and indicators.

Figure 16 shows a general view of the beam being tested and the certified power bench during the testing and Figure 17 shows the support area of the beam with dial gauges.

### 4.3 Test results

According to Table 39* [16] the category of crack resistance requirements, imposed on the VTK-33u bridge beam, is - 2b, in which the formation of cracks is allowed under the action of the design loads.

The control loads for testing the pilot beam were determined in accordance with the requirements of GOST 8829-94 [18] and [19].

According to the project, the experimental deflection

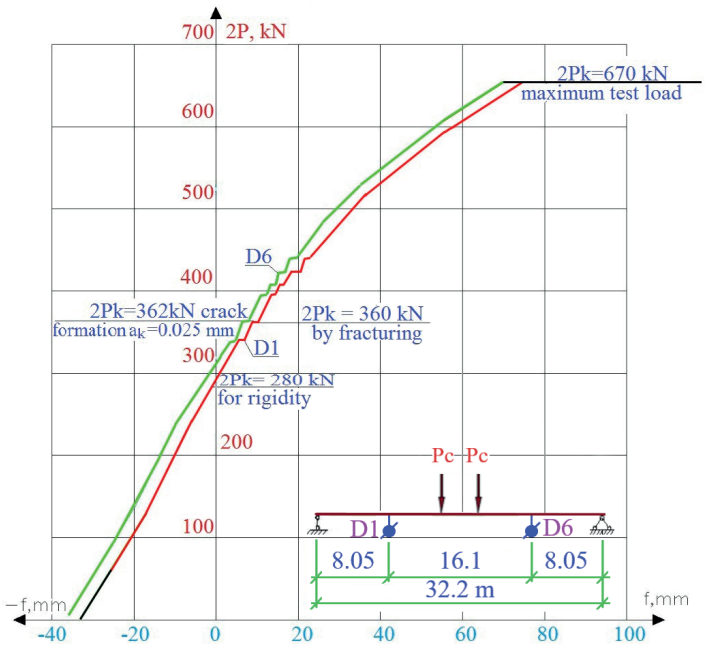


***Figure 18*** *Deflection curves at a distance of 8.05 m from the middle of the span: D1 and D6 - deflectometers*

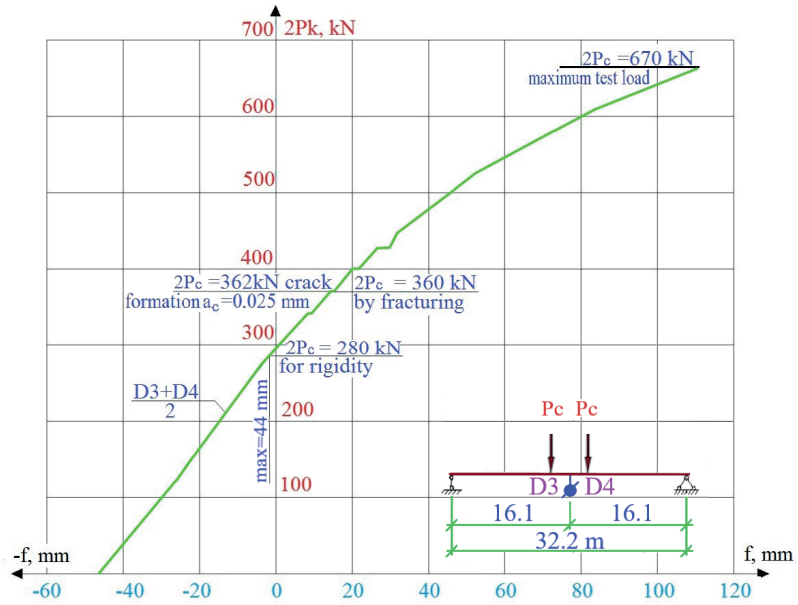


***Figure 19*** *Mid-Span Deflection Graphs: D3 and D4 - deflectometers*

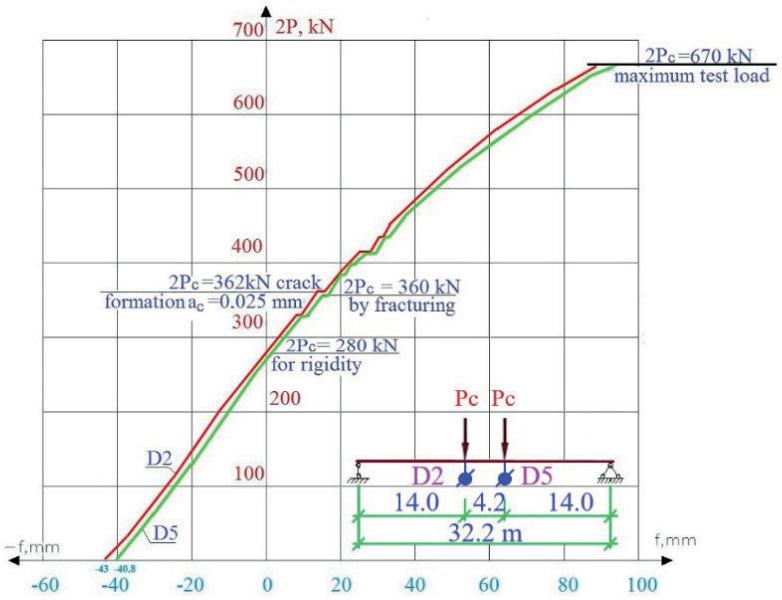


***Figure 20*** *Deflection curves at a distance of 2.1 m from the middle of the span: D2 and D5 - deflectometers*

value, under the action of the control load on stiffness, should not exceed the value equal to $f_c$ = 59.2 mm and the crack extension width, under the action of the control load on crack resistance, should not exceed the value equal to $a_{cr}$ = 0.09 mm.

Figures 18, 19 and 20 show graphs of deflections during testing of the VTK-33 bridge beam.

At the first stage of testing, the stiffness of the beam was evaluated. With a control load in terms of rigidity equal to $2P_c$ = 280 kN, the control deflection of the beam should not exceed a value equal to $f_c$ = 59.2 mm. Upon reaching this load, the experimental deflection in the middle of the span of the beam had a value equal to $f_{exp}$ = 44.0 mm, which made 74.3 % of the control deflection.

At the second stage of testing, the crack resistance of the beam was evaluated and the crack extension width was controlled. One of the main indicators, characterizing the reliability of the bridge beams, is their crack resistance, since this primarily affects their durability and, ultimately, strength. According to the design, with a control load of $2P_c$ = 360 kN, the experimental crack extension width should not exceed the control value equal to $a_{cr}$ = 0.09 mm. When the control load 2*Pc* = 360 kN was reached during the testing, there were no cracks in the concrete of the beam.

At the third stage of testing, the strength of the beam was evaluated. When checking the strength of the beam, the ultimate load, at which the bearing capacity of the experimental structure is estimated, is the control load equal to the value 2 $P_c$ = 630 kN. At a load of 2 $P_c$ = 362 kN, a crack was formed with an extension width $a_{cr}$ = 0.025 mm. With further loading and reaching a load equal to 2 $P_{exp}$ = 432.9 kN, the experimental width of the crack extension did not exceed the value $a_{cr}$ = 0.09 mm. An assessment of the stress-strain state of the VTK-33u beam at a load value of 2 $P_c$ = 670 kN, indicated that the limit state had not been reached in it and the experimental design had a reserve of the bearing capacity.

During the tests, the possible displacement of bundles of prestressing reinforcement, relative to the concrete of the beam, was monitored. At all the stages of loading the beam, there was no displacement (pulling) of the bundles of prestressing reinforcement relative to the concrete of the beam, which indicated the reliability of the working reinforcement coupling with concrete.

Experimental tests of the reduced model of reinforced concrete beam from 24 m to 18 m are given in [19]. The research was carried out in cooperation with Prefa Sucany, Inc., the University of Zilina and Projstar PK, Ltd. As a result of the tests the sufficient load-bearing capacity of the beam was confirmed for the design load.

## 5 Calculation of the span in the finite element program “Lira”

The accepted design scheme of the bridge deck is an idealized mathematical model, which is used in the finite element method (FEM), in which a building structure is represented as a set of rod, plane or volume finite elements having common points - nodes. The more finite elements the computation scheme has, the more accurate the results will be.

In the considered case, the calculated span of the VTK-33u girder is 32.2 m. The span was divided lengthwise into 20 equal parts - 1.61 m each.

In this example, the reinforced concrete span is considered without considering the reinforcement. This can be explained by the fact that the difference between the given geometrical characteristics of the reinforced concrete section and the geometrical characteristics of the concrete section in determining the forces has little effect on the accuracy of the forces. However, this greatly

simplifies the input of initial data and speeds up the calculation time.

After assigning the type of stiffness to the plates and rods, the scheme of the span becomes physically meaningful (Figure 21).

The slab does not go on top of the beams because in the calculation scheme, i.e. in the mathematical model in Lira, all the elements are combined by their centers of gravity (Figure 21). The flanges of the beams are not actually joined together in the computational scheme. This is a conditional simplification of the computational scheme - the joint work of the beams in the transverse direction is ensured by the plate passing through the centers of gravity of the beams. This will have absolutely no effect on the accuracy of the calculation (determination of forces in the beams). The span slab redistributes the load between the beams: it will be affected by the temporary load and the load from the bridge deck.

The next step is to set the boundary conditions, i.e. the span support conditions. To calculate the forces in the superstructure elements, it is not necessary to specify the supports precisely enough (i.e. take into account elastic properties of rubber-metal bearing parts; this can be considered when calculating the bridge abutments). In this case, it is assumed that at one edge there are linear-moving support parts and at the other edge - linear-non-moving ones.

The results of the deflections calculation in the three stages of the span test are shown in Figures 22-24.

The criterion for the positive performance of the overpass spans is the design factor determined by the formula:

$$K = \frac{f_e}{f_{cal}}, \quad (1)$$

where:

$f_e$ is the experimental deflection in the beam from the test load;

$f_{cal}$ - design deflection in the beam from the test load.

Table 4 shows the results of acceptance tests of the overpass.

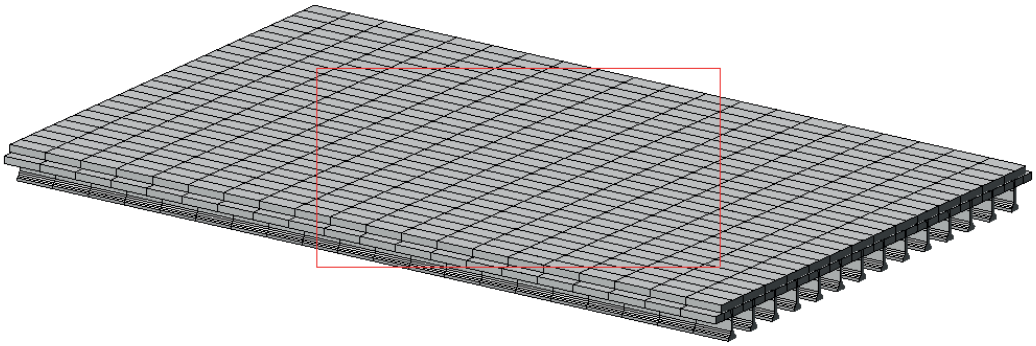

***Figure 21*** *Spatial model of the bridge span*

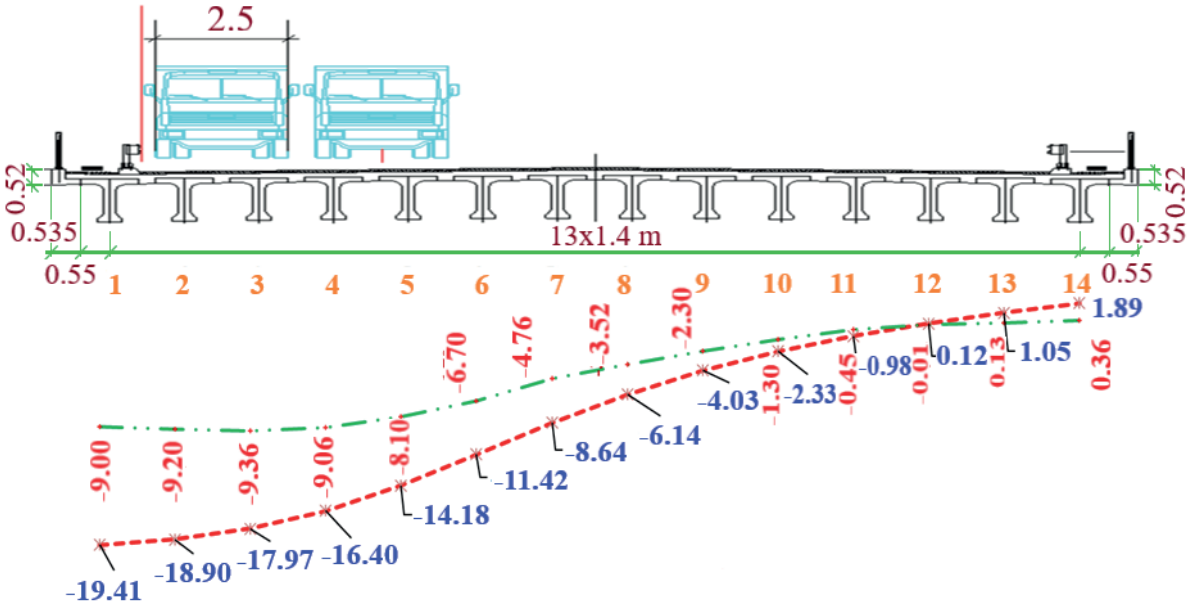


***Figure 22*** *Deflections in the beams of the span in the first stage [1]:*
*-·-· maximum deflection according to the test results, - - - design deflection*

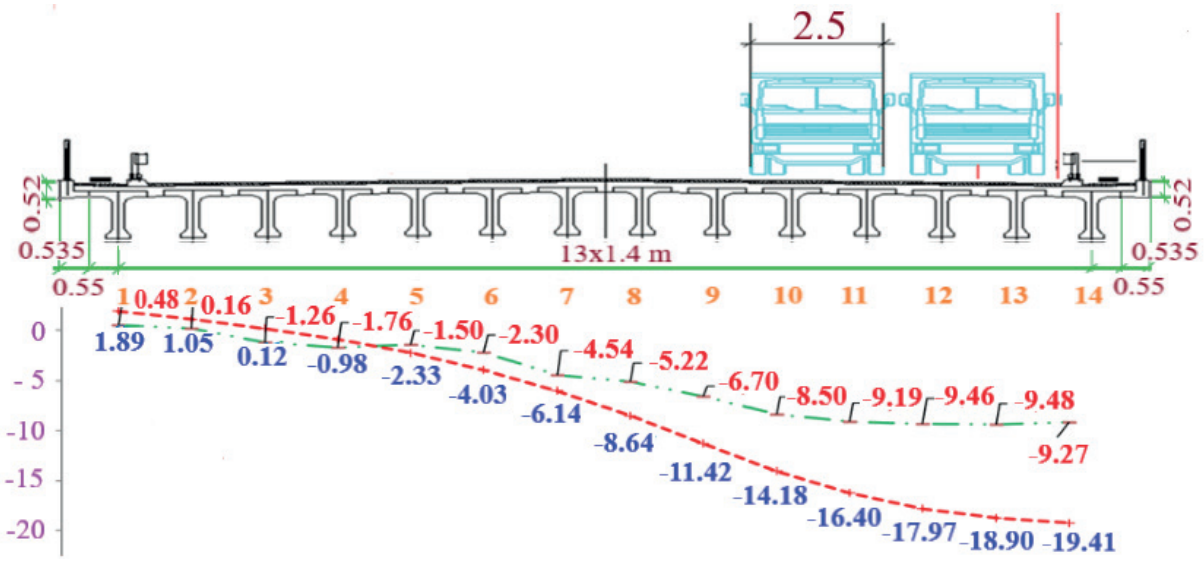


***Figure 23*** *Deflections in the beams of the span in the second stage [1]:*
*-·-· maximum deflection according to the test results, - - - design deflection*

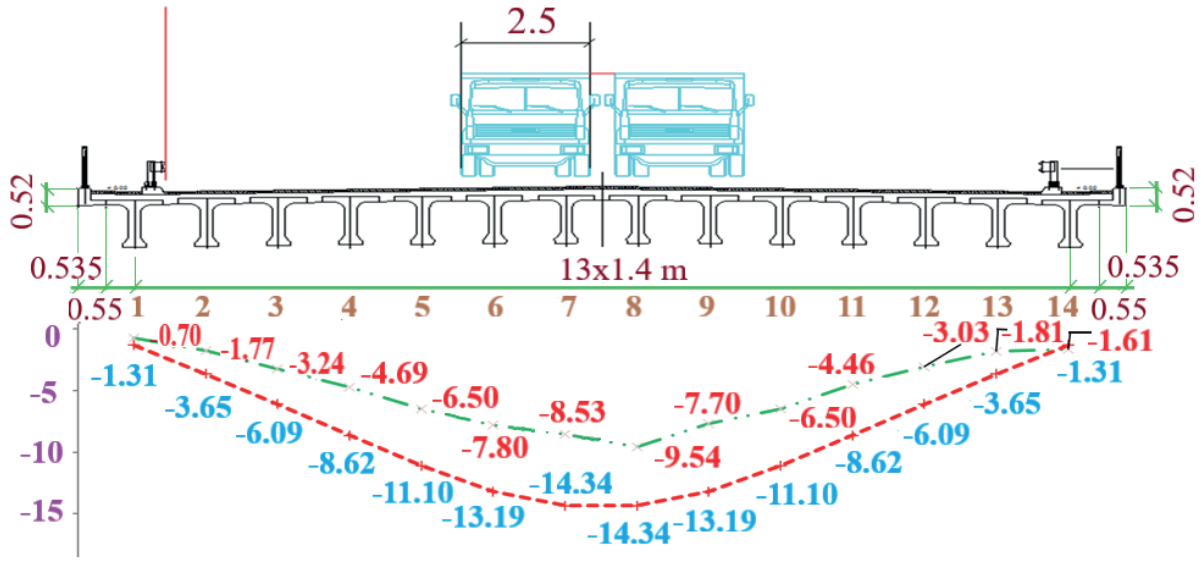


***Figure 24*** *Deflections in the beams of the span in the third stage:*
*-·-· maximum deflection according to the test results, - - - design deflection*

***Table 4*** *Values of experimental and design deflections and the design coefficients*

| Overpass | Actual maximum deflection, $f_e$, mm | Calculated maximum value of deflection, $f_{cal}$, mm | Design factor, K |
|---|---|---|---|
| First stage of tests | 9.36 (Figure 23) | 17.97 (Figure 23) | 0.52 |
| Second stage of testing | 9.48 (Figure 24) | 18.90 (Figure 24) | 0.50 |
| Third stage of tests | 9.54 (Figure 25) | 14.34 (Figure 25) | 0.67 |

According to the results of static tests, the value of the structural coefficient K, according to [18] for the elements of the spans, in which the calculations do not take into account the joint work of the main beams with the elements of the roadway and pavement, as a rule, is from 0.5 to 0.7.

The obtained values of structural coefficients indicate that the tested span structure works according to the design models accepted in the project.

Theoretical aspects and numerical implementation of the stress sensitivity analysis of a beam, centered on the cross-section parameters and implemented in the Matlab package are presented in [20].

The article [21] presents the results of modeling of the concrete and rod elements, reinforcement by the three-dimensional finite-element models taking into account the crack opening. The calculation was performed by the finite element method in the SCAD program. The

method made it possible to obtain values of the crack opening, taking into account the work of longitudinal reinforcement located in the tensile and compressed zones of the structure and transverse reinforcement. These results are more difficult or practically impossible to obtain in the calculation according to the existing standards.

## 6 Conclusions

1. A close inspection of the VTK-33u beams of the superstructure No. 1 of the Almaty-Kapshagay highway, damaged by vehicle impacts, was carried out.
2. In beam 1, a rib is destroyed, the lower part is widened and breaks in wires and K-7 strands are found. Beam 1 was not subjected to repair and was dismantled.
3. The superstructure beams were repaired. Given the responsibility of performing this type of repair work, especially the injection of beam into cracks, it was entrusted to an expert organization with a prior license.
4. Beams 5, 6, 7, 8, 9 and 10 were repaired by restoring the widened lower part with EMACO FAST TIXO, manufactured by BASF.
5. In beams 2, 3, 4, 11, 12, 13 and 14, along with the destruction of the lower part, longitudinal cracks of various lengths were also found, followed by significant decrease of their bearing capacity. Those beams were completely dismantled and replaced by the new ones.
6. An experimental bridge beam VTK-33u was manufactured using the bench technology at the production base of Magnetik LLP (Zarechny village, Almaty region, Kazakhstan).
7. The control load upon examination of the beam stiffness was 2 $R_k$ = 280 kN. With a given load, the experimental deflection should not exceed the control deflection equal to $f_k$ = 59.2 mm. With a control load equal to 2$P_c$ = 280 kN, the experimental deflection in the beam had a value equal to $f_{exp}$ = 44 mm, which amounted to 74.3 % of the control deflection equal to $f_c$ = 59.2 mm.
   The stiffness grade of the VTK-33u bridge beam complies with the requirements of GOST 8829-94 standard, the project and norms of Construction Directives and Rules 2.05.03-84* “Bridges and pipes”.
8. The control load upon examination of the VTK-33u bridge beam crack resistance was 2 $P_c$ = 360 kN. Under this load, the experimental crack extension width should not exceed the control value equal to $a_{cr}$ = 0.09 mm. When the control load of 2 $P_c$ = 360 kN was reached during testing, no signs of cracks are found in the concrete of the beam.
   The crack resistance of the VTK-33u bridge beam complies with the requirements of GOST 8829-94 standard, the project and norms of Construction Directives and Rules 2.05.03-84* “Bridges and pipes”.
9. The control load upon examination of the VTK-33u bridge beam strength was 2 $P_c$ = 630 kN. An assessment of the stress-strain state of the VTK-33u beam at a load value of 2 $P_c$ = 670 kN indicated that the limit state had not been reached in it and the experimental design had a reserve of the bearing capacity.
   The strength grade of the VTK-33u bridge beam complies with the requirements of GOST 8829-94 standard, the project and norms of Construction Directives and Rules 2.05.03-84 * “Bridges and pipes”.

## References

[1] JALAIROV, A., KUMAR, D., KASSYMKANOVA, K.-K., MURZALINA, G., JANGULOVA G. Ensuring operational reliability of overpass on “Almaty-Kapshagai” highway section in Kazakhstan. *Communications - Scientific letters of the University of Zilina* [online]. 2021, **24**(1), p. D23-D36. ISSN 1335-4205, eISSN 2585-7878. Available from: https://doi.org/10.26552/com.C.2022.1.D23-D36

[2] MISKIEWICZ, M., BRUSKI, D., CHROSCIELEWSKI, J., WILDE, K. Safety assessment of a concrete viaduct damaged by vehicle impact and an evaluation of the repair. *Engineering Failure Analysis* [online]. 2019, **106**, 104147. ISSN 1350-6307. Available from: https://doi.org/10.1016/j.engfailanal.2019.104147

[3] MORAVCIK, M., KOTES, P., BRODNAN, M., KOTULA, P. Some Experience from the Analysis of Existing 40 Years Old Prestressed Bridges in the North of Slovakia. *Communications - Scientific letters of the University of Zilina* [online]. 2014, 16(4*)*, p. 4-8. ISSN 1335-4205, eISSN 2585-7878. Available from: https://doi.org/ 10.26552/com.C.2014.4.4-8

[4] MANSOUR, D. M. M., MOUSTAFA, I. M., KHALIL, A. H., MAHDI, A. H. An assessment model for identifying maintenance priorities strategy for bridges. *Ain Shams Engineering Journal* [online]. 2019, **10**(4), p. 695-704. ISSN 2090-4479. Available from: https://doi.org/10.1016/j.asej.2019.06.003

[5] ZHU, Z., LI, Y., MA, C. Damage analysis of small box girder bridges under car explosion. *Engineering Failure Analysis* [online]. 2021, **120**, 105104. ISSN 1350-6307. Available from: https://doi.org/10.1016/j.engfailanal.2020.105104

[6] SUN, P., HOU, X., ZHENG, W., QIN, H., SHAO, G. Risk assessment for bridge structures against blast hazard via a fuzzy-based framework. *Engineering Structures* [online]. 2021, **232**, 111874. ISSN 0141-0296. Available from: https://doi.org/10.1016/j.engstruct.2021.111874

[7] HUTHWOHL, P., BRILAKIS, I. Detecting healthy concrete surfaces. *Advanced Engineering Informatics* [online]. 2018, **37**, p. 150-162. ISSN 1474-0346. Available from: https://doi.org/10.1016/j.aei.2018.05.004

[8] VICAN, J., GOCAL, J., MELIS, B., KOTES, P., KOTULA, P. Real Behaviour and Remaining Lifetime of Bridge Structures. *Communications - Scientific Letters of the University of Zilina [online]*. 2008, **10**(2), p. 30-37. ISSN 2093-8829, eISSN 2234-1765. Available from: https://doi.org/ 10.26552/com.C.2008.2.30-37

[9] GHAFFARY, A., MOUSTAFA M. A. Synthesis of repair materials and methods for reinforced concrete and prestressed bridge girders. *Materials* [online]. 2020, **13**(18), 4079. eISSN 1996-1944. Available from: https://doi.org/10.3390/ma13184079

[10] PSHINKO, O., SHCHERBAK, A., RUDENKO, D. Research of operational properties of modified specialized concrete for transport constructions. *Communications - Scientific Letters of the University of Zilina* [online]. 2019, **21**(4), p. 90-96. ISSN 1335-4205, eISSN 2585-7878. Available from: https://doi.org/10.26552/com.C.2019.4.90-96

[11] BANTHIA, N., ZANOTTI, C., SAPPAKITTIPAKORN, M. Sustainable fiber reinforced concrete for repair applications. *Construction and Building Materials* [online]. 2014, **67**(C), p. 405-412. ISSN 0950-0618. Available from: https://doi.org/10.1016/j.conbuildmat.2013.12.073

[12] NASER, M. Z., HAWILEH, R. A., ABDALLA, J. A. Fiber-reinforced polymer composites in strengthening reinforced concrete structures: a critical review. *Engineering Structures* [online]. 2019, **198**, 109542. ISSN 0141-0296. Available from: https://doi.org/10.1016/j.engstruct.2019.109542

[13] Interstate Standard GOST 26633 - 2015 Heavy-weight and sand concretes. Specifications (in Russian). Moscow, 2019.

[14] GOST 13840-68 Steel reinforcing ropes 1x7. Specifications.

[15] GOST 34028-2016 Reinforcing rolled products for reinforced concrete constructions. Specifications.

[16] SNiP 2.05.03-84* Bridges and pipes.

[17] GOST 22690-88 Concrete. Determination of strength by mechanical methods of non-destructive testing.

[18] GOST 8829-94 Reinforced concrete and prefabricated concrete building products. Loading test methods. Assessment of strength, rigidity and crack resistance.

[19] SP RK 3.03-113-2014 Bridges and culverts. Rules of examination and test.

[20] MORAVCIK, M. The Load Testing and Numerical Verifying of the Precast Prestressed Girder. *Communications - Scientific Letters of the University of Zilina* [online]. 2007, **9**(3), p. 56-62. ISSN 1335-4205, eISSN 2585-7878. Available from: https://doi.org/10.26552/com.C.2007.3.56-62

[21] SAGA, M., VASKO, M. Stress Sensitivity Analysis of the Beam and Shell Finite Elements. *Communications - Scientific Letters of the University of Zilina* [online]. 2009, **11**(2), p. 5-12. ISSN 1335-4205, eISSN 2585-7878. Available from: https://doi.org/10.26552/com.C.2009.2.5-12

[22] NAZARENKO, S., N., Galina A. GRUDCINA, G., A. Method of the Finite-Element Model Formation Containing the 3D Elements for Structural Calculations of the Reinforced Concrete Structures Considering the Crack Opening. *Communications - Scientific Letters of the University of Zilina* [online]. 2021, **23**(1), p. 15-25. ISSN 1335-4205, eISSN 2585-7878. Available from: https://doi.org/10.26552/com.C.2021.1.D15-D25

# ASSESSMENT OF TRAFFIC CONGESTION UNDER INDIAN ENVIRONMENT - A CASE STUDY

**Satya Ranjan Samal** [1,*], **Malaya Mohanty** [1], **Moses Santhakumar Selvaraj** [2]

[1]KIIT Deemed to be University, Bhubaneswar, India
[2]National Institute of Technology, Tiruchirappalli, India

*E-mail of corresponding author: satya.samalfce@kiit.ac.in

***Resume***

Traffic congestion is a major problem around the globe. The prime reason for congestion is unavailability of traffic infrastructure to meet the traffic demand. Road users are forced to face undesirable delay, which influences the economy, environment and health. The present study examines the congestion in the urban roads of Bhubaneswar, a smart city in India. Travel time for various categories of vehicles was estimated and congestion indices in terms of buffer index were evaluated. Multiple linear regression modeling has been used to evaluate the congestion parameters. The p-value for all the independent variables in the developed model is < 0.05. Four elements, namely Strict traffic law implementation, Adequate parking facilities, Decentralization and Controlling the road side activities are required to improve the serviceability and mobility of urban road networks.

***Article info***

Received 13 April 2022
Accepted 2 September 2022
Online 27 September 2022

***Keywords:***

traffic congestion
buffer index
travel time
economy

Available online: https://doi.org/10.26552/com.C.2022.4.D174-D182

ISSN 1335-4205 (print version)
ISSN 2585-7878 (online version)

## 1 Introduction

The development of any country, especially the country like India, is largely dependent on the transportation infrastructures. As the number of vehicles increased rapidly, the existing road infrastructure is not able to accommodate the present capacity, which leads to congested traffic environment [1]. In a developing country congestion has been the major setback for road users. Normally, congestion means that the present traffic demand is exceeding the existing roadway capacity. Congestion is not only affecting the travel time but it is also having an impact on human health, which leads to adverse traffic environment [2]. The traffic congestion results in stress of drivers, which leads to road crashes [3]. Growth of population as well as the number of vehicles and shifting of human resources from rural to urban networks, are the most contributing factors for the traffic congestion [4]. Unlike several major issues, such as indigence, starvation, poor education, etc. congestion is constantly suffered , day by day by millions of road users across the globe [5]. Faulty traffic infrastructures, insufficient human resources, limited roadway width and overtaking proneness of drivers fabricate extended congestion [6]. While the recurring congestion is based on saturated flow and behavioral traits, the non-recurring congestion is based on construction, crashes or crisis with different causes, but having similar effects [7]. The socio-economic irregularities have been observed due to the covid-19 pandemic, which has affected the travel behavior on the road network [8]. Congestion impact can be associated to extra fuel consumption costs, additional transportation costs in terms of vehicle maintenance and operating costs, human health and environment associated problems [6]. Traffic congestion analysis can be done by using the parameters like level of service (LOS), lane-mile duration index and roadway congestion index [9]. Traffic congestion reduction strategies can be achieved by using congestion pricing techniques [10-13]. The utilization of suitable models, associated with road user behavior, can be effective for congestion reduction in terms of travel time, fuel consumption and emission [14].

Due to increase in human resources and number of vehicles, the existing transportation framework is not enough to tackle the present condition. In India, there is a little investigation put up with regard to congestion. Additionally, heterogeneous environments are making things difficult. This research is focused on the congestion indices to recognize the functional effectiveness of the roadway system and the practical congestion mitigation techniques are proposed.

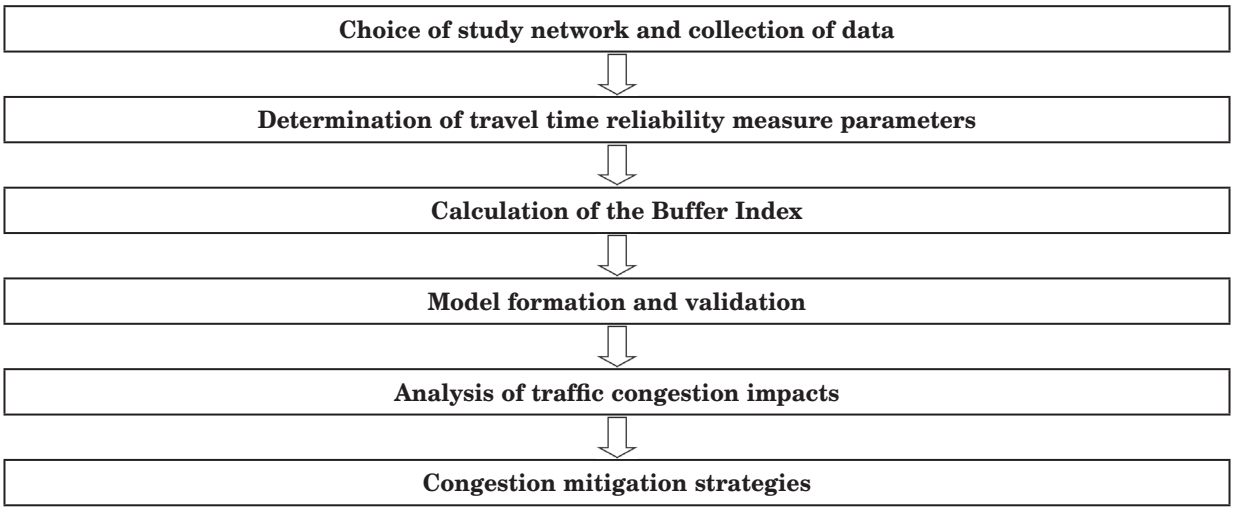


***Figure 1*** *Methodology flowchart*

## 2 Definition of traffic congestion

It would be essential to have a clarity regarding the way someone define the traffic congestion, before analyzing the elements associated with the congestion and its impact. Several definitions of congestion have been reported before. According to the Highway Capacity Manusal (HCM, 2016) [15], congestion is measured using various parameters like mean trip speed, volume to capacity ratio, demand to capacity ratio etc. Along with the HCM (2016), other studies [1-10], related to congestion, reveal that road congestion can be defined based on three categories as follows:

a. Based on demand and capacity,
b. Based on travel time and
c. Based on costs.

## 3 Study approach

The methodology is one of the most important aspects in any research for obtaining the desired results. The present study has adopted the following study approach, which is shown below in tabular format in Figure 1.

## 4 Data collection and analysis

The primary work for any study is the data collection. Majority of the research related to traffic start with the data collection, which gives an outline of the collected data followed by its analysis.

### 4.1 Travel time calculation and measures for travel time reliability

For determination of the buffer index, the travel time plays an important parameter. The time taken from origin to destination was referred as the travel time. It can be calculated by using simple analytical approach or by computer software. In this research, information has been gathered by video graphic techniques and extracted manually with the help of Kinovea software, which plays the video at frame per second. The software can be used to capture, slow down, compare, annotate and measure motion in videos. The camera used for the study has a precision level of 25 frames per second. The travel time reliability measures play an important factor for the congestion analysis and has been calculated in this study.

### 4.2 Congestion indices

The congestion indices are the upgraded version of the V/C ratio. The V/C ratio is mainly focused on construction of the additional road infrastructure to meet the present traffic demand, whereas, the congestion indices are focused on the functional effectiveness based on mobility, serviceability and accessibility.

According to Lyman, and Bertini (2008) [16], the congestion indices are categorized as (a) Buffer Time Index, (b) Travel Time Index and (c) Planning Time Index whose general formulae and general descriptions are provided below.

$$\text{Buffer time Index} = (95^{\text{th}} \text{ percentile travel time} - \text{Mean travel time})/\text{Mean travel time} \quad (1)$$

$$\text{Travel time Index} = \text{Mean Travel time}/\text{Off peak travel time} \quad (2)$$

$$\text{Planning time Index} = 95^{\text{th}} \text{ percentile travel time}/\text{Off peak travel time} \quad (3)$$

$$Buffer\ time\ Index = \frac{95th\ percentile\ travel\ time - Mean\ Travel\ time}{Mean\ travel\ time} Travel\ time\ Index$$
$$= \frac{Mean\ Travel\ time}{Off\ peak\ travel\ time} Planning\ time\ Index$$
$$= \frac{95th\ percentile\ travel\ time}{Off\ peak\ travel\ time}$$

- **95th Percentile Travel Time** refers to the travel time where the passenger is behind the average time only one out of every twenty outings.
- **Buffer Time Index (BTI)** The supplementary time that passengers add to travel to make sure that they are on time. It is usually determined by subtracting the 95th percentile travel time from the mean travel time and then divided by the mean travel time.
- **Travel Time Index (TTI):** The mean time that is required to travel during the rush hours as compared to off peak hours is TTI. It is calculated by dividing the mean travel time with off peak travel time.
- **Planning Time Index (PTI):** The total time required to plan for an on-time arrival 95% of the time, calculated as the 95th percentile travel time divided by off peak travel time.

The researchers [16-20], though discussed about all congestion indices, but considered the buffer time index for the analysis. The BTI has been considered as congestion index in the current study. It can be identified that the buffer time index gives satisfactory result as compared to other two indices. This research was primarily concentrated on the buffer time index due to the heterogeneous traffic environment.

### 4.3 Choice of road network

The road network selection is the important and foremost step in the research. The requirement of research directly depends on the study area consideration. The urban road of the Bhubaneswar city is considered for the present study. Two locations were selected from the Bhubaneswar road network to analyze the congestion index whose attributes are given in Table 1. Road 1: Patia - Infocity road and road 2: Jaydevvihar -Nandankanan road (Figure 2). The locations were selected such that the traffic flow at those sites is not influenced by horizontal curvature, the presence of downstream or upstream intersection, bus stop, parked vehicles, pedestrian movements, or any kind of side friction.

Patia - Infocity road is a commercial road in Bhubaneswar city connecting Patia Junction and Infocity Junction. The road is a six-lane divided roadway with a footpath on either side of it and on-street parking on either side of the road along with the raised kerb on either side of the road.

Jaydevvihar - Nandankanan road is a main road in Bhubaneswar city connecting Jaydevvihar Junction and Barang Junction. The road is a six-lane divided roadway with a footpath on either side of it and on-street parking on either side of the road along with the raised kerb on either side of the road.

Two locations were taken for the present study. From 8 AM to 11 AM are considered as morning rush periods and from 2 PM to 3 PM are considered as morning off-peak hours. Video graphic survey was executed for the


***Figure 2*** *Location of data collection (I) and (II) Patia- Infocity road; (III) and (IV) Jaydevvihar-Nandankanan road*

***Table 1*** *Roadway parameters used in the study*

| Roadway | Category | Lane attributes |
|---|---|---|
| Selected roadway 1 | Arterial | 6 lanes divided |
| Selected roadway 2 | Arterial | 6 lanes divided |

***Table 2*** *Buffer Time Index (%) of the selected roadway*

| Roadway | Movement | Buffer Time Index (%) |
|---|---|---|
| Selected Roadway1 | Upward | 26 |
| | Downward | 28 |
| Selected Roadway2 | Upward | 36 |
| | Downward | 33 |

data collection in the selected roads. Considering the movements' direction, the buffer time index has been calculated as presented in Table 2. Although the other congestion indices were discussed by various researcher, in this research the buffer time index was taken as the congestion index due to the heterogeneous traffic environment and no lane discipline. The lesser the buffer time index, the better the serviceability of the roadway network.

## 5 Travel time modeling

The current research tried to establish a travel time model by considering the various elements associated with the traffic congestion. The main elements, which influence the travel time are speed of the vehicle and volume of traffic. The travel time model is considered for the congestion prediction. The observed value and the estimated value have to be compared and should be validated with minimum percentage error. The travel times were obtained for the peak hour of from 8.30 AM to 9.30 AM.

### 5.1 Model estimation

A regression model estimates the dependent variable from one or additional independent variables, which affect the dependent variable. The study tried to develop a multiple linear regression model by considering the travel time as a dependent variable, speed and traffic volume as independent variables.

The obtained equation is as follows:

$$\begin{aligned} TT &= 28.173 - (0.676 * A1) - (0.004 * A2) \\ &= 28.173 - (0.676 * A1) - (0.004 * A2) \end{aligned} \quad (4)$$

in which: TT = Mean travel time, s,
A1 = Speed of vehicle, m/s,
A2 = Traffic volume, PCU/h.

Model was evaluated considering the traffic volume and vehicle speed. The developed equation is valid for an operating speed greater than 5 m/s (18 km/h) and the traffic volume of more than 500 PCU/h. The p-value for all the regression coefficients has been provided in Table 3. It can be seen that the p-value for all the independent variables is less than 0.05, which indicates their significance at 5% level of significance. It shows that there is a significant difference between all the independent variables. Therefore, each independent variable has a significant effect on the outcome of dependent variable. Hence, it can be said that the regression is well fitted and the model developed is statistically correct.

***Table 3*** *Statistical parameters of the regression analysis*

| (Constant) | Coefficients | P Value |
|---|---|---|
| | 28.173 | 0.000 |
| Speed | -00.676 | 0.000 |
| Traffic Volume | -00.004 | 0.045 |

***Table 4*** *Percentage of error in the process of validation*

| Timing | Observed travel time, s | Predicted travel time, s | Percentage error (%) | Average percentage error (%) |
|---|---|---|---|---|
| 8.30 AM - 8.45 AM | 18.29 | 18.04 | 1.36 | 3.5 |
| 8.45 AM - 9.00 AM | 13.48 | 12.49 | 7.3 | |
| 9.00 AM - 9.15 AM | 13.48 | 13.40 | 0.59 | |
| 9.15 AM - 9.30 AM | 20.56 | 19.58 | 4.76 | |

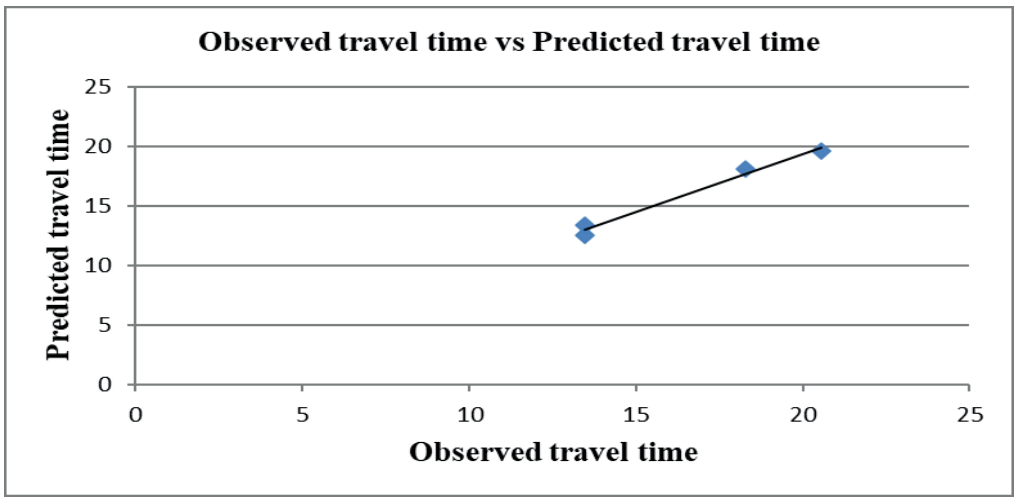


***Figure 3*** *Variation of the observed travel time and predicted travel time*

### 5.2 Model validation

Validation of the model is done by the comparison of the estimated value and observed value as shown in Table 4. The validation of model signifies its accountability to replicate in actual traffic scenario. Further, the variation of observed travel time with predicted travel time is presented in Figure 3. To validate the model, percentage errors, comparing observed travel time and predicted travel time, were evaluated. Model should be considered as fit if the difference of error percentage were within 10 %.

To validate the proposed travel time model, the travel times computed by the model have been compared to those obtained from the field data. For the validation purpose, separated field data were collected from various locations of the six-lanes divided arterial road other than the location used for the model development. This ensures that the equation developed is not localized and can be utilized for the travel time estimation at various other locations. Table 4 shows the comparison of average travel time of all the categories of vehicles estimated from the proposed model and observed travel time as obtained from the field data. From Table 4, it can be observed that the values obtained from the proposed model are in close agreement with the observed field values. The average percentage error was found to be 3.5 %. Therefore, it can be concluded that the proposed model is good enough to predict the travel time.

## 6 Traffic congestion impacts

Traffic congestion propagates significant difficulties to road users in Bhubaneswar city. Congested traffic extents lack of sureness in journey heading to tension and dangerous traffic environments. Due to traffic congestion people are suffering economically, physically and even mentally. The impact of traffic congestion on Bhubaneswar city may be viewed in various aspects including economy aspects, environment aspects and health aspects. For the present study the required data has been gathered from different sources, e.g. discussion, survey, field observation, personal communication and peer reviewed publications on the related affairs to identify the effect of traffic congestion on several elements.

### 6.1 Impact on economy

Due to the congestion, the road users were suffering in many ways. The majority suffering can be of spoiling time, increase in transportation price, increase in fuel expenditure, vehicle operating and maintenance costs. The study considered peak 1 hour for the delay cost survey for a section of 100 m. The delay time has been observed by differentiating between the mean travel time for the off-peak period and rush/peak period. The details of the delay costs are presented in Tables 5

***Table 5*** *Statistics for buses*

| Roadway (1) | Buses (2) | Mean strength (Individuals/ Vehicle) (3) | Computed delay for 1 bus (Second/vehicle) (4) | Computed delay for 1 bus (Hour/vehicle) (5) = (4) / 3600 | Costs of 1 h in Rupees (USD) (6) | Computed delay costs of buses for 1 h in Rupees (USD) (7) = (6) x (5) x (3) x (2) |
|---|---|---|---|---|---|---|
| Chosen Roadway 1 | 30 | 43 | 7 | 0.0019 | 39.5 (0.49) | 97 (1.21) |
| Chosen Roadway 2 | 60 | 43 | 11 | 0.003 | 39.5 (0.49) | 306 (1.21) |
| COMPUTED COSTS OF DELAY FOR BUSES FOR 1 HOUR IN RUPEES 403 ( 5.07 Euro and 5.05 Dollar) | | | | | | |

***Table 6*** *Statistics for four wheelers*

| Roadway (1) | 4-W (2) | Mean strength (Individuals/ Vehicle) (3) | Computed delay for 1 Four wheelers (Second/ vehicle) (4) | Computed delay for 1 4-W (Hour/vehicle) (5) | Costs of 1 h in Rupees (USD) (6) | Computed delay costs of four wheelers for 1 h in Rupees (USD) (7) |
|---|---|---|---|---|---|---|
| Chosen Roadway 1 | 154 | 4.8 | 8 | 0.002 | 62.5 (0.78) | 93 (1.16) |
| Chosen Roadway 2 | 237 | 4.8 | 9 | 0.003 | 62.5 (0.78) | 214 (2.68) |
| COMPUTED COSTS OF DELAY FOR FOUR WHEELERS FOR 1 HOUR IN RUPEES 307 ( 3.86 Euro and 3.84 Dollar) | | | | | | |

***Table 7*** *Statistics for motorcycles*

| Roadway (1) | Motorcycles (2) | Mean strength (Individuals/ Vehicle) (3) | Computed delay for 1 motorcycle (Second/ vehicle) (4) | Computed delay for 1 motor cycle (h/vehicle) (5) | Costs of 1 h in Rupees (USD) (6) | Computed delay costs of motor cycles for 1 h in Rupees (USD) (7) |
|---|---|---|---|---|---|---|
| Chosen Roadway 1 | 700 | 1.5 | 7 | 0.002 | 32 (0.4) | 68 (0.85) |
| Chosen Roadway 2 | 1140 | 1.5 | 8 | 0.002 | 32 (0.4) | 110 (1.38) |
| COMPUTED COSTS OF DELAY FOR MOTORCYCLES FOR 1 HOUR IN RUPEES 178 (2.24 Euro and 2.23 Dollar) | | | | | | |

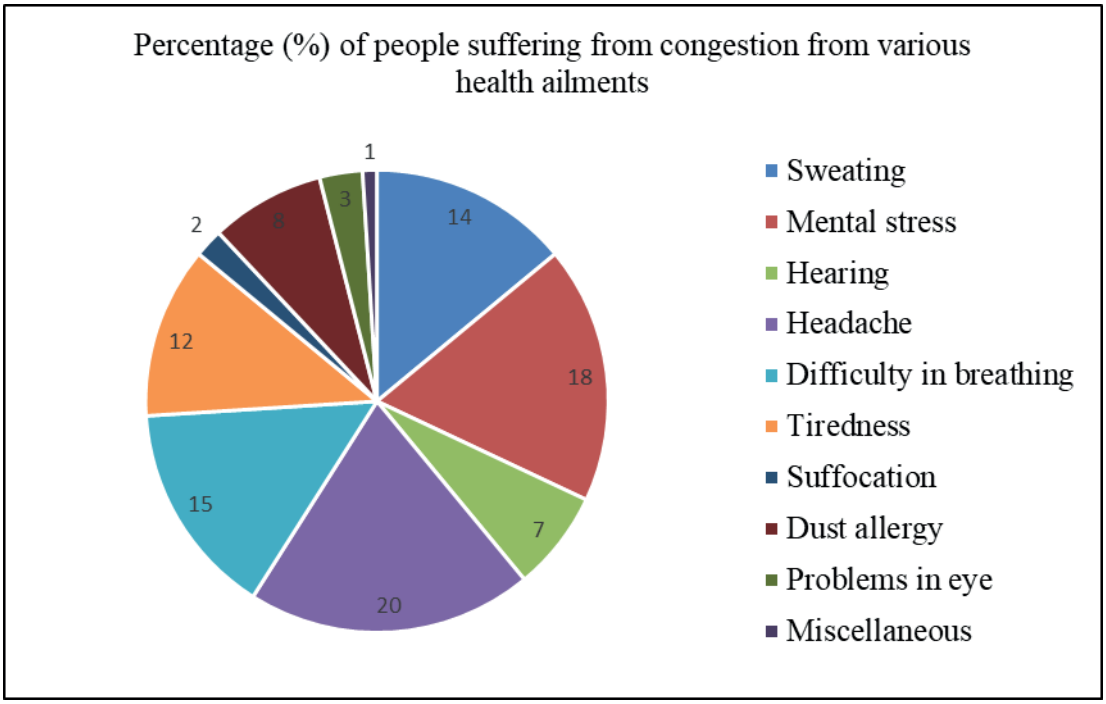


***Figure 4*** *Classified symptoms of congestion*

through 7 for various categories of vehicles. The delay costs' survey has been conducted according to [21].

The delay costs for the buses, four wheelers and motorcycles are computed for the chosen roads by considering rush one hour in a 100 m section based on Indian Roads Congress, Special Publication (IRC SP) 30 (2010). The delay costs or buses was estimated as Rupees (Rs.) 403/hour. The delay costs for four wheelers were estimated as Rs (Rupees). 307/hour and for the motorcycles the costs were around Rs. 178/hour in a 100m section by only considering the rush hour. If the length of the road is more than the costs of the delay

***Table 8*** *Categorizations of congestion reduction strategies*

| Elements | Response (%) | Ranking |
|---|---|---|
| Public awareness | 3 | Rank IV |
| Building flyovers | 11 | Rank II |
| Proper usage of public transport | 7 | Rank III |
| Execution of firm traffic laws | 16 | Rank I |
| Reshuffling of timings for government/private sectors | 4 | Rank IV |
| Removing Non-Motorized Vehicle | 2 | Rank IV |
| Decentralization | 17 | Rank I |
| Managing roadside activities | 17 | Rank I |
| Discourage to use private vehicles | 1 | Rank IV |
| Excessive parking costs | 3 | Rank IV |
| Improving pedestrian safety | 2 | Rank IV |
| Sufficient parking provision | 17 | Rank I |

The ranking: < 5% Rank IV; 6-10% Rank III; 11- 15% Rank II and > 15% Rank I

will be more. During the congested period, the motorist must apply the brake and clutch frequently. Due to this, the fuel consumption increases and the serviceability and durability of the vehicle decreases. Thus, the Vehicle operating costs are directly proportional to congestion.

### 6.2 Impact on health

Due to congestion individuals have to occupy more hours on the roadway, which is straightway influencing the health of the inhabitants. The adverse effect on health due to congestion should not be ignored. The study has classified the symptoms in various manner, whose classification is shown in the pie chart form in Figure 4.

It can be observed that the general public are largely facing health issues associated with headache (20 %), mental stress (18 %), breathing issues (15%) and sweating (14%) due to traffic congestion. According to perception of road users, hearing (7%) and dust allergy (8%) are felt moderately during a traffic congestion. Issues like suffocation (2 %), Eye problem (3 %), etc. are rarely exhibited by the road users as an effect of congestion.

### 6.3 Impact on environment

Capacity of the roadway is up to full extent at the congested traffic. The extent of the congestion is directly proportional to the environmental pollution. The sound and air pollution are the important environmental pollutions caused by the congested traffic. The environment takes major part in the traffic congestion. The harmful gases like $SO_2$, CO, $CO_2$, and $NO_2$ are released from the vehicles during the congested traffic. From the study conducted by [22], it can be identified that 97% of scholars are disrupted due to honking, 86% of the residents influenced by the noise pollution, 78% undergo annoyance, 49% bad temperament, 43% of the public are facing difficulties in focusing and sleeping, 33% of the inhabitants are struggling for hearing and 45% of vehicle operators are blowing horn constantly in the congested traffic.

## 7 Proposed congestion reduction strategies

The present study was primarily concentrated on upgrading of the current traffic framework with minimum costs and efforts. Various elements have been considered as the congestion reduction strategies. The information was received from several prospects, such as common public, specialist, resource persons, educationists, engineers, roadside vendors etc. The categorization of congestion reduction strategies has been tabulated in Table 8.

Importance has not been considered for building the new infrastructures, as the present study was primarily concentrated on upgrading of the current traffic framework with minimum costs consideration. This study was aimed for the ranking approach, based on the feedback collected from the various sources. The lesser the rank, the higher the consideration needed for the elements, e.g. the elements categorized as Rank I, have to be executed instantly for the better outcomes. Majority of the inhabitants gave a strong recommendation mostly on the four elements that include Execution of firm traffic laws, Sufficient parking provision, Decentralization and Managing the road side activities. So, for the improvement in the serviceability and mobility of the urban road network these above-mentioned elements need to be implemented immediately. Because of the growth of motorcycle the number of non-motorized vehicles are become obsolete now a days. Other elements are also effective for the congestion reduction but for the instant results the

elements such as Execution of firm traffic laws, Sufficient parking provision, Decentralization and Managing the road side activities have to be taken seriously and proper execution need to be done at the earliest.

## 8 Conclusions and recommendations

The current research was focused on the congestion analysis and the negative impact of the traffic congestion. Necessary information was gathered from selected roads under Indian traffic environment and the congestion reduction strategies have been proposed. The level of congestion is varying depending upon the category of the vehicles and lane distribution. To evaluate the level of congestion and to identify the negative impact of the traffic congestion on various factors were analyzed. Congestion prediction under Indian environment is being complicated and cannot be totally eliminated due to the increase in numbers of the two wheelers and four wheelers, especially the passenger cars.

The buffer Index has been considered to analyze the congestion level on the selected road network. Due to the congested traffic, inhabitants are enforced to waste more hours on roadway. Therefore, the effect of the traffic congestion is negatively affecting the overall economy of the country. In addition, the environment and human health are being troubled because of the traffic congestion. Travel time model was demonstrated by considering various parameters influencing the travel time. The percentage error was observed below 10 %, so the general model is appropriate and it certifies the analytical significance of the estimate model. Delay costs for various categories of vehicles are computed for the chosen roads by considering rush one hour in a 100 m section based on IRC SP 30 (2010). The delay costs for buses were estimated as Rs. 403/hour. The delay costs for four wheelers were estimated as Rs. 307/per hour and for the motorcycle the costs were around Rs. 178/hour in a 100 m section, by considering the rush hour only. If the length of the road were bigger, than the costs of the delay would be higher. During the congested period, the motorist must apply the brake and clutch frequently. Due to that, the fuel consumption increases and the serviceability and durability of a vehicle decreases. So, the vehicle operating costs are straightly related to congestion.

Majority of the inhabitants gave a strong recommendation mostly on the four elements that includes Strict traffic law implementation, Adequate parking facilities, Decentralization and Controlling the road side activities. So, for improvement in the serviceability and mobility of the urban road network, the above mentioned elements need to be implemented immediately. In developing countries, like India, heterogeneous traffic environment further complicated the situations. Due to the huge traffic congestion, the situation might sometimes be related to life and death and that cannot be compensated. Proper coordination between various organizations, starting from the research, planning, execution and practical implementation, has to be addressed with immediate effect to tackle the world's most debatable topic i.e. the traffic congestion.

## References

[1] DUBEY, P. P., BORKAR, P. Review on techniques for traffic jam detection and congestion avoidance. In: 2015 2nd International Conference on Electronics and Communication Systems ICECS 2015: proceedings [online]. IEEE. 2015. eISBN 978-1-4799-7225-8, p. 434-440. Available from: https://doi.org/10.1109/ECS.2015.7124941

[2] PADIATH, A., VANAJAKSHI, L., SUBRAMANIAN, S. C., MANDA, H. Prediction of traffic density for congestion analysis under Indian traffic conditions. In: 12th International IEEE Conference on Intelligent Transportation Systems ITSC 2009: proceedings [online]. IEEE. 2009. ISBN 9781424455195, p. 78-83. Available from: https://doi.org/10.1109/ITSC.2009.5309716

[3] HENNESSY, D. A., WIESENTHAL, D. L. Traffic congestion, driver stress, and driver aggression. *Aggressive Behavior: Official Journal of the International Society for Research on Aggression* [online]. 1999, **25**(6), p. 409-423. eISSN 1098-2337. Available from: https://doi.org/10.1002/(SICI)1098-2337(1999)25:6<409::AID-AB2>3.0.CO;2-0

[4] UDDIN, A. Traffic congestion in Indian cities: challenges of a rising power. Naples: Kyoto of the Cities, 2009.

[5] DOWNS, A. *Stuck in traffic: coping with peak-hour traffic congestion*. Brookings Institution Press, 2000. ISBN 081571923X.

[6] MAHMUD, K., GOPEAND, K., CHOWDHURY, S. M. Possible causes and solutions of traffic jam and their impact on the economy of Dhaka City. *Journal of Management and Sustainability* [online]. 2012, **2**(2), p. 112-135. ISSN 1925-4725, eISSN 1925-4733. Available from: https://doi.org/10.5539/jms.v2n2p112

[7] MCGROARTY, J. Recurring and non-recurring congestion: causes, impacts, and solutions. University of Cincinnati: Neihoff Urban Studio-W10, 2010.

[8] MACIOSZEK, E., KUREK, A. Extracting road traffic volume in the city before and during COVID-19 through video remote sensing. *Remote Sensing* [online]. 2021, **13**(12), 2329. eISSN 2072-4292. Available from: https://doi.org/10.3390/rs13122329

[9] RAO, A. M., RAO, K. R. Measuring urban traffic congestion-a review. *International Journal for Traffic and Transport Engineering* [online]. 2012, **2**(4), p. 286-305. ISSN 2217-544X, eISSN 2217-5652. Available from: http://dx.doi.org/10.7708/ijtte.2012.2(4).01

[10] QINGYU, L., ZHICAI, J., BAOFENG, S., HONGFEI, J. Method research on measuring the external costs of urban traffic congestion. *Journal of Transportation Systems Engineering and Information Technology* [online]. 2007, **7**(5), p. 9-12. ISSN 1570-6672. Available from: https://doi.org/10.1016/S1570-6672(07)60035-X

[11] VAN WOENSEL, T., CRUZ, F. R. A stochastic approach to traffic congestion costs. *Computers and Operations Research* [online]. 2009, **36**(6), p. 1731-1739. ISSN 0305-0548. Available from: https://doi.org/10.1016/j.cor.2008.04.008

[12] ZHILI, L., CHUNYAN, L., CHENG, L. Traffic impact analysis of congestion charge in mega cities. *Journal of Transportation Systems Engineering and Information Technology* [online]. 2009, **9**, p. 57- 61. ISSN 1570-6672. Available from: https://doi.org/10.1016/S1570-6672(08)60088-4

[13] DE PALMA, A., LINDSEY, R. Traffic congestion pricing methodologies and technologies. *Transportation Research Part C: Emerging Technologies* [online]. 2011, **19**(6), p. 1377-1399. ISSN 0968-090X. Available from: https://doi.org/10.1016/j.trc.2011.02.010

[14] MACIOSZEK, E., IWANOWICZ, D. A back-of-queue model of a signal-controlled intersection approach developed based on analysis of vehicle driver behavior. *Energies* [online]. 2021, **14**(4), 1204. eISSN 1996-1073. Available from: https://doi.org/10.3390/en14041204

[15] Transportation research board. HCM (Highway Capacity Manual). Washington, DC: National Academics of Sciences, Engineering, Medicine, 2016.

[16] LYMAN, K., BERTINI, R. L. Using travel time reliability measures to improve regional transportation planning and operation. *Transportation Research Record: Journal of the Transportation Research Board* [online]. 2008, **2046**(1), p. 1-10. ISSN 0361-1981, eISSN 2169-4052. Available from: https://doi.org/10.3141/2046-01

[17] SATHYA PRABHA, R., MATHEW, S. Evaluation of operational efficiency of urban road network using travel time reliability measures. 2013.

[18] SAMAL, S. R., DAS, A. K. Evaluation of traffic congestion parameters under heterogeneous traffic condition: a case study on Bhubaneswar City. In: *Transportation research lecture notes in civil engineering* [online]. MATHEW, T., JOSHI, G., VELAGA, N., ARKATKAR, S. (eds.). Vol. 45. Singapore: Springer, 2020. ISBN 978-981-32-9041-9, eISBN 978-981-32-9042-6. Available from: https://doi.org/10.1007/978-981-32-9042-6_53

[19] SAMAL, S. R., KUMAR, P. G., SANTHOSH, J. C., SANTHAKUMAR, M. Analysis of traffic congestion impacts of urban road network under Indian condition. *IOP Conference Series: Materials Science and Engineering* [online]. 2020, **1006**(1), 012002. ISSN 1757-8981, eISSN 1757-899X. Available from: https://doi.org/10.1088/1757-899X/1006/1/012002

[20] SAMAL, S. R., MOHANTY, M., SANTHAKUMAR, S. M. Adverse effect of congestion on economy, health and environment under mixed traffic scenario. *Transportation in Developing Economies* [online]. 2021, **7**(2), p. 1-10. ISSN 2199-9287, eISSN 2199-9295. Available from: https://doi.org/10.1007/s40890-021-00125-4

[21] IRC SP-30. Manual on economic evaluation of highway projects in India. New Delhi: Indian Road Congress, 2010.

[22] DEY, A. R., KABIR, N., EFROYMSON, D. Noise pollution: research and action. Work for a Better Bangladesh. Dhaka, 2002.

# STUDIES ON COMPRESSIVE STRENGTH MICROSTRUCTURAL ANALYSIS OF SELF-COMPACTING MORTAR WITH BACTERIA

**Middela Sravanthi [1], S. Venkateswara Rao [1], Kanthala Krishnaveni [2,*], Venkata Kamal Lal Meenuga [2], Sujana Kariveda [3]**

[1]Department of Civil Engineering, National Institute of Technology, Warangal, Telangana, India
[2]Department of Civil Engineering, Anurag University, Telangana, India
[3]Department of Biotechnology, Osmania University, Telangana, India

*E-mail of corresponding author: krishnavenikanthala@gmail.com

***Resume***

This research proposed bacteria-treated concrete, which is highly desirable because the mineral precipitation induced from microbial activities is pollution free and natural. This study investigates the effects of Bacillus Licheniformis, Bacillus Cohnii and mixed bacteria on compressive strength, ultrasonic pulse velocity test, rapid chloride penetration test, microstructural analysis and bacteria cell concentration of 10 $^{5}$cell/ml of normal and self-compacting mortars made with and without fly ash for 7 and 28 days. With self-compacting mortar, the compressive strength of Bacillus Licheniformis improved by 30.3% and by adding Bacillus Cohnii in 28 days, the ion penetration value decreased. Finally, it was observed that the deposition of calcium carbonate in mortar improved compressive strength using SEM-EDS and XRD with compound polymorphisms of calcite, vaterite, quartz, and Hautirite.

***Article info***

Received 29 April 2022
Accepted 14 September 2022
Online 17 October 2022

***Keywords:***

self-compacting mortar
compressive strength
bacillus licheninformis
bacteria cohnii
class-c fly ash
durability test

Available online: https://doi.org/10.26552/com.C.2022.4.D183-D200

ISSN 1335-4205 (print version)
ISSN 2585-7878 (online version)

## 1 Introduction

In the field of civil engineering for the construction of modern buildings, concrete has the highest compressive strength compared to steel [1]. It is also the most affordable. Due to its many properties, such as high compressive strength, durability and rigidity, concrete is the most commonly used building material [2]. Workable concrete is defined as concrete that has been laid and compacted uniformly without bleeding or segregation. Microbiologically Induced Calcite Precipitation (MICP) is a natural bio-mineralization process in which live microorganisms (such as bacteria) generate layers of Calcium Carbonate ($CaCO_3$) that fill cracks and improve concrete's strength and durability [3].

Numerous kinds of research have been conducted and more are being conducted to determine the use of bacteria in self-repairing cracked concrete. A new generation of bio-additives for Self-Compacting Concrete (SCC) was recently created using this ground-breaking technology [4-6]. Self-Compacting Concrete is a flowable self-consolidating concrete mixture. The concrete's durability is reduced due to cracking and is more prone to corrosion. Cracks in concrete surfaces are often repaired with cement paste, penetrating cement grout, or epoxy grout [7-8].

Self-healing concrete self-heals by forming a lime layer with the help of moisture and air from the environment. The reaction between cement and water is exothermic and the heat release is called heat of hydration. The heat of hydration is one of the well-known methods to measure reactivity. Concerning the heat of hydration study, 50% of the total heat is released between 1 and 3 days, 75% in 7 days and 83-91% in 28 days for Ordinary Portland Cement (OPC). The age at which 20-30% hydration will be completed depends on the water-to-cement ratio, relative humidity, curing method and temperature and cement composition. The non-hydrated cement will hydrate when cracks emerge on the concrete surface [9-10]. The lime particles in cement will then react with the moisture in the air, filling up the fissures. When the crack width is between 0.05 and 0.1 mm, the crack may automatically fill. Alternative repair procedures, based on chemical healing agents, can be employed for crack widths less than 0.3 mm when the crack width reaches 0.1mm. The use of biological healing agents can also be incorporated into this approach [11]. Bacterial activity produces

calcium carbonate or other calcium-based chemicals, which are then utilized to fill fissures. Microbiologically Induced Calcium Precipitation (MICP) is the name for this concept [12-13]. The MICP generates $CO_2$ in the presence of water by microbial metabolism, leading to formation of carbonate ions. Calcium carbonate is formed when the carbonate ion interacts with calcium ions under the right conditions [14-17].

The MICP is influenced by the bacterial concentration, ionic strength, availability of water, air space and nutrients, the matrix's pH and the presence of nucleation sites. Some of these essential criteria are built into concrete, while others can be easily achieved. *Bacillus subtilis (B. subtilis*), a common soil Gram-positive bacteria, is extremely effective in MICP when utilized in concrete. *B. subtilis* attaches to cement particles' surfaces and produces MICP nucleation sites [18-19]. Existing research provides information on the role of bacteria in successful crack restoration and improving concrete's mechanical and durability properties, which are explained as follows:

Sushree et al. [20] used an alkali-activated Ground Granulated Blast-furnace Slag (GGBS) and fly ash to replace cement in self-compacting concrete mixes. The authors look at the effects on the fresh and hardened properties of Self-Compacting Geopolymer Concrete (SCGC) mixtures due to *Bacillus Licheniformis*. Moreover, Mohd Nasim et al. [21] have investigated the effect of crystalline admixture (CA), fly ash (FA) and PVA fibre on the ability of early-age cracks in concrete to self-heal. M1 is the control mix, M2 is the 0.1 percent Polyvinyl Acetate (PVA) fibre by volume mix, M3 is the 20% partial cement replacement with fly ash mix and M4 is the 2% CA by cement mass mix; these are the four mixes used. Then, Tsampali et al. [22] investigated the qualities of the self-healing cement paste compositions comprising nano-CaO and nano-$SiO_2$ at 1.5% w/w, as well as a combination of the two, with 0.5 percent NL and 1% NS.

Glass Fibre Reinforced Concrete (GFRC) is used by Guzlena et al. [23] to investigate concrete that has been assisted to heal by the addition of crystals. The GRC was chosen due to the fibre reinforcement, which allowed the breadth of the crack to be controlled during the pre-cracking of the sample. Moreover, Dongsheng et al. [24] enhanced the self-healing efficiency of cemented coral fine aggregate by using Urea Formaldehyde (UF) microcapsules. Further, Manvith et al. [25] looked into various methods for employing mineralizing bacteria to improve the structural strength of concrete. Then, Pavan et al. [26] provided a quick overview of the many features of bacterial concrete. Microcracks are essentially present in concrete.

Luhar et al. [27stated that autonomous crack sealing using microorganisms in the concrete without human intervention is a possible solution to the problem of long-term concrete improvement. Algaifi et al. [28] used Gene Expression Programming (GEP) modelling a new predicted mathematical formula for compressive strength of bacterial concrete was established using 69 experimental tests with various amounts of calcium nitrate tetra-hydrate, yeast extract, urea, bacterial cells and time. Almohammed et al. [29] utilized M5P, Random Tree (RT), Reduced Error Pruning Tree (REPT), Random Forest (RF) and Support Vector Regression (SVR) techniques were evaluated and compared to Multiple Linear Regression (MLR) -based models for predicting the compressive strength of concrete (with bacteria). Ramagiri et al. [30] disclosed that since the primary goal of creating these blends is to reduce environmental impact, a full Life Cycle Analysis (LCA) is required.

Moreover, *Bacillus Licheniformis* has been studied in self-compacting geopolymer concrete, but no research on *Bacillus Licheniformis, bacillus cohnii*, or mixed bacteria in mortar, has been done. Very little research has focused on impact of the self-compacting concrete on *bacillus cohnii's* self-healing mechanism under various curing conditions. Concrete that self-compacts, when *Bacillus Licheniformis* bacteria are added, is not the subject of much research. The main contribution of this research is as follows:

*Bacillus Licheniformis and Bacillus cohnii*, a laboratory cultured bacteria, are used in this research. Thus, this research investigated the new properties, Ultrasonic Pulse Velocity (UPV) test and compressive strength of self-compacting and normal mortars with bacteria incorporation using single and mixed bacteria. Microstructural and durability evaluations of self-compacting and normal mortars with bacterial integration utilized single and mixed bacteria.

The following sections are laid out: The materials and their properties are covered in Section 2, along with a thorough account of the experimental work. The outcome and a discussion of the suggested strategy are presented in Section 3. The paper is concluded in Section 4.

## 2 Materials and methods

The following materials and methods were utilized in this research.

### 2.1 Materials

Materials such as cement, fine aggregate, water, admixture and bacteria (nutrient broth, nutrient agar) were gathered from local sources. The chemical and physical properties of collected materials are examined in the laboratory and tabulated as follows.

#### 2.1.1 Cement

Cement is the most essential and crucial material that regulates mortar performance since it is required

***Table 1*** *Physical properties of cement*

| Properties | Result | Permissible limits |
|---|---|---|
| Fineness | 8% | It should not be more than 10 |
| Specific gravity | 3.12 | 3.1-3.16 |
| Normal consistency | 34% | 25-35% |
| Initial setting time | 35min | It should not be less than 30 min |

***Table 2*** *Chemical Composition of Cement*

| Oxide | Concentration (%) |
|---|---|
| CaO | 63.3 |
| $SiO_2$ | 21.8 |
| $Al_2O_3$ | 4.8 |
| $Fe_2O_3$ | 3.8 |
| MgO | 0.9 |
| $SO_3$ | 2.2 |
| $K_2O$ | 0.46 |
| $TiO_2$ | 0.13 |
| $Na_2O$ | 0.17 |

***Table 3*** *Fineness of Sand*

| IS sieve size (mm) | Weight of retained (g) | % of retained | Cumulative % of retained | % of passing | As per IS383:1970 Specification limit | | | |
|---|---|---|---|---|---|---|---|---|
| | | | | | I | II | III | IV |
| 10 | 0 | - | | 100 | 100 | 100 | 100 | 100 |
| 4.75 | 10 | 1 | 1 | 99 | 90-100 | 90-100 | 90-100 | 95-100 |
| 2.36 | 18 | 1.8 | 2.8 | 97.2 | 60-95 | 75-100 | 85-100 | 95-100 |
| 1.18 | 106 | 10.9 | 13.7 | 86.6 | 30-70 | 55-90 | 75-90 | 90-100 |
| 0.6 | 358 | 35.7 | 49.4 | 50.8 | 15-34 | 35-59 | 60-79 | 80-100 |
| 0.3 | 498 | 49.8 | 98.2 | 1 | 5-20 | 8-30 | 12-40 | 15-50 |
| 0.15 | 10 | 1 | 100.2 | 0 | 0-10 | 0-10 | 0-10 | 0-15 |
| | | | 265.3 | | | | | |

***Table 4*** *Physical Properties of Fine Aggregate*

| Properties | Result |
|---|---|
| Fineness modulus | 2.65 |
| Zone | II |
| Specific gravity | 2.62 |
| Bulk density (loose) | 1550 kg/m$^3$ |
| Bulk density (compacted) | 1692 kg/m$^3$ |

to bond sand and aggregate. According to IS 12269-2013, this research utilized Ordinary Portland cement 53 grade (OPC-53). Table 1 shows the physical properties of cement, such as fineness, specific gravity, normal consistency and the first setting time. The OPC 53 grade cement results are compared to IS 4031-1988.

Table 2 shows the chemical characteristics of cement, such as Calcium Oxide (CaO), Aluminum Oxide ($Al_2O_3$), Silicon Dioxide ($SiO_2$), Ferric Oxide ($Fe_2O_3$), MgO (Magnesium Oxide), Sulphur Trioxide ($SO_3$), Titanium Oxide ($TiO_2$), Potassium Oxide ($K_2O$) and Sodium oxide ($Na_2O$), examined in this research.

### 2.1.2 Fine aggregate

Aggregate material helps in the compacting of cementitious materials. It minimizes cement and water usage while contributing to the mechanical strength of mortar and it is an essential component in the

construction process. In this research, river sand easily available nearby was collected and processed. According to IS.2386:1963, specific gravity and fineness are evaluated based on equation (1), which is stated in Table 3.

Fineness modulus= (Cumulative percentage of retained)/100 (1)

The fine aggregate chosen has a fineness modulus of 2.65 and confirms Zone-II, according to the results. The sand was rinsed and screened on-site to remove harmful elements before being tested according to IS: 2386-1963. The physical properties of fine aggregate results are illustrated in Table 4.

### 2.1.3 Water

The mortar unit bond is reduced when water in the mortar mix evaporates or is absorbed by the masonry units and wet mixes that are simple to deal with, yielding the highest bond strengths. According to IS.456: 2000, in this research the fresh potable water was used for curing and mixing. For both vibrated and self-compacting mortar, the water-cement (w/c) ratio utilized in this research is 0.4.

### 2.1.4 Bacteria

This research utilizes laboratory-cultured bacterium such as *Bacillus Lechiniformis* and *Bacilluscohnii*, where the class and order of the bacteria are illustrated in Tables 5 and 6

*Cultivation of Bacteria:* The features of pure bacteria from the microbial culture collection are listed below. *Bacillus Licheniformis* and *Bacillus cohnii* are sorts of bacteria found in soil. They are commonly observed on ground-dwelling birds (like sparrows) and aquatic species' feathers, specifically the plumage on the chest and back (like ducks). It is a mesophilic gram-positive bacterium. It thrives at temperatures around 50 °C but can withstand much higher temperatures. The ideal temperature for enzyme secretion is 37 °C.

*Nutrient Broth:* Nutrient broth is a liquid medium, which is depicted in Figure 1. It is essential for the faster growth of bacteria, in which an autoclave, oven, conical flask, test tubes, glass rod and cotton are employed to prepare and sterilize nutrient broth. Moreover, for 500 ml, peptone 2.5 g, beef extract 1.50 g, NaCl 2.5 g/l and distilled water are all the ingredients of nutrient broth. Combine the ingredients in a mixing bowl, heat and shake properly to dissolve them. Then, add distilled water to reach the desired volume and partially dilute each test tube or conical flask with the medium. After dilution, cotton plugs should be placed in all flasks. After that, sterilize the prepared solutions for 15 minutes in an autoclave at 121 °C. Finally, Remove the flasks and preserve them at room temperature until suitable to use.

*Nutrient Agar:* Nutrient agar is the nutrient broth shown in Figure 2; the only difference is that it is hardened with agar. The ingredients are Peptone 5 g/l, NaCl 5 g/l, Meat extract 1.50 g/l, Agar 15 g/l and Yeast extract 1.20 g. Except for the agar, all ingredients are dissolved in distilled water in the correct ratio. The agar powder is added to the medium and heated to dissolve the agar, obtaining a clear liquid. Then, the media is

***Table 5*** *Class and Order of Bacillus Licheniformis*

| Class of Bacillus Licheniformis | Order of Bacillus Licheniformis |
|---|---|
| MTCC number | 2588 |
| Genes/species | *Bacillus Licheniformis* |
| Growth condition | Aerobic |
| Subculturing period | 30 days |
| Temperature | 37°C |
| Incubation | 36 h |
| Growth media number | 3 |

***Table 6*** *Class and Order of Bacillus cohnii*

| Class of Bacillus cohnii | Order of Bacillus cohnii |
|---|---|
| MTCC number | 3616 |
| Genes/species | *Bacillus cohnii* |
| Growth condition | Aerobic |
| Subculturing period | 5days |
| Temperature | 37°C |
| Incubation | 24 h |
| Growth media number | 239 |


***Figure 1*** *Nutrient Broth*

***Figure 2*** *Nutrient Agar*

uniformly distributed in the tubes or slants covered with cotton. After that, sterilize the prepared solutions for 15 minutes in an autoclave at 121 °C. Finally, cool the tube in a slanting position.

### 2.1.5 Admixtures

Ingredients added to the concrete batch right before or during the mixing are admixtures. In this research, fly ash and superplasticizer are used as admixtures, of which the chemical and physical properties are explained as follows:

*Fly ash:* Fly ash is a fine grey powder primarily made up of spherical, glassy particles and produced as a by-product of coal-fired power plants. This research discovers the quality standards for fly ash according to IS 3812-2003. Fineness, low carbon content and strong reactivity are the characteristics of good fly ash. Sub-bituminous coal usually produces fly ash with a CaO value of more than 10 %. Moreover, fly ash from class C possesses both pozzolanic and cementitious characteristics. Thus, this research utilized class C fly ash. Class C fly ash's chemical and physical properties are illustrated in Tables 7 and 8.

*Super Plasticizer:* Superplasticizers (SPs) are a type of additive used in the production of high-strength concrete. They are also known as high-range water reducers. Plasticizers are chemicals that allow concrete to be made with up to 15 % less water. Water content can be reduced by as much as 30 %. Chemical admixtures are concrete additives that improve the concrete's strength and longevity by increasing penetration, lowering the amount of water in the concrete and improving the concrete's strength and longevity. They decrease the amount of water in the product while maintaining its workability. Table 9 shows the physical characteristics of the superplasticizer.

***Table 7*** *Physical Properties of Class C Fly ash*

| Properties | Results Obtained |
|---|---|
| Normal consistency | 28 % |
| Initial setting time | 50min |
| Specific gravity | 2.10 |

***Table 8*** *Chemical Properties of Class C Fly ash*

| Oxide | Percent content |
|---|---|
| Calcium Oxide (CaO) | 16 |
| Silicon Dioxide ($SiO_2$) | 40 |
| Aluminum Oxide ($Al_2O_3$) | 17 |
| Ferric Oxide ($Fe_2O_3$) | 6 |
| Magnesium Oxide (MgO) | 1.81 |
| Sulphur Trioxide ($SO_3$) | 3 |
| Potassium Oxide ($K_2O$) | 2.19 |
| Titanium Oxide ($TiO_2$) | 0.94 |
| Sodium Oxide ($Na_2O$) | 0.62 |

***Table 9*** *Physical Properties of Super Plasticizer*

| Base | Sulphonated Naphthalene formaldehyde |
|---|---|
| Specific gravity | 1.23 - 1.25 |
| Sight appearance | Dark brown |
| Solid content | 40 % |
| pH | > 6 |
| Dosage | 1to2 to litresper100kg of Cement |

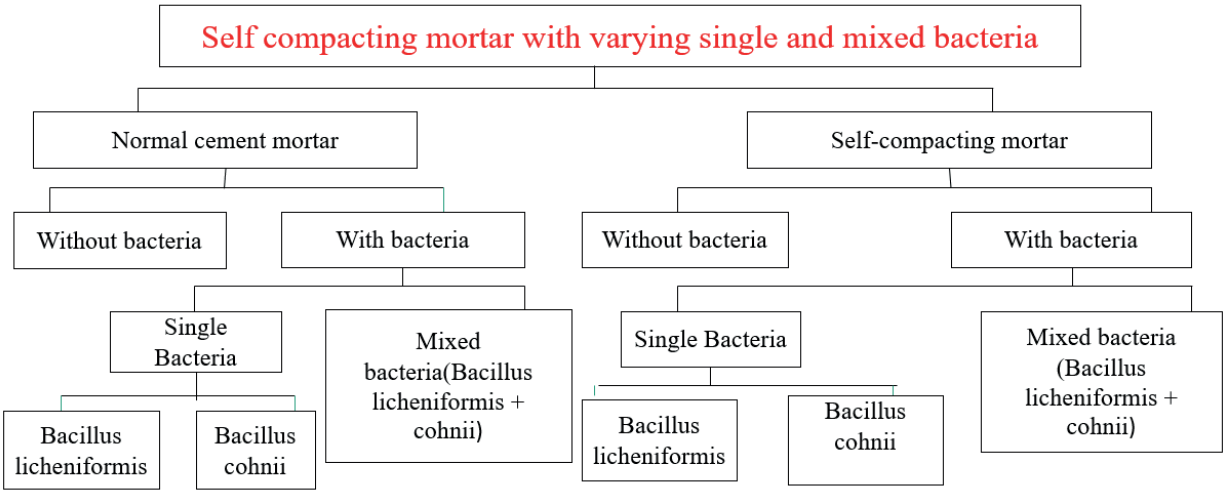


***Figure 3*** *Architecture of Self-compacting mortar with single and mixed bacteria*

## 2.2 Methods

The testing was performed using the following mix compositions - cement, fine aggregate, water and admixtures for the preparation of self-compacting mortar. Mix proportions for various combinations of mineral admixtures were evaluated using the cement replacement materials. The Mini v-funnel and Mini slump are all used to determine the workability of concrete. Mechanical Properties such as the non-

***Table 10*** *Mix Proportion of Normal Mortar*

| Mix proportions | | CEMI | Fly ash | Sand | Water | Bacteria (cells/ml) |
|---|---|---|---|---|---|---|
| 1:1 | Weight (kg/m$^3$) | 760 | 190 | 970 | 0.30 | $10^5$ |
| | Volume (m$^3$) | 0.243 | 0.09 | 0.37 | 0.230 | |

***Table 11*** *Mix Proportion of Self-Compacting Mortar*

| Mix proportions | | CEMI | Fly ash | Sand | Water | W/C | Sp | Bacteria (cells/ml) |
|---|---|---|---|---|---|---|---|---|
| 1:1 | Weight (kg/m$^3$) | 760 | 190 | 970 | 300 | 0.4 | 3.0 | $10^5$ |
| | Volume (m$^3$) | 0.243 | 0.09 | 0.37 | 0.3 | | 0.00244 | |

(a) Casting Concrete (b) Curing Concrete

***Figure 4*** *Preparation of Test Specimen*

destructive test, Compressive strength test and durability test of SCM mixes were tested using various degrees of cement replacement material with a constant aggregate and water-binder ratio. The following Figure 3 shows the architecture of the proposed approach.

### 2.2.1 Mix proportions

The mixing process greatly impacts the fresh-state properties of self-compacting mortars when it comes to efficiently utilizing superplasticizers. They indicated that the ratio of time spent mixing before adding the superplasticizer has no effect on its effectiveness and, as a result, modifies the self-compatibility of these mortars. The overall mixing process takes 10 minutes and begins with addition of fine aggregates (sands) and fine materials, followed by one minute of mixing. The initial water fraction, equivalent to 80% of the total mixing water, is gradually added to optimize homogenization without pausing the mixing process for another minute. The second water component (the remaining 20 %), combined with the superplasticizer, is gradually put into the mix without interfering. The mixing continues at its constant speed for another 5 minutes. After that, the mixer is turned off, giving the mixture two minutes to settle. If necessary, take this step to clean the mixer's paddle. Self-compacting mortar is selected 1:1 ratio for this research. The water-cement ratio in this mix is 0.4, with fly ash replacing 20% of the cement. The following Tables 10 and 11 describe the mixed proportion of normal and self-compacting mortar. This research evaluated the mix design, which is discussed in Appendix-I.

### 2.2.2 Preparation of test specimen

The specimens were made in cast-iron moulds measuring 70.6mm x 70.6mm x 70.6mm, in which oil was sprayed within the moulds to facilitate easier removal. The specimens are cast with and without bacteria and then demoulded and cured in fresh water in the curing tank after 24 hours. Finally, the specimens were removed and stored in the shade after completing the curing period. Figure 4 shows the casting concrete and curing concrete.

### 2.3 Test performed on SCM

The test was performed on self-compacting mortar in both fresh and hardened states. In fresh SCM, Mini-cone slump-flow test for SCM, Mini V-funnel test for SCM are conducted as well as in hardened SCM Compression Test, Ultrasonic Pulse Velocity Test; Rapid Chloride Penetration Test is performed. Scanning

Electron Microscopy and X-Ray Diffraction Analysis are conducted for the microstructure analysis.

### 2.3.1 Ultrasonic pulse velocity test

The ultrasonic pulse velocity test operates on the principle that an electro-acoustical transducer induces an ultrasonic pulse into the concrete, which then generates multiple reflections at the different material phase boundaries of the concrete specimen. The PUNDIT (Portable Ultrasonic Non-destructive Digital Indicating Tester) is used. The PUNDIT instrument is made in Switzerland by Proceq. The ultrasonic pulse velocity approach is used to evaluate the mortar for homogeneity, fractures, voids and other flaws. The ultrasonic waves' passage through the hardened mortar specimens was timed in microseconds. The pulse velocity was calculated by dividing the time required by the distance travelled.

### 2.3.2 Rapid chloride penetration test

After 28 days of curing, a rapid chloride penetration test was performed on mortar specimens 100 mm in diameter and 50 mm thick for proportions of standard mortar and self-compacting mortar with and without fly ash. After effectively attaching the tank and preparing the samples, this test was performed by ASTM C 1202-19 without any leaks. The diffuser cell contains two terminals, one of which is positive and the other negative. A 3.0 % sodium chloride (NaCl) solution was added to the tank connected to the positive terminal. In contrast, a 0.3 N solution of sodium hydroxide (NaOH) was added to the tank attached to the negative terminal. A 60 V current was then supplied for six hours to both reservoirs. The initial reading is obtained and further readings were taken every 30 minutes up to 360 minutes.

### 2.3.3 Scanning electron microscopy

A specimen of fractured concrete is examined using the scanning electron microscopy. This investigation was carried out to examine the morphology of mortar. The SEM images of the fillers detected in sample cracks. The fragmented specimen is initially fixed to either metal or a graphite stub using a rapid fading adhesive. The stub was covered with glue or double-sided tape before the mortar powder was sprinkled. The sample was then compressed with aluminium sheets to remove the loose granules. Cement paste and concrete need to be coated in a thin layer of electrically conductive substance, such as gold plated, because they are typically non-conductive. The specimens were prepared for the SEM analysis once the coating was finished and the thickness on the specimen surface had been applied.

### 2.3.4 X-ray diffraction analysis

This research uses X'Pert High Score Plus software to determine the crystalline material phase and their chemical compositions to analyze X-ray diffraction. Amorphous to Crystalline nature is indicated by XRD patterns with scan ranges of 3° to 80° ($2\theta$). For this examination, a powder sample was taken from mortar specimens that had been crushed while being tested for mechanical qualities. Calcite, Vaterite, Quartz and Hematite are some of the hydration products of Crystalline that develop in mortar.

## 3 Result and discussions

This section describes different test results from the proposed approach, such as workability, compressive strength, ultrasonic pulse velocity test and microstructural analysis.

### 3.1 Performance evaluation

The workability of self-compacting mortar is evaluated using the Mini-cone slump-flow test and the Mini V-funnel test for SCM. Furthermore, Compression strength with and without bacteria, mixed bacteria, ultrasonic pulse velocity and rapid chloride penetration tests are conducted.

### 3.1.1 Workability of self- compacting mortar

The workability of the self-compacting mortar is evaluated by mixing different ratios of cement, fine aggregate and water, in which the water-cement ratio is constant. The new properties of mortar are evaluated by Mini slump cone and V funnel slump.

Table 12 illustrates values for the Mini Slump and Mini V-Funnel test on self-compacting mortar. According to the research findings, incorporating bacteria into the mortar has no impact on its workability. Table 12

***Table 12*** *Workability Test Results*

| S. No | Mix (1:1) | | | | Workability | |
|---|---|---|---|---|---|---|
| 1. | Water | Cement | Fine aggregate | W/C | Mini slump (mm) | Mini V-Funnel (s) |
| | 120 ml | 300 | 300 | 0.4 | 260mm | 8 s |


***Figure 5*** *Ultrasonic pulse velocity test setup*

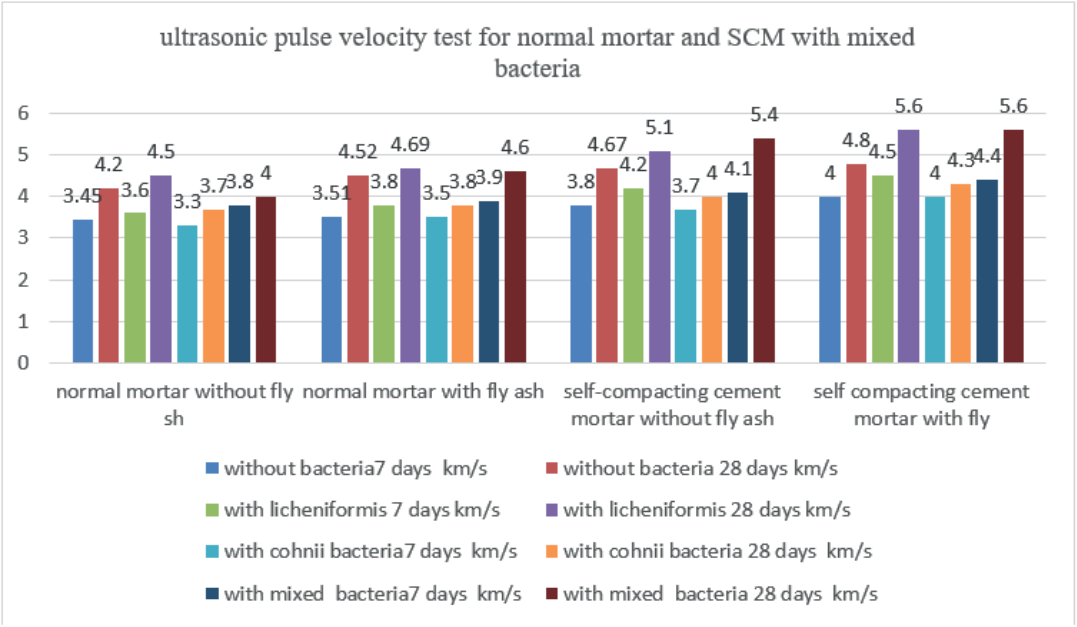


***Figure 6*** *Ultrasonic pulse velocity test for normal mortar and SCM with mixed bacteria*

shows that the workability of bacterial mortar mixes is determined by the slump; Mini V-Funnel is 260 mm and 8 s when the dose of cell concentration of bacteria is $10^5$ cells/ml.

### 3.1.2 Ultrasonic pulse velocity test

Ultrasonic pulse velocity tests were conducted on mortar specimens measuring 70.6 mm x 70.6 mm x 70.6 mm that had been cured in water for 7 days and 28 days. The test configuration for UPV is shown in Figure 5.

The mortar can be examined for homogeneity, cracks, voids and other faults using the ultrasonic pulse velocity method.

Figure 6 compares the ultrasonic pulse velocity test without fly ash for 7 days and 28 days. Compared to the normal mortar, the self-compacting mortar has a high pulse velocity of 5.4 km/s for *bacteria Licheniformis* in the $4^{th}$ week. The ultrasonic pulse velocity results were obtained using fly ash in normal and self-compacting mortar for 7 days and 28 days. Compared to the normal mortar with fly ash, the self-compacting mortar with fly ash has a high pulse velocity of 5.6 km/s *bacteria Licheniformis* and mixed bacteria at 28 days. Furthermore, all the bacterial mortar specimens had ultrasonic pulse velocities greater than 3.0 km/s. Therefore, the bacterial mortar can efficiently enhance mortar strength.

***Figure 7*** *Compression strength test setup*

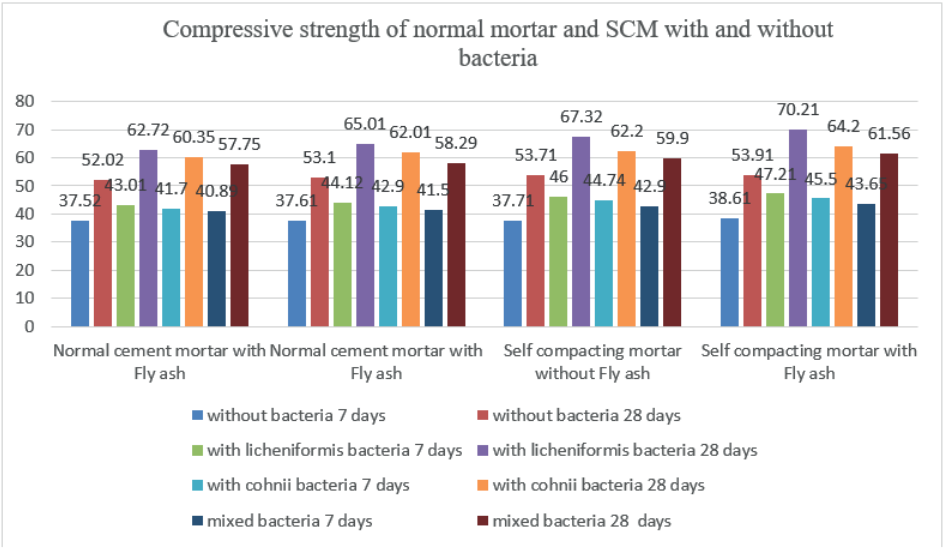


***Figure 8*** *Compressive strength of normal mortar and SCM with and without bacteria*

### 3.1.3 Compression strength

Compressive testing equipment with a 2000 kN capability was used to measure the compression strength of normal and bacterial mortar. The tests were performed once the specimen was centered in the testing apparatus. Once the dial gauge needle had just begun to change direction, the loading process was continued. The direction of the needle's motion has changed, indicating that the specimen has failed. The current dial gauge value was used to calculate the maximum load. The ultimate load, divided by the specimen's cross-sectional area, yields the ultimate cube compressive strength. The test configuration for compressive strength on a bacterial concrete cube specimen is shown in Figure 7.

The compressive strength test was performed on the normal and self-compacting mortar after curing for 7 and 28 days. The test setup for the compressive strength on a bacterial concrete cube specimen is shown in Figure 7.

In Figure 8, Compressive strength on self-compacting mortar without bacteria is 38.61 N/mm$^2$ and 53.91 N/mm$^2$ for 7 days and 28 days, respectively. Compared to the normal mortar, the compressive strength with and without fly ash increases in self-compacting mortar. Compared the seven days of curing and 28 days of curing enhances the strength of the self-compacting mortar. The Compressive strength on normal mortar with *Bacillus* Licheninformis bacteria, with and without fly ash for 7 days and 28 days are 43.01 N/mm$^2$, 44.12 N/mm$^2$, 67.32 N/mm$^2$, 65.01 N/mm$^2$. Compressive strength on self-compacting mortar with *Bacillus Licheniformis bacteria*, with and without fly ash for 7 days and 28 days are 46 N/mm$^2$, 47.21 N/mm$^2$, 67.32 N/mm$^2$, 70.21 N/mm$^2$. As a result, self-compacting mortar with fly

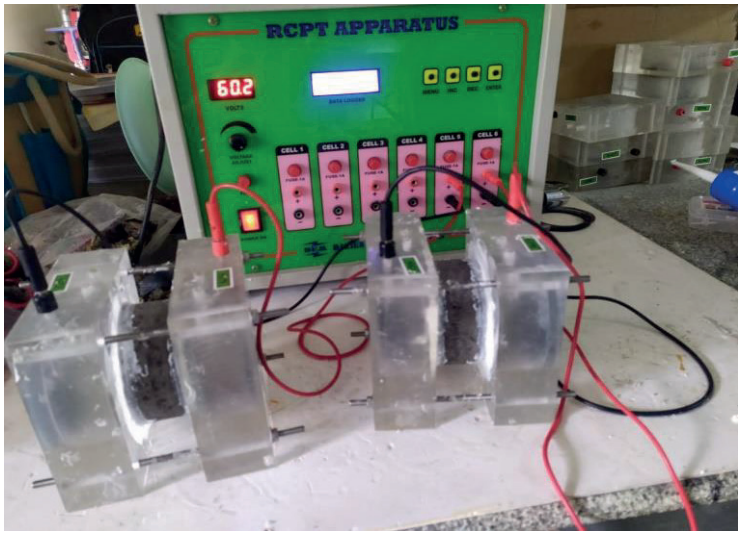


***Figure 9*** *Rapid chloride penetration test setup*

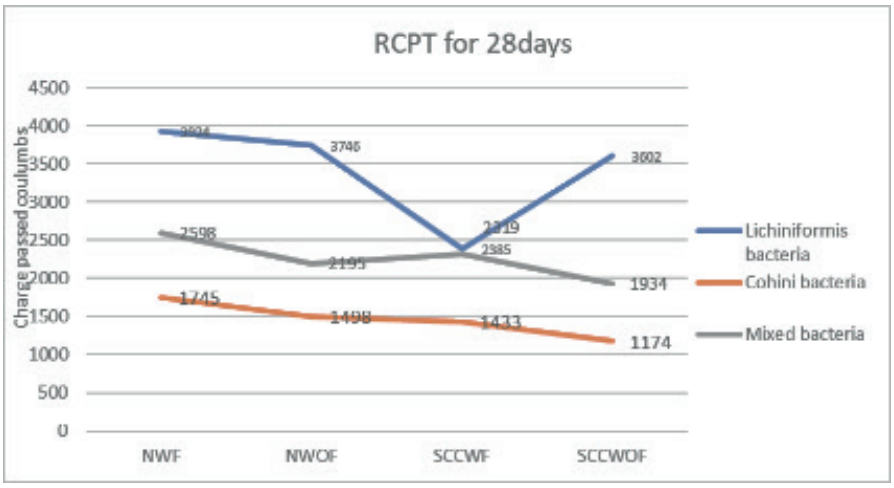


***Figure 10*** *Rapid chloride penetration test results*

ash and *Bacillus Lichneniformis bacteria* has a higher compressive strength of 70.21 N/mm² at 28 days.

The Compressive strength on normal mortar with *bacteria Cohnii*, with and without fly ash for 7 days and 28 days, is 41.7 N/mm², 42.9 N/mm², 60.35 N/mm² and 62.01 N/mm². Compressive strength on self-compacting mortar with *bacteria Cohnii*, with and without fly ash, for 7 days and 28 days, is 44.74 N/mm², 45.5 N/mm², 62.2 N/mm² and 64.2 N/mm². As a result, self-compacting mortar with fly ash and *bacteria Cohnii* has a higher compressive strength of 64.2 N/mm² at 28 days.

A compressive strength test was conducted on normal mortar and self-compacting mortar with mixed bacteria such as *Bacillus Licheniformis* and *Bacteria Cohnii*. Compressive strength on normal mortar with mixed bacteria, with and without fly ash for 7 days and 28 days, is 40.89 N/mm², 41.5 N/mm², 57.75 N/mm² and 58.29 N/mm². Compressive strength on self-compacting mortar with mixed bacteria, with and without fly ash, for 7 days and 28 days, is 42.9 N/mm², 43.65 N/mm², 59.9 N/mm² and 61.56 N/mm². As a result, self-compacting mortar with fly ash and mixed bacteria attains higher compressive strength of 61.56 N/mm² at 28 days.

The result of the compression strength test shows that *Bacillus Licheniformis bacteria* has the highest compressive strength in 7 and 28 days when compared to all other control mortars and bacteria.

### 3.1.4 Rapid chloride penetration test

After 28 days of curing, a rapid chloride penetration test was conducted on mortar specimens with a diameter of 100 mm and a thickness of 50 mm for proportions of normal mortar and self-compacting mortar, with and without fly ash. The test configuration for RCP is shown in Figure 9.

Figure 10 shows the rapid chloride penetration test of *Bacillus Licheninformis*, *Bacteria Cohnii* and *Mixed Bacteria*. The *Bacillus Licheninformis* has a higher penetration value than the *bacteria cohnii*, mixed bacteria and other mortar mixes. According to the test results, bacillus Cohnii has much lower chloride permeability than other bacteria.

### 3.1.5 Micro-structural analysis

The microstructure of bacterial mortar specimens can be examined using a scanning electron microscope (SEM) and an X-ray diffractometer. The SEM images, X-ray diffraction patterns and energy dispersive X-ray spectra of mortar samples, acquired from testing specimens, are described as follows.

*SEM-EDS:* Scanning electron microscopy can be used to examine a cracked concrete specimen. The goal of this study was to look into the morphology of mortar. A scanning electron microscope (SEM) was used to examine the microstructure of the concrete mixes, allowing the microstructure of the hydrated cement paste to be observed.

The formation of calcium carbonate crystals, the precipitation of calcite crystals within the mortar and the filling of pores are all visible. In this research, SEM analysis of bacteria mortar revealed unique calcite crystals included in the mortar. The presence of crystalline calcite in the form of CaCO3 in bacterial mortar specimens with fly ash was confirmed by high calcium levels. The presence of calcium (Ca) and the weight fraction of calcium are indicated by the Energy Dispersive X-Ray (EDX) spectrum of bacteria mortar. Moreover, the SEM-EDS test results include *Bacillus Licheniformis bacteria* with and without fly ash, *Bacteria Cohnii* with and without fly ash and mixed bacteria with and without fly ash of self-compacting mortar, are shown in Figures 11-16.

*X-Ray Diffraction Analysis:* The microstructure of various mixes was examined using an X-Ray Diffraction test and the peaks of graphs were utilized to identify minerals such as Quartz, Gypsum and C-S-H gel. In mortar mixtures, quartz aids in the development of bonding qualities. Gypsum is primarily important for controlling the time required for mortar to set. Calcite is a crucial component in the development of mortar strength qualities. Calcium silica hydrates gel improves mortar's strength while making it more durable and workable. Moreover, the X-ray diffraction test results include *Bacillus Licheniformis* bacteria with and without fly ash, *Bacteria Cohnii* with and without fly ash and Mixed bacteria with and without fly ash of self-compacting mortar, as shown in Figures 17-19

Microbes considerably impact the characteristics of bacteria in mortar, as demonstrated by SEM and XRD. According to the test results, self-compacting mortar with fly ash produces more calcium carbonate or calcite. XRD measurements revealed a higher percentage of calcite in Bacillus Licheniformis fly ash specimens with a cell concentration of $10^5$ cells/ml. Bacteria mortar contains a lot of calcite, CH and C-S-H, as well as fly ash.

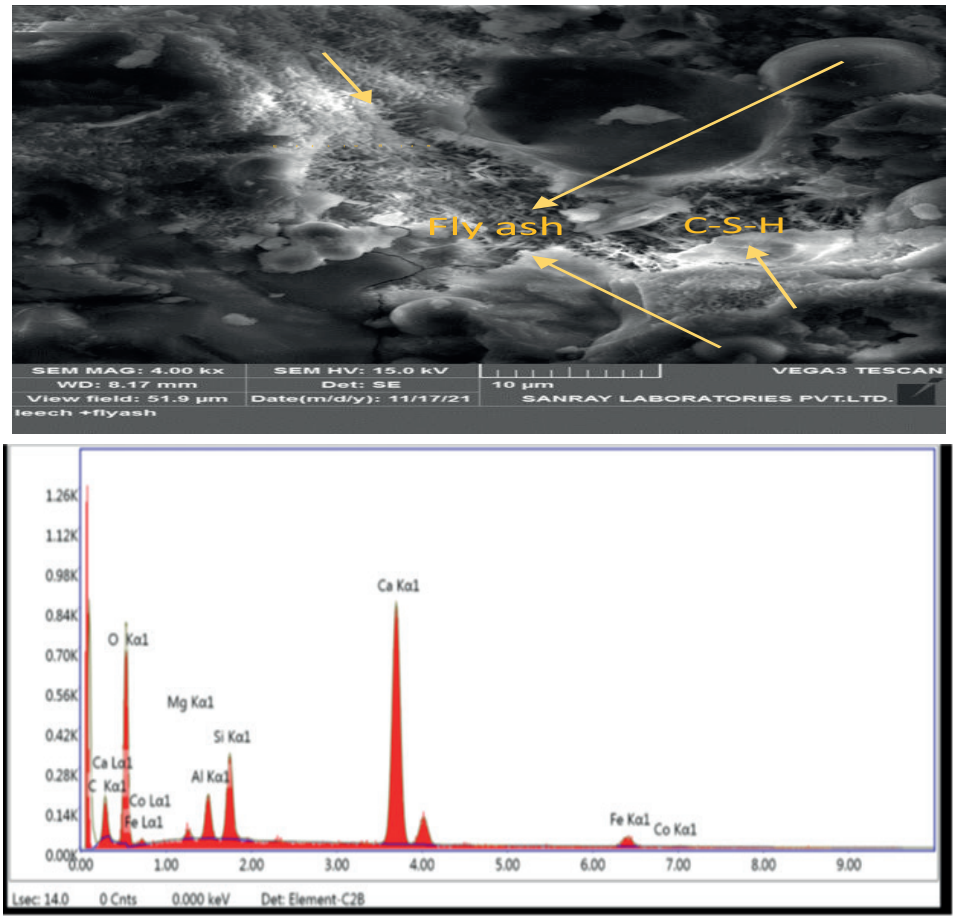


***Figure 11*** *Bacillus Licheniformis bacteria with fly ash SEM and EDS after 28 days of curing*

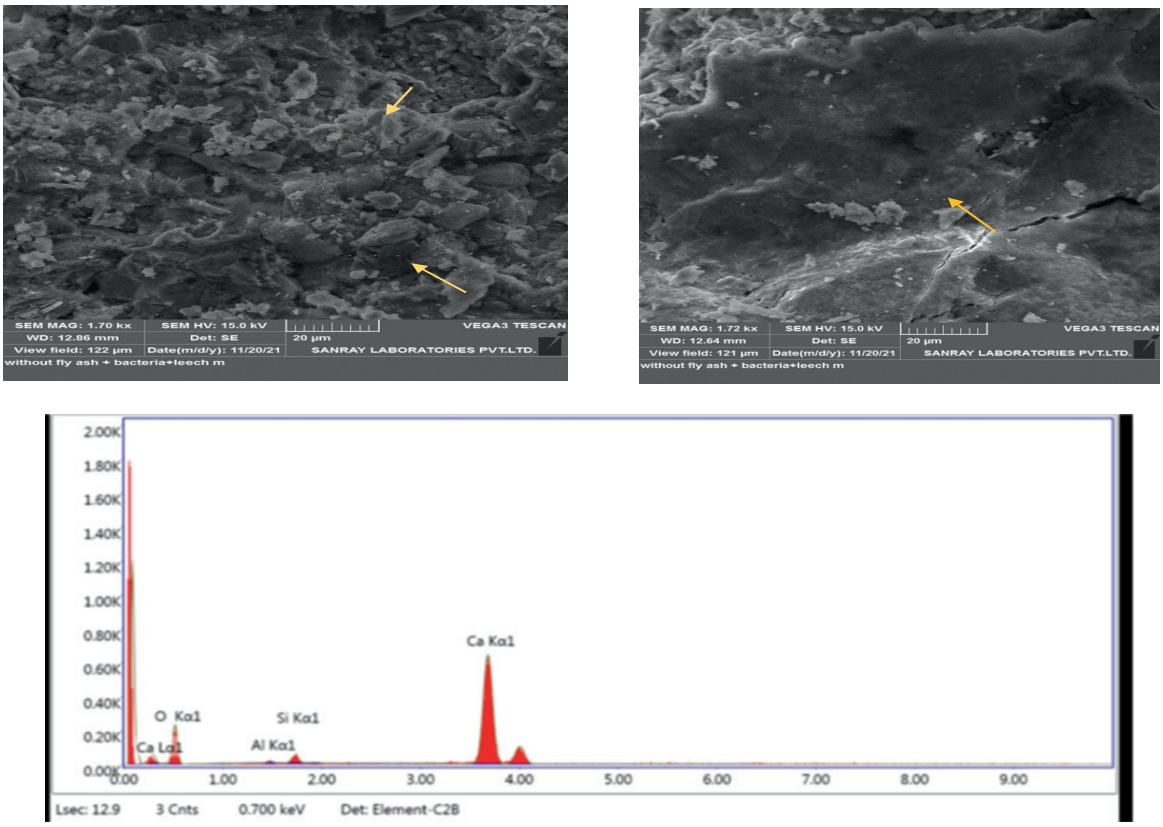


***Figure 12*** *Bacillus Licheniformis bacteria without fly ash SEM and EDS after 28 days of curing*

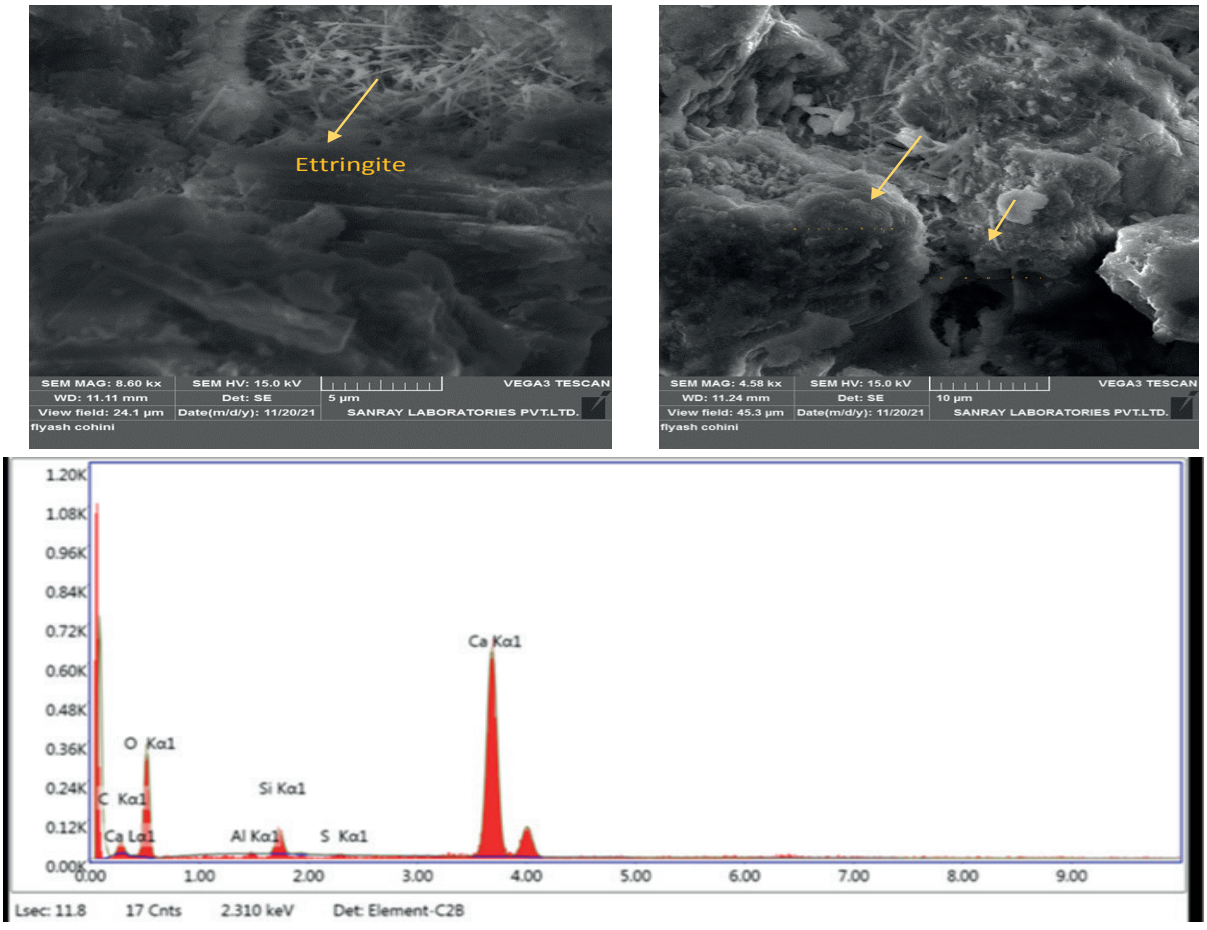


***Figure 13*** *Bacteria Cohnii with fly ash SEM and EDS after 28 days of curing*

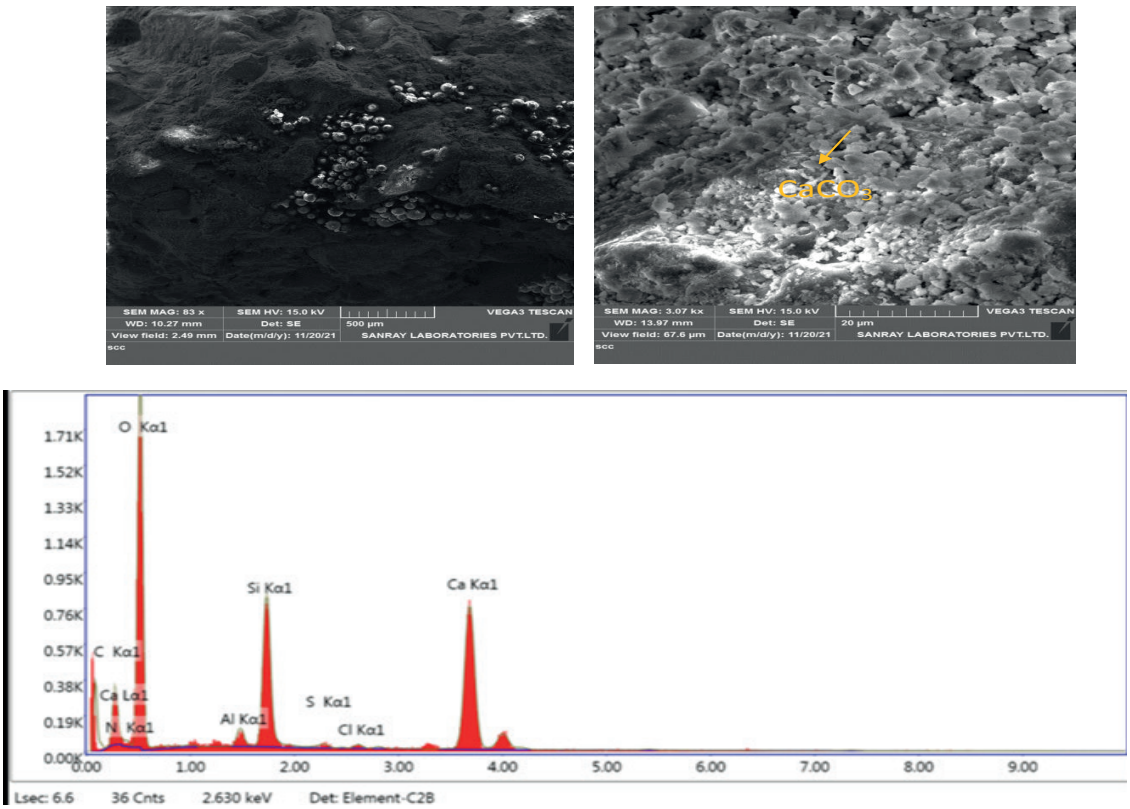


***Figure 14*** *Bacteria Cohnii without fly ash SEM and EDS after 28 days of curing*

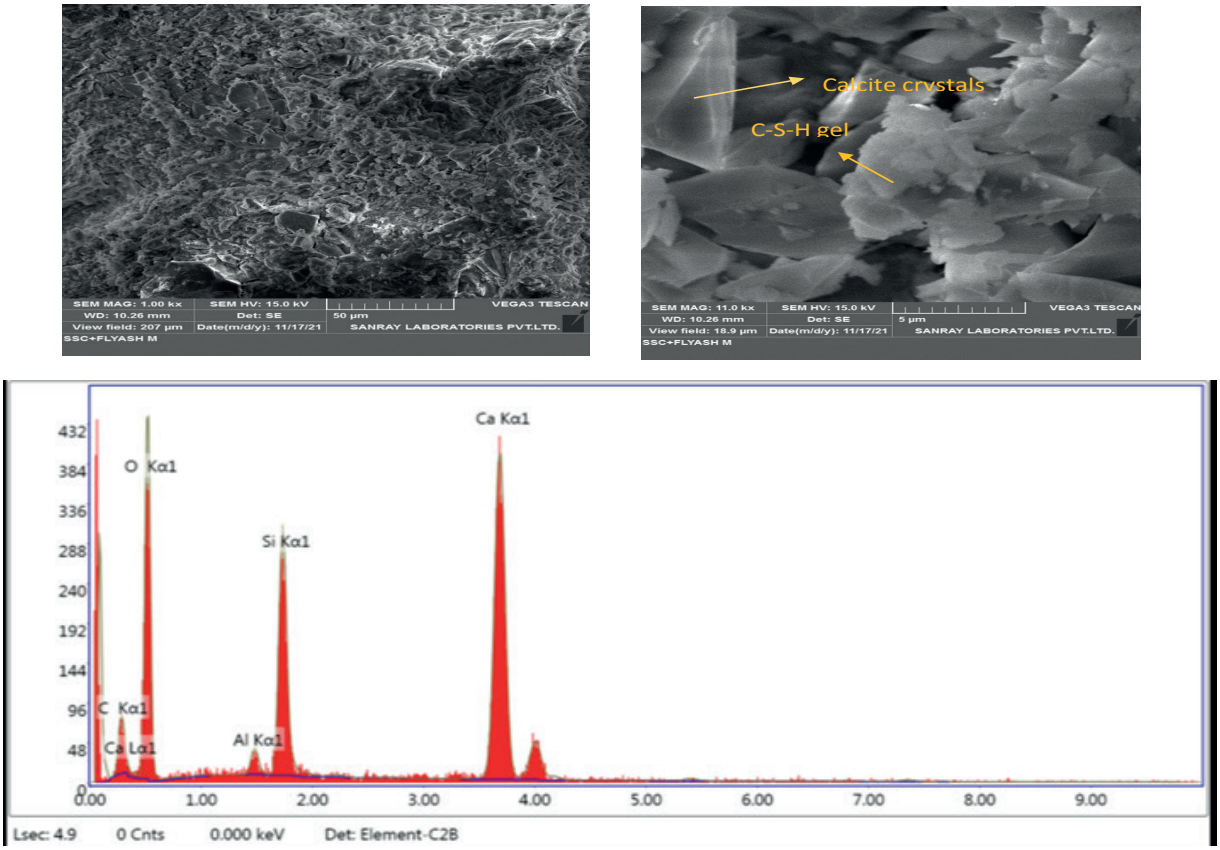


***Figure 15*** *Mixed Bacteria with fly ash SEM and EDS after 28 days of curing*

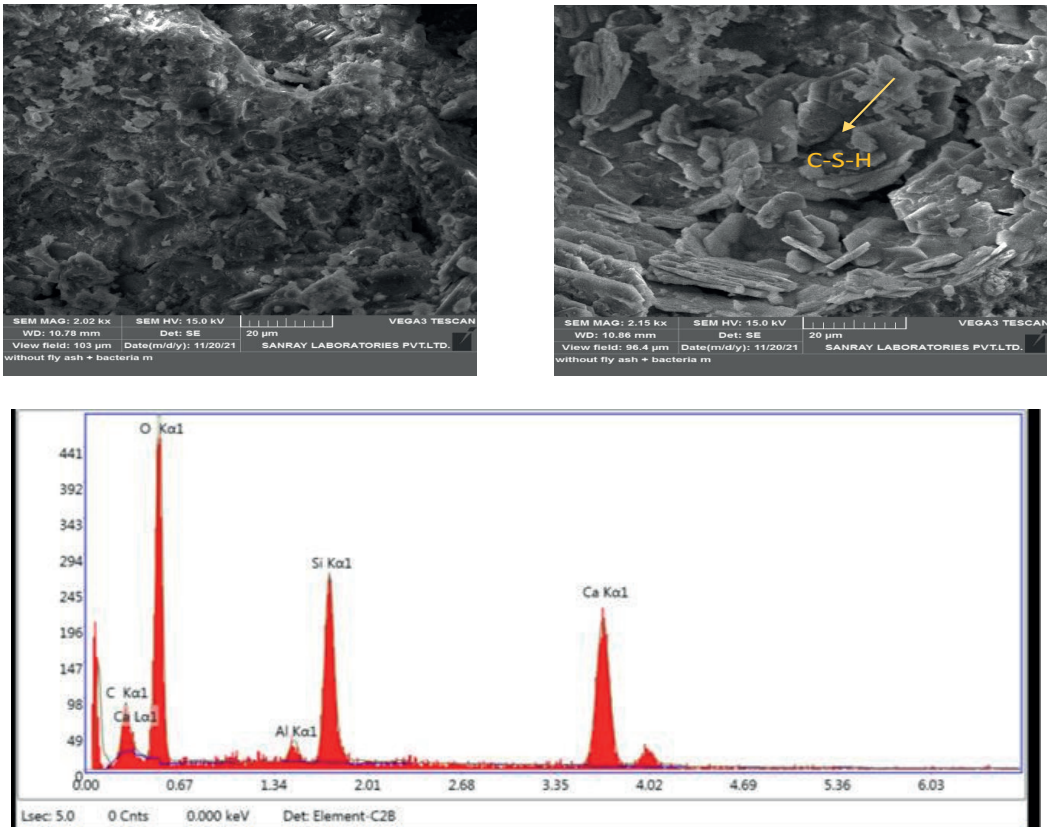


***Figure 16*** *Mixed Bacteria without fly ash SEM and EDS after 28 days of curing*

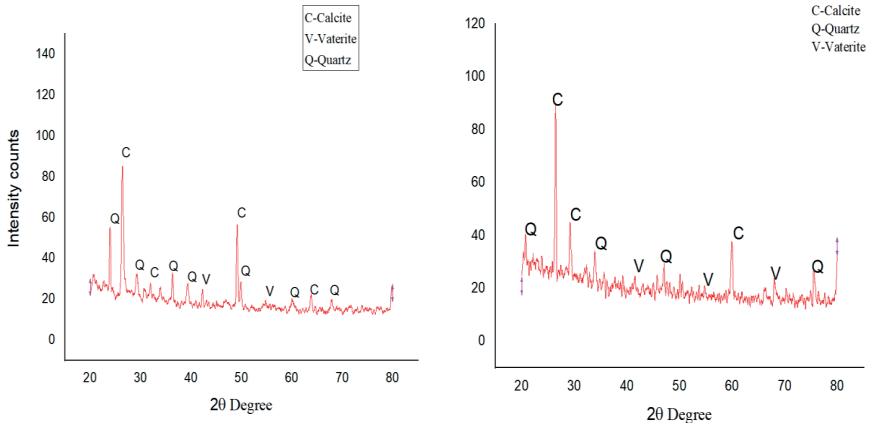


***Figure 17*** *X-ray diffraction for Bacillus Licheniformis with and without fly ash*

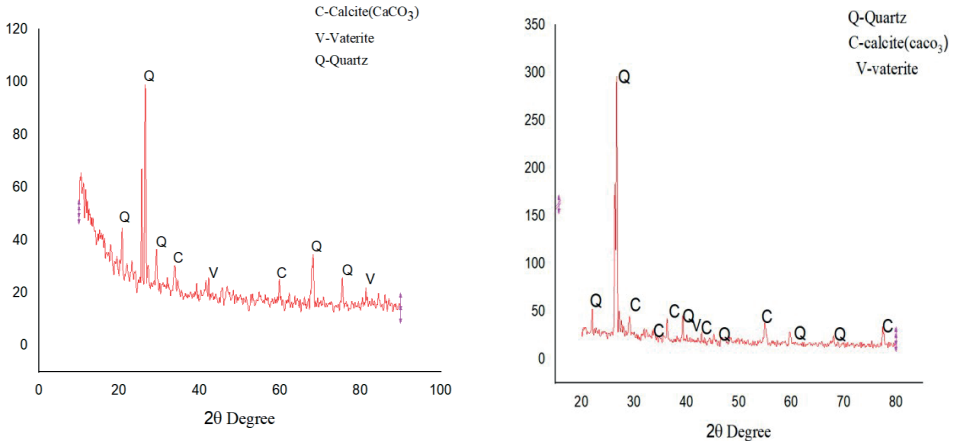


***Figure 18*** *X-ray diffraction for Bacteria Cohnii with and without fly ash*

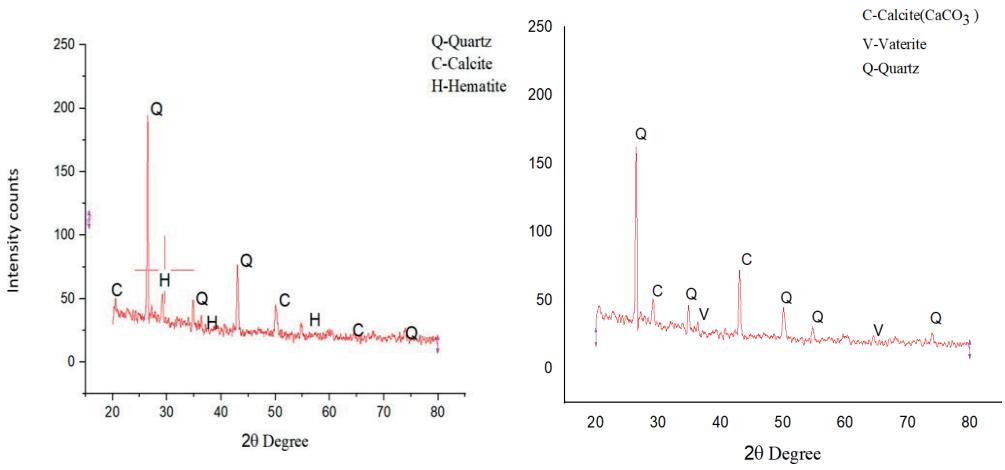


***Figure 19*** *X-ray diffraction for Mixed Bacteria with and without fly ash*

## 4 Conclusion

- *Bacillus Licheniformis* significantly increases the compressive strength up to 30 % for SCM by adding fly ash compared to normal mortar at 28 days. *Bacillus Licheniformis*, *Bacillus cohnii and mixed bacteria (Licheniformis + cohnii)* increased compressive strength by 30 %,19.08 % and 14.19 %, respectively. There is an increase in compressive strength due to the settlement of calcite as a filling material in the inner portion of cracks on the concrete surface.
- The non-destructive testing studies, i.e. the Ultrasonic pulse velocity test, could identify microbes' crack healing nature by understanding the variation in pulse velocity. It is observed that the quality of the normal mortar and SCM specimens with bacteria is excellent compared to normal mortar and SCM without bacteria. There is an increase in the velocity of waves by the increased $CaCo_3$ formation of nucleation effect of bacterium cell walls.
- SEM-EDX analysis showed the crystals of calcium carbonate morphology and C-S-H gel. It was confirmed through the elemental composition of mortar samples, which showed the presence of C, O and Ca elements in EDX, indicating the presence of $CaCO_3$.
- The XRD analysis observed the presence of calcite, quartz and vaterite mineral phases. The presence of calcite ($CaCO_3$) improves the strength. Previous studies also revealed the formation of vaterite and calcite due to self-healing, confirming the presented results. In the future, concrete mixes could incorporate mineral admixtures such as silica fume, GGBS and their combinations, chemical admixtures and microorganisms.

Self-Compacting Mortar has many benefits over traditional abiotic reinforced concrete. It can heal cracks caused by water with no human intervention and lasts much longer. Moreover, traditional concrete is expensive to manufacture and difficult to recycle effectively, whereas bacterial concrete is environmentally friendly nor economically feasible. In the long term, the self-healing concrete saves money on construction costs and minimizes the waste generated during the demolition of traditional concrete structures because it may regenerate itself and increase the lifespan of the buildings it comprises.

## References

[1] DEGLOORKAR, N. K., PANCHARATHI, R. K. Investigating microstructure characterization of mortars from 800 years old heritage structures in the Southern part of India. *Journal of Archaeological Science: Reports* [online]. 2020, **34**(A), 02634. ISSN 2352-409X. Available from: https://doi.org/10.1016/j.jasrep.2020.102634

[2] DEGLOORKAR, N. K., PANCHARATHI, R. K. Characterization of ancient mortar for sustainability of an 800-year-old heritage site in India. *Materials Today: Proceedings* [online]. 2020, 32(4), p. 734-739. ISSN 2214-7853. Available from: https://doi.org/10.1016/j.matpr.2020.03.472

[3] RAO, S., SILVA, P., DE BRITO, J. Experimental study of the mechanical properties and durability of self-compacting mortars with nanomaterials (SiO2 and TiO2). *Construction and Building Materials* [online]. 2015, **96**, p. 508-517. ISSN 0950-0618. Available from: https://doi.org/10.1016/j.conbuildmat.2015.08.049

[4] GHOSH, P., MANDAL, S., CHATTOPADHYAY, B. D., PAL, S. Use of microorganism to improve the strength of cement mortar. *Cement and Concrete Research* [online]. 2005, **35**(10), p. 1980-1983. ISSN 0008-8846. Available from: https://doi.org/10.1016/j.cemconres.2005.03.005

[5] SHASHANK, B. S., NAGARAJA, P. S. Durability studies on low-strength bacterial concrete [online]. In: *Advances in Sustainable Construction Materials*. BISWAS, S., METYA, S., KUMAR, S., SAMUI, P. (eds.). Lecture Notes in Civil Engineering. Vol. 124. Singapore: Springer, 2021. ISBN 978-981-33-4589-8, eISBN 978-981-33-4590-4, p. 639-650. Available from: https://doi.org/10.1007/978-981-33-4590-4_60

[6] SHASHANK, B. S., NAGARAJA, P. S. Fracture behaviour study of self-healing bacterial concrete. *Materials Today: Proceedings* [online]. 2022, **60**(1), p. 267-274. ISSN 2214-7853. Available from: https://doi.org/10.1016/j.matpr.2021.12.520

[7] CHAHAL, N., SIDDIQUE, R., RAJOR, A. Influence of bacteria on the compressive strength, water absorption and rapid chloride permeability of fly ash concrete. *Construction and Building Materials* [online]. 2012, **28**(1), p. 351-356. ISSN 0950-0618. Available from: https://doi.org/10.1016/j.conbuildmat.2011.07.042

[8] TAYEBANI, B., MOSTOFINEJAD, D. Penetrability, corrosion potential and electrical resistivity of bacterial concrete. *Journal of Materials in Civil Engineering* [online]. 2019, **31**(3), 04019002. ISSN 0899-1561, eISSN 1943-5533. Available from: https://doi.org/10.1061/(ASCE)MT.1943-5533.0002618

[9] REDDY, P. Y., RAMESH, B., KUMAR, L. P. Influence of bacteria in self-healing of concrete-a review. *Materials Today: Proceedings* [online]. 2020, **33**, p. 4212-4218. ISSN 2214-7853. Available from: https://doi.org/10.1016/j.matpr.2020.07.233

[10] ZHENG, T., QIAN, C. Self-healing of later-age cracks in cement-based materials by encapsulation-based bacteria. *Journal of Materials in Civil Engineering* [online]. 2020, **32**(11), 04020341. ISSN 0899-1561, eISSN 1943-5533. Available from: https://doi.org/10.1061/(ASCE)MT.1943-5533.0003437

[11] STANASZEK-TOMAL, E. Bacterial concrete as a sustainable building material? *Sustainability* [online]. 2020, **12**(2), 696. eISSN 2071-1050. Available from: https://doi.org/10.3390/su12020696

[12] REDDY, B. M., REVATHI, D. An experimental study on effect of Bacillus sphaericus bacteria in crack filling and strength enhancement of concrete. *Materials Today: Proceedings* [online]. 2019, **19**, p. 803-809. ISSN 2214-7853. Available from: https://doi.org/10.1016/j.matpr.2019.08.135

[13] NGUYEN, T. H., GHORBEL, E., FARES, H., COUSTURE, A. Bacterial self-healing of concrete and durability assessment. *Cement and Concrete Composites* [online]. 2019, **104**, 103340. ISSN 0958-9465. Available from: https://doi.org/10.1016/j.cemconcomp.2019.103340

[14] SEIFAN, M., BERENJIAN, A. Application of microbially induced calcium carbonate precipitation in designing bio self-healing concrete. *World Journal of Microbiology and Biotechnology* [online]. 2018, **34**(11), 168. ISSN 0959-3993, eISSN 1573-0972. Available from: https://doi.org/10.1007/s11274-018-2552-2

[15] AMERI, F., SHOAEI, P., BAHRAMI, N., VAEZI, M., OZBAKKALOGLU, T. Optimum rice husk ash content and bacterial concentration in self-compacting concrete. *Construction and Building Materials* [online]. 2019, **222**, p. 796-813. ISSN 0950-0618. Available from: https://doi.org/10.1016/j.conbuildmat.2019.06.190

[16] LORS, C., DUCASSE-LAPEYRUSSE, J., GAGNE, R., DAMIDOT, D. Microbiologically induced calcium carbonate precipitation to repair microcracks remaining after autogenous healing of mortars. *Construction and Building Materials* [online]. 2017, **141**, p. 461-469. ISSN 0950-0618. Available from: https://doi.org/10.1016/j.conbuildmat.2017.03.026

[17] DUCASSE-LAPEYRUSSE, J., GAGNE, R., LORS, C., DAMIDOT, D. Effect of calcium gluconate, calcium lactate and urea on the kinetics of self-healing in mortars. *Construction and Building Materials* [online]. 2017, **157**, p. 489-497. ISSN 0950-0618. Available from: https://doi.org/10.1016/j.conbuildmat.2017.09.115

[18] ZHANG, L. V., SULEIMAN, A. R., ALLAF, M. M., MARANI, A., TUYAN, M., NEHDI, M. L. Crack self-healing in alkali-activated slag composites incorporating immobilized bacteria. *Construction and Building Materials* [online]. 2022, **326**,126842. ISSN 0950-0618. Available from: https://doi.org/10.1016/j.conbuildmat.2022.126842

[19] BAYATI, M., SAADABADI, L. A. Efficiency of bacteria-based self-healing method in alkali-activated slag (AAS) mortars. *Journal of Building Engineering* [online]. 2021, **42**, 102492. ISSN 2352-7102. Available from: https://doi.org/10.1016/j.jobe.2021.102492

[20] RAUTRAY, S. S., MOHANTY, B. N., DAS, M. R. Performance of self-compacting geopolymer concrete using Bacillus Licheniformis. *Materials Today: Proceedings* [online]. 2020, **26**, p. 2817-2824. ISSN 2214-7853. Available from: https://doi.org/10.1016/j.matpr.2020.02.587

[21] NASIM, M., DEWANGAN, U. K., DEO, S. V. Effect of crystalline admixture, fly ash and PVA fibre on self-healing capacity of concrete. *Materials Today: Proceedings* [online]. 2020, **32**, p. 844-849. ISSN 2214-7853. Available from: https://doi.org/10.1016/j.matpr.2020.04.062

[22] TSAMPALI, E, STEFANIDOU, M. Effect of nano-SiO2 and nano-CaO in autogenous self-healing efficiency. *Materials Today: Proceedings* [online]. 2021, **37**, p. 4071-4077. ISSN 2214-7853. Available from: https://doi.org/10.1016/j.matpr.2020.09.253

[23] GUZLENA, S., SAKALE, G. Self-healing of glass fibre reinforced concrete (GRC) and polymer glass fibre reinforced concrete (PGRC) using crystalline admixtures. *Construction and Building Materials* [online]. 2021, **267**, 120963. ISSN 0950-0618. Available from: https://doi.org/10.1016/j.conbuildmat.2020.120963

[24] XU, D., CHEN, W., FAN, X. Experimental investigation of particle size effect on the self-healing performance of microcapsule for cemented coral sand. *Construction and Building Materials* [online]. 2020, **256**, 119343. ISSN 0950-0618. Available from: https://doi.org/10.1016/j.conbuildmat.2020.119343

[25] REDDY, C. M., RAMESH, B., MACRIN, D. Influence of bacteria Bacillus subtilis and its effects on flexural strength of concrete. *Materials Today: Proceedings* [online]. 2020, **33**, p. 4206-4211. ISSN 2214-7853. Available from: https://doi.org/10.1016/j.matpr.2020.07.225

[26] JOGI, P. K., LAKSHMI, T. V. Self-healing concrete based on different bacteria: a review. *Materials Today: Proceedings* [online]. 2021, **43**, p. 1246-1252. ISSN 2214-7853. Available from: https://doi.org/10.1016/j.matpr.2020.08.765

[27] LUHAR, S., LUHAR, I., SHAIKH, F. U. A Review on the performance evaluation of autonomous self-healing bacterial concrete: mechanisms, strength, durability and microstructural properties. *Journal of Composites Science* [online]. 2022, **6**(1), 23. eISSN 2504-477X. Available from: https://doi.org/10.3390/jcs6010023

[28] ALGAIFI, H. A., ALQARNI, A. S., ALYOUSEF, R., BAKAR, S. A., IBRAHIM, M. W., SHAHIDAN, S., IBRAHIM, M., SALAMI, B. A. Mathematical prediction of the compressive strength of bacterial concrete using gene expression programming. *Ain Shams Engineering Journal* [online]. 2021, **12**(4), p. 3629-3639. ISSN 2090-4479. Available from: https://doi.org/10.1016/j.asej.2021.04.008

[29] ALMOHAMMED, F., SIHAG, P., SAMMEN, S. S., OSTROWSKI, K. A., SINGH, K., PRASAD, C. V., ZAJDEL, P. Assessment of soft computing techniques for the prediction of compressive strength of bacterial concrete. *Materials* [online]. 2022, **15**(2), 489. eISSN 1996-1944. Available from: https://doi.org/10.3390/ma15020489

[30] RAMAGIRI, K. K., CHINTHA, R., BANDLAMUDI, R. K., DE MAEIJER, K. P., KAR, A. Cradle-to-gate life cycle and economic assessment of sustainable concrete mixes-alkali-activated concrete (AAC) and bacterial concrete (BC). *Infrastructures* [online]. 2021, **6**(7), 104. eISSN 2412-3811. Available from: https://doi.org/10.3390/infrastructures6070104

# REDUCTION IN ENTRY CAPACITY OF ROUNDABOUT UNDER THE INFLUENCE OF PEDESTRIANS IN MIXED TRAFFIC CONDITIONS

**Chintaman Bari, Ashish Dhamaniya***

Department of Civil Engineering, Sardar Vallabhbhai National Institute of Technology, Surat, India

*E-mail of corresponding author: adhamaniya@gmail.com

***Resume***

Models developed in Highway Capacity Manual (HCM) are not suitable to cater to the effects of mixed traffic conditions and hence, its use is unjustifiable. This research investigates such a challenging problem as the effect of undesignated pedestrian crossings on the entry capacity of roundabouts. For the present study, field survey data were collected using video cameras from three roundabouts such that the base section (roundabout without pedestrian influence) and non-base sections (with pedestrian influence), both scenarios, were captured. A modified HCM equation was developed to estimate entry capacity and further, the reduction in capacity with respect to pedestrian volume is determined. Lastly, a relationship was developed to check the effect of pedestrian crossflow on the entry capacity. The relation shows that capacity reduced to 1841 Passenger Car Unit (PCU/h) when the pedestrian flow increased to 288 pedestrians/hour.

***Article info***

Received 7 May 2022
Accepted 15 September 2022
Online 19 October 2022

***Keywords:***

roundabout
pedestrian
entry capacity
critical gap
follow-up time

Available online: https://doi.org/10.26552/com.C.2022.4.D201-D214

ISSN 1335-4205 (print version)
ISSN 2585-7878 (online version)

## 1 Introduction

Nowadays, the safety of pedestrians has become a part of public apprehension. Pedestrian crossing, especially at undesignated places, causes two-fold effects. One, the crossing pedestrians forced the vehicles to reduce their speed to find sufficient gaps to cross the road and consequently reduced the capacity of the section [1]. Two, the pedestrians put themselves at risk in the collision with running vehicles [2]. A way to ensure the right level of the road traffic safety is designing a safe road infrastructure. Roundabout intersections are a good example of a point road infrastructure that increases the road safety [3-4]. A circular intersection with the central island in which continuous traffic movement is observed (clockwise direction in the left-hand drive) is called a roundabout. The roundabouts necessitate the entering traffic to give way to traffic already in the circle and observe various design rules to increase safety. At roundabouts, the pedestrian visual gets widen as the exiting traffic from a roundabout advances in a single direction rather than in multiple directions. Further, it improves the understanding of the drivers' movements compared to the perpendicular junctions. Additionally, it lowers the queueing condition due to the absence of traffic lights. Moreover, the traffic conflict points and thus the damages due to crashes reduce due to the installation of the roundabouts instead of the conventional intersections [5-6]. In addition, the lower conflict points are observed as compared to other point facilities [4]. It is due to the merging and diverging of vehicles at small angles at lower speeds causing less potential for accidents [7]. Further, speed reduction when crossing the intersection, low loss of time for drivers at inlets, etc., contribute significantly to ensuring the appropriate level of road safety at a given point of the network transport [8].

Hence, they are mostly accepted worldwide as a replacement to the conventional intersection for every traffic scenario, i.e. homogeneous and mixed traffic. A decrease in idling time is observed at roundabouts compared to signalized intersections as the vehicles are continuously in motion for crossing the roundabout.

Pedestrians interact with vehicles at the roundabout while crossing in places where there is no provision for pedestrian crossings. In the absence of traffic signals and markings, the complexity and flexibility of pedestrian behaviour is observed more than that of vehicles at roundabouts. Therefore, this study aims to determine the effect of the pedestrian crossing on

a roundabout capacity where the pedestrian has not provided any entry facility such as marking or foot over bridge at roundabouts. Under such conditions, pedestrians force the vehicle to make sufficient gaps and reduce entry capacity. The well-recognized manual for traffic operations and planning, i.e. the United States Highway Capacity Manual (US HCM), is widely followed in India, irrespective of its transferability for mixed traffic conditions, [9-10]. The objectives of the present study are twofold, one is to determine the approach leg entry capacity at a roundabout operating under highly heterogeneous and quasi-lane discipline scenarios and the second is to determine the effect of the undesignated pedestrian crossing on the roundabout's entry capacity. The outcome of the present study can be useful for providing some insights for the revision of the Indian Highway Capacity Manual [11].

The remainder of the study is as follows. Section 2 describes the detailed literature review of the studies carried out at roundabouts in developed and developing countries. Next, Section 3 describes the detailed objectives and methodology of the present study. Section 4 describes the data collection and the preliminary data analysis, including traffic composition, traffic and pedestrian volume. Section 5 focused on determining Passenger Car Units (PCU), which are further used for estimating entry capacity, as discussed in Section 6. After that, Section 7 describes the critical gap analysis, which is finally used to derive the capacity of the non-base section, discussed in Section 8. Lastly, Conclusions are given in Section 9.

## 2 Literature review

Various researchers worldwide focused on roundabout entry capacity research, including the US, Germany, United Kingdom (UK), etc. The researchers have given various models for evaluating the traffic operations at the roundabout, which can be broadly categorized into two groups. Out of two, one deals with the empirical methodology based on the intersection geometry and the other depends purely on the gap acceptance process. Many researchers used a simulation approach to study the roundabout capacity [12-16]. The Indian standard document, referred to as Indian Roads Congress (IRC) [17], gives the formula for estimation of the entry capacity of the roundabout. The method is purely based on empirical approach and uses the principles of Wardrop. According to the US HCM [9], roundabouts' entry capacity ($Q_e$) equation is given based on the circulating flow ($Q_c$). On the other hand, the HCM [10], proposed the formulas for determining the entry capacity of a roundabout based on the critical gap and follow-up time. Schroeder and Rouphail [18] developed the pedestrian delay model based on the probability of crossing for the single-lane roundabout. Meneguzzer and Rossia [19] studied the effect of a pedestrian on the entry capacity of roundabouts in Italy. Firstly, a nonlinear relationship was developed between the percent occupancy and pedestrian volume, which is further used to develop the equation for entry capacity. A simulation approach using SIDRA INTERSECTION software was applied by [20] to assess the roundabout capacity given HCM. Al-Ghandour et al. [21] analyzed the single-lane roundabout with slip lanes with pedestrian volumes using microsimulation. The results showed that there is an increase of 28.1s/veh of delay if the vehicles yield 100 pedestrians per hour in high traffic conditions. A comparative evaluation of roundabout capacity by UK method, US method, Swiss method, IRC method and German method was carried out by Chandra and Rastogi [22]. They concluded that the IRC method estimated a higher capacity value when compared to the other methods. Various shortcomings of the HCM [9] roundabout capacity model listed in HCM [10] and some related model extensions provided by the SIDRA INTERSECTION software are discussed regarding the future development of the HCM roundabout capacity model. Kang et al. [23] used the microsimulation approach to evaluate the effect of a pedestrian on the entry capacity of the roundabout. It was found that the installation of a splitter island at entry enhances pedestrian safety and the entry capacity roundabout. Ahmad and Rastogi [24] developed the static Passenger Car Units (PCUs) for roundabouts under mixed traffic conditions. They developed the heterogeneity equivalency factor (H-Factor) for converting flow from vehicles per hour to PCUs/h. Osei et al. [25] studied the effect of roundabout signalization on the capacity of roundabout using microsimulation. The results showed that the capacity enhanced by 50 % due to signalization at the roundabouts.

From the aforementioned literature, it can be seen that a lot of work is carried out in developed countries where the traffic has lesser heterogeneity and with lane discipline. Further, the countries where the study was done had well-planned pedestrian crossing facilities. However, the conditions in developing countries differ from those of developed nations with a highly heterogeneous nature of traffic with quasi-lane discipline nature. Further, well-designated pedestrian facilities are not provided at intersections in developing countries and hence, the models developed in developed nations cannot justify the true nature of the traffic in developing countries. Thus, there is indeed a need to study the effect occurring on the traffic operations at roundabouts due to the undesignated pedestrian crosswalks under the mixed traffic scenario.

## 3 Objectives and the methodology of the present study

As the literature review implies, the studies related to developing countries are scarce where the pedestrian

himself forces the vehicle to find the sufficient gap under mixed traffic conditions. The activity of pedestrian crossing on the road is purely a gap acceptance phenomenon. Here, the pedestrian will estimate the available gap on all the lanes for crossing the road. Then, the pedestrian will accept or reject the gap depending on the lane traffic volume and perception. As the number of pedestrian's increases, there ought to be a reduction in the capacity and a reduction in the entry speed of the vehicles approaching the roundabout, thus increasing delays. This must be analyzed because a significant increase in delay would be detrimental to the idea of using roundabouts. Thus, the objectives of the present study are two-fold (a) to estimate the entry capacity of the roundabout under mixed traffic conditions and (b) to determine the effect of crossing pedestrians on the entry capacity of the roundabout. However, it has been assumed that drivers' behavior is consistent throughout the observation period at all the study roundabouts.

Initially, roundabout sections were selected on arterial/sub-arterial roads without gradient and curvature to determine the capacity loss. The basic consideration in selecting a section will be that it should be free from the bus stop, parked vehicles, curvature, gradient, pedestrian movement and any other side friction. Further, roundabouts with significant pedestrian crossings are considered for the study to determine the effect of the pedestrian crossing on the capacity of the roundabout, as well. Finally, the reduction factor due to crossing pedestrians is calculated.

## 4 Data collection

Field studies are carried out to study the prevailing traffic characteristics and operation at roundabouts. For the present study, three roundabouts with four legs and diameters ranging from 20 to 25 m were selected from the different regions of the country. Two of the three roundabouts are considered the base roundabouts, located in Jaipur (Northern region) and Trivandrum (Southern region). The third one is having a significant number of crossing pedestrians, located in Surat (Western region), which is considered for the comparative study. All the candidate roundabouts have a four-lane divided carriageway in all directions. Field data has been collected using high resolution video cameras keeping cameras at a high vantage point in order to capture the whole roundabout area. The data related to entry, exit flows from each lane, circulatory flow and the crossings pedestrians were captured in the video camera. Field data was collected on a typical weekday in normal weather conditions for more than twelve hours, covering both off-peak and peak hours for each roundabout.

Along with the videographic survey, details of the geometry of all the candidate roundabouts were collected, as shown in Table 1.

The whole survey data was compiled to get the traffic data in the desired format. Then, the data extraction was done in the laboratory by replaying the recorded traffic video on a large screen and the data related to traffic volume and composition, accepted gap, rejected gap and follow-up time were extracted manually using AVIDEMUX software and recorded for further analysis.

### 4.1 Traffic composition

The traffic was divided into seven vehicle classes for dealing with mixed traffic scenarios for the present

***Table 1*** *Inventory details of the candidate roundabouts*

| Inventory details | Chomu House Circle (Jaipur) | | | | Chakka roundabout (Trivandrum) | | | | Keval Chowk | | | |
|---|---|---|---|---|---|---|---|---|---|---|---|---|
| | Leg 1 | Leg 2 | Leg 3 | Leg 4 | Leg 1 | Leg 2 | Leg 3 | Leg 4 | Leg 1 | Leg 2 | Leg 3 | Leg 4 |
| Entry Width (m) | 8.5 | 11.2 | 9.4 | 11.6 | 8.5 | 8.5 | 8.5 | 8.5 | 9.4 | 8.5 | 10.7 | 7 |
| Exit Width (m) | 8.5 | 14 | 10.3 | 9.6 | 9.0 | 10.5 | 10 | 10.5 | 10.9 | 8.5 | 8.9 | 7 |
| Approach Width (m) | 6.25 | 10.5 | 5.3 | 10 | 6.5 | 7.0 | 6.5 | 7 | 9.4 | 8.5 | 10.7 | 7 |
| Departure Width (m) | 6.25 | 10.5 | 5.3 | 8.2 | 7.0 | 7.5 | 7.0 | 9.0 | 12.4 | 15.6 | 12.2 | 14.2 |
| Circulating Roadway width (m) | 14 | 10.5 | 10.2 | 12.3 | 9.5 | 9 | 10.2 | 9.5 | 14 | 10.5 | 14 | 12 |
| Weaving Length (m) | 34.8 | 24.8 | 24.8 | 30.6 | 17.5 | 21.9 | 18.2 | 22.1 | 9.4 | 8.5 | 10.7 | 7 |
| Central Island Diameter (m) | 24.9 | | | | 23.4 | | | | 24.8 | | | |
| Central Island Perimeter (m) | 78.5 | | | | 73.5 | | | | 77.87 | | | |

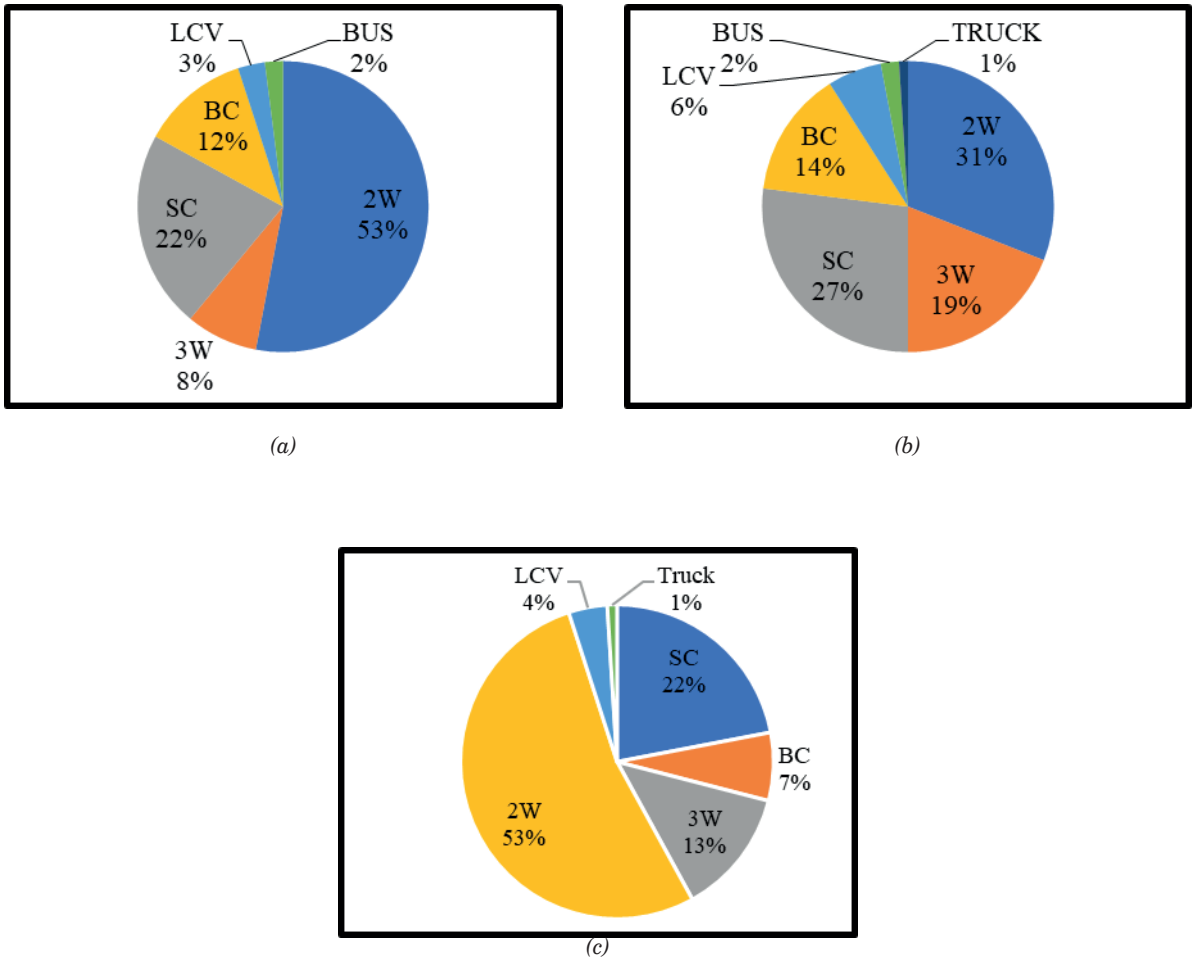


***Figure 1*** *Traffic Composition (a) Chomu House Circle (b) Chakka Roundabout (c) Kewal Chowk*

study. The classification includes motorized two-wheeler, motorized three-wheeler, Small Car, Big Car, Light Commercial Vehicle (LCV), Bus and Truck. The small car includes vehicles with a capacity of engine less than 1400 cc and the big cars include vehicles having more than an engine capacity of 1400 cc. The small cars are mostly hatchbacks and sedans, while the big cars include sports utility vehicles and cross utility vehicles. As all the candidate roundabouts were in the urban road network, a lower proportion of trucks were observed and hence, trucks were combined with vehicle class buses for the present study. After extracting filed survey data for all three locations collected using video cameras it was observed that most of the share is acquired by two-wheelers at the base section. Motorized two-wheeler share was maximum in Jaipur and Surat (53%) and minimum in Trivandrum (31 %). On the other hand, the share of small cars at all the three candidate locations is nearly the same, 22% in Jaipur and Surat and 27% in Trivandrum. Motorized three-wheelers proportion was maximum in Jaipur (19%) and minimum in Surat (13 %). The proportion of LCV is 4% in Surat and both truck and bus found less than 1% in the observed traffic mix. Figure 1 shows the traffic composition at three locations.

### 4.2 Pedestrian volume

To study the pedestrian flow effect on the roundabout, it is essential to study the pedestrian volume that crosses the roadway. Figure 2 illustrates the variation of pedestrian volume observed in the roundabout area during different hours of the selected time.

### 4.3 Traffic volume

Traffic volume is a quantitative flow measure, with vehicles per day and vehicles per hour being the most frequent units. Traffic volume observed at three different roundabouts is analyzed per approach lane.

## 5 Determination of passenger car units (PCU)

For highly heterogeneous and quasi-lane discipline traffic, the estimation of capacity in vehicles per hour (vph) is not justifiable and hence, there is a need to develop the equivalency factors for different vehicle classes to represent capacity in equivalent terms. Passenger Car Unit (PCU) is the multiplying factor

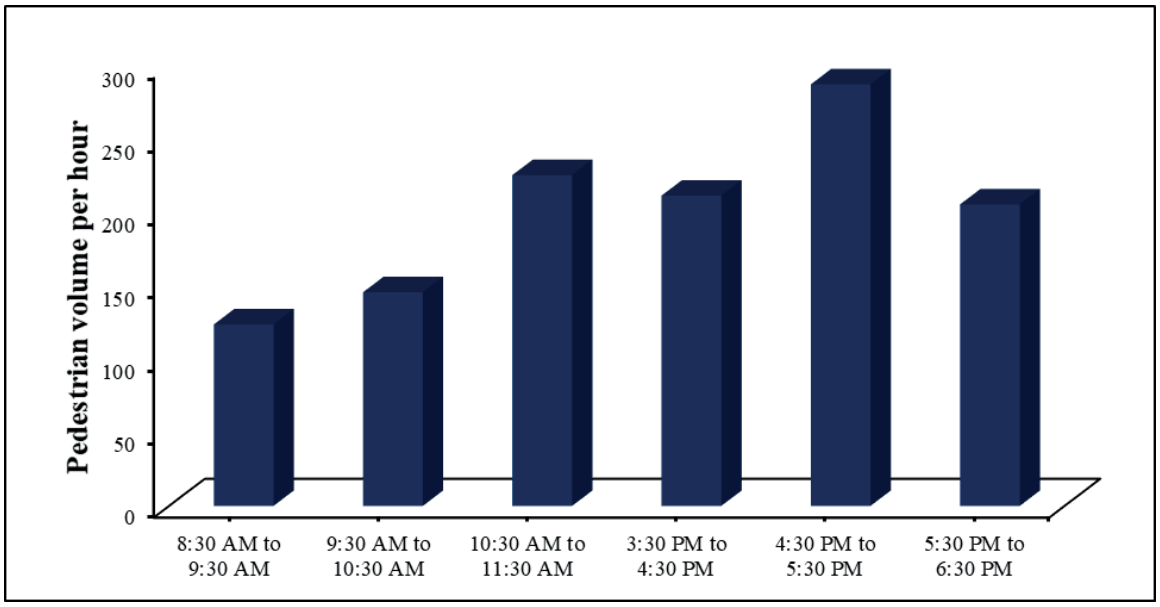


***Figure 2*** *Number of pedestrians crossings at different time intervals*

that differs for each vehicle class, which gives the traffic in equivalent terms, i.e. PCU/h. For the present study, the time occupancy method developed by Sonu et al. [26] is used to determine the PCU for each vehicle class at roundabouts. In the time occupancy method, the ratio of time required to pass from one arm to another arm for the i-th vehicle to the time required for the same car movement is considered. The occupancy time is considered here as it is a representative factor that takes into the effect caused due to variation in roadway geometry and the traffic characteristics of a vehicle during a particular movement in a roundabout. Additionally, it can clearly represent the interaction between the considered vehicle class and the standard vehicle class (here, small car) for determining the PCU.

PCU values for the present study are used for each movement separately, i.e. the left turn, straight and right-turn movement. Interestingly, no significant difference was found in the PCU values for all the movements of motorized two-wheelers and three-wheelers; thus, the constant values are adopted as 0.22 and 0.67, respectively. As a small car was taken as the base category, the PCU value was obtained as 1.00 for it. On the other hand, for big cars, the PCU value varies from 1.52 to 1.65 for the left-turn and right-turn movement, with 1.58 for the straight movement. Similarly, for LCV and bus, the PCU values are 1.75 and 4.04 for the left-turn, 1.81 and 4.43 for the straight movement and 1.93 and 4.64 for the right-turn, respectively. These values are used for capacity estimation and to determine the reduction in entry capacity at the non-base location.

## 6 Estimation of entry capacity

In the present study, the entry capacity is found using the relationship between the entry flow and the circulatory/conflicting flow. For the requirement of the circulatory flow, the data from the candidate roundabout located in Jaipur (base section) is considered since the significant delay and queue formation was captured during the data collection. First, the entry flow and circulatory flows are converted in equivalent terms, i.e. PCU/h using the vehicle class-wise PCU values mentioned in the previous section. Separate values for the right, left and straight turning vehicles are used for the present study to convert the traffic flow into equivalent PCU flow. Entry capacity for the roundabout is the maximum equivalent flow in PCU/h when the conflicting flow exists in the roundabout area. Here, the conflicting flow consists of all the other turning movements in front of the leg for which entry capacity is to be found. For this, the relationship is developed between the entry flow and conflicting flow, which was further compared to the relationship given in HCM [10]. For the present study, a negative polynomial relationship is found to exist between the entry flow and the circulatory flow. Moreover, the same reference value can be employed to compare capacity values at the non-base locations (locations with a significant pedestrian crosswalk) as well. The HCM [10] model for entry capacity is formulated as given in:

$$Qe = f_{HVe} * f_p * f_A * A * e^{\left(\frac{B}{f_B}\right)Qc}. \tag{1}$$

whereas parameters $A$ and $B$ are related to the follow-up time and critical gap, it can be expressed as:

$$Q_e = A * e^{BQ_c}, \tag{2}$$

where $A = \frac{3600}{t_f}$ $B = \frac{tc - 0.5t_f}{3600}$

$Qe$-Entry capacity, $Qc$-circulatory flow, $t_f$ - follow up time, $t_c$ - critical gap

From Equation (2), it is evident that the entry capacity of a roundabout is conspicuously influenced by the value of critical gap and follow-up time. So, a profound analysis of the critical gap and related parameters is conducted to study the effect of the undesignated pedestrian crosswalk on roundabout capacity needs.

## 7 The Gap Analysis for the base and non-base section

The estimation of critical gaps from observed traffic flow patterns is one of the most challenging tasks in the case of roundabouts. Concerning the traffic rules, there is no minimum delays to major stream vehicle at the roundabout. However, for the minor stream vehicle, the delay may occur, as the minor stream vehicle can only enter the conflict area at the roundabout if the safe passage zone through the complete conflict area is available to the driver in the aspect of the major stream vehicle. Here, the critical gap plays an important role, which can be defined as the least possible time interval that an entering vehicle can take to merge into the circulating stream safely. It can be said that the driver cannot make the gap less than the critical gap for maneuvering, but he can take the gap more than that for the safe maneuver. The probability Equilibrium Method (PEM) is used in the present study to estimate the critical gap for each vehicle class. After that, the equivalent stream critical gap was derived to deal with the highly heterogeneous traffic conditions observed in the field.

### 7.1 Accepted and rejected gaps

Data related to the classified vehicular gap was extracted purposefully considering the major stream vehicles in the weaving zone while the minor vehicle enters the major stream. The accepted and rejected gap by the drivers is observed to be influenced by the type of vehicle. This can be understood by the graph shown in Figure 3 for the average values of accepted and maximum rejected gaps at both study locations. A general trend of increase in average gap size with the increase in the size

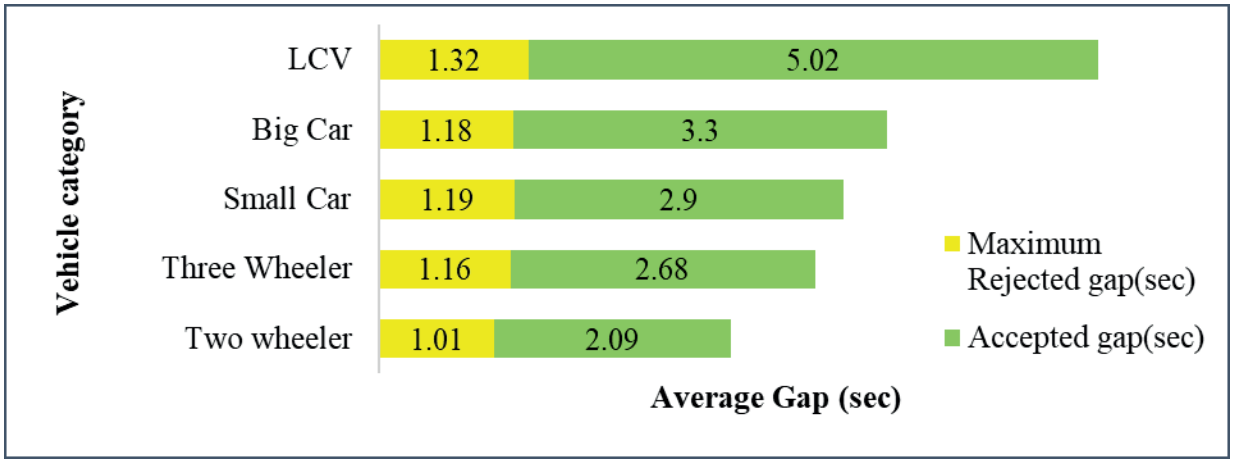


*(a) Chakka Trivandrum*

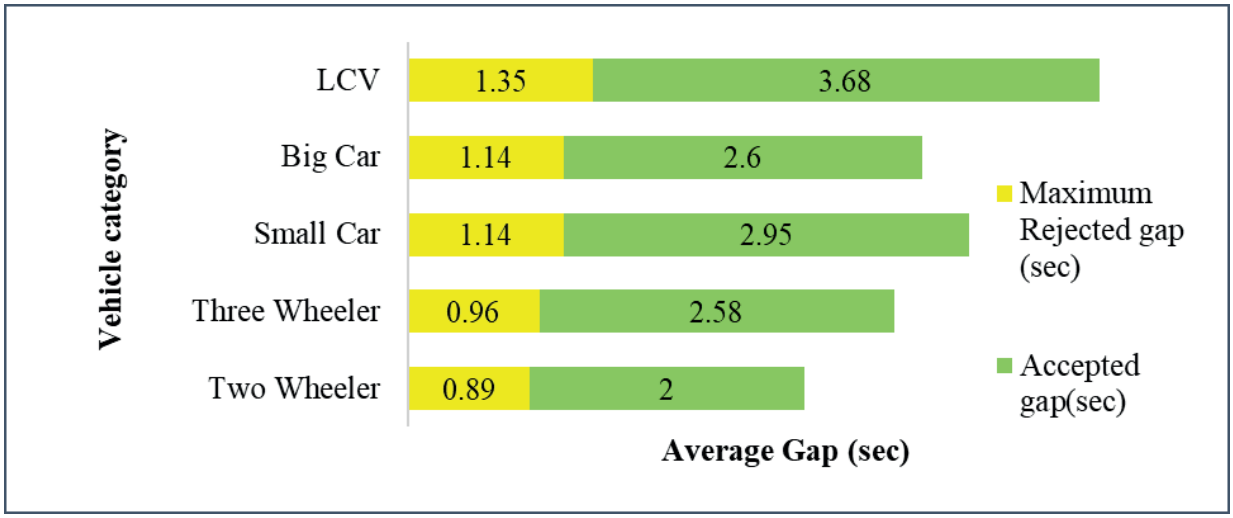


*(b) Chomu House Jaipur*

***Figure 3*** *Average accepted and rejected gaps at base sections*

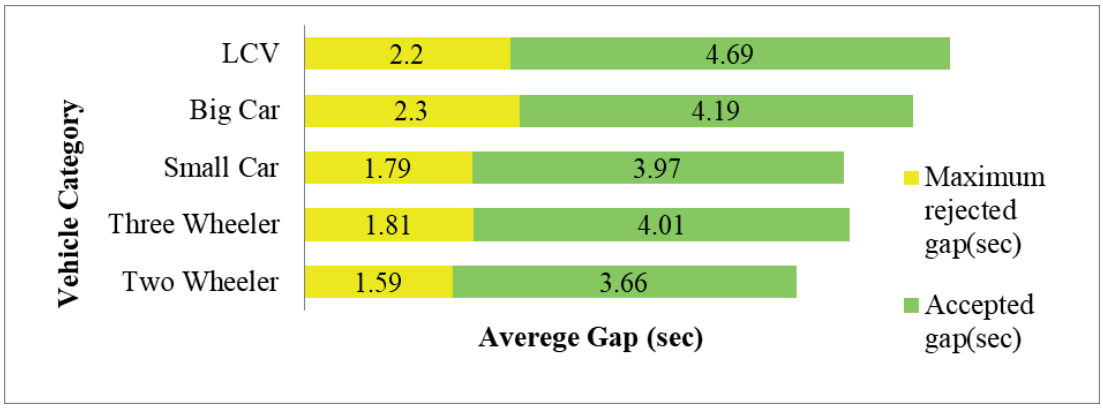


***Figure 4*** *Average accepted and rejected gaps at the non-base section (Keval Chowk)*

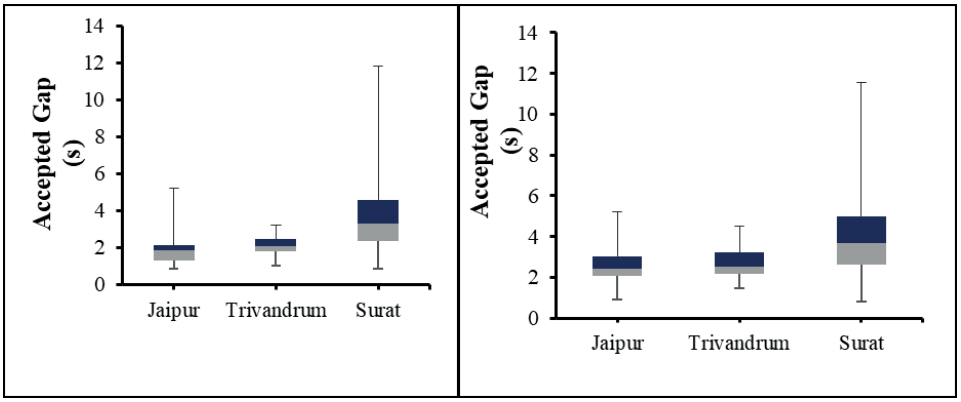


*(a) Motorized two-wheeler* *(b) Motorized three-wheeler*

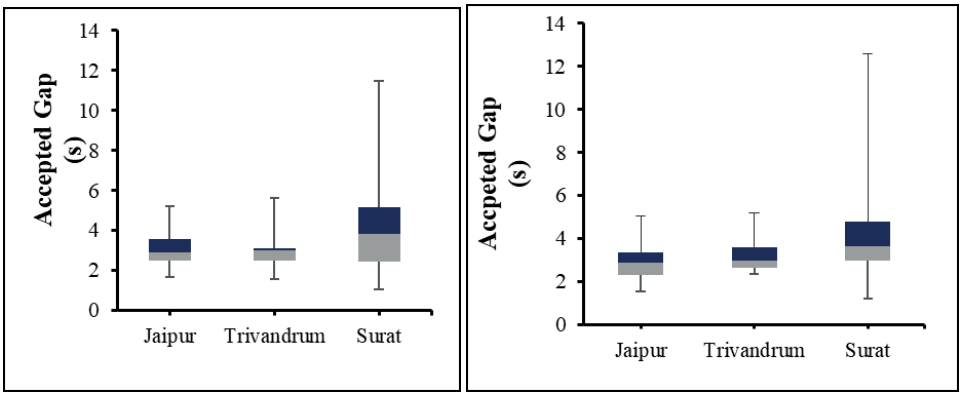


*(c) Small Car* *(d) Big Car*

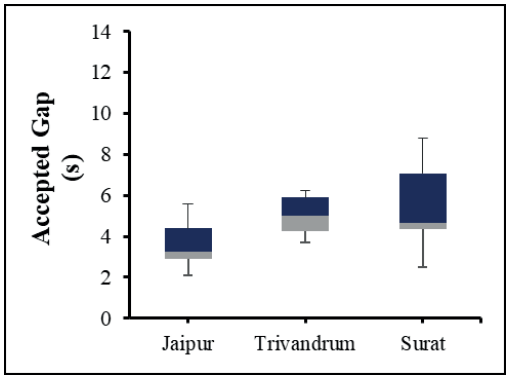


*(e) LCV*

***Figure 5*** *Accepted Gap variations for each category of vehicles*

of subject vehicle type exists at selected roundabouts. As the size increases, the drivers tend to enter larger gaps. The samples available for trucks and buses at the selected roundabout are relatively low; hence, the gap analysis of such vehicles is not considered in the study.

Similar analysis has been performed in the non-base section as well, to comprehend the observed variation in accepted and maximum rejected gap values. From the analysis shown in Figure 4, it is envisaged that there is a reasonable variation in the accepted and rejected gap at the non-base section, where pedestrian crossings are recurrent. This also focuses on pedestrians' influence (hindrance created by vehicular movement) in the selected study zone. Furthermore, the statistical analysis clearly designates the substantial variation in the accepted gap at the location with significant pedestrian movement.

When discussing the pedestrian-vehicle interaction at the roundabout, it is common that some percentage

***Table 2*** *ANOVA test statistics*

| Type of a vehicle | Base Section Vs. Base section | | | Base section Vs. Non-base section | | |
|---|---|---|---|---|---|---|
| | F- statistical | F-critical | p- value | F-statistical | F-critical | p- value |
| Two-wheeler | 1.010 | 3.920 | 0.320 | 74.000 | 3.860 | 0.000 |
| Three-wheeler | 0.170 | 3.980 | 0.680 | 22.761 | 3.954 | 0.000 |
| Small Car | 0.620 | 3.980 | 0.430 | 10.336 | 3.882 | 0.001 |
| Big Car | 1.810 | 4.050 | 0.180 | 9.817 | 3.990 | 0.003 |
| LCV | 0.840 | 4.300 | 0.370 | 8.926 | 4.210 | 0.006 |

*(a)* *(b)*

*(c)* *(d)*

***Figure 6*** *Pedestrian crossing movement at the roundabout area*

of drivers is expected to yield to a waiting pedestrian, which depends on vehicle speed and driving behavioral attributes. To understand this possible extent of variation in behavioural attributes of pedestrian and driver at selected locations, a broad analysis has been performed to analyze the variation of the accepted gap for each individual category of vehicles. The results of the analysis are illustrated as a box-whisker diagrams shown in Figure 5.

From the above analysis, it is observed that the variation in the accepted gap is found to be very high in the location with significant pedestrian movement. To construe such a finding, an Analysis of Variance (ANOVA) test has been performed for accepted gap values extracted from both the base sections, such as the Chomu House roundabout (Jaipur) and Chakka roundabout (Trivandrum). The results shown in Table 2 clearly depict that there is no variation between the accepted gaps at both the study location. Similarly, the same analysis showed a significant difference between the accepted gap values between the base and non-base section, which substantiates the earlier finding that a notable influence of pedestrians exists in the roundabout.

The rigorous analysis of the collected video disclosed a steady propensity that the pedestrian movements create a larger gap in the circulating traffic stream as the pedestrian is creating a hindrance to circulatory flow. Moreover, the minor stream vehicle also follows the same course, impeding the major stream movement in a weighty manner. Figure 6 illustrates the pedestrian crossing attributes in the roundabout area. Thus, the performance of the roundabout was altered to a significant extent. To quantify the aftermaths on roundabout performance, it is necessary to analyze parameters such as circulating flow, critical gap and follow-up time, as they are considered the influencing entry capacity parameters.

### 7.2 Method of the critical gap estimation

The critical gap can be eloquently defined as the least possible time interval that an entering vehicle can take to merge into the circulating stream safely. In the present study, the critical gap is estimated by the method developed by Wu [27], known as Probability Equilibrium Method (PEM). The foundation of this method is based on the probability equilibrium theory that considers both the accepted and rejected gaps. The cumulative distribution functions (CDFs) of accepted (Fa(t)) and rejected gaps (Fr(t)) is used in this method to find out the critical gap.

Now, according to PEM,

Observed probability that a gap of length t is accepted = $1 - F_a(t)$

Observed probability that a gap of length t is not accepted = $F_a(t)$

Observed probability that a gap of length t is rejected = $1 - F_r(t)$

Observed probability that a gap of length t is not rejected = $F_r(t)$

Therefore, from above equations follows:

$F_r(t) \neq 1 - F_a(t)$ and $1 - F_r(t) \neq F_a(t)$.

Thus, it can be said that the accepted gap is always greater than the actual critical gap [28].

### 7.3 Estimation of the critical gap

The wide variety of vehicles in a mixed traffic stream and diversity in their size and speed over a wide

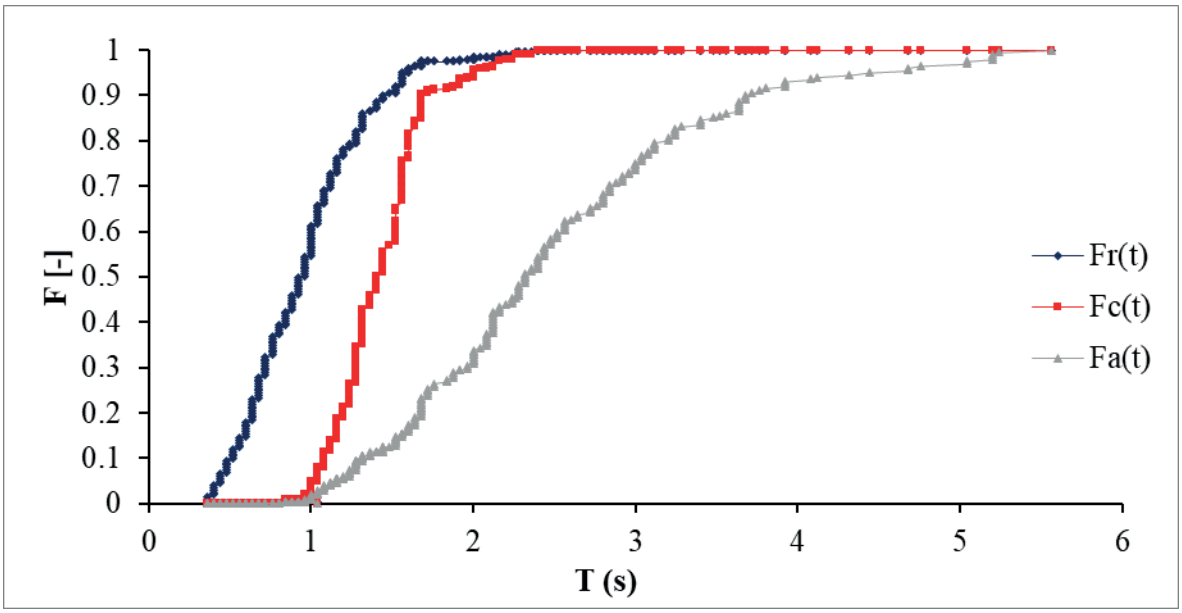


***Figure 7*** *Schematic relationships between the PDFs for rejected gaps, accepted gaps and estimated critical gaps from PEM*

range makes it extremely complex to study the driver behavior aspects, like the critical gap at intersections under prevailing traffic conditions. The critical gap is one of the major parameters for gap acceptance models. The accuracy of the critical gap mainly determines the accuracy of the capacity estimation. This study focuses on implementing the probability equilibrium method to find out the driver's critical gap in heterogeneous traffic scenarios as MLM does not efficiently produce any result as the maximized value did not converge due to the widespread between the accepted and maximum rejected gaps at the location with significant pedestrian influence. This simplified approach also shows that the probability density function (PDF) of the critical gap always lies between the functions of accepted and rejected gaps shown in Figure 7.

The reliable capacity of the roundabout can be found with help of the critical gap and follow-up time. The critical gap obtained from the PEM method is 1.58 s for the candidate roundabout in Jaipur, while it is 1.62 s for the candidate roundabout in Trivandrum. Similarly, the critical gap was also derived for the different time intervals with the varying pedestrian flow at the non-base location to assess the reduction in entry capacity due to the same. Now, the second component for the capacity estimation, i.e. follow-up time, is also evaluated at the roundabout under the queueing conditions, i.e. saturation condition. If the two consecutive vehicles from the minor stream enter the roundabout using the same gap, then the minimum time gap between the two consecutive vehicles is known as the follow-up time. Various factors affect the variation of the follow-up time, including the type of the vehicle, the number of vehicles queued behind, the traffic volume position of the vehicle in the queue and the drivers' personal parameters. In the present study, vehicle category-wise follow-up time in the queued condition is found by considering the following vehicle as to the subject vehicle. As discussed earlier, a substantial amount of delay and queue formation is observed at the candidate roundabout in Jaipur, i.e. the Chomu House roundabout; the follow-up time estimation analysis for the base section was carried out. The results showed that the weighted average follow-up time is 1.24 s. Similarly, the analysis has been extended to a non-base location and the follow-up time is estimated for varying pedestrian flow levels. The estimated critical gap and follow-up time values at the non-base location are shown in Table 3.

## 8 Estimation of reduction in entry capacity due to pedestrian cross flow

As mentioned in Equation (1), the entry capacity by the HCM method depends upon the critical gap ($t_c$) and follow-up time ($t_f$) values. The HCM has given values for $t_c$ and $t_f$ as 4.5 s and 2.7 s, respectively. In a comparison of these values to values obtained in the present study for candidate roundabouts (Table 3), the values are found to be lower. This can be attributed to the maximum share of Motorized two-wheelers in the traffic stream and the absence of heavy vehicle traffic at the candidate roundabouts. From the previous section, the values of $t_c$ and $t_f$ are obtained as 1.58 s and 1.24 s, respectively. These values are obtained by the weighted average depending upon the present traffic composition. With the use of these values and the field circulatory flow values, the entry capacity of the roundabout is estimated using the HCM equation. The results showed that the entry capacity value by using the present study values and the HCM method is lower than the field capacity value observed in the equivalent units, i.e. PCU/h. The mean absolute percentage error (MAPE) is found to be 11.80%. Hence, it can be concluded that the HCM cannot be used directly for Indian conditions and there is a need to develop an adjustment factor for estimation of capacity for Indian conditions. The ratio of the entry flow value to the value given by HCM is taken as the adjustment factor [29]. A range of the adjustment factors is obtained that varies between 0.98 and 1.25. Hence, the average value of all the adjustment factors is suggested for evaluating capacity in mixed traffic conditions. The adjustment factor of 1.10 for HCM equation gives the same value of entry capacity observed in the field. This adjustment factor is used with field data and a modified plot for entry capacity is shown as illustrated in Figure 8. Thus, Equation (3) portrays the entry capacity estimation equation for roundabouts operating under a mixed traffic environment.

***Table 3*** *Estimated entry capacity values at the base and non-base locations*

| Sr. No. | Pedestrian volume (peds/h) | Critical gap (s) | Follow up time (s) | Entry Capacity (PCU/h) | Reduction in entry capacity |
|---|---|---|---|---|---|
| Base Section - Chomu House Roundabout | Nil | 1.58 | 1.24 | 3223 | Base |
| 1 | 124 | 2.07 | 1.17 | 2715 | 15.76% |
| 2 | 146 | 2.46 | 1.1 | 2740 | 14.98% |
| 3 | 206 | 1.80 | 1.29 | 2355 | 26.93% |
| 4 | 212 | 3.35 | 1.18 | 2200 | 31.74% |
| 5 | 288 | 1.78 | 1.65 | 1841 | 42.87% |

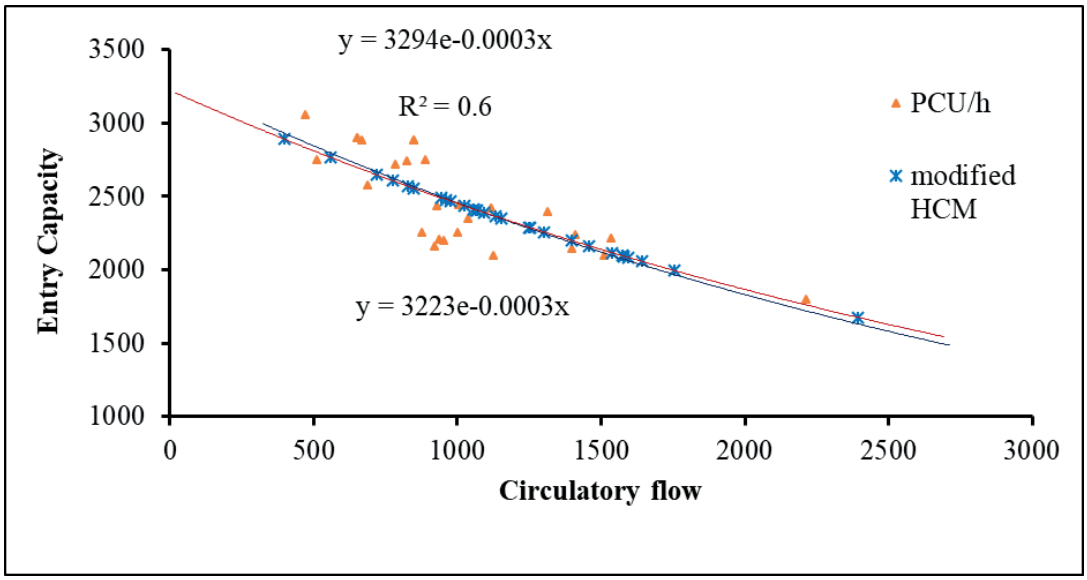


***Figure 8*** *Modified HCM model for heterogeneous traffic condition*

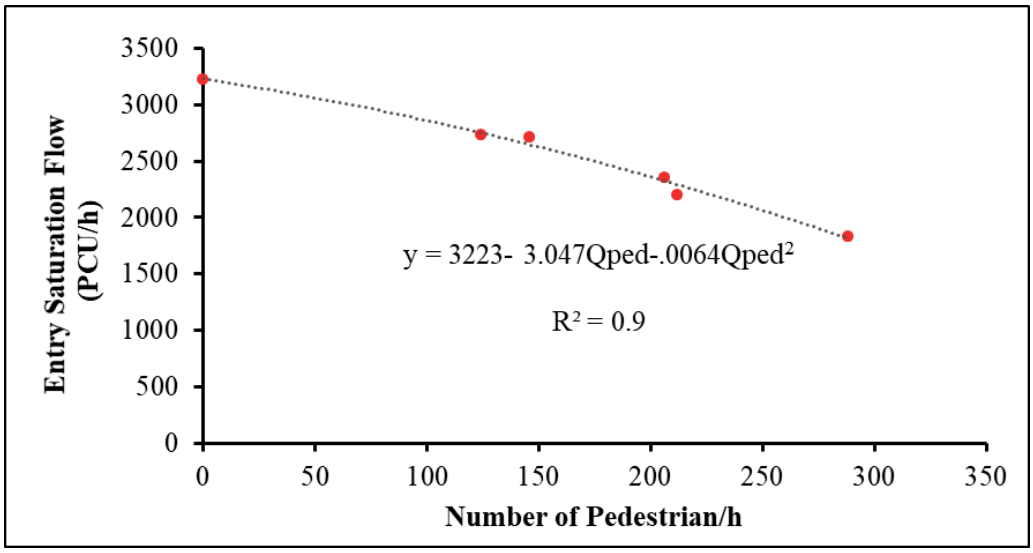


***Figure 9*** *Reduction in entry capacity of the roundabout with respect to pedestrian volume*

$$Q_e = 3223e^{-0.0003Qc}. \quad (3)$$

The number of pedestrians crossing that particular leg can affect the entry capacity. As the number of pedestrians increases, the entry capacity might probably reduce. In the present study, entry saturation flow was found and compared to the pedestrian volume at the roundabout with significant pedestrian movement (Surat Location) shown in Table 3. Further, the entry capacity value has been compared to the base value generated by the modified HCM Method.

To find out the trend in reduction of entry saturation flow due to the undesignated crosswalk of pedestrians, a plot has been generated between the pedestrian volume and entry capacity, shown in Figure 9. The relationship between entry saturation flow and pedestrian volume is found to be negative second-degree polynomial relation, indicating that with an increase in pedestrian flow rate, the entry capacity of the roundabout decreases at a second-degree polynomial rate. The $R^2$ value of Equation (4) is strong enough to capture the variation.

$$Entry\ capacity = 3223 - 3.047(Q_{ped}) - \\ - 0.0064(Q_{ped})^2. \quad (4)$$

The entry capacity taking account of pedestrians, is then

$$Q_{e,ped} = \begin{pmatrix} 3223 - 3.047(Q_{ped}) - \\ - 0.0064(Q_{ped})^2 \end{pmatrix} e^{-0.0003Q_c}. \quad (5)$$

It is better to use a reduction factor like

$$Q_{e,ped} = \begin{pmatrix} 3223 - 3.047(Q_{ped}) - \\ - 0.0064(Q_{ped})^2 \end{pmatrix} e^{-0.0003Q_c}. \quad (6)$$

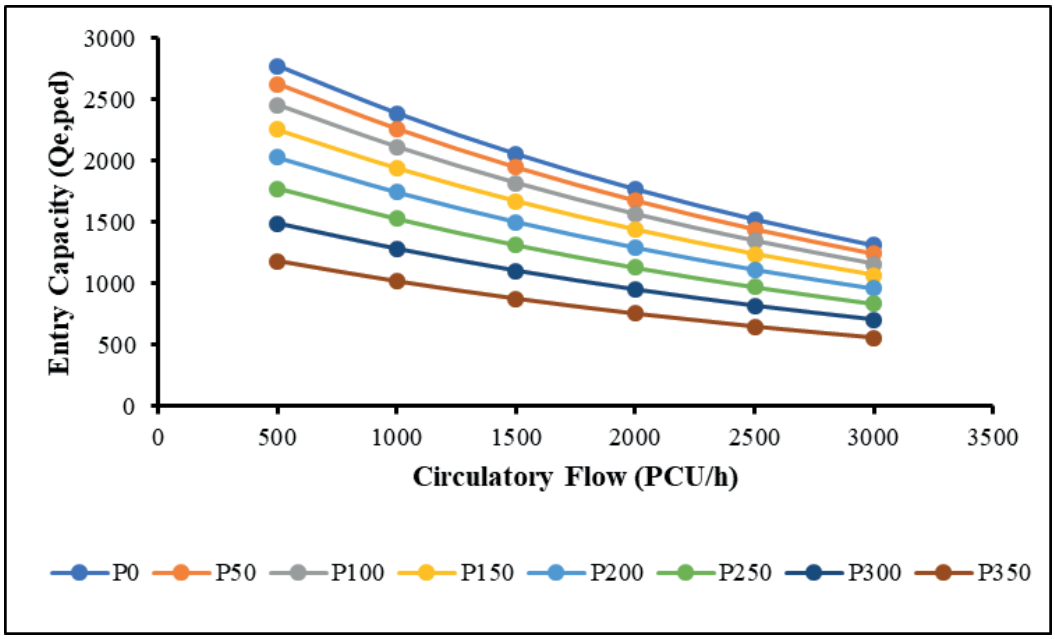


***Figure 10*** *Entry capacity of the roundabout with respect to pedestrian volume*

This reduction factor can be applied to all the possible capacity values.

The entry capacity taking account of pedestrians is then

$$Q_{e,ped} = Q_e * f_{ped} . \quad (7)$$

Figure 10 shows the effect of pedestrian flow on the roundabout entry capacity.

## 9 Conclusions

The present study has been taken up with the prime objective to determine reduction in the entry capacity of a roundabout due to influence of the crossing pedestrians in the roundabout area. Selected roundabouts are operating under mixed traffic conditions as prevails in India and pedestrian are crossing at grade in the roundabout area without any marked crosswalk in order to access their point of interest. Such conditions are not uncommon in developing countries like India. Three roundabouts in different regions of the country have been selected for the study to quantify the influence of pedestrian flow on roundabout capacity. Two of the selected roundabouts have no pedestrian cross flow and hence are termed as the base sections, whereas the third roundabout has the significant number of crossing pedestrians during the observation time and is termed as the non-base section. The entry capacity of a roundabout for the base sections has been determined using the HCM equation. The HCM equation takes into account two parameters i.e. the critical gap and follow up time. The accepted and rejected gaps have been determined from field collected data and the critical gap has been estimated using the PEM method. The follow up time is also determined from the field data. It is observed that the critical gap is 1.58 s, whereas the follow up time is 1.24 s for the base section. Values of the critical gap and follow up time are quite lower than the values suggested by the HCM [10]. The lower values of critical gap and follow up time are attributed to the high proportion of the two wheelers and very low proportion of the heavy vehicles in the traffic stream. The two wheelers accepted a very lower gap for merging in the circulatory stream what ultimately brings down the low values of critical gap. These low values of the critical gap and follow up time lead to the higher capacity values, as compared to those determined from the HCM equation and therefore a correcting factor of 1.10 is presented in this study. Further, it is observed that with the pedestrian cross flow the accepted gap and follow up time values are increasing due to the fact that presence of pedestrians yields the entry vehicle and the accepted gap size (value in time) higher than those of the base conditions. The higher values of the critical gap and follow up time ultimately result in the lower capacity values. It is observed that the entry capacity reduces with increase in pedestrians' cross flow. A negative second-degree polynomial equation has been proposed to determine the entry capacity relation to number of crossing pedestrians. It is observed that initially the reduction is low at smaller number of crossing pedestrians and the reduction in capacity increases with the increase in pedestrians' cross flow. This is attributed to the fact that more pedestrians are causing more hindrance to the entry vehicle.

**References**


[1] GOLAKIYA, H. D., DHAMANIYA, A. Modeling speed and capacity estimation at urban midblock sections under the influence of crossing pedestrians. *Journal of Transportation Engineering, Part A: Systems* [online]. 2019, **145**(9), 04019036. ISSN 2473-2907. Available from: https://doi.org/10.1061/jtepbs.0000260

[2] GOLAKIYA, H. D., PATKAR, M., DHAMANIYA, A. Impact of midblock pedestrian crossing on speed characteristics and capacity of urban arterials. *Arabian Journal for Science and Engineering* [online]. 2019, **44**(10), p. 8675-8689. ISSN 2191-4281. Available from: https://doi.org/10.1007/s13369-019-03786-x

[3] MACIOSZEK, E. Roundabout entry capacity calculation - a case study based on roundabouts in Tokyo, Japan and Tokyo surroundings. *Sustainability* [online]. 2020, **12**(4), 1533. ISSN 2071-1050. Available from: https://doi.org/10.3390/su12041533

[4] SEVERINO, A., PAPPALARDO, G., CURTO, S., TRUBIA, S., OLAYODE, I. O.. Safety evaluation of flower roundabout considering autonomous vehicles operation. *Sustainability* [online]. 2021, **13**(18), 10120. ISSN 2071-1050. Available from: https://doi.org/10.3390/su131810120

[5] RODEGERDTS, L. *Roundabouts in the United States*. Washington, D. C.: Transportation Research Board, 2007. ISBN 9780309098748.

[6] KHAN, A., DHAMANIYA, A., ARKATKAR, S. Modification in HCM delay model for roundabout for mixed traffic conditions - a pilot study. *Communications - Scientific Letters of the University of Zilina* [online]. 2022, **24**(2), p. D92-D104. ISSN 1335-4205, eISSN 2585-7878. Available from: https://doi.org/10.26552/COM.C.2022.2.D92-D104

[7] TROUTBECK, R. J., BRILON, W. Unsignalized intersection theory. In: *Traffic-flow theory*. 2001. p. 1-47.

[8] MACIOSZEK, E. The comparison of models for critical headways estimation at roundabouts [online]. In: *Contemporary challenges of transport systems and traffic engineering*. MACIOSZEK, E., SIERPINSKI, G. (eds.). Lecture notes in networks and systems. Vol. 2. Cham: Springer, 2017. ISBN 978-3-319-43984-6, eISBN 978-3-319-43985-3, p. 205-2019. Available from: https://doi.org/10.1007/978-3-319-43985-3_18

[9] Highway Capacity Manual (HCM). Special Rep. No. 209. 4. ed. Washington, D. C.: Transportation Research Board, 2000.

[10] Highway Capacity Manual (HCM). Washington, D. C.: Transportation Research Board, National Research Council, 2010.

[11] Indo-HCM. Indian Highway Capacity Manual. 2017.

[12] CHUNG, E., YOUNG, W., AKCELIK, R. Comparison of roundabout capacity and delay estimates from analytical and simulation models. In: 16th Conference of the Australian Road Research Board: proceedings. Vol. 16(5). 1992. ISSN 0572-1431, p. 369-385.

[13] LI, Z., DEAMICO, M., CHITTURI, M. V., BILL, A. R., NOYCE, D. A. Calibration of VISSIM roundabout model: a critical gap and follow-up headway approach. In: 92nd Annual Meeting of Transportation Research Board: proceedings. 2013. p. 1-22.

[14] GALLELLI, V., VAIANA, R. Roundabout intersections: evaluation of geometric and behavioural features with VISSIM. In: TRB National Roundabout Conference: proceedings. 2008. p. 1-19.

[15] SHAABAN, K., KIM, I. Comparison of SimTraffic and VISSIM microscopic traffic simulation tools in modeling roundabouts. *Procedia Computer Science* [online]. 2015, **52**, p. 43-50. ISSN 1877-0509. Available from: https://doi.org/10.1016/j.procs.2015.05.016

[16] ECHAB, H., EZ-ZAHRAOUY, H., LAKOUARI, N. Simulation study of interference of crossings pedestrian and vehicle traffic at a single lane roundabout. *Physica A: Statistical Mechanics and its Applications* [online]. 2016, **461**, p. 854-864. ISSN 0378-4371. Available from: https://doi.org/10.1016/j.physa.2016.06.006

[17] IRC-65. Recommendation practice for traffic rotaries. New Delhi: Indian Road Congress, 1976.

[18] SCHROEDER, B. J., ROUPHAIL, N. M. Mixed-priority pedestrian delay models at single-lane roundabouts. *Transportation Research Record: Journal of the Transportation Research Board* [online]. 2010, **2182**, p. 129-138. ISSN 0361-1981, eISSN 2169-4052. Available from: https://doi.org/10.3141/2182

[19] MENEGUZZER, C., ROSSIA, R. Evaluating the impact of pedestrian crossings on roundabout entry capacity. *Procedia-Social and Behavioral Sciences* [online]. 2011, **20**, p. 69-78. ISSN 1877-0428. Available from: https://doi.org/10.1016/j.sbspro.2011.08.012

[20] AKCELIK, R. An assessment of the highway capacity manual 2010 roundabout capacity mode. In: International Roundabout Conference of Transport Research Board: proceedings. 2011.

[21] AL-GHANDOUR, M., SCHROEDER, B., RASDORF, W., WILLIAMS, B. Delay analysis of single-lane roundabout with a slip lane under varying exit types, experimental balanced traffic volumes and pedestrians, using microsimulation. *Transportation Research Record: Journal of the Transportation Research Board* [online]. 2012, **2312**(1), p. 76-85. ISSN 0361-1981, eISSN 2169-4052. Available from: https://doi.org/10.3141/2312-08

[22] CHANDRA, S., RASTOGI, R. Mixed traffic flow analysis on roundabouts. *Journal of the Indian Roads Congress*. 2012, **73**(1), p. 69-77. ISSN 0258-0500.

[23] KANG, N., NAKAMURA, H., ASANO, M. Estimation of roundabout entry capacity under the impact of pedestrians by applying microscopic simulation. *Transportation Research Record: Journal of the Transportation Research Board* [online]. 2014, **2461**, p. 113-120. ISSN 0361-1981, eISSN 2169-4052. Available from: https://doi.org/10.3141/2461-14

[24] AHMAD, A., RASTOGI, R. An approach to deal with heterogeneity on roundabouts. *International Journal of Civil Engineering* [online]. 2017, **15**(4), p. 585-598. ISSN 2383-3874. Available from: https://doi.org/10.1007/s40999-017-0189-4

[25] OSEI, K. K., ADAMS, CH. A., ACKAAH, W., OLIVER-COMMEY, Y. Signalization options to improve capacity and delay at roundabouts through microsimulation approach: a case study on arterial roadways in Ghana. *Journal of Traffic and Transportation Engineering* [online]. 2021, **8**(1), p. 70-82. ISSN 2095-7564. Available from: https://doi.org/10.1016/j.jtte.2019.06.003

[26] SONU, M., DHAMANIYA, A., ARKATKAR, S., JOSHI, G. Time occupancy as measure of PCU at four legged roundabouts. *Transportation Letters* [online]. 2016, latest articles, p. 1-12. ISSN 1942-7867, eISSN 1942-7875. Available from: https://doi.org/10.1080/19427867.2016.1154685

[27] WU, N. Total approach capacity at signalized intersections with shared and short lanes; generalized model based on a simulation study. *Transportation Research Record: Journal of the Transportation Research Board* [online]. 2007, **2027**, p. 19-26. ISSN 0361-1981, eISSN 2169-4052. Available from: https://doi.org/10.3141/2027-03

[28] WU, N. A new model for estimating critical gap and its distribution at unsignalized intersections based on the equilibrium of probabilities. In: 5th International symposium on Highway Capacity and Quality of Service of Service: proceedings. 2006. p. 1-10.

[29] MAHESH, S., AHMAD, A., RASTOGI, R. An approach for the estimation of entry flows on roundabouts. *Transportation Research Procedia* [online]. 2016, **17**, p. 52-62. ISSN 2352-1465. Available from: https://doi.org/10.1016/j.trpro.2016.11.060

# CRITICAL GAP ESTIMATION AND ITS IMPLICATION ON CAPACITY AND SAFETY OF HIGH-SPEED UN-SIGNALISED T-INTERSECTION UNDER HETEROGENEOUS TRAFFIC CONDITIONS

**Khushbu Bhatt** [1,*], **Ninad Gore** [2], **Jiten Shah** [1]

[1]Civil Engineering Department, Institute of Infrastructure, Technology Research and Management, Ahmedabad, Gujarat, India
[2]Civil Engineering Department, Toronto Metropolitan University (Formerly Ryerson University), Toronto, Canada

*E-mail of corresponding author: k22112011@gmail.com

***Resume***
In India, priority rules at un-signalized intersections are often ignored by drivers. The present paper reports the applicability of deterministic and probabilistic methods for estimating the critical gaps at high-speed un-signalized T-intersections. The critical gap is estimated for different vehicle types and crossing movements. The study quantifies the implication of critical gap values on the capacity and safety values at un-signalized T-intersections. The results point to conclusion that the value obtained for the critical gap using deterministic methods is lower than that estimated by the probabilistic method. The gap values estimated using the Binary Logit Regression method are similar to those computed using the equation reported in Indo-HCM (2017). It was concluded that a lower value of the critical gap yields a higher capacity value and a higher value of risk probability.

***Article info***
Received 9 July 2022
Accepted 22 September 2022
Online 20 October 2022

***Keywords:***
critical gap
un-signalized intersections
safety, capacity
probability of risk

Available online: https://doi.org/10.26552/com.C.2022.4.D215-D228

ISSN 1335-4205 (print version)
ISSN 2585-7878 (online version)

## 1 Introduction and background

Drivers' gap acceptance behavior significantly affects the traffic operation and the safety of un-signalized intersections. While manoeuvering through the intersection, the driver accepts or rejects the available gap. The characteristics of the approaching or conflicting vehicle, traffic volume, intersection characteristics (type of control, intersection characteristics) and the characteristics of the offending vehicle (subject vehicle performing crossing manoeuvers) affect the driver's decision to accept or reject an available gap [1]. Further, heterogeneity due to drivers' demographics, like age, gender, experience and driving behavior results in the dynamic nature of accepted gaps. Poor acceptance of gaps is a major reason for crashes at un-signalized intersections [2]. The magnitude of the accepted gap governs the risk while manoeuvering through the intersection. For instance, a driver accepting larger gaps is at lower risk than drivers accepting smaller gaps.

The critical gap, the derived value of a gap, is the most used indicator to estimate the safety and capacity at un-signalized intersections. The critical gap is defined as "the minimum gap that all the drivers in the traffic stream are assumed to accept at similar locations" [3]. "Generally, it is assumed that the driver's critical gap is greater than the largest gap rejected and shorter than the accepted gap for that driver." Generally, the drivers accept all the gaps greater than the critical gap and reject gaps lesser than the critical gap. This definition holds if the drivers in the traffic stream are homogeneous. However, considering heterogeneity in drivers due to perception-reaction time, risk-taking behavior and demographics, a certain proportion of drivers accept a gap smaller than the critical one. It implies that the value of the critical gap could be used as a measure in addition to accepted gaps to gauge the prevailing levels of safety at un-signalized intersections.

The critical gap value varies from driver to driver, among the intersection, as per the traffic movements and traffic situations. Incorrect estimates of the critical gap value led to inappropriate design of the road components. Different methods were developed in the past for estimating values of the critical gaps at

intersections\. Broadly, the methods for critical gap estimation can be categorized into (a) deterministic methods and (b) probabilistic methods. These methods are developed for homogeneous and lane-disciplined based traffic conditions.

Raff's method was developed in the early '50s to analyze the lag data and it can be used for small traffic volumes [4]. The result is highly dependent on the conflicting traffic volume [5-6]. The modified method of the previous method was the lag method, which requires sufficient lag data for each interval of time, which is not easily available and needs longer observation periods. Raff's method rejects the major valuable data and does not consider the gap data. This results in the over-representation of aggressive behavior of the driver and it is the major drawback of this method [6-8]. In 1968, the Ashworth method was developed to overcome the negative aspects of Raff's method. The Ashworth method illustrated the empirical distribution function considering the mean and standard deviation of the accepted gap. This method disregarded the biased results by using the probability distribution curve. This method assumes that the gap is exponentially distributed and that the critical gap is normally distributed. In this method, the value of the critical gap is highly dependent on the major street traffic volume, which is the major limitation [6].

A method that represents the critical gap, based on a histogram by using the total number of the gap acceptances and rejections is known as the Greenshields Method. The same extent of acceptances and rejections is obtained for the critical gap value estimation. The critical gap value is acquired as the mean value of acceptance and rejection. This method considers only a smaller quantity of samples leading to misinterpretation of the results and this is the major limitation of this method [9-11].

Similar to the lag method, a harder's method is developed, which considers only the value of the accepted gap and average floating value rather than lag. This method assumes that the gap value lies within the interval of 1 to 21 seconds. It overestimates the critical gap value when only the gap data is considered, but the result improvises when the lag value is also included [6-8]. The critical gap shows the properties of the cumulative distribution function and the value fluctuates, which is the major drawback of this method [11].

A logit model can be characterized using the binary logit model as a utility function, which is an alteration in the safety and reduction in delay time. This model generally deals with the gap acceptance behavior of the driver and it obtains the optimum value of critical gap as per past research studies [12]. Seigloch method requires the vehicle count of the major street under continuous queuing. The value of the critical gap estimated using this method is stochastic. However, it is not suitable for estimating the values for different turning movements and under saturated traffic conditions. Hence, its practical application is impossible.

The most predominant method used for estimating the critical gap values over the last two decades is the Maximum likelihood method [3-4, 6, 13]. This method assumes that the driver behavior is homogeneous and consistent. This method estimates the value based on probability of lying between the accepted and rejected gap. However, this method is unsuitable for heterogeneous traffic conditions and overestimates the value of a cautious driver [8]. A simple alternative method, the Probability Equilibrium Method (PEM), was established, which does not include any complex calculation. The concept is based on the probability equilibrium of accepted and rejected gaps by the cumulative distribution function. The advantage of this method is that it applies to a smaller sample size [14-15]. An advanced method is the Acceptance curve, based on empirical and theoretical considerations [11]. The disadvantage of this method is that for fewer gap data intervals, it will not provide S- a shaped curvilinear curve. The values will float, resulting in an inaccurate estimation of the critical gap [16]. A Probit method is based on fitting a weighted linear regression line to gap data after dividing the time interval [16]. It is unreliable and gives biased results compared to other methods [4]. Another method is Hewitt, which is an iteration method to estimate the value of a critical gap, however there is a doubt on its applicability for heterogeneous traffic conditions.

A Clearing Time Approach method is similar to Raff's method and estimates the value based on the cumulative distribution curve of accepted gap ($F_a$) and Clearing time ($F_r$). The clearing time is defined as the time interval required by the vehicle to cross the conflict area of the intersection. However, the limitation of this method is that the critical gap is a function of the accepted and rejected gap [8]. An Occupancy Time Method is an improved version of the clearing time approach method [17]. It includes the cumulative distribution of accepted gap and occupancy time, based on the traffic condition. An advantage of this method is that it is applicable for heterogeneous, as well as homogeneous traffic conditions. All the existing methods used to estimate the critical gap are described briefly above. A summary of the methods, their advantage, limitation, data requirements and applicability can be found in detail in [18-19].

The literature review reveals that various methods were developed for estimating critical gap values. The applicability of various methods and their comparative appraisal is widely studied for homogeneous traffic conditions. Few studies have estimated the critical gap values for un-signalized intersections [8, 11, 20]. However, very few studies in the past have estimated the critical gaps for the high-speed un-signalized intersections under mixed traffic conditions. The critical gap value influences the capacity and safety at un-signalized

intersections. Therefore, the variation in the critical gap value ought to influence the capacity and safety at un-signalized intersections. However, to the best of the authors' knowledge, the implication of a critical gap on capacity and safety at un-signalized intersections is not well reported. With the following inspiration, the purpose of the present study is framed as below.

(a) To estimate the critical gap values by vehicle type and crossing movement at the high-speed un-signalized intersections.
(b) To analyze the implication of the critical gap value on capacity and safety of the high-speed un-signalized intersections.

## 2 Critical gap estimation methods

In the present study, four methods, i.e., Raff's, Ashworth, Occupancy Time and Binary Logit, are adopted to estimate the critical gap for the high-speed un-signalized intersections. Raff's, Ashworth's and Occupancy time methods fall under deterministic methods, whereas the Binary Logit method is considered as a probabilistic method. The methods are discussed next.

### 2.1 Raff's method

Raff's method was introduced in 1950 for estimating the value of the critical gap [21]. Due to its simple application, several authors have used the Raff method to estimate the critical gap for homogenous and heterogeneous traffic conditions. The cumulative sum of the accepted and the rejected gap equals 1 [22]. However, the limitation of this method is that it does not consider the lag data. Lag is the time interval between the arrival of a yielding vehicle and the way of the next priority stream vehicle. Therefore, the Raff's method was modified, also known as Modified Raff's method. The mathematical representation of this method is:

$$F_a(t) + F_r(t) = 1. \tag{1}$$

As per this method, the value of the critical gap is the gap for which the accepted gap is larger than the critical gap and gaps shorter than the critical gap are rejected gaps. In Equation (1), $F_a$ and $F_r$ are the cumulative probabilities of the accepted and the rejected gaps. The intersecting point of the cumulative distribution curve of the accepted and rejected gaps is a critical gap.

### 2.2 Ashworth method

In 1968, the Ashworth method was developed to estimate the critical gap by using the mean and standard deviation values of the accepted gap. These result in the elimination of the unfair results obtained by the probability distribution curve. The gap follows the exponential distribution and the critical gap value follows the normal distribution obtained by this method. As per NRC (National Research Council, 1966), the estimation of the critical gap can be done using the following equation,

$$t_c = \mu - p\sigma_a^2, \tag{2}$$

where $\mu$ is the mean accepted gap, $\sigma_a$ is the standard deviation, $p$ is the traffic volume in vehicles per second and $t_c$ is the critical gap value. The main limitation of this method is that the value obtained for the critical gap is highly correlated with the major street traffic volume [6].

### 2.3 Occupancy time method

Under the prevailing mixed traffic condition, priority rules at unsignalised intersections are violated in India. The drivers perceive equal priority from major and minor approaches, resulting in high risk at intersections. The driver's aggressive behavior during the turning from minor to major is observed due to accepting smaller gaps and rolling over to the major traffic stream. The available gap gets altered due to this type of aggressive behavior of the driver while manoeuvering. Therefore, the occupancy time method is proposed and advocated to estimate the critical gap in this kind of aggressive crossing behavior [16].

The occupancy time method is the modified form of the clearing time approach method [8]. It is generally defined as the „total time required by a vehicle executing the priority movement to occupy the conflict area". The occupancy time is influenced by driver behavior, intersection geometry, type of subject vehicle and opposing vehicular traffic [1, 6, 23].

The Occupancy Time Method states that "*for a low priority movement to clear the intersection area through the gap in conflicting flow, the following inequality must be satisfied*" [1]:

$$P(t_a > t) \geq P(ot \leq t)), \tag{3}$$

where, $P$ is the probability of an event, $t_a$ is the accepted gap, $t$ is the time gap and *ot* is the occupancy time.

Based on the above equation, the critical gap is the intersection point of intersection of the cumulative frequency curves of accepted gaps (1 - $F_a$) and occupancy time ($F_{ot}$). Moreover, the speed of the conflicting vehicle significantly affects the gap size and critical gap. However, this method does not explicitly account for the effect of speed on the critical gap value and, therefore, forms a major limitation.

### 2.4 Binary logit regression method

The decision for the available gap (to accept or reject) varies among the drivers and is random and discrete. Therefore, choice of the modelling methods can be extended to model drivers' decisions and estimate the critical gap value. The deterministic term of observed utility is a function of different variables that influence the gap acceptance behavior at an uncontrolled intersection. The utility function is defined in the mathematical form below:

$$V_i = \alpha + \beta_1 x_1 + \beta_2 x_2 + \cdots + \beta_n x_n\,, \tag{4}$$

where $V_i$ is the deterministic component of the utility of selecting a particular substitute. α is constant, $x_1$, $x_2$ ….. $x_n$ are independent variables and $\beta_1$, $\beta_2$……$\beta_n$ are the weighted coefficients.

If the model is developed for rejected gaps, then the probability of rejection using the binary logit model can be calculated as:

$$P = \frac{\exp(V_i)}{1 + \exp(V_i)}. \tag{5}$$

The gap corresponding to a 50% probability of acceptance or rejection is termed a critical gap. As per different studies, the researchers concluded that the value obtained from this method is the smallest [12]. It is reported that better results may be obtained if only the gap data is used. However, the method would provide underestimated critical gap value if the lag data is considered, as well [6]. Moreover, the method enables to study of the effect of waiting time on the critical gap [24]. In the present study, the decision to a gap, i.e., accepted or rejected, was modelled as a function of the gap size, the waiting time of the following vehicle and the speed of the conflicting vehicle. The critical gap was estimated for two types of crossing movements (major to the minor street and minor to the major street) and for four classified vehicle types to represent the heterogeneous traffic conditions.

## 3 Data

As per the MORTH (2020) [25] statistics on road accidents in India, 20.7% of intersection-related crashes are contributed by uncontrolled intersections. Further, uncontrolled T-intersections contributed to 35% of the intersection-related fatalities among all the intersection types. Therefore, un-signalized T-intersections were the main focus of the analysis. The traffic data for three un-signalized T-intersections were collected using videography on rural highways with similar geometry. The snapshots of the selected study locations are shown in Figure 1. The intersections are sufficiently away from the upstream and downstream of the other intersections, ensuring that the traffic flow is unaffected by the nearby intersections. In addition to that, during the data collection, each intersection approach was free from adjacent encroachments. The geometric and traffic details of the selected study intersections are summarized in Table 1. Traffic video for the subject study intersections was collected by


***Figure 1*** *Snapshot of study sections and position of the camera*


***Figure 2*** *Methodology for the extraction of (a) gap (b) occupancy time*

placing a high-definition camera (frame rate of 33 frames per second) near a high-rise building to serve as a vantage point. The traffic video was collected to capture the natural driving behavior. The data was collected on a weekday in November and December under fair weather conditions for 12 hours (9:00 AM to 9:00 PM). All the physical dimensions of the intersections were measured manually during the free-flow traffic conditions with the aid of the traffic police. The videos were recorded such that at least 200 m on major roads and 100 m on minor roads are visible. The camera location for collecting the traffic data is illustrated in Figure 1.

The selected intersections are represented as L1, L2 and L3, respectively. The three traffic movements are classified as M1, M2 and M3, where M1 represents the traffic from the major stream manoeuvering to minor stream and M2 is the traffic movement from minor stream to major stream; both M1 and M2 are the right-turning movements and are critical at un-signalized intersections. The major and minor streams are categorized and defined as per the Indian Highway Capacity Manual [26]. M3 is the approach comprised of the major through traffic. Figure 1 represents the snapshots of the study section.

### 3.1 Data extraction

In countries like India, the left-turning movement at the intersection is free. Therefore, the gap in acceptance for the right turning movement from major and minor approaches, which are the critical movements at the intersection. Hence, data for the right-turning movements are only extracted and analyzed. In the absence of a trustworthy automatic traffic data extractor, the gap, occupancy and speed data were extracted manually by repeatedly playing the video file in the laboratory. Figure 2 illustrates the conceptual diagram for extracting gap and occupancy time data. The gap and occupancy time was measured in 1/100$^{th}$ of a second.

#### 3.1.1 Extracting the gap size and driver‘s decision

The gap is referred to as the time headway between the two consecutive vehicles in the major and minor traffic stream, as shown in Figure 2(a) [8]. The gap data (size and decision) was extracted from the recorded video. The data extraction resulted in 868 gaps for the major right turn and 622 for the minor right turn (including both accepted and rejected gaps) for the subject study locations. Both accepted and rejected gaps by vehicle type and crossing movements were extracted for all three locations.

#### 3.1.2 Extracting the occupancy time

Occupancy time is defined as the „time occupied by the vehicle in the conflicting area until the driver accepts the gap for manoeuvering through the intersection“ [27]. Figure 2b shows the conflict area of the intersection where the two traffic streams interact.

#### 3.1.3 Extracting the speed of the conflicting vehicle

For each location, depending upon the visual clarity and appropriateness of the data requirements, trap lengths of 37, 46 and 50 m were marked on the approach to calculate the speed of conflicting vehicles. The speed of the conflicting vehicle is calculated by noting the time difference a vehicle takes to clear the trap length of the respective length. The speed is then calculated by dividing the length of the intersection by the time taken to clear the trap.

#### 3.1.4 Extracting the waiting time of offending vehicle

The waiting time of the vehicle is extracted by noting the time until the right-turning vehicle accepts

the gap and merges into the traffic stream. If the driver approaches the intersection and accepts the first gap, then in such cases, the waiting time of the right-turning driver is recorded as zero.

## 4 Results and discussion

### 4.1 Preliminary analysis

The traffic composition at all three intersections was classified under six categories, which are motorized two-wheelers (M2W), motorized three-wheelers (M3W), four-wheelers (Cars), light commercial vehicles (LCV), buses and trucks. A summary of classified traffic configuration is illustrated in Table 2.

M2W dominates the traffic composition at the study intersections with a share of 50-63 %, followed by 4W (17-30 %) and 3W (5-17 %). For L-3, the proportion of heavy vehicles (including LCVs, buses and trucks) is 14.8 %, whereas the same for L-1 and L-2 was 4.05 % and 6.01 %. Table 2 summarizes the descriptive statistics of gap and occupancy time data.

The accepted gap and occupancy time vary significantly by crossing movement and vehicle type (Table 3). For instance, drivers of M2W and M3W accept the smaller gaps compared to the drivers of cars and heavy vehicles, which can be attributed to the easy manoeuverability of motorized two-wheeler and three-wheeler. This implies that drivers of 2W and 3W tend to roll over and accept smaller gaps, highlighting aggressive driving behavior. The variation in the values of occupancy time corroborates the observation (lower value of occupancy time for 2W and 3W compared to 4W and HV). A smaller value of occupancy time also highlights aggressive driving behavior [1].

A lower value of accepted gap can be noted for drivers performing right turning movement from major to minor stream. On the contrary, drivers accept larger gaps when performing right turning movement from a minor to a major approach. At high speed, un-signalized T-intersections, the vehicle along the major approach travels at a higher speed. Therefore, the drivers of the minor approach exhibit safe and cautious gap-acceptance behavior. The safe driving behavior can also be seen from the higher values of occupancy time for the minor approach compared to the major approach. The variation in the magnitude of accepted gaps and occupancy time, by type of vehicle and crossing movement, significantly influences the critical gap value. Therefore, in the present study, the critical gap is estimated by the type of vehicles and the right-turning movements. The estimation of the critical gap using different methods is explained in further sections.

### 4.2 Critical gap estimation

#### 4.2.1 Raff's method

Raff's method is one of the oldest methods for estimating the value of the critical gap. As per Raff's method, the critical gap is the point of intersection of the cumulative percentile curves of accepted gaps F (a) and rejected gaps 1-F(r), as shown in Figure 3. Here, the critical gap for L1 is shown as an example. From Figure 3, 2.72 s represents the critical gap for L1. The critical gap is estimated by the type of vehicle and right-turning movement for each location. The results are summarized in Table 4.

#### 4.2.2 Ashworth method

This method is very simple and effortless to apply. The three different types of input are required to estimate the critical gap. This section calculates the critical gap for all three locations for the vehicle type by following the procedure explained earlier. The extracted accepted gap was used to evaluate the mean and standard deviation for different vehicle types for each location. The critical gap is estimated by type of the vehicle and the right-turning movements for each location and the results are summarized in Table 4.

***Table 2*** *Descriptive statistics of the gap and occupancy time by crossing movement and vehicle type*

| Vehicle Type | Accepted Gap (s) | | | | Occupancy Time (s) | |
|---|---|---|---|---|---|---|
| | Major Right Turn | | Minor Right Turn | | Major Right Turn | Minor Right Turn |
| | N | Mean (SD) | N | Mean (SD) | Mean (SD) | Mean (SD) |
| M2W | 326 | 3.52(1.70) | 214 | 3.45(1.56) | 5.09(1.74) | 5.45(2.02) |
| M3W | 233 | 3.49(1.36) | 194 | 3.61(1.42) | 5.06(1.70) | 5.22(1.93) |
| Cars | 234 | 3.87(1.34) | 159 | 4.12(1.47) | 5.92(2.74) | 5.62(1.92) |
| HV | 75 | 4.76(1.51) | 55 | 5.03(1.40) | 6.87(2.42) | 7.12(2.52) |

Note: N: Number of samples; SD: Standard deviation; M2W: motorized two-wheelers; M3W: motorized three-wheelers; HV: Heavy vehicles (LCV, buses and trucks combined)

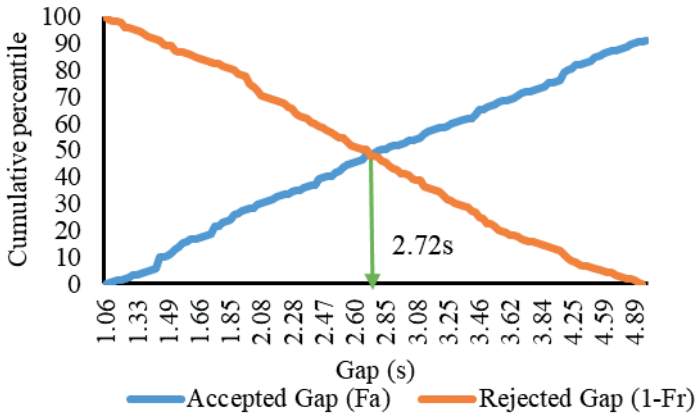


***Figure 3*** *Critical gap for location 1 by the Raff's method*

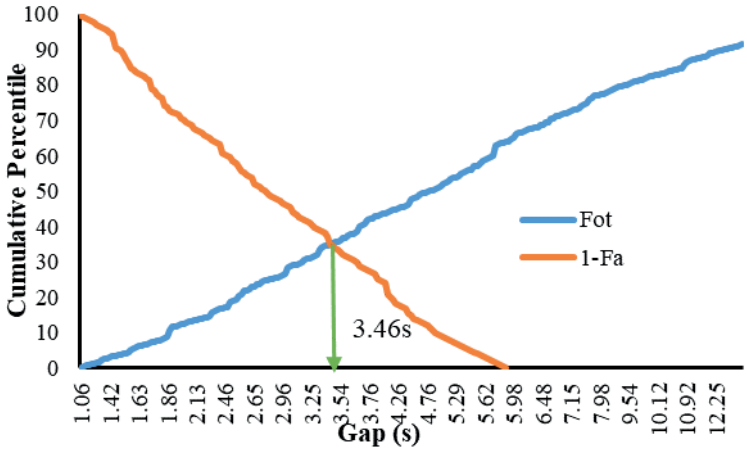


***Figure 4*** *Critical gap for location 1 by occupancy time method*

***Table 3*** *Binary logit model by vehicle type and crossing movement*

| Major Right Turning Movement | | | | |
|---|---|---|---|---|
| Variable | Vehicle Type | | | |
| | 2W | 3W | 4W | HV |
| Constant (SE) | 3.820 (0.736) | 2.879 (0.828) | -1.066 (0.765) | 4.366 (0.452) |
| G (SE) | -1.125 (0.150) | -1.623 (0.266) | -1.230 (0.206) | -0.324 (0.315) |
| WT (SE) | -0.216 (0.131) | -0.542 (0.217) | -0.580 (0.148) | -0.201 (0.209) |
| CS (SE) | 0.012 (0.015) | 0.010 (0.016) | 0.086 (0.020) | 0.41 (0.031) |
| Log-likelihood function | -295.153 | -225.771 | -234.434 | -81.826 |
| Cox and Snell R squared | 0.336 | 0.323 | 0.304 | 0.152 |
| Nagelkerke R squared | 0.455 | 0.431 | 0.405 | 0.205 |
| Minor Right Turning Movement | | | | |
| Variable | Vehicle Type | | | |
| | 2W | 3W | 4W | HV |
| Constant (SE) | 4.255 (0.835) | 4.446 (0.947) | -0.212 (0.046) | 6.242 (.156) |
| G (SE) | -0.726 (0.154) | -1.433 (0.287) | -0.528 (0.160) | -0.280 (0.310) |
| WT (SE) | -0.194 (0.109) | -0.324 (0.214) | -0.0390 (0.118) | -0.359 (0.251) |
| CS (SE) | 0.013 (0.017) | 0.030 (0.017) | 0.085 (0.023) | 0.081 (0.040) |
| Log-likelihood function | 218.346 | 186.525 | 174.398 | 155.956 |
| Cox and Snell R squared | 0.275 | 0.311 | 0.241 | 0.215 |
| Nagelkerke R squared | 0.37 | 0.415 | 0.321 | 0.289 |

Note: G: Gap Size (s); WT: Waiting Time (s); CS: Speed of Conflicting vehicle; SE: Standard error. All variables are significant at 95% CI

#### 4.2.3 Occupancy time method

An occupancy time method (OTM) effectively estimates critical gaps under mixed traffic conditions [1]. This method incorporates aggressive driving behavior for estimating critical gaps. According to the occupancy time, the critical gap is the intersecting point of the cumulative frequency curves of accepted gaps ($1\text{-}F_a$) and occupancy time ($F_{ot}$), as shown in Figure 4.

Here, 3.46 s represents the critical gap value for L-1 (location-1). The critical gap is estimated by the type of a vehicle and the right-turning movements for each location. The results are summarized in Table 4.

#### 4.2.4 Critical gap estimation using the Binary Logit Regression Method (BLRM)

In the present study, the drivers' decision for gap i.e. to accept or reject an available gap, was modelled as a function of the gap size, waiting time of the offending vehicle and the speed of the conflicting vehicle using the binary logit regression. The model summary is shown in Table 3.

For all the models developed in the present study, a negative coefficient can be noted for the gap size. It implies that as the gap size increases, the probability of rejection decreases, or the probability of acceptance increases. Similarly, a positive sign for the speed of the conflicting vehicle can be noted. This highlights that as the speed of the conflicting vehicle increases, the probability of rejecting a gap increases. Consistent observations can be noted for both crossing movements and different vehicle types.

A negative coefficient can be noted for the waiting time. This implies that the probability of rejection decreases as the waiting time increases. This highlights that as the waiting time increases, the drivers become impatient and force themselves into the traffic stream by accepting and rolling over smaller gaps to manoeuver through the intersection. Consistent observations can be noted for both crossing movements and different vehicle types. The present study is the first to report the effect of the waiting time of offending vehicles on the gap-acceptance phenomenon under the mixed traffic conditions.

The critical gap is estimated by calculating the gap corresponding to the 50% probability of acceptance or rejection. The estimated value of the critical gap by vehicle type and crossing movement is summarized in Table 4.

#### 4.2.5 Critical gap estimation using Indo-HCM

The average critical gap is evaluated using the base critical gap, which depends on the geometry of the section, the proportion of large vehicles and an adjustment factor depending on the movement and vehicle type as per Indo-HCM -2017 and then based on the Equation (6) the critical gap is estimated.

$$t_{cx} = t_{cb} + f_{lv} * \ln(P_{lv}). \quad (6)$$

The critical gap is estimated by vehicle type and crossing movement for each location and the results are summarized in Table 4.

Table 4, illustrates that the critical gap varies significantly by type of a vehicle and the right-turning movements. For instance, lower critical gap values can be noted for M2Ws (1.18 sec) and M3Ws (1.62 s) compared to cars (2.08 s) and HVs (2.54 s). This implies that drivers of different vehicle types, i.e. M2Ws and M3Ws exhibit aggressive driving behavior (accept and rollover smaller gaps) compared to cars and HV. The results of the critical gap corroborate the observations deduced from Table 4 for different categories of vehicles and the right turning movements. The lower value of the critical gap also highlights that drivers of M2Ws and M3Ws are at a higher risk than drivers of cars and HVs. Consistent observation can be noted for the critical gap estimated using different methods.

Further, the lower critical gap values can be noted when drivers from a major approach take a right turn to merge into the minor stream (Refer to Table 4). This highlights that drivers from the major approach exhibit aggressive crossing behavior (accepting smaller gaps and lower occupancy time) as the priority rules at unsignallised intersection are not followed. On the contrary, drivers of the minor stream reveal cautious gap-acceptance behavior. This can be attributed to the fact that at high-speed un-signalized T-intersections, the vehicle along the major approach travels at a higher speed. Therefore, the drivers of the minor approach exhibit safe and cautious gap-acceptance behavior. This can be witnessed from the values of occupancy time and the accepted gap. Consistent observation can be deduced using different methods of critical gap estimation. It can also be observed that the critical gap varied between the subject study locations for a given vehicle type and crossing movement. The variation in the critical gap can be attributed to variation in traffic volume, speed of the vehicles and driving behavior characteristics.

From Table 4, it is evident that the critical gap estimated using different methods varies significantly. For instance, the lower value of the critical gap for different vehicle types and crossing movements was estimated using Ashworth's method compared to other methods. However, larger values of the critical gap are estimated using the BLRM. It is important to note that the values of the critical gap, estimated using deterministic methods (Raff's method, Ashworth method and Occupancy time method) are lower than the critical gap estimated using the probabilistic method (BLRM). The critical gap estimated using the BLRM is in close agreement with the values estimated using the Indo-

***Table 4*** *Critical gap by vehicle type and crossing movements*

| Major Right Turning | | | | | | |
|---|---|---|---|---|---|---|
| Location | Vehicle Type | Raff's Method | Ashworth Method | Occupancy Time method | Indo-HCM | BLRM |
| L1 | M2W | 1.60 | 1.56 | 1.64 | 2.78 | 2.24 |
| | M3W | 1.86 | 1.75 | 2.56 | 3.07 | 3.18 |
| | Cars | 2.52 | 2.25 | 3.52 | 3.50 | 3.59 |
| | HV | 2.96 | 2.54 | 4.36 | 4.28 | 3.92 |
| | Average | 2.23 | 2.02 | 3.02 | 3.40 | 3.23 |
| L2 | M2W | 1.82 | 1.62 | 2.20 | 2.53 | 2.76 |
| | M3W | 2.08 | 1.81 | 2.26 | 2.72 | 3.12 |
| | Cars | 2.37 | 2.37 | 2.59 | 3.28 | 3.62 |
| | HV | 2.76 | 2.83 | 3.45 | 3.96 | 4.18 |
| | Average | 2.25 | 2.15 | 2.62 | 3.12 | 3.42 |
| L3 | M2W | 2.18 | 2.09 | 2.18 | 2.88 | 2.84 |
| | M3W | 2.42 | 2.26 | 2.52 | 3.32 | 3.26 |
| | Cars | 2.87 | 2.54 | 3.16 | 3.65 | 3.48 |
| | HV | 3.53 | 3.39 | 3.48 | 4.04 | 3.62 |
| | Average | 2.75 | 2.57 | 2.83 | 3.47 | 3.30 |
| Minor Right Turning | | | | | | |
| Location | Vehicle Type | Raff's Method | Ashworth Method | Occupancy Time method | Indo-HCM | BLRM |
| L1 | M2W | 1.96 | 1.18 | 2.06 | 2.56 | 2.54 |
| | M3W | 2.23 | 2.02 | 2.85 | 3.44 | 3.38 |
| | Cars | 3.58 | 2.24 | 3.85 | 3.62 | 3.94 |
| | HV | 3.05 | 2.68 | 4.07 | 4.05 | 4.18 |
| | Average | 2.71 | 2.03 | 3.21 | 3.42 | 3.51 |
| L2 | M2W | 1.90 | 1.26 | 1.45 | 2.32 | 2.45 |
| | M3W | 2.14 | 1.65 | 2.86 | 3.46 | 3.82 |
| | Cars | 2.42 | 2.08 | 3.25 | 3.85 | 3.96 |
| | HV | 2.86 | 2.57 | 3.84 | 4.16 | 4.28 |
| | Average | 2.33 | 1.89 | 2.85 | 3.45 | 3.63 |
| L3 | M2W | 2.25 | 1.44 | 2.08 | 3.14 | 2.48 |
| | M3W | 2.68 | 1.62 | 2.16 | 3.58 | 3.26 |
| | Cars | 2.96 | 2.25 | 3.54 | 4.06 | 3.88 |
| | HV | 3.17 | 2.89 | 4.29 | 4.22 | 4.15 |
| | Average | 2.77 | 2.05 | 3.02 | 3.75 | 3.44 |

Note: All values in seconds (s)

HCM [25]. It is important to mention that the critical gap estimated using the BLRM explicitly considers different factors such as gap size, waiting time of the offending vehicle and speed of the conflicting vehicle on the drivers' decision and hence, the critical gap. Therefore, the critical gap estimated using the probabilistic method could be deemed robust and consistent [17]. The impact of varying critical gap values on capacity and safety is discussed next.

### 4.3 The implication of critical gap to capacity

The critical gap is the most popularly used to estimate the capacity of the un-signalized intersection and further identify the section's level of service (LOS). The intersection's capacity enables planners and engineers to comprehend the prevailing LOS. The capacity of un-signalized intersections depends on the value of critical gap and follow-up time, conflicting volume and road geometric features. The capacity for un-signalized intersection is as:

$$C_x = a * V_{cx} \frac{e^{-Vcx(tcx-b)}/3600}{1-e^{-Vcx \cdot tfx}/3600}, \quad (7)$$

where, $C_x$ is Capacity of movement (in PCU/h); $V_{cx}$ is conflicting volume corresponding to the movement in PCU/hr, $t_{cx}$ is the critical gap in seconds (s), $t_{fx}$ is follow-up time in seconds (s); $a$ and $b$ are the adjustment factors based on intersection geometry.

***Table 5*** *Capacity in PCU/h using different methods of critical gap estimation*

| Location | Raff's Method | Ashworth Method | OTM | Indo-HCM | BLRM |
|---|---|---|---|---|---|
| Major Right Turn | | | | | |
| L-1 | 1866 | 2213 | 1053 | 815 | 903 |
| L-2 | 1809 | 1955 | 1340 | 928 | 754 |
| L-3 | 1106 | 1293 | 1033 | 612 | 702 |
| Minor Right Turn | | | | | |
| L-1 | 1000 | 1680 | 708 | 618 | 582 |
| L-2 | 1250 | 1824 | 835 | 545 | 483 |
| L-3 | 747 | 1429 | 605 | 337 | 429 |

Note: All values in PCU/h

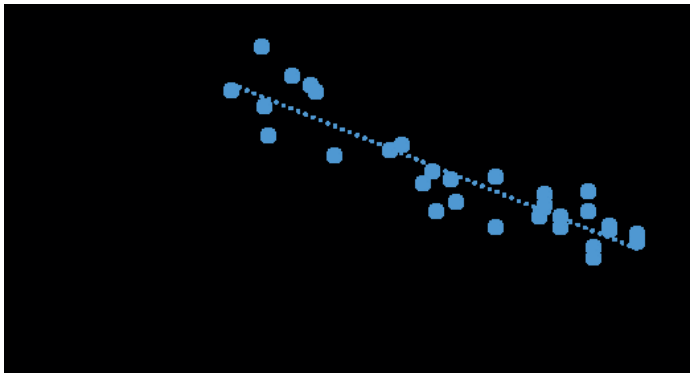

***Figure 5*** *Variation in capacity with the critical gap*

Un-signalized intersections are characterized by frequent merging, diverging and crossing operations. The presence of heterogeneity and non-lane-based aggressive traffic complicates the traffic operations. Crossing operations are the most critical at un-signalized intersections compared to other legal movements [27]. A crossing operation involves turning for merging into a major stream or diverging into a minor stream. Therefore, the present section estimates capacity values only for the right-turning operations. Table 5 summarizes the capacity values estimated using different methods of critical gap estimation by crossing movement.

From Table 5, a significant variation in capacity values obtained using different methods of the critical gap, is evident. Higher capacity values can be noted for critical gap values estimated using Ashworth's method (1293-2213 PCU/h). The capacity value obtained from the deterministic method is quite high (605-2213 PCU/h). However, the critical gap estimated using the BLRM yields a lower capacity value (429-582 PCU/h) for the minor right turn than (702-903 PCU/h) for major right turn. Further, for different crossing movements, smaller capacity values can be noted for the minor approach compared to the major approach. Further, a significant variation in capacity between the subject study locations can be noted. The variation in capacity values by crossing movement, study locations and different methods can be attributed to variation in critical gap values. To probe further, the variation in capacity with the critical gap is analyzed using a scatter plot, as shown in Figure 5. Here, the results obtained using different methods are merged.

A negative correlation between capacity and the critical gap is estimated in Figure 5. The lower value of the critical gap yields the higher value of the capacity. It is observed that with a lower critical gap, the majority of the drivers accept lower gap values. As a result, higher capacity values can be noted.

### 4.4 The implication of the critical gap on safety

The decision to cross the intersection is measured using the gap (i.e. accepted or rejected). In general, the drivers often reject the smaller gap and accept the larger gap. Thus, a driver accepting a larger gap endures lesser risk than a driver accepting a smaller one in the traffic stream. This implies that risk (R) is an inverse function of the magnitude of the accepted gap. Therefore, mathematically risk can be represented as:

$$Risk(R) = \frac{1}{Accepted\ gap(s)}. \tag{8}$$

Based on the above equation, a smaller value of the accepted gap indicates the higher risk and vice-versa. The concept of Probability of Critical Crossing Conflicts (PCCC) is used as an indicator of operational risk at un-signalized intersections [27]. The PCCC is derived by

modelling the post encroachment time (PET) data using the extreme value theory (EVT). In the present study, Probability of Risk (POR), an indicator of operational risk based on accepted gaps, is derived. The computation of POR is explained next.

The Generalized Pareto (GP) and Generalised Extreme Value (GEV) are the two most popular extreme value distributions used by researchers to model the variation of different traffic conflict indicators. Past studies have reported that the best-fitted distribution to model the variation in the risk is the generalized extreme value (GEV) distribution [28-36].The safety of an un-signalized intersection has been evaluated using the EVT. The technique has shown potential for use in safety-related studies and is now widely used in conflict and crash-related studies. Recently, researchers have demonstrated the applicability of EVT theory in estimating the number of crashes [30-32]. Therefore, the GEV distribution is used to derive the POR in the present study.

Consider X1, X2, X3,…Xm as independent random variables (in the present case, the value of risk) with a similar probability distribution, where Yn = max (X1, X2, X3,…., Xm). When n→∞, the Yn will converge to a GEV distribution [27], as shown:

$$f(x) = \frac{1}{\sigma}\exp\left(-(1+kz)^{-\frac{1}{k}}(1+kz)^{-\frac{1}{k}}\right)^{-1-\frac{1}{k}} \quad k \neq 0, \tag{9}$$

where, $z = (x - \mu)/\sigma$, $\mu$ is the location parameter, $\sigma$ is the scale parameter and $k$ is the shape parameter.

The POR is defined as an area under the probability density function of GEV distribution between the thresholds of gap representing serious conflicts. The POR can be computed using the following

$$Probability\ of\ risk\,(POR) = \int_{LL}^{ULL} f(x)dx\,, \tag{10}$$

where, $f(x)$ is the probability density function of GEV distribution, *LL* and *UL* represent the Lower and Upper limits of risk, representing the critical conflicts, respectively.

Recently, the critical gap could characterize the risk of crossing conflicts. Based on the critical gap value, the risk of crossing conflict was characterized as serious and non-serious conflicts [36]. Therefore, the critical gap value was used in the present study to evaluate the POR of the un-signalized T-intersections.

Considering the critical gap as a threshold to define serious conflict, the Equation (11) to estimate POR can be rewritten as:

$$Probability\ of\ risk\,(POR) = \int_{\min imum\ risk}^{risk\ at\ critical\ gap} f(x)dx\,. \tag{11}$$

A higher value of POR indicates that most of the crossing manoeuvers are serious and hence, the safety is poorer. The value of POR can facilitate monitoring of the level of operational risk at un-signalized intersections. Intersections with a higher POR value are riskier and unsafe than intersections with a lower POR value. The probability of risk (POR), obtained using different critical gap estimation methods, is summarized in Table 6 by location and type of crossing movement.

When different methods are compared to each other, the POR values revealed a wide variation. A higher value of POR was observed for the Ashworth method, whereas lower values of POR can be noted for BLRM and Indo-HCM methods. The difference in POR can be recognized by the critical gap value. The POR estimated for Indo-HCM and BLRM method is similar and statistically insignificant, attributed to the similar critical gap values (Refer to Table 5). Further, it can be noted that the POR varied between different crossing movements. A lower value of the probability of risk can be noted when drivers of the minor approach accept the gap to merge into the major approach. At high speed, un-signalized T-intersections, the vehicle along the major approach travels at a higher speed. Therefore, the drivers of the minor approach exhibit safe and cautious gap-acceptance behavior. On the contrary, drivers of the major stream accept and roll over smaller gaps and, thus, endure higher risk.

The variation in POR with the critical gap was analyzed using a scatter plot, as shown in Figure 6. A negative correlation between the probability of risk and the critical gap value is evident. For location 3, from Tables 5 and 6 lowering the value (2.77 sec) of the critical gap results in a higher (62%) probability of risk for location 3. Therefore, intersections with a higher

***Table 6*** *Probability of Risk using different critical gap estimation methods*

| | | Major Right Turn | | | |
|---|---|---|---|---|---|
| Location | Raff's Method | Ashworth Method | OTM | Indo-HCM | BLRM |
| L-1 | 0.70 | 0.77 | 0.42 | 0.36 | 0.36 |
| L-2 | 0.66 | 0.72 | 0.52 | 0.26 | 0.26 |
| L-3 | 0.56 | 0.65 | 0.54 | 0.37 | 0.37 |
| | | Minor Right Turn | | | |
| L-1 | 0.41 | 0.64 | 0.28 | 0.22 | 0.22 |
| L-2 | 0.73 | 0.88 | 0.53 | 0.30 | 0.30 |
| L-3 | 0.62 | 0.88 | 0.52 | 0.37 | 0.37 |

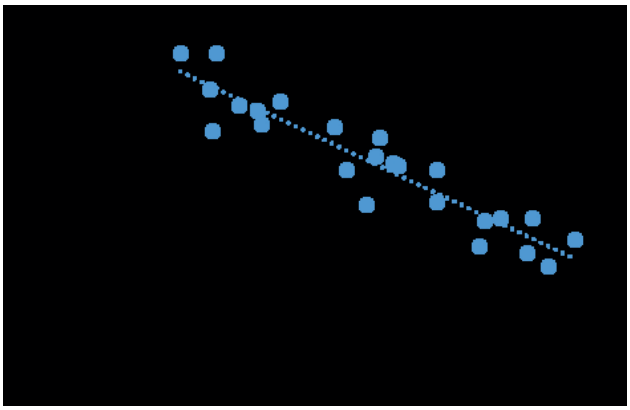

***Figure 6*** *Variation in the probability of risk with critical gap*

critical gap (3.44 sec) have a risk of (37 %) and are safer than intersections with a lower critical gap value. Overall, it can be concluded that the magnitude of the accepted gap and the value of the critical gap jointly influence the safety of un-signalized T-intersections.

## 5 Conclusions and way forward

At un-signalized T- intersections in India, a significant number of crashes and fatalities are recorded as compared to other types of intersections. Crossing conflict is one of the severe types compared to other types at un-signalized intersections. Driver's gap acceptance behavior influences traffic operations and safety at un-signalized intersections. A driver accepts or rejects the available gap for crossing movement through the intersection. The present paper explores and compares different methods of the critical gap for the high-speed un-signalized T-intersection under heterogeneous traffic conditions. The study also explores the implication of the critical gap value on the capacity and safety at an un-signalized T-intersection. The traffic data is collected for three high-speed un-signalized T-intersections and the critical gap for the study area is estimated using deterministic (Raff's, Ashworth's, and Occupancy Time Method) and probabilistic methods (Binary Logit Regression method) The comparative analysis of the estimation of the critical gap is illustrated. Some of the important conclusions, drawn from the present study, are discussed below:

1. The critical gap varies significantly by vehicle type. A lower value of the critical gap was noted for motorized two-wheelers (1.18 s) and motorized three-wheelers (1.62 s) compared to cars (2.08 s) and heavy vehicles (2.54 s). This implies that motorized two-wheelers and motorized three-wheelers manoeuver through the intersection by accepting the smaller gaps in the traffic stream, thereby enduring higher risks.
2. The critical gap values vary significantly by crossing movement. A higher value of the critical gap was noted when drivers from the minor approach performed the right-turning operation to merge into the major approach than the drivers performing the right-turning operations from the major approach. This can be attributed to the fact that at high-speed un-signalized T-intersections, the vehicle along the major approach travels at a higher speed. Therefore, the drivers of the minor approach exhibit safe and cautious gap-acceptance behavior.
3. The critical gap estimated using different methods varies significantly. For a given vehicle type and crossing movement, a lower value (1.56 s) of the critical gap (from Table 5) was derived using Ashworth's method, whereas a relatively higher value (2.24 s) of the critical gap was derived using the Binary Logit Regression method. Consistent observations were noted for different vehicle types and crossing movements.
4. For various vehicle types and crossing movement, a lower value of the critical gap is derived using the deterministic methods (Raff's method, Ashworth's method and Occupancy Time method) compared to the critical gap derived using the probabilistic method (Binary Logit Regression method). Moreover, the gap values estimated using the Binary Logit Regression method are similar to those computed using equation reported in Indo-HCM (2017).
5. The value of the critical gap significantly influences the capacity and safety of un-signalized intersections. A higher capacity value (2213 PCU/h) was noted for smaller critical gap values (2.02 s). On the other hand, a higher probability of risk (POR) (77 %) was observed for smaller critical gap values.

The estimated critical gaps do not capture the effect of the age, gender of the driver, passenger occupancy, other physical activities, variation in climate and traffic encroachments on the gap acceptance behavior. The effect of the factors mentioned above on the critical gap can be studied. The selected study areas are on high-speed un-signalized T-intersections. Therefore, the transferability of different critical gap estimation methods to un-signalized intersections in an urban area can be studied. The probability of risk can be evaluated by the vehicle type and varying traffic volume

levels. The derived POR values can be modelled as a function of traffic flow and intersection geometry-related characteristics. The severity of the crossing conflict could be quantified by correlating the size of the accepted gap and the speed of the conflicting vehicle. Further, drivers' dilemmas at un-signalized intersections can be modelled and the implication of the length of the dilemma on safety can be quantified. The study can be extended to analyze the variation in the gap acceptance based on the traffic volume by collecting more data on the sites and at different time durations.

## Data availability

Some or all data, models, or codes that support the findings of this study are available from the corresponding author upon reasonable request.

## References


[1] MOHAN, M., CHANDRA, S. Three methods of PCU estimation at unsignalized intersections. *Transportation Letters* [online]. 2018, **10**(2), p. 68-74. ISSN 1942-786, eISSN 1942-7875. Available from: https://doi.org/10.1080/19427867.2016.1190883

[2] BRILON, W., WU, N. *Unsignallised intersections - a third method for analysis* [online]. Adelaide, Australia: Pergamon-Elsevier Publications, 2002. ISBN 978-0-080-43926-6, eISBN 978-0-585-47460-1. Available from: https://doi.org/10.1108/9780585474601-009

[3] TROUTBECK, R., BRILON, W. *Unsignalized intersection theory*. US: Federal Highway Administration, 1997.

[4] MILLER, A. Nine estimators of gap acceptance parameters. *Traffic Flow and Transportation*. 1972, **0**, p. 215-235.

[5] HURWITZ, D. Connecting gap acceptance behavior with crash experience. In: 3rd International Conference on Road Safety and Simulation: proceedings. 2011.

[6] BRILON, W., MILTNER, T. Capacity at intersections without traffic signals. *Transportation Research Record: Journal of the Transportation Research Board* [online]. 2005, **1920**(1), p. 32-40. ISSN 0361-1981, eISSN 2169-4052. Available from: https://doi.org/10.1177/03611981051920001

[7] CHANDRA, S., MOHAN, M., GATES, T. Estimation of the critical gap using intersection occupancy time. In: 19th International Conference of Hong Kong Society for Transportation Studies: proceedings. 2017.

[8] ASHALATA, R., CHANDRA, S. Critical gap through clearing behavior of drivers at unsignalised intersections. *KSCE Journal of Civil Engineering* [online]. 2011, **15**(8), p. 1427-1434. ISSN 1226-7988, eISSN 1976-3808. Available from: https://doi.org/10.1007/s12205-011-1392-5

[9] HARWOOD, D., MASON, J., FITZPATRICK, K., HARWOOD, D., Field observations of truck operational characteristics related to intersection sight distance. *Transportation Research Record: Journal of the Transportation Research Board*. 1990, **1280**, p. 163-172. ISSN 0361-1981, eISSN 2169-4052.

[10] GATTIS, J., LOW, S. Gap acceptance at a typical stop-controlled intersection. *Journal of Transportation Engineering* [online]. 1999, **125**(3), p. 201-205. ISSN 2473-2907, eISSN 2473-2893. Available from: https://doi.org/10.1061/(ASCE)0733-947X(1999)125:3(201)

[11] AMIN, H., MAURYA, A. A review of critical gap estimation approach at an uncontrolled intersection in case of heterogeneous traffic conditions. *Journal of Transport Literature* [online]. 2015, **9**(3), p. 5-9. eISSN 2238-1031. Available from: https://doi.org/10.1590/2238-1031.jtl.v9n3a1

[12] VASCONCELOS, A., SECO, A., SILVA, A. Comparison of procedures to estimate critical headways at roundabouts. *Promet - Traffic and Transportation* [online]. 2013, **25**(1), p. 43-53. ISSN 0353-5320, eISSN 1848-4069. Available from: https://doi.org/10.7307/ptt.v25i1.1246

[13] TROUTBECK, R. J. Estimating the critical acceptance gap from traffic movements. Brisbane: Queensland University of Technology, Queensland University of Technology. Physical Infrastructure Centre. 1992.

[14] ELANGO, S., RAMYA, A., RENITA, A., RAMANA, M., REVATHY, S., RAJAJEYAKUMAR, M. An analysis of road traffic injuries in India from 2013 to 2016: a review article. *Journal of Community Medicine and Health Education* [online]. 2018, **8**(2), p. 601-609. ISSN 2161-0711. Available from: https://doi.org/10.4172/2161-0711.1000601

[15] PAUL, M., GHOSH, I. Speed-based proximal indicator for the right-turn crash at unsignalized intersections in India. *Journal of Transportation Engineering, Part A: Systems* [online]. 2018, **144**(6). ISSN 2473-2907, eISSN 2473-2893. Available from: https://doi.org/10.1061/JTEPBS.0000139

[16] MOHAN, M., CHANDRA, S. Critical gap estimation at two-way stop-controlled intersections based on occupancy time data. *Transportmetrica A: Transport Science* [online]. 2018, **14**(4), p. 316-329. ISSN 2324-9935, eISSN 2324-9943. Available from: https://doi.org/10.1080/23249935.2017.1385657

[17] BHATT, K., SHAH, J. An impact of gap acceptance on road safety: a critical systematic review. *Journal of Sustainable Development of Transport and Logistics* [online]. 2022, **7**(1), p. 6-22. ISSN 2520-2979. Available from: https://doi.org/10.14254/jsdtl.2022.7-1/1

[18] BHATT, K., SHAH, J. Driver's risk compelling behavior for crossing conflict area at a three-legged uncontrolled intersection. In: *Intelligent Infrastructure in Transportation and Management* [online]. SHAH, J., ARKATKAR, S. S., JADHAV, P. (eds.). Studies in Infrastructure and Control. Singapore: Springer, 2022. ISBN 978-981-16-6935-4, eISBN 978-981-16-6936-1. Available from: https://doi.org/10.1007/978-981-16-6936-1_4

[19] PATIL, G., SANGOLE, J. Gap acceptance behavior of right-turning vehicles at T- intersections - a case study. *Journal of the Indian Roads Congress*. 2015, p. 44-54. ISSN 0258-0500.

[20] MOHAN, M., CHANDRA, S. A review and assessment of techniques for estimating critical gap at two-way stop-controlled intersections. *European Transport / Trasporti Europei*. 2016, **61**(61), p. 1-18. ISSN 1825-3997.

[21] RAFF, M., HART, J. *A volume warrant for urban stop signs*. Saugatuck, USA: Eno Foundation for Highway Traffic Control, 1950.

[22] MOHAN, M., CHANDRA, S. Capacity estimation of unsignallised intersections under heterogeneous traffic conditions. *Canadian Journal of Civil Engineering* [online]. 2019, **47**(6), p. 651-662. ISSN 0315-1468, eISSN 1208-6029. Available from: https://doi.org/10.1139/cjce-2018-0796

[23] POLUS, A., LAZAR, S., LIVNEH, N. Critical gap as a function of waiting time in determining roundabout capacity. *Journal of Transportation Engineering* [online]. 2005, **129**(5), p. 504-509. ISSN 2473-2907, eISSN 2473-2893. Available from: https://doi.org/10.1061/(ASCE)0733-947X(2003)129:5(504)

[24] Road accidents in India. Ministry of Road Transport and Highways, 2019.

[25] Indian highway capacity manual. New Delhi: Council of Scientific and Industrial Research (CSIR), 2012.

[26] MOHAN, M., CHANDRA, S. Investigating the influence of conflicting flow's composition on critical gap under heterogeneous traffic conditions. *International Journal of Transportation Science and Technology* [online]. 2021, **10**(4), p. 393-401. ISSN 2046-0430. Available from: https://doi.org/10.1016/j.ijtst.2021.01.004

[27] GOYANI, J., PAUL, A., GORE, N., ARKATKAR, S., JOSHI, G. Investigation of crossing conflicts by vehicle type at unsignallised t- intersection under varying roadway and traffic condition in India. *Journal of Transportation Engineering, Part A Systems* [online]. 2021, **147**(2) p. 05020011: 1 -18. ISSN 2473-2907, eISSN 2473-2893. Available from: https://doi.org/10.1061/JTEPBS.0000479

[28] GOYANI, J., PAWAR, N., GORE, N., ARKATKAR, S. Investigation of traffic conflicts at unsignalized intersection for reckoning crash probability under mixed traffic conditions. *Journal of Eastern Asia Society for Transportation Studies* [online]. 2019, **13**, p. 2091-2110. ISSN-l 1341-8521, eISSN 1881-1124. Available from: https://doi.org/10.11175/easts.13.2091

[29] WANG, C., STAMATIADIS, N. Evaluation of a simulation-based surrogate safety metric. *Accident Analysis and Prevention* [online]. 2014, **71**, p. 82-92. ISSN 0001-4575. Available from: https://doi.org/10.1016/j.aap.2014.05.004

[30] ZHENG, L., SAYED, T. Application of extreme value theory for before-after road safety analysis. *Transp. Res. Rec* [online]. 2019, **2673**(4), p. 1001-1010. Available from: https://doi.org/10.1177/03611981198415

[31] ZHENG, L., SAYED, T. Comparison of traffic conflict indicators for crash estimation using peak over threshold approach. *Transportation Research Record: Journal of the Transportation Research Board* [online]. 2019, **2673**(5), p. 493-502. ISSN 0361-1981, eISSN 2169-4052. Available from: https://doi.org/10.1177/0361198119841556

[32] SONGCHITRUKSA, P., TARKO, A. The extreme value theory approach to safety estimation. *Accident Analysis and Prevention* [online]. 2006, **38**, p. 811-822. ISSN 0001-4575. Available from: https://doi.org/10.1016/j.aap.2006.02.003

[33] ZHENG, L., SAYED, T. From univariate to bivariate extreme value models: Approaches to integrate traffic conflict indicators for crash estimation. *Transportation Research Part C: Emerging Technologies* [online]. 2019, **103**, p. 211-225. ISSN 0968-090X. Available from: https://doi.org/10.1016/j.trc.2019.04.015

[34] ZHENG, L., SAYED, T., ESSA, M. Validating the bivariate extreme value modelling approach for road safety estimation with different traffic conflict indicators. *Accident Analysis and Prevention* [online]. 2019, **123**, p. 314-323. ISSN 0001-4575. Available from: https://doi.org/10.1016/j.aap.2018.12.007

[35] CHAUHAN, R., DHAMANIYA, A., ARKATKAR, S. Driving behavior at signalized intersections operating under disordered traffic conditions. *Transportation Research Record: Journal of the Transportation Research Board* [online]. 2021, **2675**(12), p. 1356-1378. ISSN 0361-1981, eISSN 2169-4052. Available from: https://doi.org/10.1177/036119812110338

[36] PAWAR, N., GORE, N., ARKATKAR, S. Examining crossing conflicts by vehicle type at unsignalised T- intersections using accepted gaps: a perespective from emarging countries. *Journal of Transportation Engineering, Part A: Systems* [online]. 2022, **148**(6). ISSN 2473-2907, eISSN 2473-2893. Available from: https://doi.org/10.1061/JTEPBS.0000665

# INVESTIGATION OF WEAR OF CUTTING PART OF POLYGONAL KNIFE CAR GRADERS IN DIFFERENT GROUND CONDITIONS

Rustem Kozbagarov [1,*], Marzhana Amanova [2], Nurbol Kamzanov [3], Lalita Bimagambetova [1], Aizhan Imangaliyeva [1]

[1]Academy of Logistics and Transport, Almaty, Republic of Kazakhstan
[2]Kazakh University of Transport Communications, Almaty, Republic of Kazakhstan
[3]Satbayev University, Almaty, Republic of Kazakhstan

*E-mail of corresponding author: ryctem_1968@mail.ru

***Resume***
The wear of cutting elements of auto graders allowed in practice causes an increase in the cutting force by 3 to 4 times, the energy intensity of the cutting process by 1.4 to 3 times, the cost of soil development by 8 to 15% with a decrease in productivity by 10 to 30%. This increases the stress state of the entire machine and reduces its operational reliability. Excessive wear of cutting elements leads to economic inexpediency or practical impossibility of further operation of machines.
The above-mentioned areas of research on the productive use of machines, the identification and creation of promising structures of working bodies have determined the task of further increasing the efficiency of auto graders based on improving the working elements taking into account their wear resistance.

***Article info***
Received 13 August 2022
Accepted 23 September 2022
Online 24 October 2022

***Keywords:***
auto grader
a cutting member
wear and tear
dump
soil
cutting forces

Available online: https://doi.org/10.26552/com.C.2022.4.D229-D238

ISSN 1335-4205 (print version)
ISSN 2585-7878 (online version)

## 1 Introduction

The main direction of improvement of the cutting part of the blade of the motor grader, as noted in the works [1-8], was the development of a reusable knife with a number of cutting faces more than four. Therefore, the object of theoretical research, first of all, were the parameters of the knife. The parameters of the dump were also investigated, which are influenced by an increase in the number of knives having smaller sizes compared to the standard ones. The results of the studies were supposed to provide initial data for choosing the optimal shape of the knife and the design of the blade cutting part.

The increase in the number of cutting faces necessitates that the knife be shaped like a polygon. In this case, the number of faces can be five, six, seven, eight. A further increase in the number of faces is obviously impractical due to an excessive decrease in the width of the face compared to the width of the knife.

In polygonal knives (Figure 1) [9-11], one of the cutting faces is the main working face, which forms the blade of the blade of the blade of the blade of the auto grader. At the same time, in order to ensure the continuity of the blade along its entire width, the knives are arranged in two rows. However, in addition to this face, two side faces, which are called the side working faces, also take part in cutting the soil or loosening it. They are located at an angle of more than 90° with respect to the main one. If the knife is the side knife of the dump [12-13], then one of its sides working faces will be the side face of the dump, and the second is, as it were, a leading step on the knife of the second row.

## 2 Materials and methods

During operation of dumps of motor graders equipped with polygonal knives, the main working faces of knives, forming the blade of the blade are subjected to the greatest wear [14-17]. The following geometric elements of the worn-out blade are installed by studies of the wear resistance of the cutting elements of the auto grader: a wear area located at a negative angle of inclination $\varphi$ to the cutting plane and characterized by width $a$ and the value of the $\varphi'$ angle, rounding of the front edge of the knife, characterized by a radius $r$. Since different wear elements ($r$ or $a$) can be determining in

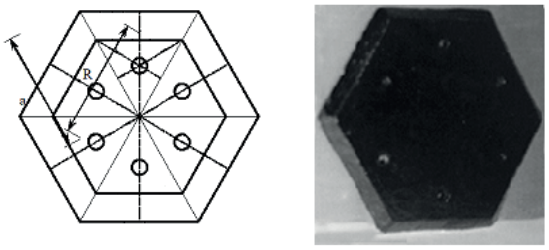


***Figure 1*** *Plate of autograder knife: a) - the diagram of the knife; b) - a general view*

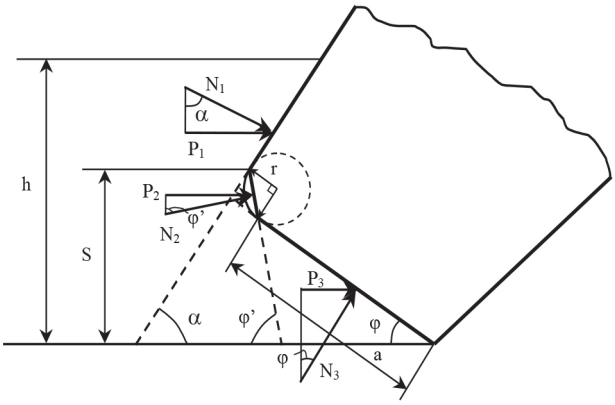


***Figure 2*** *Additional resistance forces generated at blade wear sites*

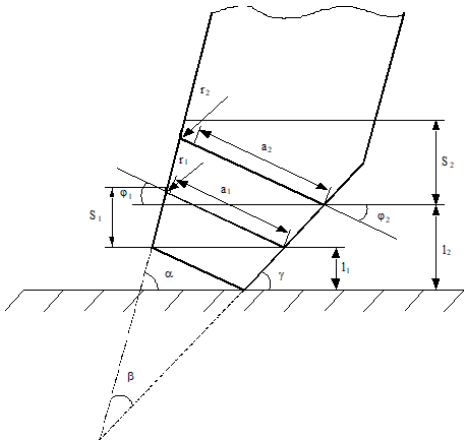


***Figure 3*** *Geometry wear of the blade of the dump of the auto grader*

different conditions, it is advisable to use the reduced wear size $S$ proposed by Kabashev [18] to expand the field of application of the derived equations, which is a complex size that takes into account both the $r$ value and the $a$ value, as well as the $\varphi$ value.

Figure 2 shows the cross-sectional diagram of the blade of a worn knife with wear zones that provide additional resistance to soil cutting. To simplify the calculation, the rounding of the front face is replaced by a flat pad at an angle 45° to the pad $a$.

Since during the knife operation all the wear areas come into contact with the ground, resistance to soil cutting of the main straight working face of the knife will be:

$$P_n' = P_1' + P_2' + P_3', \tag{1}$$

where $P'_1$ - resistance to soil cutting in the unworn blade area (above wear zones); $P'_2$ - resistance to soil cutting on the site replacing the rounded wear zone $r$; $P'_3$- resistance to soil cutting at the wear site $a$.

The ultimate resistance to cutting will be:

$$P_{Pk} = P_n' + 2P_\kappa' = P_1' + P_2' + P_3' + 2P_\kappa', \tag{2}$$

here $P'_1$ corresponds to $P'_n$, but its range is limited by the width of the site $(h - S)/2$,
where $h$ - is the depth of the soil cutting.

$$P_1' = B_n \cdot (h - S) \cdot \left(1 + f \cdot \sqrt{\frac{1}{\sin^2\varphi'} - 1}\right) = N_2 \cdot \sin(\varphi + 45^0) \cdot \left(1 + f \cdot \sqrt{\frac{1}{\sin^2(\varphi + 45^0)} - 1}\right), \tag{3}$$

or one gets:

$$P_1' = N_1 \cdot \sin\alpha \cdot \left(1 + f \cdot \sqrt{\frac{1}{\sin^2\alpha} - 1}\right), \tag{4}$$

$$P_2' = N_2 \cdot \sin\varphi' \cdot \left(1 + f \cdot \sqrt{\frac{1}{\sin^2\varphi'} - 1}\right) = N_2 \cdot \sin(\varphi + 45^0) \cdot \left(1 + f \cdot \sqrt{\frac{1}{\sin^2(\varphi + 45^0)} - 1}\right), \tag{5}$$

where $\varphi'$ - is the inclination angle of the platform $r$ to the cutting plane.

$$P_3' = N_3 \cdot \sin\varphi \cdot \left(1 + f \cdot \sqrt{\frac{1}{\sin^2\varphi} - 1}\right). \tag{6}$$

In general, the $P_{P\kappa}$ value will be:

$$P_{P\kappa} = B_n \cdot \left[(h - S) \cdot \left(1 + f \cdot \sqrt{\frac{1}{\sin^2\alpha} - 1}\right) + \frac{r}{\cos 45^0}\left(1 + f \cdot \sqrt{\frac{1}{\sin^2(\phi + 45^0)} - 1}\right)\right] \times \frac{1 - \sin\rho \cdot \cos 2\phi_H}{1 + \sin\rho \cdot \cos 2\phi_H} \cdot \left\{3 \cdot C_0 \cdot \cos\rho + \gamma_n \times \left[\frac{h - S}{2} + \frac{r \cdot \sin(\phi + 45^0)}{2 \cdot \cos 45^0} + \frac{a \cdot \sin\phi}{2}\right]\right\} + 2 \cdot [K_S \cdot B_\kappa \cdot h \cdot \mu + \varepsilon \cdot B_\kappa \cdot h \cdot \mu \cdot v^2]. \tag{7}$$

***Figure 4*** *Investigation of the wear pattern of motor grader dumps blades in production conditions*

***Table 1*** *Change of geometrical parameters of motor graders knives during operation in various soils*

| No. | Soil conditions and type of work | Classes of soil $C$ | Average development volume soil $V$ (thousand m$^3$) | Dull radius $r$ (mm) | Wear and tear area $a$ (mm) | Wear area inclination angle $\varphi$ (degree) | Reduced size wear $S$ (mm) |
|---|---|---|---|---|---|---|---|
| 1 | Development and movement of sandy soils | 3-5 | 1.5 | 0 | 17 | 22 | |
| | | 3-5 | 3.0 | 0 | 20 | 16 | |
| | | 3-5 | 9.9 | 0 | 27 | 6 | |
| 2 | Development and movement of sandy loam soils | 10-15 | 1.5 | 3.0 | 14 | 20 | 9.0 |
| | | 10-15 | 3.0 | 3.5 | 18 | 13 | 10.2 |
| | | 10-15 | 7.2 | 4.5 | 21 | 9 | 13.3 |
| 3 | Development and movement of loams | 14-16 | 1.5 | 3.5 | 10 | 14 | 8.0 |
| | | 14-16 | 3.0 | 4.0 | 12 | 17 | 9.5 |
| | | 14-16 | 8.5 | 6.0 | 17 | 20 | 14.5 |
| 4 | Development and movement of heavy loams and clays | 18-20 | 1.5 | 3.0 | 9 | 10 | 8.0 |
| | | 18-20 | 3.0 | 4.0 | 10 | 16 | 9.5 |
| | | 18-20 | 14.4 | 8.0 | 16 | 18 | 20.0 |
| 5 | Development of clays, loams with inclusions | 20-30 | 1.5 | 6.0 | 9 | 19 | |
| | | 20-30 | 3.0 | 8.0 | 12 | 22 | |
| | | 20-30 | 3.8 | 10.0 | 11 | 30 | |

An expression was obtained that can be used to calculate the ground resistance forces to cutting and the corresponding cutting efficiency coefficients at different values of the dull sites.

However, it is not yet known what values of the dull parameters should be taken as criteria and used in calculations. In order to determine these criteria, as well as to expand the field of use of the obtained formula, using it, in particular, for the reduced dull size, it is necessary to investigate the wear patterns of the blades of the dump of auto graders.

As noted above, an auto grader cutting element having a wedge-shaped cross-section may be characterized by the following wear geometries: a rounded wear area of the front face of the wedge or angular wear measured by the radius of rounding $r$, a flat dull area located at a negative angle $\varphi$ to the cutting plane and a measured width of the area $a$. In addition, wear can be characterized by a loss of blade height or linear wear $l$, as well as a complex wear parameter - the reduced size $S$, combining the values $r$, $a$ and $\varphi$ (Figure 3).

The study of the wear nature of the blades of the dump of motor graders was carried out at the construction and repair facilities of the roads of JSC

Roads of Kazakhstan [2, 15] (Figure 4). Initially, all dimensions of the wear elements were recorded, with the exception of $S$. The data obtained are shown in Table 1.

However, it turned out that in different soil conditions, different wear elements play a decisive role. To take into account all these cases with a single formula, it is necessary to use the complex reduced wear size - $S$.

In order to link the reduced wear size $S$ with the radius of rounding $r$, the wear pad $a$ and the slope of the pad $\varphi$, consider the worn blade diagram in Figure 5.

As one can see from the diagram, the dimension $S$ is made up of lines

$$S = bc + cd + de, \quad (8)$$

where $bc = nc\cos\alpha = r\cos\alpha$; $cd = ck\cos\varphi = r\cos\varphi$; $de = kp = km\sin\varphi = a\sin\varphi$.

Then

$$S = bc + cd + de = r\cos\alpha + r\cos\varphi + a\sin\varphi, \quad (9)$$

from where

$$S = r(\cos\alpha + \cos\varphi) + a\sin\varphi. \quad (10)$$

Equation (10) can be simplified by establishing the relationship of the change values $r$, $a$ and $\varphi$. This can be done if the regularities of their change are known depending on the amount of work performed in different categories of soils. These patterns can also be used to predict the nature of the wear of knives during their operation and control this process. Therefore, based on the data of Table 1, graphs were plotted and equations of the above dependencies were derived.

Figures 6 and 7 show the graphs of the radius of rounding of the blade $r$ and the wear site $a$ dependences on the volume of excavated soil $V$, respectively. The obtained regression equations are summarized in Table 2.

The following conclusions can be drawn from the analysis of regression graphs and equations:

- clay-containing rocks (loams and clays) without inclusions have close relationships $r = f(V)$ and $a = f(V)$;
- loams and clays with inclusions are characterized by a more intensive increase in the radius of rounding of the blade $r$ with an increase in the volume of mined soil $V$ and a significant spread of data, which is due, apparently, to the chaotic

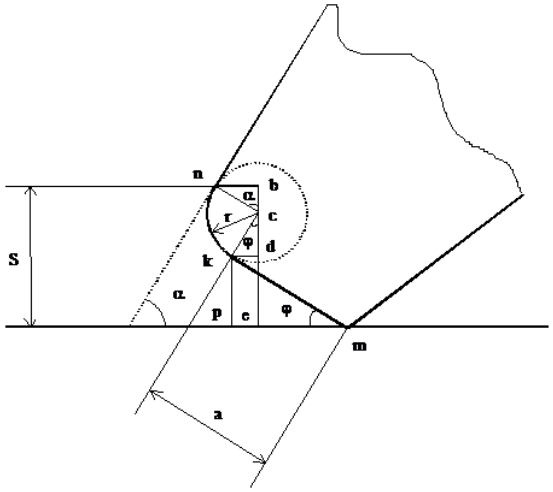


***Figure 5*** *Diagram for determination of the reduced wear size*

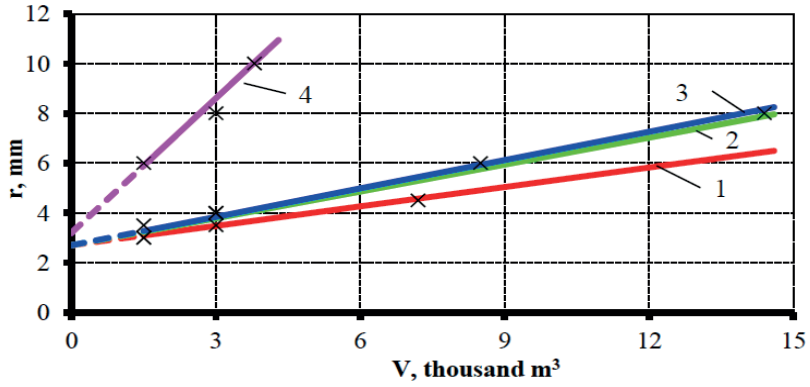


***Figure 6*** *Dependence of the rounding radius r on volume of the worked-out soil V for different soil types: 1 - sandy loam - r = 2.7 + 0.26V; 2 - loams - r = 2.7 + 0.36V ; 3 - heavy loams and clays - r = 2.7 + 0.38V; 4 - loam with inclusions - r = 3.2 + 1.80V*

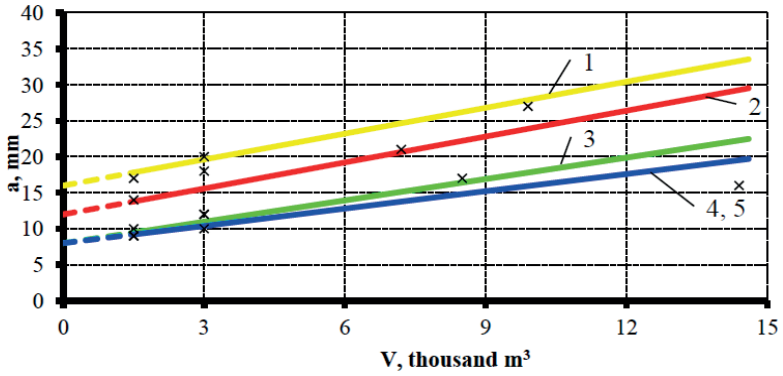


***Figure 7*** *Dependence of the wear site a on volume of mined soil V for various soil types: 1 - sandy soil - a = 16 + 1.20V; 2 - sandy loam soil - a = 12 + 1.20V; 3 - loams - a = 8 + 0.99V; 4 - heavy loams and clays - heavy loams and clays a = 8 + 0.80V; 5 - loam with inclusions - a = 8 + 0.85V*

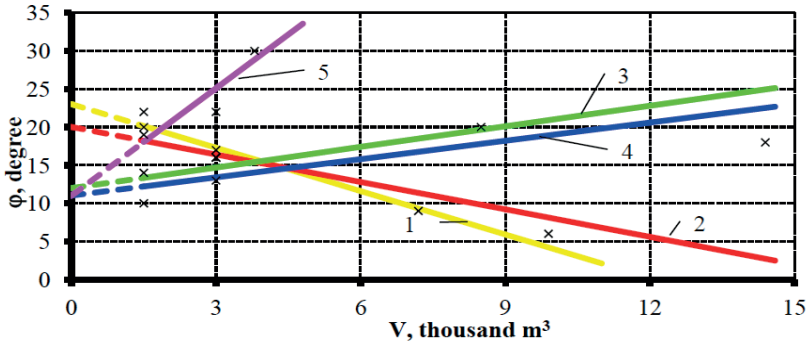


***Figure 8*** *Dependence of the slope angle a of the wear site on the volume of mined soil V for various soil types: 1 - sandy soil - $\phi = 23 - 1.90V$; 2 - sandy loam - $\phi = 20 - 1.20V$; 3 - loams - $\phi = 12 + 0.90V$; 4 - heavy loams and clays - $\phi = 11 + 0.80V$; 5 - loam with inclusions - $\phi = 11 + 4.70V$*

***Table 2*** *Regression equations for determining the geometric parameters of wear of motor graders knives*

| No. | Soil conditions | Radius blurring $r$ | Platform wear $a$ | Wear area inclination angle $\varphi$ |
|---|---|---|---|---|
| 1 | Sand | $r = 0$ | $a = 16 + 1.20V$ | $\varphi = 23 - 1.90V$ |
| 2 | Sandy loam | $r = 2.7 + 0.26V$ | $a = 12 + 1.20V$ | $\varphi = 20 + 1.20V$ |
| 3 | Loams | $r = 2.7 + 0.36V$ | $a = 8 + 0.99V$ | $\varphi = 12 + 0.90V$ |
| 4 | Heavy loams and clays | $r = 2.7 + 0.38V$ | $a = 8 + 0.80V$ | $\varphi = 11 + 0.80V$ |
| 5 | Loam and clay with inclusions | $r = 2.7 + 1.80V$ | $a = 8 + 0.85V$ | $\varphi = 11 + 4.70V$ |

nature of inclusions, which reduces the reliability of the calculation results according to the obtained formulas;

- wear along the radius of rounding r of the knife blades during operation in sandy soils does not appear, and in sandy loams it appears with less intensity than in the clay-containing soils. The change in the wear site in sands and sandy loams also differs in intensity from clay-containing soils.

Figure 8 shows graphs of the dependence of the inclination angle of the wear site to the cutting plane (angle of $\varphi$) on the volume of the developed soil. The regression equations obtained are shown in Table 2.

The given graphs and equations confirm the earlier conclusions that the change in wear elements in the clay-containing soils can be expressed by generalized formulas. In addition, it can be seen that in sandy and sandy loam soils the $\varphi$ value decreases with increasing $V$, and in clay-containing soils it increases.

However, in general, the limits of variation of the $\varphi$ value for all the soils, with the exception of soils with inclusions, are small. If one takes all the obtained values as a sample of random variables, then the average sample is $\varphi = 15.08°$. With corrected mean quadratic deviation $S_{isp} = 0.8°$, determine with reliability $\gamma = 0.95$ limits of confidence interval of true value of $\varphi$ inclination angle. At $\gamma = 0.95$ and $n = 12$ according to the reference book [6] one finds the value $t$ expressed in

fractions of the mean quadratic error $\sigma$, $t$ = 2.13. The accuracy of estimate of $\delta$, given that at $n \leq 30$ $\sigma \approx S_{isp}$ is found.

$$\delta = \frac{t \cdot \sigma}{\sqrt{n-1}} = \frac{t \cdot S_{isp}}{\sqrt{n-1}} = \frac{12.3 \cdot 0.8}{\sqrt{12-1}} = 0.51^{\circ}.$$

The confidence interval is defined as: ($\varphi$ - 0.51; $\varphi$ + 0.51) and its limits are:

$$\varphi - 0.51 = 15.08 - 0.51 = 14.57 \approx 14.6^{\circ};$$
$$\varphi + 0.51 = 15.08 + 0.51 = 15.59 \approx 15.6^{\circ}.$$

So, with a reliability of $\gamma$ = 0.95, that is, in 95 cases out of 100, the true value of the inclination angle $\varphi$ is in the confidence interval $14.6^{\circ} \leq \varphi_{\circ ist} \leq 15.6^{\circ}$. Therefore, it is permissible to accept for all the soils, with the exception of soils with inclusions, the average value of the angle $\varphi$ = 15°.

Substituting the average value of the angle $\varphi$ in Equations (5) and (6) one obtains:

$$P_2' = B_n \cdot 1.43r \cdot (1 + 0.574f) \times \times \frac{1 - \sin \cdot \rho \cdot \cos 2\varphi_H}{1 + \sin \cdot \rho \cdot \cos 2\varphi_H} \cdot (C_O \cdot \cos\rho + \gamma_n \cdot 0.62r). \quad (11)$$

$$P_3' = B_n \cdot a \cdot (1 + 3.73f) \cdot \frac{1 - \sin \cdot \rho \cdot \cos 2\varphi_H}{1 + \sin \cdot \rho \cdot \cos 2\varphi_H} \times \times (C_O \cdot \cos\rho + \gamma_n \cdot 0.13r). \quad (12)$$

In general, the $P_{P\kappa}$ value will be:

$$P_{P\kappa} = B_n \cdot \left[(h-s) \cdot \left(1 + f \cdot \sqrt{\frac{1}{\sin^2\alpha} - 1}\right) + + 1.43r \cdot (1 + 0.574f) + a(1 + 3.73f)\right] \times \times \frac{1 - \sin \cdot \rho \cdot \cos 2\varphi_H}{1 + \sin \cdot \rho \cdot \cos 2\varphi_H} \cdot \left[3 \cdot C_0 \cdot \cos\rho + \gamma_n \times \times \left(\frac{h-S}{2} + 0.62r + 0.13a\right)\right] + 2 \cdot (K_S \cdot B_\kappa \cdot h \cdot \mu \times \times \varepsilon \cdot B_\kappa \cdot h \cdot \mu \cdot \upsilon^2). \quad (13)$$

Equation (10) can be represented as:

$$S = r(\cos\alpha + \cos 15^{\circ}) + a \sin 15^{\circ}, \quad (14)$$

from here

$$S = r(0.966 + \cos\alpha) + 0.26a \quad (15)$$

The equations found $r = f(V)$ and $a = f(V)$ are substituted in Equation (15).

For sandy loam soils, we get:

$$S = 2.7(2.13 + \cos\alpha) + 0.26V(2.16 + \cos\alpha). \quad (16)$$

Consider that $2.16 \approx 2.13$. Then

$$S = (2.7 + 0.26V)(2.13 + \cos\alpha). \quad (17)$$

Similarly, for the clay-containing soils after transformations, one obtains:

$$S = (2.7 + 0.38V)(1.70 + \cos\alpha). \quad (18)$$

Verification of the obtained equations became possible when the data on the wear of knives were obtained at the objects of the trust Construction mechanization LLP (Figure 9), given in Table 3. Here, not only the parameters $r$ and $a$ were recorded, but the complex size $S$, as well, when working in the clay-containing soils. The results of measurements were compared with the calculated data obtained from equations given in Table 2 and Equations (17) and (18). As one can see, the average error of the measured and calculated values is about 5%, and the maximum - does not exceed 11%, which is permissible in such unorganized processes as wear of the cutting elements of the auto grader.

After checking the formulas, Table 1 was supplemented with the calculated values of $S$ and

***Table 3*** *Change of geometric parameters of wear of motor grader dumps blades at the objects of Construction mechanization LLP trust*

| No. | Soil conditions | Soil development volume V (thousand m³) | Magnitude of wear geometric parameters (mm) | | | | | |
|---|---|---|---|---|---|---|---|---|
| | | | *r* | | *a* | | S | |
| | | | by measurement | settlement | by measurement | settlement | by measurement | settlement |
| 1 | Loams | 10 | 6 | 6.3 | 20 | 18.0 | 15 | 16.0 |
| | | 15 | 8 | 8.1 | 22 | 22.8 | 20 | 20.6 |
| | | 20 | 10 | 9.9 | 30 | 27.8 | 25 | 25.3 |
| | | 25 | 12 | 11.7 | 34 | 32.7 | 30 | 30.0 |
| 2 | Heavy loams and clays | 10 | 7 | 6.5 | 18 | 16.8 | 17 | 16.0 |
| | | 15 | 9 | 8.4 | 20 | 20.2 | 22 | 20.6 |
| | | 20 | 10 | 10.3 | 25 | 24.0 | 26 | 25.3 |
| | | 25 | 13 | 12.2 | 30 | 28.1 | 32 | 30.0 |

***Figure 9*** *Wear of motor graders knives at the facilities of the trust Construction mechanization LLP*

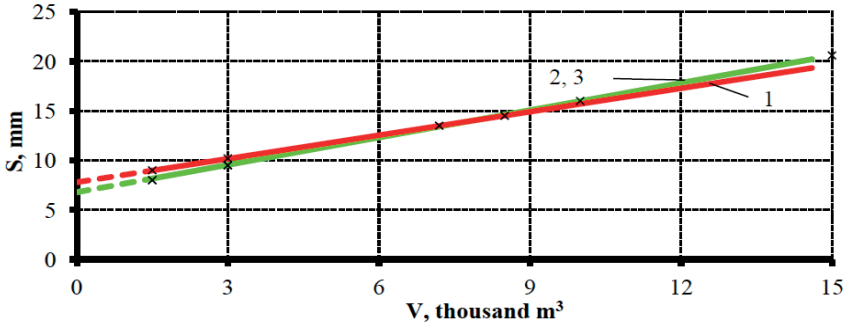


***Figure 10*** *Dependence of the reduced dull size S on the volume of mined soil V for various soil types: 1 - sandy loam; 2 - loams; 3 - heavy loams and clays*

***Table 4*** *Pair correlation equations for calculations of wear parameters depending on the reduced wear size for different soil types*

| Soil type | $r = f(S)$ | $a = f(S)$ |
|---|---|---|
| Sandy | $r = 0.35S$ | $a = 0.6 + 1.63S$ |
| Clay-containing | $r = 0.42S$ | $a = 1.8 + 0.84S$ |

graphs of the change $S$ in clay-containing and sandy loam soils, shown in Figure 10, were drawn on them.

It can be seen that with an increase in the volume of developed soil $V$, wear $S$ in sandy loam soils first exceeds wear in clay-containing soils, but its growth intensity is smaller and after mining 6.0 - 6.5 thousand m$^3$ of soil, the wear value in clay-containing soils becomes larger.

Equations (17) and (18) can be used in workflow planning and control in production conditions.

## 3 Results and discussions

Thus, theoretically, Equation (10) is derived, expressing the relationship of the reduced size $S$ with the wear parameters $r$, $a$ and $\varphi$. The relationship of these parameters in the production process was experimentally investigated, which made it possible to clarify Equation (10) and obtain the Equation (15). The values of $S$, corresponding to the initial data $r$ and $a$ in production experiments (Table 3) and Equations (17) and (18), expressing the dependence of $S$ on $V$, made it possible to plan and control the process of working the blade elements are obtained.

Now it is possible to establish a pair of correlation relationship between $r$ and $S$, $a$ and $S$, which is necessary to transform the Equation (18) in order to universalize it.

The data obtained correspond to equations given in Table 4.

Substituting the obtained expressions into Equations (11) and (12), one gets:

- for sandy loam soils:

$$P_2' = 0.5 \cdot B_n \cdot S \cdot (1 + 0.574f) \times \times \frac{1 - \sin\beta \cdot \cos 2\varphi'_H}{1 + \sin\beta \cdot \cos 2\varphi'_H} \cdot (C_O \cdot \cos\rho + 0.22 \cdot \gamma_n \cdot S), \quad (19)$$

$$P_3' = B_n \cdot (0.6 + 1.63S) \cdot (1 + 3.73f) \times \times \frac{1 - \sin\beta \cdot \cos 2\varphi_H''}{1 + \sin\beta \cdot \cos 2\varphi_H''} \cdot (C_O \cdot \cos\rho + 0.22 \cdot \gamma_n \cdot S), \quad (20)$$

$$P_{P\kappa} = P_1' + P_2' + P_3' = B\Big\{(h - s) \times \times \Big(1 + f \cdot \sqrt{\frac{1}{\sin^2\alpha} - 1}\Big) \cdot \frac{1 - \sin\beta \cdot \cos 2\varphi_H''}{1 + \sin\beta \cdot \cos 2\varphi_H''} \times \times \big[C_0 \cdot \cos\rho + 0.5 \cdot \gamma_n \cdot (h - S)\big] + (C_0 \cdot \cos\rho + + 0.22 \cdot \gamma_n \cdot S) \cdot \Big[0.5S \cdot (1 + 0.574f) \times \times \frac{1 - \sin\beta \cdot \cos 2\varphi_H''}{1 + \sin\beta \cdot \cos 2\varphi_H''}\Big]\Big\} + 2(K_S \cdot B_\kappa \cdot h \cdot \mu + + \varepsilon \cdot B_\kappa \cdot h \cdot \mu \cdot \upsilon^2), \quad (21)$$

- for clay soils:

$$P_2' = 0.6 \cdot B_n \cdot S \cdot (1 + 0.574f) \times \times \frac{1 - \sin\beta \cdot \cos 2\varphi_H'}{1 + \sin\beta \cdot \cos 2\varphi_H'} \cdot (C_O \cdot \cos\rho + 0.26 \cdot \gamma_n \cdot S), \quad (22)$$

$$P_2' = B_n \cdot (1.8 + 0.84S) \cdot (1 + 3.73f) \times \times \frac{1 - \sin\beta \cdot \cos 2\varphi_H''}{1 + \sin\beta \cdot \cos 2\varphi_H''} \times \big[C_O \cdot \cos\rho + \gamma_n \cdot (0.23 + 0.11S)\big], \quad (23)$$

$$P_{P\kappa} = P_1' + P_2' + P_3' = B_n \cdot \Big\{(h - S) \times \times \Big(1 + f \cdot \sqrt{\frac{1}{\sin^2\alpha} - 1}\Big) \cdot \frac{1 - \sin\beta \cdot \cos 2\varphi_H''}{1 + \sin\beta \cdot \cos 2\varphi_H''} \times \times \big[C_o \cdot \cos\rho + 0.5 \cdot \gamma_n \cdot (h - S)\big] + 0.6S \times \times (1 + 0.574f) \cdot \frac{1 - \sin\beta \cdot \cos 2\varphi_H'}{1 + \sin\beta \cdot \cos 2\varphi_H'} \times \times (C_o \cdot \cos\rho + 0.26 \cdot \gamma_n \cdot S) + (1.8 + 0.84S) \times \times (1 + 3.73f) \cdot \frac{1 - \sin\beta \cdot \cos 2\varphi_H''}{1 + \sin\beta \cdot \cos 2\varphi_H''} \times \times \big[C_O \cdot \cos\rho + \gamma_n \cdot (0.23 + 0.11S)\big]\Big\} + 2(K_S \cdot B_\kappa \cdot h \cdot \mu + \varepsilon \cdot B_\kappa \cdot h \cdot \mu \cdot \upsilon^2) \quad (24)$$

According to Equation (5), the coefficients $K_c$ of the unaffected blade of the knife as compared to the blunted blade will be:

$$K_c = \frac{P_{P\kappa}'/A}{P_{P\kappa}/A} = \frac{P_{P\kappa}'}{P_{P\kappa}}, \quad (25)$$

where $P_{P\kappa}'$ - is resistance to cutting with an unaffected knife; $P_{P\kappa}$ - resistance to cutting by blunted knife with reduced wear size $S$; $A$ - projection of the contact area of working faces of knife with soil in a vertical plane.

Then:

- for sandy loam soils:

$$K_c = \frac{B_n \times \left\{\begin{array}{l}(h - S) \cdot \Big(1 + f \cdot \sqrt{\frac{1}{\sin^2\alpha} - 1}\Big) \times \\ \times \frac{1 - \sin\beta \cdot \cos 2\varphi_H}{1 + \sin\beta \cdot \cos 2\varphi_H} \cdot \left[\begin{array}{l} C_0 \cdot \cos\rho + \\ + 0.5 \cdot \gamma_n \times \\ \times (h - S) \end{array}\right] + \\ \times \left\{ + \left[\begin{array}{l} 0.5S \cdot (1 + 0.574f) \times \\ \times \frac{1 - \sin\beta \cdot \cos 2\varphi_H'}{1 + \sin\beta \cdot \cos 2\varphi_H'} + \\ + (0.6 + 1.63S) \times \\ \times \frac{1 - \sin\beta \cdot \cos 2\varphi_H''}{1 + \sin\beta \cdot \cos 2\varphi_H''} \end{array}\right] + \right. \\ \left. + (C_0 \cdot \cos\rho + 0.22 \cdot \gamma_n \cdot S) \right\} + \\ + 2(K_S \cdot B_\kappa \cdot h \cdot \mu + \varepsilon \cdot B_\kappa \cdot h \cdot \mu \cdot \upsilon^2) \end{array}}{B_n \cdot h \cdot \Big(1 + f \cdot \sqrt{\frac{1}{\sin^2\alpha} - 1}\Big) \cdot \frac{1 - \sin\beta \cdot \cos 2\varphi_H}{1 + \sin\beta \cdot \cos 2\varphi_H} \times \times (C_0 \cdot \cos\rho + 0.5 \cdot \gamma_n \cdot h) + 2 \cdot \Big(\begin{array}{l} K_S \cdot B_\kappa \cdot \mu + \\ + \varepsilon \cdot B_\kappa \cdot \mu \cdot \upsilon^2 \end{array}\Big)} \quad (26)$$

- for clay soils:

$$K_c = \frac{B_n \times \left\{\begin{array}{l}(h - S) \cdot \Big(1 + f \cdot \sqrt{\frac{1}{\sin^2\alpha} - 1}\Big) \times \\ \times \frac{1 - \sin\beta \cdot \cos 2\varphi_H}{1 + \sin\beta \cdot \cos 2\varphi_H} \cdot [C_0 \cdot \cos\rho + \\ + 0.5 \cdot \gamma_n \cdot (h - S)] + 0.6S \times \\ \times (1 + 0.574f) \frac{1 - \sin\beta \cdot \cos 2\varphi_H'}{1 + \sin\beta \cdot \cos 2\varphi_H'} \times \\ + (C_0 \cdot \cos\rho + 0.26\gamma_n S) + \\ + (1.8 + 8.84S) \cdot (1 + 3.73f) \times \\ \times \frac{1 - \sin\beta \cdot \cos 2\varphi_H''}{1 + \sin\beta \cdot \cos 2\varphi_H''} \cdot [C_0 \cdot \cos\rho + \\ + \gamma_n (0.23 + 0.11S)] \end{array}\right\} \times \times 2(K_S \cdot B_\kappa \cdot h \cdot \mu + \varepsilon \cdot B_\kappa \cdot h \cdot \mu \cdot \upsilon^2)}{B_n \cdot h \cdot \Big(1 + f \cdot \sqrt{\frac{1}{\sin^2\alpha} - 1}\Big) \cdot \frac{1 - \sin\beta \cdot \cos 2\varphi_H}{1 + \sin\beta \cdot \cos 2\varphi_H} \times \times (C_0 \cdot \cos\rho + 0.5 \cdot \gamma_n \cdot h) + 2 \cdot \Big(\begin{array}{l} K_S \cdot B_\kappa \cdot \mu + \\ + \varepsilon \cdot B_\kappa \cdot \mu \cdot \upsilon^2 \end{array}\Big)} \quad (27)$$

***Table 5*** *Coefficients $K_c$, characterizing the increase in soil resistance to cutting as a result of blunting of the blade of the knife, measured by the reduced size S*

| *Dull value S (mm)* | *Soil* | |
|---|---|---|
| | *sandy loam* | *loams* |
| *5* | *0.60* | *0.72* |
| *10* | *1.18* | *1.35* |
| *15* | *1.90* | *2.08* |
| *20* | *2.36* | *2.76* |
| *25* | *3.04* | *3.54* |
| *30* | *3.62* | *4.28* |

Results of $K_c$ coefficient calculation at $\alpha$ = 40°, $f$ = 0.7 and $h$ = 80 mm are given in Table 5.

As one can see, when the reduced wear size S increases to 30 mm, the soil resistance increases in 3 to 4 times, which reduces productivity and increases the costs of work of the auto grader.

## 4 Conclusions

1. Production experiments were carried out, as a result of which regularities of changes in geometric parameters of wear of dump of auto graders in various soils were established: the radius of rounding of the blade $r$ from the volume of mined soil $V$; wear sites $a$ from the volume of excavated soil $V$; the angle of inclination of the wear area to the cutting plane $\varphi$ of the volume of excavated soil $V$; reduced wear size $S$ of volume of excavated soil $V$; wear elements $r$ and $a$ of the reduced wear size $S$. The corresponding equations are obtained.
2. It has been established, that in clay-containing soils - loams and clays without inclusions, close relationships $r = f(V)$, $a = f(V)$ and $\varphi = f(V)$, are obtained, which makes it possible to use generalized regression equations for these soils.
3. In loams and clays with inclusions, the obtained experimental data are characterized by significant variation and the dependencies obtained from them differ from the corresponding dependencies for other clay-containing soils. Therefore, the proposed formulas for clay-containing soils cannot be used for clay-containing soils with inclusions and the obtained dependencies for these soils cannot be recommended for wide use due to the weak correlation of design and experimental data due to the large dispersion of the latter.
4. In sandy soils, wear of the blade along the radius $r$ does not occur. The regression equations of the above dependencies in sands and sandy loams have a different character than in clay-containing soils. So, the wear $r$ in sandy loam is manifested with less intensity, and the wear site $a$ in sands and sandy loam increases more intensively; the angle of $\varphi$ decreases with increasing $V$, while in clay-containing soils it increases. For sands and sandy loams there are proposed formulas different from those proposed for the clay-containing soils.
5. It has been found that the angle of the wear site $\varphi$ varies within insignificant limits and its average value can be taken 15°. With a reliability of $\gamma = 0.95$ this value is contained in the confidence interval $14.6° < \varphi < 15.6°$.
6. A formula is proposed for determining the reduced wear size $S$ through $r$, $a$, $\varphi$ and $\alpha$, cutting angle, specified using the obtained results of experimental studies.
7. A formula is proposed for determining the reduced wear size $S$ depending on $V$, which makes it possible to plan and control the process of working blade cutting elements.

## References


[1] DOTSENKO, A. I., KARASEV, G. N., KUSTAREV, G. V., SHESTOPALOV, K. K. *Machines for earthworks.* Moscow: Bastet, 2012. ISBN 978-5-903178-28-5.

[2] LUKASHUK, O. A., KOMISSAROV, A.P., LETNEV, K.YU. *Machines for soil development. Design and calculation*. Ekaterinburg: Ural University Publishing House, 2018. ISBN 978-5-7996-2386-9.

[3] VOLKOV, D. P., KRIKUN, V. Y., TOTOLIN, P. E., GAEVSKAYA, K. S. *Earthwork machines.* Moscow: Mechanical Engineering, 1992. ISBN 5-217-01973-5.

[4] KOZBAGAROV, R. A., KAMZANOV, N. S., AKHMETOVA, S. D., ZHUSSUPOV, K. A., DAINOVA, Z. K. Improving the methods of milling gauge on highways. *News of the National Academy of Sciences of the Republic of Kazakhstan, Series of Geology and Technical Sciences* [online]. 2021, 3(447), p. 87-93. ISSN 2518-170X. Available from: https://doi.org/10.32014/2021.2518-170X.67.

[5] KOZBAGAROV, R. A., ZHUSSUPOV, K. A., KALIYEV, Y. B., YESSENGALIYEV, M. N., KOCHETKOV, A. V. Determination of energy consumption of high-speed rock digging. *News of the National Academy of Sciences of the Republic of Kazakhstan, Series of Geology and Technical Sciences* [online]. 2021, 6(450), p. 85-92. ISSN 2518-170X. Available from: https://doi.org/10.32014/2021.2518-170X.123.

[6] MESHCHERYAKOV, V.A., WEBER, V.V. Setpoint optimization for the control system of the motor grader in heavy load mode. *The Russian Automobile and Highway Industry Journal* [online]. 2018, 15(4), p. 502-513. ISSN 2658-5626. Available from: https://doi.org/10.26518/2071-7296-2018-4-502-513

[7] POLYARUS, A., PASCHENKO, R., POLIAKOV, E., LEBEDINSKYI, A. Analysis of motor-grader loading on the basis of fractal dimension. *Automobile Transport* [online]. 2016, 39, p. 47-53. ISSN 2309-981X. Available from: https://doi.org/10.30977/AT.2219-8342.2016.39.0.47.

[8] FEDOROV, D. I. *Working bodies of earth-moving machines*. Moscow: Mechanical Engineering, 1977. ISBN 5-217-00490-8.

[9] BALOVNEV, V. I. *Modeling of interaction processes with the environment of working bodies of road construction machines*. Moscow: Higher School, 1981, ISBN 5-217-02343-0.

[10] KOZBAGAROV, R. A., TARAN, M. V., ZHUSSUPOV, K. A., KANAZHANOV A. E., KAMZANOV, N. C., KOCHETKOV, A. V. Increasing the efficiency of motor graders work on the basis of working elements perfection. *News of the National Academy of Sciences of the Republic of Kazakhstan, Series of Geology and Technical Sciences* [online]. 2021, 1(445), p. 98-105. ISSN 2518-170X. Available from: https://doi.org/10.32014/2021.2518-170X.14.

[11] KOZBAGAROV, R. A., SHALBAYEV, K. K., ZHIYENKOZHAYEV, M. S., KAMZANOV, N. S., NAIMANOVA, G. T. Design of cutting elements of reusable motor graders in mining. *News of the National Academy of Sciences of the Republic of Kazakhstan, Series of Geology and Technical Sciences* [online]. 2022, 3(453), p. 128-141. ISSN 2518-170X. Available from: https://doi.org/10.32014/2022.2518-170X.185.

[12] SHEVCHENKO, V., CHAPALYGINA, O. Determination of indexes of the motor grader course stability on the basis of studying its analytical model of movement. *Bulletin of Kharkov National Automobile and Highway University* [online]. 2020, 2(88), p. 43-50. ISSN 2521-1773. Available from: https://doi.org/10.30977/BUL.2219-5548.2020.88.2.43.

[13] SHERBAKOV, A. P., PUSHKAREV, A. E., MAKSIMOV, S. E. Replacement working body material as a way to increase reliability of road construction machines. *The Russian Automobile and Highway Industry Journal* [online]. 2021**,** 18(6), p. 646-661. ISSN 2658-5626. Available from: https://doi.org/10.26518/2071-7296-2021-18-6-646-661.

[14] ALIPOV, G. I. Effect of soil pressure on wear of excavator bucket teeth. *Construction and Road Machines*. 1966, 4. p. 16-17. ISSN 0039-2391.

[15] ARTEMYEV, K. A., BELOKRYLOV, V. G., UGRYUMOV, A. A. The form of wear of scraper knives. *Construction and Road Machines*. 1976, 10, p. 17-18. ISSN 0039-2391.

[16] ZHUSSUPOV, K., TOKTAMYSSOVA, A., ABDULLAYEV, S., BAKYT, G., YESSENGALIYEV, M., BAZARBEKOVA, M. Investigation of the stress-strain state of a wheel flange of the locomotive by the method of finite element modeling. *Mechanika* [online], 2018, 24(2), p. 174–181. ISSN 1392–1207. Available from: https://doi.org/10.5755/j01.mech.24.2.17637.

[17] YANHUA, S., TAOHUA, Z., CHUN, J. Simulation based analysis of articulated steer grader with six motor-driven wheels. *Advanced Materials Research* [online]. 2012, 455-456, p. 1090-10957. ISSN 1662-8985. Available from: DOI:10.4028/www.scientific.net/AMR.455-456.1090.

[18] TURGUMBAEV, S. Z., KABASHEV, R. A. The results of experimental research of the process of soil digging by modernized working blades under hydrostatic pressure. *The Russian Automobile and Highway Industry Journal* [online]. 2017, 2(54), p.36-42. ISSN 2071-7296. Available from: https://doi.org/10.26518/2071-7296-2017-2(54)-36-42.

Project

# Research on the effects of short-term aging on the properties of asphalt materials (RESTAAM).

## is co-financed by Slovak Research and Development Agency by the Ministry of Education, Science, Research and Sport of the Slovak Republic

**Project objective:**
The aim of the project is to expand knowledge about the aging processes of asphalt mixtures and asphalt binders with special emphasis on the implementation of modern technologies for their production, characterized by reduced production temperatures, such as foam bitumen technology. The following objectives of research project will be addressed:

- assessment of the impact of modification of laboratory process of short-term aging of bitumen and asphalts on their technical and rheological properties,
- assessment of the effect of application of foam bitumen on the properties of bitumen and asphalts in the context of short-term aging methods,
- investigation of the dependence between changes in the properties of bitumen and asphalts exposed to short-term aging under different conditions.

**Project description:**
The project is focused on basic research of relationships between the intensity of aging process of binders in asphalt by short-term oxidative aging and bitumen exposed to heat and air on a rolling thin film that undergoes in asphalt mixing plant and that is essential and critical to the expected service-life. These relations are of considerable importance in terms of the technologies of hot mix asphalt and warm mix asphalt and application for the construction of a road pavement wearing course at reduced temperature and the bitumen used for its production.

**Partner of the project:** Kielce University of Technology

**Project duration:** 1/1/2022 – 31/12/2023

**Project code:** SK-PL-21-0070

# THE RESEARCH AND IMPACT EVALUATION OF ECO-DRIVING STRATEGY ON SPECIFIC ENERGY CONSUMPTION IN A PASSENGER VEHICLES

**Piotr Gorzelańczyk [1,*], Piotr Piątkowski [2]**

[1]Stanislaw State Staszic University of Applied Sciences in Pila, Pila, Poland
[2]Koszalin University of Technology, Koszalin, Poland

*E-mail of corresponding author: piotr.gorzelanczyk@puss.pila.pl

***Resume***

The article presents the results of an assessment of the impact of Eco-driving on the achieved emission parameters and performance characteristics of vehicles, with a particular focus on energy efficiency. The first part of the article presents the main principles of Eco-driving and then presents the results of experimental tests carried out on two vehicles powered by conventional fuel in the form of gasoline and substitute (unconventional) fuel in the form of LPG. The vehicles were operated under different traffic conditions. Based on the analysis of the experimental results, final conclusions were formulated. The analysis of the test results made it possible to demonstrate differences in the on-road energy consumption of the vehicles depending on the driving technique used and, in addition, the results obtained were compared to the energy intensity of electric vehicles as reported by their manufacturers.

***Article info***

Received 17 March 2022
Accepted 20 June 2022
Online 12 August 2022

***Keywords:***

eco-driving strategy
specific energy consumption (SEC)
vehicle

Available online: https://doi.org/10.26552/com.C.2022.4.E122-E133

ISSN 1335-4205 (print version)
ISSN 2585-7878 (online version)

## 1 Introduction

Currently one can observe an over the world trend for changing of energy sources for vehicle powertrain system [1-2]. The main direction of these changes is an electric power system [3], however, now and in the closest future, still are and will be used vehicles with conventional power systems equipped with internal combustion engines [4]. Most of combustion engines, which have been applied for transportation vehicles are the four stroke engines. These engines can be divided in two types, like compression ignition engines (CI - mostly used in commercial vehicles) and spark ignition engines (SI). Presently, both of these engines can be powered by conventional (as technological results of crude oil distillation) or unconventional (for example; biogas, biodiesel, hydrogen, ethanol, etc.) fuels. Besides the vehicles with internal combustion engines (ICE) now automotive manufacturers offer their products equipped with alternative power systems like; battery electric vehicles (BEVs), hybrid electric vehicles (HEVs), plug-in hybrid electric vehicles (PHEVs) and fuel cell vehicles (FCVs). So, nowadays, the automotive's clients have a wide scope of vehicles to choose at local and world markets, but when they have to make a decision - to buy a new car, they have to calculate summary investment costs and administration requirements connected with the areas where the vehicles will be used. It is a result of critical use of the conventional powered vehicles in the cities and overall "decarbonisation" of all the transport sections.

The presented data in Figure 1 show that the most of nowadays vehicle buyers and users of passenger cars are choosing vehicles, which are equipped with SI engine. Vehicles with diesel engines (CI) have only 20 % where SI engines have almost 42 % share of a new vehicle market in the second quarter of 2021. The main reason of these decisions can be connected with increase in environmental awareness or administration limits connected with "clean" zones located in the cities. Sometimes consumers decisions result from the overall economical balance between all the investment and maintenance costs and predicted exploitation period. They make a calculation, how much time, or how much mileage have to be done to lose a gap of investment cost between vehicles equipped with CI and SI engine, where vehicle with CI engine is mostly about 10÷15% more expensive than SI. This lets one to state that predicted

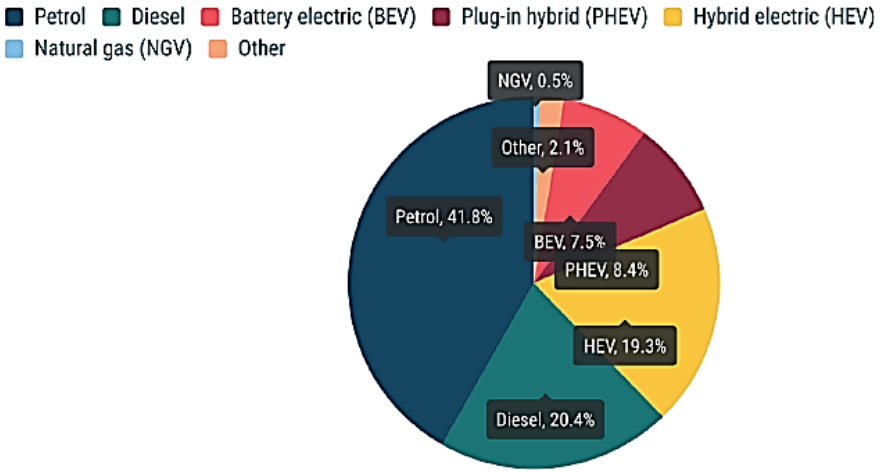


***Figure 1*** *Percentage share of registrations of the new passenger cars for Europe in the 2nd quarter of 2021 by the type of powertrain systems [5]: BEV - battery electric vehicles, HEV - hybrid electric vehicles, PHEV - plug-in hybrid electric vehicles, NGV - Natural gas vehicles*

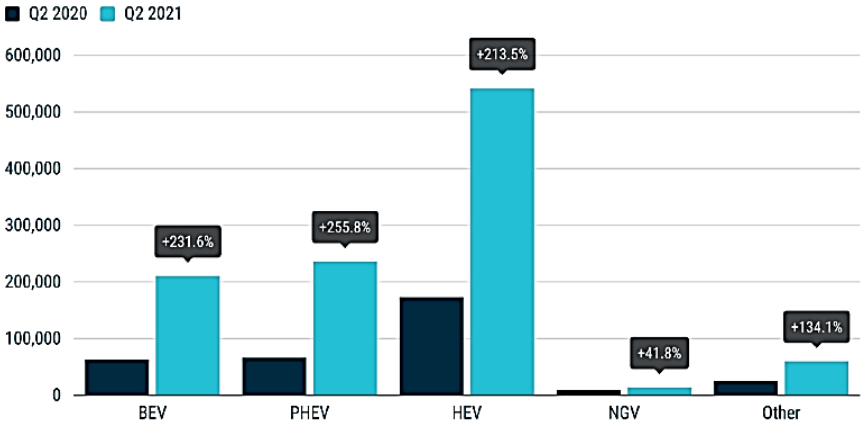


***Figure 2*** *Amount and dynamics of increase in registration of the new passenger cars for EU in the 2nd quarter of 2021, powered alternatively by oil-related fuels [5]; BEV - battery electric vehicles, PHEV - plug-in hybrid electric vehicles, HEV - hybrid electric vehicles, NGV - natural gas vehicles, other - mainly LPG vehicles*

exploitation time of vehicles with CI engine will be much longer than that of the SI engines, i.e. the CI vehicles will be used much more intensive - yearly mileage will mostly be more than 50 000 km. Moreover, the users of vehicles with the SI engines sometimes decide to install an LPG/CNG fuel system to convert their vehicle to a cheaper fuel for reducing the operation costs.

Nowadays, increasingly appear vehicles that are powered by electricity, but they do have a share on European market over 10% (all together BEVs, HEVs and PHEVs) - Figure 2. It seems to be expected that in a next 20 years this share should be much more significant. It could be caused by climate change and policy of decrease in GHG emission dedicated to all the mean of transport - for commercial and private usage. Some troubles, related to the electric vehicles' implementation were presented in [6-9]. based on these publications one can conclude that these troubles are strongly related to the user's economic status and availability of electric grid infrastructure equipped with the charger stations. The usage of a gaseous type of fuels (like LPG) for engine feeding, besides reducing the operating costs, has the significant impact on decrease of the exhaust fumes' toxic ingredients emission, as well, what, on the other hand causes significant impact on environmental destruction related to the conventional fuels [10-12].

The market for vehicles with conventional internal combustion engines is also subject to change due to emissions and powertrain efficiency requirements. Currently, internal combustion engines are fuelled with gas in the form of natural gas or a mixture of propane and butane (LPG). In addition to the economic effects, such measures also improve the environmental balance by reducing exhaust emissions.

The work by Chapman and Patil [13] presents the results of a study of the parameters of an internal combustion engine fuelled with a mixture of gases in the form of hydrogen and methane (in a volume proportion of 0 to 20% $H_2$). The researchers showed that under full-load conditions, increasing the hydrogen content to 20% allows a reduction in $CO_2$ emissions by about 20% compared to an engine fuelled with methane. At the same time, they observed a decrease in engine torque

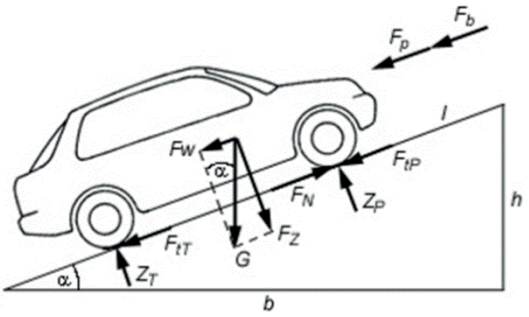


***Figure 3*** *The scheme for a forces impact on moving vehicle on a hill; α - inclination of the road-upward, l - length of the road-upward, h - hill height, $Z_T$ - surface reaction for the rear axle wheels, $F_{tT}$ - rolling resistance forces of the rear axle wheels, $F_N$ - driving force, $Z_p$ - surface reaction of the front axle wheels, $F_{tP}$ - rolling resistance forces of the front axle wheels, $F_p$ - air resistance force, $F_b$ - inertia resistance force, $F_w$ - road-upward resistance force, $F_Z$ - normal component of the vehicle's gravity force*

values (above 10 %$H_2$), which resulted from a change in the energy density of the fuel mixture supplied. Hence, in addition to use of unconventional fuels, actions are also necessary to adapt and modernise contemporary and future vehicle propulsion systems to the requirements of increasing the generally understood efficiency.

In the work of Wang et al. [14], a detailed energy and exegetical analysis of a compression ignition internal combustion engine used in trucks was carried out. One of the main conclusions of the presented research was demonstration of significance of influence of parameters controlling the process of creating a combustible mixture on exergy losses, where the injection advance angle and thermodynamic parameters of the supplied working agents (fuel and air) were indicated as the key factor and the appropriate selection and control of these parameters for the engine load made it possible to obtain the value of the thermal efficiency index at the level of almost 48%. Therefore, it can be concluded that the elements of the energy efficiency assessment are often the basis for the already mentioned modernisation of the propulsion systems of vehicles and their engines. Such a detailed analysis of possible changes and trends in these systems is presented in the work by Friedla et al. [15]. The authors of this study indicate that the tendency to increase the requirements regarding reduction of combustion engine emissions, obtained as a result of the type-approval tests, will make the test results more realistic in relation to the actual emission parameters obtained by vehicle users. In addition, the authors point out that electrification and synergy in the retrofitting of many vehicle assemblies will, in the near future, make it possible to achieve near-zero environmental impact of internal combustion engines and they will be able to complement the range of powertrains available on the market.

The work by Leach et al. [16] provides an overview of currently available methods for retrofitting internal combustion engines to achieve an increase in efficiency ratings while reducing exhaust emissions, especially harmful and toxic components. Apart from elements of the engine construction technology and fuel combustion system analysis, the article also points to some limitations in development of contemporary competitive electric drives, where the problems related to electricity generation, distribution and storage, as well as administrative regulations uniform in various countries, have been pointed out as crucial. In turn, the work by Tsiakmakis et al. [17] presents an analysis of the emission performance of vehicles powered from various energy sources (from conventional combustion engines to electric drives). Their conclusions make it possible to state that the coexistence of multiple propulsion sources is of key importance for the diversification of energy consumption from various sources. The authors also point out that the use of a specific propulsion system, adapted to the conditions of use, makes it possible to achieve the lowest possible values of environmental impact and, at the same time, to obtain relatively high values of indicators corresponding to efficiency of the energy conversion processes. At the same time, the paper points out that, apart from technological issues, which are important from the point of view of vehicle design, the nature of the load variability and its value are of the key importance for the obtained values of emissions and energy consumption, which directly translates into the obtained profile of driving speed.

## 2 Vehicle movement resistances

When the vehicle is moving, then there are forces, which result in different kinds of resistance. The main of these forces are [18-19];

- rolling resistance ($F_t$),
- air resistance ($F_p$),
- hill resistance ($F_w$),
- inertia forces for mass at translation and circular motion ($F_b$),
- trailer drag force ($F_u$).

The scheme of chosen forces, which have been impacted on moving vehicle was presented in Figure 3.

The forces balance for determined and fixed vehicle velocity could be described as

a difference of the driving force ($F_N$) and the overall resistance forces ($\Sigma F_o$) and can be expressed by:

$$F_N - \sum F_o = 0\,, \tag{1}$$

where, based on Figure 3, overall movement resistance forces are:

$$\sum F_o = F_t + F_p + F_b + F_w\,. \tag{2}$$

So, for this forces' balance for vehicle moving with fixed velocity one can express the balance of power as:

$$N_e - \sum F_o \cdot \frac{ds}{dt} = 0\,, \tag{3}$$

where:
$N_e$ - engine effective power,
$s$ - length of route travelled in time ($t$).

In the case of a lack in power balance in Equation (3), the vehicle is going to change its velocity (if the engine power has overcome an overall resistance power, then the velocity will increase and decrease otherwise).

## 3 Energetic movement balance

For an analysis of vehicle movement from the energetic point of view, a situation was taken into account where only the engine torque is responsible for a vehicle motion. In this case, an engine torque directly depends on in-cylinder mean effective pressure (MEP), which depends on efficiency of the fuel heat conversion to mechanical energy. Amount of input energy mainly results from the effectiveness of combustion process, mass of fuel and its calorific value. The energy obtained by the fuel combustion can be used for a change of vehicle movement parameters (increase in velocity, acceleration, etc.) and are dissipated as loses of energy (effect of natural dissipation of a vehicle movement energy) and imperfection of mechanical energy conversions by the powertrain system. This energy scheme can be described as a ratio of specific energy consumption (SEC) or overall energy consumption. Currently, it is called as tank-to-wheel (*TTW*) coefficient [10, 20]. The energy balance can be described as:

$$G_s \cdot W_d = E + \Delta E_s + \Delta E_p\,, \tag{4}$$

where:
$G_s$ - mean mass of the road fuel consumption [kg/km],
$W_d$ - fuel's energetic value [J/kg],
$E$ - kinetic energy of vehicle movement [J],
$\Delta E_s$ - change of energy loses for engines conversion processes [J],
$\Delta E_p$ - change of energy loses for vehicles powertrain energy conversion processes [J].

Further considering that the energy required to overcome the resistance of deceleration motion comes from the mechanical work during (at time Tn) driving the vehicle wheels by the vehicle engine.Then, the energy consumption of a vehicle moving along the road ($s$), with a known length of its section ($L_n$), can be defined as:

$$E = \int_0^{L_n} F_n ds\,, \tag{5}$$

and further, taking into account the dependence of time and path, it can be written that:

$$E = \int_0^{T_n} F_n v dt\,. \tag{6}$$

It should also be remembered that the components of the balance in Equation (4), such as hill resistance and inertia resistance, can take both positive and negative signs (when this component of the balance causes a decrease in velocity or an increase in velocity).

Taking into account the equivalence of work and energy, the main components included in the sum of the factors describing the energy consumption of the vehicle motion and referring to the quantity that characterizes the road ($s$), their individual components can be written as:

- energy necessary to overcome the rolling resistance ($E_t$),
- energy necessary to overcome the air resistance ($E_p$),
- the energy necessary to overcome the resistance to ascent ($E_w$),
- the kinetic energy of the vehicle ($E_k$) or its change.

Hence, taking into account the balance of forces acting on the vehicle in Equation (1) and based on the assumption of some of its components' variability, the general form of the energy balance for a specific road section can be written as:

$$G_s W_d = E_t + E_p \pm E_w \pm E_k + \Delta E_s + \Delta Ep \tag{7}$$

where:
$\Delta E_s$ - change of energy due to the gravity force (change of the potential energy),
$\Delta E_p$ - change of energy due to the air resistance force.

Then, the energy balance equation for a single phase of motion (for each elementary road profile) can be described in the form:

$$E = mg\int_0^{L_n} f_t ds + c_x A\varepsilon \int_0^{L_n} v^2 ds + m\int_0^{L_n} a ds\,, \tag{8}$$

where:
$f_t$ - rolling resistance coefficient on the $n$-th road section,
$c_x$ - air resistance coefficient on the $n$-th road section,
$a$ - acceleration on the $n$-th road section.

Taking into account the components, which are describing the energy consumption of the vehicle motion, recommendations can be made as to what kind of actions to control the vehicle should be performed in order to obtain the lowest possible energy demand to cover the

road section as;

- in terms of reducing the value of the rolling resistance forces;
  - choosing a road with the least possible deformable surface,
  - choosing tires with the minimum possible width for the vehicle,
  - keeping of the highest possible pressure in the tires,
  - choosing the shape of the tire tread pattern (smooth and full),
  - selection of the tyre stiffness and tread hardness,
- reducing the value of the air resistance forces;
  - selection of the vehicle speed to the engine load characteristics and torque characteristics,
  - the use of aerodynamic spoilers to obtain laminar airflow,
- reduction of inertia resistances by:
  - avoiding the sudden accelerations,
  - using the engine also for the braking process, appropriately anticipating road events,
  - keeping the actual vehicle weight as low as possible (without unnecessary load).

Such formulated recommendations can be called the main assumptions of the ecological and economic operation of a vehicle, which is nowadays referred to as Eco-driving.

An important aspect of the Eco-driving is keeping the car in a proper technical condition, where vehicle manufacturers, in addition to determining the principles of organizing maintenance and repair of vehicles, indicate the vehicle's operational features that can significantly change the value of fuel consumption [21-24]. The first comprehensive representative study on ecological and economic driving in Poland, conducted by TNS OBOP, shows that 90% of drivers in Poland declared their willingness to move in accordance with the principles of the Eco-driving [22]. The skills and knowledge of the respondents regarding Eco-driving were assessed highly and over 79% of the respondents say that they would be driving vehicles in accordance with these principles.

## 4 Vehicle traffic energy consumption studies

The aim of the research was to estimate the energy consumption of the vehicle traffic in given real operating conditions and to relate the obtained results to the energy consumption of currently promoted electric vehicles (EVs). The energy consumption of the traffic of the tested vehicles was determined indirectly based on the fuel consumption measurements, both for vehicles operating in the real urban and outside of urban traffic conditions - the so-called mixed cycle.

### 4.1 Research objects

The subjects of the research were two passenger cars of different design and functional types. These vehicles were designed to transport no more than 5 passengers, while at the time of measurements, only drivers were in the vehicles. The vehicles were equipped with standard tires, typical for each model. The technical and operational characteristics of the tested objects are presented in Table 1.

The characteristics of the power of air resistance as a function of changes in the velocity of vehicle movement for the tested vehicles are shown in Figure 4.

Taking into account the change in the value of the air resistance force, as an effect of the influence of geometric features and the shape of the body structure, it can be concluded that despite the completely different

***Table 1*** *Technical data of the tested vehicles - according to the manufacturers' data.*

| No. | Property | Vehicle No. 1 | Vehicle No. 2 |
|---|---|---|---|
| 1. | Vehicle frontal area | 2.48 $m^2$ | 2.26 $m^2$ |
| 2. | Vehicle body air resistance coefficient $c_x$ | 0.32 | 0.31 |
| 3. | Engine volume | 1870 $cm^3$. | 2461 $cm^3$ |
| 4. | Body shape and type | single-body / MPV | two-box / station wagon |
| 5. | Engine maximum power at rotation | 75 kW @ 4000 rpm | 103 kW @ 4000 rpm |
| 6. | Engine maximum torque at rotation | 200 Nm @ 1500 rpm | 290 Nm @ 1900 rpm |
| 7. | Engine type/ Type of Charger | CI engine, DI, CR I fuel system/turbo | CI engine, DI, CR I fuel system/ turbo |
| 8. | Arrangement and number of cylinders / valves | R4/8V | R5/10V |
| 9. | Type of tyres | 195/65 R15<br>Barum Bravuris 5HM/ energy class C | 205/65 R16<br>Hankook Ventus Prime3 K125/ energy class C |
| 10. | The main gear ratio/ gear box ratio for 5th | 4.35/0.947 | 4.77/1.02 |
| 11. | Average fuel consumption - mixed cycle [NEDC] | 5.9 $dm^3$/100km | 6.6 $dm^3$/100km |
| 12. | Net weight of the vehicle | 1365 kg | 1555 kg |

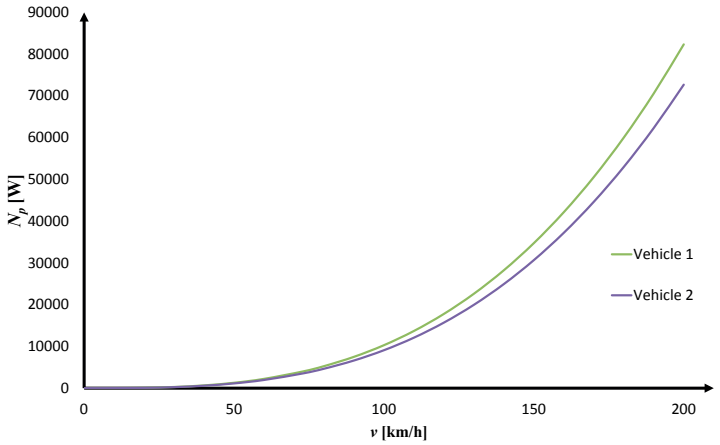


***Figure 4*** *Computational characteristics of the air resistance power ($N_p$) in relation to the movement velocity for the tested vehicles*

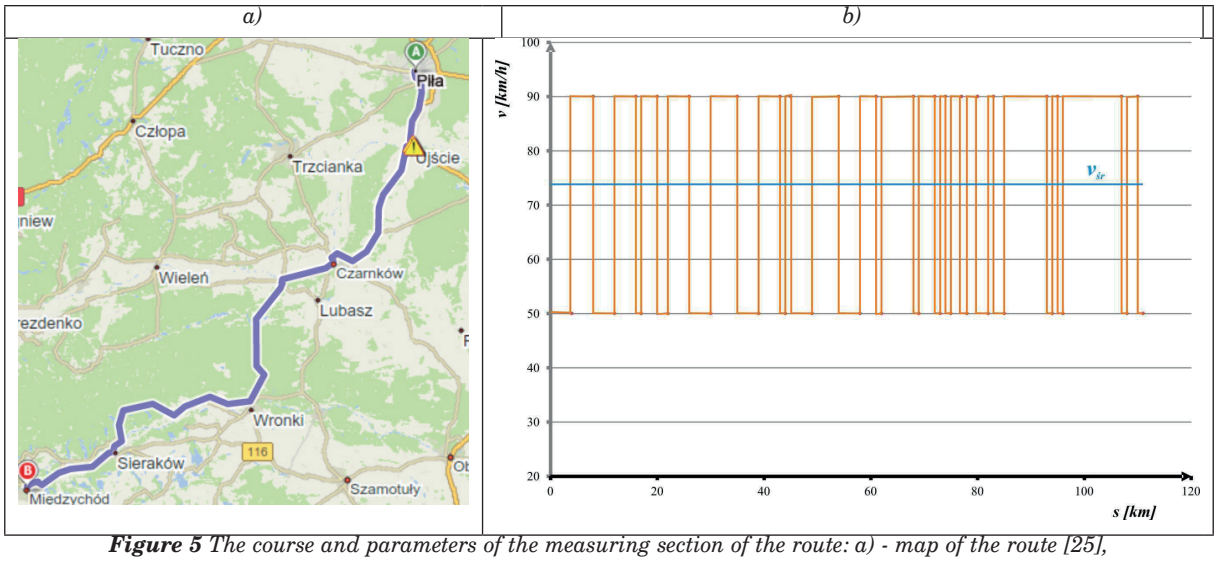


***Figure 5*** *The course and parameters of the measuring section of the route: a) - map of the route [25], b) possible maximum speeds on elementary sections of the route*

market segment of these vehicles, the characteristics of air resistance, in terms of the speed of movement covered by the test, do not differ in relative values by no more than 12% and that results mainly from the different values of the air resistance coefficient and the frontal area of the tested vehicles.

### 4.2 The research methodology

The research was carried out for the two adopted driving strategies. The first test was carried out in terms of real traffic conditions, where the driver steered the vehicle in such a way as to adjust the traffic parameters (speed, acceleration and braking) to the road conditions enabling the shortest possible travel time, while maintaining the local speed limits. It was supposed to reflect the typical behavior of the driver on the road. The second attempt was similar to the first type, with the difference that the driver used the principles of Eco-driving as far as it was possible.

Based on the measurement of the fuel consumption available on board the tested vehicles using the system of automatic acquisition of data about the vehicle motion parameters, with which the tested vehicles were equipped - i.e. the reading of the average road fuel consumption recorded by the vehicle diagnostic and control system. Based on the obtained data on fuel consumption, conversions were made into the value of the waveform energy consumption (unit energy consumption). The value of estimation error was determined by the standardized method, where, based on t analysis of the measurement systems' components, it was determined that the maximum value of the measurement error should not exceed ± 5% of the measured value. The route was carried out three times (back and forth) for each of the vehicles and each trial version. The route covered a 111*km* section of the country road no 11 and voivodship road no 182 road between the towns of Pila and Miedzychod (Figure 5a). The total distance of each vehicle was 1332*km* and the specific data are presented in Table 2.

***Table 2*** *Route-specific data*

| | Road property | Value |
|---|---|---|
| 1. | Length of the AB section of the route | 111 km |
| 2. | Maximum speed for sections of the route outside the populated areas | 90 km/h |
| 3. | Maximum speed for sections of the route in the populated areas | 50 km/h |
| 4. | The computational average velocity of the movement of vehicles on the route | 73 km/h |
| 5. | Computational travel time of AB section for average velocity | 95 min |
| 6. | The share of the sum of the route sections for the traffic with a speed limit of up to 50 km/h | 35.1% |
| 7. | The share of the sum of the route sections for the traffic with a speed limit of up to 90 km/h | 64.9% |
| 8. | The difference in altitude of the beginning and end of the route | 20 m |

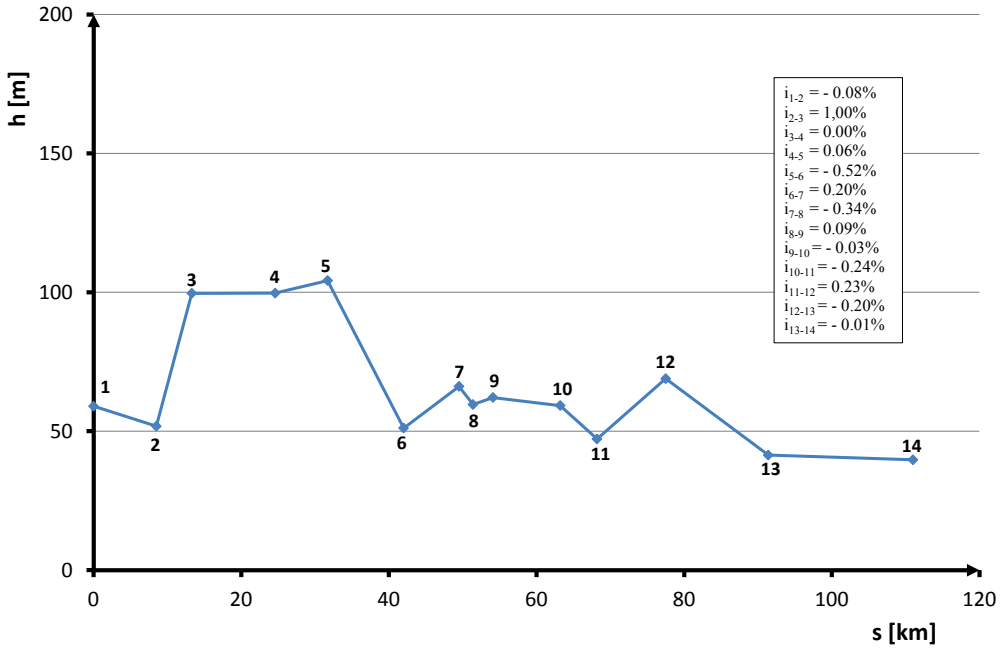


***Figure 6*** *Scheme of the configuration simplified to the critical points of the longitudinal profile of the measurement path from the starting point (1) to the end point (14) together with determination of the longitudinal slopes of the road (i); h - height of the path's points location relative to sea level, s - distance from the starting point A of the route*

During the road tests, there were no significant disruptions to the vehicle traffic. There were stable weather conditions, i.e. wind speed below 4 m/s, ambient temperature 20 °*C*, pressure 101.5 *kPa* and no renovation or cleaning works were carried out on the road that could significantly change the achieved velocity profile. The route covered both populated, field and forest areas, where there were few local speed limits. On the other hand, the longitudinal profile of the control route for the travel direction from A to B, simplified to reference points and the determination of longitudinal slopes, is shown in Figure 6.

For analysis of the obtained measurement data values, the value of the arithmetic mean obtained for the trip in both directions for all tests was taken. When analyzing the nature of the traffic, it was noticed that between the individual elementary sections of the route there was a cyclical change in speed caused by a change in the value of the ascent resistance force ($F_w$), which could have influenced the obtained values of the measured parameters. Hence, the analysis also took into account the features related to the route. Then, using the relationship describing the strength of resistance to ascent in the form:

$$F_w = m \cdot g \cdot \sin\alpha\,, \tag{9}$$

the total value of the hill resistance force for the entire length of the control route can be determined and written in the form of the equation:

$$\sum F_w = \sum_{j=1}^{k} F_n = \sum_{j=1}^{k} m \cdot g \cdot \sin\alpha_j \tag{10}$$

where:
$k$ - number of the last leg of the route,
$j$ - number of the next section of the route,
$\alpha j$ - longitudinal slope angle of the next section of the route.

Then, taking into account that for small values of the rise/fall angle of the road section, it is close to the

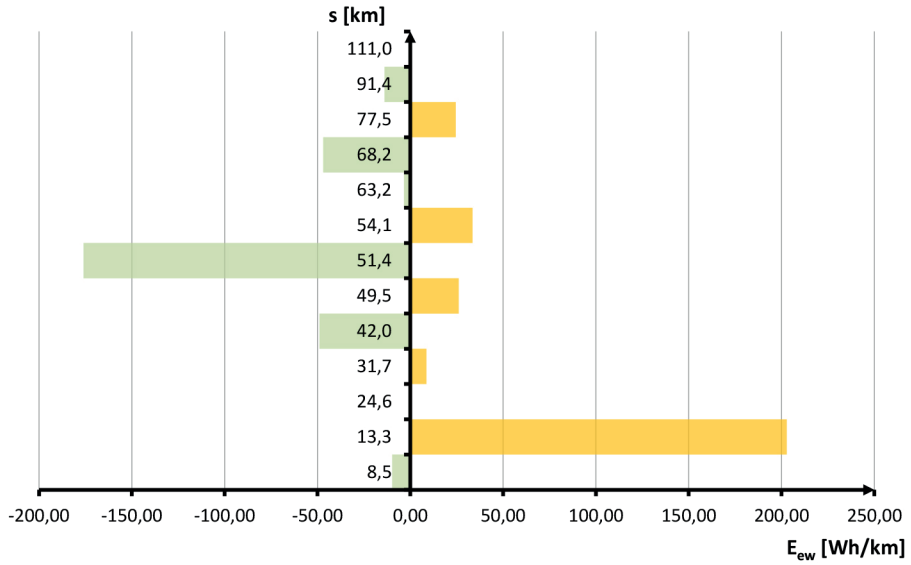


***Figure 7*** *The results of calculations of the specific energy demand for overcoming the sections of ascents and descents for the average speed of forward motion (73 km/h) - based on experimental data; vehicle weight 1365 kg, slopes according to the longitudinal profile of the route*

longitudinal gradient of the road that:

$$\sin\alpha_j \cong i_j ,$$

where, $i_j$ is the longitudinal slope of the $j$-th road section defined as the change of height above sea level at the beginning and end of the section ( $\Delta h$ ) along its length ($l$):

$$i_j = \frac{\Delta h}{l} \cdot 100\% .$$

Equation (10) can then be written in its final form as:

$$\sum F_w = \sum_{j=1}^{k} m \cdot g \cdot i_j . \tag{11}$$

Hence, the total value of energy ($E_{ew}$), necessary to perform the mechanical work in order to overcome the segmental resistance to motion of a vehicle caused by longitudinal road inclinations (potential energy increase) can be presented as:

$$E_{ew} = \sum_{j=1}^{k} m \cdot g \cdot i_j \cdot l_j . \tag{12}$$

In the case of assuming a constant value of the average speed of movement of the tested vehicle along the length of the test route, the power of the ascent resistance forces will be; on sections of slopes - reduction of energy demand by the vehicle engine, while in the case of the road slopes - an increase in energy demand.

Thus, in the case of the conducted experimental tests, the power supplied by the engine, necessary to overcome the total power of the ascent resistance ($N_{ew}$), can be described by the relation:

$$\sum N_{ew} = \frac{\sum E_{ew}}{t} = \frac{\sum_{j=1}^{k} mgi_j l_j}{t} . \tag{13}$$

or taking into account the speed of movement of the vehicle on each section of the road ($V_j$):

$$\sum N_{ew} = \sum_{j=1}^{k} F_{wj} \cdot V_j . \tag{14}$$

Then, taking into account the nature of the traffic (speed variability, speed of movement) and the load of the vehicle, it can be concluded that the power of the resistances to the uphill (road longitudinal inclination) has a significant impact on the energy balance of traffic and at the same time on the energy consumption necessary for the vehicle's movement. Taking into account the travel time of individual sections of ascents / descents, the angle of longitudinal slope and their length, it is possible to estimate the unit value of the energy necessary to overcome the hill due to the difference in height (change of potential energy $E_p$).

The results of calculations of the road distribution of the demand for unit energy necessary to overcome the slopes ($E_{ew}$) for the control section and the assumed constant speed of the vehicle movement are shown in Figure 7.

When analyzing the distribution of the specific energy demand for overcoming the resistance of slopes along the length of the control sections of the route (Figure 7), it can be noticed that the values of the demand are closely related to the value of the longitudinal slope of individual road sections. The obtained distribution refers to the value of the average speed of forward motion for the entire length of the route. This means that in the event of an increase in the demand for traffic energy (also supplied to the engine), the driver reduced the vehicle velocity - increasing the value of the gear ratio so much that it was possible to climb this hill. In addition, it should also be noted that the negative values of the specific energy consumption refer to cases where

***Table 3*** *Basic properties of the fuel [26]*

| | Fuel property/parameter | Value of parameter for fuel | |
|---|---|---|---|
| | | ON1 | ON2 |
| 1. | Density w 15˚C [g/m$^3$] | 822 | 832 |
| 2. | Self-ignition temperature [˚C] | > 260 | >255 |
| 3. | Kinematic viscosity @ 40°C [mm$^2$/s] | 1.5÷4.5 | 2.0÷4.5 |
| 4. | Calorific value [MJ/m$^3$] | 34.77 | 35.94 |
| 5. | Vapour pressure @ 40°C [kPa] | 0.4 | 0.4 |

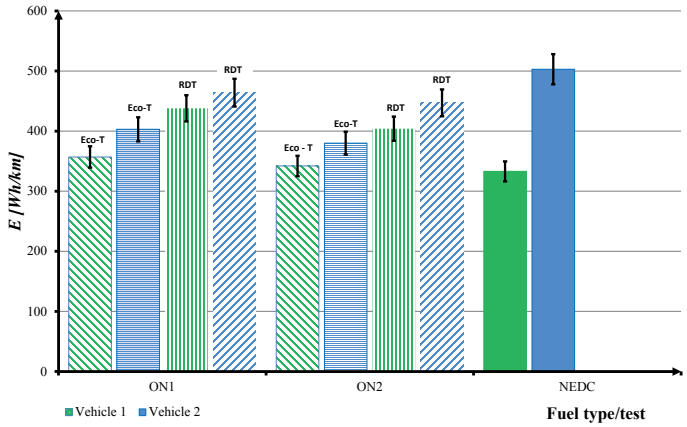


***Figure 8*** *Average specific energy consumption on the control path depending on the type of fuel and the driving method of vehicle control: Eco-T - Eco-driving mode, RDT - driving mode according to road conditions, ON1 - standard diesel oil, ON2 - enhanced diesel oil, NEDC - energy consumption data based on the vehicle manufacturer's data*

the longitudinal road slope causes the conversion of the tangent component of the gravity force, i.e. the drag force is converted into a driving force. This ultimately means that the driver can significantly reduce the energy consumption of the engine and at the same time can start using the resistance of the vehicle powertrain to generate braking force.

This is particularly important when planning one-way travel routes and when changing the actual weight of the vehicle or the volume and parameters of road traffic. On the other hand, when the mass of the vehicle is unchanged (electric vehicles) or only to a small extent (mass change due to fuel consumption) and the journey is to be carried out in both directions, the impact of the power of slopes on the energy balance can be considered negligible. The reason for this is that during the travel in both directions (back and forth), the vectors of the vectors of the resistance forces of the elevations change for each pass, which results in the mutual cancellation of the impact of these forces on the vehicle motion.

Due to the fact that the research was carried out for two directions of traffic, a balanced system of hill resistance forces was adopted in the further part of the study. Moreover, for the purposes of analyzing the energy consumption of the traffic of the tested vehicles, it was assumed that vehicle engines were used for braking, which in the overall balance will allow to partially compensate for the increase in fuel consumption in the acceleration phase.

The fuel in the form of standard diesel oil (ON1) and enhanced oil (ON2) was used to power the engines of the tested vehicles. The enriching additives were to directly affect the engine cleaning process and result in the improvement of the quality of the created combustible mixture and reduction of the harmful and toxic exhaust components' emission. The basic properties of these fuels are presented in Table 3.

### 4.3 Research results

The results of experimental studies of the average road energy consumption are presented in Figures 8 and 9. The analysis of the results of the average specific road energy consumption tests presented in Figure 8 allows to conclude that both in the case of Vehicle 1 and Vehicle 2, the lower energy consumption (fuel) was obtained when the driver was using recommendations resulting from the principles of Eco-driving. It should be noted, however, that the obtained values relate to the test performed in determined traffic and environmental conditions. However, the presented data of vehicle manufacturers were for reference only and are intended only for reference purposes. In addition, it should also be noted that the shape of the road may significantly

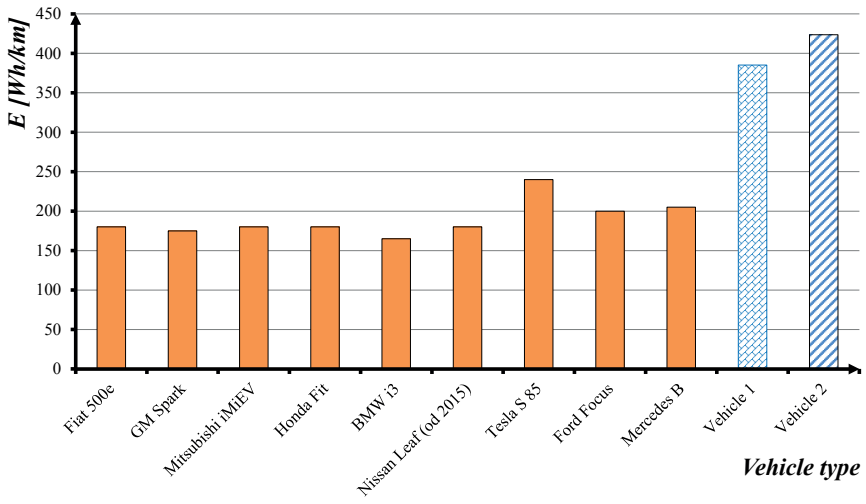


***Figure 9*** *Comparison of the average value for the test of specific energy consumption (E) of the traffic of passenger cars subjected to road tests and cars with electric drive based on manufacturers' data (by the product of battery capacity and range according to the EPA test)*

affect the increase in energy consumption, which in the analyzed case may constitute almost a double increase in relation to the specific energy consumption value.

The demonstrated reduction in energy consumption by about 10% in Eco mode (Figure 8) seems to be obvious due to the reduction of idling times of engines, as well as more effective use of the available torque and power of the engines in terms of achieving and maintaining the assumed velocity of movement. Moreover, it can be noticed that in the analyzed case, the use of enriched diesel oil did not significantly affect the result of the average specific energy consumption and the obtained differences are within the scope of measurement errors. Hence, it can be concluded that in the case of diesel fuels, the essence of reducing the energy consumption concerns driving techniques and road conditions. Enriched fuel significant advantage, related to the effects of cleaning the fuel supply system and the combustion chamber, could rather be observed in the perspective of vehicle mileage greater than that achieved in the study.

In the comparison presented in Figure 8, it should be noted that the calculated average specific energy consumption (based on the manufacturer's data on road fuel consumption) for the vehicle No. 1 indicates the comparability of the factory data and the obtained results of energy consumption under "economic" driving conditions. In the case of the car of vehicle no. 2, the manufacturer's data on energy consumption is similar to the results obtained from tests carried out in the real traffic conditions (without the key application of Eco-driving principles). This may indicate that during the road tests for these cases, traffic conditions similar to the NEDC test conditions occurred. Moreover, it can also be concluded that in the remaining cases the main reasons for the discrepancies in the obtained measurement results are the road factors forcing non-standard vehicle traffic conditions during the test. At the same time, it can be concluded that in the daily operation of the vehicle, the specific energy (fuel) consumption will be up to about 20% higher than the values obtained in the NEDC tests. At the same time, as a result of the research, it was observed that it is also possible to obtain lower unit energy consumption - vehicle No. 2.

A comparison of the average road energy consumption of the tested passenger cars in relation to those powered by electricity (Figure 9) calculated based on the test data on the electric battery capacity and range determined according to the EPA test for a combined cycle (EPA-Environmental Protection Agency of United State of America).

Taking into account the results of research and analysis (Figure 9), it can be concluded that compared to the tested cars, all the presented electric cars are almost twice more effective than ICE vehicles. This situation results from the fact that the energy consumption resulting from the consumption of energy supplied ($Q_d$) to perform the work and to generate the torque necessary to obtain the driving force on the wheels of the vehicle driving axle, where taking into account the internal resistances and losses of the drive train ($\eta$) for a specific road section, which can be written in the following form:

$$E = \frac{Q_d \cdot \eta}{s}. \tag{15}$$

In the case of electric vehicles, due to the relatively high efficiency of the electricity conversion process (over 90 %), it can be shown that the overall efficiency of the energy conversion processes is greater than the energy conversion processes in the case of vehicles with engines powered by conventional fuels (less than 50 %). The main reason for this difference is the efficiency of chemical into mechanical energy conversion processes taking place in internal combustion engines. In this case, taking into account the delivered energy conversion efficiency index, it is possible to record the dependence

on the energy consumption of traffic for vehicles with conventional drive:

$$E = \frac{Q_d \cdot \eta_e \cdot \eta}{s} \tag{16}$$

and an energetic efficiency can be expressed as:

$$\eta_e = \frac{1}{g_e \cdot W_u}, \tag{17}$$

where:
$g_e$ - specific fuel consumption, $kg/kWs$,
$W_u$ - calorific value of fuel, $kJ/kg$.

Hence, the relationship in Equation (16) describes the relation of the energy consumption of the vehicle motion, taking into account the properties of the fuel (energy supplied), the efficiency of its conversion by the engine and the generation of the driving force on the vehicle wheels. At the same time, this relationship allows to understand the essence of differences in values of the average road energy consumption for the selected and tested vehicles (Figure 9), where the key processes seem to be the processes occurring during the conversion of energy supplied to mechanical energy transmitted to the wheels of the driving axle. Taking this into account, it can also be stated that, regardless of the type and features of the vehicle propulsion system, it is important to minimize the energy consumption to use it efficiently for the purposes and processes serving the user.

On the other hand, in the case of electrically powered cars, Equation (16) should take into account, apart from the efficiency of the engine and losses in the powertrain, the losses arising in the process of charging the battery and losses resulting from the self-discharge of the battery, as well. Only this approach and taking them into account will make it possible to realistically compare the energy consumption of electric and conventional vehicles, which basically refers to resistance to motion. These, in turn, result mainly from the geometric and mechanical properties of the vehicle, therefore they should not constitute significant differences in the analysis of the energy consumption of the vehicle movement.

## 5 Summary

Taking into account the theoretical analysis and the obtained research results of fuel consumption measurements and based on that calculated a specific energy consumption of vehicle traffic, it can be concluded that:

The application of the principles of Eco-driving allows for the reduction of energy consumption and this change may reach even 10 % of the average SEC value and at the same time contribute to reduction of the exhaust gas emissions.

The longitudinal profile of the road significantly influences the change in the average specific energy consumption and the intensity of this change depends directly on the longitudinal gradient of the road and the actual weight of the vehicle.

Even a simplified form of analysis of the longitudinal profile of the route allows to effectively influence the route planning process and the appropriate planning of routes for laden vehicles to shape the longitudinal profile (use of slopes) allows to significantly reduce energy consumption and thus transport operation costs.

Showing the higher energy consumption of the traffic of vehicles with conventional propulsion is burdened with losses on the side of energy conversion, while the specific energy consumption of the traffic itself depends directly on the resistance to motion of a vehicle and not on the method of its propulsion.

## References

[1] LI, Y., BAI, X.-S., TUNER, M., IM, H. G., JOHANSSON, B. Investigation on a high-stratified direct injection spark ignition (DISI) engine fueled with methanol under a high compression ratio. *Applied Thermal Engineering* [online]. 2019, **148**, p. 352-362. ISSN 1359-4311. Available from: https://doi.org/10.1016/j.applthermaleng.2018.11.065

[2] CHEN, W., PAN, J., FAN, B., LIU, Z., PETER, O. Effect of injection strategy on fuel-air mixing and combustion process in a direct injection diesel rotary engine (DI-DRE). *Energy Conversion and Management* [online]. 2017, **154**, p. 68-80. ISSN 0196-8904. Available from: https://doi.org/10.1016/j.enconman.2017.10.048

[3] ZHANG, F., COOKE, P. The green vehicle trend: electric, plug-in hybrid or hydrogen fuel cell? [online] [accessed 2019-02-21]. Available from: https://www.esci-ksp.org/wp/wp-content/uploads/2012/04/The-Green-Vehicle-Trend-Electric-Plug-in-hybrid-or-Hydrogen-fuel-cell.pdf

[4] LONG, A., BOSE, A., O'SHEA, R., MONAGHAN, R., MURPHY, J. D. Implications of European Union recast renewable energy directive sustainability criteria for renewable heat and transport: case study of willow biomethane in Ireland. *Renewable and Sustainable Energy Reviews* [online]. 2021, **150**, 111461. ISSN 1364-0321. Available from: https://doi.org/10.1016/j.rser.2021.111461

[5] Registrations of the new passenger cars - www.acea.auto [online] [accessed 2021-06-12]. 2021. Available from: https://www.facebook.com/cartrackPL/

[6] ADEYANJU, A. A. *Electric vehicle economics*. LAP LAMBERT Academic Publishing, 2020. ISBN 978-620-2-52668-5.

[7] ROTARIS, L., GIANSOLDATI, M., SCORRANO, M. The slow uptake of electric cars in Italy and Slovenia. Evidence from a stated-preference survey and the role of knowledge and environmental awareness. *Transportation Research Part A: Policy and Practice* [online]. 2021, **144**, p. 1-18. ISSN 0965-8564. Available from: https://doi.org/10.1016/j.tra.2020.11.011

[8] BOBETH, S., KASTNER, I. Buying an electric car: a rational choice or a norm-directed behavior? *Transportation Research Part F: Traffic Psychology and Behaviour* [online]. 2020, **73**, p. 236-258. ISSN 1369-8478. Available from: https://doi.org/10.1016/j.trf.2020.06.009

[9] FEVANG, E., FIGENBAUM, E., FRIDSTROM, L., HALSE, A. H., HAUGE, K. E., JOHANSEN, B. G., RAAUM, O. Who goes electric? The anatomy of electric car ownership in Norway. *Transportation Research Part D: Transport and Environment* [online]. 2021, **92**, 102727. ISSN 1361-9209. Available from: https://doi.org/10.1016/j.trd.2021.102727

[10] KHAN, M. I. Comparative well-to-tank energy use and greenhouse gas assessment of natural gas as a transportation fuel in Pakistan. *Energy for Sustainable Development* [online]. 2018, **43**, p. 38-59. ISSN 0973-0826. Available from: https://doi.org/10.1016/j.esd.2017.12.004

[11] GUZEL, T. D., ALP, K. Modeling of greenhouse gas emissions from the transportation sector in Istanbul by 2050. *Atmospheric Pollution Research* [online]. 2020, **11**(12), p. 2190-2201. ISSN 1309-1042. Available from: https://doi.org/10.1016/j.apr.2020.08.034

[12] DUC, K. N., DUY, V. N. Study on performance enhancement and emission reduction of used fuel-injected motorcycles using bi-fuel gasoline-LPG. *Energy for Sustainable Development* [online]. 2018, **43**, p. 60-67. ISSN 0973-0826. Available from: https://doi.org/10.1016/j.esd.2017.12.005

[13] CHAPMAN, K. S., PATIL, A. Performance, efficiency and emissions characterization of reciprocating internal combustion engines fueled with hydrogen/natural gas blends [online]. Final technical report. Manhattan: Kansas State University, National Gas Machinery Laboratory, 2008. Available from: https://www.osti.gov/servlets/purl/927586

[14] WANG, B., PAMMINGERB, M., WALLNERA, T. Impact of fuel and engine operating conditions on efficiency of a heavy-duty truck engine running compression ignition mode using energy and exergy analysis [online]. Available from: www.osti.gov/servlets/purl/1606254 - dostęp. 08.06.2022 r

[15] FRIEDL, H., FRAIDL, G., KAPUS, P. Highest efficiency and ultra-low emission - internal combustion engine 4.0. *Combustion Engines* [online]. 2020, **180**(1), p. 8-16. ISSN 2300-9896, eISSN 2658-1442. Available from: https://doi.org/10.19206/CE-2020-102

[16] LEACH, F., KALGHATGI, G., STONE, R., MILES, P. The scope for improving the efficiency and environmental impact of internal combustion engines. *Transportation Engineering* [online]. 2020, **1**, 100005. ISSN 2666-691X. Available from: https://doi.org/10.1016/j.treng.2020.100005

[17] TSIAKMAKIS, S., FONTARAS, G., CUBITO, C., PAVLOVIC, J., ANAGNOSTOPOULOS, K., CIUFFO, B. From NEDC to WLTP: effect on the type-approval $CO_2$ emissions of light-duty vehicles [online]. EUR 28724 EN. Luxembourg: Office of the European Union, 2017. ISBN 978-92-79-71643-0, eISBN 978-92-79-71642-3. Available from: https://doi.org/10.2760/93419

[18] WACHOWIAK, P., GORZELANCZYK, P., KALINA, T. Analysis of the effectiveness of shock absorbers in the light of the applicable legal regulations in Poland and Slovakia (in Polish). *Coaches. Technology, Operation, Transport Systems* [online]. 2018, 19(6), p. 764-770. ISSN 1509-5878, eISSN 2450-7725. Available from: https://doi.org/10.24136/atest.2018.172

[19] GORZELANCZYK, P. Tire wear characteristics of public transport buses in the city of Pila (in Polish). *Coaches. Technology, Operation, Transport Systems*. 2017, 18(12), p. 891-896. ISSN 1509-5878, eISSN 2450-7725.

[20] EDWARDS, R., LARIVE, J.-F., RICKEARD, D., WEINDORF, W. Well-to-wheels analysis of future automotive fuels and powertrains in the European context [online]. Luxemburg: Office of the European Union, 2014. ISBN 978-9279-21395-3. Available from: https://doi.org/10.2788/79018

[21] SILKA, W. *Car traffic energy consumption* (in Polish). Warszawa: Scientific and Technical Publishers, 1997. ISBN 8320420377

[22] Principles of ecodriving [online] [accessed 2021-06-12]. 2021. Available from: http://dopierwszego.pl/2018/ecodriving-czyli-ekologiczny-styl-jazdy-poznaj-jego-8-glownych-zalozen/

[23] MERKISZ, J., PIELECHA, I., PIELECHA, J., BRUDNICKI, K. *Alternative vehicle drives*. Poznan: Poznan University of Technology Publishing House, 2006. ISBN 978-83-7143-260-6

[24] GORZELANCZYK, P., MICHAS, D. The impact of eco-driving on the operation of vehicles (in Polish). *Coaches. Technology, Operation, Transport Systems* [online]. 2019, **1-2**, p. 216-219. ISSN 1509-5878, eISSN 2450-7725. Available from: https://doi.org/10.24136/atest.2019.039

[25] Maps Google [online] [accessed 2021-06-12]. 2021. Available from: http://www.mapsgoogle.pl

[26] Properties of the fuel [online] [accessed 2021-06-12]. 2021. Available from: https://www.shell.pl

# DEVELOPING NOVEL REGISTRATION OF ROAD TRAFFIC ACCIDENTS

**Jamshid Sodikov, Quvonchbek Musulmonov, Dilshod Imamaliev ***

Department of "Construction and Maintenance of Automotive Roads", Tashkent State Transport University, Tashkent, Uzbekistan

*E-mail of corresponding author: dilimshod@gmail.com

***Resume***

The paper reviews the road traffic accident registration form and discusses existing practices carried out in Uzbekistan. The popularity of mobile phones/tablets and internet technologies in daily use and their increasing power in terms of speed and memory could assist efficiency and accuracy in the road traffic accident data collection. The authors review up-to-date mobile/internet technologies for the road accident data registration and propose a novel approach that covers various data sources including police data, hospital data, road department data, insurance company data, transport company data and social media data. The proposed approach integrates all the data into a single system (database), which can be used for public audit and research purposes.

***Article info***

Received 23 February 2022
Accepted 17 June 2022
Online 25 August 2022

***Keywords:***

road traffic accidents
registration form
geolocation
mobile/internet technologies

Available online: https://doi.org/10.26552/com.C.2022.4.F62-F71

ISSN 1335-4205 (print version)
ISSN 2585-7878 (online version)

## 1 Introduction

The likelihood of the road traffic accidents (RTA) is random because road traffic accidents happen due to several factors or a combination of factors that characterize its randomness. It is customary to consider the driver-vehicle-road system as the main factor influencing the occurrence of an accident. The lion's share of accidents of these factors lies with the driver, about 80 %. The road traffic accidents are one of the most important social problems at present. With improvement of the welfare and growth in the level of motorization, the growth rate of accidents on the roads increases every day.

According to the latest data from the World Health Organization (WHO, 2018) [1], 1.35 million people die every year around the world, in other words, almost 3,700 people die every day on the world's roads and about 20-50 million people sustain various non-fatal injuries, more than half of all deaths and injuries happen to vulnerable road users such as pedestrians, cyclists and motorcyclists and their passengers. Young people are particularly vulnerable on the world's roads and the road traffic injuries are the leading cause of death for children and young people aged 5-29. Young men under the age of 25 are more likely to be involved in the road traffic crashes than women, with 73 of all the road traffic deaths occurring in young men of this age. Developing countries have higher rates of road traffic injuries, with 93 % of deaths occurring in the low- and middle-income countries. In addition to the human suffering, caused by road traffic injuries, they also carry a heavy economic burden on victims and their families, both due to the cost of treating the injured and the loss of productivity of those killed or disabled. More broadly, the road traffic injuries have a major impact on the national economy, costing countries 3% of their annual gross domestic product, both due to the cost of treating the injured and due to the loss of productivity of the killed or disabled.

According to the concept of ensuring road safety in the Republic of Uzbekistan for 2018 - 2022, statistical indicators show that annually on the territory of the Republic of Uzbekistan there are on average about 9-10 thousand road accidents, including more than 2000 of the - human victims (Directive 377, 2018) [2].

## 2 Literature review

Accounting for the road traffic accidents plays an important role, since based on the data it is possible to identify the road sections with the highest number of

***Table 1*** *Road accident data collection state of the art*

| No. | Research paper/report | Authors | Findings |
|---|---|---|---|
| 1 | Design and development of a prototype mobile geographic information system for real-time collection and storage of traffic accident data (thesis), 2016 [10] | Peter Markus | Researcher reviewed existing STRADA crash database used in Sweeden, highlighted shortcomings. Based on that author proposed the smartphone-based crash data collection and layout web application for visualization and data analysis. |
| 2 | Critical Review of the International Crash Databases and Proposals for Improvement of the Italian National Database, 2012 [11] | Alfonso Montella, David Andreassen, Andrew P. Tarko, Shane Turner, Filomena Mauriello, Lella Liana Imbriani, Mario A. Romeroc, Rohit Singh | Authors critically reviewed the crash data base in developed countries and point out weaknesses of existing Italian crash database. They stressed out the following key points: consistency in crash data collection by police officers, national crash database should include all the relevant information and recommended improvements of the highway police practice. |
| 3 | Development and evaluation of a web-based software for crash data collection, processing and analysis, 2017 [12] | Alfonso Montella, Salvatore Chiaradonna, Giorgio Criscuolo, Salvatore De Martino | Researchers overview state of the art road accident data collection around the world and pinpoint main issues and prospects for improvement. They mentioned key aspects of software framework, structure of database, features of the system. Authors proposed ReGIS web-based software platform-independent, for the crash data collection, processing and analysis, which can be used as mobile and desktop application. |

road traffic accidents (RTA), that is, their concentration. The probable cause of the origin can be also determined; the accident itself is a probable phenomenon, therefore, the causes of origin are indirectly probabilistic. It is generally known that the occurrence of an accident is due to the three classic factors driver-car-road, some researchers also suggest taking into account the environment.

For a correct assessment of the road safety, an electronic accident database should be available. Additionally to create an electronic database of road accidents, an electronic road accident registration system should be introduced. At present, accidents in Uzbekistan are recorded in paper format but stored in an electronic database. The disadvantage of this approach is that when converting from a paper to an electronic version, there is a high probability of subjective factors that affect the quality and reliability of the data entered. There is also a time lag when one needs to get the latest reports in real-time. One of the main disadvantages of this method of accounting for accidents is that it is impossible to accurately determine the location of an accident since when filling out a registration card, the location is tied to the closest object, for example, a school, store, building etc.

Consequently, the relevance of the electronic registration development of the road accidents is increasing, with existing technologies, such as tablets, smartphones and other devices that are connected to the Internet, which have built-in GPS modules that allow to effectively solve the problems of electronic registration of road accidents. It is also important how much data is required to collect the crash data. Since the more data is required to collect, the more time and money is required to collect. Sodikov, 2018 [3] provides a table of the existing road traffic accident registration card. It consists of 12 forms of filling out by an employee of an internal affairs body (traffic police officer) such as 1. General information, 2. Location (village, town), 3. Location of an accident on the road, 4. Road condition, 5. Violation of traffic rules by pedestrians, 6. Driver information, 7. Vehicle information, 8. The ownership of the vehicle, 9. Victim information, 10. Additional information, 11. Description and diagram of the accident, 12. Measures taken.

Since the existing accident registration requires the collection of a lot of data, therefore, the time spent on filling it out increases. Software for photo recognition (computer vision), machine learning (big data processing and forecasting) and others are already available and widely used. Therefore, to improve the productivity and accuracy of data collection, it is necessary to timely introduce new information technologies. In this direction, scientific prerequisites have been proposed by a number of researchers [4-9]. In addition, the researchers listed in Table 1 worked on this issue and offered their recommendations on the approach to registering road accidents. Currently, the traffic safety authorities keep records of accidents according to the corresponding forms, in a handwritten form. Traffic accident data collection requires a lot of time, sometimes for a district or city scale a few days and for a country level a week and sometimes more. Electronic registration of the road accidents with the use of geoinformation technologies has been proposed, [10-12]. A tablet computer running android or IOS is proposed for the data collection. The proposed electronic card for the traffic accidents has several advantages and will save the employee's time. First of all, after arriving at the scene of the accident, the employee takes a photo with the geolocation function,

***Table 2*** *Main sources of data on road accidents*

| Source | Data type | Remarks |
|---|---|---|
| State Traffic Safety Administration of the Ministry of Internal Affairs of the Republic of Uzbekistan. | 1. General information, 2. Location (village, town), 3. Location of an accident on the road, 4. Road condition, 5. Violation of traffic rules by pedestrians, 6. Driver information, 7. Vehicle information, 8. The ownership of a vehicle, 9. Victim information, 10. Additional information, 11. Description and diagram of the accident, 12. Measures taken. | Access to the road traffic accident database is internal and limited. There are assumptions about the underreporting of road accidents. There is a database, but there is no subsystem for identifying causes and effects. No electronic exchange with other state organizations. |
| Road organizations | According to MKN 15-2007 „Rules for the registration and analysis of road accidents on highways“, attention is mainly paid to the assessment of road conditions | Access is limited, there is no electronic database. No electronic exchange with other state organizations. |
| Vehicle fleets and transport companies | Road traffic accidents registered by transport organizations whose vehicles were involved in an accident. | Access is limited, there is no electronic database. No electronic exchange with other state organizations. |
| Ministry of Health | Number of road traffic accidents, number of fatalities, number of non-fatal injuries, age and gender of victims, driver‘s condition, age, occupation registered. | The base is not systematized, there are various discrepancies, incomplete data. Access is limited. No electronic exchange with other state organizations. |
| Insurance companies | Fatal and non-fatal injuries, damage to vehicles, cost of claims | There is no electronic database. Access is limited, no electronic exchange with other state organizations. |
| Social media | Mainly photography, from where one can determine the time of the incident and the types of vehicles | Access is not limited, but there is no systematic collection of data |

which will allow visualizing the given accident in an electronic map (QGIS, ArcGIS, or Google Fusion). After that, one can use the electronic driver's license database to determine the characteristics of the driver/vehicle or to recognize the photo. The built-in scheme library can be used for drawing the road accident diagram.

Vision Zero, adopted in 1995, represented a fundamentally new way of looking at road safety problems and their solutions. Vision Zero is a multinational road safety project that aims to create a road system without fatal or serious traffic-related injuries. It started in Sweden and was approved by their parliament in October 1997. The core principle of the vision is that "Life and health can never be exchanged for other benefits in society" rather than the more traditional cost-benefit comparison, in which life and health are valued in monetary terms and then this value is used to decide how much money to spend on the road network to reduce risk. Vision Zero means that ultimately no one will be killed or seriously injured in the transport system, [13]. Currently, the zero-mortality concept has been introduced in countries such as Canada, the Netherlands, the United Kingdom, the United States, Norway and other countries.

The Zero Death Concept views the road transport system as a whole, whose components - roads, vehicles and pedestrians - work together to the ensure safety. This holistic approach is fundamentally new in the field of the road safety. The concept of zero deaths implies a new perspective on responsibility. The primary responsibility for safety rests with the creators of the road transport system - road services, vehicle manufacturers, carriers, politicians, government officials, legislators and the police. The concept of zero mortality consists of many components, each of which contributes to improving road safety: these are ethical principles, human qualities, responsibility and scientific data.

## 3 Methods

Accidents are recorded by several government agencies. Those are the State Traffic Safety Inspectorate of the Republic of Uzbekistan, the Ministry of Health, Road services. However, there is a problem of data exchange between government organizations. Table 2 lists the main sources of crash data. As can be seen from Table 2, despite the fact that there are various sources of collection and recording of road accidents, there are several problems such as the incompleteness of data, lack of a single electronic database, lack of electronic data exchange between government departments and causes underreporting of road accidents.

Regardless of the data source on road accidents, there are certain problems associated with recording and collecting data. The most complete base, in terms of storing and processing data, can be considered the electronic database of the State Traffic Safety Inspectorate of the Ministry of Internal Affairs, which currently more or less meets modern requirements.

However, the main drawback is the paper-based crash accounting method, which prevents accurate and timely crash registration. Therefore, a methodology for electronic data collection using modern tablet computers should be developed. A unified electronic system for collecting, storing and analyzing data on road accidents

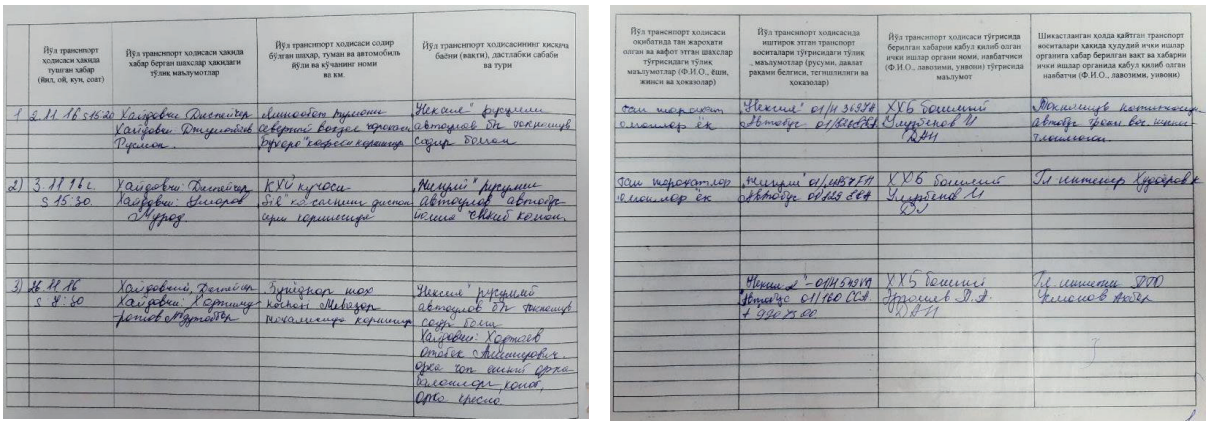

***Figure 1*** *Registration journal of vehicle fleets accidents*
*(source: Bus Park No. 1 of the Yashnabad district of Tashkent city, [3])*

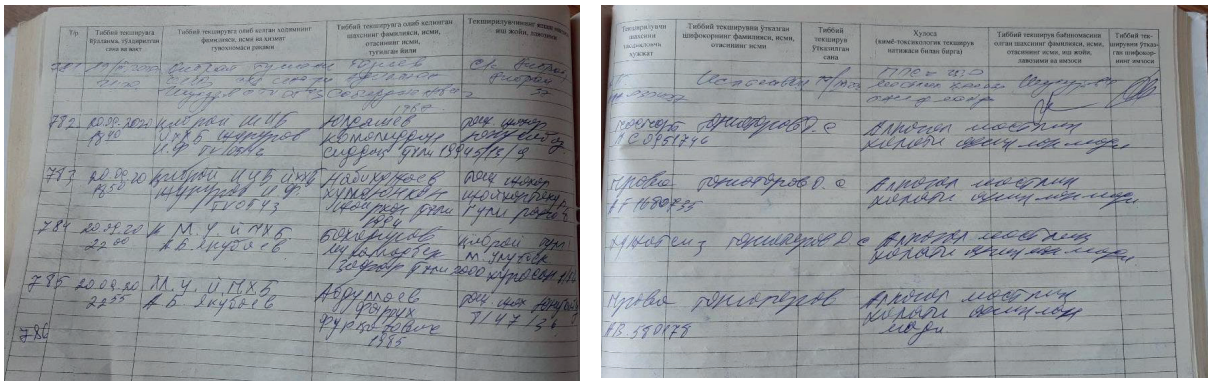

***Figure 2*** *Registration journal of medical examination of drivers involved in road accidents*
*(source: Republican Scientific Center of Emergency Medical Care, Tashkent, [3])*

would increase the efficiency of employees of public services and would increase the accuracy and quick data transmission in the real-time, as well. This, in turn, would facilitate timely decision-making before and after the accidents on the roads and streets. Based on real and reliable data, it is possible to develop measures to eliminate or prevent accidents in a more adequate and timely manner. Existing data collection methods do not meet modern requirements and impede the adoption of appropriate measures to prevent the road accidents. One of the main problems of the paper method is that when registering an accident, the location indicates the nearest structure, be it a store or a building that can be demolished after a certain time. Consequently, it would be difficult to determine the exact location of the accident. This information is very important when determining the most dangerous sections of streets and roads, that is, places of concentration (black spots).

On the other hand, the road organizations keep their records of accidents. The main focus is on taking into account the location of accidents and road conditions and the geometric parameters of the roads. Based on these data, it can be assumed that one or another road condition could have provoked an accident. However, it is well known that an accident occurs due to a combination of several factors that can arise under uncertain circumstances, which is why an accident is considered as a probabilistic phenomenon. Road organizations store data in the paper form, moreover, these data are not transferred to the traffic police for further study, that is, there is no electronic data exchange. Identification of problems, associated with the exchange of data, their accuracy, as well as reliability has an important role in determining the causes and consequences of road accidents.

Fleets and transport companies also keep records of accidents involving their vehicles. Figure 1 shows the pages of the traffic accident log of the city fleet. It takes into account vehicle technical condition, driver's condition (sober/drunk) and other characteristics. Just like in road organizations, in-vehicle fleets and transport companies, accidents are stored in the paper form and are not exchanged with other organizations and departments that keep records of accidents.

Departments of the Ministry of Health also keep records of the road accidents when victims are admitted to hospitals and also when checking vehicle drivers for sobriety. As in previous cases, accidents are recorded in the paper form and there is no electronic exchange with other departments. The pages of the registration log of the medical examination of drivers involved in road accidents are shown in Figure 2. The most frequently

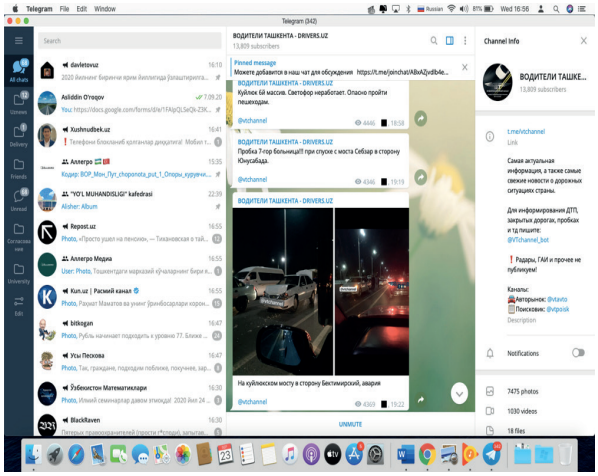

***Figure 3*** *Photo report of the accident (source: page of the group "Drivers of Tashkent" of the social platform "Telegram", [3])*

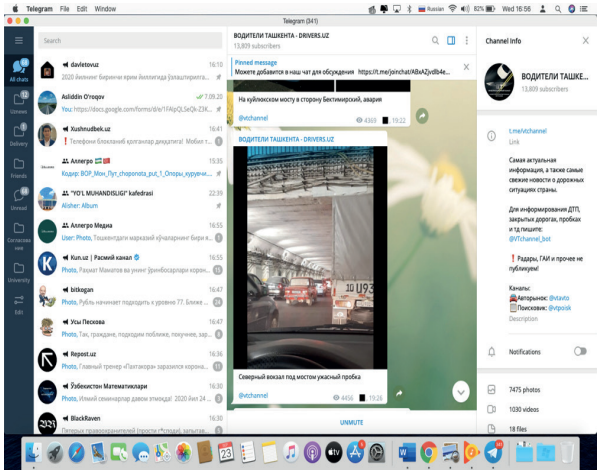

***Figure 4*** *Traffic jam photo report (source: page of the group "Drivers of Tashkent" of the social platform "Telegram", [3])*

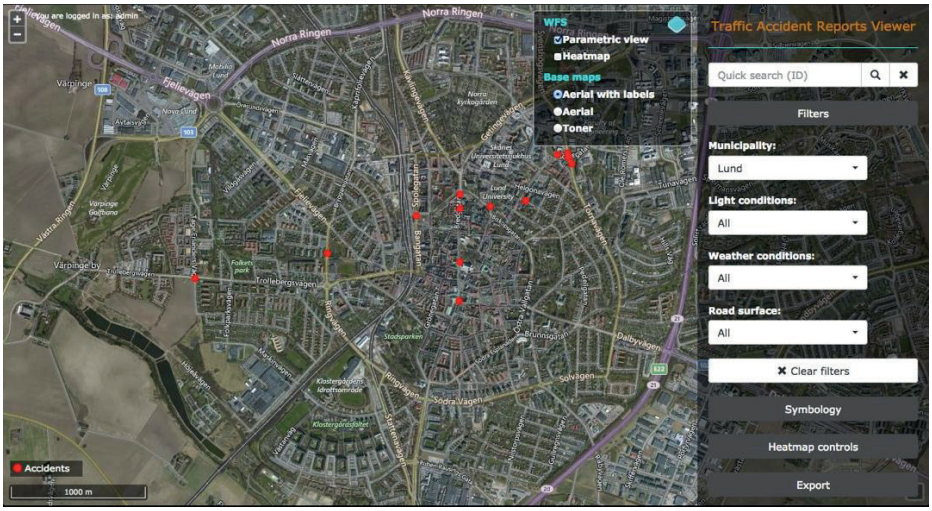


***Figure 5*** *An example of visualization of the location of an accident, [10]*

cited definition of a fatal road traffic accident is "any person who is killed immediately or died within 30 days in a road traffic accident (Preliminary report, 2003) [14]. However, there are different periods to determine the days after which a person can be considered killed due to an accident. For example, the European Union, Greece, Portugal and Spain use 24 hours, France uses 6 days, Italy uses 7 days and other countries use 30 days (Mackay, 2006) [15].

Insurance companies keep records of accidents in terms of fatal and non-fatal injuries, vehicle damage and the costs of claims. In addition, there is no electronic registration nor the data exchange for further analysis of the consequences of road accidents.

The development of information technology, as well as the penetration into the daily life of social networks, makes it possible to register the events taking place in real-time. Existing telegram channels/communities such as "Drivers of Tashkent", "Behind the Wheel" and others allow keeping records directly during the accident or immediately after the accident. The pages of the publication of posts about road accidents on the social network "Telegram" in the group "Drivers of Tashkent" are shown in Figures 3, 4. Therefore, in this direction, attention should be paid to creation of a traffic accident registration boot, which would allow collecting preliminary information about incidents.

Sweden is a leader in the road safety with the lowest death rate of 3 per 100,000 inhabitants. The number of road traffic fatalities per 100,000 inhabitants in Sweden fell by 52 % between 2000 and 2018. In 2018, there were 3.2 deaths per 100,000 inhabitants, up from 6.7 in 2000. For comparison, the European Union average is 4.9 deaths per 100,000 inhabitants in 2018 (Road Safety Annual Report, 2019) [16].

Studies carried out by Markus, 2016 [10] and Sjoo and Ungerback, 2007 [17] in Sweden have shown that the use of outdated crash data collection methods revealed the following disadvantages: reporting delays, reports with insufficient information such as attribute

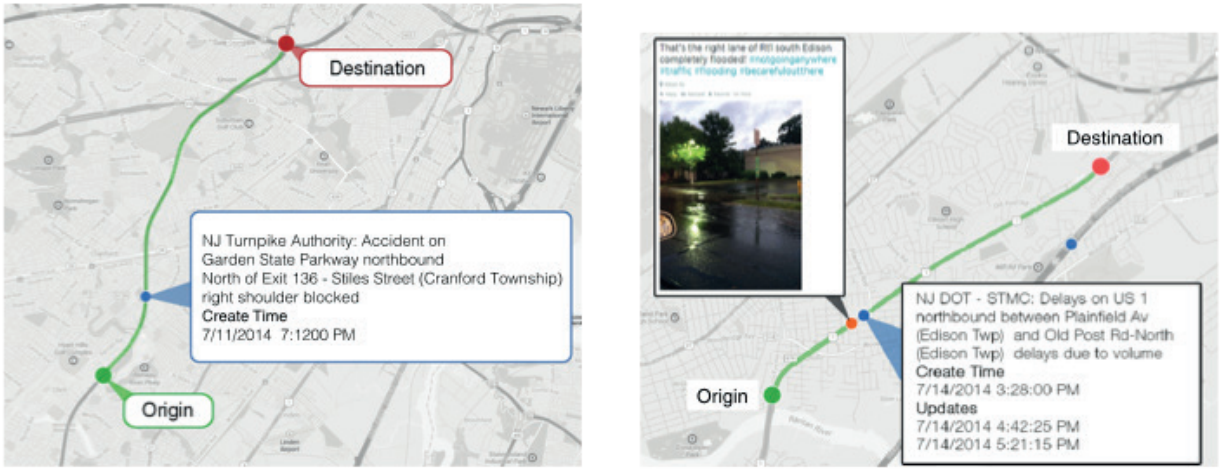


***Figure 6*** *An example of visualization of accidents and road problems in the state of New Jersey, [18]*

data and inaccurate location. According to researchers [3, 9 and 10] using a GPS device could increase the accuracy of the location of an accident. Figure 5 provides an example of visualization of an accident, as well as the area, lighting, weather conditions, type of coverage. This application is based on an open-source software that allows to develop additional functions for statistical analyzes and construction of various thematic maps, such as the concentration of road accidents, zones of hazardous areas (heatmaps) and others.

A review of the literature shows that, even the country with the lowest number of the road accidents per 100,000 people, is at the stage of developing electronic accounting and analysis of road accidents.

Several researchers have attempted to collect data using internet technology. For example, the state of New Jersey used the social network Twitter to collect data on traffic conditions and accidents. The popularity of alternative data collection procedures among researchers in various fields has increased, especially with the development of mobile and wireless devices over the past two decades. Authors of [18] highlighted an improved data collection method, which was presented for analyzing traffic conditions and traffic accidents. An integrated database system using the open online data sources for real-time traffic information. At the same time, the main goal of the study is to collect and use data for sections of the transport network where the physical sensor infrastructure is limited at best. Figure 6 shows an example how in the real-time it is possible to get data from the social networks and visualize. Although the data that is collected in this way does not allow obtaining detailed data on road accidents, it plays a huge role in the timely response of the police and ambulance.

The sections of the road where an accident occurred can be determined in the real-time. A photo of the scene can be also obtained if the user posted it on his Twitter account.

When switching from paper technology, or a semi-computerized road accident accounting system, to a complete electronic accounting system using mobile devices (smartphones, tablets), it can increase accuracy, timeliness, describe the incident in more detail using audio, video, photos, sketches and geolocation. It shows that outdated methods of collecting data on road accidents do not provide data promptly, at times it can reach up to 50 days from the time of registration of the road accidents at the scene of the accident until the storage to a central database for further processing and development of measures to prevent the occurrence of road accidents. Accordingly, this entails not only incompleteness of the database but underreporting of road accidents, as well.

Underreporting of road accidents is relevant even in developed countries. In all the countries, there is a problem of underreporting road accidents with victims. In the Scandinavian countries, where the accounting system is at a high level, an average of about 50 % of road traffic accidents with injuries are recorded. In the UK, only 60 % of accidents are recorded, in which drivers or passengers of vehicles were injured, in Australia - about 70 %, in New Zealand and Spain – 67 %. In Russia, there is also an underestimation of road accidents with victims and is about 10-20 % according to [19].

Mortality due to road accidents is a special object of statistical research and is characterized by specific features that are directly related to its accounting.

- Firstly, the number of deaths includes both persons who died at the scene of a road traffic accident and those who died from its consequences within 30 next days.
- Second, the road traffic deaths are estimated based on a large number of structural characteristics. The death toll will be distributed according to standard demographic characteristics (gender, age) as well as non-standard, original characteristics. The latter include the distribution of the number of fatalities in the road accidents due to the causes of road accidents (for example, road accidents and

victims due to the unsatisfactory condition of streets and roads etc.); distribution of the number of deaths in road accidents by subjects of road traffic accidents (for example, road accidents and victims of traffic violations by pedestrians, road accidents and victims of traffic violations by drivers of vehicles in condition etc.); distribution of the number of fatalities in road accidents by category of vehicle owners guilty of road accidents (for example, road accidents and victims of traffic violations by drivers of vehicles of legal entities etc.) etc.

- Thirdly, some special factors affect the intensity of mortality due to road accidents. Among them: time of the day and period of the year; roadway lighting; length and coverage of highways; traffic capacity of highways; traffic intensity and many others, [20]. In Kazakhstan, the software "Accident" was developed with the following functions:
  - ❑ search, entry, change and removal from the database of statistical data from road traffic accidents cards
- Search for the required card according to one or several specified criteria (date of the accident, vehicle state number, the name of the vehicle owner, victim etc.);
  - ❑ statistical analysis of road accidents (quantitative, qualitative and topographic);
  - ❑ filtration of data by one or several criteria (up to four), combined with the use of logical operators, which allows to select a certain range from the total volume of statistical information;
  - ❑ forming and printing out various forms of reporting, analysis results, individual accident cards;
  - ❑ the use of specialized dictionaries when entering information into the database, allowing to unambiguously identify the input object and reduce the size of the database.

A review of scientific literature shows that there is a need to develop an automated accounting system and real-time data transfer to a central electronic database, as well as electronic data exchange between departments, such as the state road safety service, road organizations, medical institutions, insurance organizations and other interested parties. organizations. The use of modern portable devices (smartphones, tablets), equipped with GPS modules, high-resolution photo/video cameras can solve the problem faced by road safety employees. Another task is to store this data in a single electronic database. In this direction, the State Traffic Safety Inspectorate of the Republic of Uzbekistan has already done a fairly large amount of work, but there are some disadvantages:

1. The electronic database has a local version;
2. Data is stored in outdated software that does not meet modern requirements;
3. Statistical analysis of crash data is very primitive;
4. There is no electronic exchange of data on road accidents between government agencies
5. Due to the manual collection of data on road accidents (record card), there are gaps (missing data), late transmission and data entry, underestimation of victims, low data accuracy.
6. There is no precise geolocation of the accident location
7. There is no visualization of the location of the accident in the electronic map
8. Manual registration of an accident scheme
9. The accident database is not connected to the driver's license and vehicle database
10. Weather conditions are not taken into account when accounting and storage accidents

## 4 Results and discussions

The existing method of accounting for the road accidents does not meet modern requirements in terms of accuracy, reliability, making the right decisions, ignoring the available mobile and internet technologies. Consequently, the development of modern methods for accounting for the road accidents is relevant in Uzbekistan. As the results of the study show, data on road accidents are stored in various state and non-state departments such as the Ministry of Internal Affairs, road organizations, the Ministry of Health, transport companies, insurance organizations and at the same time they do not exchange data with each other. Many questions arise, what this data is stored for and what is the use of it, what measures are being taken to reduce the number of fatal and injury accidents. To solve the above tasks and problems, a computerized system should be developed for collecting, storing, transferring and analyzing. A theoretical basis for the collection, storage, analysis and recommendation should be created, which would form the basis of a unified automated electronic system for registering, analysis and recommending of road accidents and would provide access and exchange of data between various departments and organizations. To solve several problems mentioned earlier, a system of automated accounting of road accidents for Uzbekistan was proposed. It consists of several subsystems, such as an accident registration system at the traffic police department, at the Ministry of Health, at the road organization, at the insurance companies, an accident accounting system in transport organizations (Figure 7). The central database would be under the control of the State Traffic Safety Inspectorate of the Ministry of Internal Affairs of Uzbekistan, where all the data related to road accidents would be stored. Each subsystem would be independent but would provide the real-time data exchange. In the event of an accident, the traffic police officer registers the accident using a tablet and assigns an ID number, which would serve as a unified link with other departments and organizations. The materials of the accident are sent to the Department of Inquiry of the

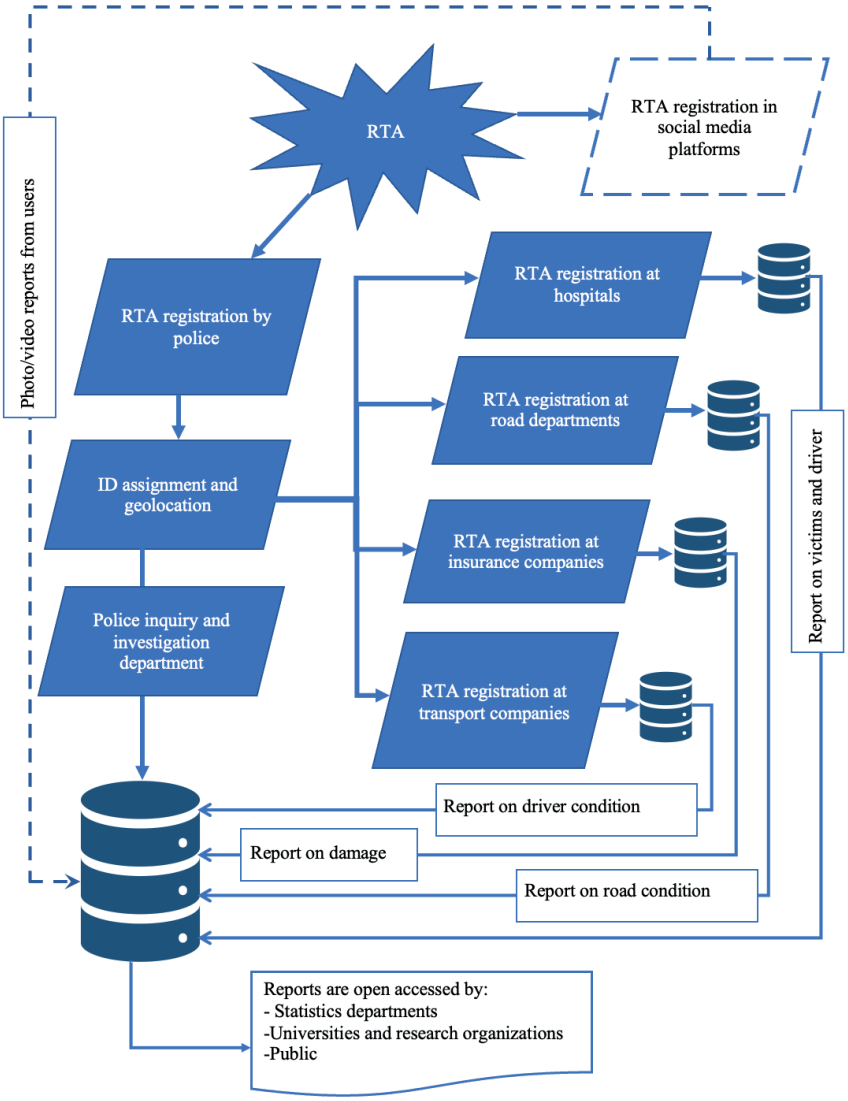


***Figure 7*** *Proposed automated accident registration system in Uzbekistan*

Road Traffic Safety Department to establish the possible cause and details of the accident and are transferred to court proceedings. If people are injured in an accident, then upon admission to the nearest hospital, the patient is registered with the same ID number that was used by the traffic police officer in automatic mode. After the patient is discharged from the hospital, the medical staff prepares a report on the condition and injuries. In addition, the subsystem takes into account data on the medical examination of drivers involved in an accident. The reports are sent to a central database for further analysis.

The ID number and location are automatically sent to the road service that operates in this section of the road, to study the impact of road conditions on the occurrence of an accident. After studying and researching the transport and operational qualities of the road, a report is drawn up and sent to the central base to study the degree of influence of road conditions. Insurance companies take into account the damage in the event of an accident, they would also use the ID number that was created by the traffic police officer. After technical expertise and damage assessment, the report is sent to a central database for analysis and assessment of all the damages. Transport companies, in turn, also use the ID number that was assigned to this accident. They assess the psychophysiological state of the driver, identify the likely cause of the accident. A report is drawn up and sent to a central database for further research.

Social networks play an important role in the registration of an accident since most users have mobile phone video recorders, which allow not only to record an accident after the occurrence but also before and during the occurrence of an accident. It serves as a quick response of traffic police officers. In addition, photo/video materials can be used in an investigation department of the traffic police. Collecting data using social networks is of a recommendatory and informative nature (dashed line in the flowchart in Figure 7).

The system of automated registration of road accidents works online and is stored in a cloud resource

to ensure the reliability and timely workflow between departments and organizations. The data in the central database is processed and analyzed. Based on this data, reports are compiled for other departments and provided to universities and research institutes for the further development of the road safety measures. Accident statistics are made available to the general public for outreach and training purposes.

## 5 Conclusions

Analysis of scientific and technical literature has shown that the methodology for the road accidents registration is outdated and does not meet modern requirements. Sweden, which has adopted the concept of zero deaths and has the lowest road traffic accident rate in the world, is developing a methodology for automated road traffic accidents using modern technology. Since 2016, authors began to create a pilot project for registering for accidents using tablets and fixing accidents in real-time. The created system for collecting, storing and processing road accident data allows to receive and analyze data on time. In Uzbekistan, large-scale transformations are being carried out to improve the road safety by introducing up-to-date technologies such as video recording of violations at the main city intersections, speed cameras recording, recording violations using tablets, data storage of road accidents in electronic form etc. Nevertheless, there are drawbacks to the road accident registration system. This is the use of outdated methods of registration for road accidents: manual/paper method of accounting for road accidents (filling out a road accident registration card). This method has several limitations, such as low data accuracy (location), data completeness (not all the data is available at the scene of the incident), untimely data transmission (late, sometimes data loss), errors and inaccuracies when entering data from paper (traffic accidents cards) to a database, not a perfect and outdated database (data is stored in a local resource, not in cloud systems). To solve these problems and tasks, this paper proposes to improve the methodology of automated accounting of road accidents data, which solves the existing problems and fills in the gaps in the system. The proposed automated system consists of several subsystems, such as the central database at the Ministry of Internal Affairs of the State Traffic Safety Inspectorate (the main database of which all data is stored), the road service subsystem provides an assessment of the impact of road conditions on the likelihood of an accident, the ambulance subsystem (Ministry of Health) performs the function of recording the state of victims in accident and driver expertise, the insurance subsystem is used to record and assess damage in the event of an accident, the transport organization subsystem studies the psychophysiological state of vehicle drivers. Based on data from the central database, open road accident data are provided for various departments and educational institutions for outreach activities. A feature of the proposed system is the synchronized exchange and transfer of data between subsystems, which increases the accuracy and reliability of data at times in comparison with the existing methodology for collecting, recording, storing and analyzing road traffic accidents data. Each subsystem is associated with an incident ID number, which allows data to be synchronized between different subsystems. This allows, at different stages of the analysis, to determine exactly where, when, what consequences, damage, culprit, road conditions and much more.

## References

[1] ISHRAT, R. Global status report on road safety 2018: summary [online]. World Health Organization, 2018. Available from: http://apps.who.int/bookorders

[2] Directive No. 377. The concept of ensuring road safety in the Republic of Uzbekistan for 2018-2022 is available (in Russian) [online]. Available from: https://lex.uz/docs/3743455

[3] SODIKOV, J. I. Electronic registration of road accidents using geoinformation technologies. *Bulletin of TashIIT*. 2018, 1. ISSN 2091-5365

[4] KHAN, M. A., KATHAIRI, A. S., GARIB, A. M. A GIS based traffic accident data collection, referencing and analysis framework for Abu Dhabi. In: World Congress: Towards more attractive urban transportation CODATU XI: proceedings. 2004.

[5] MATTSSON, K., UNGERBACK, A. Traffic accidents: tutorial for reporting / Vagtrafikolyckor: handledning vid rapportering (in Swedish). Borlange: Transportstyrelsen, 2013. ISSN 1401-9612.

[6] DERDUS, K. M., & OZIANYI, V. G. A mobile solution for road accident data collection. *Proceedings of the 2nd Pan African International Conference on Science, Computing and Telecommunications, PACT 2014*, 115–120. https://doi.org/10.1109/SCAT.2014.7055140

[7] ADNAN, M., ALI, M. S. (2014). An effective methodology for road accident data collection in developing countries [online]. In: *Data science and simulation in transportation research*. JANSSENS, D., YASAR, A.-U.-H., KNAPEN, L. (Eds.). IGI Global, 2014. ISBN 9781466649200, eISBN 9781466649217, p. 103-114. Available from: https://doi.org/10.4018/978-1-4666-4920-0.CH006

[8] MAHOVA, O. A. Theoretical questions of the applied analysis of mortality in road accidents (in Russian). *Statistics and Economics / Statistika i Ekonomika* [online]. 2016, **0**(6), p. 183-187. ISSN 2500-3925. Available from: https://doi.org/10.21686/2500-3925-2014-6-183-187

[9] SODIKOV, J. Road traffic accident data analysis and visualization in R. *International Journal of Civil, Structural, Environmental and Infrastructure Engineering Research and Development* [online]. 2018, 8 (3), p. 25-32. ISSN 2249-6831, eISSN 2249-7943. Available from: https://doi.org/10.24247/IJCSEIERDJUN20184

[10] MARKUS, P. Design and development of a prototype mobile geographic information system for real-time collection and storage of traffic accident data. Student thesis series Ines. 2016.

[11] MONTELLA, A., ANDREASSEN, D., TARKO, A., TURNER, S., MAURIELLO, F., IMBRIANI, L., ROMERO, M., SINGH, R. Critical review of the international crash databases and proposals for improvement of the Italian national database. *Procedia - Social and Behavioral Sciences* [online]. 2012, 53, p. 49-61. ISSN 1877-0428. Available from: https://doi.org/10.1016/j.sbspro.2012.09.859

[12] MONTELLA, A., CHIARADONNA, S., CRISCUOLO, G., DE MARTINO, S. Development and evaluation of a web-based software for crash data collection, processing and analysis. *Accident Analysis and Prevention* [online]. 2019, 130, p. 108-116. ISSN 0001-4575. Available from: https://doi.org/https://doi.org/10.1016/j.aap.2017.01.013

[13] BELIN, M., JOHANSSON, R., LINDBERG, J. E., TINGVALL, C. *The Vision Zero and its consequences*. In: 4th International Conference on Safety and the Environment in the 21st Century: proceedings. 1997. p. 1-14.

[14] Working party on passive safety. *Preliminary report on the development of a global technical regulation concerning pedestrian safety* [online]. Brussels: United Nations Economic Commission for Europe, Inland Transport Committee, 2003. Available from: https://unece.org/DAM/trans/doc/2003/wp29grsp/ps-36.pdf

[15] MACKAY, M. Quirks of mass accident data bases. *Traffic Injury Prevention* [online]. 2006, **6** (4), p. 308-310. ISSN 1538-9588, eISSN 1538-957X. Available from: https://doi.org/10.1080/15389580500253737

[16] International transport forum. *Road safety annual report* [online]. Paris: OECD Publishing, 2019. eISSN 2312-4571. Available from: https://doi.org/10.1787/23124571

[17] SJOO, B., UNGERBACK A. New national information system for injuries and accidents in the whole carriage system. STRADA final report - Transportstyrelsen / Nytt nationellt informationssystem for skador och olyckor inom hela vagtransportsystemet. STRADA slutrapport - Transportstyrelsen (in Swedish) [online]. 2022. Available from: https://www.transportstyrelsen.se/sv/publikationer-och-rapporter/rapporter/vag/Nytt-nationellt-informationssystem-for-skador-och-olyckor-inom-hela-vagtransportsystemet-/

[18] KURKCU, A., MORGUL, E., OZBAY, K. Extended Implementation method for virtual sensors. *Transportation Research Record: Journal of the Transportation Research Board* [online]. 2019, 2528, p. 27-37. ISSN 0361-1981, eISSN 2169-4052. Available from: https://doi.org/10.3141/2528-04

[19] FATTAKHOV, T. A. *Sources of information about road accidents and accounting of road traffic injuries in Russia*. Demographic Review, 2014. 1(3), 127-143. https://doi.org/10.17323/DEMREVIEW.V1I3.1811

[20] MAKENOV, A. A., NAUMIK, O. V. Improvement of the road accident registration system in the traffic police units. *Bulletin of AKSTU*. 2009, 3, p.83-88. ISSN 1609-1825.

# SAFETY IN CITIES AND TRANSPORT THROUGH SOUND MONITORING

**Dalibor Smažinka, Martin Hrinko ***

College CEVRO Institute, Prague, Czech Republic

*E-mail of corresponding author: martin.hrinko@seznam.cz

***Resume***

This paper deals with the use of modern technology for security purposes, focusing on the situation in cities (urban noise and shooting) and in transport (passenger rail). The authors aimed to highlight the possibilities and capabilities of installation of technology in the field of applied physical acoustics (sensors, evaluation system with the possibility of setting sensitive sensing filters, end output) and the possibilities of monitoring, including the response of security forces or security measures to the detected danger. In the paper, the authors also include graphical representations of the energy-normalized spectra of the different sound backgrounds and classification classes of acoustic events and types of acoustic events to clarify the differences of the selected monitored events.

***Article info***

Received 15 February 2022
Accepted 16 August 2022
Online 14 September 2022

***Keywords:***

urban safety
traffic safety
sound events
sound classification
video surveillance
audio surveillance
safety system response

Available online: https://doi.org/10.26552/com.C.2022.4.F72-F81

ISSN 1335-4205 (print version)
ISSN 2585-7878 (online version)

## 1 Introduction:

For years, the world's security forces have been concerned with the use of modern technology to strengthen their response to dangers that may arise, either intentionally or negligently, from the weakest link in the security chain, the human factor. The authors of this paper present a description of one such modern and now available technology, the essence of which is the use of applied physical acoustics in the installation of systems in the streets and squares of cities, with the ability to evaluate and compare the specified criteria as correct or incorrect. All this according to the sounds that a modern sensitive acoustic sensor, through set filters of monitored sounds (acoustic events), placed at target locations in the city, evaluates and transmits the information either to the operator or autonomously evaluates as a danger and triggers protective measures. Some examples, among many that can give the readers of this paper a better overview, include the recognition of the sound of gunshots on a busy street, in a square, in a means of transport etc. Further, for example, detecting the sound of a railway train passing through a location, whereby the correct time of passage can be compared at a time when the barriers are to be lowered, or evaluating the sound of a railway train passing through a section at a time when no passage through that location is expected. Reaction and the so-called checking or comparison checking with the described technology will thus help to prevent collision of rail trains directed to one track, check the lowered barriers, alert security forces to firearms firing at a particular location etc. All these measures are aimed at saving the life and health of the public and the efficiency of security forces and measures. Nowadays, one is increasingly encountering the so-called "smart cities", but behind this label, in the vast majority of cases, one only find a system that counts parking spaces in car parks in parts of cities, near hospitals or shopping centres. That is why the authors were looking at a new way of strengthening the security.

## 2 Goal

The aim of this paper was to discuss, describe and investigate the evolution of sound detection and its application for security, starting from the original knowledge about the origin and physical characteristics of sound, to the current multifunctional use of modern technologies and systems. Based on several studies from the transportation field, the authors evaluated the current potential of using the sound event detection (SED) systems specifically for the purpose of improving

the transportation safety in practice and present their conclusions to the readers.

## 3 The use of applied physical acoustics in the traffic safety and smart cities

Scientific experiments with sound date back to ancient Greece, when scientists and philosophers were concerned with locating the sources of sound. However, the modern study of this topic did not begin until the late 19th century, motivated by the desire to scientifically describe the principle by which the human brain is able to locate the direction of sound. The first experiments described were conducted by Lord Rayleigh in his garden, trying to locate the position of talking people. The result of his investigations was the conclusion that the phenomenon that makes this possible is binaural hearing, the fact that humans have two organs of hearing. Simply put, the human brain has the ability to evaluate the delay of individual sound signals in both ears to locate the source [1]. This type of experiment began the modern investigation of acoustic cues used to source and localize sound.

In the first half of the 20th century, other psycho-acousticians such as Jeffress, Mills, Newman, Rosenzweig, Wallach and many others joined in and came up with further research that underpins today's understanding of sound source localization [2].

The results of research in acoustics were used as early as World War I for sound detection and location systems to identify and locate potential firing incidents and to set up an appropriate response. Those systems grew from simple microphone configurations used for position estimation to complex arrays that relatively accurately located gunfire at long range [3].

In later years, methods for audio pattern recognition and audio signal analysis, data pre-processing, feature extraction and classification algorithms were added. There has been a shift from audio analysis of recorded audio to real-time audio analysis.

Such advanced systems can now be used as an effective means of audio monitoring, i.e. detecting, locating and classifying audio events for security purposes. They can significantly increase the efficiency and effectiveness of security systems and contribute to prevention, especially when integrated with other security technologies, such as video surveillance systems, alarm systems or active voice loudspeakers.

Modern audio detection systems can reliably detect sound, identify its source from a selected list, locate its position and transmit this data in real time either directly to security guards or trigger a subsequent automated process through integration with downstream communication or security systems. Category lists of detected sounds for security purposes most commonly include gunshots, explosions, human screams, glass breaking and various alarm sounds such as car or security system alarms.

The application of security audio-detection systems is suitable in public areas of cities and towns, in the premises of transport hubs and public transport vehicles, in buildings such as schools, hospitals, banks, office centres, shopping centres etc. Complementing the traditional security technologies, used in public areas outside or inside buildings with sound detection significantly improves their effectiveness. It brings a much greater situational awareness, brings a proactive approach to these systems and thus contributes to preventative security. It also contributes to more efficient communication and work of security forces and emergency services personnel. By providing additional situational awareness, sound detectors are also an important factor in eliminating false alarms when integrated with other security technologies.

The integration of security technologies into cooperating units has the great economic benefits for the operator, as well. Seemingly higher input costs bring savings in the long run, because some damages do not occur at all due to prevention. This is true when it comes to protecting assets. When it comes to protecting health or human life, the benefit is obvious.

## 4 Benefits of sound detection for security purposes

The vast majority of security monitoring systems are based on video surveillance using cameras. This has the great advantage of providing visual information, which is the most conclusive material (we trust what we see). However, the use of audio detection and monitoring systems has some undeniable advantages over video monitoring.

The biggest advantage is that while standard cameras have a limited angular field of view, microphones can be omnidirectional, i.e., with a spherical monitoring field. (Eyes can only see in one direction, ears can hear in all directions)

The second important factor that speaks in favour of use of the audio monitoring systems is the fact that some audio events, important for surveillance, such as screams or gunshots, have little or no visual counterpart. These are events that have little or no visual manifestation.

Other advantages are the independence of sound from lighting conditions and visibility, for example in adverse weather conditions or in the dark. Although the video technology has undergone great developments in recent years, using technologies such as thermal imaging and highly sensitive image sensors to advance the use of video technology even in very poor visibility, it is still limited in this respect. Another advantage of audio monitoring systems is their low costs of transmission over a data network. The bitrate of the processed audio is smaller than the video bitrate. This can be an advantage for larger installations of audio

detectors, for example in urban environments where the complicated conditions for data signal transmission are expected.

It could also be noted here that from a psychological point of view, audio surveillance is perceived as less invasive than video surveillance and can be a valid substitute in all the situations where privacy is a concern. To this end, it is important to note that audio surveillance does not usually involve automatic speech recognition [4].

## 5 Forms of audio detection from a data network architecture perspective

Historically, the digital audio monitoring systems have evolved architecturally by processing data streams from audio sensors on separate dedicated servers with software developed for this purpose. Such an architecture with a central server brings the advantage of high computing power for audio processing and analysis. However, it also has many disadvantages. The sound detected by the sensor has to be transmitted to this server over the data network. However, there may not be a good data link between the monitoring site and the server itself and transmission with minimal loss is expected for reliable sound detection and analysis. In recent years, with development of the small computers and the rise of edge computing, a new variant of network architecture is also coming to the fore for audio monitoring systems. The audio is analysed in a distributed manner directly at the point of detection and only the metadata in the form of extracted information and alarms is sent to a central server. This architecture saves the computing power of the server and is also significantly less demanding on the capacity of the transmission network between the detector and the server. However, this option requires each sensor to be equipped with hardware with computing power, power and data connectivity.

Considering the facts stated in the previous two options, a third option is logically offered, which uses other security system equipment already installed at the location of the intended audio monitoring of events. The use of surveillance cameras is offered as the best solution for several reasons. Firstly, they are already electrically powered devices, equipped with data connectivity and in some cases also an application platform with computing power ready to run additional applications directly on the camera. Currently, some manufacturers of security surveillance cameras offer such an open environment [5].

Another significant advantage is the possibility of logical integration of events detected by audio analysis with video verification directly at the level of the camera and transferring this information to the monitoring center or security control room comprehensively. This aspect is further discussed in the following section.

## 6 Technical aspects of the use of sound detection and classification

### 6.1 Noise and signal level of detected sounds

For an initial assessment for possibility of deploying and successfully using the sound detection and classification for security purposes, it is important to first map the acoustic environment of the site where the sound detection is planned to be used. This is particularly the case for common ambient sounds, as noisy environments make sound detection difficult. Considerably higher success rates can be expected in indoor environments where the amount of background sounds (noise) is limited or known. In outdoor environments, especially in urban environments, detection accuracy will be limited by the amount and intensity of background sounds. In addition, in outdoor environments, sounds caused by weather conditions must be considered. Many factors influence the quality and thus the success rate of sound event detection. Sound pressure levels in decibels (dB) typical in different acoustic environments and for some specific sound sources (measured at a distance of 1 m) are visualized in Figure 1.

The most important is the so-called signal to noise ratio (SNR). This is a measure that compares the level of the desired signal with the level of background noise. The SNR is defined as the ratio of signal power to noise power expressed in decibels. The SNR is affected by several factors. The most important ones are the background noise level, the signal power of the event being monitored and the distance of the microphone from the sound source. All these factors make the problem of background sound subtraction a challenging task [4].

### 6.2 Measuring the accuracy of sound detection and classification

The detection, classification and localization of acoustic events for security purposes are the focus of many researchers. Experiments focus on the accuracy of detections in different acoustic environments while using different audio analysis algorithms. For accuracy tests, four different well-known audio detectors, based on different sound processing algorithms, are most commonly used:

***Impulse detector*** - detects sound based on short-term signal levels - used mainly to detect sudden, loud impulse sounds.

***Speech detector*** - detects sound based on the harmonicity of the signal - mainly used to detect speech and human screams.

***Variance detector*** - detects sound based on changes in signal characteristics over time - particularly suitable for detecting sudden narrowband changes in the signal being analysed

***Histogram detector*** - detects sound based on the the differences in the energy distributions for the signals

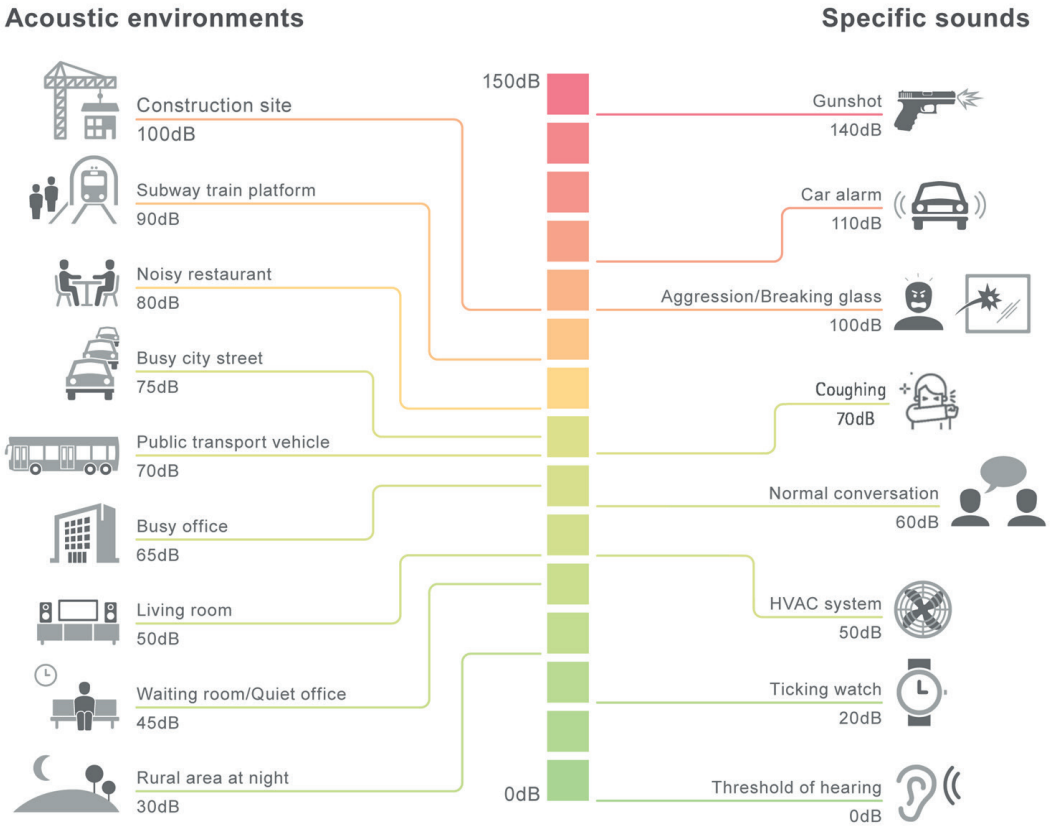


***Figure 1*** *Sound pressure levels in decibels (dB) typical in different acoustic environments and for some specific sound sources (measured at a distance of 1 m), [6]*

overall difference between the event and background spectra - particularly suitable for detecting any abnormal sounds (uses a histogram in 1/3 octave frequency bands to model the spectrum of the acoustic background).

For example, Polish researchers from the Technical University of Gdansk in their experiment investigated the accuracy of detection, classification and localization of sound events [7]. To test the detection and classification accuracy, they used four classification classes of threatening events C1 to C4 and one classification class of non-threatening events C5 (other sounds).

For the background sound, the test used four simulated environments with typical background sounds, two outdoor and two indoor:

- outdoor scene with traffic noise recorded on a busy street (traffic)
- outdoor scene with railway traffic noise recorded at the station (railway)
- indoor scene with noise from cocktail parties recorded in the university dining hall (cocktail-party)
- indoor scene with noise recorded in the main auditorium of the university (indoor).

Each sound background has its own characteristics. To compare them, it is necessary to normalize their sound spectra energetically. As can be seen in Figure 2, used are clearly visible. The sound background typical of the indoor scene has energy concentrated in the middle part of the spectrum (200 Hz-2000 Hz). The very high level of tonal components for the railway noise was due to the train braking.

They used recordings of typical sounds of hazardous situations - gunshot, explosion, broken glass and human scream - as the types of sound events they investigated [7]. They used the ratio of True Positive (TP) and False Positive (FP) detections to determine the detection accuracy rate. The detection rate is then equal to the number of correctly detected events (TP) that match the events in the Ground Truth (GT) reference list divided by the total number of events in this list. A correct detection (TP) is then understood if the difference between the detection time and the event time in the GT reference list is less than 1 second. An incorrect detection (FP) is understood when an event is detected that does not match an event in the GT reference list and is classified as one of the four event types of the reference list (C1 to C4) [7].

Figure 3 shows the correct detection rates for different classification classes and types of acoustic events. It can be seen that, on average, the detectors perform best in the presence of cocktail-party noise compared to other types of disturbance signals. The

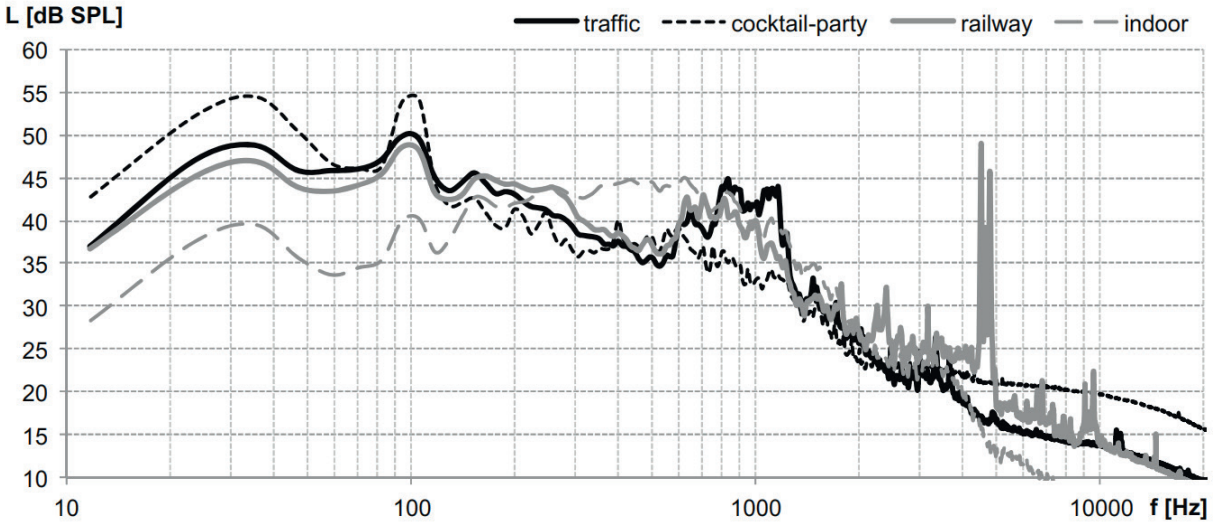


***Figure 2*** *Energy-normalized spectra of individual background sounds, [7]*

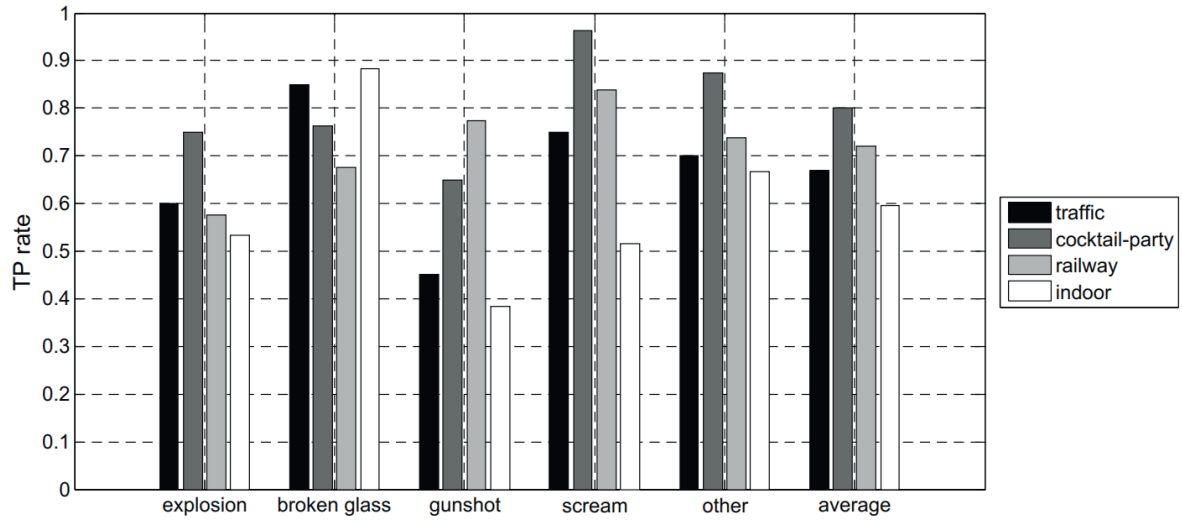


***Figure 3*** *Correct detection (TP) rates for different acoustic event classification classes and types of acoustic events. [7]*

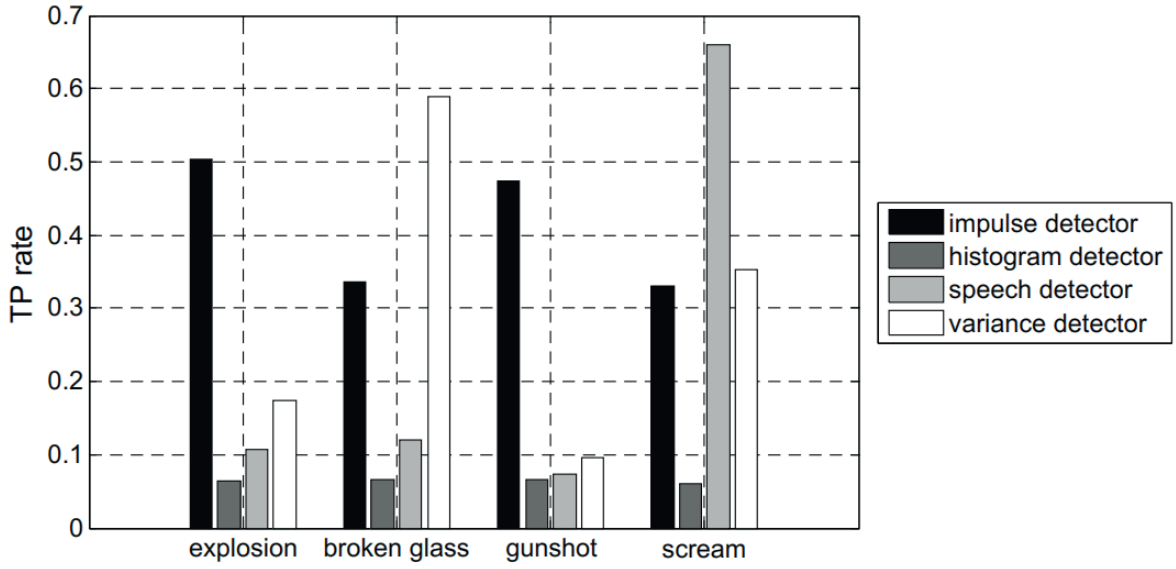


***Figure 4*** *Correct detection (TP) rates for different classification classes and types of acoustic events, [7]*

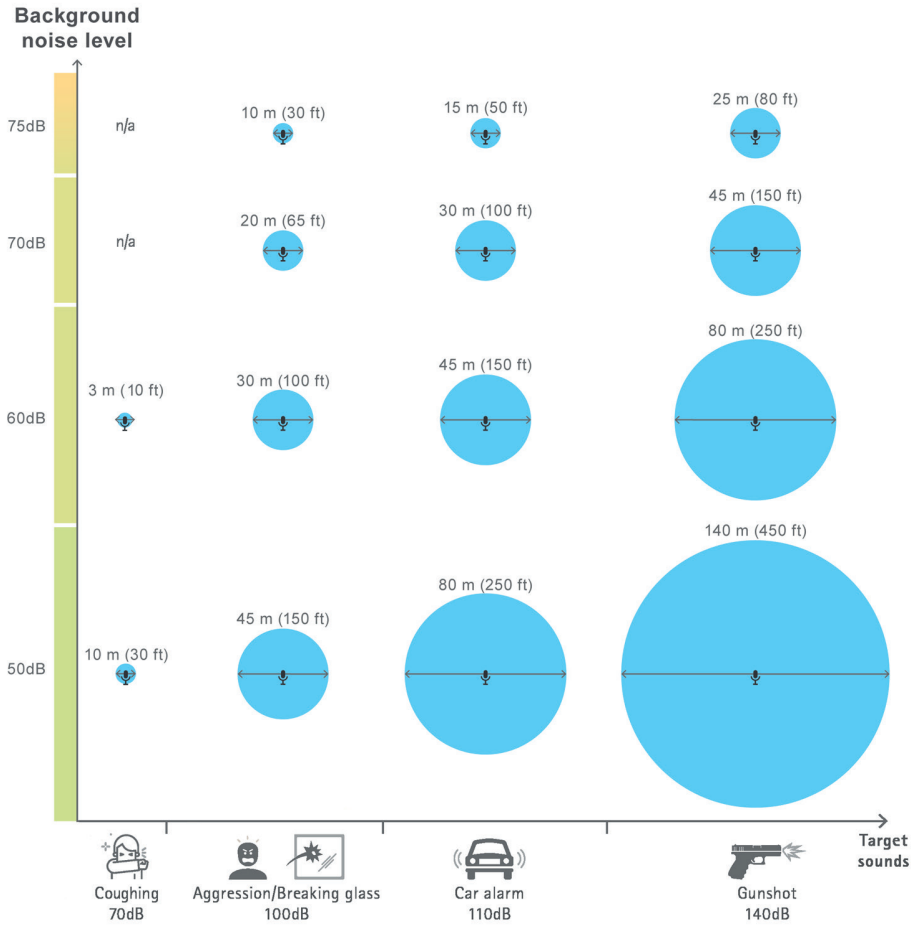


***Figure 5*** *Typical sizes of areas covered by effective sound detection for security purposes for different cases based on experience, [6]*

worst detection rates are achieved in simulated noise typical of indoor environments. (Indoor) It can also be observed that some classes of acoustic events are strongly masked by specific noise types. For example, gunshots have a TP level of 0.45 in the presence of the traffic noise (traffic) and 0.74 in the presence of the railway noise (railway).

Figure 4 shows how different detection algorithms performed in the test in recognizing different event classification classes. The results in the graph indicate the average precision detection rates (TP) for all SNR values. The presented dependencies show that the different detection algorithms used are complementary and suitable for recognizing the specific types of events. For example, the speech detector responds to the tonality present in screams, while the variance detector responds to sudden changes in sound features associated with a glass breaking event [7].

### 6.3 Spatial coverage by sound detection

The size of the microphone coverage area depends to a large extent on the signal-to-noise ratio (SNR). The diameter of the circle around the microphone is used to measure the detection coverage, i.e. the area where the microphone can detect sounds. When the background noise (noise) increases, detection coverage decreases. Sounds that are desirable to detect, such as aggressive voices or gunfire, must be 10-30 dB higher than the background noise level. The information below is intended as an informative guide and is based on many years of experience of implementing the sound detection solutions, (Figure 5). The X-axis shows the most commonly detected sound sources for security purposes and the Y-axis indicates increasing ambient noise levels in the detected area.

## 7 Integration with surveillance system

Improving the safety and security of the public transport system is a top priority for transport companies, which are installing camera systems for this purpose. However, the number of these surveillance cameras is constantly increasing and their monitoring requires too much workload for operators to maintain a high level of attention and short reaction times. Over the last decades, many software developers and researchers have been involved in developing image processing tools that

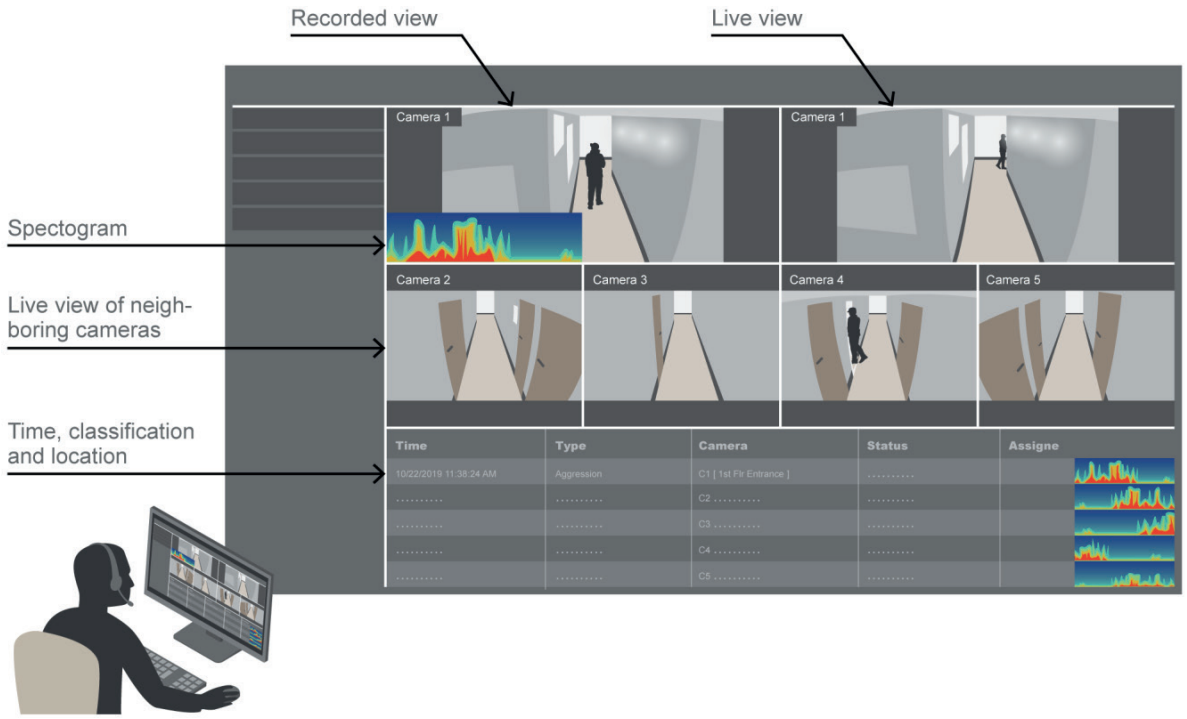


***Figure 6*** *Example of integration of audio monitoring with a video surveillance system in a surveillance center, [6]*

help the operator to automatically detect suspicious and dangerous situations. Many video analytics software applications, specifically designed for the transportation environment, have been created and have been validated in the real-world situations [8]. Analyzing audio events in a very effective way increases the efficiency of these surveillance systems.

As already mentioned, the combination and integration of safety technologies significantly increases their efficiency, reliability and preventive effect. The integration of audio monitoring with a video surveillance system brings the greatest synergy. In general, during the security incident, the situation can evolve rapidly and is usually not static. The security operator should be able to visually verify the situation quickly and easily. To achieve this, it is recommended to automatically link alarms triggered by the sound detection with live and recorded video provided by the CCTV system. If only live footage is displayed during detection, it may be that the perpetrator has already moved out of the field of view of the camera. Therefore, it is important to display the recorded video starting a few seconds before detection (video buffer) and a live view of surrounding cameras that cover the locations where the perpetrator may have moved. This is shown in Figure 6, where one can see the surveillance wall in the security operations center and the recorded view and live view windows at the top of the wall when an alarm triggered by a sound detector is detected. Below them, one can see automatically displayed windows with live view of surrounding cameras to get a situational overview. Below them, the recorded alarm data time, sound source classification and location are displayed for the quick response and future possible forensic analysis. As additional information, a spectrogram is also displayed on the screen and recorded for a visual representation of sound levels at different frequencies over time.

## 8 Existing studies on acoustic event detection (SED) for the traffic safety purposes

Historically, there have been several studies that focus on combining audio and video analytics to enhance security. Some of them even directly in the traffic environment. This section examines these in order to evaluate the suitability of using audio and video analysis to enhance safety in traffic and to describe the current limitations.

In 2007, a team of three researchers from the University of Verona addressed the question of whether the recognition and detection of audio and visual patterns in a scene and the subsequent integration and synchronization of this audio and visual data are possible and which method is effective. Experimental results on real sequences showed promising results [9].

Separate audio and video signals were processed using the two different adaptive modules aimed at accounting for audio and visual information in a unique way, using only one camera and one microphone. Then, the two models were integrated using the concept of synchronization to achieve audio-video event recognition. This fusion was implemented using the AVC matrix, a feature that allows both to detect and

***Table 1*** *Accuracy of audio event classification for four different scenarios [9]*

| Scenario | Audio | Video | Audio-Video |
|---|---|---|---|
| A | 100.00% | 83.35% | 100.00% |
| B | 60.87% | 95.65% | 95.65% |
| C | 95.24% | 85.71% | 95.24% |
| D | 62.12% | 66.67% | 89.39% |

segment AV events as well as to discriminate between them. Experimental results on real sequences showed that detection of this type is applicable in practice. From today's perspective of using neural networks and deep learning, these are early experiments, but they were already applicable. Table 1 shows the classification accuracy of audio and video analysis in four scenarios with increasing complexity. The results show a relatively high level of accuracy.

A team of researchers from France has investigated the effectiveness of a combined audio-video surveillance system for an automatic monitoring in public transport vehicles. This was in 2006, as a part of the SAMSIT (Systeme d'Analyse de Medias pour une Securite Intelligente dans les Transports publics) project, which aimed to design a solution for automatic surveillance in public transport vehicles (e.g. trains and metro cars) by analysing human behaviour based on interpretation of the audio-video stream. Its aim was to take into account the specific transport environment for the design of effective security surveillance systems.

The system consisted of six modules: face detection and tracking, audio event detection and audio-video scenario recognition. The audio event detection module detected abnormal audio events, which were precursors for detecting security incident scenarios that were predefined by end users. The audio-video scenario detection module performed the high-level interpretation of observed objects by combining audio and video events based on spatio-temporal reasoning. System performance was evaluated for a series of predefined audio, video and combined events.

Their study concluded that despite the challenging visual conditions, the system was able to successfully recognize several scenarios. They further stated that much work is still needed to develop video and audio algorithms to obtain a reliable system. They further stated that the future direction lies in improving the ability of the video algorithms in particular to cope with the complex lighting conditions in moving vehicles [9].

An interesting study in this regard was presented by a group of researchers from Ankara Science University in 2018 at the 6th International Conference on Control Engineering and Information Technology (CEIT). For their research, authors developed deep neural network (DNN) models for scream and traffic accident recognition. Tests of their models showed that they can be reliably used in real-world applications and in transportation [10].

However, they also pointed out that although there are already a number of papers that show the possibility of using audio as a source for video surveillance security, there are still few studies that address cost, scalability and practicality. In general, recent work tends to perform such tasks on supercomputers equipped with powerful GPUs and using complex neural network architectures. Thus, for wider use in practice, algorithms and, more importantly, their computational power requirements will need to be streamlined. A suitable solution is to distribute these algorithms from the central servers directly to sensors (cameras, microphones). The most modern terminal devices already allow this with their performance and chipset architecture.

In the last few years, Intelligent Traffic Monitoring Systems (ITS) have also been developed, which, among other things, aim to improve the road safety by ensuring a timely response to events such as traffic accidents and congestion.

The research on the effectiveness of different algorithms for audio detection in traffic, specifically within the framework of Intelligent Traffic Monitoring Systems (ITS), is the subject of a 2020 paper by a team of researchers from the University of Skopje, who conducted a comparative study of different audio algorithms suitable for practical use for these purposes. Their goal was to design a robust system capable of detecting traffic audio events in a real environment. At the core of this system is a deep learning model capable of detecting anomalous events and classifying them based on their acoustic characteristics. The results showed that the proposed model can be successfully applied in practice and that algorithms using the convolutional neural networks (CNN) are the most suitable for the detection of acoustic events [11].

## 9 Conclusion and future work

The aim of this paper was to discuss, describe and investigate the evolution of sound detection and its application for security, starting from the original knowledge about the origin and physical characteristics of sound to the current multifunctional use of modern technologies and systems. Based on several studies from the transportation field, the authors evaluated the current potential of using sound event detection (SED) systems specifically for the purpose of improving the transportation safety in practice and present its

conclusions to the readers. The idea of combining video and sound to make security surveillance and warning systems more effective has been the subject of several research in history. Some of them even directly in the transport environment. The aim was to evaluate their suitability for use and to describe their current limitations.

Over decades of development and research in the field of physical acoustics, a number of algorithms have been developed that can be effectively applied in different cases and environments. The outcome of most of the research has been the realization that improvements in the performance of the algorithms are necessary for an effective use. For audio analytics algorithms, this is primarily reliability in background noise environments, i.e., an increase in the signal-to-noise ratio (SNR). For video analytics algorithms, this is primarily their ability to cope with complex lighting conditions in the image, which is typical in moving vehicles, for example [12].

In this respect, technology has advanced significantly in the last few years. This is mainly due to the multiplication of computational power in surveillance cameras due to more powerful graphics cards chipsets (GPU) and thus improved image parameters for video analysis. Development of video and audio analysis algorithms has also advanced significantly, mainly due to the use of artificial intelligence principles such as deep learning and neural networks. Thus, the use and effectiveness of the combination of audio and video detection and recognition for security purposes, not only in transport, has moved forward significantly.

In the last few years, Intelligent Traffic Monitoring Systems (ITS) have also been developed to, among other things, improve the road safety by ensuring a timely response to events such as traffic accidents and congestion. This field is also beginning to make significant use of a combination of audio and video detection for the automated acquisition of reliable traffic data.

Sound events detection systems are proving to be a very effective technology for improving traffic and city safety with a strong preventive effect. Especially in conjunction with video surveillance systems, they theoretically provide an exceptionally effective safety tool. Over decades of development and research in the field of physical acoustics, several algorithms have been developed that can be effectively applied in a variety of cases and environments. It is surprising that acoustic detection, classification and localization has not been used widely and massively to a similar extent as the video surveillance systems have been over the decades. According to information on urban and traffic security systems, the use of audio detection systems is very poor. For example, according to a survey of 110 small and medium-sized municipalities in the Czech Republic in 2020 and 2021, not one of them is considering deploying an audio detection system for their city and traffic safety, even though all of them either already have or are planning to build a video surveillance system [13].

This paper dealt with the problem of audio event detection and its combination with video surveillance systems purely from a technological point of view. Legislation and processes applicable to the transport sector will certainly be another important factor in expanding their use.

Further research is suggested here in the form of finding out the reasons for such a low deployment of audio detection systems in transport and cities, as well as research into the percentage increase in safety in specific use cases in transport and urban public spaces when audio detection technology is deployed in conjunction with video surveillance systems or other technologies.

## References

[1] BORING, E. G. *Sensation and perception in the history of experimental psychology*. New York: Appleton-Century-Crofts, 1942.

[2] BLAUERT, J. *Spatial hearing: the psychophysics of human sound localization*. Cambridge: MIT press, 1997. ISBN 0-262-02413-6.

[3] GRAVES, J. R. Audio gunshot detection and localization systems: history, basic design and future possibilities. ProQuest Dissertations and Theses. Denver: University of Colorado at Denver, 2012.

[4] CROCCO, M., CRISTANI, M., TRUCCO, A., MURINO, V. Audio surveillance: a systematic review. *ACM Computing Surveys* [online]. 2016, **48**(4), 52. ISSN 0360-0300, eISSN 1557-7341. Available from: https://doi.org/10.1145/2871183

[5] AXIS camera application platform (ACAP) - Axis Communications [online]. White paper. 2021. Available from: https://www.axis.com/files/tech_notes/wp_ACAP_en_2103.pdf.

[6] Audio analytics for professionals - Sound Intelligence Design Guide [online]. 2021. Available from: https://www.soundintel.com/

[7] LOPATKA, K., KORTUS, J., CZYZEWSK, A. Detection, classification and localization of acoustic events in the presence of background noise for acoustic surveillance of hazardous situations. *Multimedia Tools*

*and Applications* [online]. 2016, **75**, p. 10407-10439. ISSN 1380-7501, eISSN 1573-7721. Available from: https://doi.org/10.1007/s11042-015-3105-4

[8] ROUAS, J. L., LOURADOR, J., AMBELLOUIS, S. Audio events detection in public transport vehicle. In: IEEE Conference on Intelligent Transportation Systems ITSC: proceedings [online]. IEEE. 2006. p. 733-738. Available from: https://doi.org/10.1109/ITSC.2006.1706829

[9] CRISTANI, M., BICEGO, M., MURINO, V. Audio-visual event recognition in surveillance video sequences. *IEEE Transactions on Multimedia* [online]. 2007, **9**(2), p. 257-267. ISSN 1520-9210, eISSN 1941-0077. Available from: https://doi.org/10.1109/TMM.2006.886263

[10] ARSLAN, Y., CANBOLAT, H. Performance of deep neural networks in audio surveillance. In: 6th International Conference on Control Engineering and Information Technology CEIT: proceedings, 2018. p. 1-5.

[11] CHAVDAR, M., GERAZOV, B., IVANOVSKI, Z., KARTALOV, T. Towards a system for automatic traffic sound event detection. In: 28th Telecommunications Forum TELFOR: proceedings [online]. IEEE. 2020. Available from: https://doi.org/10.13140/RG.2.2.19496.29448

[12] VU, V.-T., BREMOND, F., DAVINI, G., THONNAT, M., PHAM, Q.-C., ALLEZARD, N., SAYD, P., ROUAS, J.-L., AMBELLOUIS, S., FLANCQUART, A. Audio-video event recognition system for public transport security. In: International Conference on Crime Detection and Prevention ICDP'2006: proceedings. 2006. p. 414-419.

[13] Help protect your town – Blind Spots / Pomozte chranit vasi obec - Slepa Mista (in Czech) [online]. 2021. Available from: https://www.slepamista.cz/

# OPTIMIZATION OF PARAMETERS FOR PEDESTRIAN SIMULATION SOFTWARE: A CASE STUDY OF EMERGENCY EVACUATION EXPERIMENTS

Hari Krishna Gaddam [1,*], Lakshmi Devi Vanumu [2], Aditya Arya[2], K. Ramachandra Rao [2]

[1]School of Planning and Design, National Rail and Transportation Institute, Under Ministry of Railways, Vadodara, Gujarat, India
[2]Department of Civil Engineering, Indian Institute of Technology, Delhi, India

*E-mail of corresponding author: harikrishnagaddam@gmail.com

***Resume***
This research study provides a new framework to optimize pedestrian simulation parameters required to replicate emergency evacuation conditions specifically observed in high rise buildings, passenger vehicles and transport terminals. The simulation experiments are performed with generalised social force model in VISWALK simulation environment. The data required for optimization are obtained by conducting several evacuation experiments. The results indicate that pedestrian behavioural aspects, such as the relaxation time, distance from the other pedestrian and force exerted by closest pedestrians, have a significant impact on total evacuation time. The outcomes are in consistence with field observations and the calibrated parameters would help in simulating future scenarios including building level simulations and further simulating emergency evacuation of passengers from transport terminals and vehicles.

***Article info***
Received 17 March 2022
Accepted 18 August 2022
Online 20 September 2022

***Keywords:***
social force model
VISWALK
pedestrian simulation
classroom evacuation
sensitivity analysis
calibration
validation

Available online: https://doi.org/10.26552/com.C.2022.4.F82-F96

ISSN 1335-4205 (print version)
ISSN 2585-7878 (online version)

## 1 Background

Evacuation of pedestrians from a building in emergency situation without any loss of life is always a challenging task. In emergency conditions, several reasons, such as physical obstruction, wrong selection of emergency exists, overcrowding, pushing and crushing, may result in injury or death of pedestrians. In addition, evacuation in closed or restricted environments is affected by several major and minor factors, such as age, gender, presence of groups, number of exists and so on. Several researchers attempted to understand the effect of pedestrian and room characteristics on evacuation behaviour using simulation and experimental methods [1-4]. Pedestrian simulation models are ordinarily used to study the evacuation characteristics of pedestrians under many circumstances. In another study [5], classroom evacuation scenarios are simulated with two exits in which a modified Cellular Automata (CA) simulation evacuation model was considered with occupant density of the exit. The study states that the phenomenon of people's hesitation and oscillation between different exits occurs in simulation when occupant density around exits was considered. Zhao and Gao [6] made an attempt to present a generalized floor field model to characterize the exit choice behaviour in rooms, which have multiple exits. Aik [7] carried out evacuation experiments and simulations in a room with two exits. To understand the evacuation process through exits the study used a modified CA evacuation model incorporating neural network decision-making for intelligent exit selection. The study results show that the exit selection behaviour of occupants depends on the density around the exits. Chen and Han [8] in their study composed a multi grid model by introducing the force concept of social force model in the lattice gas model. They used finer lattice to enable pedestrians to occupy multiple grids in place of a single grid and studied the behaviour of the pedestrians while evacuating from a single door of a big room. The results revealed that with increase in the width of the door, the time of evacuation decreases but it is not linear. Li et al. [9] studied the escape panic of a classroom evacuation in real-life 2013 Ya'an earthquake in China using the social force model. The model parameters are calibrated and optimized using differential evolution

algorithm to reproduce the non-linear evacuation speed, which is consistent with observed video data. Results show that the trained evacuation leader and number of available exits have tremendous impact on evacuation process. Gu et al [10] studied the evacuation behaviour of school students in normal and emergency conditions through regression modelling. From the analysis it is observed that students‘ cumulative departures in normal conditions is a linear function, while in emergency it is a convex function and further students' reaction time increases substantially in emergency conditions.

It is a great challenge to conduct practical evacuation experiments without risking the lives of the people participating in the experiments. Therefore, evacuation modelling using the simulation technique is a great alternative to conducting evacuation experiments. Evacuation modelling is a branch of science concerned with simulating human behaviour in an emergency condition. Even though the empirical data is compulsory for setting up a simulation model, it has an advantage when it comes to creating various alternative scenarios. Simulations with good calibrated parameters help in more accurate forecasting. The simulation methodology not only produce accurate results but also saves money.

Transport security and passenger safety during evacuation from vehicles and terminals cane be addressed using the simulation software. In transportation domain, computer-based simulation models with suitable parameters replicate passenger behaviour from passenger terminals and transport vehicles. They are used for economical way of evaluating in various conditions. Simulation models have been developed for assessing passengers boarding and alighting behaviours, evacuation behaviours using various methods. Najmanová et al. [11] explored the impact of various factors on passengers' evacuation from the rail coach to a station platform during emergency. In total, 15 evacuation experiments were conducted in a double decker train in Czech Republic and 91 passengers were called for the experiments that were conducted under various scenarios by varying widths, exit types and exit methods. Wang [12] studied the evacuation of passengers from the two floor metro station subway and station hall using pathfinder simulation model. In another study [13], an agent-based simulation model is used to handle the evacuation procedure in transit stations for various scenarios. They explored the impact of different factors on total evacuation time of passengers from the transit station.

The present study aims to evaluate the classroom evacuation scenarios in emergency conditions, using the VISWALK (PTV) simulation tool [14], which particularly suits the simulation for the fatal build-up of pressure observed during the emergency evacuations. To represent the real-world behaviour of the pedestrians, the model parameters need to be calibrated and validated. Therefore, the suitable empirical data is to be collected, either from the real world observations, or from experimental studies. As availability of observed pedestrian data is difficult, researchers mainly relied on experimental studies [15-19]. These studies are useful in collecting pedestrian behavioural information, such as choice of route selection, individual travel times, individual speeds, trajectories and so on.

So far very few studies [20-21] attempted to validate the social force model parameters in VISSIM and VISWALK simulation environment. Kretz et al. [20] validated the social force model parameters in VISSIM simulation framework using the experimental data. In this study, pedestrian flow through bottlenecks in normal conditions have been simulated and found that default parameters given in VISSIM manual is sufficient to simulate the normal behaviour of pedestrians. Marten and Henningsson [21] in their study verified and validated the VISWALK pedestrian simulation model for the use as a building evacuation model. In the validation, results from VISWALK are compared to four real life experiments, including a corridor, classroom, theatre lobby and a staircase. The results confirmed that, with default parameter settings, speeds and travel times of the occupants are totally deviating from the actual results. This study suggests that model predictions will be close to experimental results if user has a good estimation of the occupant demographics and is aware of the limitations of the model. However, the literature review confirmed that the detailed discussion on influential parameter sets for emergency evacuations and their optimization procedure is nearly non-existent. Thus, the present study is an attempt to fill this gap.

The paper is organised as follows: section 2 discusses the concept of generalised social force model and the important VISWALK parameters. Section 3 introduces the methodology adopted for this study. Sections 4 and 5 cover the sensitivity analysis and calibration procedures respectively. Section 6 is about validation of parameters and some predictions. Finally, section 7 concludes the paper.

## 2 Social force model and VISWALK parameters

In the present study, PTV VISWALK-7.0 is used to simulate the emergency evacuation of pedestrians. The simulation tool is built on the concept of Generalised Social Force Model (GSFM) [22], which permits to investigate the distinctive degrees of panic. Moreover, the GSFM is able to predict the collective phenomenon of escape panic in the framework of self-driven many particle systems. Further, it is also good at representing the typical human behaviour in emergency conditions, such as arching, jamming and overcrowding. Simulation models, developed based on the social force model, have helped in developing several emergency evacuation strategies for different types of facilities in natural and human made disasters for instance earthquakes, fire, bottleneck conditions and so on [9, 14, 22]. The

***Table 1*** *Description about VISWALK parameters [14]*

| No | VISWALK Parameter | Description | Range | Remarks |
|---|---|---|---|---|
| 1 | Tau (τ) | Represents the relaxation time of pedestrian. Its value is inversely proportional to force between pedestrians | 0-1 | Default Value is 0.4. if τ < 0.4 then the pedestrian will be aggressive and similarly if τ > 0.4 then pedestrian will be relaxed. |
| 2 | Lambda (λ) | The parameter in the model judges how people at one's back will behave | 0-1 | Default Value is 0.176. If λ increases, pushing from other pedestrians also increases. |
| 3 | Grid size (D) | Conveys the meaning that the maximum distance at which pedestrians have an effect upon each other | ≥ 0 | Default value is 5. If D decreases, it increases the influence on the other pedestrian. Units are meters. |
| 4 | Noise | The greater this parameter value, the stronger the random force that is added to the systematically calculated forces | 0-2 | With noise is equivalent to zero, the so called pedestrian „arches" will form and remain stable. If the noise value lies within the range of 0.8 to 1.4, one of the pedestrians will step back after a while and another one will pass through. |
| 5 | React to N | During the calculation of total force for a pedestrian, only the influence exerted by the *n* closest pedestrians was taken into account | ≥ 0 | Default value is 8. React to N is inversely proportional to density. |
| 6 | VD | This parameter defines how individual will response to group in counter flow. | ≥ 0 | Default value VD is 3.0.It means there is less avoidance from opposite flow. |

acceleration equation of generalised social force model is as follows.

$$m_i \frac{dv_i}{dt} = m_i \frac{v_i^0(t)e_i^0(t) - v_i(t)}{\tau_i} + \sum_{j(\neq i)} f_{ij} + \sum_W f_{iW}. \quad (1)$$

Here, pedestrian $i$ of mass $m_i$ wishes to attain his or her desired speed $v_i^0$ in a certain direction $e_i^0$ and actual velocity $v_i$ with a relaxation time $\tau_i$. Simultaneously, each pedestrian tries to maintain velocity dependent distance from other pedestrian's $j$ and walls $W$. Corresponding interaction forces are $f_{ij}$ and $f_{iW}$ respectively. For detailed information on „interaction forces" refer to [22]. Table 1 describes VISWALK pedestrian simulation parameters with their default values [14].

## 3 Methodology

Unlike other studies, simulation model development for emergency evacuation is a complicated one, where evacuation times for different classroom sizes with different door widths have to be predicted accurately using a specific parameter set. Therefore, a new methodological approach is proposed to obtain those values. Step by step procedure involved in this methodology is discussed below.

### 3.1 Experiments

The very first step in simulation model development is the collection of suitable input data from suitable experiments. In this study, fifteen experiments have been carried out in a classroom environment for different age groups and varying door widths. In total of fifteen experiments, fourteen experiments data is used for calibration of parameters and one experiment data is used for validation of optimized parameter set. To consider different age groups of pedestrians (Post-graduate, Under-graduate and higher secondary school) with all the possible scenarios, data was collected at two different places, such as university classroom and public-school classroom, Delhi, India. Table 2 describes different characteristics of classrooms, whereas sketches of the classrooms are depicted in Figure 1 and Figure 2.

The first set of experiments were conducted at a Lancers convent public school, in which 43 students of the 6$^{th}$ grade participated, with 86 % class occupancy and an average age of 11.14 years. The classroom consists of movable tables and chairs on a leveled floor. There was only one exit provided at the entrance of the classroom. The second set of experiments were conducted in the same school and in a similar kind of classroom in which 36 students of the 9$^{th}$ grade had participated, with 75 % class occupancy and an average age of 14.56 years. The experiments conducted in the school classrooms consider different scenarios as shown in Table 3. The third set of experiments were conducted in the lecture hall complex in Indian Institute of Technology (IIT), Delhi in which 38 students had participated, with 63 % class occupancy. The classroom consists of arrangment of movable tables and chairs on a leveled floor with two exits. The forth set of experiments were also conducted in the lecture hall complex of IIT Delhi in which 12 students had participated (LH-605), with 40 % class occupancy. The experimental scenarios considered for the study are

***Table 2*** *Characteristics of classrooms*

| Description | Lancers Convent Public School, Delhi | | Lecture Hall Complex, IIT Delhi | |
|---|---|---|---|---|
| | 6th grade | 9th grade | Undergraduate (UG) LH - 611 | Post-Graduate (PG) LH - 605 |
| Area of classroom ($m^2$) | 46.65 | 46.2 | 87.86 | 38.97 |
| Classroom Capacity | 50 | 48 | 60 | 30 |
| No of Exits | 1 | 1 | 2 | 2 |
| Placement of exits | Front | Front | Front | Back |
| Desk and chair arrangement | Movable | Movable | Movable | Movable |

***Table 3*** *Different experiment scenarios in Lancers Convent Public School*

| No. | Door Width (m) | 6th grade | 9th grade |
|---|---|---|---|
| 1 | 0.8 | S1 (big door) | S1 (big door) |
| 2 | 1.1 | S2 (both door) | S2 (both door) |
| 3 | 0.3 | S3 (small door) | S3 (small door) |
| 4 | 0.8 | Govt. Guidelines | Govt Guidelines |

***Table 4*** *Different experiment scenarios in lecture hall complex, IIT Delhi*

| No. | Door Width (m) | UG class | PG class |
|---|---|---|---|
| 1 | 1.2 | S1 (2 small door open) | S1 (2 small door open) |
| 2 | 1.8 | S2 (2 big doors open) | S2 (2 big doors open) |
| 3 | 1.5 | S3 (1 big and 1 small) | S3 (1 big and 1 small) |
| 4 | 1.5 | S4 (only 1 exit) | S4 (only 1 exit) |
| 5 | 3 | S5 (both doors open) | S5 (both doors open) |

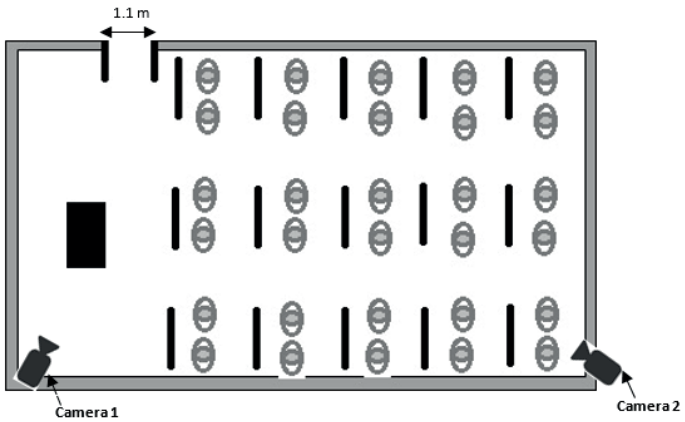


***Figure 1*** *Sketch of a classroom experimental scenario in Lancers Convent Public School, Delhi*

given in Table 4. In all these experiments, students were instructed to evacuate the room from the shortest path to the exit. The evacuees are informed about the evacuation procedure before conducting the study and asked them to behave as if they are in emergency situation.

The data collection for the study was performed using the video graphic technique. As shown in Figure 1, videos were recorded from convenient vantage points and then data was extracted using MATLAB® based tool [23]. Data analysis was carried out using Microsoft Excel and R statistical tool [24]. Snapshots of evacuation experiment and evacuation time details of the 6th grade classroom and undergraduate classroom is depicted in Figure 3. The data obtained from the evacuation experiments, such as flow, composition, individual travel times, individual speeds and total evacuation times, were obtained and used in simulation model development, parameters calibration and validation. The details of evacuation experiments are given in Table 5. More details on data collection procedure and development of evacuation models can be found in [2].

***Figure 2*** *Sketch of a classroom experimental scenario in Lecture Hall Complex, IIT Delhi (here Corridor width 1800 mm, between benches (from left to right 720 mm, 450 mm and 630 mm respectively)*

*(a)*

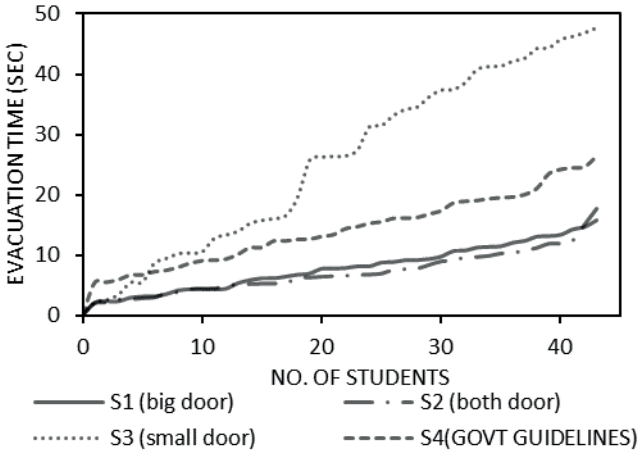


*(b)*

*(c)*

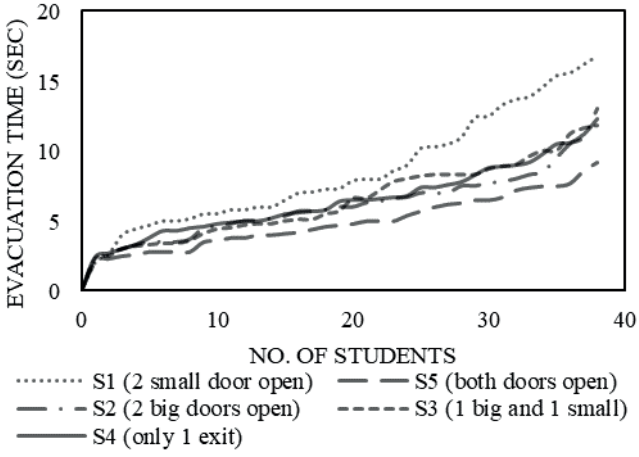


*(d)*

***Figure 3*** *(a) and (b) - Snapshot of the 6th grade and their cumulative evacuation times for different door widths respectively; (c) and (d) - Snapshot of the undergraduate class and their cumulative evacuation times for different door widths respectively (In Figure 2 (b): big door = 0.8 m, both doors =1.1 m, small door = 0.3 m, In Figure 2 (d): two small door = 1.2 m, both doors = 3.0 m, two big doors = 1.8 m, 1 big and 1 small = 1.5 m)*

***Table 5*** *Comprehensive view of evacuation experiments*

| No | Grade / class | Class occupancy (classroom capacity) | Door width (m) | Average age | Proportion of women | Classroom area ($m^2$) | Total Evacuation time (s) | Speed distribution ($\mu^*$,$\sigma^*$) |
|---|---|---|---|---|---|---|---|---|
| 1 | $6^{th}$ | 43 (50) | 0.8 | 11.14 | 41.80 | 46.65 | 15.70 | 0.93, 0.29 |
| 2 | $6^{th}$ | 43 (50) | 1.1 | 11.14 | 41.80 | 46.65 | 17.76 | 1.01, 0.27 |
| 3 | $6^{th}$ | 43 (50) | 0.3 | 11.14 | 41.80 | 46.65 | 47.60 | 0.36, 0.26 |
| 4 | $6^{th}$ | 43 (50) | 0.8 | 11.14 | 41.80 | 46.65 | 26.47 | 0.50, 0.15 |
| 5 | $9^{th}$ | 36 (48) | 1.1 | 14.56 | 41.66 | 46.2 | 14.21 | 0.99, 0.23 |
| 6 | $9^{th}$ | 36 (48) | 1.1 | 14.56 | 41.66 | 46.2 | 12.64 | 1.10, 0.32 |
| 7 | $9^{th}$ | 36 (48) | 0.3 | 14.56 | 41.66 | 46.2 | 33.03 | 0.51, 0.27 |
| 8 | $9^{th}$ | 36 (48) | 1.1 | 14.56 | 41.66 | 46.2 | 31.60 | 0.45, 0.16 |
| 9 | UG* | 38 (60) | 1.2 | 23.80 | 10.50 | 87.86 | 16.80 | 0.93, 0.38 |
| 10 | UG | 38 (60) | 1.8 | 23.80 | 10.50 | 87.86 | 13.00 | 1.26, 0.42 |
| 11 | UG | 38 (60) | 1.5 | 23.80 | 10.50 | 87.86 | 11.80 | 1.23, 0.34 |
| 12 | UG | 38 (60) | 1.5 | 23.80 | 10.50 | 87.86 | 12.30 | 1.43, 0.32 |
| 13 | UG | 38 (60) | 3.0 | 23.80 | 10.50 | 87.86 | 9.20 | 1.53, 0.38 |
| 14 | PG* | 12 (30) | 1.2 | 25.42 | 33.30 | 38.97 | 9.00 | 0.89, 0.25 |
| 15 | PG | 12 (30) | 1.8 | 25.42 | 33.30 | 38.97 | 5.77 | 1.03, 0.20 |
| 16 | PG | 12 (30) | 1.5 | 25.42 | 33.30 | 38.97 | 6.00 | 0.99, 0.22 |
| 17 | PG | 12 (30) | 3.0 | 25.42 | 33.30 | 38.97 | 7.20 | 1.33, 0.66 |

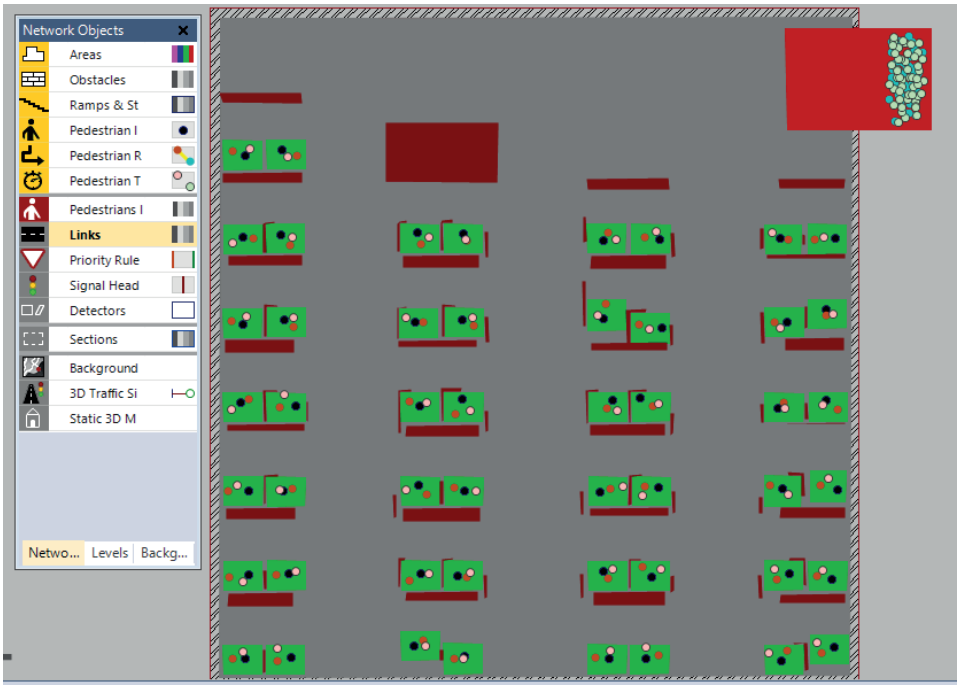


***Figure 4*** *Snapshot of the VISWALK simulation model setup for the $6^{th}$ grade*

### 3.2 Simulation model development

In the next step, AutoCAD drawings (.dwg) of the classroom area chosen for the study is used as a background image to the VISWALK Simulation model (e.g. Figure 4 for Grade 6 classroom). Then, different pedestrian facilities are created (e.g. walking area, exit area, table and chairs etc.) and pedestrian inputs were given to prepare the simulation model. To evaluate the model performance, Total Evacuation Time (TET) is chosen as a measure of performance (MOP); cumulative absolute residual error (CARE) and GEH1 statistics are chosen as goodness of fit (GOF) measures. Subsequently, the initial evaluation of VISWALK model was carried out using the default parameter set and the model performance is evaluated. It was found that the default parameter cannot satisfy the required criteria, where those parameters mainly meant for representing the

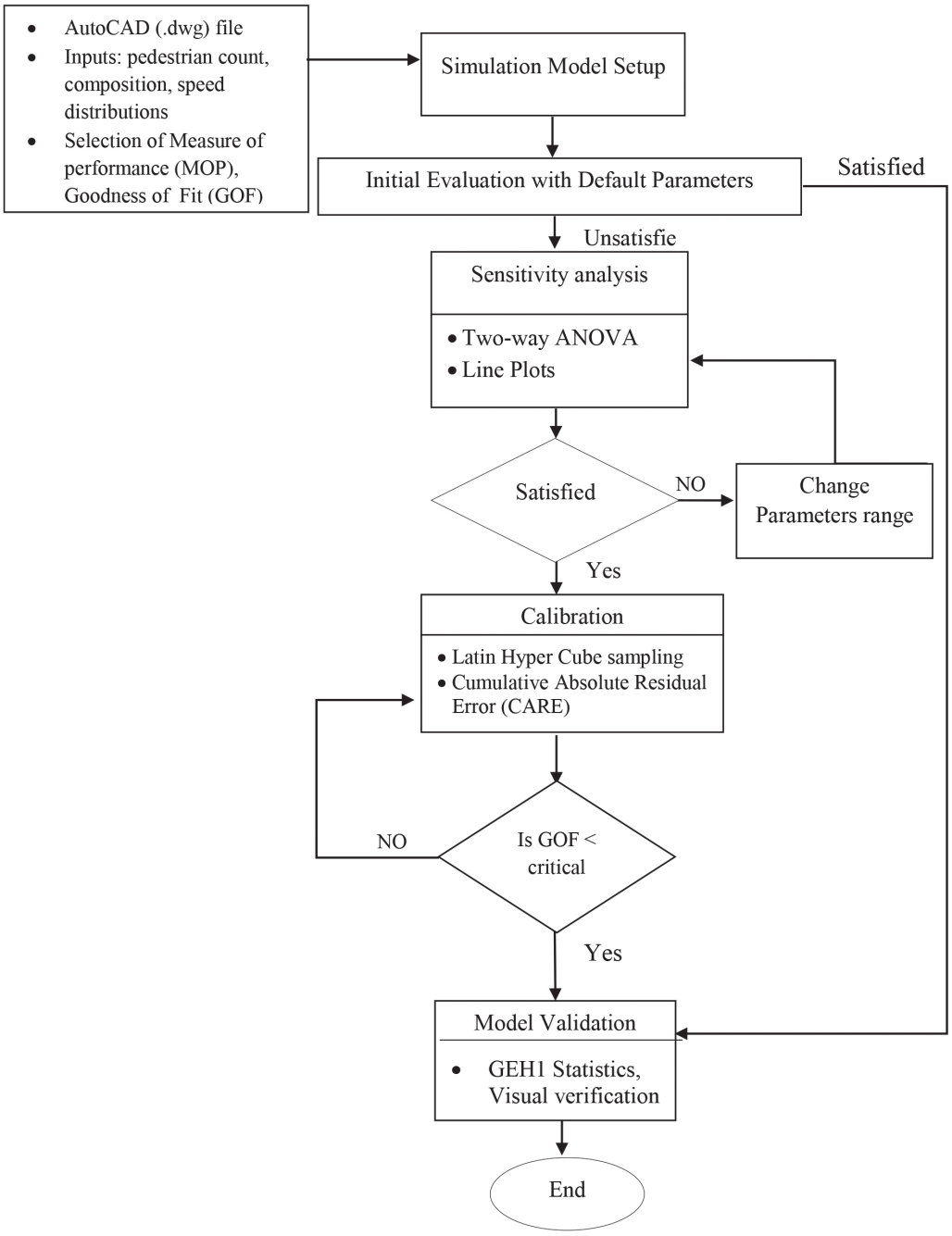


***Figure 5*** *Methodology for calibration and validation of the VISWALK evacuation model*

normal behaviour of pedestrians. Sensitivity analysis of walking behaviour parameters was done by the two-way analysis of variance (ANOVA) (without replications) and line plots to identify the most influential parameters of the model. The detailed analysis is given in section 4. If the output from the sensitivity analysis is in accordance with the observed data, then the analysis is moved to calibration level otherwise sensitivity analysis step will be repeated until the desired ranges are achieved.

In the calibration step, optimum set of model parameters are identified by minimizing the differences between simulated and observed values. To minimize the computational time, suitable parameter sets are generated using Latin Hypercube Sampling (LHS) algorithm in which several sets of parameters are generated and the error value is estimated using the cumulative absolute residual error (CARE) and regression plots. The best parameter set will be the one, which produces the least error. More information on LHS and the outcomes are given in section 5. In the final stage, validation is carried out for the optimized parameter set to check its adoptability and to quantify the approximate error it is produced. Because the validated outcome is a single value, the GEH1 statistic was adopted to evaluate the model performance. Further, visual observations are also used to check the model accuracy in representing some of the pedestrian behaviour at bottlenecks in emergency conditions, such

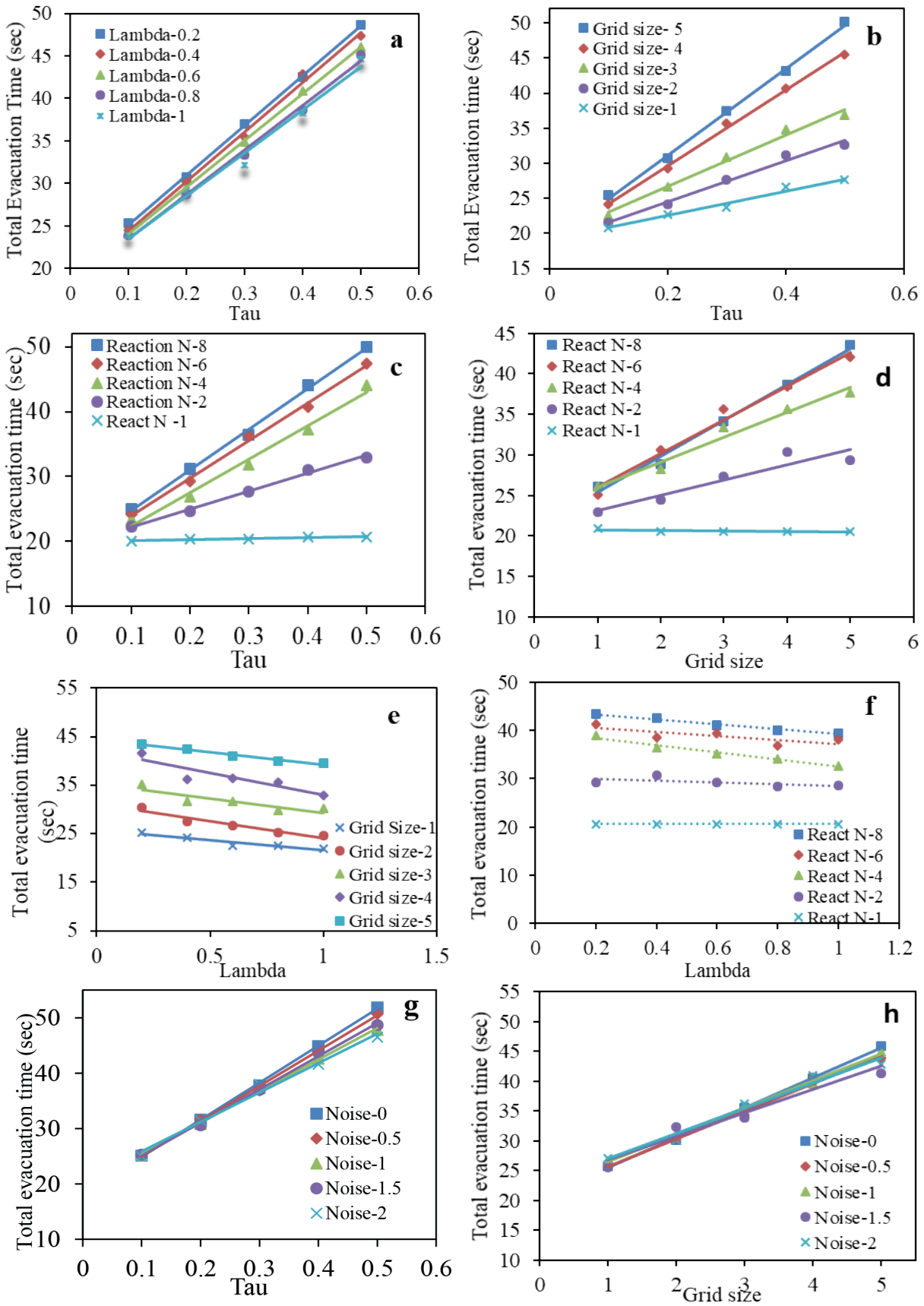


***Figure 6*** *Estimated marginal means of the Total Evacuation Time between different pedestrian simulation parameters*

as arching and clogging. The complete methodology flowchart used for calibration and validation is given in Figure 5.

## 4 Sensitivity analysis

The sensitivity analysis plays a major role while handling a lot of variables in which few parameters are redundant. It helps in determining their relative importance and thus aids in identifying the variable(s) of interest. The sensitivity analysis for the VISWALK walking behavioural parameters is performed to know how, with a small change in the respective parameter values the individual results will behave [25]. In the present study, the two-way ANOVA method without replication is used to conduct pairwise sensitivity analysis. In this approach, simulations are carried out by varying selected two parameter values and keeping other parameters constant. Individual and combined effect of the two parameters on Total Evacuation Time (TET) was evaluated. Parameter VD value is taken as default as there is no opposite flow in experimental studies. The outcomes of the sensitivity analyses are presented in Figure 6 and Table 6.

Following conclusions can be drawn from the sensitivity analysis.

The results shows that $\tau$ and $\lambda$ have individual and combined effect on simulation output i.e., TET. Here, the TET values increase with increasing $\tau$ and $\lambda$ value. However, at lower values of $\tau$, there is not much deviation in the output (Figure 6a). The two-way ANOVA results (Table 6) also proved the same. Figure 6b conveyed a meaning that there is a significant deviation in the TET values for different $\tau$ and D values. However, for small values of D there is not much change in the TET for varying $\tau$ values.

React to N and $\tau$ values have significant effect on TET, which can be concluded through Figure 6c. The ANOVA results also proved the above statement clearly (Table 6). However, for the lower React to N values there is no change in TET. It can be seen from Figure 6d that the parameter D with React to N has a significant relation with TET. The ANOVA results also proved it to be true (Table 6). However, for lower React to N values there is no change in TET. Figure 6e shows that parameters $\lambda$ and D have a combined effect on simulation outcomes, however, the TET is not much affected while increasing $\lambda$ value and keeping the parameter D constant. From the ANOVA results (Table 6) and Figure 6f can be seen that parameters $\lambda$ and React to N show a significant impact on outcome, but there is no much difference in TET with increase in $\lambda$ value when React to N is constant. From Figure 6g it is observed that with the increase in $\tau$ value, the TET is increased but Noise parameter does not have any influence on altering pedestrian behaviour. From Figure 6h is also shown that with increase in the D value the TET increased but the Noise parameter does not have any effect on pedestrian behaviour and the same can be observed from the ANOVA results.

From the sensitivity analysis, it is observed that parameters, such as $\tau$, D, React to N have significant impact on evacuation results. It may also suggest that those parameters are more influential in capturing pedestrian behaviour in emergency conditions. Further, it is also proved that $\lambda$ has less influence and Nosie parameter has no influence on simulation outcomes. Therefore, the noise parameter is considered to be constant in the calibration procedure.

## 5 Calibration

In calibration, the difference between simulated and observed variables are minimized by finding an optimum set of model parameters. In this study, a new approach has been adopted for the parameter calibration. In this approach, a large sets of walking parameters (sample sets are given in Table 7) were generated using the Latin Hypercube Sampling (LHS) algorithm using MATLAB® program. Then, each parameter set was supplied to the VISWALK model to simulate 14 evacuation scenarios simultaneously. The difference between estimated total evacuation time and observed evacuation time is considered as a measure of effectiveness. The parameter set, which produces the least error can be considered as effective one and will be used in further validation purpose and evaluating alternative scenarios. Several GOF measures, such as paired t-test, regression, MAPE etc. have been tested to estimate the error. However, none of them can suitably assess the model prediction accuracy. Therefore, the cumulative absolute residual error (CARE) was adopted as a goodness of fit measure (GOF). Calibration methodology adopted in this study is presented in Figure 7.

Latin hypercube sampling (LHS) is a stratified random sampling procedure that provides an efficient way of sampling variables from their multivariate distributions. It provides a full coverage of the range of each variable by maximally stratifying the marginal distribution. It was initially developed for the purpose of the Monte-Carlo simulation, where it is efficiently selecting input variables for computer models [26-27].

Table 8 shows twenty-three sample (including default parameter set) sets of parameters generated by the LHS, which were used to run simulations for different door widths and area of the classroom. Results given in Table 8 show that the R-square as an evaluation method is obsolete (high $R^2$ value can result in high residual error, e.g. set 23 in Table 8, while moderate R-square value scenario P-1 gives the least residual error). This study proposed Cumulative Absolute Residual Value (CARE) to identify the best parameter set from the analysis. Parameters are displayed in the table sorted on the basis of the error value in ascending order. The

***Table 6*** *ANOVA without replication between different groups*

| No. | Source of Variation | SS | df | MS | F statistic | P-value | F critical |
|---|---|---|---|---|---|---|---|
| 1 | λ | 37.25 | 4 | 9.31 | 15.74 | 0.00 | 3.00 |
| | τ | 1511.19 | 4 | 377.79 | 638.55 | 0.00 | 3.00 |
| | Error | 9.46 | 16 | 0.59 | | | |
| | Total | 1557.91 | 24 | | | | |
| 2 | D | 575.10 | 4 | 143.77 | 17.16 | 0.00 | 3.01 |
| | τ | 796.09 | 4 | 199.02 | 23.75 | 0.00 | 3.01 |
| | Error | 134.04 | 16 | 8.37 | | | |
| | Total | 1505.24 | 24 | | | | |
| 3 | React to N | 933.53 | 4 | 233.38 | 14.08 | 0.00 | 3.01 |
| | τ | 814.96 | 4 | 203.74 | 12.29 | 0.00 | 3.01 |
| | Error | 265.13 | 16 | 16.57 | | | |
| | Total | 2013.63 | 24 | | | | |
| 4 | React to N | 693.03 | 4 | 173.25 | 19.05 | 0.00 | 3.01 |
| | D | 367.53 | 4 | 91.88 | 10.10 | 0.00 | 3.01 |
| | Error | 145.44 | 16 | 9.09 | | | |
| | Total | 1206.01 | 24 | | | | |
| 5 | D | 1048.74 | 4 | 262.18 | 331.73 | 0.00 | 3.01 |
| | λ | 85.29 | 4 | 21.32 | 26.97 | 0.00 | 3.01 |
| | Error | 12.64 | 16 | 0.79 | | | |
| | Total | 1146.68 | 24 | | | | |
| 6 | React to N | 1382.82 | 4 | 345.70 | 277.58 | 0.00 | 3.01 |
| | λ | 28.46 | 4 | 7.11 | 5.71 | 0.00 | 3.01 |
| | Error | 19.92 | 16 | 1.24 | | | |
| | Total | 1431.21 | 24 | | | | |
| 7 | Noise | 10.25 | 4 | 2.56 | 2.34 | 0.09 | 3.00 |
| | τ | 1808.77 | 4 | 452.19 | 412.71 | 0.00 | 3.00 |
| | Error | 17.53 | 16 | 1.09 | | | |
| | Total | 1836.56 | 24 | | | | |
| 8 | Noise | 3.20 | 4 | 0.80 | 0.65 | 0.63 | 3.00 |
| | D | 1011.21 | 4 | 252.80 | 207.41 | 0.00 | 3.00 |
| | Error | 19.50 | 16 | 1.21 | | | |
| | Total | 1033.91 | 24 | | | | |

SS = sum of squares, df = degree of freedom, MS = mean squares

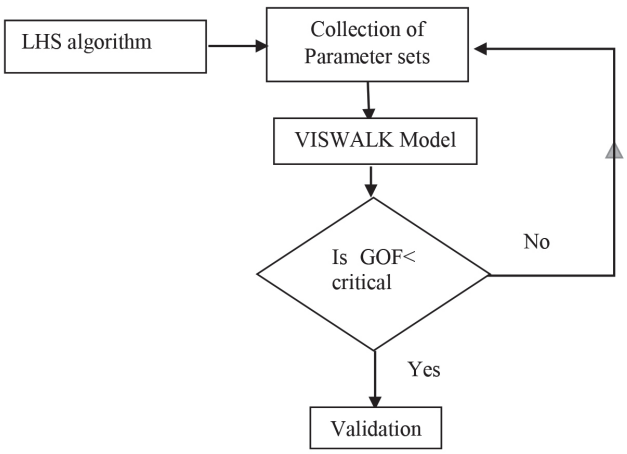


***Figure 7*** *Flowchart for calibration procedure*

best parameter set observed from the calibration is P1 and the same parameter set is used for the validation purpose. Results show that variables, such as door width and number of students, are crucial in representing evacuation time of the classroom. It is found that the relationship between the total evacuation time (TET) and door width is represented by a power function (Figure 8). This is in contrast to the findings of Liao et al. [28], which show that the relationship between the flow and a door width is linear. Results of this study can be best supported by the fact that TET is exponentially varying with the door width until a particular value and remains constant for further increase in door width, which is realistic in nature. As depicted in Figure 8, there is a good agreement between the total evacuation time values obtained from empirical and simulated values.

## 6 Validation

In the validation procedure simulation results are compared to the experimental values collected for undergraduate classroom with 38 number of students for the door width of 1.5 m. The TET and visual confirmation, such as arching behaviour, are used as measure of performance. As the TET is a single value in this case, GEH1 (Equation (2)) statistics is used as goodness of fit measure [25, 29], GEH < 1 indicates good fit. In present scenario, the GEH 1 statistic value is 0.27676 and it shows that there is no difference between actual and simulated values.

$$GEH1 = \sqrt{\frac{2(x_i - y_i)^2}{x_1 + y_i}}, \tag{2}$$

where $x_i$ is the observed value and $y_i$ is the estimated value. If GEH value < 1, it can conclude that there is no significant difference between the observed and simulated values.

Finally, using an optimized parameter set values, the future scenarios for the two classrooms in university environment are simulated considering full occupancy. It would be interesting to know how much time it will take to evacuate the rooms in any emergency situation. Total evacuation time values, obtained from the simulation runs, are shown in Table 9. These values are also compared to outputs from the regression model and they were found to be satisfactory.

## 7 Discussion

The impetus behind this research work is to develop a new framework to optimize the simulation model parameters and further to use the simulation model for suggesting solutions in an emergency. The

***Table 7*** *Sample LHS Parameter set*

| No | τ | λ | D | React to N | Noise | VD |
|---|---|---|---|---|---|---|
| 1 | 0.291 | 0.261 | 0.649 | 4 | 0.200 | 3 |
| 2 | 0.067 | 0.916 | 1.058 | 2 | 0.200 | 3 |
| 3 | 0.467 | 0.947 | 1.251 | 5 | 0.200 | 3 |
| 4 | 0.492 | 0.598 | 2.537 | 2 | 0.200 | 3 |
| 5 | 0.368 | 0.138 | 2.214 | 4 | 0.200 | 3 |
| 6 | 0.332 | 0.351 | 2.016 | 2 | 0.200 | 3 |
| 7 | 0.192 | 0.434 | 0.852 | 2 | 0.200 | 3 |
| 8 | 0.422 | 0.828 | 2.444 | 4 | 0.200 | 3 |
| 9 | 0.209 | 0.051 | 1.384 | 5 | 0.200 | 3 |
| 10 | 0.133 | 0.103 | 0.800 | 1 | 0.200 | 3 |
| 11 | 0.407 | 0.269 | 2.995 | 6 | 0.200 | 3 |
| 12 | 0.251 | 0.697 | 2.709 | 5 | 0.200 | 3 |
| 13 | 0.160 | 0.765 | 1.583 | 3 | 0.200 | 3 |
| 14 | 0.277 | 0.651 | 1.920 | 3 | 0.200 | 3 |
| 15 | 0.095 | 0.501 | 1.683 | 3 | 0.200 | 3 |
| 16 | 0.400 | 0.300 | 0.620 | 4 | 0.200 | 3 |
| 17 | 0.200 | 0.800 | 0.994 | 2 | 0.200 | 3 |
| 18 | 0.200 | 0.200 | 1.112 | 3 | 0.200 | 3 |
| 19 | 0.200 | 0.400 | 1.000 | 4 | 0.200 | 3 |
| 20 | 0.100 | 0.800 | 0.992 | 1 | 0.200 | 3 |
| 21 | 0.300 | 0.400 | 1.213 | 4 | 0.200 | 3 |
| 22 | 0.300 | 0.176 | 2.200 | 6 | 0.200 | 3 |

***Table 8*** *Calibrated parameter sets*

| No. | Scenario | Parameter Set | | | | | | $R^2$ | Cumulative Absolute Residual Value (CARE) |
|---|---|---|---|---|---|---|---|---|---|
| | | τ | λ | D | React to N | Noise | VD | | |
| 1 | P1 | 0.400 | 0.300 | 0.620 | 4 | 0.200 | 3 | 0.8913 | 40.45 |
| 2 | P2 | 0.200 | 0.800 | 0.994 | 2 | 0.200 | 3 | 0.7238 | 56.05 |
| 3 | P3 | 0.100 | 0.800 | 0.992 | 1 | 0.200 | 3 | 0.6731 | 67.99 |
| 4 | P4 | 0.200 | 0.200 | 1.112 | 3 | 0.200 | 3 | 0.8103 | 49.85 |
| 5 | P5 | 0.300 | 0.400 | 1.213 | 4 | 0.200 | 3 | 0.8197 | 109.15 |
| 6 | P6 | 0.300 | 0.176 | 2.200 | 6 | 0.200 | 3 | 0.8729 | 112.49 |
| 7 | P7 | 0.200 | 0.400 | 1.000 | 4 | 0.200 | 3 | 0.8041 | 49.05 |
| 8 | P8 | 0.291 | 0.261 | 0.649 | 4 | 0.200 | 3 | 0.5964 | 50.85 |
| 9 | P9 | 0.067 | 0.916 | 1.058 | 2 | 0.200 | 3 | 0.6119 | 68.61 |
| 10 | P10 | 0.467 | 0.947 | 1.251 | 5 | 0.200 | 3 | 0.6073 | 60.85 |
| 11 | P11 | 0.492 | 0.598 | 2.537 | 2 | 0.200 | 3 | 0.5901 | 117.09 |
| 12 | P12 | 0.368 | 0.138 | 2.214 | 4 | 0.200 | 3 | 0.7498 | 104.89 |
| 13 | P13 | 0.332 | 0.351 | 2.016 | 2 | 0.200 | 3 | 0.7735 | 50.55 |
| 14 | P14 | 0.192 | 0.434 | 0.852 | 2 | 0.200 | 3 | 0.6885 | 55.95 |
| 15 | P15 | 0.422 | 0.828 | 2.444 | 4 | 0.200 | 3 | 0.7568 | 104.89 |
| 16 | P16 | 0.209 | 0.051 | 1.384 | 5 | 0.200 | 3 | 0.7133 | 48.55 |
| 17 | P17 | 0.133 | 0.103 | 0.800 | 1 | 0.200 | 3 | 0.5886 | 65.31 |
| 18 | P18 | 0.407 | 0.269 | 2.995 | 6 | 0.200 | 3 | 0.4731 | 163.89 |
| 19 | P19 | 0.251 | 0.697 | 2.709 | 5 | 0.200 | 3 | 0.7204 | 63.05 |
| 20 | P20 | 0.160 | 0.765 | 1.583 | 3 | 0.200 | 3 | 0.6972 | 56.19 |
| 21 | P21 | 0.277 | 0.651 | 1.920 | 3 | 0.200 | 3 | 0.7426 | 53.05 |
| 22 | P22 | 0.095 | 0.501 | 1.683 | 3 | 0.200 | 3 | 0.6396 | 53.05 |
| 23 | Default | 0.400 | 0.176 | 5.000 | 8 | 0.200 | 3 | 0.9183 | 228.69 |

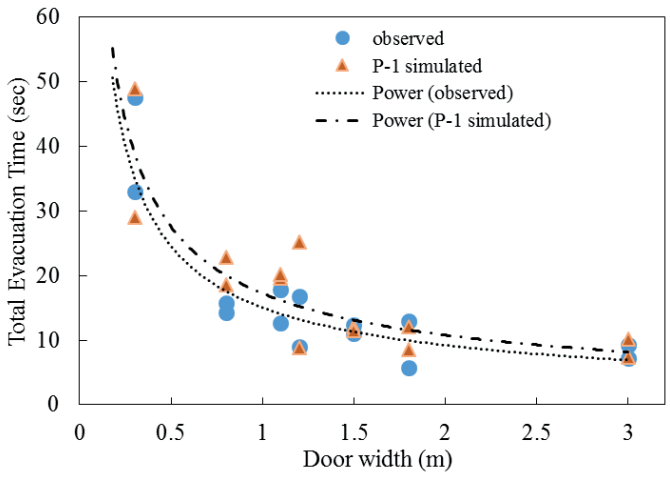


***Figure 8*** *Comparing observed results to simulation results*

***Table 9*** *Future Scenarios for full occupancy for door width 3.0 m (University Scenario)*

| Condition: when class is fully occupied | Simulated TET (sec) |
|---|---|
| PG classroom | 12.9 |
| UG classroom | 18 |
| Parameter set for the simulation: τ = 0.4, λ = 0.3, D = 0.6, React to N = 4, VD = 3, Noise = 0.2 | |

proposed methodology includes real world experiments in classrooms; identifying the suitable parameters, using sensitivity analysis; calibration and validation of selected parameters, using advanced techniques and finally testing of the model for future scenarios. Data availability is the major hurdle in fine tuning the simulation model and further it is extremely difficult to get the data from emergency evacuation incidents happened around the world in various conditions. As the first attempt in India, especially in classroom set-up, evacuation data was collected for different geometric configurations and involving students of diverse age groups. Before conducting the experiments, instructions were given to students in such a way that they behave as if they were in emergency situations.

In the next step, the sensitivity analyses were carried out to identify the most influential parameters, because these parameters mostly govern the outcome of the model. In the proposed method, the two-way ANOVA and two-dimensional line plots were involved in sensitivity analysis. Considering the problem at hand and the model parameters, fourteen classroom scenarios are simulated simultaneously using the parameter sets generated through the Latin Hypercube Sampling algorithm. The goodness of fit for the parameters is measured using cumulative residual error, which is an appropriate method to compare observed and empirical data. The validation of the optimized parameter set proved that they mimic the emergency conditions satisfactorily. The optimized parameters will help in simulating future scenarios including building level simulations.

From the simulation results it is found that the relationship between the total evacuation time and classroom door widths is non-linear. Initial observation shows that there is a little change in evacuation times with increasing door widths. However, there is a huge drop in evacuation time with a little increasing of door widths. Those results are commensurate with already published results, such as Chen and Han [8] and Gu et al. [10]. Results from Chen and Han [8] study show that with increase in the width of door, the time of evacuation decreases but it is not linear [8]. From the Gu et al. [10] study it is observed that students‘ cumulative departures in normal conditions is a linear function while in emergency it is a convex function and further students’ reaction time increases substantially in emergency conditions. Similar studies are also observed in the transportation domain. For instance, Najmanova et al. [11] research study emphases on assessing the several characteristics of passengers by the means of laboratory based controlled experiments. Evacuation experiments were conducted in a double decker train in Czech Republic and the experiments were conducted under various scenarios by varying widths, exit types and exit methods. Results show that the evacuation time reduces with increasing door width, number of exits and their location. Passenger characteristics, like speeds and exit flow rates as well as human behaviours were evaluated. In the other study by Kim et al. [30], a model suitable for the domestic environment is established, based on the data measured and tested in Korea and related formulas and variables are derived to predict the effect of reducing the boarding and alighting time when the door width is increased.

In addition to the existing knowledge, the present study provided the data about response of the students (i.e. the total evacuation time) of various categories with different characteristics for varying door widths in emergency; with simulations it is proved that door width has a tremendous impact on evacuation time. It is believed that the calibrated and validated parameters for VISWALK identified through a well-designed methodology, would help in developing solutions for various problems in infrastructure related domains, including the transportation.

## 8 Limitation of the study

In this study, evacuation data was collected for different geometric configuration and involving students of diverse age groups. Prior to conducting the experiments, instructions were given to students in such a way that they behave as if they were in emergency situations. It is difficult to obtain 100 % accuracy in instil human responses during the emergency evacuation experiments. The factors, such as anxiety/fear and reaction times were captured partially in the present study. Using the basic data available from experiments, simulation models can be better calibrated and used for mimicking the real behaviour of evacuees by adjusting parameters and in the case of sensitivity analysis, to identify the most influential parameters, 15 combinations have to be verified. In this study authors explored only 8 combinations, considering the importance of the parameters in modelling. More research is possible in this direction.

## 9 Conclusions and future scope

This study is an attempt to establish the procedure for optimizing the simulation model parameters using the real-world data for emergency evacuation conditions. The proposed methodology is suitable for calibrating and validating any kind of pedestrian simulation model for normal and emergency scenarios. Conducting experiments on humans is arduous and perilous task and may leads to accidents as well. The authors have taken all the precautions to avoid incidents while conducting the experiment. Getting the data from recorded incidents is immensely useful and will further improve the quality of work. However, obtaining such data is hard and in most of the conditions it will not be available. In emergency evacuation, pedestrian behaviour plays a major role

and, in this study, pedestrian behavioural aspects, such as the relaxation time, distance from the other pedestrians and force exerted by the closest pedestrians, have a significant impact on total evacuation time from the classroom. Using the basic data available from experiments, simulation models can be better calibrated and used for mimicking the real behaviour of evacuees by adjusting parameters.

The methodology proposed in this study is very precise in considering all the necessary steps to optimize the pedestrian simulation parameters required to replicate emergency evacuation conditions, specifically in some practical applications, such as high-rise buildings, passenger vehicles and transport terminals. The proposed method assists in developing the suitable evacuation plans for emergency conditions and helps in improving the safety during the evacuations.

In line with the present study, in future, the authors would like to explore the application of the non-conventional optimization procedures, such as Genetic Algorithm (GA) or Differential Evolution (DA) in parameter estimation. In addition, number of doors and door position influence on total evacuation time needs to be evaluated using the calibrated models. In the future, authors will extend this work to public transport vehicles and terminals where emergency evacuation of passengers from vehicles and terminals can be studied, using the simulation tools, such as VISWALK, PATHFIDNER and so on. From the experiments, it is observed that aggressiveness of the evacuees is the potential threat to the safety in panic conditions. Preparedness of the pedestrians for emergency situations is very important and continuous mock-drills for those conditions are mandatory.

## Acknowledgements

This research did not receive any specific grant from funding agencies in the public, commercial, or not-for-profit sectors. The authors would like to thank the Lancers Convent Public School authority, New Delhi, for necessary permissions to conduct the evacuation drills.

## References

[1] YANG, X., YANG, X., WANG, Q., KANG, Y., PAN, F. Guide optimization in pedestrian emergency evacuation. *Applied Mathematics and Computation* [online]. 2020, **365**, 124711. ISSN 0096- 3003. Available from: https://doi.org/10.1016/j.amc.2019.124711.

[2] VANUMU, L. D., ARYA, A., GADDAM, H. K., RAO, K. R. Modelling emergency evacuation of classroom with different age profiles. *Collective Dynamics* [online]. 2020. **5**, p. 374-381. ISSN 2366-8539. Available from: https://doi.org/10.17815/CD.2020.96

[3] LI, X., XU, X., ZHANG, J., JIANG, K., LIU, W., YI, R., SONG, W. Experimental study on the movement characteristics of pedestrians under sudden contact forces. *Journal of Statistical Mechanics: Theory and Experiment* [online]. 2021, **2021**, 063406. eISSN 1742-5468. Available from: https://doi.org/10.1088/1742-5468/ac02c7

[4] JAIN H., VANUMU L. D., RAMACHANDRA RAO, K. Identifying a suitable pedestrian simulation software - a case study on emergency evacuation of classroom. In: *Recent advances in traffic engineering* [online]. ARKATKAR, S., VELMURUGAN, S., VERMA, A. (eds.). Lecture Notes in Civil Engineering. Vol. 69. Singapore: Springer, 2020. ISBN 978-981-15-3741-7, eISBN 978-981-15-3742-4. Available from: https://doi.org/10.1007/978-981-15-3742-4_34

[5] LIU, S., YANG,L., FANG, T.AND LI, J. Evacuation from a classroom considering the occupant density around exits. *Physica A: Statistical Mechanics and its Applications* [online]. 2009, **388**(9), p. 1921-1928. ISSN 0378-4371. Available from: https://doi.org/10.1016/j.physa.2009.01.008

[6] ZHAO, H., GAO, Z. Reserve capacity and exit choosing in pedestrian evacuation dynamics. *Journal of Physics A: Mathematical and Theoretical* [online]. 2010, **43**(10), 105001. ISSN 1751-8113, eISSN 1751-8121. Available from: https://ui.adsabs.harvard.edu/link_gateway/2010JPhA...43j5001Z/doi:10.1088/1751-8113/43/10/105001

[7] AIK, L. E. Exit-selection behaviors during a classroom evacuation. *International Journal of Physical Sciences* [online]. 2011, **13**(6), p. 3218-3231. ISSN 1992-1950. Available from: https://doi.org/10.5897/IJPS10.466

[8] CHEN, M., HAN, D. Simulation of evacuation processes using a multi-grid model. In: *Recent advances in computer science and information engineering* [online]. QIAN, Z., CAO, L., SU, W., WANG, T., YANG, H. (eds.). Lecture Notes in Electrical Engineering. Vol. 126. Berlin, Heidelberg: Springer, 2012. ISBN 978-3-642-25765-0, eISBN 978-3-642-25766-7. Available from: https://doi.org/10.1007/978-3-642-25766-7_42

[9] LI, M., ZHAO, Y., HE, L., CHEN, W., XU, X. The parameter calibration and optimization of social force model for the real-life 2013 Ya'an earthquake evacuation in China. *Safety Science* [online]. 2015, **79**, p. 243-253. ISSN 0925-7535. Available from: https://doi.org/10.1016/j.ssci.2015.06.018

[10] GU, Z., LIU, Z., SHIWAKOTI, N., YANG, M. Video-based analysis of school students' emergency evacuation behavior in earthquakes. *International Journal of Disaster Risk Reduction* [online]. 2016, **18**, p. 1-11. ISSN 2212-4209. Available from: https://doi.org/10.1016/j.ijdrr.2016.05.008

[11] NAJMANOVA, H., KUKLIK, L., PESKOVA, V., BUKACEK, M., HRABAK, P., VASATA, D. Evacuation trials from a double-deck electric train unit: experimental data and sensitivity analysis. *Safety Science* [online]. 2022, **146**, 105523. ISSN 0925-7535. Available from: https://doi.org/10.1016/j.ssci.2021.105523

[12] WANG, F. Multi-Scenario Simulation of Subway Emergency Evacuation Based on Multi-Agent. *International Journal of Simulation Modelling* [online]. 2021, **20**(2), p. 387-397. ISSN 1726-4529. Available from: https://doi.org/10.2507/ijsimm20-2-co8

[13] LEI, W., LI, A., GAO, R., HAO, X., DENG, B. Simulation of pedestrian crowds' evacuation in a huge transit terminal subway station. *Physica A: Statistical Mechanics and Its Applications* [online]. 2012, **391**(22), p. 5355-5365. ISSN 0378-4371. Available from: https://doi.org/10.1016/j.physa.2012.06.033

[14] PTV group. PTV Vissim 7 User Manual. PTV AG, 2013.

[15] DAAMEN, W., HOOGENDOORN, S. Emergency door capacity: influence of population composition and stress level. In: Fifth International Conference on Pedestrian and Evacuation Dynamics: proceedings. New York: Springer, 2010. ISBN 978-1-4419-9724-1.

[16] DAAMEN, W., HOOGENDOORN, S. Calibration of pedestrian simulation model for emergency doors for different pedestrian types. In: Transportation Research Board 91st Annual Meeting: proceedings. 2012.

[17] YAMASHITA, T., MATSUSHIMA, H., NODA, I. Exhaustive analysis with a pedestrian simulation environment for assistant of evacuation planning. *Transportation Research Procedia* [online]. 2014, **2**, p. 264-272. ISSN 2352-1465. Available from: https://doi.org/10.1016/j.trpro.2014.09.047

[18] ZHU,W.,WANG,Y., MA,Y.,.KONG,Y., ZHOU,X., DU, B. Experimental study on evacuation behavior of crowds in emergency situation. In 5th International Conference on Risk Analysis and Crisis Response: proceedings. CRC Press, 2015. eISBN 9780429226403.

[19] NICOLAS, A., BOUZAT,S., KUPERMAN, M. N. Pedestrian flows through a narrow doorway: Effect of individual behaviours on the global flow and microscopic dynamics. *Transportation Research Part B: Methodological* [online]. 2017, **99**, p. 30-43. ISSN 0191-2615. Available from: https://doi.org/10.1016/j.trb.2017.01.008

[20] KRETZ, T., HENGST, S., VORTISCH, P. Pedestrian flow at bottlenecks-validation and calibration of vissim's social force model of pedestrian traffic and its empirical foundations. *arXiv preprint* [online]. 2008, arXiv:0805.1788. Available from: https://doi.org/10.48550/arXiv.0805.1788

[21] MARTEN, J. B., HENNINGSSON, J. Verification and validation of viswalk for building evacuation modelling. Report 5481. Lund, Sweden: Department of Fire Safety Engineering, Lund University, 2014. ISSN 1402-3504.

[22] HELBING, D., FARKAS, I., VICSEK, T. Simulating dynamical features of escape panic. *Nature* [online]. 2000, **407**(6803), p. 487-490. ISSN 0028-0836, eISSN 1476-4687. Available from: https://doi.org/10.1038/35035023

[23] SINGH, M. K., GADDAM, H., VANUMU, L. D., RAO, K. R. Traffic data extraction using MATLAB® based tool. In: International Conference TPMDC-2016: proceedings. 2016.

[24] R core team. R: a language and environment for statistical computing - R Foundation for Statistical Computing [online]. Vienna, Austria, 2015. Available from: https://www.R-project.org/

[25] DAAMEN, W., BUISSON, C., HOOGENDOORN, S. P. *Traffic simulation and data: validation methods and applications* [online]. 1. ed. Boca Raton: CRC Press, 2014. ISBN 9780429161902. Available from: https://doi.org/10.1201/b17440

[26] MCKAY, M. D., BECKMAN, R. J., CONOVER, W. J. A Comparison of three methods for selecting values of input variables in the analysis of output from a computer code. *Technometrics* [online]. 1979, **21**, p. 239-245. ISSN 0040-1706, eISSN 1537-2723. Available from: https://doi.org/10.1080/00401706.1979.10489755

[27] IMAN, R. L., CONOVER, W. J. A distribution free approach to inducing rank correlation among input variables. *Communications in Statistics - Simulation and Computation* [online]. 1982, **11**(3), p. 311-334. ISSN 0361-0918, eISSN 1532-4141. Available from: http://dx.doi.org/10.1080/03610918208812265

[28] LIAO, W, TORDEUX, A, SEYFRIED, A, CHRAIBI, M, DRZYCIMSKI, K, ZHENG, X, ZHAO, Y. Measuring the steady state of pedestrian flow in bottleneck experiments. *Physica A Statistical Mechanics and its Applications* [online]. 2016, **461**, p. 248-261. ISSN 0378-4371. Available from: https://doi.org/10.1016/j.physa.2016.05.051

[29] HOLLANDER, Y., LIU, R. The principles of calibrating traffic microsimulation models. *Transportation* [online]. 2008, **35**(3), p. 347-362. ISSN 0049-4488, eISSN 1572-9435. Available from: https://doi.org/10.1007/s11116-007-9156-2

[30] JUNGTAI, K., MOO, S. K., JAE, S. H., YONG, H. C., TAESIK K. An analysis of boarding and alighting times for urban railway vehicles. *Journal of the Korean Society for Railway* [online]. 2014, **17**(3), p. 210-215. ISSN 1738-6225, eISSN 2288-2235. Available from: https://doi.org/10.7782/JKSR.2014.17.3.210

# MODELING THE INTELLIGENT TRANSPORT SYSTEMS ELEMENTS FUNCTIONALITY TESTING PLAN: A CASE STUDY

**Ján Ližbetin *, Jan Pečman, Jiří Hanzl, Ondrej Stopka**

Department of Transport and Logistics, Institute of Technology and Business in Ceske Budejovice, Ceske Budejovice, Czech Republic

*E-mail of corresponding author: lizbetin@mail.vstecb.cz

***Resume***

Autonomous control and the associated development of relevant intelligent control systems have become an issue of interest in the automotive sector decades ago. This article deals with the issue of subsystem validation planning. The theoretical part describes the issue, characterizes the current state of the researched issues in selected scientific publications and characterizes the data and methods with which the authors work. The practical part of the article analyzes a case study in the form of a model project, its structure, testing requirements and design of a test campaign plan. The output is a calculation and decision tree, which determines the optimal variant of the number of vehicles so that the validation is completed, while minimizing time and financial resources.

***Article info***

Received 21 March 2022
Accepted 12 September 2022
Online 30 September 2022

***Keywords:***

autonomous management
testing
planning
intelligent transport systems

Available online: https://doi.org/10.26552/com.C.2022.4.F97-F108

ISSN 1335-4205 (print version)
ISSN 2585-7878 (online version)

## 1 Introduction

The autonomous operation of road vehicles, which will no longer be operated by a natural person, has become increasingly specific in recent decades, with developers being able to discover and validate a number of technologies relevant to this issue. However, the implementation of these systems was preceded by extensive research and development. Only then were the individual intelligent systems gradually delivered to pre-specified and controlled series of vehicles and tested [1]. Now, those technologies are slowly becoming the standard of comfort, as well as an element for increasing car safety. It can be assumed that the growing demand and pressure to ensure that vehicles equipped in this way are standardly delivered worldwide would increase in the coming years. For the manufacturer of a given vehicle type, this means creating a specification that meets the widest possible range of operating conditions. These, of course, vary considerably from one part of the world to another, so there is a need to ensure that these systems work properly and safely wherever the vehicle is operated, or that the user is informed of limited uses.

The article deals with the proposal of an optimized testing plan for intelligent transport systems (ITS) for autonomous management. This is a model in which the testing requirements are fixed. These are mainly the number of kilometers, the type of road, different lighting conditions and driving speed. According to the specific driving plan, the final decision on the number of used test vehicles is determined using the so-called decision tree method. The input information is, for example, the purchase price of the test car and possible sanctions in the case of non-compliance with the delivery date of the final product to the customer [2-3]. Proper testing is a key prerequisite for validation of any developed system. In the case of ITS for autonomous vehicle control, it is a question of verifying the correctness of the system's response to a given traffic situation. The validation procedure consists of the design and assembly of the test vehicle, the analysis of testing requirements, the planning of the test campaign, its implementation, the subsequent analysis and the synthesis of the collected data. The article also defines the individual terms that relate to the topic and provides links to other areas that affect validation. It is an explanation of the essence of ITS for the software management and testing automation, outlining the methodology of creating the testing requirements and a description of the practical implementation of tests.

## 2 Literature review

The issue of the ITS and autonomous vehicle management has been discussed very often in recent

years and countless erudite and professional articles have been published. Much of the research and published output is devoted to ITS testing. Most published professional articles focus on development, testing and evaluation of autonomous systems. For example [4] deals with the so-called intelligent vehicle. In their Intelligent Vehicle Lab at the Technical University of Cartagena, authors designed a vehicle navigation application that provides a clear and reliable platform for the development of autonomous driving technologies as well as for the testing purposes. The open and modular architecture is able to easily integrate a wide range of sensors and actuators that can be used to test vehicle control algorithms and strategies. Algorithms are used to perform the global and local route planning on board autonomous vehicles.

A similar procedure is characterized, for example, in [5]. The article defines a path planning algorithm based on potential fields. Potential models are modified so that their behavior is appropriate to the surroundings and dynamics of the car and they can face almost any unexpected scenarios. The response of the system takes into account the characteristics of the road (e.g. maximum speed, lane curvature etc.) and the presence of obstacles and other users. The algorithm was tested on an automated vehicle equipped with a GPS receiver, a measuring unit and a computer vision system in real environments.

In publication [6], the authors discuss the problem of the method of "stereo" depth estimation into a model designed for in-depth learning of an autonomous vehicle control system using the neural networks. The authors came up with a "self-improving" pyramid stereo network that can obtain direct regression disparity without complicated post-processing. In addition, online learning can not only solve the problem of data reduction, but also save time spent on training and hardware resources in practice. At the same time, the proposed model has the ability to self-improve new scenes, which can quickly adjust the model according to test data over time and improve prediction accuracy.

Other selected publications directly address the design and the ITS system, but they do not directly address the way and procedure of testing these elements and systems. In other articles, the ITS testing is dealt with, for example, [7-11] or [12].

The publication [7] presents a complete framework capable of testing each component involved in the ITS and which is able to control the interoperability of all the components. This framework provides for testing the conformity of all the ITS components in terms of their specifications (especially communication protocols that ensure interoperability at different layers), as well as testing the interoperability of these components to ensure their proper functioning where they work together. It also notes that some standard specifications (either protocols or test case specifications) need to be improved.

In publications [8-10], the authors address simulation as a tool for the ITS testing and evaluation because it provides a cost-effective and safe alternative to testing and evaluation. A combination of simulators can be used to create accurate and realistic test scenarios, especially if the systems being tested are complex. Interconnected and automated driving in the context of the ITS is another area of research on the transport systems, dealt with in [9]. In the article, authors present a simulation framework consisting of driving, traffic and network simulators for testing and evaluating ITS applications. Examples of adaptive cruise control applications that are used as the test cases for the simulation framework, as well as for development of the real scenarios of its use, are given. Authors examined the reliability of communication tools in the vehicle, between vehicles and between the vehicle and the transport infrastructure or transport equipment, [10].

However, the issue of planning the scope of testing such systems is addressed very marginally. Most authors discuss either the systems themselves, the design of these systems, the method and possibilities of testing the reliability of ITS, but they no longer address the planning of the scope of testing. When planning the testing, the financial and operational capabilities of the development company must be taken into account, as well as customer requirements for reliability guarantees and system delivery dates. The publication [13] is closest to this topic. The authors present a checklist of critical steps and considerations that are part of successful ITS planning and implementation.

According to authors interesting is study [14] that tested some elements of intelligent transport systems, namely elements of adaptive cruise control in conjunction with passive safety features.

The results revealed that driver and passenger interaction with the seatbelt reminder system led to large and significant decreases in the percentage of trips where occupants were unbelted, in the percentage of total driving time spent unbelted and in the time taken to fasten a seatbelt in response to system warnings. The seatbelt reminder system was rated by drivers as being useful, effective and socially acceptable and led to a decrease in drivers' subjective workload.

The analysis of the examined documents shows that the issue of the ITS testing planning optimization is insufficiently addressed in the available scientific literature and the authors deal with it only marginally. This topic is addressed to a limited extent, which is considered a gap in articles published in professional and scientific journals. The topic of the ITS testing planning optimization is not sufficiently researched and analyzed. This proves and highlights the topicality of the researched subject and the fact that there is still room for further research in this area. The authors outline the possibility of optimizing the ITS s testing plan using the so-called decision tree and Gantt charts. The authors

did not identify this view of the ITS testing planning in any of the analyzed literature.

## 3 Data and methods

Intelligent transport systems ensure active safety and increased comfort for drivers and other passengers while driving. Those systems can partially or completely interfere with the steering of the vehicle, while some maneuvers can be performed by the vehicle independently. It is another step towards autonomous driving, where the driver will not have to control the vehicle and will be able to engage in other activities. Individual ITS are based on monitoring the environment by sensors, mainly based on laser, radar, ultrasound, camera and their mutual cooperation. Individual sensors collect data from the environment and can detect individual objects. If the object is close to the vehicle, the sensor sends a message to the control unit, which passes this information on and ensures, for example, braking or adjusting the position of the vehicle in the lane.

Development of these systems is very time and money consuming and consists of several parts. After the development itself, the testing phase begins. First it is necessary to test the sensor and function on simulations, then in a test vehicle on a closed test polygon and then it is necessary to verify the correctness of the system functionality in real conditions [15]. This phase is called the final system validation and usually takes place in several countries and under different conditions. Testing requirements are usually determined by the purpose of the function. If this is a function to keep the vehicle in the lane on the highway, most of the test campaign will take place on the highways. However, if it is a parking assistant, the test campaign will focus on the greatest possible variability of parking spaces and scenarios that the end user can encounter. The data that uploaded as a part of the test campaign is then analyzed and the results are passed to the customer to verify the reliability and proper functioning of the system.

### 3.1 ITS software testing

Software is a very important part of ITS, although far from the only one. However, the final testing phase of the system focuses mainly on the results of the software, as the other parts were tested before they were put into operation. The final validation is therefore a check of the functionality of the unit with an emphasis on software.

The software testing is an integral part of its development and accounts for up to 50 % of the time and costs of its development. If the software is not tested, errors or even a complete malfunction of the device could occur. Thorough testing of the software is therefore intended to ensure its smooth and correct functioning [16].

Due to the integration of software into virtually every aspect of life, great emphasis is placed on the proper testing to the satisfaction of the end user. In order to avoid all the malfunctions, the software would have to be tested several times longer than it took to develop and it would still not be possible to detect every bug. It is therefore necessary to find the point of the optimal level of testing so that all the fundamental errors are detected and at the same time software development still pays off economically. This point describes [17].

### 3.2 Testing procedure

Testing is defined as the process of assessing whether a particular system meets the originally specified requirements defined by the client or user. The test result is a report describing the difference between the expected and actual result.

During the testing, code errors and missing or incomplete requirements coverage are searched. The result demonstrates the quality of the product as a whole. There are several steps and levels in the testing process. The three basic steps are unit testing, integration testing and system testing. Software development is divided into several modules and each module is worked on by a different person or team of developers. Those modules are then tested separately and are unit testing. Integration tests check the correct assembly of modules. This step often reveals errors that make the modules incompatible. The development of individual modules separately is important especially so that the entire software is not tied to one person. In the event of termination of cooperation, the entire development project would be jeopardized. The individual modules must meet the given standards and requirements and must be mutually compatible and follow each other. The third step is system testing, in which all the aspects of the software as a whole are tested. When testing complicated and branched software with a large number of combinations, it is appropriate to incorporate testing automation [17].

The testing itself takes place in cycles, which consist of planning, analysis and preparation of tests, execution and evaluation and final monitoring of defects. In the planning phase, a project analysis is performed and it is defined which aspects are to be checked and evaluated within the testing, i.e. how the tests are to be performed. Of course, it is also necessary to consider human and financial resources and, based on these inputs, subsequently create a timetable. The output of this phase is a test plan, which indicates the division of roles and responsibilities, the timetable and the financial estimate of the activity [18].

### 3.3 Security of ITS functions

To ensure security testing, a statistical model needs to be defined. The statistical model is a term that defines the number of hours or kilometers in each condition to be tested. Vendor Functional Safety Specialists ITS functions, in collaboration with the customer-side experts, jointly create testing requirements to cover all the test scenarios and ensure maximum safety according to ISO 26262 and ISO 21448 [19-20]. The customer's requirements for the function of the ITS system are also included in this analysis. Based on this thorough analysis, a table is created with a combination of given conditions. The number of hours or kilometers, required to verify safety, is determined based on calculations by functional safety experts so that the individual risks are statistically covered.

This statistical model also serves as a basis for testing planning. It can contain conditions such as the road type, driving speed, number of lanes, lighting, weather conditions, as well as many others. The greater the number of basic conditions, the greater the final number of hours or kilometers that need to be recorded and the higher the costs associated with testing. The basic conditions should be defined in such a way that the basic possible combinations of conditions are covered and at the same time that they are achievable and their upload is not in conflict with the law. If it is necessary to upload a combination of conditions that does not occur so often and it is impossible or very difficult to upload the conditions, it is possible to simulate these conditions. This step is again associated with increased costs. Therefore, the proper preparation and a plan designed to minimize the time required to work with other participants, such as the profession of fire brigade or the closure of a public road, should be carried out.

ISO 26262 and 21448 standards are the basic pillars of the safety of the ITS functions and their scope covers all aspects of these functions in the development and subsequent operation phase on public roads. This topic is very sensitive, as it is a new issue and the public is still skeptical about the credibility of ITS systems. It can be assumed that the ITS functions will become the standard in transport over time and life without them will be difficult to imagine. Responsibility for the lives of drivers, crew members and other road users is an integral part of this issue and therefore safety always comes first [21].

### 3.4 Practical implementation of tests

To perform the tests, it is necessary to equip the vehicle with systems that can collect data for subsequent evaluation. These are mainly the tested sensor, the reference sensors and the computer that collects all this data. Reference sensors are sensors with greater accuracy than the tested sensor and are already available on the market. Based on the comparison of the recorded data, it is possible to compare the data recording results of the reference and tested sensor or a prototype.

## 4 Case study

The model project described in the feasibility study is a fictitious project that does not have its own project structure, customer or final product design. It is a universal model to which it is possible to apply all the processes of real projects without the risk of leakage of sensitive information. This project does not provide any specific functions, but collects general information from the real projects.

The aim of the study is a practical illustration of the testing process. In this part of the article, the authors want to explain to readers how and under which conditions data collection and evaluation would take place. Each test plan is developed primarily from customer requirements. The customer defines what he wants to test, what test results he expects and under what conditions the test should take place. Subsequently, a testing plan is compiled that reflects all the input factors defined by the customer. The reader will thus get a more specific idea of the testing process and how to evaluate the obtained data.

### 4.1 Requirements from customers

The selected model project is focused on several functions of autonomous management. Testing requirements are therefore composed of the real requirements for individual functions for specific customers. As the areas of operation of the individual functions are very different, the final conditions for testing cover a wide range of possibilities and their mutual combinations. The purpose of testing autonomous control functions is to cover as many combinations of conditions as possible that a vehicle can get in normal traffic on public roads [22-24]. Covering all the entered combinations at a given time requires very detailed planning and knowledge of transport conditions in other countries.

One of the basic building blocks for creating a statistical model is the type of road. In this case, the road type can be defined by three basic categories: "Rural", "Urban", "Highway". These are rural roads, urban roads, the so-called district roads and motorways.

Another group of conditions are lighting

***Table 1*** *Overview of testing requirements, [27]*

| | Description | % | Number of hours |
|---|---|---|---|
| Traffic orientation | Left-sided | 30 | 300 |
| | Right-sided | 70 | 700 |
| Country | Germany | 20 | 200 |
| | France | 10 | 100 |
| | Czech Republic | 10 | 100 |
| | Hungary | 10 | 100 |
| | Denmark | 10 | 100 |
| | Belgium | 10 | 100 |
| Light conditions | Day | 80 | 800 |
| | Night | 15 | 150 |
| | Low light | 5 | 50 |
| Type of road | Urban | 15 | 150 |
| | Rural | 15 | 150 |
| | Highway | 70 | 700 |
| Total | | 100 | 1000 |

conditions. Some sensors change their behavior based on the lighting conditions. This can be caused by poor visibility at dusk and at night, glare from public lights or oncoming vehicles. Each function needs to be tested in all the variants of lighting conditions to minimize the risk of malfunction that could lead to an accident. The lighting conditions have three categories: "Day", "Night" and "Low light". The individual conditions are precisely defined by the Meteorological and Astronomical Institute. The Low light category includes civil, nautical and astronomical dawn and dusk, as well as the golden hour. Civil dawn and dusk are defined by the position of the center of the solar disk, which is located 6° below the horizon. At this time, it is possible to perform most common daily activities without artificial lighting. Nautical dawn and dusk take place when the center of the sun's disk is between 6° and 12° below the horizon. The first stars are beginning to be seen and the horizon is also very noticeable. Astronomical dawn and dusk are the moment of the first or last rays of the sun. The stars are clearly visible in the dark sky and the center of the sun's disk is located 18° below the horizon. The golden hour is the part of the day when the center of the sun's disk is between 10° and 12° above the horizon. The golden hour is often accompanied by golden lighting. Sunrise and sunset are events when the center of the sun's disk crosses the horizon. The day is therefore the part of the day from the time when the sun is 12° above the horizon in the morning until 12° above the horizon again in the evening. The night runs from astronomical twilight to astronomical dawn [25-26].

For the purposes of the model project, it is also important whether it is right-hand or left-hand traffic. Although the left-hand traffic is associated mainly with Japan and the United Kingdom, it affects more than seventy countries around the world. They will probably not be so significant in terms of overall size or population, but the fact that the number is more than a third of all the states is certainly worth noting. This is also one of the biggest differences in the road transport one can find in the world. In such a case, it is necessary to at least know the shortcomings of the functions of autonomous control, in the best case to verify that the function works properly even in such changed conditions and is able to adapt. Table 1 lists all the parts of the statistical model that are applicable for each country. Only European countries were chosen for the purposes of the model project, but it is no exception that data needs to be uploaded in the USA, China, Japan, South Korea and many other areas.

The total number of recordings must be at least 1000 hours. At least 30% of the total must be on the left-hand drive roads. The volume of data uploaded in Germany must be double that of other right-handers. The volume of data for the remaining countries must be evenly distributed. Other countries, where data upload and subsequent function validation are required, are: France, the Czech Republic, Hungary, Denmark and Belgium. The required distribution of data from individual types of roads is as follows: Urban = 15%, Rural = 15%, Highway = 70%. The distribution of data recorded in individual lighting conditions is as follows: Day = 80%, Night = 15%, Low light = 5%.

### 4.2 Draft test activity plan

Based on customer requirements, it is then necessary to create a specific plan for the test campaign. This plan may change during the campaign. The reason

***Table 2*** *Length of recording in individual countries, [27])*

| Country | Hours of recording | Days of recording | Weeks of recording | Estimated number of km |
|---|---|---|---|---|
| Great Britain | 380 | 64 | 13 | 32200 |
| Germany | 252 | 42 | 9 | 21320 |
| France | 131 | 22 | 5 | 11000 |
| Czech Republic | 131 | 22 | 5 | 11000 |
| Hungary | 131 | 22 | 5 | 11000 |
| Denmark | 131 | 22 | 5 | 11000 |
| Belgium | 131 | 22 | 5 | 11000 |
| Total | 1287 | 216 | 47 | 108520 |

for changing the plan may be, for example, specifying or changing some requirements or changing the start of the campaign due to delays in previous development steps. Another possible stimulus for change may be the sudden occurrence of an unexpected event, such as an accident or breakdown of a test vehicle, natural influences and disasters, or a loss of human resources. It is necessary to respond to each of these facts operatively, but it is not necessary to include them in the planning. The test campaign plan includes a Gantt chart, a plan of each path to be uploaded and the estimated financial amount of the entire campaign.

The maps.google.com server was used to plan accurate routes due to its worldwide reach and ease of use. For the purposes of this test campaign, the assumed average speed was set at 100 $km.h^{-1}$ for the Highway condition, 70 $km.h^{-1}$ for the Rural condition and 30 $km.h^{-1}$ for the Urban condition. The total estimated mileage and length of recording in each country are shown in Table 2.

As an example of testing in individual European countries, the article presents the test in Germany. The complete course of testing in all the selected European countries is detailed in [27].

Germany is the second country in terms of the total number of hours needed to validate the system. For the Rural condition, the estimated number of kilometers to meet the requirement is almost 3,000 km. To meet this requirement, one only needs to upload the defined route once. The Highway condition is represented by a larger number of hours, so the expected number of recorded kilometers is also higher. In the case of Germany, it is 17,500 km. To meet the requirement, the selected route needs to be uploaded four times. Again, it is possible to use both directions of one route to increase the variability of the recorded data.

The following cities were selected for the Urban condition: Berlin, Munich, Stuttgart, Hamburg, Dresden, Cologne and Frankfurt. Only one day will be recorded in each of these cities. These are cities that are important not only for their history, but especially for their technical sophistication and are therefore also important for development of autonomous management.

The number of hours required to record does not vary in other countries. Individual countries differ in the composition of the infrastructure and the area, which affects the total number of repetitions of individual routes, but this is not important in the case of a model project.

However, some specific projects may regulate the number of iterations. It is also necessary to incorporate the requirements of lighting conditions into the planning of individual shifts. During the eight-hour shift, six hours are expected to be used effectively for recording. The loss of two hours is expected due to the need to prepare and calibrate the in-vehicle recording system, report daily results and upload data samples for inspection. The distribution of shifts under lighting conditions depends on the exact location and time. In the case of covering the Day, Low light and Night conditions, it is advisable to schedule afternoon shifts during which all the three categories of light conditions will be met on an ongoing basis. Due to the organization of accommodation and breaks between the shifts, this option is more suitable than planning several night shifts. Due to the constant shifts, night shifts are inappropriate. If the shift ends at 6:00, for example, accommodation would have to be paid for two days and the costs would double. In exceptional cases, it is possible to insert a night shift if the crew stays in the same location for several days. If the night shifts are not planned for the whole week, it is advisable to include them at the end of the working week in order to observe the rest periods and, at the same time, to make efficient use of the time during the working week. The plan of individual campaigns also needs to be monitored in terms of time.

For the project management, it is important to have an overview of when which vehicle will move in each location. Not only for these purposes, the Gantt chart will be used, which provides a simple weekly overview of ongoing activities. For the needs of the model project, only the length of individual variants of the test campaign is determined, as its beginning is not specified. The project requirement is that the total duration of the test campaign does not exceed twenty weeks. If this limit is exceeded, a fine would be imposed for non-compliance with the agreed deadlines with the customer, which is subsequently included in the decision tree [28].

## 5 Results

The performance of the whole static model of testing and the processing of the obtained data was done within the diploma thesis [27]. The student of the combined form of study worked in an unnamed company, which deals with development of elements of intelligent transport systems and was given the task to process the requirements and testing plan. She worked in the team that implemented the test plan and was able to obtain a relevant amount of data. Based on the entry requirements and the developed plan, she processed the obtained results of individual tests within her diploma thesis.

If only one test vehicle was used for the entire test campaign, this activity would last 54 weeks. In such a case, the set limit would be exceeded more than twice and high fines would be imposed. It can therefore be assumed that this option will not be suitable for the implementation of the campaign. Table 3 contains a Gantt chart of the testing process with one test vehicle.

If the two vehicles are used, the total length of the campaign will be reduced to 27 weeks (Table 4). In this variant, the set limit will also be exceeded, but the difference is not as significant as in the first variant with one vehicle. As the number of vehicles increases, the total number of kilometers travelled by one vehicle decreases, thus reducing the risk of a serious fault.

The variant, in which three test vehicles are available, is reduced to a total length of 19 weeks. This is the first option in which the set limit is observed without the need to pay a fine for non-compliance with the agreed deadline for submission of the project. If exceeding the limit would mean the final unsuccessful completion of the project, there would be a minimum number of three vehicles with which this deadline can be met. The total length of the test campaign was reduced by eight weeks (Table 5). Saving eight weeks can have a major impact on the overall progress of the project and can be a key factor leading to the final successful completion of the project.

Using four test vehicles would only use sixteen weeks out of a total limit of twenty weeks per test campaign. The four-week reserve is relatively large and would probably not be used. It would be possible to shorten the total time, but in this case, there would be long inefficient vehicle crossings, which is not necessary in this case due to not using the entire set time for the test campaign. The total inefficient time spent in the service is again six weeks. Therefore, adding another

***Table 3*** *Gantt chart for one test vehicle (TV 1), [27])*

| Week | 1 | 2 | 3 | 4 | 5 | 6 | 7 | 8 | 9 | 10 | 11 | 12 | 13 | 14 |
|---|---|---|---|---|---|---|---|---|---|---|---|---|---|---|
| TV 1 | | | CZ | | | H | service | | | H | | | DK | service |
| Week | 15 | 16 | 17 | 18 | 19 | 20 | 21 | 22 | 23 | 24 | 25 | 26 | 27 | 28 |
| TV 1 | | DK | | | D | | service | | | | D | | | service |
| Week | 29 | 30 | 31 | 32 | 33 | 34 | 35 | 36 | 37 | 38 | 39 | 40 | 41 | 42 |
| TV 1 | | | F | | | BE | service | | | BE | | | GB | service |
| Week | 43 | 44 | 45 | 46 | 47 | 48 | 49 | 50 | 51 | 52 | 53 | 54 | | |
| TV 1 | | | | GB | | | service | | | GB | | | | |

Note: CZ - Czech Republic, H - Hungary, DK - Denmark, D - Germany, F - France, BE - Belgium, GB - Great Britain

***Table 4*** *Gantt chart for two vehicles, [27])*

| Week | 1 | 2 | 3 | 4 | 5 | 6 | 7 | 8 | 9 | 10 | 11 | 12 | 13 | 14 |
|---|---|---|---|---|---|---|---|---|---|---|---|---|---|---|
| TV 1 | | | F | | | BE | service | | | BE | | | GB | service |
| TV 2 | | | CZ | | | H | service | | | H | | | D | service |
| Week | 15 | 16 | 17 | 18 | 19 | 20 | 21 | 22 | 23 | 24 | 25 | 26 | 27 | |
| TV 1 | | | | GB | | | service | | | GB | | | | |
| TV 2 | | | | D | | | service | D | | | DK | | | |

***Table 5*** *Gantt chart for three vehicles, [27])*

| Week | 1 | 2 | 3 | 4 | 5 | 6 | 7 | 8 | 9 | 10 | 11 | 12 | 13 | 14 |
|---|---|---|---|---|---|---|---|---|---|---|---|---|---|---|
| TV 1 | | | CZ | | | BE | service | | | BE | | | GB | service |
| TV 2 | | | H | | | F | service | | | F | | | GB | service |
| TV 3 | | | DK | | | D | service | | | | D | | | service |
| Week | 15 | 16 | 17 | 18 | 19 | | | | | | | | | |
| TV 1 | | | GB | | | | | | | | | | | |
| TV 2 | | GB | | | | | | | | | | | | |
| TV 3 | D | | | | | | | | | | | | | |

***Table 6*** *Gantt chart for four vehicles, [27])*

| Week | 1 | 2 | 3 | 4 | 5 | 6 | 7 | 8 | 9 | 10 | 11 | 12 | 13 | 14 |
|---|---|---|---|---|---|---|---|---|---|---|---|---|---|---|
| TV 1 | | | | GB | | | service | | | GB | | | | service |
| TV 2 | | | | D | | | service | | D | | | DK | | service |
| TV 3 | | | BE | | | F | service | | | F | | | | |
| TV 4 | | | CZ | | | H | service | | | H | | | | |
| Week | 15 | 16 | | | | | | | | | | | | |
| TV 1 | GB | | | | | | | | | | | | | |
| TV 2 | | DK | | | | | | | | | | | | |
| TV 3 | | | | | | | | | | | | | | |
| TV 4 | | | | | | | | | | | | | | |

***Table 7*** *Gantt chart for eight vehicles, [27])*

| Week | 1 | 2 | 3 | 4 | 5 | 6 |
|---|---|---|---|---|---|---|
| TV 1 | | | CZ | | | |
| TV 2 | | | H | | | |
| TV 3 | | | | D | | |
| TV 4 | | D | | | F | |
| TV 5 | D | | | DK | | |
| TV 6 | | | BE | | | F |
| TV 7 | | | | GB | | |
| TV 8 | | | | GB | | |

vehicle does not result in the more efficient use of vehicles (Table 6).

Another variant is set at eight vehicles (Table 7). In this variant, there is no need to service the vehicles during the campaign and therefore the time is used most efficiently. The entire test campaign could be implemented in just six weeks, which is the same time that the vehicles spent in service on the previous three variants. In this variant, there are also minor changes in the composition of countries. It is not a condition that one vehicle records a single area, so it is possible to combine individual countries. Two vehicles can be allocated to the UK to speed up the test campaign. The route to be loaded will then be split between the two vehicles, so the vehicles do not have to travel together. In a shorter time, they will be able to cover most of the required route.

Each vehicle is associated with the costs of its purchase, purchase of test equipment and subsequent installation. Specific prices are very sensitive information for all the companies. Therefore, the prices were converted to the number of units. Factors such as the price of the data upload itself, the price of the test car and its equipment, the price of the vehicle service and the possible amount of the fine in the case of non-compliance with the set deadline are included in the price calculation. Detailed calculations and characteristics of individual items for individual testing variants are given in [27].

## 6 Discussion

The performance of the whole static model of testing and processing of the obtained data was done in [27]. The student of the combined form of study works in an unnamed company, which deals with the development of elements of intelligent transport systems and was given the task to process the requirements and testing plan. She worked in the team that implemented the test plan and was able to obtain a relevant amount of data. Based on the entry requirements and the developed plan, she processed the obtained results of individual tests. Based on those results, a decision tree was compiled.

The final tool for deciding on the number of vehicles to be used for the model project test campaign is the decision tree. The decision tree (Figure 1) takes into account different variants and compares them to each other in order to minimize the costs [28-30]. The options that can ultimately be chosen are the choice of one, two, three, four or eight test vehicles. Based on this decision, it is also necessary to adapt the specific plan for each shift and to ensure sufficient human resources to carry out this campaign, as well.

Based on the decision tree, it is necessary to decide how many test vehicles will be used for the test campaign. It is possible to choose from variants 1, 2, 3, 4 and 8 vehicles. The number of service operations is determined based on the interval in the Gantt chart for each variant. Seven service tasks are required for

one vehicle; for a variant of 2 to 4 vehicles it is six service operations. In the case of eight vehicles, there is no need to interrupt the test campaign due to the necessary service and all maintenance on the vehicles can be carried out after the end of the test campaign at the expense of another project, if the vehicles continue to be used.

If the service intervals are not observed, there is a risk of more serious breakdowns on the vehicle and the consequent higher costs of servicing. It is assumed that the time saved by neglecting regular service would subsequently have to be used to carry out emergency service during the campaign, so the overall length of the campaign is unlikely to change. If the time limit of 20 weeks is exceeded, there is a fine for not meeting the deadline. The number of weeks for the one-vehicle variant is 54, for two vehicles it is 24 weeks, for three vehicles 19 weeks, for four vehicles 16 weeks and for eight vehicles only 6 weeks. There are no penalties or benefits for the earlier termination of the project.

The evaluation of the decision tree in individual nodes is as follows:

1) Step 1 - testing or termination (7-16): 3 900 < 22 500
2) Step 2 - with service or without service (2 - 6):
   a) (3 900 + 420 = 4 320) < (3 900 + 450 = 4 350)
   b) (3 900 + 360 = 4 260) < (3 900 + 900 = 4 800)
   c) (3 900 + 360 = 4 260) < (3 900 + 1350 = 5 250)
   d) (3 900 + 360 = 4 260) < (3 900 + 1800 = 5 700)
   e) (3 900 + 0 = 3 900) = (3 900 + 0 = 3 900)
3) Step 3 - number of testing vehicles:
   a) 4 320 + 4 500 + 35 700 = 44 520
   b) 4 260 + 9 000 + 7 350 = 20 610
   c) 4 260 + 13 500 + 0 = 17 760
   d) 4 260 + 18 000 + 0 = 22 260
   e) 3 900 + 36 000 + 0 = 39 900
   f)

Based on evaluation of the decision tree and taking into account all the risks, the optimal number of vehicles was determined to be three. In this variant, the time set for the completion of the test campaign is sufficiently used and at the same time it is possible to coordinate the operation of all three vehicles without major difficulties [31-32].

Based on the result, it can be noted that it is more advantageous to adhere to regular service intervals of vehicles, so as not to cause more serious failures, the repair of which would be many times higher. Although the service life of the test vehicle is around five years, it

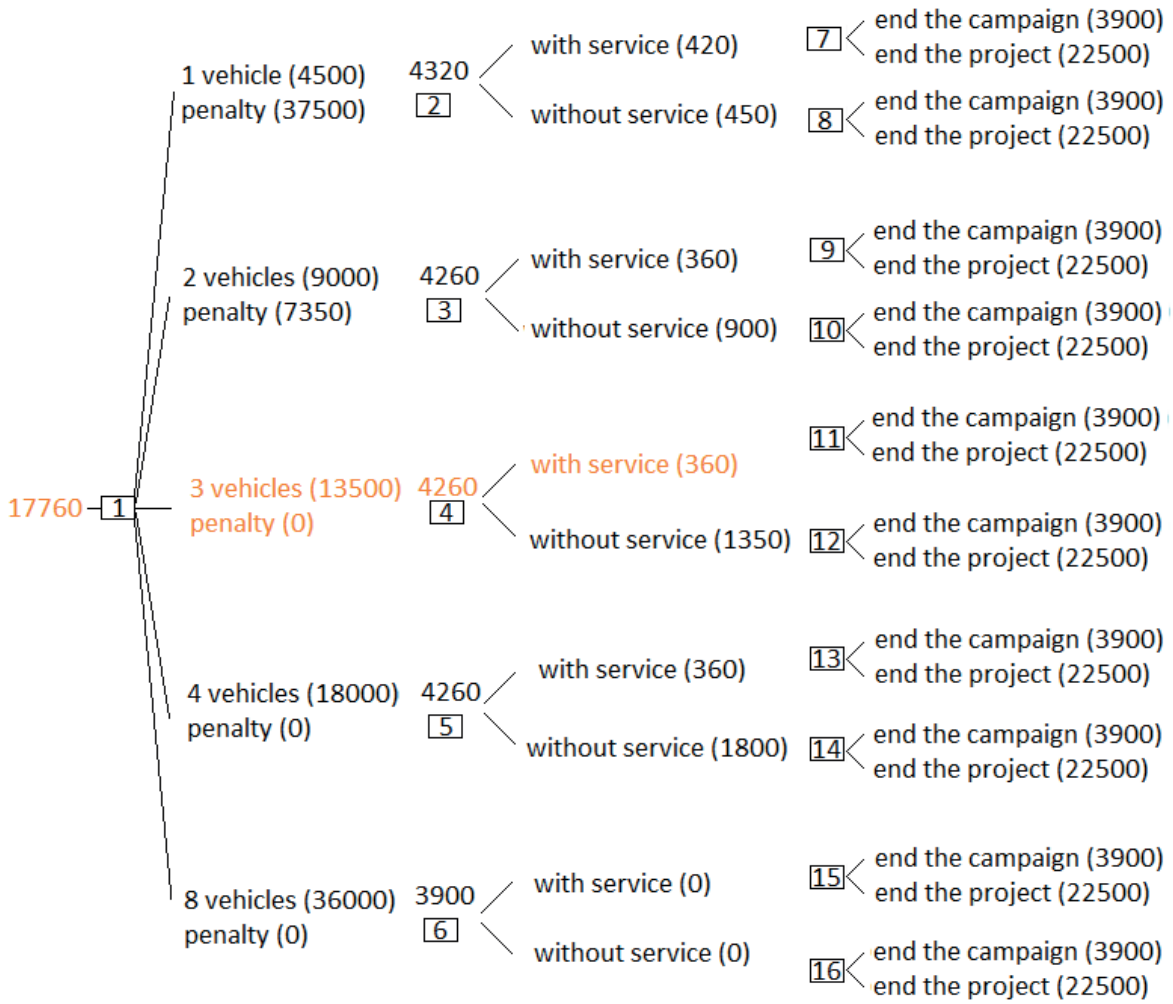


***Figure 1*** *Resulting decision tree, [27])*

is very undesirable to encounter an unexpected vehicle failure during the test campaign. Risks arising from unplanned repairs are, for example, insufficient service capacity or unavailability of spare parts. Those risks can jeopardize the entire course of the test campaign and thus the entire project.

At the same time, it was also found that in the case of this model project, the fines for exceeding the set deadline are so high that it pays to invest in the acquisition of more test vehicles and thus meet the deadline. For another project, however, it could be the other way around. This decision depends on the amount of the fine for non-compliance with the deadline and price of the vehicle and its equipment, so it is necessary to find out at the beginning of the project what factors could affect the final result and what the impact could be on the whole project.

The three-vehicle test campaign will last 19 weeks and will require a total of 6 test crew members. The total costs of the test campaign are 17760 units. The variant of one vehicle was in the total amount of 44520 units, and it is therefore the most expensive variant. By increasing the number of vehicles to three, the total costs were reduced by 60 %.

During this campaign, each of the vehicles will undergo a total of two regular services, which will ensure a sufficient service life of the vehicle throughout the test campaign. After the end of the test campaign, the vehicles can be used on another project, or as obstacles to testing functions on the test site. Vehicles that have been modified and equipped with test technology must not be returned to normal operation. If no other activity is found for the vehicle, it will have to be eliminated. The test equipment can also be used on other vehicles.

## 7 Conclusions

Intelligent transport systems help the driver to control the vehicle and their main task is to increase the road safety and driving comfort. Examples of these functions are parking assistant, traffic congestion assistant and automatic emergency braking. Those functions are usually based on sensors that collect information about the environment and then take control or warn of possible obstacles. In the automotive field, laser and ultrasonic sensors, cameras and radars, or combinations thereof, are used for this purpose. The combination of multiple sensors ensures greater reliability of functions. If one of the sensors does not have sufficiently accurate data about the vehicle's environment, the other sensor can replace it, or they compare the information collected from the environment and evaluate the whole situation together.

The development of these systems is very time and money consuming and consists of several parts. After the development itself, the testing phase begins. The data that is uploaded as a part of the test campaign is then analyzed and the results are passed to the customer to verify the reliability and proper functioning of the system.

The article deals with creation of a plan for the final verification of the functionality of intelligent transport systems, taking into account the minimization of time for vehicle testing and minimization of testing costs. After creating five proposed variants, one variant was selected based on the decision tree. Using this option, the test campaign will be completed within the set time limit. This limit is twenty weeks of uploading and the three-vehicle variant will cover the entire test campaign in as little as nineteen weeks. The test campaign will take place in the United Kingdom, Germany, France, the Czech Republic, Hungary, Denmark and Belgium. It is estimated that over 100,000 km will be recorded during this campaign, divided into different road conditions and lighting conditions.

The solution that was originally expected to be the most economical was to use a less than optimal number of vehicles. It would be necessary to pay a fine for not meeting the agreed deadline, but the total costs could still be lower. This assumption was not confirmed and despite the high purchase price of the test vehicle and other equipment, the three-vehicle variant was less costly. From the customer's point of view, meeting the deadline is also a sign of reliability.

In conclusion, the authors state that the aim of this article has been achieved. The case study, which is part of the article, provided an insight into the issue of creating a plan for testing elements of intelligent transport systems so that it brings relevant data for the customer. This data also serves the customer as a basis for declaring the functionality and reliability of its components. In the final evaluation of the achieved results, the authors state that the overall results of reliability and functionality testing limit two basic factors - the total costs of the test room and the time required to perform a sufficient number of tests. It is very difficult to optimize the total costs of testing while maintaining the required time range. A possible further goal of the research could be the study and design of a more exact testing methodology, which would bring a sufficient amount of relevant data needed to state the reliability, namely the system unreliability.

## Acknowledgment

Contribution has been prepared based on the grant: Ministry of education, youth and sports of the Czech Republic 04SVV22 - Research of the influence of road height profile on fuel consumption during vehicle acceleration.

**References:**


[1] COLLELA SHAOUT, D., AWAD, S. Advanced driver assistance systems - past, present and future. In: 7th International Computer Engineering Conference ICENCO' 2011: proceedings [online]. IEEE. 2011. ISBN 978-1-4673-0730-7, eISBN 978-1-4673-0731-4, p. 72-82. Available from: https://doi.org/10.1109/ICENCO.2011.6153935

[2] CABAN, J., RYBICKA, I. The use of a plate conveyor for transporting aluminum cans in the food industry. *Advances in Science and Technology Research Journal* [online]. 2020, **14**(1), p. 26-31. ISSN 2299-8624. Available from: https://doi.org/10.12913/22998624/113283

[3] CATALAO, F. P., CRUZ, C. O., SARMENTO, J. M. The entanglement of time and cost deviations in public projects. *Annals of Public and Cooperative Economics* [online]. 2021, early view. eISSN 1467-8292. Available from: https://doi.org/10.1111/apce.12364

[4] BORRAZ, R., NAVARRO, P. J., FERNANDEZ, C., ALCOVER, P. M. Cloud incubator car: a reliable platform for autonomous driving. *Applied Sciences-Basel* [online]. 2018, **8**(2), 303. eISSN 2076-3417. Available from: https://doi.org/10.3390/app8020303

[5] MARTINEZ, C., JIMENEZ, F. Implementation of a potential field-based decision-making algorithm on autonomous vehicles for driving in complex environments. *Sensors* [online]. 2019, **19**(15), 3318. eISSN 1424-8220. Available from: https://doi.org/10.3390/s19153318

[6] TIAN, Y. L., DU, Y. B., ZHANG, Q. S., CHENG, J., YANG, Z. Depth estimation for advancing intelligent transport systems based on self-improving pyramid stereo network. *IET Intelligent Transport Systems* [online]. 2020, **14**(5), p. 338-345. eISSN 1751-9578. Available from: https://doi.org/10.1049/iet-its.2019.0462

[7] FOUCHAL, H., WILHELM, G., BOURDY, E., WILHELM, G., AYAIDA, M. A testing framework for intelligent transport systems. 2016 In: IEEE Symposium on Computers and Communication ISCC: proceedings [online]. 2016. ISBN 978-1-5090-0680-9, eISBN 978-1-5090-0679-3, p. 180-184. Available from: https://doi.org/10.1109/ISCC.2016.7543736

[8] ARAMRATTANA, M., ANDERSSON, A., REICHENBERG, F., MELLEGARD, N., BURDEN, H. Testing cooperative intelligent transport systems in distributed simulators. *Transportation Research Part F - Traffic Psychology and Behaviour* [online]. 2019, **65**, p. 206-216. ISSN 1369-8478. Available from: https://doi.org/10.1016/j.trf.2019.07.020

[9] ARAMRATTANA, M., LARSSON, T., JANSSON, J., NABO, A. A simulation framework for cooperative intelligent transport systems testing and evaluation. *Transportation Research Part F - Traffic Psychology and Behaviour* [online]. 2019, **61**, p. 268-280. ISSN 1369-8478. Available from: https://doi.org/10.1016/j.trf.2017.08.004

[10] MARE, R. M., MARTE, C. L., CUGNASCA, C. E., GOGLIANO-SOBRINHO, O., DOS SANTOS, A. S. Feasibility of a testing methodology for visible light communication systems applied to intelligent transport systems. *IEEE Latin America Transactions* [online]. 2021, **19**(3), p. 515-523. eISSN 1548-0992. Available from: https://doi.org/10.1109/TLA.2021.9447702

[11] VERHOEFF, L., VERBURG, D. J., LUPKER, H. A., KUSTERS, L. J. J. VEHIL: A full-scale test methodology for intelligent transport systems, vehicles and subsystems. In: IEEE Intelligent Vehicles Symposium 2000: proceedings [online]. 2000. eISBN 0-7803-6363-9, p. 369-375. Available from: https://doi.org/10.1109/IVS.2000.898371

[12] WOO, J. W., YU, S. B., LEE, S. B. Design and simulation of a vehicle test bed based on intelligent transport systems. *International Journal of Automotive Technology* [online]. 2016, **17**(2), p. 353-359. ISSN 1229-9138, eISSN 1976-3832. Available from: https://doi.org/10.1007/s12239-016-0036-7

[13] REGAN, M. A., RICHARDSON, J. H. Planning and implementing field operational tests of intelligent transport systems: a checklist derived from the EC FESTA project. *IET Intelligent Transport Systems*. 2009, **3**(2), p. 168-184. eISSN 1751-9578.

[14] YOUNG, K. L., REGAN, M. A., TRIGGS, T. J., STEPHAN, K., MITSOPOULOS-RUBENS, E., TOMASEVIC, N. Field operational test of a seatbelt reminder system: effects on driver behaviour and acceptance. *Transportation Research Part F - Traffic Psychology and Behaviour*. 2008, **11**(6), p. 434-444. ISSN 1369-8478.

[15] BRUMERCIK, F., LUKAC, M., CABAN, J., KRZYSIAK, Z., GLOWACZ, A. Comparison of selected parameters of a planetary gearbox with involute and convex-concave teeth flank profiles. *Applied Sciences* [online]. 2020, **10**, 1417. eISSN 2076-3417. Available from: https://doi.org/10.3390/app10041417

[16] MYERS, G. J., SANDLER, C., BADGETT, T. *The art of software testing*. 3. ed. Hoboken: John Wiley, 2012. ISBN 978-1-118-13313-2.

[17] ARUMUGAM, A. K. Software testing techniques and new trends, *International Journal of Engineering Research and Technology (IJERT)* [online]. 2019, **8**(12), p. 708-713. eISSN 2278-0181. Available from: https://doi.org/10.17577/IJERTV8IS120318

[18] ZELINKA, B. Software testing. Unicorn Systems [online] [accessed 2021-10-27]. 2013. Available from: http://docplayer.cz/30077481-Testovani-softwaru-10-dubna-borek-zelinka.html
[19] ISO 26262-1:2011 Road vehicles - Functional safety - Part 1: Vocabulary. Geneva, Switzerland: International Organization for Standardization, 2018.
[20] ISO/PAS 21448:2019 Road vehicles - Safety of the intended functionality. Geneva, Switzerland: International Organization for Standardization, 2019.
[21] BELLAIRS, R. Why SOTIF (ISO/PAS 21448) is key for safety in autonomous driving [online] [accessed 2021-10-30]. 2019. Available from: https://www.perforce.com/blog/qac/sotif-iso-pas-21448-autonomous-driving
[22] STEPHENS, R. *Beginning software engineering*. Indianapolis: John Wiley, 2015. ISBN 978-1-118-96914-4.
[23] WANG, M., THOBEN, K. D. Sustainable urban freight transport: analysis of factors affecting the employment of electric commercial vehicles., In: *Dynamics in Logistics* [online]. FREITAG, M., KOTZAB, H., PANNEK, J. (eds.). 2017. p. 255-265. Cham: Springer, 2017. ISBN 978-3-319-45116-9, eISBN 978-3-319-45117-6. Available from: https://doi.org/10.1007/978-3-319-45117-6_23
[24] MALEK, A., CABAN, J., SARKAN, B. Research on low-emission vehicle powered by LPG using innovative hardware and software. *The Archives of Automotive Engineering - Archiwum Motoryzacji* [online]. 2020, **89**(3), p. 19-36. eISSN 2084-476X. Available from: https://doi.org/10.14669/AM.VOL89.ART2
[25] OSTROWSKA, I., ROSA, G., SLUPINSKA, K., GRACZ, L. The impact of written correspondence on building customer relationship. In: 36th International Scientific Conference on Economic and Social Development ESD 2018: proceedings. 2018. p. 454-463.
[26] BETKIER, I., ZAK, J. K., MITKOW, S. Parking lots assignment algorithm for vehicles requiring specific parking conditions in vehicle routing problem. *IEEE Access* [online]. 2021, **9**, p. 161469-161487. eISSN 2169-3536. Available from: https://doi.org/10.1109/ACCESS.2021.3131480
[27] KNOBOVA, V. Design of an optimized intelligent transport systems functionality testing plan [online] [accessed 2022-02-24]. 2021. Available from: https://is.vstecb.cz/th/hicvl/
[28] BARTA, D., GALLIKOVA, J., CABAN, J. Maintenance system of semi-trailer and risk priority number. *The Archives of Automotive Engineering - Archiwum Motoryzacji* [online]. 2019, **86**(4), p. 101-109. eISSN 2084-476X. Available from: https://doi.org/10.14669/AM.VOL86.ART7
[29] HITKA, M., ZAVADSKA, Z., JELACIC, D., BALAZOVA, Z. Qualitative indicators of employee satisfaction and their development in a particular period of time. *Drvna Industria* [online]. 2015, **66**(3), p. 235-239. ISSN 0012-6772, eISSN ISSN 1847-1153. Available from: https://doi.org/10.5552/drind.2015.1420
[30] TUDORICA, A., BANACU, C. S., COLESCA, S. E. Literature review regarding the application of multi-criteria analysis in transport infrastructure projects. *Management Research and Practice*. 2021, **13**(2), p. 36-59. ISSN 2067-2462.
[31] BRUMERCIKOVA, E., BUKOVA, B., NEDELIAKOVA, E. A proposal for the account-based ticketing application in passenger transport in the Slovak Republic: a case study. *Sustainability* [online]. 2020, **12**(14), 5491. eISSN 2071-1050. Available from: https://doi.org/10.3390/su12145491
[32] FEDORKO, G., MOLNAR, V., STROHMANDL, J., VASIL, M. Development of simulation model for light-controlled road junction in the program technomatix plant simulation. In: International Conference Transport Means 2015: proceeding. Vol. 169. 2015. p. 466-499.

# FEASIBILITY STUDY OF TSUNAMI EVACUATION ROUTES BASED ON ROAD PERFORMANCE USING THE INDONESIAN HIGHWAY CAPACITY MANUAL

Cut Mutiawati, Fitrika Mita Suryani*, Muhammad Isya, Lulusi, Renni Anggraini, Vimia Nabila Putri, Riky Rivinaldi

Civil Engineering, Syiah Kuala University, Banda Aceh, Indonesia

*E-mail of corresponding author: fitrika_mitasuryani@unsyiah.ac.id

***Resume***

Earthquake and tsunami preparedness is important to plan, especially in the earthquake and tsunami-prone areas, such as Banda Aceh. This study evaluates the tsunami evacuation routes' performance using the width of the road, travel time and the Degree of Saturation (DS) parameter. Some of the Degree of Saturation (DS) of the road segment surprisingly reach 1.0 to 3.18, exceeding the recommended 0.75 standard DS ratio. That indicates that the existing roads cannot accommodate traffic flow during evacuation. This study recommends the evacuation process by walking. Thus, developing the pedestrian routes according to evacuation safety requirements is strongly encouraged. Further, more escape buildings reachable within 15 minutes of evacuation time should be planned in the area. The pedestrian routes need to be designed separately from that of the traffic flow.

***Article info***

Received 13 April 2022
Accepted 4 October 2022
Online xx

***Keywords:***

evacuation route performance
travel time
degree of saturation

Available online: https://doi.org/10.26552/com.C.2022.4.F109-F119

ISSN 1335-4205 (print version)
ISSN 2585-7878 (online version)

## 1 Introduction

Geographically, Aceh is prone to earthquake and tsunami disasters as it lies at the confluence of the two tectonic plates that can affect the earthquake and tsunami. The earthquake and tsunami on 26 December 2004 in the western seas of Sumatra Island near the island of Simeuleu were in Aceh. This earthquake triggered a tsunami killing more than 225,000 people in 11 countries and causing devastating destruction in many coastal areas [1]. One of the areas badly hit by the earthquake and tsunami is the Kuta Raja Sub-district in Banda Aceh. In 2012, another earthquake occurred, but without a tsunami. Yet, it caused traffic congestion in many places. Helderop and Grubesic [2] explored the implications of network disturbance in their study to provide vulnerability analysis and emergency response in the event of an exacerbation of an alternative network that maintains important information in the network.

To reduce the possible victims in an earthquake in any city or region, it would be necessary to assess the performance of the transportation network in response to demands to provide relief to travelers following an earthquake. One of the issues, mostly faced by cities worldwide, is natural disasters [3-4]. Most new technologies allow users to select the best route depending on numerous factors, including road length, grade and speed [5]. Travel time during crises, such as earthquakes and tsunamis, is an important factor. Recker et al. [6] stated that the sudden demand on the network, with the aim of uncertain travel, especially in times of crisis, is also a matter of considering the travel time reliability.

Some research on evacuation routes has been conducted [7], performing real-time shortest path prediction, excluding route blockage by fire. Meanwhile, the duration of river flooding was researched by Takahashi, Nakagawa and Higashiyama [8] and Inoue, Nakatani and Yabe [9]. Sakata, Hirano and Arikawa [10] focused on selecting the shortest path of each route that will not be traversed by the refugees caught in the anticipated tsunami. Optimization of the ant colony, modeling the natural food gathering behavior of ants, can search the shortest path in the shortest time, considering the absence of route blockages [11-12].

Understanding and institutionalizing the seamless link between critical urban infrastructure and disaster management have helped the developed world to establish

effective disaster management processes. However, this link is conspicuously missing in developing countries, where disaster management has been more reactive than proactive [13]. Indonesia is one of the developing countries prone to disasters, such to earthquakes and tsunamis. Communities urgently need disaster mitigation efforts to minimize casualties and damage in the event of a tsunami. Planning should pay attention to the evacuation flows to avoid congestion to speed up the evacuation process. This research aimed to conduct a study on tsunami evacuation routes, including identifying the locations suitable as the evacuation sites when a tsunami occurs, as well as the road sections feasible for evacuation routes in the event of a tsunami based on the width of the road, velocity and degree of saturation (V/C).

The walking velocity of a group of elderly people is 0.751 m/sec, the slowest speed that can reach the evacuee speed. It is assumed that if they can reach the evacuation destination, other evacuees moving faster can also reach the evacuation shelter.

The widening of roads in urban areas with high densities needs to be done to facilitate evacuation [14]. In addition to road widening, there is a need for building new roads from urban areas with a high density to safe places. Those roads are corridor roads from downtown that can reduce congestion points at the intersection of roads due to the grid-shaped road network pattern and overcapacity.

The width of the road for evacuation depends on the road types, such as primary arterial road (minimum road width of 10 meters); secondary artery road (minimum road width of 8 meters), secondary collector road (minimum road width of 8 meters), secondary local road (minimum road width of 4 meters) and neighborhood road (minimum road width of 4 meters) [15].

The following are the evacuation route planning requirement [16]:

1) The 6 m standard road width is allowed to 4 m when a smaller capacity is required
2) The river stream is one of the disaster-prone areas.
3) Transportation system identification is based on the field observation, so the road used to evacuate can be determined and wide enough to accommodate refugees.
4) The building is the shortest and the nearest to the shelter. The route chosen must be the shortest to the safe area. In addition, the route chosen should not have many intersections. Most evacuation traffic delays occur at the intersection [17- 18].

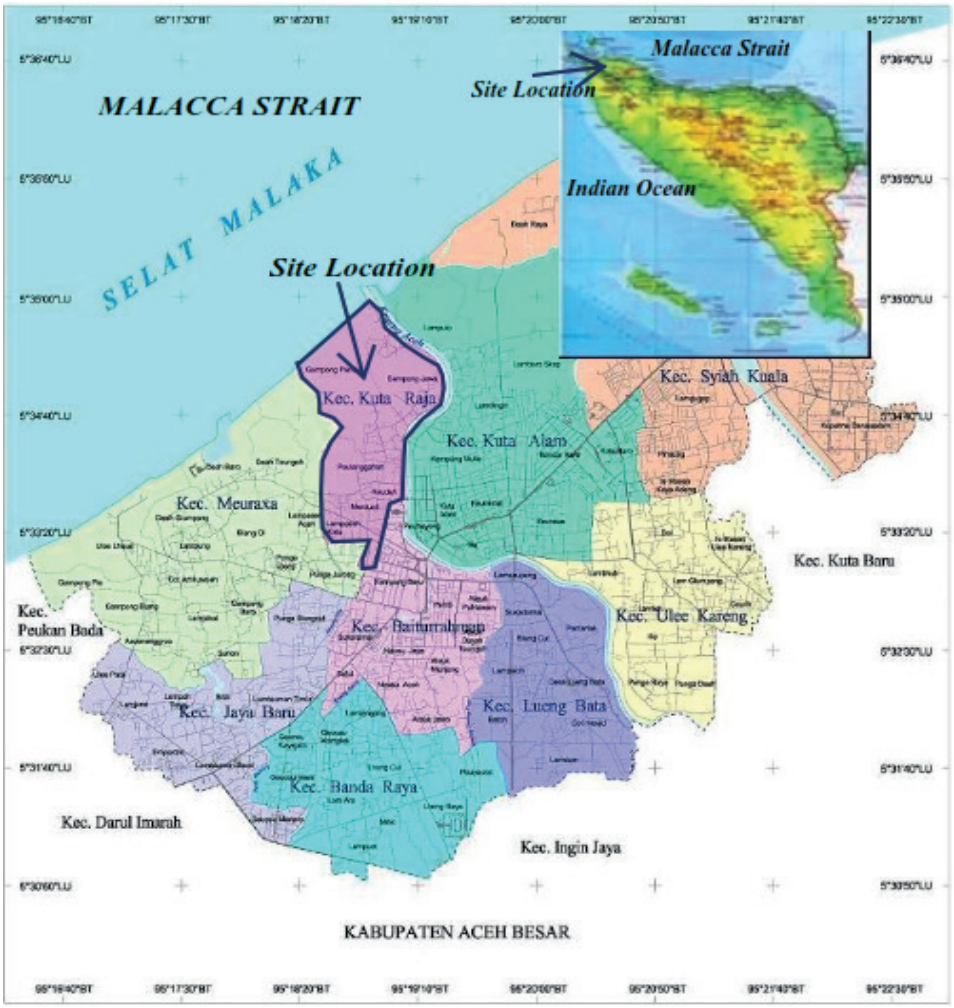


***Figure 1*** *Research Location*

***Table 1*** *The number of research samples*

| Name of Village | Number of Households | Number of Samples |
|---|---|---|
| 1. Gampong Jawa | 557 | 55 |
| 2. Gampong Pande | 199 | 20 |
| 3. Gampong Pelanggahan | 639 | 63 |
| 4. Gampong Keudah | 433 | 43 |
| 5. Gampong Merduati | 923 | 90 |
| 6. Gampong Lampaseh Kota | 548 | 54 |
| 7. Gampong Alue Deah Teungoh | 389 | 38 |
| 8. Gampong Lampaseh Aceh | 585 | 57 |
| 9. Gampong Deah Baro | 197 | 20 |
| 10. Gampong Deah Glumpang | 258 | 38 |
| Total sample | 4.728 | 478 |

The human response capability depends on the estimated time of arrival (ETA) of a tsunami, the time at which technical or natural warning signs (ToNW), determined by Institutional Decision Time (IDT) and Notification Time INT, can be received by the population), the Reaction Time (RT) of the population and the Evacuation Time (ET). The actual available Response Time (RsT) is then obtained by Post et al. [19].

Indonesia Tsunami Early Warning System (Ina-TEWS), as cited by Muhajir [20], the tsunami period following the earthquake is 43 minutes, with 8 minutes for institutional decision and notification, 10 minutes for community reaction, 17 minutes for travel time to reach safe evacuation point and 8 minutes to the higher floor (vertical evacuation). Therefore, evaluation of road performance as an evacuation route is crucial. This evaluation is useful for people's safety when earthquakes and tsunamis re-occur.

An indicator of the road performance in the Indonesian Highway Capacity Manual (IHCM) is the Degree of Saturation (DS). It is the value ratio between the traffic volume and the capacity of the road in units (pcu/h) [21]. Interaction with pedestrians is one of the main factors determining the road performance [22]. IHCM accommodates the pedestrian factor as side friction that will reduce the puck road performance.

## 2 Research methods

### 2.1 Location

The research is located in Kuta Raja Sub-district, Banda Aceh City, consisting of six villages, i.e. Gampong Jawa, Gampong Pande, Gampong Peulanggahan, Gampong Merduati, Gampong Keudah and Gampong Lampaseh Kota. This Sub-district is directly adjacent to the sea in the North. It is also located in the red zone of the tsunami (dangerous) with severe impacts during the 2004 tsunami [23]. The map of the research location can be seen in Figure 1. The borders of the Kuta Raja Sub-district are as follows [24-25]: - North: Malacca Strait

- South: Baiturrahman Sub-district
- West: Meuraxa Sub-district
- East: Kuta Alam Sub-district

### 2.2 Research samples

The data on the transport modes used for evacuation, the point of origin and the destination of evacuation were obtained by distributing questionnaires to the respondents (n = 478), the people in each village in the Kuta Raja sub-district. In addition, four villages in the District Meuraxa conduct evacuation through the Kuta raja sub-district. The number of respondents in each village is divided proportionally based on the number of households [25]. Table 1 presents the number of samples in each village and Figure 2 shows the flow chart of the research.

### 2.3 Data collection and processing

This research required data on the mode of transport used for evacuation, vehicle ownership, the number of households, the point of origin and destination of evacuation (safe points for evacuation purposes), the distance used to calculate evacuation time, the width of roads as the evacuation routes and the number of residents and buildings eligible for evacuation. The data of transport mode, population, vehicle ownership, origin and destination were required to predict the number of evacuation flows. Those data were obtained through questionnaires. Distance and road width was obtained by measuring the distance needed to calculate the evacuation time, while the width of the road was used to calculate the capacity of the evacuation route. Population data were used to obtain the city size adjustment factor (FCcs) to calculate the road capacity.

The data analysis steps are as follows:

1. Identifying the safe locations for tsunami evacuation

***Table 2*** *Average Speed Evacuation, [29]*

| Walking Condition | Average Speed, m/s |
|---|---|
| - A Person pushing a perambulator | 1.070 |
| - A person with a child | 1.020 |
| - Independent walking elderly person | 0.948 |
| - A group of walking elderly people | 0.751 |

***Table 3*** *Street transport Quality Index*

| Route performance | DS = V/C ratio | Index |
|---|---|---|
| Very favorable | < 0.350 | A |
| Favorable | 0.350 - 0.500 | B |
| Fairly favorable | 0.500 - 0.750 | C |
| Unfavorable | 0.750 - 0.900 | D |
| Very unfavorable | 0.900 - 1.000 | E |
| Obstruction and Congestion | > 1.000 | F |

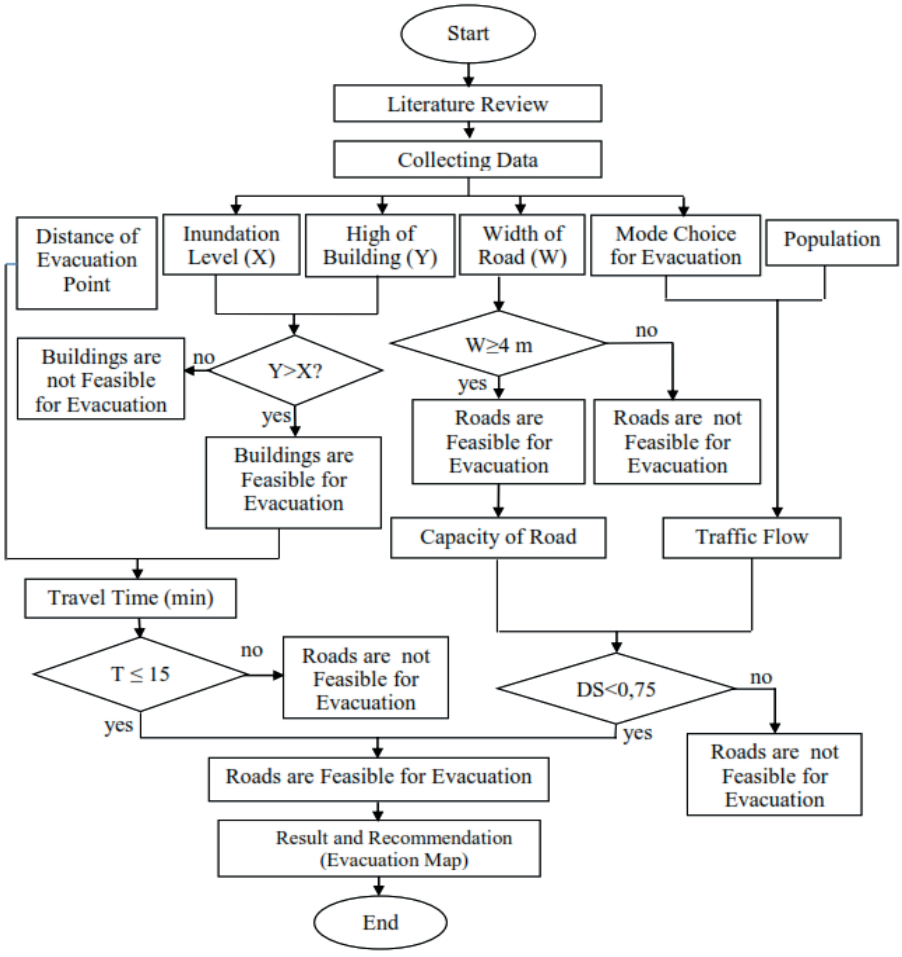


***Figure 2*** *Flow Chart of Research*

(high ground or vertical evacuation) based on the inundation height during the 2004 tsunami. A vertical evacuation from a tsunami is a building or earthen mound with sufficient height to elevate evacuees above the level of tsunami inundation. It is designed and constructed with the strength and resiliency needed to resist the effects of tsunami waves. Buildings for evacuation shelters can be single-purpose, multi-purpose facilities, single-hazard and multi-hazard considerations [26-27].

2. Identifying appropriate roads for evacuation routes based on the road width.
3. Calculating the distance and travel time of each road, assuming the speed was 14 km/h for motor

vehicles and 2.5 km/h for people on foot [28]. The Japan Institute for Fire Safety and Disaster Preparedness overviews the walking condition and average walking speed in disaster evacuation, as shown in Table 2 [29].

4. Calculating evacuation flows (V) on the evacuation route based on the mode of transport used by the community, assuming that all people would evacuate.
5. Calculating the capacity of each road segment. Road capacity (C) is calculated by IHCM:

$$C = Co * FCw * FCsp * FC_{SF} * FC_{CS}, \quad (1)$$

where:

Co = base capacity for the urban road,
FCw = coefficient factor of the road width for capacity,
FCsp = coefficient factor of separator for capacity,
$FC_{SF}$ = coefficient of the factor of side friction for capacity,
$FC_{CS}$ = coefficient factor of city size for capacity.

6. Calculating the performance of the evacuation routes. Indicator of the road performance to the Indonesian Highway Capacity Manual (IHCM) is the Degree of Saturation (DS), the ratio between the volume of traffic (V) and the capacity of a road (C) in passenger car units per hour (pcu/h) or V/C ratio [21]. Assessment of the road performance for evacuation routes in this study uses indicators as shown in Table 3.

## 3 Results and discussion

This study discusses the modes the community uses for evacuation, appropriate evacuation places and the feasibility of evacuation routes based on the road width and travel time road performance.

### 3.1 The transport mode for evacuation

The residents of Kuta Raja Sub-district used four types of vehicles: cars, pedicabs, motorcycles and foot, during the evacuation. The dominant mode of transport, chosen by the community to evacuate, was a motorcycle (72 %), followed by a car (9 %), pedicab (1%) and foot (18 %). Figure 3 illustrates the number of people using each type of transportation.

### 3.2 Safe location for evacuation

The evacuation site for the people of Kuta Raja Sub-district was a one to five-story building, whereas an evacuation site of empty fields and hills was unavailable in this area. The buildings selected for evacuation were government-owned, while private/personal-owned buildings were not used, although they were safe. These safe buildings for evacuation consisted of one to five-story buildings located within or outside Kuta Raja Sub-district. The buildings within Kuta Raja

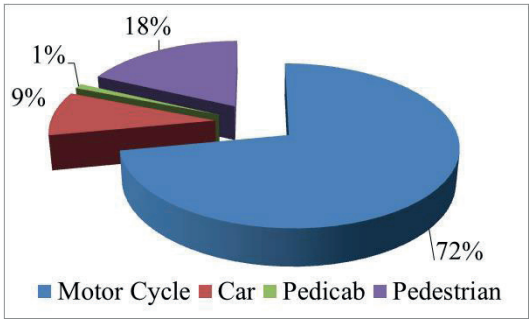


***Figure 3*** *Vehicle choices for evacuation*


***Figure 4*** *(a) Public Elementary School 70 (SD), (b) Public Junior High School 12 (SMP), (c) Public Senior High School 13 (SMA), (d) Tgk. Dianjong Mosque, (e) Low-cost Rental Apartments, (f) Cut Mutia Hospital, (g) Hotel Lading, (h) State Electricity Company, (i) Pasar Aceh Building, (j) Baiturrahman Mosque*

Sub-district were Public Elementary School 70, Public Junior High School 12, Public Senior High School 13, Tgk. Dianjong Mosque and low-cost rental apartments. Meanwhile, the evacuation sites outside the Kuta Raja Sub-district were Cut Mutia Hospital, Hotel Lading, State Electricity Company (PLN), Pasar Aceh building and Baiturrahman Mosque located in Baiturrahman Sub-district. Safe locations for tsunami evacuation for the people of the Kuta Raja Sub-district are illustrated in Figure 4.

The one-story building was the Baiturrahman Great Mosque, which was safe for evacuation during the 2004 tsunami. Two-story (a, b, c, d, h), three-story (f), Four- story (g, i) and five-story (e). The location of the buildings was feasible due to the water height of the 2004 tsunami below the building floor height.

### 3.3 The feasibility of evacuation routes based on the width and travel time

According to SDC [15] the minimum width of the evacuation route for local roads is 4 m, while the evacuation time is 17 minutes of 43 minutes of the total Tsunami evacuation [9]. Meanwhile, the disaster evacuation time in Aceh was only 35 minutes, so the evacuation travel time was also reduced. This study assumed a travel time of 15 minutes, assuming the evacuation speed of 14 km/h for motor vehicles and 2.5 km/h for pedestrians [3]. The feasibility result of the evacuation route based on the travel time revealed that the safe points for evacuation could only be reached by motor vehicles and almost all the routes were not feasible for evacuation on foot. Therefore, the number of evacuation sites in the form of multi-story buildings needs to be added as they are reachable on foot. The safe points for evacuation in each village are as follows.

1) Gampong Jawa
   The people in Gampong Jawa could evacuate to ten evacuation points, with three points located in the Gampong Jawa area and seven points situated outside Gampong Jawa. Based on the travel time of the evacuation route, the people of Gampong Jawa had 12 feasible routes for motor vehicles and two routes for pedestrians. The route for pedestrians was safe because the evacuation points were close, located in Gampong Jawa and a village next to it. It showed that people willing to evacuate on foot are unsafe if they choose a place of evacuation outside the location of the residence because it takes longer.
2) Gampong Pande
   Gampong Pande had ten evacuation points with ten routes for motor vehicles. However, there was no proper evacuation route for pedestrians as the travel time to reach the evacuation point exceeded 15 minutes. Since the Gampong Jawa did not have evacuation buildings, people had to evacuate out of the village, which took > 15 minutes. Gampong Pande evacuation sites, which are safe according to the government, were similar to Gampong Jawa, including Public Elementary School 70, Public Junior High School 12, Public Senior High School 13, Tgk. Dianjong Mosque, low-cost rental apartments (Rusunawa), Cut Mutia Hospital, Hotel Lading, State Electricity Company (PLN) Banda Aceh, Pasar Aceh Building and Baiturrahman Mosque.
3) Gampong Peulanggahan
   Gampong Peulanggahan had seven evacuation points with 11 feasible routes based on the travel time for motor vehicles and two routes for pedestrians. The feasible evacuation points for pedestrians were located in Gampong Peulanggahan. It means that their distance and travel time was shorter compared to other villages.
4) Gampong Keudah
   Gampong Keudah had five evacuation points with eight routes for motor vehicles and no proper route for pedestrians. That was because the evacuation points were located outside the Gampong Keudah, as well.
5) Gampong Lampaseh Kota
   Gampong Lampaseh Kota had two evacuation points with five routes suitable for motor vehicles, but there was no proper route for pedestrians. Both of these evacuation points were located outside the Gampong Lampaseh Kota.
6) Gampong Merduati
   Gampong merduati had four evacuation points with six evacuation routes for motor vehicles and one evacuation route for pedestrians. The proper evacuation points for pedestrians were located in Gampong Merduati, so the travel time was shorter.

### 3.4 Routes feasibility based on the road performance

The calculation of the road capacity, traffic flow and degree of saturation was carried out to obtain the performance of the roads in the evacuation routes. The degree of saturation parameter was used to measure the performance of the road. The road performance calculation in this study assumes a one-way road. During a tsunami emergency, all the roads should be one-way and traffic flow to the red zone should be stopped. Traffic control points should be installed to prevent traffic flow to the red zone and direct it toward the evacuation site. The road feasibility, based on performance, was calculated by the degree of saturation parameter obtained by dividing the vehicle flows by the road capacity, the results are illustrated in Table 5.

1) Capacity of Road

The road capacity calculated was the roads the people went through to the planned evacuation site. The capacity was obtained by multiplying the basic capacity of the road segment (Co) with the Adjustment

factor values due to side frictions (FCsf), the city size adjustment factor (FCcs), the road width adjustment factor (FCw) and the road type adjustment factor (FCsp). This research assumed that the side frictions were very high and the roads type for evacuation were one-way and effective lane widths of 3-4 m. The Road Capacity on the Evacuation route can be seen in Table 4.

2) Degree of Saturation

The evacuation flows of Rama Setia Street and Diponegoro Street are not only from the Kuta Raja Sub-district, but from some villages in Meuraxa Sub-district as well, i.e. Gampong Lampaseh Aceh, Gampong Baro, Gampong Deah Teungoh and Gampong Deah Glumpang. These evacuation flows include motorcycles, cars and pedicabs (tricycles). IHCM considers it pedestrian side friction because it will inhibit the movement of evacuation flows due to low pedestrian speed. Side frictions are not only pedestrians but the parking vehicles and vehicles coming out from the left and right sides, as well. In this study, the side friction is assumed to be very high.

The survey found some roads with no traffic flow because no respondent chose those roads to the evacuation place: Krueng Geudong street segment 1, Raja Siuroe street, Tuanku Raja Keumala street and Panglateh street. Krueng Geudong street segment 1 is located in the swamp area, with no population. Though the Tuanku Raja Keumala street is located in a housing area and can be used to evacuate to Low-cost Rental Apartments, no respondent chose it as an evacuation site. The building is located near the sea, so the people feel unsafe to evacuate to the building. Some people were using the access routes for evacuation, as well.

The results of the road performance calculations, based on the degree of saturation (DS), can be seen in Table 5. The results showed that most of the main roads used for evacuation were very bad because the value was above 0.75 and exceeded 1.0 (Saturated/gridlock/vehicle cannot move). Poorly performing roads were not only arterial and collector roads, but the access roads, as well, such as Tgk. Dianjong street and T. Muda street. Tentara Pelajar street was safe because of the change of the two-way street into one direction when the evacuation widened the road and some communities evacuated to the PLN office (State Electricity Company) on that road. The road performance of Rama Setia street, Cut Mutia street and Diponegoro street was terrible (gridlock), with the DS ratio of the road segment reaching > 1.0 to 3.18. This shows that the roads are at the Service level F [21]. The gridlock increases when the flow is so high and vehicles get very close to each other. The total gridlock occurs when vehicles have to stop or move very slowly [30-31]. Improving the performance of roads can be done by widening some roads that still have space.

The result of DS shows that the existing roads cannot accommodate traffic flow during the evacuation. This study recommends the evacuation process by walking. Thus, developing the pedestrian routes, according to evacuation safety requirements, is strongly encouraged. Further, more escape buildings reachable within 15 minutes of evacuation time should be planned in the area. The pedestrian routes need to be designed separately from that of the traffic flow. Mixed traffic was hazardous in evacuation routes, as it causes accidents between pedestrians and motor vehicles.

According to SDC [15], the minimum width of the evacuation route for local roads is 4 meters. In the mixed traffic, the road capacity is divided by two, resulting in two 2-meter-wide lanes. According to Melkova [32] and

***Table 4*** *Road Capacity*

| Street | Width (m) | Co | FCw | FCsp | FCsf | FCcs | Capacity |
|---|---|---|---|---|---|---|---|
| Jl. Krueng Geudong | 4 | 1,650 | 1.08 | 1.00 | 0.73 | 0.90 | 1,170.77 |
| Jl. Tgk. Dianjong | 5 | 2,900 | 0.56 | 1.00 | 0.73 | 0.90 | 1,344.22 |
| Jl. Pawang Hitam | 5 | 2,900 | 0.56 | 1.00 | 0.73 | 0.90 | 1,344.22 |
| Jl. Hamzah Yunus | 4 | 1,650 | 1.08 | 1.00 | 0.73 | 0.90 | 1,170.77 |
| Jl. Raja Siuroe | 3.5 | 1,650 | 1.00 | 1.00 | 0.73 | 0.90 | 1,084.05 |
| Jl. Bangka | 4 | 1,650 | 1.08 | 1.00 | 0.73 | 0.90 | 1,170.77 |
| Jl. Tuanku Raja Keumala | 5 | 2,900 | 0.56 | 1.00 | 0.73 | 0.90 | 1,344.22 |
| Jl. T. Muda | 5 | 2,900 | 0.56 | 1.00 | 0.73 | 0.90 | 1,344.22 |
| Jl. Cut Mutia | 10 | 4,950 | 0.92 | 1.00 | 0.73 | 0.90 | 2,688.44 |
| Jl. Tgk. Dikandang | 6 | 3,300 | 0.92 | 1.00 | 0.73 | 0.90 | 1,994.65 |
| Jl. Malem Dagang | 5 | 2,900 | 0.56 | 1.00 | 0.73 | 0.90 | 1,344.22 |
| Jl. Kamboja | 4 | 1,650 | 1.08 | 1.00 | 0.73 | 0.90 | 1,170.77 |
| Jl. Tentara Pelajar | 14 | 6,600 | 0,96 | 1.00 | 0.73 | 0.90 | 4,336.20 |
| Jl. Taman Siswa | 5.5 | 2,900 | 0,56 | 1.00 | 0.73 | 0.90 | 1,430.95 |
| Jl. Panglateh | 5 | 2,900 | 0.56 | 1.00 | 0.73 | 0.90 | 1,344.22 |
| Jl. Rama Setia | 7 | 3,300 | 1.00 | 1.00 | 0.73 | 0.90 | 2,168.10 |
| Jl. Diponegoro 1 | 8 | 3,300 | 1.08 | 1.00 | 0.73 | 0.90 | 2,341.55 |
| Jl. Diponegoro 2 | 12 | 4,950 | 0.92 | 1.00 | 0.73 | 0.90 | 3,512.32 |

***Table 5*** *Degree of Saturation for Evacuation Routes*

| Street | Capacity | Capacity (C) | Traffic Flow (Q) | Degree of Saturation |
|---|---|---|---|---|
| | Pcu/h | Pcu/15 min | | Q/C |
| Jl. Kreung Geudong Segmen 1 | 1,170.77 | 292.69 | 0.00 | 0.00 |
| Jl. Kreung Geudong Segmen 2 | 1,170.77 | 292.69 | 65.00 | 0.22 = A |
| Jl. Kreung Geudong Segmen 3 | 1,170.77 | 292.69 | 51.00 | 0.17 = A |
| Jl. Kreung Geudong Segmen 4 | 1,170.77 | 292.69 | 30.85 | 0.11 = A |
| Jl. Tgk. Dianjong Segmen 1 | 1,066.97 | 266.74 | 303.97 | 1.14 = F |
| Jl. Tgk. Dianjong Segmen 2 | 1,066.97 | 266.74 | 351.78 | 1.32 = F |
| Jl. Tgk. Dianjong Segmen 3 | 1,066.97 | 266.74 | 497.63 | 1.87 = F |
| Jl. Tgk. Dianjong Segmen 4 | 1,066.97 | 266.74 | 557.80 | 2.09 = F |
| Jl. Tgk. Dianjong Segmen 5 | 1,066.97 | 266.74 | 667.73 | 2.50 = F |
| Jl. Pawang Hitam | 1,066.97 | 266.74 | 34.15 | 0.13 = A |
| Jl. Hamzah Yunus | 1,170.77 | 292.69 | 20.56 | 0.07 = A |
| Jl. Raja Siuroe | 1,084.05 | 271.01 | 0.00 | 0.00 |
| Jl. Bangka | 1,170.77 | 292.69 | 66.61 | 0.23 = A |
| Jl. Tuanku  Raja Keumala | 1,066.97 | 266.74 | 0.00 | 0.00 |
| Jl. T. Muda Segmen 1 | 1,066.97 | 266.74 | 344.81 | 1.29 = F |
| Jl. T. Muda Segmen 2 | 1,066.97 | 266.74 | 193.96 | 0.73 = C |
| Jl. Cut Mutia Segmen 1 | 2,991.98 | 747.99 | 919.78 | 1.23 = F |
| Jl. Cut Mutia Segmen 2 | 2,991.98 | 747.99 | 758.70 | 1.01 = F |
| Jl. Cut Mutia Segmen 3 | 2,991.98 | 747.99 | 992.15 | 1.33 = F |
| Jl. Tgk. Dikandang Segmen 1 | 1,994.65 | 498.66 | 169.65 | 0.34 = A |
| Jl. Tgk. Dikandang Segmen 2 | 1,994.65 | 498.66 | 238.40 | 0.48 = B |
| Jl. Malem Dagang | 1,066.97 | 266.69 | 225.97 | 0.85 = D |
| Jl. Kamboja | 1,170.77 | 292.69 | 23.47 | 0.08 = A |
| Jl. Tentara Pelajar segmen 1 | 4,162.75 | 1,040.65 | 254.46 | 0.24 = A |
| Jl. Tentara Pelajar segmen 2 | 4,162.75 | 1,040.65 | 501.91 | 0.48 = B |
| Jl. Taman Siswa Segmen 1 | 1,066.97 | 266.69 | 200.20 | 0.75 = D |
| Jl. Taman Siswa Segmen 2 | 1,066.97 | 266.69 | 70.00 | 0.26 = A |
| Jl. Panglateh | 1,066.97 | 266.69 | 0.00 | 0.00 |
| Jl. Rama Setia Segmen 1 | 2,168.10 | 542.03 | 717.60 | 1.32 = F |
| Jl. Rama Setia Segmen 2 | 2,168.10 | 542.03 | 1,480.42 | 2.73 = F |
| Jl. Rama Setia Segmen 3 | 2,168.10 | 542.03 | 1,720.99 | 3.18 = F |
| Jl. Diponegoro Segmen 1 | 2,991.98 | 585.39 | 1,176.72 | 2.01 = F |
| Jl. Diponegoro Segmen 2 | 2,991.98 | 747.99 | 1,409.21 | 1.88 = F |

Kramarova [33], the width of space needed for one person to walk is 0.85 meter, while the comfortable width for two people to walk ranges from 2.0 meters - 2.5 meters. Meanwhile, the 2-meter-wide lane for motorized vehicle mode is only sufficient for motorcycles. One motorbike requires width space of 1.3 meters [10], with details of the motorbike being 0.8 meter wide and 0.25 meter for the free space width on each side. For two motorcycles, it usually takes 2.1 meters. If the large space is available, pedestrian paths should ideally be on both sides of the road to minimize accidents between pedestrians and motorized vehicles due to people crossing the road.

According to Lawalata et al. [34], the width of small passenger vehicles ranges from 1.46 meter - 1.97 meter, excluding free space on both sides of the mode. Thus, cars are not recommended as an evacuation mode due to insufficient road width. In addition, cars tend to cause potential congestion during evacuation. Figure 5 illustrates the evacuation route map at the Kuta Raja Sub-district.

## 4 Conclusions

The research indicates that existing roads are unable to accommodate evacuation flow. Some of the DS ratios of the road segment reach 1.0 to 3.18, exceeding the recommended standard DS ratio value of 0.75. It is dangerous to public safety. Therefore, this study recommends that evacuation using a motorized vehicle should be minimized or avoided. Thus, the pedestrian route needs to be made by the evacuation

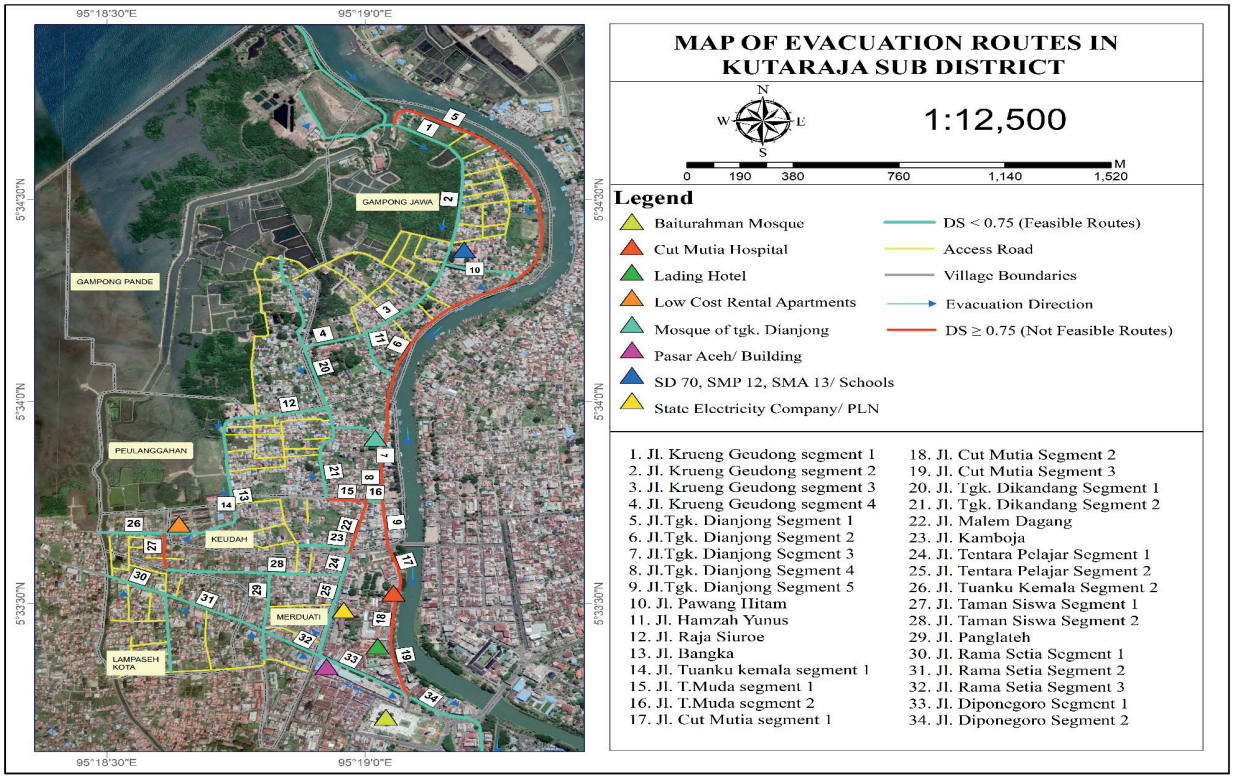


***Figure 5*** *Map of Evacuation Routes in Kuta Raja Sub-district*

safety requirements and the safe evacuation points in the form of buildings (vertical evacuation) need to be added by considering the evacuation travel time of 15 minutes. This pedestrian route also separates the pedestrians flow of evacuation from the motor vehicles' flow, to minimize the accident rate between pedestrians and motor vehicles.

**Acknowledgments**

Authors would like to thank The Ministry of Research, Technology and Higher Education which has funded this research, the surveyors who have helped the data collection and all those who have helped complete this research.

**References**

[1] National plan for disaster management year 2010-2014 - National Board of Disaster Management [online] [accessed 2017-07-21]. Available from: https://www.bnpb.go.id/uploads/renas/1/BUKU%20RENAS%20PB.pdf

[2] HELDEROP, E., GRUBESIC, T. H. Streets, storm surge and the frailty of urban transport systems: a grid-based approach for identifying informal street network connections to facilitate mobility. *Transportation Research Part D: Transport and Environment* [online]. 2016, **77**, p. 337-351. ISSN 1361-9209. Available from: https://doi.org/10.1016/j.trd.2018.12.024

[3] NTZEREMES, P., KIRYTOPOULOS, K. Evaluating the role of risk assessment for road tunnel fire safety: a comparative review within the EU. *Journal of Traffic and Transportation Engineering* [online]. 2019, **6**(3), p. 282-296. ISSN 2095-7564. Available from: https://doi.org/10.1016/j.jtte.2018.10.008

[4] ALMASI, S. A., KHABIRI, M. M., TAFTI, F., AKBARZADEH, M. Optimal route determination to provide relief following an earthquake using the traffic density ratio (case study: Isfahan's fire stations). *Communications - Scientific Letters of the University of Zilina* [online]. 2021, **23**(1), p. 20-32. ISSN 1335-4205, eISSN 2585-7878. Available online: https://doi.org/10.26552/com.C.2021.1.F20-F32

[5] SIUHI, S., MWAKALONGE, J. Opportunities and challenges of smart mobile applications in transportation. *Journal of Traffic and Transportation Engineering* [online]. 2016, **3**(6), p. 582-592. ISSN 2095-7564. Available from: https://doi.org/10.1016/j.jtte.2016.11.001

[6] RECKER, W., CHUNG, Y., CHEN, A., PARK, J., WANG, L., JI, Z., LIU, H., HORROCKS, M., OH, J.-S. Considering risk-taking behavior in travel time reliability. California Partners for Advanced Transit and Highways (PATH). Research report. Berkeley: University of California, 2005. ISSN 1055-1425.

[7] MOCHIO, T., KITAHARA, Y. Application of ant colony optimization technique to real time search of optimal evacuation route after severe earthquake (in Japanese). *Journal of Japan Association for Earthquake Engineering* [online]. 2016, **16**(5), p. 5_93-5_110. eISSN 1884-6246. Available from: https://doi.org/10.5610/jaee.16.5_93
[8] TAKAHASHI, T., NAKAGAWA, H., HIGASHIYAMA, M. Assessment of evacuation system based on the simulation of inundation and action of residents. *Annuals of Disaster Prevention Research Institute, Kyoto University* [online]. 1989, **32**(B-2), p. 757-780. ISSN 0386-412X. Available from: http://hdl.handle.net/2433/72188
[9] INOUE, T., NAKATANI, T., YABE, H. Development of evacuation route search method that considers the temporal changes of inundation area (in Japanese). In: 61st Hokkaido Development Bureau Technological Research Presentation Meeting: proceedings [online]. 2017. Available from: https://thesis.ceri.go.jp/db/files/14081870595b3b137db5df1.pdf
[10] SAKATA, Y., HIRANO, H., ARIKAWA, T. Development of evacuation route selection method depending on the level of tsunami. *Journal of Japan Society of Civil Engineers Ser B2 (Coastal Engineering)* [online]. 2018, **74**(2), p. I_397-I_402. ISSN 1884-2399, eISSN 1883-8944. Available from: https://doi.org/10.2208/kaigan.74.I_397
[11] FORCAEL, E., GONZALEZ, V., OROZCO, F., VARGAS, S., PANTOJA, A., MOSCOSO, P. Ant colony optimization model for tsunamis evacuation routes. *Computer-Aided Civil and Infrastructure Engineering* [online]. 2014, **29**(10), p. 723-737. eISSN 1467-8667. Available from: https://doi.org/10.1111/mice.12113
[12] KITAMURA, F., INAZU, D., IKEYA, T., OKAYASU, A. An allocating method of tsunami evacuation routes and refuges for minimizing expected casualtiess. *International Journal of Disaster Risk Reduction* [online]. 2020, **45**, 101519. ISSN 2212-4209. Available from: https://doi.org/10.1016/j.ijdrr.2020.101519
[13] BALOYE, D. O., PALAMULENI, L. G. Modelling a critical infrastructure-driven spatial database for proactive disaster management: a developing country context. *Jamba - Journal of Disaster Risk Studies* [online]. 2016, **8**(1), p. 1-14. ISSN 2027-845x, eISSN 1996-1421. Available from: https://doi.org/10.4102/jamba.v8i1.220
[14] COBURN, A. W., SPENCE, R. J. S. *Earthquake protection*. 3. ed. London: John Wiley and Sons, 2002. ISBN 978-0-470-84923-1.
[15] Sea Defense Consultants. Tsunami refuge planning guideline-SDC-R-70022. Agency for Rehabilitation and Reconstruction, 2007.
[16] SITTI, F. S., TUNINITYAS, A. R., ADIPANDANG, Y. Evacuation route planning in Mount Gamalama Ternate Island - Indonesia. *Procedia Environment Sciences* [online]. 2013, **17**, p. 344-353. ISSN 1878-0296. Available from: https://doi.org/10.1016/j.proenv.2013.02.
[17] SOUTHWORTH, F. Regional evacuation modeling in the United States: a state-of-the-art review. Report No. ORNL-TM/11740. Oak Ridge: Oak Ridge National Laboratory, 1991.
[18] XIE, CH., TURNQUIST, M. A. Integrated evacuation network optimization and emergency vehicle assignment. *Transportation Research Record: Journal of the Transportation Research Board* [online]. 2009, **2091**, p. 79-90. ISSN 0361-1981, eISSN 2169-4052. Available from: https://doi.org/10.3141/2091-09
[19] POST, J., WEGSCHEIDER, S., MUCK, M., ZOSSEDER, K., KIEFL, R., STEINMETZ, T., STRUNZ, G. Assessment of human immediate response capability related to tsunami threats in Indonesia at a sub-national scale. *Natural Hazards Earth System Science* [online]. 2009, **9**(4), p. 1075-1086. ISSN 1561-8633. Available from: https://doi.org/10.5194/nhess-9-1075-2009
[20] MUHAJIR, A. Utilization of geographic information system for route determination and evacuation building case study: Syiah Kuala District of Banda Aceh. Thesis. Technology Institute of Sepuluh Nopember Surabaya, 2013.
[21] Directorate of Urban Road. Indonesia highway capacity manual (IHCM). Directorate General of Highways. Jakarta: Directorate of Urban Road, 1997.
[22] CHEN, X., ZHAN, F. B. Agent-based modelling and simulation of urban evacuation: relative effectiveness of simultaneous and staged evacuation strategies. *Journal of the Operational Research Society* [online]. 2008, **59**(1), p. 25-33. ISSN 0160-5682, eISSN 1476-9360. Available from: https://doi.org/10.1057/palgrave.jors.2602321
[23] FAUZIAH, FATIMAH, E., SYAMSIDIK, Assessment of the tsunami disaster risk level for the Banda Aceh City area. *Journal of Civil Engineering - Unsyiah*. 2014, **3**(2), p. 145-156. ISSN 2088-9321. Available from: http://jurnal.unsyiah.ac.id/JTS/article/view/5580/4611
[24] Statistic of Kuta Raja Sub district. Kuta Raja sub district in figure. Statistics Indonesia. Banda Aceh, 2016.
[25] Statistic of Kuta Raja Sub district. Kuta Raja Sub District in figure. Statistics Indonesia. Banda Aceh, 2015.
[26] FEMA. Guidelines for design of structures for vertical evacuation from tsunamis [online] [accessed 2015-06-21]. 2008. Available from: https://www.FEMA.gov/media-library-data/20130726-1641-20490-9063/femap646.pdf
[27] DEWI, R. S. A gis based approach of an evacuation model for tsunami risk reduction. *Journal of Integrated Disaster Risk Management* [online]. 2012, **2**(2), p. 108-139. ISSN 2185-8322. Available from: http://doi.org/10.5595/idrim.2012.0023

[28] JUN, L., HATOYAMA, K., IEDA, H. Formulation of tsunami evacuation strategy to designate routes for the car mode - lesson from the three cities in Tohoku Area, Japan. In: The Eastern Asia Society for Transportation Studies: proceedings. 2013.

[29] BUDIARJO, A. Evacuation shelter building planning for tsunami-prone area: a case study of Meulaboh City - Indonesia. Thesis. Enschede, The Netherlands: International Institute for Geo-Information Science and Earth Observation, 2006.

[30] TAMIN, O. Z. Transportation planning and modelling: theory, case study and applications. Bandung: ITB Press, 2008. ISBN 979-8591-67-4.

[31] SUSILO, B. H., IMANUEL, I. Traffic congestion analysis using travel time ratio and degree of saturation on road sections in Palembang, Bandung, Yogyakarta and Surakarta. *MATEC Web of Conferences* [online]. 2018, **181**, 06010 eISSN 2261-236X. Available from: https://doi.org/10.1051/matecconf/201818106010

[32] MELKOVA, P. *Prague public space design manual* (in Czech). Prague: Institute of Planning and Development of the Capital City of Prague, 2014. ISBN 978-80-87931-09-7.

[33] KRAMAROVA, Z. Search for requirements for the width of pedestrian roads in the context of the classification of public space. *IOP Conference Series: Materials Science and Engineering* [online]. 2021, **1203**, 032050. ISSN 1757-8981, eISSN 1757-899X. Available from: http://doi.org/10.1088/1757-899X/1203/3/032050

[34] LAWALATA, G. M., FAISAL, R., IDA, R. S., VERA, G., SRI, A., HARLAN, P. P. Design vehicle for geometric highway design in Indonesia. *Road and Bridge Journa*l. 2019, **36**(2), p. 117-131. eISSN 2527-8681.


1953
70
2023
ŽILINSKÁ UNIVERZITA V ŽILINE
ŽILINSKÁ UNIVERZITA V ŽILINE
BiotechUSA
SOM VEDEC
Strojnícka fakulta
BA BB
E 499 062

# THE SMART CITY CONCEPT TO INCENTIVIZE PUBLIC TRANSPORT IN THE V4 COUNTRIES IN THE POST-COVID-19 PERIOD

**Milan Kubina, Oliver Bubelíny ***

University of Zilina, Zilina, Slovakia

*E-mail of corresponding author: oliver.bubeliny@fri.uniza.sk

***Resume***

The attractiveness of public transport is not high and therefore it is obvious that private transport is the preferred mode of transport. The interest in public transport has declined even more since the outbreak of the COVID-19 pandemic, during which passengers feared the rapid spread of the disease in public vehicles. As a result, the habit of traveling individually has increased. This paper highlights the massive increase in private transport in the V4 Countries by the use of private vehicles and the related decrease in use of public transport. It also presents some of the relevant tools of the Smart City concept that could improve the use of public transport in cities. This paper is aimed at highlighting the current use of public bus transport (including public transport) in the V4 countries vis-a-vis the ongoing COVID-19 pandemic and highlighting the information and communication technology (ICT) - related means of incentivization.

***Article info***

Received 5 May 2022
Accepted 17 August 2022
Online 26 October 2022

***Keywords:***

public transport
management
smart city
strategy
COVID-19

Available online: https://doi.org/10.26552/com.C.2022.4.G15-G23

ISSN 1335-4205 (print version)
ISSN 2585-7878 (online version)

## 1 Introduction

Transport is one of the sectors that have major impacts on the environment of all countries. Industry emissions have been gradually declining since 1990, but the transport emissions are constantly on the rise. Overall, passenger cars, vans, trucks and buses account for 70% of the total greenhouse gas emissions generated by transport. The other 30% comes mainly from the aviation and shipping sectors. Road transport, therefore, has a significant environmental impact. Air pollution from traffic can be mainly seen in urban areas that are exposed to higher concentrations. Currently, the European Union is moving towards reducing the air pollution from transport, in particular through the introduction of fuel quality standards and the promotion of electromobility. The other traffic environmental impacts - high noise and landscape disturbance - should also be taken into account [1]. Cities, as well as individual countries, are committed to reducing the impact of transport on air quality through the adoption of European Union standards. Improving the air quality in cities creates a better climate for living in cities and conurbations. The significant increase in private transport and the low use of public transport is also a problem. The share of private transport in 2018 in Slovakia raised to 73.6%. The remaining share was taken by road, rail and public transport [2]. The OECD estimate indicates an ambitious opportunity to reduce the emissions produced by urban transport by 80% compared to 2015 if the right urban policies were adopted [3].

The COVID-19 pandemic has also caused a huge drop in passenger motivations to use the public transport. Quarantine mandates have significantly reduced mobility. Fears and anxieties about using the public transport have again sparked the increase in private transport. The solution to reducing emissions in cities is to create sustainable and reliable public transport. It is this type of transport that is currently greatly aided by the Smart City concept, which uses information and communication tools to make urban areas, including transport, more efficient. In addition to the Smart City concept, cities need to adopt other measures to promote the public transport, such as creating emission zones, expanding infrastructure for urban micromobility etc. [3].

***Table 1*** *Advantages and disadvantages of the public transport*

| Advantages | Disadvantages |
|---|---|
| major reduction of air pollution | maybe slower |
| fewer traffic jams in cities | need to overcome the ‚Last kilometer' |
| high availability | lower comfort |
| less parking spaces | lower flexibility |
| higher safety | lower privacy |
| plenty of time while travelling | higher risk of infection |

## 2 Theoretical review

Public transport, in general, can be considered as any transport for a fee paid to the operator. From the city and region perspective, the public transport should be designed to be friendly to inhabitants. Development of the motor transport and the availability of motor vehicles have made private transport the preferred mode over public transport. In the 90s of the 20th century, private transport began to rise already by up to 90%. Currently, this trend continues, although an increase in public transport passengers has also been observed since the COVID-19 pandemic. In her research, Steg pointed out that avid car users are the primary opponents of public transport. For them, the vehicle is a symbol of prestige and independence. Thus, the car is not only a means of transport for them, but it also represents certain cultural and psychological values. Conversely, casual car users had a much more positive attitude towards the public transport [4].

The pandemic has brought great uncertainty to public transport with passengers' fear of a potential outbreak. As a result, the public transport is going through a major decline in general (rail, road, private, primarily urban transport). On the other hand, no significant increase in private transport was observed, primarily due to the introduction of quarantine mandates, which decreased the mobility of the population. Most employees worked from home and the students switched to online learning. A number of publications, focusing on public transport and COVID-19, have highlighted the significant impacts of individual governments concerning public transport. Wielechovski et al. pointed to the adverse impact of governmental measures on urban mobility. They also pointed out that the interconnection between the increase in individual cases and the use of public transport had not been confirmed [5]. Rasca highlights the impact of the measures on mobility in their article also. They point to the relationship of individual restrictive measures to the strong impact on the number of passengers in public transport (lockdown, open schools in some regions etc.) [3]. When deciding between the private transport or micromobility, people mainly took their feeling of safety into account. They saw public transport as an area where the disease could spread faster. Beck et al. in their study from Australia highlighted the relationship between the use of public transport and its safety from a hygienic perspective. People with greater concerns about hygiene showed less interest in using the public transport. For this reason, they perceived it as a risk [6]. Similar studies have been carried out in different European cities with very similar results. Residents use private transport more and their perception of public transport has deteriorated, e.g. in terms of comfort and quality [7-8].

Public transport has thus become a negatively perceived mode of transport in many cities around the globe. Given the many benefits of public transport, cities need to incentivize their residents to use it. Table 1 shows several general advantages and disadvantages of the public transport.

Most of the advantages above are the result of the large capacity of vehicles. A public transport vehicle can carry a number of passengers who would otherwise use cars. All this generates traffic jams, which in turn has a negative impact on air quality. Conversely, the disadvantages are a large number of people in the vehicle and the need to cover the "last kilometer" from the public transport stop.

The incentive for the residents towards the frequent use of public transport can come in the form of different tools rendered by the Smart City concept. In general, a Smart City can be defined as a city that uses information and communication means to improve the quality of life of its residents, support the economy and address the traffic problems in order to build a sustainable city with lower environmental impacts. The individual components of the Smart City can include smart economy, smart public administration, smart housing, smart population, smart transport and smart environment. Smart transport can be generally defined as a way of managing traffic in a city that can use information and communication means to ensure the smooth mobility of the city residents. These are the possibilities of building a sensor network, building the signal preference of public transport vehicles and solving micromobility issues. The deployment of information and communication means in the city traffic management brings valuable information to city officials in the form of real-time data collection. Subsequently, this facilitates ad-hoc decisions or other managerial decisions with regard to the strategic management of the city [9].

## 3 Materials and methods

This paper is aimed at highlighting the current use of public bus transport in the V4 countries *vis-a-vis* the ongoing COVID-19 pandemic and highlighting ICT-related means of incentivization. The view of use of the public transport is complemented by the view of registered motor vehicles in the V4 Countries. The term "V4 Countries" refers to the countries of the Visegrad Group: Slovakia, Czech Republic, Hungary and Poland. These are Slovakia's neighbors, which are part of the European Union. The following research questions were defined to produce this paper and achieve its goal.

RQ1: Did the COVID-19 pandemic - together with different governmental mandates - affect the volume of public transport in the cities of the V4 Countries?

RQ2: Is there a negative correlation between the use of public transport and private vehicles in the V4 Countries?

RQ3: Do any measures (tools) exist in the Smart Cities concept that can incentivize passengers to use public transport?

This paper uses data taken from the V4 Countries' statistical data. The period under examination was 2012–2020. The Statistical Office of the Slovak Republic does not keep accurate information on the number of people transported by the urban public transport; therefore the data for Slovakia are counted together with the suburban transportation. For the rest of the paper, a content analysis of scientific papers (assessment of public transport during the pandemic around the globe) was used, as well as other publications and websites that are directly focused on building the smart cities.

## 4 Results

The data collected were analyzed and presented in MS Excel. The data were normalized to a common reference scale in millions of passengers and millions of private cars. The data were subsequently used to analyze and provide answers to the presented research questions:

*RQ1 Did the COVID-19 pandemic - together with different governmental mandates - affect the volume of public transport in the cities of the V4 Countries?*

This research question can be divided into two sub-questions with a focus on public and private transport for easier interpretation:

- RQ1a: Did the COVID 19 pandemic and the relevant governmental measures affect the public transport?
- RQ1b: Did the COVID 19 pandemic and the relevant governmental measures affect the private transport concerning the number of registered vehicles in the V4 Countries?

With regard to RQ1a, it can be stated that the reduction in the number of public transport passengers was apparent in all the V4 Countries. Until the outbreak of the pandemic in 2020, the number of public transport passengers was fluctuating. In 2020, there was a massive drop due to the COVID-19 pandemic. This came due to the introduction of governmental measures, such as lockdown, quarantine mandates and the like, higher reluctance to use public transport due to hygienic safety, or increased use of non-motorized means of transport. Figure 1 shows the progress of the number of passengers in the V4 Countries.

With regard to RQ1b, to analyze the private transport, it is possible to use the indicator of registered vehicles of individual countries. Figure 2 shows the increases in passenger motor vehicles (4-wheel motor vehicles used for passenger transport). It follows that the increase in the number of vehicles is not just the result of the pandemic. The increase in the number of registered vehicles happens constantly across the period under analysis. However, no significant increase in the number of registered vehicles was observed in 2020.

The reason why there was no sharp increase in motor vehicles may also be the introduction of lockdown and the resulting reduced mobility and small imports

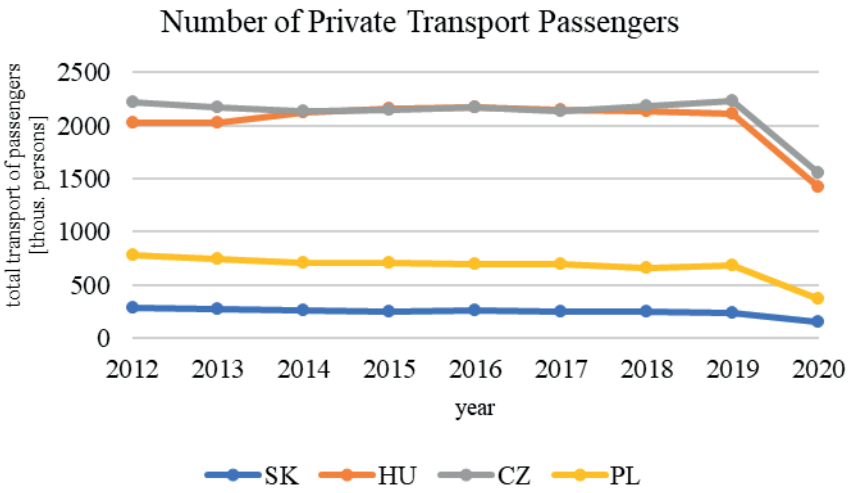


***Figure 1*** *Number of Private Transport Passengers, [7, 10-12]*

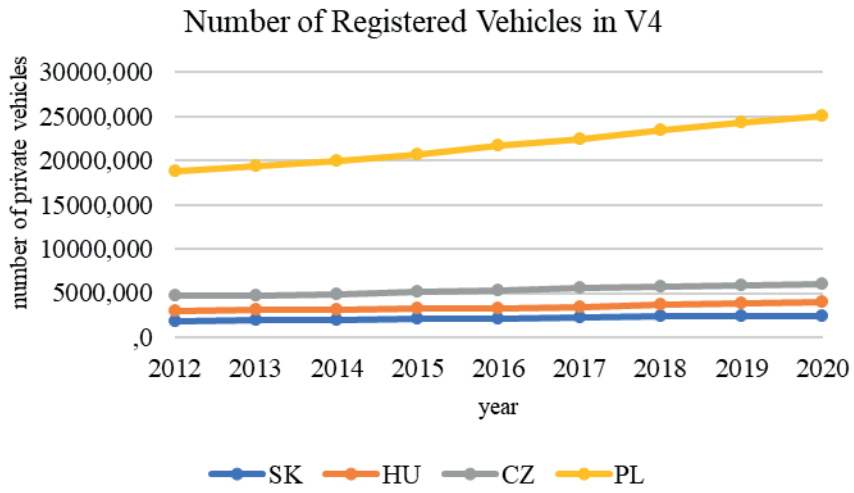


***Figure 2*** *Number of Registered Vehicles in V4, [7, 10-12]*

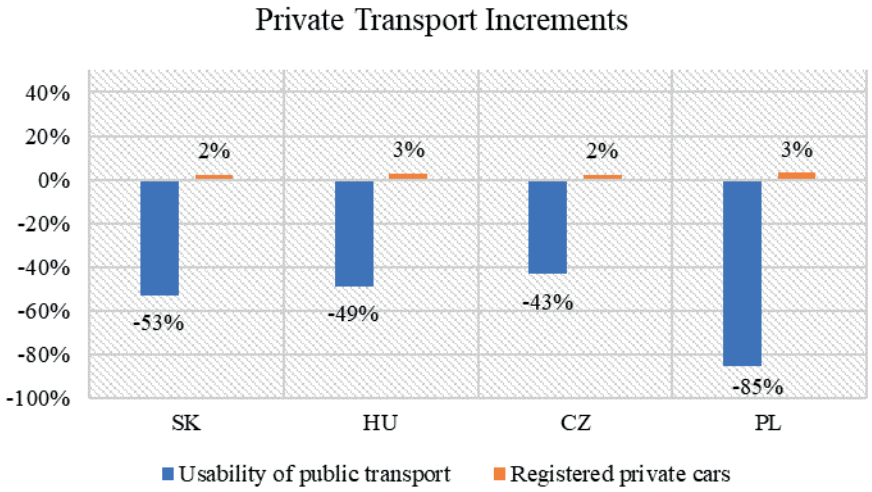


***Figure 3*** *Private Transport Increments, [7, 10-12]*

of used cars. Other reasons could be a job loss or fear of buying new vehicles. Figure 3 shows a comparison of the percentage shift of increments of registered vehicles and the number of transported passengers in the V4 Countries.

From the above, it can be stated that the increments of new vehicles were relatively low. However, the drop in the use of public transport in 2020 compared to 2019 was significant. In 2020, motor vehicles raised by 2% in Slovakia, which means that additional 46409 vehicles were registered in the country. However, vehicle registration is not the only indicator of the number of motor vehicles; it is also the number of vehicles imported into the country from abroad. Hungary recorded a 3% increase in 2020, an increase of more than 100, 000 vehicles, the Czech Republic a 2% increase, which represents an increase of more than 120,000 vehicles and in Poland, it was an increase of more than 700,000 vehicles. Figure 4 shows the percentage change (increments in individual years) of registered vehicles across the V4 Countries. Conversely, Poland experienced the most significant decline. The differences in the declines in public transport could just have led to a variety of governmental pandemic regulations. Some countries have taken measures lasting a longer period of time (e.g. longer school closures, which drastically reduces city mobility). Different countries have also experienced different pandemic developments.

The RQ1 research question can be answered with respect to its sub-questions RQ1a and RQ1b. The RQ1a question, whether the COVID-19 pandemic had an impact on public transport in the V4 Countries, can be answered with a resounding yes. Drastic restrictions on movement of population through the quarantine mandates and lockdowns, or working from home, have significantly reduced the number of public transport passengers, which is indicated in Figure 1 and Figure 3, showing the apparent drop in the number of public transport passengers. On the other hand, the RQ1b sub-question cannot be answered with a definite yes. The increasing trend in the number of registered vehicles is apparent in the long run. However, since 2017, the

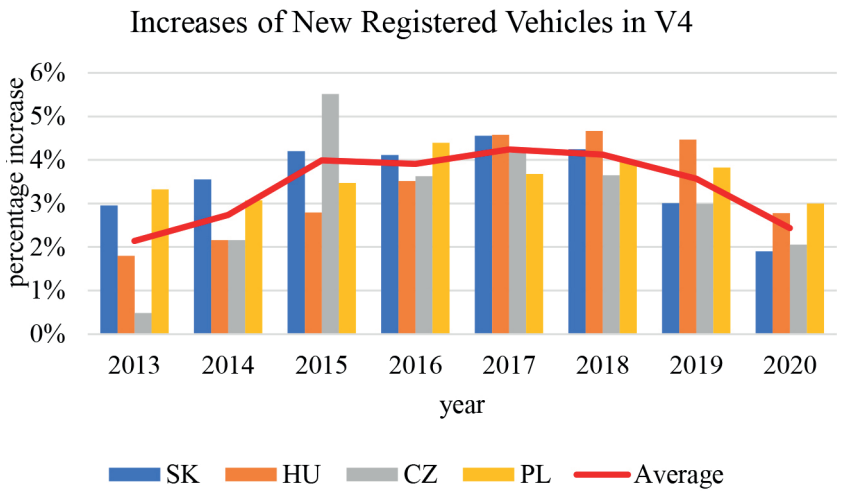


***Figure 4*** *Increases of New Registered Vehicles in V4, source: [7, 10-12]*

***Table 2*** *Results of linear regression*

| Country | Pearson coefficient (R) | P-value |
|---|---|---|
| Slovakia | -0.79 | 0.010863 |
| Czech Republic | -0.48 | 0.184542 |
| Hungary | -0.47 | 0.192737 |
| Poland | -0.73 | 0.023747 |

growth has been gradually slowing down and the increments of registered vehicles are becoming smaller every year. The mean value of the V4 Countries has been declining since 2017. This trend continues even during the COVID-19 pandemic. For this reason, it is not possible to state whether the pandemic had an impact on decline in registered vehicles in the V4 Countries.

RQ2: Is there a negative correlation between the use of public transport and private vehicles in the V4 Countries?

The data were evaluated using correlation and regression analysis. The relationship between the long-term and constant growth of motor vehicles lowering the use of public transport can be confirmed by a negative correlation of variables. Pearson's sample correlation coefficient was used for this confirmation:

$$r_{x,y} = \frac{\overline{x \cdot y} - \overline{x} \cdot \overline{y}}{\sqrt{\overline{x^2} - (\overline{x})^2} \cdot \sqrt{\overline{y^2} - (\overline{y})^2}}, \quad (1)$$

where:

$r$ is Pearson koeficient,

$x$ is number of transported passengers by public bus transport,

$y$ is number of vehicles.

For this coefficient, the higher the number is, the stronger the linear relationship between the variables becomes and vice versa. The results of the calculated Pearson correlation coefficient for individual V4 Countries are shown in Table 2. The coefficient was highly negative in Slovakia and Poland. Hungary and the Czech Republic have a correlation coefficient halved, which really means that in addition to this private transportation increase impact; there are other undefined variables with the same effect. With regard to the created ANOVA model, which represents the analysis of variance, it is possible to monitor the p-value (the level of model significance). Within the veracity of individually created models for the individual country dependencies, it is possible to draw a conclusion. In Slovakia and Poland, the models are statistically significant; in other models, statistical significance was not confirmed.

It can be argued that other factors enter into the relationship of these dependencies, such as the availability of public transport services, the possibility of using micromobility (e-scooters, bicycle-sharing), or dissatisfaction with the quality of public transport - low safety, poor onward connections etc.

As a result of this examination, the research question can be answered affirmatively. A degree of dependency exists between these relationships. However, it is necessary to add that other variables enter into this dependence that has not been examined. This is confirmed by the Pearson coefficient itself, but also by the results of the analysis of variance and the ANOVA model.

RQ3: Do any measures exist in the Smart Cities

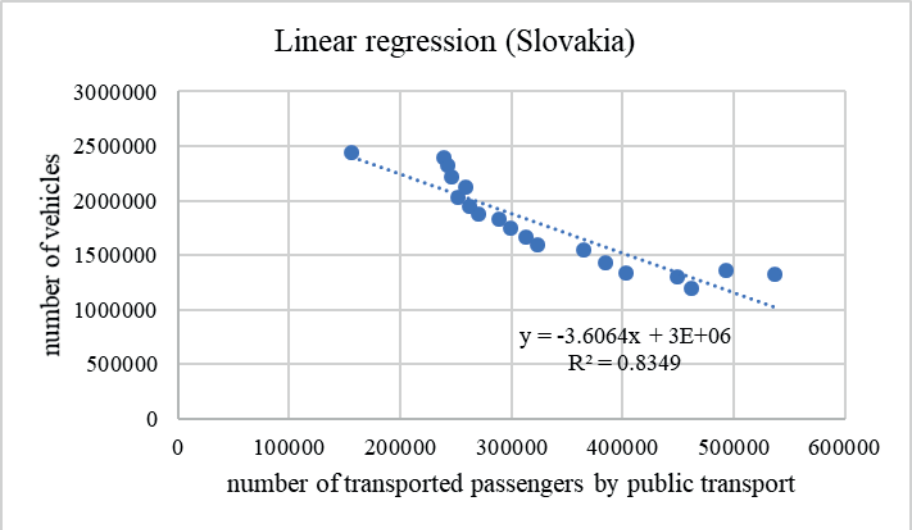


***Figure 5*** *Example of Linear Regression (case Slovakia)*

concept that can incentivize passengers to use public transport?

The effects of information and communication means are observed everywhere. The term and concept of the Smart City deal with use of these resources in practical terms. The goal is definite - to facilitate different management processes in the city, as well as to improve the quality of life of the residents, considering the long-term city sustainability. Internet of Things tools create the space for generating large amounts of data for further analysis and the basis for further decision-making processes. In order to incentivize residents to use public transport more intensively, it is necessary to take such measures that can simplify the purchase of transport tickets, provide route search and speed up the transport itself. Such measures may include:

## 5 Mobility as a service (MaaS)

This type of service comes as a brand new business model to cities. It integrates services of different kinds into one comprehensive platform. The MaaS provider facilitates different transport options and aligns them with customers' requirements. This includes primarily public transport, but it also integrates bicycle sharing, e-scooter sharing, availability of taxis, sharing of motor vehicles etc. A major added value is availability of the city mobility application for customers. Through a single platform, a customer is able to satisfy their transportation needs in several ways by making a payment through this application. This streamlined city transport planning and payment is a clear benefit for the customer. On the other hand, the MaaS provider can collect a huge amount of information and data that can then be used to improve their services. The basic goal of this service is to provide passengers arriving in the cities with a suitable alternative to the private mode of transport [13]. An important part of the functionality of this service is the existing infrastructure - 3G/4G/5G networks and their security, daily updated information on the availability of individual services, timely information on updating schedules, availability of payment systems [14]. To meet the demanding service infrastructural requirements, the cooperation of individual service representatives is key, such as the city management, telecommunication companies, payment service providers, public transport providers and providers of shared services [15]. Another important part is the city's data service providers providing the website and MaaS mobile application. It is this component that is essential to generate a large volume of data, which is used for further analysis and subsequent management. Carrier and shared service providers are key stakeholders to MaaS. With regard to this type of service, third parties, such as Uber, are coming under the spotlight [16].

## 6 Park and ride

It is a parking lot, or a system of parking lots, which are located on the city outskirts connected to the public transportation network. Residents coming to the cities thus park their vehicles on the city outskirts and continue to the city by using the public transport. The advantage of this type of parking is that it reduces the number of motor vehicles entering the city center, which improves air quality and the quality of life of city residents in general. On the other hand, it saves time for drivers to find a parking space. Thus, the time it takes them to get to their destination may be the same. Macziosek and Kurek [17] made an analysis of the use of such car parks in Krakow, Poland. They highlighted the importance of building such parking lots and the right incentivization of drivers, e.g. through free parking if they purchase a public transport ticket. In their research, they also pointed out that the most important element for the use of this type of car park is the

proximity of the public transport spot at the destination and the quality of public transport itself. This system, together with the MaaS interconnection, can ideally affect the number of vehicles in downtowns. Such car parks exist in all V4 Countries. In Slovakia, it is built mainly in locations around the capital with a connection to the railway directly to the city center].

## 7 Public transport preference and bus lanes

Another measure that can be used in individual cities is giving preference to public transport vehicles with traffic lights. Traffic jams and slowdowns at traffic lights are common problems. Again, the problem is the high intensity of private transport, which significantly affects the fluidity of public transport. In the end, its attractiveness is reduced by for instance frequent delays. Another possibility is to build a sensor network on light signals with controllers and transmitters installed in public transport vehicles, which signals when a public transport vehicle is arriving at an intersection and prioritizes it with traffic lights. Several tactics that govern such intersections exist. It can be done in the form of suspending the green lights in the intended path of the approaching public transport vehicle or accelerating the switching of different traffic lights to improve the fluidity of public transport. Many tactics that can switch traffic lights exist and they depend mainly on the use of the intersection and the intensity of the private and public traffic in it [18].

A more fundamental option is to create public transport lanes, which can speed it up and get faster to intersections. However, the basic problem lies in the existing infrastructure, which significantly limits the construction of new lanes in cities (e.g. surrounding buildings, urban greenery etc.).

It is also possible to take restrictive measures with regard to urban mobility. These may include, for instance, the **creation of low emission zones.** Motor vehicles that do not meet the defined requirements are not allowed to enter these zones. It can be a specific emission class (euro 4-6), or it can only be vehicles that are powered by an alternative type of fuel. Many European cities are currently making decisions to build such zones. The aim is primarily to create good and clean air in downtowns. Air quality can also be observed through the Smart City concept, through sensors installed in different parts of the city. According to a case study from Madrid, after the introduction of the low-emission zone, the air quality in the city has significantly improved and the noise, generated by the traffic, was reduced. Other restrictions may include the adoption of parking restrictions, making changes in parking policies, or increasing parking fees [19].

The answer to the RQ3 research is that the Smart City concept has many tools that can be used to increase the share of public transport in cities. However, the implementation of these measures depends on the established city strategy. However, this also depends on other attributes, such as the financing of individual measures, the complexity of interconnection of individual stakeholders, the relative limitedness of the infrastructure, political beliefs etc. Then, it is up to the individual cities and their representatives to what extent they will try to rebuild the city in line with the concept. However, it can be proven that in the city the results after implementation are observable relatively quickly [19].

## 8 Discussion and conclusion

This paper was aimed at highlighting the current use of public bus transport in the V4 countries *vis-a-vis* the ongoing COVID-19 pandemic and highlighting ICT-related means of incentivization. Three research questions were posed with regard to its goal, related to individual and public transportation amidst the ongoing COVID-19 pandemic. The results are positive answers to individually defined questions. The V4 Countries recorded a decline in the number of public transport passengers. On the other hand, the number of registered cars in the countries is constantly increasing, although, in recent years, the increase has a declining nature. The link between the reductions in vehicle registration in relation to the pandemic has not been shown. The relationship between the number of passengers transported by public transport and the number of registered vehicles in the V4 Countries was also examined. Looking at each country individually, there was a minor dependence between the two variables. However, this minor dependence also pointed to the fact that other variables also affect this relationship; namely the availability of motor vehicles, the use of micromobility/bicycle sharing. The last question regarded the City Smart concept. The impact of information and communication means is also apparent in the urban sphere. They bring new possibilities for managing all the parts of the city in line with this concept. Its actual development in cities depends on individual representatives and their interest in deployment. If they were to opt-in, then they would have to comply with several strategic principles from the strategic management perspective [20-21]. It is mainly about planning, project preparation, project implementation and at the same time, implementation follow-ups according to a suitable methodology [22]. The deployment of the entire concept means a real change for the city and several fundamental actions would have to be implemented from a managerial point of view. These include finding sufficient financial resources to create sufficient technical and technological infrastructure in the city (includes the installation of various types of sensors, security cameras etc.). However, the advantage remains that the well-built infrastructure is then suitably applicable in several city management areas.

The aim of the infrastructure is to collect a lot of usable data, which through a suitable system leads to long-term sustainability and competitiveness of the city and provides the city with an advantageous position in relation to other stakeholders [22-23].

From the transport perspective, the aim of the Smart City concept is to incentivize the public transport through a sound infrastructure. Subsequently, the quality of the selected public transport provider and miscellaneous city micromobilities - based on the sharing of electric scooters or bicycles - also contribute to this. Intelligent velomobility and modern e-velomobility, i.e. electrically-powered bicycles, also come to the fore as a part of the Smart City concept [21]. This mode of transport also contributes to reducing emissions in the city and the only question left is to motivate residents and visitors to use them. Smart City as a transport concept must be adopted gradually with regard to functioning of the city ecosystem. It is necessary to emphasize the conviction of the city officials and the willingness to develop the city. However, city officials are often elected for only a certain period and therefore, they refuse to take unpopular measures, which would ultimately have a significant positive effect. These include car prohibitions to enter downtowns, the construction of city outskirts car parks connected to public transport grid, or the digitization of car parks with the temporary exclusion of their operation. However, the communication of this development is the actual communication with the residents who must be informed of these planned changes. It is also essential to involve all other stakeholders [24-25].

Smart City, as a concept for improving the quality of life of the residents, is also a transport solution. Its advantage is the possibility of making public transport more attractive, mainly by simplifying the search for onward connections, purchasing travel tickets and preferring the public transport vehicles at traffic lights. It is necessary to emphasize that it is not only the Smart City concept that is aimed at incentivizing the use of public transport. It is also about, for instance, constantly increasing travel comfort, adjusting onward connections, availability of stops, raising hygiene standards. The future that cities face truly lies in public transport to create a clean environment improving the quality of life of its residents. Cities will thus face the important task of creating a place for people to live that will increase their overall attractiveness. In general, other stakeholders, such as the local or state government, will need to prioritize public transport in order to reduce emissions. After demanding technological and infrastructural solutions and implementation of the concept, the role of cities will thus also include the need to shift the opinion of their residents towards the public transport to become an attractive and comfortable mode of transport.

## References


[1] European Environment Agency [online]. 2020. Available from: https://www.eea.europa.eu/themes/transport/intro

[2] Enviroportal [online]. 2019. Available from: https://www.enviroportal.sk/indicator/detail?id=761&print=yes

[3] OECD iLibrary [online]. 2021. Available from: https://www.oecd-ilibrary.org/sites/316ba973-en/index.html?itemId=/content/component/316ba973-en

[4] STEG, L. Can public transport compete with the private car? *IATSS Research* [online]. 2003, **27**, p. 27-35. ISSN 0386-1112. Available from: https://doi.org/10.1016/S0386-1112(14)60141-2

[5] WIELECHOVSKI, M., CESKA, K., GRZEDA, L. Decline in mobility: public transport in Poland in the time of the COVID-19 pandemic. *Economies* [online]. 2020, **8**(4), 78. ISSN 2227-7099. Available from: https://doi.org/10.3390/economies8040078

[6] BECK, M. J., HENSHER, D. A., NELSON, J. D. Public transport trends in Australia during the COVID-19 pandemic: an investigation of the influence of bio-security concerns on trip behaviour. *Journal of Transport Geography* [online]. 2021, **96**, 103167. ISSN 0966-6923. Available from: https://doi.org/10.1016/j.jtrangeo.2021.103167

[7] Passenger transport - time series - Czech statistical office [online] [accessed 2021-11-15]. Available from: https://www.czso.cz/csu/czso/passenger_transport_time_series

[8] EISENMANN, C., NOBIS, C., KOLAROVA, V., LENZ, B., WINKLER, C. Transport mode use during the COVID-19 lockdown period in Germany: the car became more important, public transport lost ground. *Transport Policy* [online]. 2021, **103**, p. 60-67. ISSN 0967-070X. Available from: https://doi.org/10.1016/j.tranpol.2021.01.012

[9] SHARIF, R. A., POKHAREL, S. Smart city dimensions and associated risks: review of literature. *Sustainable Cities and Society* [online]. 2022, **77**, 103542. ISSN 2210-6707. Available from: https://doi.org/10.1016/j.scs.2021.103542

[10] Transport - Hungarian central statistical office [online]. 2021. Available from: https://www.ksh.hu/transport

[11] Urban transport - Poland [online]. 2021. Available from: https://bdl.stat.gov.pl/BDL/dane/podgrup/temat

[12] Summary indicators for transport and mail - Statistical Office of the Slovak Republic [online]. 2021. Available from: http://datacube.statistics.sk/#!/view/sk/VBD_SK_WIN/do1003rs/v_do1003rs_00_00_00_sk

[13] What is MaaS? - MaaS Alliance [online] [accessed 2021-11-15]. Available from: https://maas-alliance.eu/homepage/what-is-maas/

[14] KUBINA, M., KOMAN, G. Big data technology and its importance for decision-making in enterprises. *Communications - Scientific letters of the University of Zilina* [online]. 2016, **18**(4), p. 129-133. ISSN 1335-4205, eISSN 2585-7878. Available from: https://doi.org/10.26552/com.C.2016.4.129-133

[15] VODAK, J., SOVIAR, J., LENDEL, V. Identification of the main problems in using cooperative management in Slovak enterprises and the proposal of convenient recommendations. *Communications - Scientific letters of the University of Zilina* [online]. 2013, **15**(4), p. 63-67. ISSN 1335-4205, eISSN 2585-7878. Available from: https://doi.org/10.26552/com.C.2013.4.63-67

[16] The rise of mobility as a service - Deloitte review [online]. 2017. Vol. 20. Available from: https://www2.deloitte.com/content/dam/Deloitte/nl/Documents/consumer-business/deloitte-nl-cb-ths-rise-of-mobility-as-a-service.pdf

[17] MACIOSZEK, E., KUREK, A. The use of a park and ride system - a case study based on the city of Cracow (Poland). *Energies* [online]. 2020, **13**, 3473. ISSN 1996-1073. Available from: https://doi.org/10.3390/en13133473

[18] MOGHIMI, B., KAMGA, C. Transit signal priority in smart cities. In: *Models and technologies for smart sustainable and safe transportation systems* [online]. DE LUCA, S., DI PACE, R., FIORI, CH. (eds.). 2021. ISBN 978-1-83880-823-5, eISBN 978-1-83880-824-2. Available from: http://dx.doi.org/10.5772/intechopen.94742

[19] LEBRUSAN, I., TOUTOUH, J. Using smart city tools to evaluate the effectiveness of a low emissions zone in Spain: Madrid Central. *Smart Cities* [online]. 2020, 3, p. 456-478. eISSN 2624-6511. Available from: https://doi.org/10.3390/smartcities3020025

[20] RASCA, S., MARKVICA, K., IVANSCHITZ, B. P. Impacts of COVID-19 and pandemic control measures on public transport ridership in European urban areas - the cases of Vienna, Innsbruck, Oslo and Agde. *Transportation Research Interdisciplinary Perspectives* [online]. 2021, **10**, 100376. ISSN 2590-1982. Available from: https://doi.org/10.1016/j.trip.2021.100376

[21] BEHRENDT, F. Why cycling matters for Smart Cities. Internet of bicycles for intelligent transport. *Journal of Transport Geography* [online]. 2016, **56**, p. 157-164. ISSN 0966-6923. Available from: https://doi.org/10.1016/j.jtrangeo.2016.08.018

[22] MORA, L., DEAKIN, M., REID, A. Strategic principles for smart city development: a multiple case study analysis of European best practices. *Technological Forecasting and Social Change* [online]. 2019, **142**, p. 70-97. ISSN 0040-1625. Available from: https://doi.org/10.1016/j.techfore.2018.07.035

[23] HOLUBCIK, M., VODAK, J., SOVIAR, J. How to manage business in collaborative environment – a case study of multinational companies. *Communications in Computer and Information Science* [online]. 2018, **877**, p. 299-311. ISSN 1865-0929, eISSN 1865-0937. Available from: https://doi.org/10.1007/978-3-319-95204-8_26

[24] ECHANIZ, E., RODRIGUEZ, A., CORDERA, R., BENAVENTE, J., ALONSO, B., SANUDO, R. Behavioural changes in transport and future repercussions of the COVID-19 outbreak in Spain. *Transport Policy* [online]. 2021, **111**, p. 38-52. ISSN 0967-070X. Available from: https://doi.org/10.1016/j.tranpol.2021.07.011

[25] SOVIAR, J., HOLUBCIK, M., VODAK, J. Regional cooperation ecosystem: case of the Zilina self-government region (Slovak republic). *Sustainability* [online]. 2018, **10**, 2219. ISSN 2071-1050. Available from: https://doi.org/10.3390/su10072219

UNIVERSITY
OF ŽILINA

1953 70 2023

In its over 70 years of successful existence, the University of Žilina (UNIZA) has become one of the top universities in Slovakia.


# Scientific conferences

## organized by University of Žilina

**11th International Conference on Air Transport – INAIR 2022 „Returning to the Skies“**
Date and venue: 9.-10. 11. 2022, Bratislava (SK)
Contact: inair@fpedas.uniza.sk
Web: www.inairportal.uniza.sk

**Solid State Surfaces and Interfaces 2022**
Date and venue: 21. - 24. 11. 2022, Smolenice (SK)
Contact: stanislav.jurecka@uniza.sk
web: https://www.savsssi.sk/scope/

**Development of the Beskydy Euroregion XVI**
Date and venue: 25. 11. 2022, Žilina (SK)
Contact: anna.padourova@fpedas.uniza.sk
Web: https://www.uniza.sk

**GISday 2022**
Date and venue: 16. 11. 2022, Žilina (SK)
Contact: jana.izvoltova@uniza.sk
Web: https://svf.uniza.sk/kgd/

**Student Scientific Conference MedIN 2022**
Date and venue: 14. 12. 2022, Žilina (SK)
Contact: veronika.mazgutova@fhv.uniza.sk
Web: https://kmkd.fhv.uniza.sk/medin/

**UNIVERSITY OF ŽILINA**
**Science & Research Department**

Univerzitná 8215/1,
010 26 Žilina,
Slovakia

Ing. Janka Macurová
tel.: +421 41 513 5143
e-mail: janka.macurova@uniza.sk

komunikácie
COMMUNICATIONS

VEDECKÉ LISTY ŽILINSKEJ UNIVERZITY
SCIENTIFIC LETTERS OF THE UNIVERSITY OF ZILINA

VOLUME 24 Number 4

October 2022



Each paper was reviewed by at least two reviewers.
Individual issues of the journal can be found on: http://komunikacie.uniza.sk
The full author quidelines are available at: https://komunikacie.uniza.sk/artkey/inf-990000-0400_Author-guidelines.php
Published quarterly by University of Žilina in EDIS - Publishing House of the University of Žilina.

Communications is currently indexed by SCOPUS, DOAJ and Index Copernicus International Journals Master list, and is icluded in portal SJR - SCImago Journal & Country Rank, EBSCO host, ROAD, Crossref (DOI), iThenticate and Google Scholar.
Communications is preserved in CLOCKSS and Portico to guarantee long-term digital preservation.

**Contact:**
Komunikácie - vedecké listy Žilinskej univerzity v Žiline
Communications - Scientific Letters of the University of Žilina
University of Žilina
Univerzitná 8215/1
010 26 Žilina
Slovakia

E-mail: komunikacie@uniza.sk
Web: https://komunikacie.uniza.sk

ISSN (print version): 1335-4205
ISSN (online version): 2585-7878

Registered No. (print version): EV 3672/09
Registered No. (online version): EV 3/22/EPP
Publisher, owner and distribution:
University of Žilina, Univerzitná 8215/1,
010 26 Žilina, Slovakia

Company identification number IČO: 00 397 563
Frequency of publishing: four times a year
Circulation: 150 printed copies per issue
Print edition price: free of charge

Publishing has been approved by:
Ministry of Culture, Slovak Republic

UNIVERSITY
OF ŽILINA

1953 70 2023

# In its over 70 years of successful existence, the University of Žilina (UNIZA) has become one of the top universities in Slovakia.


The mission of UNIZA is to develop education on the basis of science, research and art activities within national and democratic traditions, to develop harmonic personality, knowledge, the good and creativity of a man and to contribute to the advancement of education, science, and culture for the welfare of the whole society.

Professional profile of UNIZA is unique and includes transport (road, railway, water, air), transport and postal services, communications, civil engineering construction, electrical engineering, telecommunications, informatics, information and communication technologies, management and marketing, mechanical engineering, materials and technologies, robotics, machinery design, energies, civil engineering, crisis and security management, civil security, fire protection, forensic engineering, applied mathematics, teacher training, library and information sciences, social pedagogy and high mountain biology. Results of science and research activities of the University have an important influence not only on the educational activities but also on the development of international cooperation or interconnection with practice.

**UNIVERSITY PARTS**
7 faculties
9 research and educational institutes and centres
3 specialized professional and training workplaces
3 information workplaces
1 economic and administrative department
4 dedicated facilities

**EDUCATION**
7 faculties:
8 000 students
more than 88 000 graduates
172 study programmes

**SCIENCE AND RESEARCH**
699 creative workers
785 000 hours, annual research capacity
190 domestic scientific projects
45 foreign projects
30 scientific and technical journals
50 scientific and professional events per year

**INTERNATIONAL COOPERATION**
The University of Žilina in Žilina has almost 50 valid university-wide bilateral agreements, and cooperates with foreign universities in the EU, Asia, America and Africa. It cooperates on foreign non-research projects and has concluded more than 300 agreements in the ERASMUS + programme.

**UNIVERSITY OF ŽILINA**
**Science & Research Department**

Univerzitná 8215/1,
010 26 Žilina,
Slovakia

Ing. Janka Macurová
tel.: +421 41 513 5143
e-mail: janka.macurova@uniza.sk